ADVANCES AND CHALLENGES OF NON-INVASIVE BRAIN STIMULATION IN AGE-RELATED NEURODEGENERATIVE DISEASES

EDITED BY: Yi Guo, Wei Wu and Junhong Zhou
PUBLISHED IN: Frontiers in Aging Neuroscience

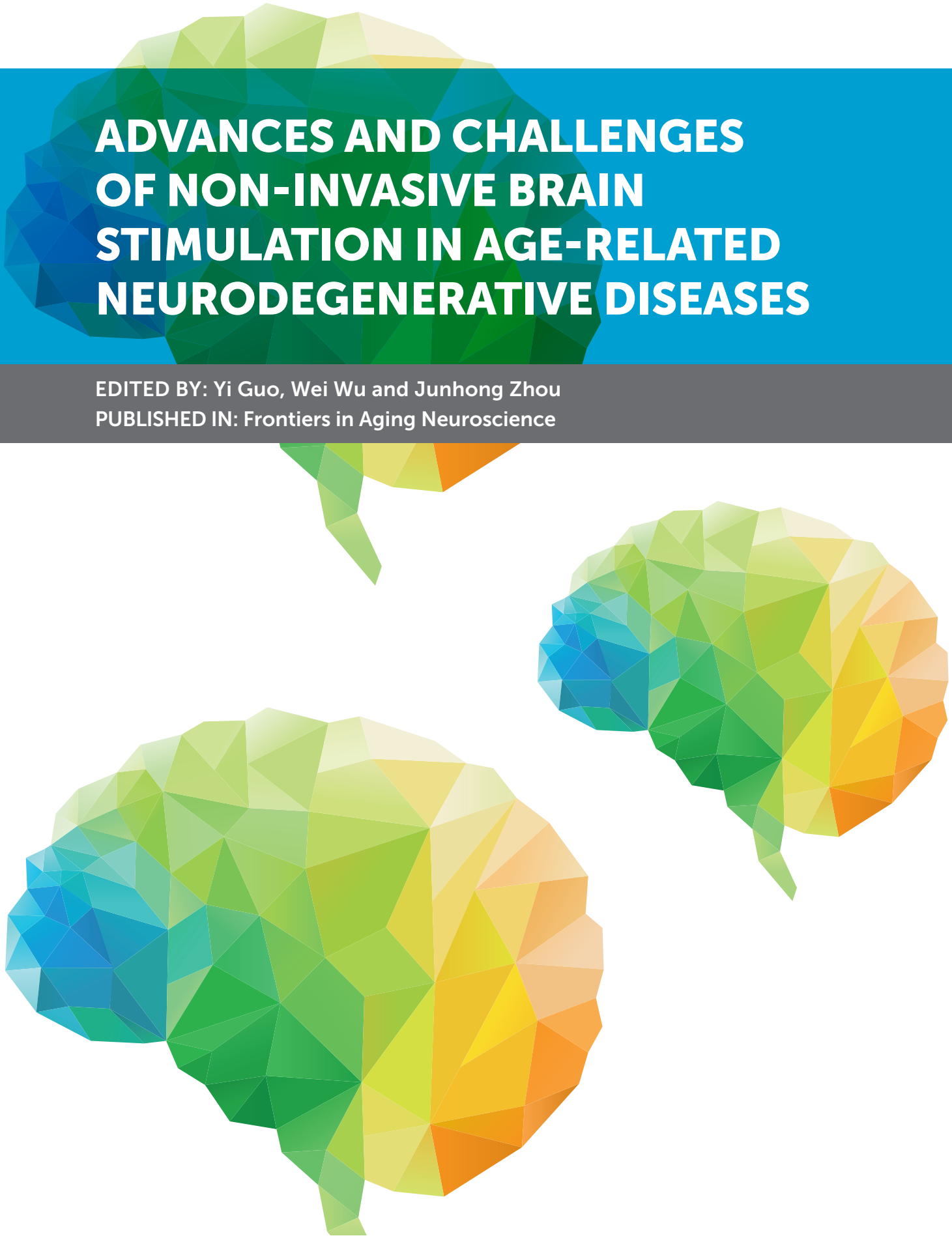

frontiers Research Topics

frontiers

ISSN 1664-8714
ISBN 978-2-88976-461-7
DOI 10.3389/978-2-88976-461-7

About Frontiers

Frontiers is more than just an open-access publisher of scholarly articles: it is a pioneering approach to the world of academia, radically improving the way scholarly research is managed. The grand vision of Frontiers is a world where all people have an equal opportunity to seek, share and generate knowledge. Frontiers provides immediate and permanent online open access to all its publications, but this alone is not enough to realize our grand goals.

Frontiers Journal Series

The Frontiers Journal Series is a multi-tier and interdisciplinary set of open-access, online journals, promising a paradigm shift from the current review, selection and dissemination processes in academic publishing. All Frontiers journals are driven by researchers for researchers; therefore, they constitute a service to the scholarly community. At the same time, the Frontiers Journal Series operates on a revolutionary invention, the tiered publishing system, initially addressing specific communities of scholars, and gradually climbing up to broader public understanding, thus serving the interests of the lay society, too.

Dedication to Quality

Each Frontiers article is a landmark of the highest quality, thanks to genuinely collaborative interactions between authors and review editors, who include some of the world's best academicians. Research must be certified by peers before entering a stream of knowledge that may eventually reach the public - and shape society; therefore, Frontiers only applies the most rigorous and unbiased reviews.
Frontiers revolutionizes research publishing by freely delivering the most outstanding research, evaluated with no bias from both the academic and social point of view. By applying the most advanced information technologies, Frontiers is catapulting scholarly publishing into a new generation.

What are Frontiers Research Topics?

Frontiers Research Topics are very popular trademarks of the Frontiers Journals Series: they are collections of at least ten articles, all centered on a particular subject. With their unique mix of varied contributions from Original Research to Review Articles, Frontiers Research Topics unify the most influential researchers, the latest key findings and historical advances in a hot research area! Find out more on how to host your own Frontiers Research Topic or contribute to one as an author by contacting the Frontiers Editorial Office: frontiersin.org/about/contact

ADVANCES AND CHALLENGES OF NON-INVASIVE BRAIN STIMULATION IN AGE-RELATED NEURODEGENERATIVE DISEASES

Topic Editors:
Yi Guo, Jinan University, China
Wei Wu, Alto Neuroscience, United States
Junhong Zhou, Harvard Medical School, United States

Citation: Guo, Y., Wu, W., Zhou, J., eds. (2022). Advances and Challenges of Non-Invasive Brain Stimulation in Age-Related Neurodegenerative Diseases. Lausanne: Frontiers Media SA. doi: 10.3389/978-2-88976-461-7

Table of Contents

frontiers in Aging Neuroscience

ORIGINAL RESEARCH
published: 15 November 2021
doi: 10.3389/fnagi.2021.766311

Computer-Delivered Cognitive Training and Transcranial Direct Current Stimulation in Patients With HIV-Associated Neurocognitive Disorder: A Randomized Trial

Raymond L. Ownby and Jae Kim*

Department of Psychiatry and Behavioral Medicine, Nova Southeastern University, Fort Lauderdale, FL, United States

Objective: HIV infection is associated with impaired cognition, and as individuals grow older, they may also experience age-related changes in mental abilities. Previous studies have shown that computer-based cognitive training (CCT) and transcranial direct current stimulation (tDCS) may be useful in improving cognition in older persons. This study evaluated the acceptability of CCT and tDCS to older adults with HIV-associated neurocognitive disorder, and assessed their impact on reaction time, attention, and psychomotor speed.

Methods: In a single-blind randomized study, 46 individuals with HIV-associated mild neurocognitive disorder completed neuropsychological assessments and six 20-min training sessions to which they had been randomly assigned to one of the following conditions: (1) CCT with active tDCS; (2) CCT with sham tDCS, or (3) watching educational videos with sham tDCS. Immediately after training and again 1 month later, participants completed follow-up assessments. Outcomes were evaluated via repeated measures mixed effects models.

Results: Participant ratings of the intervention were positive. Effects on reaction time were not significant, but measures of attention and psychomotor speed suggested positive effects of the intervention.

Conclusion: Both CCT and tDCS were highly acceptable to older persons with HIV infection. CCT and tDCS may improve cognitive in affected individuals.

Clinical Trial Registration: [www.ClinicalTrials.gov], identifier [NCT03440840].

Keywords: ranscranial direct current stimulation, computer-delivered cognitive training, human immunodeficiency virus, cognition, HIV-associated neurocognitive disorder, mild neurocognitive disorder

OPEN ACCESS

Edited by:
Wei Wu,
Alto Neuroscience, United States

Reviewed by:
David Eugene Vance,
University of Alabama at Birmingham, United States
Maximilian Achim Friehs,
University College Dublin, Ireland

****Correspondence:***
Raymond L. Ownby
ro71@nova.edu

Received: *28 August 2021*
Accepted: *20 October 2021*
Published: *15 November 2021*

Citation:
Ownby RL and Kim J (2021) Computer-Delivered Cognitive Training and Transcranial Direct Current Stimulation in Patients With HIV-Associated Neurocognitive Disorder: A Randomized Trial. Front. Aging Neurosci. 13:766311. doi: 10.3389/fnagi.2021.766311

INTRODUCTION

While there has been significant progress in the treatment of HIV infection using multiple antiretroviral medications, HIV-association neurocognitive disorders (HANDs) continue to be seen in affected individuals, even when their viral loads are non-detectable (Heaton et al., 2010). HANDs are clinically significant because of their impact on patients' everyday functioning

(Thames et al., 2011a,b, 2013), medication adherence (Hinkin et al., 2002, 2004; Thames et al., 2013), and quality of life (Tozzi et al., 2003; Degroote et al., 2013, 2014; Moore et al., 2014). In older persons, HANDs may have an additive or even synergistic effect in older persons, combining the influences of chronic HIV infection and cognitive aging (Valcour et al., 2004; Wendelken and Valcour, 2012).

Few treatments are available for HAND. Stimulants can improve cognition in HAND but may be abused by vulnerable individuals and have undesirable adverse effects (Hinkin et al., 2001). Other medication treatments have been studied, but none has demonstrated clear efficacy (Antinori et al., 2007; Schifitto et al., 2007, 2009; Sacktor et al., 2011; Nakasujja et al., 2013; Decloedt et al., 2016). Other researchers have suggested that computer-delivered cognitive training (CCT) may be useful in HAND (Vance et al., 2012, 2019; Cody and Vance, 2016), but specialized CCT software is not always readily available or affordable. Further, many programs created for CCT are not inherently interesting, reducing users' motivations for continued use after completing a study for which they were compensated. Another approach may be to use computer gaming software that is already available as a CCT intervention (Zelinski and Reyes, 2009; Bonnechère et al., 2020). CCT software developers have sought to increase the inherent interest in their programs through gamification (Green and Seitz, 2015) to enhance their inherent interest, but many computer games are on the market now and often available at little or no cost. In addition, existing games depend on sustained use by players for their commercial success. Games such as these are interesting to players and include elements that engage them. First-person shooters (in which players use weapons to shoot at fictional enemies) can affect sustained attention and reaction time (Green and Seitz, 2015), however, some players may object to this type of game's violent content (Wu and Spence, 2013; Green and Seitz, 2015).

Another established genre are games that provide players the simulated experience of car racing. These games require attention and psychomotor speed while using content that may be less objectionable. Use of one car racing game, created for a research study, was associated with better mental functioning in older persons (Anguera et al., 2013). Other researchers have commented on the possible usefulness of commercial computer games in addressing mental functioning in persons 50 years of age and older (Basak et al., 2008; Zelinski and Reyes, 2009; Belchior et al., 2012, 2016; Bavelier and Green, 2016). Car racing games can engage and hold players' interest, potentially allowing them to continue cognitive training over extended periods. Researchers have shown that an off-the-shelf game that demanded mental speed resulted in longer use by older individuals when compared to a typical CCT program (Belchior et al., 2012, 2016). Game play has been related to long-term mental training results, with effects evident in other cognitive domains besides those specifically trained (Cardoso-Leite and Bavelier, 2014). Gaming has been shown, for example, to have a positive impact on the ability to regulate and direct mental processes (Anguera et al., 2013). Games may thus be effective for training and can engage users in a sustained fashion.

Players' adherence to regular game play, however, may also be limited even if games are more engaging that other forms of cognitive training. Recent research on ways to encourage users of self-help software has shown that specific game characteristics, such as daily activities to be completed, can help users establish regular play in brief sessions (e.g., 15 min) (Alexandrovsky et al., 2019, 2021). In addition, the effect of type of game play on player motivation may vary across the lifespan (Birk et al., 2017).

Transcranial direct current stimulation (tDCS) in combination with CCT has been shown to improve cognitive functioning (Coffman et al., 2012; Martin et al., 2013, 2014; Trumbo et al., 2016; Lawrence et al., 2017, 2018; Leshikar et al., 2017). tDCS is implemented by applying moistened sponge electrodes to a person's scalp and passing through a very small direct current (1–2 mA). tDCS research has shown that it can have a positive impact on various mental abilities, including verbal problem solving (Cerruti and Schlaug, 2009), working memory (Fregni et al., 2005; Zaehle et al., 2011; Heimrath et al., 2012), and learning (Clark et al., 2012; Floel et al., 2012).

How tDCS affects mental function is not definitively established, however, it has been shown to stimulate brain-derived neurotrophic growth factor (BDNF) in the motor cortex (Fritsch et al., 2010). This may be especially relevant in treating persons with HAND as BDNF is affected in HIV infection (Bachis et al., 2012; Avdoshina et al., 2013), and implicated in cognitive decline in older persons (Buchman et al., 2016). Increases in BDNF might be expected to exert a positive effect on mental functioning in persons with HAND. It may be noted, however, that multiple mechanisms for the effect of tDCS on cognition have been suggested (Yamada and Sumiyoshi, 2021).

We previously completed a pilot study of game-based CCT comparing its combination with active and sham tDCS in persons 50 years and older with HAND (Ownby and Acevedo, 2016). Results suggested that the intervention was acceptable to participants and that it may have had positive effects on their attention and working memory. In the follow-up study reported here, we further explore the acceptability and efficacy of a game-based CCT intervention combined with tDCS in older persons with HIV infection. We hypothesized that CCT with tDCS would be acceptable to persons 50 years of age and older with HAND. We also hypothesized that CCT would be associated with improved reaction time, psychomotor speed, and attention and that the combination of active tDCS with CCT would be superior to CCT alone.

MATERIALS AND METHODS

Participants

Participants were individuals 50 years of age and older with HIV infection. Diagnosis of HAND was established through review of recent laboratory results, clinical evaluation, and neuropsychological testing. All participants stated they subjectively experienced cognitive difficulties and, after assessment, were found to have impairment of mental functioning in two or more cognitive domains while not having dementia, thus meeting Frascati criteria for mild

neurocognitive disorder (Antinori et al., 2007). Potential participants were excluded if they had characteristics that might have increased risk to them from tDCS, such as seizures or bipolar disorder (Galvez et al., 2011; Brunoni et al., 2013). Use of many psychotropic medications was also an exclusion criterion, as the pharmacologic activity of many of these drugs can affect tDCS (Medeiros et al., 2012; McLaren et al., 2018). Medications that were exclusions included those affecting serotonin, such as many antidepressants, dopamine, such as stimulants and antipsychotics, and gamma-amino butyric acid, such as benzodiazepines. Left-handed participants were excluded as our intent was to stimulate the dominant dorsolateral prefrontal cortex.

Procedures

Recruitment and Determination of Eligibility

Participants were first recruited from individuals who had been in a previous study. We also recruited from local service providers for persons with HIV. A number of participants referred friends or acquaintances. We distributed flyers in several areas of Broward County, Florida, known to have a high prevalence of HIV infection, as well as advertising in a local newspaper and creating a Facebook page.

Interested individuals were contacted for a telephone interview to establish that they had complaints of cognitive difficulties, using questions published by the European AIDS Clinical Society (European AIDS Clinical Society, 2015). In this interview, we inquired about use of medications that might lead to exclusion, and whether the person was willing to be in a study of CCT and tDCS. All were being treated for HIV infection and had been on their current medication regimen for at least the past month. Individuals who, from this telephone interview, appeared likely to be eligible were asked to come to our offices for individual assessment.

At this assessment, potential participants completed a series of cognitive assessments (marked with an asterisk in **Table 1**). The battery was selected to allow evaluation of areas often affected in HANDs (Woods et al., 2009). Attention and working memory were evaluated with the Digit Span subtests of the Wechsler Adult Intelligence Scale, 4th edition, or WAIS-IV (Wechsler, 2008). Psychomotor speed was evaluated with the Coding subtest of the WAIS-IV and Grooved Pegboard Test (Lafayette Instrument Company, 2002). Executive function was measured with the Trail Making Test, Part B (Lezak, 2004). Verbal fluency was assessed with the Verbal Fluency test of the Delis-Kaplan Executive Function System (Delis et al., 2001). Verbal learning and memory were assessed with the Hopkins Verbal Learning Test—Revised or HVLT-R (Brandt and Benedickt, 2001), and visual learning and memory with the Brief Visuospatial Memory Test, or BVMT-R (Benedict et al., 1996).

Cognitive impairment for the purpose of establishing the diagnosis of mild neurocognitive disorder was defined as a score in at least two ability areas that was below population norms by at least one standard deviation. Participants were treated for HIV infection that included ongoing laboratory measures of treatment effects (HIV-1 viral load and CD4 cell counts). Individuals in the study brought recent laboratory results, allowing us to verify their HIV status and know their current treatment and immune status. All medications were also brought to this visit to allow verification of current medication use. Persons who met entry criteria then completed the additional assessments as described in the next section.

Acceptability

We used several strategies to evaluate the feasibility and acceptability of the CCT with tDCS intervention to participants. We used a questionnaire based on the Technology Acceptance Model, or TAM (Venkatesh et al., 2003; Venkatesh and Bala, 2008), the dimensions of which have received substantial support for use with digital health technologies

TABLE 1 | Cognitive and functional measures used.

Domain	Measure
Reaction time	*California computerized assessment package (CalCap)* (Venkatesh and Bala, 2008)
Attention	**Wechsler adult intelligence scale, 4th Ed.,* digit span subtest (Molero-Chamizo et al., 2018)
	Wechsler memory scale, 4th ed., symbol span subtest (Seidel and Ragert, 2019)
Psychomotor speed	**Wechsler adult intelligence scale,* 4th ed., coding subtest (Coppens et al., 2019)
	*Trail making test, part A (Rourke et al., 1999)
	*Grooved pegboard (Buchman et al., 2016)
Premorbid function	Wechsler test of adult reading (Santos et al., 2018)
Executive function	*Trail making test, part B (Rourke et al., 1999)
	*Verbal and design fluency from D-KEFS (Lawrence et al., 2017)
	Stroop color word test (Cerruti and Schlaug, 2009)
	Iowa gambling task (Hinkin et al., 2001)
Learning and memory	*Hopkins verbal learning test—revised (Antinori et al., 2007)
	*Brief visuospatial memory test—revised (Sacktor et al., 2011)
Functional status	Medication management test—revised (Thames et al., 2011a)
	University of California San Diego performance-based skills assessment (Albert et al., 1999; Atkinson et al., 2004)

Measures used to establish eligibility are marked with an asterisk.

(Binyamin and Zafar, 2021). The model specifies that users' perceptions of an application's ease of use and usefulness are related to their future intention to use the application. We hypothesized that if the intervention were viewed favorably by participants, their average rating on the Usefulness and Ease of Use scales of this questionnaire would be significantly different from the midpoint of the scale in a positive direction. Participants rated subscale items on a seven-point Likert-type scale anchored at one end with "strongly disagree" and at the other "strongly agree."

Another scale was developed based on a model balancing risks and benefits of a treatment was used to develop a questionnaire assessing users' perceptions of the balance between an intervention's risks and benefits (Atkinson et al., 2004, 2005). Participants were asked, for example, if they experienced benefits from the intervention and adverse effects from it. They were then asked to provide an overall judgment as to whether the benefits of the intervention outweighed its adverse effects. Spontaneous comments about the intervention made by participants during training sessions were recorded verbatim.

Cognitive Measures

In order to evaluate possible cognitive effects of the intervention more comprehensively, participants additional assessments after determination of their eligibility. Use of these measures allowed tests of the study's hypothesis that participants receiving the active interventions would display better performance than control participants in reaction time, attention, and psychomotor speed.

In order to evaluate intervention effects on participants' reaction time, they completed the California Computerized Assessment Package (Miller, 2013). To further evaluate the effects of the intervention on executive functions, participants also completed the Stroop Color Word Test (Golden, 1978), the Iowa Gambling Task (Bechara et al., 2005), and the Design Fluency subtest of the Delis-Kaplan Executive Function System (Delis et al., 2001). Finally, to assess whether the intervention had an impact on everyday functional performance, participants completed the Medication Management Test—Revised, a measure of the person's ability to understand and carry out medication-related tasks (Albert et al., 1999) and the University of San Diego Scales of Observed Performance (Patterson et al., 2001), assessing their ability to perform everyday tasks such as making a medical appointment and paying a bill. Finally, in order to provide an estimate of participants' premorbid level of functioning, they completed the Wechsler Test of Adult Reading (Wechsler, 2001).

Other Self-Report Measures

The assessment battery also included the Patient's Assessment of Own Functioning or PAOF (Chelune et al., 1986). This measure asks the individual to self-report their experience of mental problems in several domains such as language, perception, and memory. It has been used in other studies of HAND (Rourke et al., 1999). We also used the Center for Epidemiological Studies Depression scale or CESD (Radloff, 1977) to assess participants' symptoms of depression. All self-report assessments were completed using computer software that read questions aloud and enabled participants to record their responses by tapping on the computer screen.

Compensation

After these initial assessments were done, individuals in the study were asked to return to begin the intervention. Participants received compensation for their involvement, US $80 for the baseline and follow-up sessions, and $40 for each intervention visit.

Computer-Based Cognitive Training

At the first training visit (after completion of baseline assessments), participants were assigned to intervention group using a computer-created randomization scheme. The scheme was generated via random numbers in a predetermined block (n = 3) randomization scheme. Participants were enrolled by the study coordinator (who was blind to treatment assignment) and assigned by the unblinded principal investigator who also conducted all training sessions.

First, procedures regarding the administration of tDCS and the use of the game controller (an Xbox game controller with USB interface to a Windows computer). The participant sat in front of and to the right of the researcher; the participant could not see the direct current device for tDCS or the researcher taking notes during training. For all participants, the anode electrode was located over the left dorsolateral prefrontal cortex (10–20 system F3) and the cathode over the right supraorbital area (FP2) (Acharya et al., 2016). This montage was used because of the likely effect of stimulation at this site on the left dorsolateral prefrontal cortex. This area of the brain was chosen for stimulation as it is known to be involved in complex executive functions such as control of cognitive processes and attention (Leh et al., 2010; Brosnan and Wiegand, 2017), and previous research has shown that its stimulation may affect relevant executive cognitive functions (Elmer et al., 2009; Javadi and Walsh, 2012; Trémolière et al., 2018; Angius et al., 2019). We also completed a computer simulation analysis of the likely current density that would result from the chosen montage (**Figure 1**) using commercially available software (HD Explore; Soterix Medical, Woodbridge NJ, United States).

Soterix EASYPads, doubled sponges with dimensions of 5 cm × 5 cm (Soterix Medical: New York) were used as electrodes. Approximately 7 cc of sterile saline was used to moisten them. They were positioned by the researcher and then fixed in place with a head band. Current for the tDCS intervention was supplied with an iontophoresis device (ActivaDose II; Gilroy, CA: Activatek). Flat rubberized carbon electrodes were inserted into the moistened sponges. Impedances were assessed before each session and kept below 20K ohms prior to stimulation.

We told people in the study that they might experience minor discomfort at the beginning of the session and that the experience might persist or fade away during the intervention (Brunoni et al., 2013). We then asked the persons in the study to pay attention to the computer while the game was set up and the tDCS intervention was begun. Individuals in the active tDCS group received a current of 1.5 mA, ramping up over 30 s and

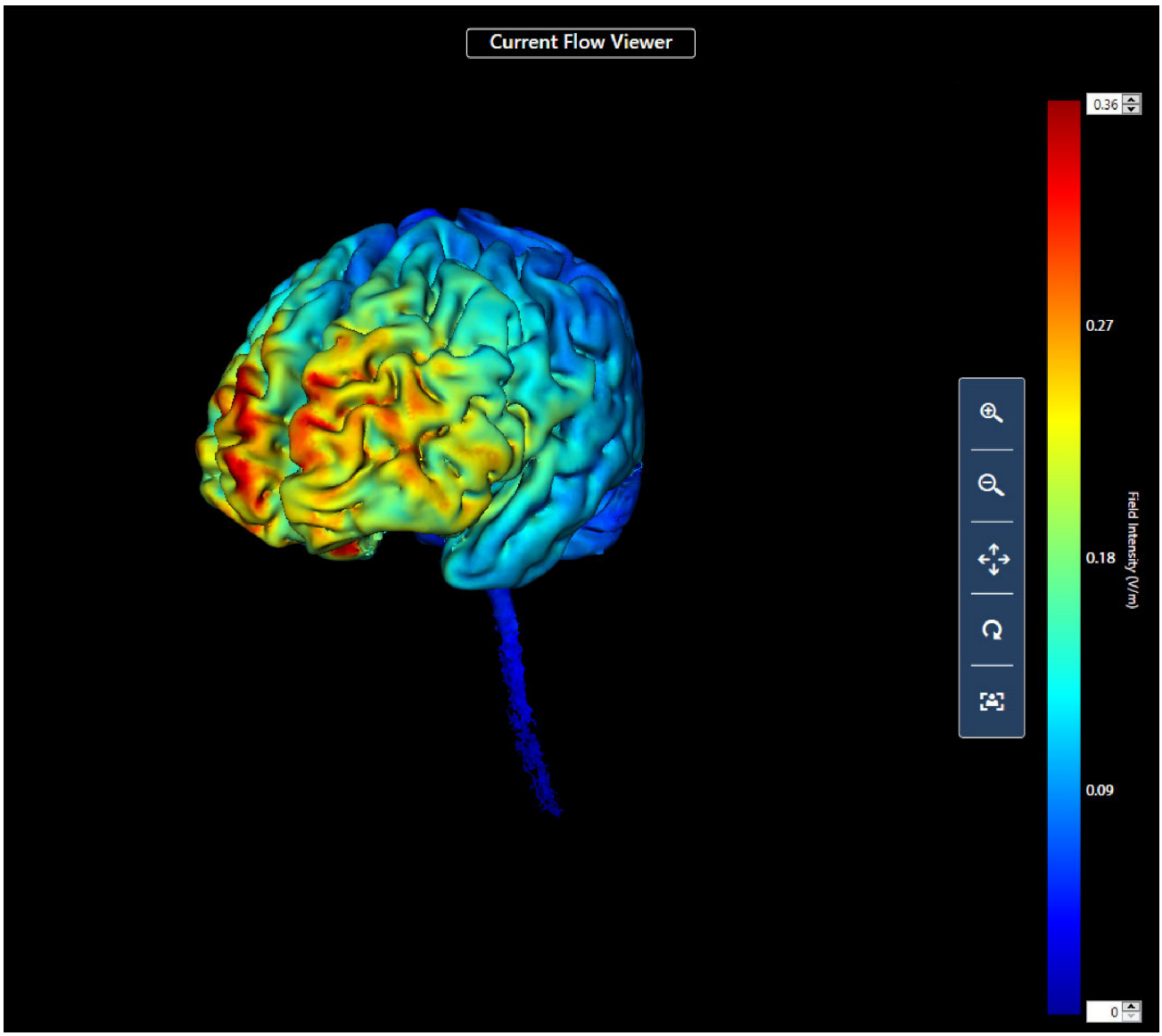

FIGURE 1 | Computer simulation of current flow.

continuing for 20 min. Individuals in the sham tDCS group and the control group received the ramping up current for 30 s which was then ramped down over 30 s.

The cognitive training intervention in this study was a commercially available car racing game *GT Racing 2* (Gameloft SE: Paris, France). This game was chosen because it was easy for most persons and was positively reviewed by a large number of users. We inferred from these characteristics that the participants in the study would find the content tolerable and might even enjoy playing the game. The game includes a several different race courses and types of races to enhance player interest. Game play required that each participant complete each course before moving on to the next. Everyone in the study randomized to CCT was able to complete at least the first four courses during six training sessions.

We encouraged participants to complete each gaming session at their desired pace, although the game imposed some restrictions on their progress. Players had to finish each race in one of the top three places, or navigate a course within a predetermined time, before moving on to the next course. We required as well that participants do each course a minimum of five times. Persons in the study completed six training sessions over a 2-week period. After each intervention session, participants were asked to provide ratings of their thinking, their mood, and how much discomfort they had experienced during the intervention.

Assessments and intervention sessions were completed within 3 weeks from the baseline evaluation. After participants finished the sixth intervention session, they returned to complete cognitive and self-report assessment. Cognitive evaluations

were completed by staff who did not know the participant's intervention group assignment. About 30 days after completing the intervention sessions and follow-up evaluations, persons in the study were asked to return to again complete assessments. All data were collected in the General Clinical Research Center at the Center for Collaborative Research on the campus of Nova Southeastern University beginning in January 2018 and ending in November 2019. The study was concluded at the end of the period of funding support.

Human Subjects Approval and Trial Registration

Study procedures were approved by the Institutional Review Board of Nova Southeastern University (protocol number 2017-410). This study was registered on ClinicalTrials.gov (NCT03440840).

Data Analyses

Planned sample size was determined prior to beginning the study using the mixed effects model simulation routine in PASS 16 (Hintze, 2018). The power analysis showed that a final sample size of 90 (30 per treatment group) would have a power of 0.88 to detect interactions of group membership with time (number of evaluations) with a small effect size (Cohen, 1988; Brydges, 2019).

Data analyses were completed in several steps. Preliminary analyses of data and descriptive statistics were obtained using SPSS version 26 (Armonk NY: IBM). Chi-square and one-way ANOVA tests evaluating the relations of participant ratings of the acceptability and feasibility of the intervention to group assignment were also completed in SPSS. Analyses of treatment effects were completed using R version 4.0.2 (R Core Team, 2020) package lme4 (Bates et al., 2015) for mixed effects models. Significance of model effects (interaction of treatment group assignment with time) was assessed using the likelihood ratio test (Kuznetsova et al., 2017). We evaluated outcomes both through tests of statistical significance as well as approximations of effect size from χ^2-values from likelihood ratio tests and *t*-values obtained in tests of between-group differences obtained using emmeans (Lenth, 2020). Effect sizes were converted to the more familiar *d* statistic using the package esc (Ludecke, 2019). As a *post hoc* assessment not included in the original study protocol the probability of finding the observed number of treatment effects in the hypothesized direction was evaluated using the exact binomial test in the package stats.

RESULTS

The study's CONSORT diagram (Moher, 1998) is presented in **Figure 2**. Demographic, educational and baseline scores for cognitive and functional measures for participants by treatment group are presented in **Table 2**. We screened 155 potential participants, and included 46 in the study. Reasons for excluding potential participants are listed in **Figure 2**. The most frequent reasons for exclusion were use of psychotropic medications, and a personal or family history of bipolar disorder. We thus were not able to include the full number of participants in the study as originally envisioned (planned $N = 30$ per group).

We explored relations of relevant covariates (age, gender, education, immune status) to mental ability variables with standard measures of association (correlations). As several of these associations were substantial and likely to create confounding relations, they were included as covariates in mixed effects random intercept models. Outcomes assessed were changes in test scores across treatment groups before and after the study intervention.

Acceptability to Participants

As hypothesized, participants rated the intervention significantly more positively than the midpoint of the Usefulness subscale of the TAM scale based on a composite of Likert-type items. The mean rating for all participants was 4.33 ($SD = 1.27$; scale range 0 "strongly disagree" to 6 "strongly agree), and this rating was significantly greater than the neutral midpoint [$t(40) = 6.71$, $p < 0.001$]. We also found that they rated its ease of use positively with a mean rating of 5.04 ($SD = 0.95$), ratings that were again significantly greater than the scale midpoint [$t(43) = 5.04$, $p < 0.001$]. Ratings suggested that overall, they enjoyed the intervention (mean = 4.73; $SD = 1.30$) and would use it again if given the opportunity (mean = 4.62; $SD = 1.25$). Participants' ratings did not vary by treatment group (all ps > 0.35).

On the scale which asked participants to assess the intervention's risks and benefits, participant ratings again suggested a positive evaluation, with a mean rating of 4.53 ($SD = 1.20$; scale range 0 "extremely dissatisfied" to 6 "extremely satisfied") on the item "overall the good outweighs the bad" and a rating of 4.70 ($SD = 1.01$) on the item "overall satisfaction." Forty-three of 46 participants (93%) indicated they were satisfied with the intervention.

Participant comments, made spontaneously during or immediately after the training sessions, were consistently positive, for example, "That was fun," "that was great," "I really enjoyed that," and "I have to get me one of these."

Cognitive and Functional Outcomes

Results of evaluations of study outcomes assessed as the interactions of intervention group across evaluations are available in **Table 3**.

We found mixed evidence across cognitive domains to support the hypothesis that CCT with and without tDCS might result in improvements in cognitive functioning relative to control. For the Digit Span Forward subtest, the interaction of treatment group by time approached statistical significance and represented a large effect size. The difference between active tDCS and the control group (**Figure 3**) also approached statistical significance [$t(61.3) = 2.19$, $p = 0.08$; $d = 0.79$]. Other subtests hypothesized to assess attention showed similar positive but non-significant interactions.

Results did not support the hypothesis that persons receiving CCT with or without tDCS would show improved reaction time. Although the observed interactions were in the hypothesized direction, they were not significant and represented at best a very small effect size.

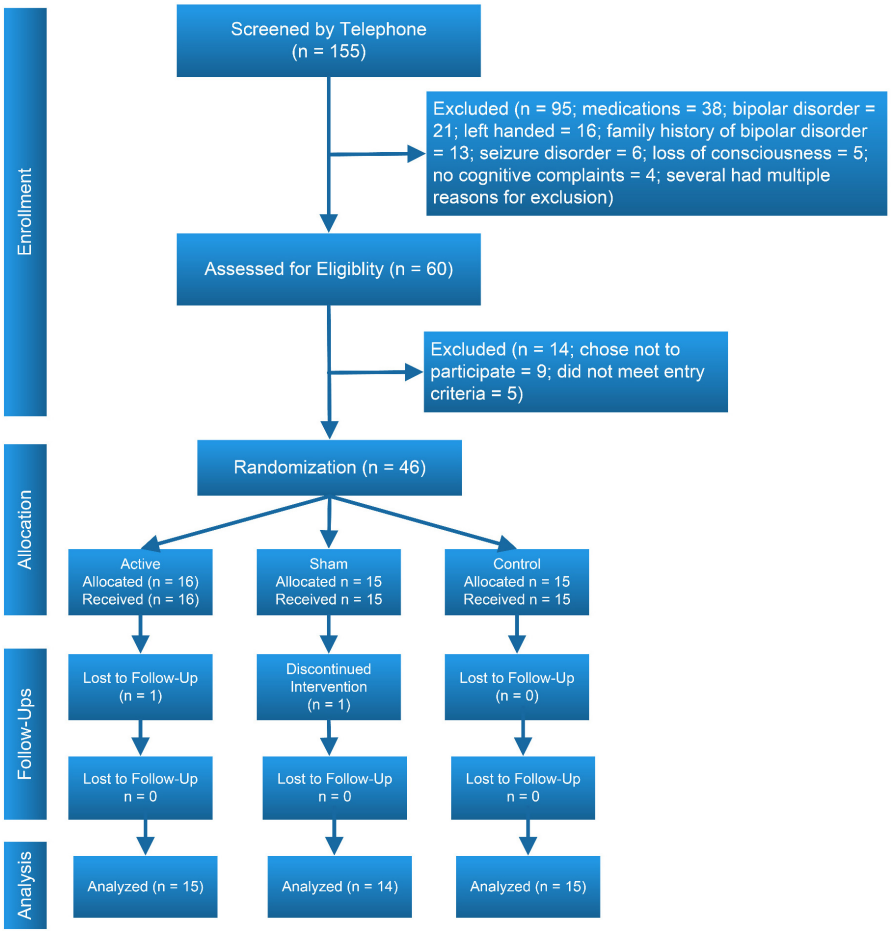

FIGURE 2 | CONSORT diagram.

Results again provided limited support for the hypothesis that CCT with tDCS might result in improved psychomotor speed compared to controls (**Figure 4**). Although the overall interaction of group by time was not significant for Trails B, the comparison of the active treatment group to control approached significance [$t(67.2) = 2.37$, $p = 0.053$; $d = 0.85$], a difference that became significant at second follow-up [$t(67.2) = 3.03$, $p = 0.01$; $d = 1.09$].

We found support for the hypothesis of improvement in psychomotor speed with a significant interaction of group by time for the WAIS-IV Coding subtest, although examination of the interaction plot suggests the effect was primarily due to the performance of persons in the CCT with sham tDCS (**Figure 5**). The between group difference from CCT + sham was not significant at immediate follow-up [$t(45.6) = 1.02$, $p = 0.57$; $d = 0.37$] but approached significance at 1-month follow-up [$t(45.6) = 2.21$, $p = 0.08$; $d = 0.79$].

This pattern was again found in results for the HVLT total score, with a significant interaction of group by time resulting from differential improvement in both treatment groups, with significant difference between the CCT + active tDCS group and control at immediate follow-up [$t(69.6) = 2.51$, $p = 0.04$; $d = 0.90$] and a substantial but no longer significant difference at 1-month follow-up [$t(69.6) = 2.05$, $p = 0.11$; $d = 0.73$; **Figure 6**].

Although we did not pose specific hypotheses for the effects of CCT with or without tDCS on executive function for this study, in exploratory analyses we evaluated the intervention's effects on this domain with several measures. A significant interaction of group by time was found for the Stroop with a large effect size, but as with several other measures, the finding was related to substantial improvement in the CCT with sham stimulation group. Other interactions were again positive but non-significant, with effect sizes in the moderate range.

As with executive function, we did not propose specific hypotheses for the two functional measures included in the assessments, but explored the intervention's effect on them. Results suggest a moderate but non-significant effect size for the MMT with a negligible effect size for the UPSA.

Given the large number of outcomes and our use of effect sizes to evaluate treatment effects, in an unplanned *post hoc* analysis, we evaluated the overall impact of the study intervention based on the number of effect sizes for cognitive variables that were in the hypothesized direction (showing an interaction of group by time favoring one of the active treatment groups).

TABLE 2 | Baseline characteristics of treatment groups.

	Active + CT(*n* = 16)		Sham + CT(*n* = 15)		Control (*n* = 15)	
Gender	**13 Men, 3 Women**		**13 Men, 2 Women**		**11 Men, 4 Women**	
Race	**5 White, 11 Black**		**7 White, 8 Black**		**5 White, 10 Black**	
	Mean	**SD**	**Mean**	**SD**	**Mean**	**SD**
Age (years)	57.06	4.99	58.80	4.13	61.07	6.28
Education (years)	11.94	3.45	14.00	3.59	13.33	3.39
WTAR VIQ[a]	96.75	14.56	102.40	16.10	95.93	14.84
WAIS-IV forward[b]	8.31	1.66	9.67	2.13	8.27	2.22
WAIS-IV backward	6.56	1.55	7.53	2.75	7.00	1.93
WAIS-IV sequence	7.44	1.97	7.73	2.69	6.93	1.98
WAIS-IV total	22.31	3.96	24.93	6.75	22.2	4.92
WMS-IV symbol span	16.13	5.10	16.07	7.42	12.53	4.05
Simple reaction time (ms)	638.31	123.37	620.87	127.66	653.84	122.89
Choice reaction time (ms)	538.63	99.33	523.33	90.75	542.64	122.29
HVLT total	21.69	3.16	20.40	5.90	19.53	3.83
HVLT delayed	6.81	2.56	6.47	2.48	5.60	2.50
BVMT total	14.50	4.66	15.13	8.63	11.80	6.93
BVMT delayed	6.38	2.78	6.40	3.46	4.53	3.44
Trails A	42.81	16.37	43.93	20.10	46.20	11.01
Trails B	98.88	33.40	117.53	40.20	117.73	37.45
Pegs R	99.50	22.96	94.73	21.35	101.47	23.05
WAIS-IV coding	48.94	9.28	51.67	13.70	46.07	15.52
Stroop	29.69	6.98	32.27	9.66	24.80	9.87
IGT	–6.67	22.84	7.73	26.70	–4.67	29.51
MMT	11.94	2.59	13.53	3.56	11.53	4.53
UPSA	79.75	10.71	80.20	16.40	76.73	13.72

[a] *WTAR VIQ, Wechsler Test of Adult Reading estimated verbal IQ.*

[b] *WAIS-IV Forward, Wechsler Adult Intelligence Scale, 4th Ed (WAIS-IV) Digit Span Forward subtest; WAIS-IV Backward, WAIS-IV Digit Span Backward subtest; WAIS-IV Sequence, WAIS-IV Sequencing subtest; WAIS-IV Total, WAIS-IV Digit Span total of three subtests; WMS-IV Symbol, Wechsler Memory Scale, 4th ed, Symbol Span subtest; Simple Reaction Time, California Computerized Assessment Package Simple Reaction task; Choice Reaction Time, California Computerized Assessment Package Choice Reaction task; HVLT Total, Hopkins Verbal Learning Test total score; HVLT Delayed, Hopkins Verbal Learning Test delayed recall score; BVMT Total, Brief Visuospatial Memory Test–Revised total score; BVMT Delayed, Brief Visuospatial Memory Test–Revised delayed recall score; Trails A, Trail Making Test, Part A; Trails B, Trail Making Test, Part B; Pegs R, Grooved Pegboard, right hand performance; WAIS-IV Coding, WAIS-IV Coding subtest; Stroop, Stroop Color-Word test score; IGT, Iowa Gambling Task Net Total score; Verbal Fluency, DKEFS Category Fluency subtest; Design Fluence, DKEFS Design Fluency subtest; MMT, Medication Management Test—Revised score; UPSA Total, UCSD Performance-Based Skills Assessment; subtest.*

The average effect size was 0.52, with 17 effects equal to or greater than 0.16, a small effect size (Brydges, 2019). The probability of this outcome compared to chance (equal distribution of positive effects across all groups) was significantly different (p = 0.04). It is thus improbable that the observed effects of the intervention were only due to chance. It should be acknowledged, that this analysis included positive effects for either treatment group and did not support the original hypothesis that the effects of CCT with active tDCS would be superior to CCT with sham tDCS.

Self-Report Outcomes

Evaluations of treatment by time interactions of participant self-report on the PAOF subscales [PAOF Memory, χ^2 (4) = 1.86, p = 0.76, d = 0.41; Cognition subscale, $\chi^2(4)$ = 0.37, p = 0.98, d = 0.18] and the CESD [$\chi^2(4)$ = 3.38, p = 0.50, d = 0.56] did not suggest the existence of between-group differences in response to the intervention. Examination of the interaction plots for the PAOF subscales (not presented) showed that mean scores for all three groups improved to a similar extent over the three evaluations. Participants reported similar levels of depression (CESD) across groups and evaluations, except participants in the active treatment group reported better mood at the 1-month follow-up evaluation. Although the test of between groups differences were not significant, the within-group change from the immediate follow-up to the 1-month follow-up for the CCT with active tDCS group approached significance and represented a large effect size [$t(78.2) = 2.17$, $p = 0.08$, $d = 0.78$].

Evaluation of participant ratings of how well they could think and remember resulted in an interaction that again approached statistical significance [$\chi^2(10) = 17.47$, $p = 0.06$, $d = 1.59$]. Examination of the interaction plot (**Figure 7**) suggests that persons in the active treatment group reported better ability to think over the final three training sessions, although between-group differences were not statistically significant [$t(106.8) = 1.57$, $p = 0.26$, $d = 0.56$].

TABLE 3 | Likelihood ratio test and effect sizes for the interaction of group by time.

	χ^2	*df*	*p*[b]	*d*
WAIS-IV forward[a]	9.03	4	***0.06***	0.99
WAIS-IV backward	2.56	4	0.82	0.38
WAIS-IV sequence	4.06	4	0.40	0.62
WAIS-IV total	6.55	4	0.16	0.82
WMS-IV symbol span	2.79	4	0.59	0.51
Simple reaction time	0.19	4	0.66	0.13
Choice reaction time	0.29	4	0.59	0.16
Trails A	1.14	4	0.89	0.32
Trails B	3.85	4	0.43	0.60
Pegs R	4.54	4	0.34	(0.66)
WAIS-IV coding	11.80	4	***0.02***	1.17
HVLT total	4.37	4	0.36	0.65
HVLT Delayed	2.13	4	0.71	0.44
BVMT total (note)	6.86	4	0.14	0.84
BVMT delayed	0.81	4	0.94	0.27
Stroop	9.64	4	***0.046***	1.03
IGT net total	5.34	4	0.25	0.73
Verbal fluency	5.84	4	0.21	0.76
Design fluency	5.94	4	0.20	0.77
MMT	2.30	4	0.68	0.46
UPSA total	2.40	4	0.66	0.02

[a]*WAIS-IV Forward, Wechsler Adult Intelligence Scale, 4th Ed (WAIS-IV) Digit Span Forward subtest; WAIS-IV Backward, WAIS-IV Digit Span Backward subtest; WAIS-IV Sequence, WAIS-IV Sequencing subtest; WAIS-IV Total, WAIS-IV Digit Span total of three subtests; WMS-IV Symbol, Wechsler Memory Scale, 4th ed, Symbol Span subtest; Simple Reaction Time, California Computerized Assessment Package Simple Reaction task; Choice Reaction Time, California Computerized Assessment Package Choice Reaction task; HVLT Total, Hopkins Verbal Learning Test total score; HVLT Delayed, Hopkins Verbal Learning Test delayed recall score; BVMT Total, Brief Visuospatial Memory Test–Revised total score; BVMT Delayed, Brief Visuospatial Memory Test–Revised delayed recall score; Trails A, Trail Making Test, Part A; Trails B, Trail Making Test, Part B; Pegs R, Grooved Pegboard, right hand performance; WAIS-IV Coding, WAIS-IV Coding subtest; Stroop, Stroop Color-Word test score; IGT, Iowa Gambling Task Net Total score; Verbal Fluency, DKEFS Category Fluency subtest; Design Fluence, DKEFS Design Fluency subtest; MMT, Medication Management Test—Revised score; UPSA Total, UCSD Performance-Based Skills Assessment; subtest.*

[b]*Probability values less than 0.10 are in bold type.*

DISCUSSION

This study's goals were to assess the acceptability of CCT using a racing game to persons 50 years of age and older with HAND. The impact of adding tDCS to CCT was also evaluated. As we had a smaller than expected sample, we assessed outcomes not only through tests of statistical significance but also through calculation of effect sizes. Results showed that the majority of participants had positive views of the intervention and believed its benefits outweighed any risks. Ratings of its usefulness and usability were positive.

Our results clearly show that participants found the intervention acceptable. The majority of ratings on factors such as usefulness and ease of use were positive, and nearly all participants indicated that they felt the benefits of the intervention outweighed any drawbacks. Further exploration of ways to make the intervention even more positive for persons with HAND appear warranted.

Assessment of mental abilities before and after training suggested that the intervention had a positive effect on learning, memory, and motor speed compared to control. Although only a few outcomes were statistically significant or approached it, those which were significant were associated with large effect sizes. Outcomes with moderate or smaller effect sizes may thus have been non-significant due to low power related to the sample size rather than a lack of effect. A *post hoc* evaluation of the probability of arriving at the observed set of effect sizes by chance suggested that our findings were not due to chance. Further, effect sizes obtained in this study are similar to those reported by other researchers, including in a meta-analysis of studies with older adults (Indahlastari et al., 2021).

Consistent with other research, the combination of cognitive training and anodal tDCS at the left dorsolateral prefrontal cortex was associated with improvement in attention as measured by digit span (Martin et al., 2013; Park et al., 2014; Santos et al., 2018). Contrary to our hypothesis, however, there was no evidence of a substantial impact of the intervention on reaction time. Others have reported that tDCS may have a facilitating effect on reaction time with anodal stimulation over primary motor cortex, but Molero-Chamizo et al. (2018) found that the effect was time dependent. Others have also failed to find an effect of tDCS (Coppens et al., 2019; Seidel and Ragert, 2019) on reaction time. Our hypothesis of an effect on reaction time was based primarily on the nature of the training task (a fast-paced computer game), but neither statistical tests nor inspection of mean plots by groups (not presented) suggested an effect for either of the active treatment groups.

We found more substantial improvements in measures of psychomotor speed, including a significant interaction of group by time for the WAIS-IV Coding subtest. Although the overall interaction for Trails B was not significant, inspection of group mean plots was consistent with relatively greater improvement on this measure for the two active treatment groups, and *post hoc* between groups tests showed a significant difference between the control and CCT + active tDCS group after treatment while none was found at baseline.

A significant effect was also found for the Stroop Color-Word Test, a measure often interpreted as assessing a person's ability to inhibit well-learned responses (Scarpina and Tagini, 2017). Others have observed a positive effect of tDCS on the Stroop task (Loftus et al., 2015; Lu et al., 2021; Perrotta et al., 2021), while Frings et al. (2018) found that cathodal stimulation of the left DLPFC disrupted Stroop performance, with the negative effect of cathodal vs. anodal stimulation expected.

We found limited support for the impact of the intervention on functional measures, with a moderate effect size but non-significant results for the Medication Management Test but no evidence of an effect on the UPSA. This is similar results reported by Vance et al. (2021) who found limited effects of cognitive training on various measures of everyday function.

Self-report measures of mood or subjective cognitive functioning did not differ between groups, with one exception. The failure to find group differences may have been related to

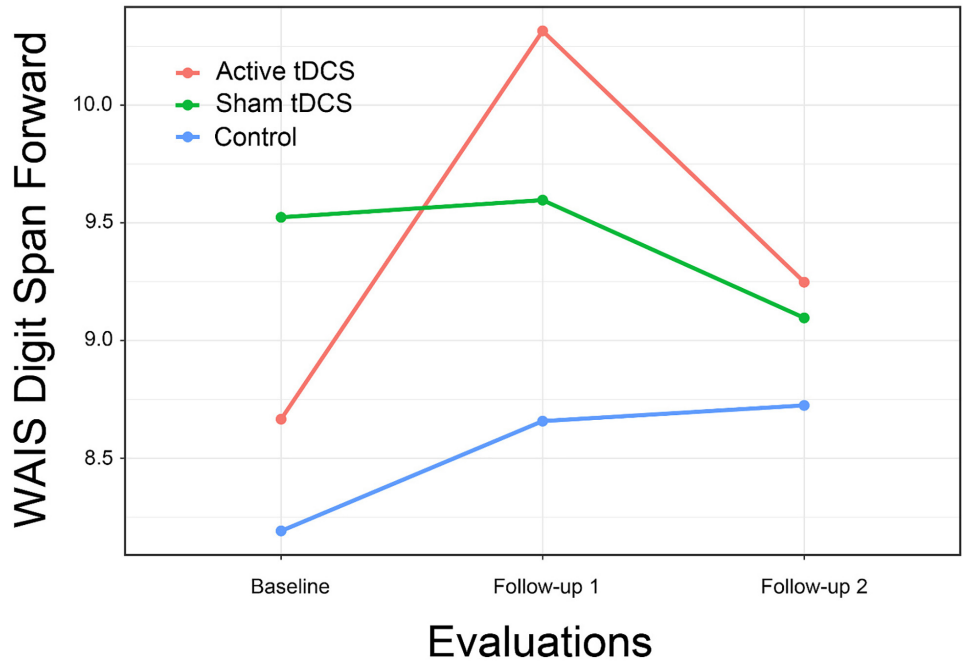

FIGURE 3 | WAIS-IV Digit Span Forward subtest score by Group and Time.

self-reported improvements across all groups, including the control. The one exception were self-reports of how well the participant perceived their thinking and memory, for which the CCT + active tDCS group gave substantially more positive reports over the last several sessions of the intervention.

The finding of possible treatment effects later during the training period suggests that the intervention's effects may have continued after training ended, with continuing improvements at 1-month follow-up in psychomotor speed (Trail Making Test, Part B; **Figure 3**) and verbal learning (Hopkins Verbal Learning Test; **Figure 5**). We also found an improvement in depression self-report (Center for Epidemiological Studies—Depression) at 1-month follow-up. This possibly delayed effect of tDCS on mood was also reported by Li et al. (2019). Given the evidence for improvement during the second week of training, it is possible that a more intensive and longer intervention might have resulted in greater effects. This possibility should be explored in future studies.

Strengths of the study include the single-blind sham-controlled design, which was effective in our pilot study as it has been in other studies (Woods et al., 2016). We collected all data using a staff member who did not know the participant's intervention assignment or by way of a computer. These measures reduced the likelihood of bias in outcomes due to

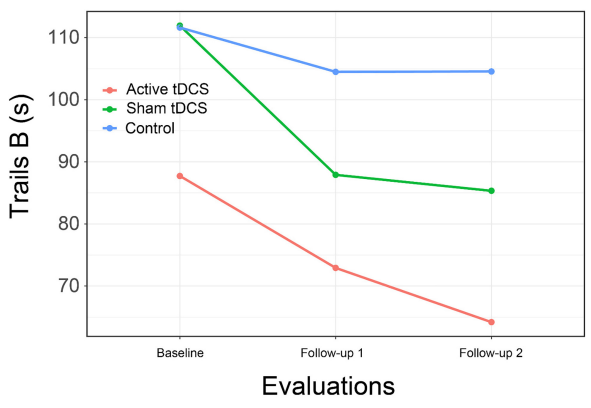

FIGURE 4 | Trail making test, part B by Group and Time. Lower scores indicate better performance.

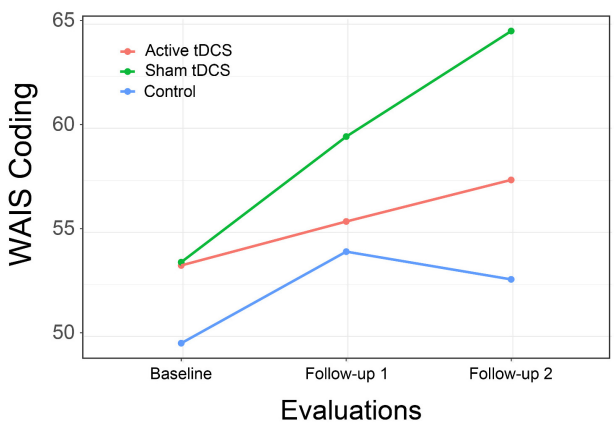

FIGURE 5 | WAIS-IV Coding subtest scores by Group and Time.

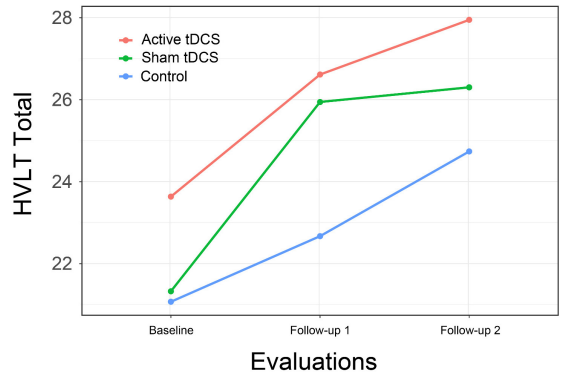

FIGURE 6 | Hopkins verbal learning test total score, Part B by Group and Time.

experimenter effects. The characteristics of participants (age, gender, education level, cognitive function) made them similar to other persons who might have HAND and be able to benefit from the intervention. Another strength is the clear characterization of study participants with respect to concurrent medication use, although this in turn limited our ability to recruit participants.

This study's limitations include the smaller than planned sample size. In spite of intensive recruiting efforts in the local community, including newspaper and online advertising, multiple contacts with community organizations and local infectious disease practitioners, and contacts with participants in previous studies we were not able to recruit the planned number of participants for the study. As shown in **Figure 1**, we were able to contact a number of potential participants that might have been adequate for planned sample size for the study, but exclusion due to validity concerns related to psychotropic medication use and safety concerns related to history of bipolar disorder, a large number of potential participants were not eligible. This limitation in turn may have affected the ability to test the statistical significance of outcomes, although in several cases when we found large effect sizes, we also found statistically significant results. Generalizing our results based only on observed effect sizes is a limitation. While the electrode montage used was chosen to stimulate the left dorsolateral prefrontal cortex via the anode, it should be acknowledged that the right frontal pole was also stimulated via the cathode (Friehs et al., 2021). Finally, it should be acknowledged that while we found a number of positive effects on cognitive measures in the two CCT groups, the original hypothesis that CCT with active tDCS would be superior to CCT with sham tDCS was not supported.

Another limitation is that this study did not employ a double-blind controlled design, raising the possibility of bias caused by the investigators. Further, it should also be noted that the timing of stimulation (concurrent with or prior to the cognitive task) may have affected study outcome. For example, Friehs and Frings (2019) showed that offline (not concurrent) stimulation of the left dorsolateral prefrontal cortex as associated with a greater impact on working memory (assessed as performance on the *n*-back task). In contrast, Martin et al. (2014) showed that concurrent stimulation was associated with skill acquisition.

As noted above, we did several things to reduce the possibility of effects related to the unblinded experimenter. These included positioning the investigator and the tDCS device out of sight of the participant during stimulation, providing neutral suggestions about what the participants might experience during stimulation, and collecting most self-report data via computer assisted self-interview with the investigators out of the room. All baseline and follow-up assessments were conducted by an assessor blind to the participant's treatment assignment or by way of a computer without the presence of a researcher. Thus, while we took a number of steps to reduce possible bias in the research design, they did not eliminate it.

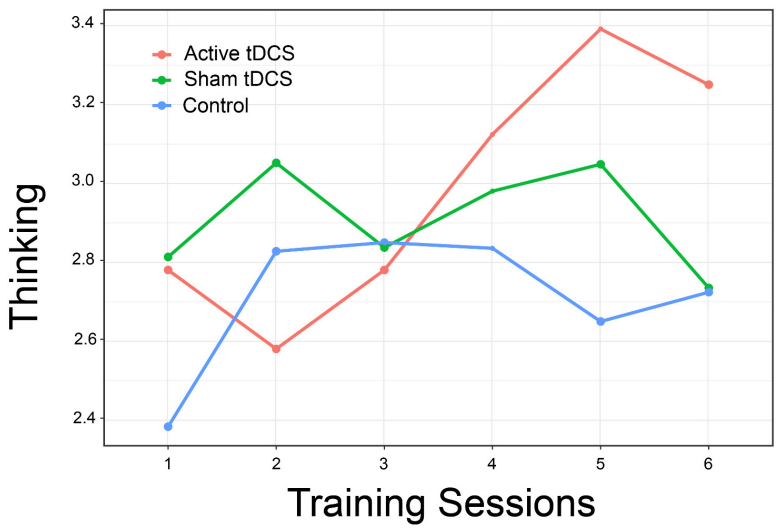

FIGURE 7 | Participants' self-rated thinking and memory by Group and Training Session.

HIV-related mental ability problems have implications for the functional status and quality of life for older persons with HAND. Our results, though limited, demonstrate the possibility that CCT with or without tDCS may have a positive impact on cognitive function. We found evidence of a moderate though non-significant effect of the intervention on a test of medication taking, a critically important skill for persons with HIV infection.

Future research should focus on continuing to explore the potential efficacy of CCT and tDCS with this population. A more detailed exploration of factors such as intensity and duration of stimulation and length and frequency of training sessions as well as the optimal timing of follow-up assessments may yield more effective treatment protocols with greater impacts on participants' functional status.

DATA AVAILABILITY STATEMENT

The raw data supporting the conclusions of this article will be made available by the authors, without undue reservation.

ETHICS STATEMENT

The studies involving human participants were reviewed and approved by the Institutional Review Board of Nova Southeastern University. The patients/participants provided their written informed consent to participate in this study.

AUTHOR CONTRIBUTIONS

RO designed the study, obtained external funding, carried out the interventions, and wrote the draft of the manuscript. JK wrote a portion of the manuscript and reviewed the complete manuscript. Both authors contributed to the article and approved the submitted version.

FUNDING

This work was supported by a grant from the US National Institutes on Aging to RO (grant R21AG056256).

REFERENCES

Acharya, J. N., Hani, A., Cheek, J., Thirumala, P., and Tsuchida, T. N. (2016). American Clinical Neurophysiology Society guideline 2: guidelines for standard electrode position nomenclature. *J. Clin. Neurophysiol.* 33, 308–311. doi: 10.1097/wnp.0000000000000316

Albert, S. M., Weber, C. M., Todak, G., Polanco, C., Clouse, R., McElhiney, M., et al. (1999). An observed performance test of medication management ability in HIV: Relation to neuropsychological status and medication adherence outcomes. *AIDS Behav.* 3, 121–128.

Alexandrovsky, D., Friehs, M. A., Grittner, J., Putze, S., Birk, M. V., Malaka, R., et al. (2021). *Serious snacking: A survival analysis of how snacking mechanics affect attrition in a mobile serious game. CHI 2021 Conference on Human Factors in Computing Systems: Making Waves, Combining Strengths; Virtual Online, Japan*. New York, NY: Association for Computing Machinery, 1–18.

Alexandrovsky, D., Friesh, M. A., Birk, M. V., Yates, R. K., and Mandryk, R. L. (2019). *Game dynamics that support snacking, not feasting. 6th ACM SIGCHI Annual Symposium on Computer-Human Interaction in Play, CHI PLAY 2019*. Barcelona: Association for Computing Machinery, 573–588.

Angius, L., Santarnecchi, E., Pascual-Leone, A., and Marcora, S. M. (2019). Transcranial direct current stimulation over the left dorsolateral prefrontal cortex improves inhibitory control and endurance performance in healthy individuals. *Neuroscience* 419, 34–45. doi: 10.1016/j.neuroscience.2019.08.052

Anguera, J. A., Boccanfuso, J., Rintoul, J. L., Al-Hashimi, O., Faraji, F., Janowich, J., et al. (2013). Video game training enhances cognitive control in older adults. *Nature* 501, 97–101. doi: 10.1038/nature12486

Antinori, A., Arendt, G., Becker, J. T., Brew, B. J., Byrd, D. A., Cherner, M., et al. (2007). Updated research nosology for HIV-associated neurocognitive disorders. *Neurology* 69, 1789–1799.

Atkinson, M. J., Kumar, R., Cappelleri, J. C., and Hass, S. L. (2005). Hierarchical construct validity of the treatment satisfaction questionnaire for medication (TSQM version II) among outpatient pharmacy consumers. *Value Health* 8(Suppl. 1), S9–S24. doi: 10.1111/j.1524-4733.2005.00066.x

Atkinson, M. J., Sinha, A., Hass, S. L., Colman, S. S., Kumar, R. N., Brod, M., et al. (2004). Validation of a general measure of treatment satisfaction, the Treatment Satisfaction Questionnaire for Medication (TSQM), using a national panel study of chronic disease. *Health Qual. Life Outcomes* 2:12. doi: 10.1186/1477-7525-2-12

Avdoshina, V., Bachis, A., and Mocchetti, I. (2013). Synaptic dysfunction in human immunodeficiency virus type-1-positive subjects: inflammation or impaired neuronal plasticity? *J. Intern. Med.* 273, 454–465. doi: 10.1111/joim.12050

Bachis, A., Avdoshina, V., Zecca, L., Parsadanian, M., and Mocchetti, I. (2012). Human immunodeficiency virus type 1 alters brain-derived neurotrophic factor processing in neurons. *J. Neurosci.* 32, 9477–9484. doi: 10.1523/jneurosci.0865-12.2012

Basak, C., Boot, W. R., Voss, M. W., and Kramer, A. F. (2008). Can training in a real-time strategy video game attenuate cognitive decline in older adults? *Psychol. Aging.* 23, 765–777. doi: 10.1037/a0013494

Bates, D., Maechler, M., Bolker, B., and Walker, S. (2015). Fitting linear mixed-effects models using lme4. *J. Stat. Softw.* 67, 1–48.

Bavelier, D., and Green, C. S. (2016). The brain-boosting power of video games. *Sci. Am.* 315, 26–31. doi: 10.1038/scientificamerican0716-26

Bechara, A., Damasio, H., Tranel, D., and Damasio, A. R. (2005). The Iowa Gambling Task and the somatic marker hypothesis: some questions and answers. *Trends Cogn. Sci.* 9, 159–162. doi: 10.1016/j.tics.2005.02.002

Belchior, P., Marsiske, M., Leite, W. L., Yam, A., Thomas, K., and Mann, W. (2016). Older adults' engagement during an intervention involving off-the-shelf videogame. *Games Health J.* 5, 151–156. doi: 10.1089/g4h.2015.0049

Belchior, P., Marsiske, M., Sisco, S., Yam, A., and Mann, W. (2012). Older adults' engagement with a video game training program. *Act. Adapt. Aging.* 36, 269–279. doi: 10.1080/01924788.2012.702307

Benedict, R. B., Schretlen, D., Groninger, L., Dobraski, M., and Sphritz, B. (1996). Revision of the Brief Visuospatial Memory Test: Studies of normal performance, reliability and validity. *Psycholog. Assess.* 8, 145–153. doi: 10.1080/13854046.2017.1288270

Binyamin, S. S., and Zafar, B. A. (2021). Proposing a mobile apps acceptance model for users in the health area: A systematic literature review and meta-analysis. *Health Inform. J.* 27:1460458220976737. doi: 10.1177/1460458220976737

Birk, M. V., Friehs, M. A., and Mandryk, R. L. (2017). *Age-based preferences and player experience: A crowdsources cross-sectional study. CHI Play '17: The annual symposium on computer-human interaction in paly*. Amsterdam: Association for Computing Machinery, 157–170.

Bonnechère, B., Langley, C., and Sahakian, B. J. (2020). The use of commercial computerised cognitive games in older adults: a meta-analysis. *Sci. Rep.* 10:15276. doi: 10.1038/s41598-020-72281-3

Brandt, J., and Benedickt, R. H. (2001). *Hopkins Verbal Learning Test–Revised: Professional manual*. Odessa, FL: Psychological Assessment Resources.

Brosnan, M. B., and Wiegand, I. (2017). The dorsolateral prefrontal cortex, a dynamic cortical area to enhance top-down attentional control. *J. Neurosci.* 37, 3445–3446. doi: 10.1523/JNEUROSCI.0136-17.2017

Brunoni, A. R., Valiengo, L., Baccaro, A., Zanao, T. A., de Oliveira, J. F., Goulart, A., et al. (2013). The sertraline vs. electrical current therapy for treating depression

clinical study: results from a factorial, randomized, controlled trial. *JAMA Psychiatry* 70, 383–391. doi: 10.1001/2013.jamapsychiatry.32

Brydges, C. R. (2019). Effect size guidelines, sample size calculations, and statistical power in gerontology. *Innov. Aging* 3:4. doi: 10.1093/geroni/igz036

Buchman, A. S., Yu, L., Boyle, P. A., Schneider, J. A., De Jager, P. L., and Bennett, D. A. (2016). Higher brain BDNF gene expression is associated with slower cognitive decline in older adults. *Neurology* 86, 735–741. doi: 10.1212/WNL.0000000000002387

Cardoso-Leite, P., and Bavelier, D. (2014). Video game play, attention, and learning: how to shape the development of attention and influence learning? *Curr. Opin. Neurol.* 27, 185–191. doi: 10.1097/wco.0000000000000077

Cerruti, C., and Schlaug, G. (2009). Anodal transcranial direct current stimulation of the prefrontal cortex enhances complex verbal associative thought. *J. Cogn. Neurosci.* 21, 1980–1987. doi: 10.1162/jocn.2008.21143

Chelune, G. J., Heaton, R. K., and Lehman, R. A. W. (1986). "Neuropsychological and personality correlates of patients' complaints of disability," in *Advances in clinical neuropsychology*, Vol. 3, eds G. Goldstein and R. E. Tarter (New York, NY: Springer), 95–126. doi: 10.1007/978-1-4613-2211-5_4

Clark, V. P., Coffman, B. A., Mayer, A. R., Weisend, M. P., Lane, T. D., Calhoun, V. D., et al. (2012). TDCS guided using fMRI significantly accelerates learning to identify concealed objects. *Neuroimage* 59, 117–128. doi: 10.1016/j.neuroimage.2010.11.036

Cody, S. L., and Vance, D. E. (2016). The neurobiology of HIV and its impact on cognitive reserve: A review of cognitive interventions for an aging population. *Neurobiol. Dis.* 92, 144–156. doi: 10.1016/j.nbd.2016.01.011

Coffman, B. A., Trumbo, M. C., and Clark, V. P. (2012). Enhancement of object detection with transcranial direct current stimulation is associated with increased attention. *BMC Neurosci.* 13:108.

Cohen, J. (1988). *Statistical power analysis for the behavioral sciences*, 2nd Edn. New York, NY: Routledge.

Coppens, M. J. M., Staring, W. H. A., Nonnekes, J., Geurts, A. C. H., and Weerdesteyn, V. (2019). Offline effects of transcranial direct current stimulation on reaction times of lower extremity movements in people after stroke: a pilot cross-over study. *J. NeuroEng. Rehab.* 16:136. doi: 10.1186/s12984-019-0604-y

Decloedt, E. H., Freeman, C., Howells, F., Casson-Crook, M., Lesosky, M., Koutsilieri, E., et al. (2016). Moderate to severe HIV-associated neurocognitive impairment: A randomized placebo-controlled trial of lithium. *Medicine* 95:e5401. doi: 10.1097/MD.0000000000005401

Degroote, S., Vogelaers, D., and Vandijck, D. M. (2014). What determines health-related quality of life among people living with HIV: an updated review of the literature. *Arch Public Health.* 72:40.

Degroote, S., Vogelaers, D. P., Vermeir, P., Mariman, A., De, R. A., Van Der Gucht, B., et al. (2013). Socio-economic, behavioural, (neuro)psychological and clinical determinants of HRQoL in people living with HIV in Belgium: a pilot study. *J. Int. AIDS Soc.* 16:18643. doi: 10.7448/IAS.16.1.18643

Delis, D. C., Kaplan, E., and Kramer, J. H. (2001). *Delis-Kaplan Executive Function System (D-KEFS)*. San Antonio, TX: The Psychological Corporation, 2001.

Elmer, S., Burkard, M., Renz, B., Meyer, M., and Jancke, L. (2009). Direct current induced short-term modulation of the left dorsolateral prefrontal cortex while learning auditory presented nouns. *Behav. Brain Funct.* 5:29. doi: 10.1186/1744-9081-5-29

European AIDS Clinical Society (2015). *Guidelines 8.0*. Brussels: European AIDS Clinical Society, 2015.

Floel, A., Suttorp, W., Kohl, O., Kurten, J., Lohmann, H., Breitenstein, C., et al. (2012). Non-invasive brain stimulation improves object-location learning in the elderly. *Neurobiol. Aging.* 33, 1682–1689. doi: 10.1016/j.neurobiolaging.2011.05.007

Fregni, F., Boggio, P. S., Nitsche, M., Bermpohl, F., Antal, A., Feredoes, E., et al. (2005). Anodal transcranial direct current stimulation of prefrontal cortex enhances working memory. *Exp. Brain Res.* 166, 23–30. doi: 10.1007/s00221-005-2334-6

Friehs, M. A., and Frings, C. (2019). Offline beats online: transcranial direct current stimulation timing influences on working memory. *Neuroreport* 30, 795–799. doi: 10.1097/WNR.0000000000001272

Friehs, M. A., Frings, C., and Hartwigsen, G. (2021). Effects of single-session transcranial direct current stimulation on reactive response inhibition. *Neurosci. Biobehav. Rev.* 128, 749–765. doi: 10.1016/j.neubiorev.2021.07.013

Frings, C., Brinkmann, T., Friehs, M. A., and van Lipzig, T. (2018). Single session tDCS over the left DLPFC disrupts interference processing. *Brain Cogn.* 120, 1–7. doi: 10.1016/j.bandc.2017.11.005

Fritsch, B., Reis, J., Martinowich, K., Schambra, H. M., Ji, Y., and Cohen, L. G. (2010). Direct current stimulation promotes BDNF-dependent synaptic plasticity: potential implications for motor learning. *Neuron* 2010:66. doi: 10.1016/j.neuron.2010.03.035

Galvez, V., Alonzo, A., Martin, D., Mitchell, P. B., Sachdev, P., and Loo, C. K. (2011). Hypomania induction in a patient with bipolar II disorder by transcranial direct current stimulation (tDCS). *J. ECT.* 27, 256–258. doi: 10.1097/YCT.0b013e3182012b89

Golden, C. J. (1978). *Stroop Color Word Test Manual*. Chicago: Stoelting.

Green, C. S., and Seitz, A. R. (2015). The impacts of video games on cognition (and how the government can guide the industry). *Policy Insights Behav. Brain Sci.* 2, 101–110. doi: 10.1177/2372732215601121

Heaton, R. K., Clifford, D. B., Franklin, D. R., Woods, S. P., Ake, C., Vaida, F., et al. (2010). HIV-associated neurocognitive disorders persist in the era of potent antiretroviral therapy: CHARTER Study. *Neurology* 75, 2087–2096. doi: 10.1212/WNL.0b013e318200d727

Heimrath, K., Sandmann, P., Becke, A., Muller, N. G., and Zaehle, T. (2012). Behavioral and electrophysiological effects of transcranial direct current stimulation of the parietal cortex in a visuo-spatial working memory task. *Front. Psychiatry* 3:56. doi: 10.3389/fpsyt.2012.00056

Hinkin, C. H., Castellon, S. A., Durvasula, R. S., Hardy, D. J., Lam, M. N., Mason, K. I., et al. (2002). Medication adherence among HIV+ adults: effects of cognitive dysfunction and regimen complexity. *Neurology* 59, 1944–1950. doi: 10.1212/01.wnl.0000038347.48137.67

Hinkin, C. H., Castellon, S. A., Hardy, D. J., Farinpour, R., Newton, T., and Singer, E. (2001). Methylphenidate improves HIV-1-associated cognitive slowing. *J. Neuropsyc. Clin. Neurosci.* 13, 248–254. doi: 10.1176/jnp.13.2.248

Hinkin, C. H., Hardy, D. J., Mason, K. I., Castellon, S. A., Durvasula, R. S., Lam, M. N., et al. (2004). Medication adherence in HIV-infected adults: effect of patient age, cognitive status, and substance abuse. *AIDS* 18(Suppl. 1), S19–S25. doi: 10.1097/00002030-200418001-00004

Hintze, J. (2018). *PASS 16*. Kaysville UT: NCSS, 2011.

Indahlastari, A., Hardcastle, C., Albizu, A., Alvarez-Alvarado, S., Boutzoukas, E. M., Evangelista, N. D., et al. (2021). A systematic review and meta-analysis of transcranial direct current stimulation to remediate age-related cognitive decline in healthy older adults. *Neuropsychiatr. Dis. Treat.* 17, 971–990. doi: 10.2147/NDT.S259499

Javadi, A. H., and Walsh, V. (2012). Transcranial direct current stimulation (tDCS) of the left dorsolateral prefrontal cortex modulates declarative memory. *Brain Stimul.* 5, 231–241. doi: 10.1016/j.brs.2011.06.007

Kuznetsova, A., Brockhoff, P. B., and Christensen, R. H. B. (2017). lmerTest package: tests in linear mixed effects models. *J. Stat. Softw.* 82, 1–26.

Lafayette Instrument Company (2002). *Grooved Pegboard Test user instructions*. Lafayette, IN: Lafayette Instrument Company.

Lawrence, B. J., Gasson, N., Bucks, R. S., Troeung, L., and Loftus, A. M. (2017). Cognitive training and noninvasive brain stimulation for cognition in Parkinson's disease: A meta-analysis. *Neurorehabil Neural. Repair.* 31, 597–608. doi: 10.1177/1545968317712468

Lawrence, B. J., Gasson, N., Johnson, A. R., Booth, L., and Loftus, A. M. (2018). Cognitive training and transcranial direct current stimulation for mild cognitive impairment in Parkinson's Disease: A randomized controlled trial. *Parkinson's Dis.* 2018:4318475.

Leh, S. E., Petrides, M., and Strafella, A. P. (2010). The neural circuitry of executive functions in healthy subjects and Parkinson's disease. *Neuropsychopharmacology* 35, 70–85. doi: 10.1038/npp.2009.88

Lenth, R. (2020). *Estimated marginal means, aka least-squares means. 2020. p. R package version 1.5.0*.

Leshikar, E. D., Leach, R. C., McCurdy, M. P., Trumbo, M. C., Sklenar, A. M., Frankenstein, A. N., et al. (2017). Transcranial direct current stimulation of dorsolateral prefrontal cortex during encoding improves recall but not recognition memory. *Neuropsychologia* 106, 390–397. doi: 10.1016/j.neuropsychologia.2017.10.022

Lezak, M. (2004). *Neuropsychological assessment, Fifth edition*. New York, NY: Oxford.

Li, M.-S., Du, X.-D., Chu, H.-C., Liao, Y.-Y., Pan, W., Li, Z., et al. (2019). Delayed effect of bifrontal transcranial direct current stimulation in patients with treatment-resistant depression: a pilot study. *BMC Psychiatry* 19:180. doi: 10.1186/s12888-019-2119-2

Loftus, A. M., Yalcin, O., Baughman, F. D., Vanman, E. J., and Hagger, M. S. (2015). The impact of transcranial direct current stimulation on inhibitory control in young adults. *Brain Behav.* 5:e00332.

Lu, H., Gong, Y., Huang, P., Zhang, Y., Guo, Z., Zhu, X., et al. (2021). Effect of repeated anodal HD-tDCS on executive functions: Evidence from a pilot and single-blinded fNIRS study. *Front. Hum. Neurosci.* 14:609. doi: 10.3389/fnhum.2020.583730

Ludecke, D. (2019). *Effect size computation for meta analysis*. Vienna: R Core Team.

Martin, D. M., Liu, R., Alonzo, A., Green, M., and Loo, C. K. (2014). Use of transcranial direct current stimulation (tDCS) to enhance cognitive training: effect of timing of stimulation. *Exp. Brain Res.* 232, 3345–3351. doi: 10.1007/s00221-014-4022-x

Martin, D. M., Liu, R., Alonzo, A., Green, M., Player, M. J., Sachdev, P., et al. (2013). Can transcranial direct current stimulation enhance outcomes from cognitive training? A randomized controlled trial in healthy participants. *Int. J. Neuropsychopharmacol.* 16, 1927–1936. doi: 10.1017/s1461145713000539

McLaren, M. E., Nissim, N. R., and Woods, A. J. (2018). The effects of medication use in transcranial direct current stimulation: A brief review. *Brain Stimulat. Basic Transl. Clin. Res. Neuromod.* 11, 52–58. doi: 10.1016/j.brs.2017.10.006

Medeiros, L. F., de Souza, I. C., Vidor, L. P., de Souza, A., Deitos, A., Volz, M. S., et al. (2012). Neurobiological effects of transcranial direct current stimulation: A review. *Front. Psychiatry* 3:110.

Miller, E. N. (2013). *California Computerized Assessment Package Manual, 2nd ed*. Palm Springs, CA: Eric N. Miller, 2013.

Moher, D. (1998). CONSORT: an evolving tool to help improve the quality of reports of randomized controlled trials. Consolidated Standards of Reporting Trials. *JAMA* 279, 1489–1491. doi: 10.1001/jama.279.18.1489

Molero-Chamizo, A., Alameda Bailén, J. R., Garrido Béjar, T., García López, M., Jaén Rodríguez, I., Gutiérrez Lérida, C., et al. (2018). Poststimulation time interval-dependent effects of motor cortex anodal tDCS on reaction-time task performance. *Cogn. Affect. Behav. Neurosci.* 18, 167–175. doi: 10.3758/s13415-018-0561-0

Moore, R. C., Fazeli, P. L., Jeste, D. V., Moore, D. J., Grant, I., and Woods, S. P. (2014). Successful cognitive aging and health-related quality of life in younger and older adults infected with HIV. *AIDS Behav.* 18, 1186–1197. doi: 10.1007/s10461-014-0743-x

Nakasujja, N., Miyahara, S., Evans, S., Lee, A., Musisi, S., Katabira, E., et al. (2013). Randomized trial of minocycline in the treatment of HIV-associated cognitive impairment. *Neurology* 80, 196–202. doi: 10.1212/wnl.0b013e31827b9121

Ownby, R. L., and Acevedo, A. (2016). A pilot study of cognitive training with and without transcranial direct current stimulation (tDCS) to improve cognition in older persons with HIV-related cognitive impairment. *Neuropsychiatr. Dis. Treat.* 12, 2745–2754. doi: 10.2147/NDT.S120282

Park, S.-H., Seo, J.-H., Kim, Y.-H., and Ko, M.-H. (2014). Long-term effects of transcranial direct current stimulation combined with computer-assisted cognitive training in healthy older adults. *Neuroreport* 2014:25. doi: 10.1097/WNR.0000000000000080

Patterson, T. L., Goldman, S., McKibbin, C. L., Hughs, T., and Jeste, D. V. U. C. S. D. (2001). Performance-Based Skills Assessment: development of a new measure of everyday functioning for severely mentally ill adults. *Schizophr. Bull.* 27, 235–245. doi: 10.1093/oxfordjournals.schbul.a006870

Perrotta, D., Bianco, V., Berchicci, M., Quinzi, F., and Perri, R. L. (2021). Anodal tDCS over the dorsolateral prefrontal cortex reduces Stroop errors. A comparison of different tasks and designs. *Behav. Brain Res.* 405:113215. doi: 10.1016/j.bbr.2021.113215

R Core Team (2020). *R: A language and environment for statistical computing*. Vienna: R foundation for statistical computing.

Radloff, L. S. (1977). The CES-D scale: A self-report depression scale for research in the general population. *Appl. Psychol. Measur.* 1, 385–481. doi: 10.1177/014662167700100306

Rourke, S. B., Halman, M. H., and Bassel, C. (1999). Neurocognitive complaints in HIV-infection and their relationship to depressive symptoms and neuropsychological functioning. *J. Clin. Exp. Neuropsychol.* 21, 737–756. doi: 10.1076/jcen.21.6.737.863

Sacktor, N., Miyahara, S., Deng, L., Evans, S., Schifitto, G., Cohen, B. A., et al. (2011). Minocycline treatment for HIV-associated cognitive impairment: results from a randomized trial. *Neurology* 77, 1135–1142. doi: 10.1212/wnl.0b013e31822f0412

Santos, V. S. D. S. D, Zortea, M., Alves, R. L., Naziazeno, C. C. D. S., Saldanha, J. S., Carvalho, S. D. C. R. D., et al. (2018). Cognitive effects of transcranial direct current stimulation combined with working memory training in fibromyalgia: a randomized clinical trial. *Sci. Rep.* 8:12477. doi: 10.1038/s41598-018-30127-z

Scarpina, F., and Tagini, S. (2017). The Stroop Color and Word Test. *Front. Psychol.* 8:557.

Schifitto, G., Yiannoutsos, C. T., Ernst, T., Navia, B. A., Nath, A., Sacktor, N., et al. (2009). Selegiline and oxidative stress in HIV-associated cognitive impairment. *Neurology* 73, 1975–1981. doi: 10.1212/wnl.0b013e3181c51a48

Schifitto, G., Zhang, J., Evans, S. R., Sacktor, N., Simpson, D., Millar, L. L., et al. (2007). A multicenter trial of selegiline transdermal system for HIV-associated cognitive impairment. *Neurology* 69, 1314–1321. doi: 10.1212/01.wnl.0000268487.78753.0f

Seidel, O., and Ragert, P. (2019). Effects of transcranial direct current stimulation of primary motor cortex on reaction time and tapping performance: A comparison between athletes and non-athletes. *Front. Hum. Neurosci.* 13:103. doi: 10.3389/fnhum.2019.00103

Thames, A. D., Arentoft, A., Rivera-Mindt, M., and Hinkin, C. H. (2013). Functional disability in medication management and driving among individuals with HIV: a 1-year follow-up study. *J. Clin. Exp. Neuropsychol.* 35, 49–58. doi: 10.1080/13803395.2012.747596

Thames, A. D., Becker, B. W., Marcotte, T. D., Hines, L. J., Foley, J. M., Ramezani, A., et al. (2011a). Depression, cognition, and self-appraisal of functional abilities in HIV: An examination of subjective appraisal aersus objective performance. *Clin. Neuropsychologist.* 25, 224–243. doi: 10.1080/13854046.2010.539577

Thames, A. D., Kim, M. S., Becker, B. W., Foley, J. M., Hines, L. J., Singer, E. J., et al. (2011b). Medication and finance management among HIV-infected adults: The impact of age and cognition. *J. Clin. Exp. Neuropsychol.* 33, 200–209. doi: 10.1080/13803395.2010.499357

Tozzi, V., Balestra, P., Galgani, S., Murri, R., Bellagamba, R., Narciso, P., et al. (2003). Neurocognitive performance and quality of life in patients with HIV infection. *AIDS Res. Hum. Retroviruses.* 19, 643–652. doi: 10.1089/088922203322280856

Trémolière, B., Maheux-Caron, V., Lepage, J.-F., and Blanchette, I. (2018). tDCS stimulation of the dlPFC selectively moderates the detrimental impact of emotion on analytical reasoning. *Front. Psychol.* 9:68. doi: 10.3389/fpsyg.2018.00568

Trumbo, M. C., Matzen, L. E., Coffman, B. A., Hunter, M. A., Jones, A. P., Robinson, C. S. H., et al. (2016). Enhanced working memory performance via transcranial direct current stimulation: The possibility of near and far transfer. *Neuropsychologia* 93, 85–96. doi: 10.1016/j.neuropsychologia.2016.10.011

Valcour, V., Shikuma, C., Shiramizu, B., Watters, M., Poff, P., Selnes, O., et al. (2004). Higher frequency of dementia in older HIV-1 individuals: the Hawaii Aging with HIV-1 Cohort. *Neurology* 63, 822–827. doi: 10.1212/01.wnl.0000134665.58343.8d

Vance, D. E., Fazeli, P., Azuero, A., Frank, J. S., Wadley, V. G., Raper, J. L., et al. (2021). Can individualized-targeted computerized cognitive training improve everyday functioning in adults with HIV-associated neurocognitive disorder? *Appl. Neuropsychol.* 2021, 1–12. doi: 10.1080/23279095.2021.1906678

Vance, D. E., Fazeli, P. L., Cheatwood, J., Nicholson, W. C., Morrison, S. A., and Moneyham, L. D. (2019). Computerized cognitive training for the neurocognitive complications of HIV infection: A systematic review. *J. Assoc. Nurses AIDS Care* 30, 51–72. doi: 10.1097/JNC.0000000000000030

Vance, D. E., Fazeli, P. L., Ross, L. A., Wadley, V. G., and Ball, K. K. (2012). Speed of processing training with middle-age and older adults with HIV: a pilot study. *J. Assoc. Nurses AIDS Care* 23, 500–510. doi: 10.1016/j.jana.2012.01.005

Venkatesh, V., and Bala, H. (2008). Technology Acceptance Model 3 and a research agenda on interventions. *Dec. Sci.* 39, 273–315. doi: 10.1111/j.1540-5915.2008.00192.x

Venkatesh, V., Morris, M. G., Davis, G. B., and Davis, F. D. (2003). User acceptance of information technology: Toward a unified view. *MIS Q.* 27, 425–478. doi: 10.2307/30036540

Wechsler, D. (2001). *The Wechsler Test of Adult Reading*. San Antonio: The Psychological Corporation, 2001.

Wechsler, D. (2008). *Manual for the Wechsler Adult Intelligence Scale–IV*. San Antonio, TX: Pearson Assessment.

Wendelken, L. A., and Valcour, V. (2012). Impact of HIV and aging on neuropsychological function. *J. Neurovirol.* 18, 256–263. doi: 10.1007/s13365-012-0094-1

Woods, A. J., Antal, A., Bikson, M., Boggio, P. S., Brunoni, A. R., Celnik, P., et al. (2016). A technical guide to tDCS, and related non-invasive brain stimulation tools. *Clin. Neurophysiol.* 127, 1031–1048. doi: 10.1016/j.clinph.2015.11.012

Woods, S. P., Moore, D. J., Weber, E., and Grant, I. (2009). Cognitive neuropsychology of HIV-associated neurocognitive disorders. *Neuropsychol. Rev.* 19, 152–168. doi: 10.1007/s11065-009-9102-5

Wu, S., and Spence, I. (2013). Playing shooter and driving videogames improves top-down guidance in visual search. *Atten. Percept Psychophys.* 75, 673–686. doi: 10.3758/s13414-013-0440-2

Yamada, Y., and Sumiyoshi, T. (2021). Neurobiological mechanisms of transcranial direct current stimulation for psychiatric disorders; neurophysiological, chemical, and anatomical considerations. *Front. Hum. Neurosci.* 15:21. doi: 10.3389/fnhum.2021.631838

Zaehle, T., Sandmann, P., Thorne, J. D., Jancke, L., and Herrmann, C. S. (2011). Transcranial direct current stimulation of the prefrontal cortex modulates working memory performance: combined behavioural and electrophysiological evidence. *BMC Neurosci.* 12:2. doi: 10.1186/1471-2202-12-2

Zelinski, E. M., and Reyes, R. (2009). Cognitive benefits of computer games for older adults. *Gerontechnology* 8, 220–235.

Conflict of Interest: The authors declare that the research was conducted in the absence of any commercial or financial relationships that could be construed as a potential conflict of interest.

Publisher's Note: All claims expressed in this article are solely those of the authors and do not necessarily represent those of their affiliated organizations, or those of the publisher, the editors and the reviewers. Any product that may be evaluated in this article, or claim that may be made by its manufacturer, is not guaranteed or endorsed by the publisher.

frontiers in Aging Neuroscience

ORIGINAL RESEARCH
published: 26 November 2021
doi: 10.3389/fnagi.2021.725013

Multifocal Transcranial Direct Current Stimulation Modulates Resting-State Functional Connectivity in Older Adults Depending on the Induced Current Density

Kilian Abellaneda-Pérez[1,2], Lídia Vaqué-Alcázar[1,2], Ruben Perellón-Alfonso[1,2], Cristina Solé-Padullés[1,2], Núria Bargalló[3,4], Ricardo Salvador[5,6], Giulio Ruffini[5,6], Michael A. Nitsche[7,8], Alvaro Pascual-Leone[9,10,11] and David Bartrés-Faz[1,2,11]**

[1] Department of Medicine, Faculty of Medicine and Health Sciences, Institute of Neurosciences, University of Barcelona, Barcelona, Spain, [2] Institute of Biomedical Research August Pi i Sunyer (IDIBAPS), Barcelona, Spain, [3] Section of Neuroradiology, Department of Radiology, Diagnostic Image Center, Hospital Clinic of Barcelona, University of Barcelona, Barcelona, Spain, [4] Magnetic Resonance Image Core Facility (IDIBAPS), Barcelona, Spain, [5] Neuroelectrics, Cambridge, MA, United States, [6] Neuroelectrics, Barcelona, Spain, [7] Leibniz Research Centre for Working Environment and Human Factors, Dortmund, Germany, [8] Department of Neurology, University Medical Hospital Bergmannsheil, Bochum, Germany, [9] Hinda and Arthur Marcus Institute for Aging Research and Deanna and Sidney Wolk Center for Memory Health, Hebrew SeniorLife, Boston, MA, United States, [10] Department of Neurology, Harvard Medical School, Boston, MA, United States, [11] Guttmann Brain Health Institute, Guttmann University Institute of Neurorehabilitation, Autonomous University of Barcelona, Badalona, Spain

OPEN ACCESS

Edited by:
Wei Wu,
Alto Neuroscience, United States

Reviewed by:
Virginia Conde,
Norwegian University of Science and Technology, Norway
Helen Carlson,
University of Calgary, Canada

***Correspondence:**
Kilian Abellaneda-Pérez
kilian.abellaneda@ub.edu
David Bartrés-Faz
dbartres@ub.edu

Received: *14 June 2021*
Accepted: *02 November 2021*
Published: *26 November 2021*

Citation:
Abellaneda-Pérez K, Vaqué-Alcázar L, Perellón-Alfonso R, Solé-Padullés C, Bargalló N, Salvador R, Ruffini G, Nitsche MA, Pascual-Leone A and Bartrés-Faz D (2021) Multifocal Transcranial Direct Current Stimulation Modulates Resting-State Functional Connectivity in Older Adults Depending on the Induced Current Density. Front. Aging Neurosci. 13:725013. doi: 10.3389/fnagi.2021.725013

Combining non-invasive brain stimulation (NIBS) with resting-state functional magnetic resonance imaging (rs-fMRI) is a promising approach to characterize and potentially optimize the brain networks subtending cognition that changes as a function of age. However, whether multifocal NIBS approaches are able to modulate rs-fMRI brain dynamics in aged populations, and if these NIBS-induced changes are consistent with the simulated electric current distribution on the brain remains largely unknown. In the present investigation, thirty-one cognitively healthy older adults underwent two different multifocal real transcranial direct current stimulation (tDCS) conditions (C1 and C2) and a sham condition in a crossover design during a rs-fMRI acquisition. The real tDCS conditions were designed to electrically induce two distinct complex neural patterns, either targeting generalized frontoparietal cortical overactivity (C1) or a detachment between the frontal areas and the posteromedial cortex (C2). Data revealed that the two tDCS conditions modulated rs-fMRI differently. C1 increased the coactivation of multiple functional couplings as compared to sham, while a smaller number of connections increased in C1 as compared to C2. At the group level, C1-induced changes were topographically consistent with the calculated electric current density distribution. At the individual level, the extent of tDCS-induced rs-fMRI modulation in C1 was related with the magnitude of the simulated electric current density estimates. These results highlight

that multifocal tDCS procedures can effectively change rs-fMRI neural functioning in advancing age, being the induced modulation consistent with the spatial distribution of the simulated electric current on the brain. Moreover, our data supports that individually tailoring NIBS-based interventions grounded on subject-specific structural data might be crucial to increase tDCS potential in future studies amongst older adults.

Keywords: aging, electric current density, multifocal transcranial direct current stimulation, resting-state functional magnetic resonance imaging, non-invasive brain stimulation (NIBS), electric modeling, neuroimaging

INTRODUCTION

The human brain is organized into complex neural networks that can be studied through resting-state functional magnetic resonance imaging (rs-fMRI; Damoiseaux et al., 2006; Smith et al., 2009; van den Heuvel and Sporns, 2013; Petersen and Sporns, 2015). Some of these neural systems have been shown to support cognition (Bressler and Menon, 2010) and change through the lifespan (Dosenbach et al., 2010; Betzel et al., 2014), as well as to be highly susceptible to aging (Tomasi and Volkow, 2012; Ferreira and Busatto, 2013; Sala-Llonch et al., 2015; Nashiro et al., 2017).

Non-invasive brain stimulation (NIBS) protocols have been used to modulate these functional systems subtending cognition in older adults (Abellaneda-Pérez et al., 2019a). The combination of NIBS with neuroimaging techniques in these populations has shed light into the network plasticity mechanisms underlying cognitive aging (i.e., Abellaneda-Pérez et al., 2019b) as well as on the putative neurobiological mechanisms underlying NIBS-induced phenotypic improvements in the elderly (i.e., Holland et al., 2011; Meinzer et al., 2013; Antonenko et al., 2018; Nilakantan et al., 2019).

In the latest years, transcranial direct current stimulation (tDCS) has been widely employed, particularly in advancing age (Perceval et al., 2016; Tatti et al., 2016). In conventional tDCS studies, which aim to target discrete cortical regions, a single anode accompanied by its corresponding cathode is used. According to our current mechanistic understanding, during tDCS, neural membrane potentials are depolarized under the anode, leading to an increase in cortical excitability, while they are hyperpolarized under the cathode, thus diminishing cortical excitability at the macroscopic level (Nitsche and Paulus, 2000; Nitsche et al., 2008). More recently, novel multifocal or network-based tDCS protocols have been developed in order to target multiple brain areas simultaneously (Ruffini et al., 2014). In multifocal tDCS, multiple electrodes with differential intensities and polarities are employed such that the resulting field aims to maximally target a specific distributed brain network and can result in higher modulatory efficacy than an otherwise similar two-electrode tDCS approach in younger samples (Fischer et al., 2017). However, in what manner multifocal tDCS entails capability to influence rs-fMRI dynamics in the aging brain, and whether this modulation is consistent with a previously targeted neural pattern, has not been previously investigated, despite the potential of network-based approaches to directly modulate a complex system rather than a concrete region. In this vein, a whole network modulation is particularly relevant in aging, since, as observed in numerous descriptive fMRI investigations, brain networks are less integrated and more segregated as a function of age (Cao et al., 2014; Chan et al., 2014; Sala-Llonch et al., 2014; Grady et al., 2016; Spreng et al., 2016), probably reflecting age-associated dedifferentiation processes (Park et al., 2012). Notably, it has been proposed within the cognitive neuroscience of aging literature that this loss of brain networks integration in the elderly relates to poorer cognitive performance (i.e., Sala-Llonch et al., 2014; Vidal-Piñeiro et al., 2014). Consequently, altering multiple neural nodes within or between specific neural circuits based on a previously simulated electrical pattern on the brain could be used to potentially restore a regular brain functioning and thus, hypothetically, ameliorate cognitive decline in advanced age.

The present study leverages from a previous investigation by our group and is based on its fMRI findings. In the stated report, we observed that distinct groups of older adults, with comparable educational attainment but different levels of white matter hyperintensities burden, can engage dissimilar brain activity patterns to successfully solve a particular working memory paradigm (for further details on the original brain patterns, see Fernández-Cabello et al., 2016). In the present study, two real tDCS conditions were designed based on those previous fMRI findings to induce two distinct electrical distribution configurations, which were expected to produce either generalized frontoparietal cortical overactivity (i.e., condition 1, or C1) or an antero-posterior dissociation aiming to enhance frontal areas whereas reducing the posteromedial cortex activity (i.e., condition 2, or C2; see section "tDCS parameters" for detailed information). It is worth noting that there is a correspondence between those brain functional configurations observed during activation and at rest (Smith et al., 2009). Hence, while C1 patterns are consistent with the classical frontoparietal circuits observed in rs-fMRI studies, the C2 anatomically resemble both the frontoparietal as well as the default-mode networks (see also Abellaneda-Pérez et al., 2020). The goals of the present study were: (I) to explore the impact of two distinct multifocal tDCS montages on rs-fMRI associated connectivity changes in older adults; (II) to examine the topographical correspondence between the tDCS-induced rs-fMRI effects and the simulated electric current distribution on the brain at the group level; and (III) to individually determine whether, and how, the observed rs-fMRI changes are associated with the calculated electric current values.

MATERIALS AND METHODS

Participants

As in our previous studies (Vidal-Piñeiro et al., 2014; Vaqué-Alcázar et al., 2017, 2020), subjects participating in the present investigation were recruited from the Fundació Institut Català de l'Envelliment. We contacted thirty-seven subjects and initially included thirty-three participants fulfilling the following criteria: aged older than 65 and neuropsychological assessment within range of normality (see below). Selected exclusion criteria were Hamilton Depression Rating Scale > 13, history of epilepsy, neurological or psychiatric disorders and any NIBS-related contraindication (Rossi et al., 2009, 2021; Antal et al., 2017) as well as for the MRI. One subject was discarded for a previous single episode of absence seizure and another volunteer was excluded due to morphine pump implantation to treat chronic pain.

Finally, thirty-one subjects met criteria to participate in this study. All participants were tDCS naïve and right-handed older adults [mean age ± standard deviation (*SD*), 71.68 ± 2.5 years; age range, 68 – 77 years; 19 females; years of education mean ± *SD*, 12.29 ± 4.0 years]. All volunteers provided informed consent in accordance with the Declaration of Helsinki (1964, last revision 2013). All study procedures were approved by the Institutional Review Board (IRB 00003099) at the University of Barcelona. For all participants, MRI images were examined by a senior neuroradiologist for any clinically significant pathology (none found).

Experimental Design

The present study was conducted in a randomized single-blind sham-controlled crossover design that consisted of four visits to our center. On the first visit (i.e., pre-experimental session; day 0), all participants underwent a comprehensive neuropsychological assessment to ensure cognitive functioning within the normal range according to age and years of education (see section "Neuropsychological assessment"). Subsequently, three experimental sessions with distinct multifocal tDCS conditions (days 1, 2, and 3) were conducted while acquiring MRI data during brain stimulation. These MRI acquisitions comprised, firstly, an arterial spin labeling (ASL) dataset (∼ 6 min), secondly, an rs-fMRI acquisition (∼ 8 min), and finally, a task-based fMRI dataset (∼ 11 min). The present study focuses on rs-fMRI images to investigate in which manner the simulated electric current distributions are associated with the actual experimentally induced effects on the aged brain when not engaged in any particular task. Furthermore, on day 1, a high-resolution three-dimensional (hr-3D; ∼ 8 min) dataset was acquired for functional data preprocessing purposes and to estimate the distribution of the induced electric current. In addition, the mentioned hr-3D acquired on day 1, and a fluid-attenuated inversion recovery (FLAIR) sequence obtained on day 2 (∼ 3 min), were used for neuroradiological assessment to exclude any brain structural abnormalities in study participants. Finally, a diffusion tensor imaging was obtained on day 3 (∼ 9 min; not used in this investigation). Therefore, the total duration of the experimental sessions was ∼ 40 min, whereof the first ∼ 5 min were used for tDCS-MRI setting preparation, and the remaining ∼ 35 min were entirely conducted within the MRI scanner. Out of the total in-scanner time, the initial 25 min were acquired during brain stimulation, and the final variable minutes were dedicated to additional acquisitions. In the experimental sessions, multifocal tDCS was applied to all participants using the two different montages referred above (i.e., C1 and C2) with real stimulation as well as a sham stimulation condition (see section "tDCS parameters" for further details). The order of the experimental sessions was counterbalanced. There was a minimum one-month wash-out between each experimental session to avoid possible prevalence of after-effects (**Figure 1**). Further, a questionnaire of tDCS-related adverse events was administered at the end of each experimental session and compared between the experimental conditions [all p-values > 0.05; for further details see **Supplementary Table 1** and **Supplementary Material**]. In addition, a very brief assessment of the quality of sham was administered (for further details, see **Supplementary Material**).

Neuropsychological Assessment

A comprehensive battery of neuropsychological tests covering all cognitive domains was administered, including the Rey-Osterrieth Complex Figure (ROCF), Rey Auditory Verbal Learning Test (RAVLT), Boston Naming Test (BNT), Semantic category evocation of animals, Number location and incomplete letters from the Visual Object and Space Perception Battery (VOSP), Trail Making Test (TMT), parts A and B, Phonemic fluency (FAS), Stroop Color Word Test, Symbol Digit Modalities Test (SDMT), and Digit span forward and backward from WAIS-III. Finally, the Vocabulary Subtest from WAIS-III was also administered to have a measure of premorbid intelligence. All participants presented a normal cognitive profile with mini-mental state examination (MMSE) scores of ≥27 and performance scores not more than 1.5 *SD* below normative data (adjusted for age and years of education) on any of the administered neuropsychological tests (i.e., they did not fulfill the criteria for mild cognitive impairment; Petersen and Morris, 2005).

Transcranial Direct Current Stimulation Parameters

Two distinct multifocal tDCS montages were designed with the Stimweaver montage optimization algorithm (Ruffini et al., 2014). The latter determines the positions and currents of the electrodes over the scalp that induce an electric field in the brain that better approximates a weighted target electric field map. We optimized for the electric field component normal (orthogonal, E_n) to the cortical surface, assuming a first order model for the interaction of the electric field with neurons in the cortex: when E_n points into/out of the cortical surface (positive/negative values of E_n in our convention), this leads to an increase/decrease in the membrane potential of the soma of pyramidal cells (and hence, cortical excitability). As mentioned, the weighted target E_n-maps used in this study were designed based on the findings obtained in

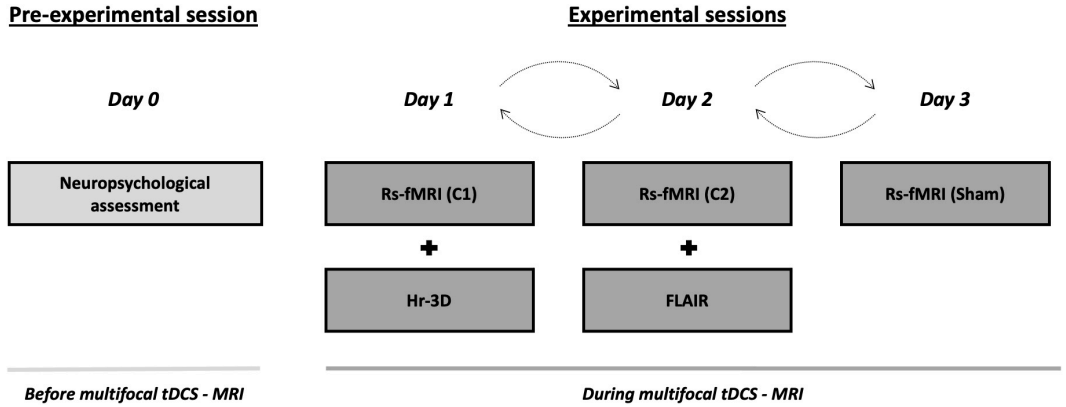

FIGURE 1 | Study protocol and timeline of the procedures accomplished before and during multifocal tDCS-MRI. On the pre-experimental session, all the subjects undertook a neuropsychological screening session to verify a normal cognitive functioning. Then, during the three consecutive experimental sessions, transcranial stimulation was delivered using differential tDCS montages (i.e., C1, C2 and sham) in a counterbalanced fashion while rs-fMRI data was acquired. A hr-3D and a FLAIR datasets were acquired for additional examinations. tDCS, transcranial direct current stimulation; MRI, magnetic resonance imaging; rs-fMRI, resting-state functional MRI; hr-3D, high-resolution three-dimensional; FLAIR, fluid-attenuated inversion recovery; C1, condition 1; C2, condition 2.

our previous fMRI study (Fernández-Cabello et al., 2016). More precisely, on the one hand, the C1 montage was grounded on an fMRI pattern of extended cortical activity, including the bilateral middle frontal gyri, the paracingulate gyri, the precuneus cortex, the bilateral supramarginal gyri and/or intraparietal sulcus area and the lingual gyri (**Figure 2A**). On the other hand, the C2 montage was derived from a second fMRI pattern including moderate activity increases in the bilateral middle frontal and the paracingulate gyri, altogether with brain activity decreases of the posterior cingulate gyrus, the ventral precuneus, and the precentral gyri (**Figure 2B**). In the optimization, the regions that registered a brain activity increase/decrease were targeted with an excitatory/inhibitory (positive/negative) target E_n field (see **Figure 2C** for C1, and **Figure 2D** for C2). Cortical maps of the magnitude of the induced electric field, in which we focused in this investigation, are shown framed in **Figure 2E** for C1 and in **Figure 2F** for C2, in the template head model used in the optimization (Colin27; Miranda et al., 2013). Stimulation was delivered via an MRI-compatible Starstim Neuroelectrics device, using 8 circular MRI Sponstim electrodes with an area of 8 cm^2. These MRI-compatible electrodes consist of a carbon rubber core and a sponger cover, both translucid materials. Hence, the core electrodes were located on the participant's scalp by fitting them inside the sponge and into the holes of a neoprene cap corresponding to the 10/10 international system for electrode placement. The central Cz position was aligned to the vertex of the head in every subject to ensure an accurate cap placement.

Based upon the foregoing, in the C1 montage the electrodes were placed in the AF7, F4, FC5, P3, P4, P7, P8 and Cz positions (see **Figure 2G** and **Table 1**), while in the C2 montage the electrodes were placed in the AF3, C3, C4, F4, FC6, Fpz, Oz and Cz positions (see **Figure 2H** and **Table 1**). For sham stimulation, either C1 or C2 montages were randomly used. The stimulator was situated outside the MRI room and the electrodes were soaked with saline solution and a thin layer of Ten20 conductive paste to ensure good conductivity and stability throughout the MRI acquisition. The current was delivered to each electrode with a wireless neurostimulator (Starstim, by Neuroelectrics Barcelona) connected to a computer via Bluetooth. For safety issues, the maximum current delivered by any electrode was 2 mA, while the maximum current injected through all the electrodes was 4 mA. In the real intervention conditions, the current was supplied during the whole rs-fMRI acquisition, starting just before the ASL acquisition and concluding at the end of the task-based fMRI dataset. In all groups, the current was initially increased and finally decreased in a 30 s ramp-up and ramp-down fashion, carefully configured to not overlap with the MRI acquisitions. For the sham condition, the current dosage was composed of an initial ramp-up of 30 s immediately followed by a 1 min ramp-down, and a final ramp-down of 30 s immediately preceded by a ramp-up of 1 min.

Magnetic Resonance Imaging Acquisition

All participants were scanned with a Siemens Magnetom Trio Tim Syngo 3 Tesla system at the MRI Core Facility (IDIBAPS) of the Hospital Clinic of Barcelona, Barcelona, Spain. In the succeeding, only the acquisitions used in this investigation, both for research purposes and clinical screening, are detailed. Three identical rs-fMRI datasets [T2*-weighted GE-EPI sequence; interleaved acquisition; repetition time (TR) = 2,700 ms; echo time (TE) = 30 ms; 40 slices per volume; slice thickness = 3.0 mm; interslice gap = 15%; voxel size = 3.0 x 3.0 x 3.0 mm; field of view (FOV) = 216 mm; 178 volumes] were acquired, one each experimental day. Furthermore, a hr-3D structural dataset [T1-weighted magnetization-prepared rapid gradient-echo (T1-weighted MPRAGE); sagittal plane acquisition; TR = 2,300 ms; TE = 2.98 ms, inversion time (IT) = 900 ms; slice thickness = 1.0 mm; voxel size = 1.0 x 1.0 x 1.0 mm; FOV = 256 mm; 240 slices] was acquired on experimental day 1. In addition, an axial FLAIR sequence

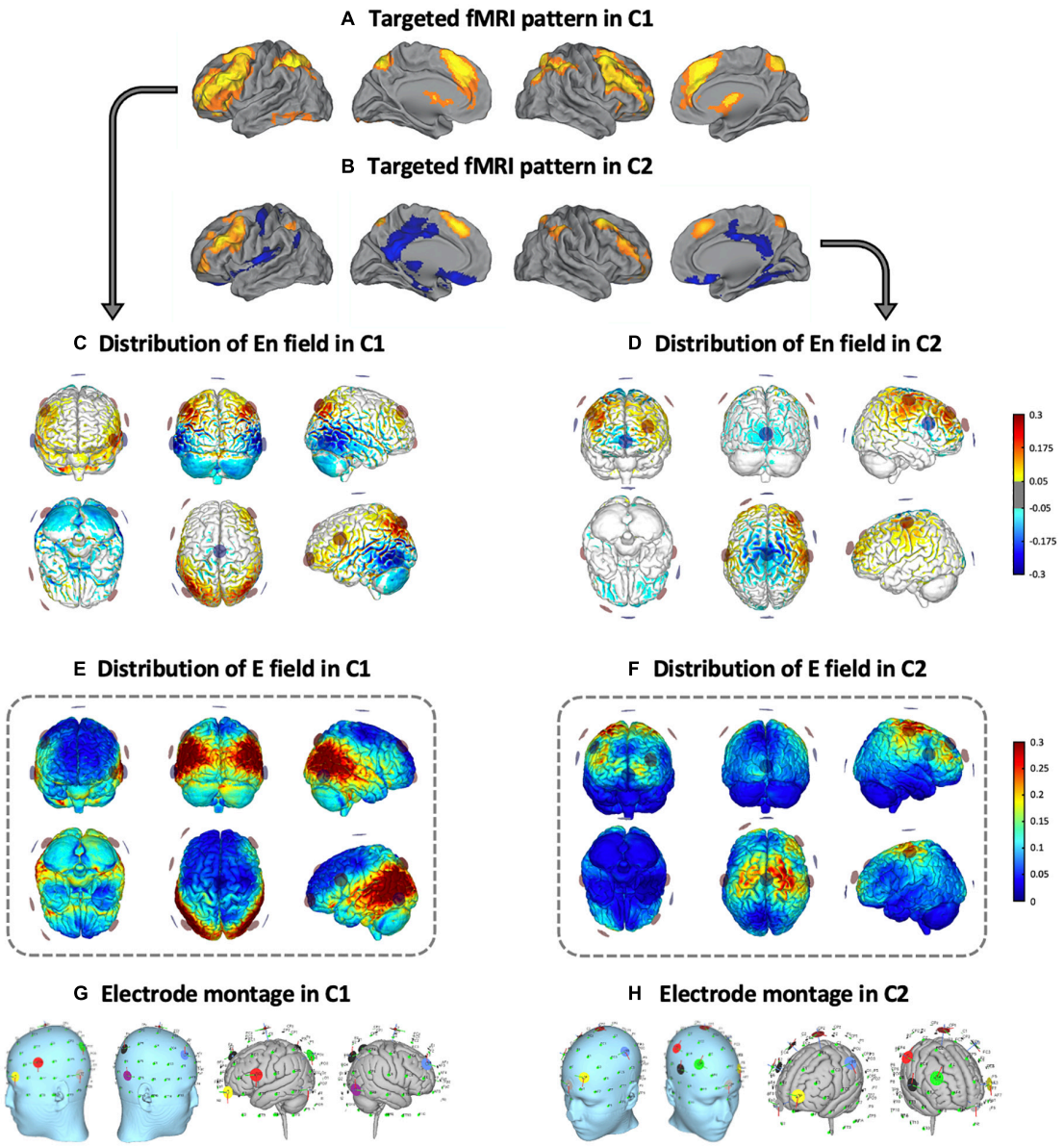

FIGURE 2 | Multifocal tDCS montages. Targeted fMRI patterns in **(A)** C1 and **(B)** C2, from Fernández-Cabello et al. (2016, adapted with permission). Distribution of the E_n field in the cortical surface in **(C)** C1 and **(D)** C2 (in V/m units). Distribution of the electric field's magnitude in the cortical surface in **(E)** C1 and **(F)** C2 (in V/m units). Representation of the electrode locations and shape on the scalp (left) and the gray matter (right) based on a Montreal Neurological Institute (MNI) head in **(G)** C1 and **(H)** C2, obtained for visual purposes. fMRI, functional magnetic resonance imaging; C1, condition 1; C2, condition 2.

(TR = 9,000 ms; TE = 96 ms; slice thickness = 3.0 mm; FOV = 240 mm; 40 slices) was obtained on experimental day 2 (see **Figure 1**).

Functional Connectivity Analyses

The FMRIB Software Library (FSL; version 6.00[1]) and the Analysis of Functional NeuroImages (AFNI[2]) were used for preprocessing and analyzing functional neuroimaging data.

Functional Connectivity Preprocessing

Resting-state functional magnetic resonance imaging (rs-fMRI) data preprocessing included the removal of the first five volumes, motion correction, skull stripping, spatial smoothing [Full Width at Half Maximum (FWHM) = 7 mm], grand mean scaling and filtering with both high-pass and low-pass filters (0.01- and 0.1-Hz thresholds, respectively). Data were then regressed with six rigid-body realignment motion parameters, mean white matter, and mean cerebrospinal fluid signal. No global signal regression was used. Normalization to MNI standard space was also applied. A visual inspection of the preprocessed rs-fMRI images was

[1]http://fsl.fmrib.ox.ac.uk/fsl/fslwiki/
[2]https://afni.nimh.nih.gov/

TABLE 1 | Electrode positions and current intensities in C1 and C2.

C1	C2
AF7: 363 μA	AF3: 864 μA
F4: 539 μA	C3: 665 μA
FC5: 385 μA	C4: 1,291 μA
P3: 1,493 μA	F4: 1,179 μA
P4: 1,220 μA	FC6: −966 μA
P7: −1,705 μA	Fpz: −998 μA
P8: −1,525 μA	Oz: −396 μA
Cz: −770 μA	Cz: −1,639 μA

thoughtfully completed before conducting further functional connectivity analyses. Moreover, as head movement may affect rs-fMRI results (Power et al., 2012, 2015; Van Dijk et al., 2012), in-scanner head motion was calculated for every subject. More precisely, two standard measures to estimate in-scanner head motion were obtained in a similar manner as described elsewhere (Power et al., 2012). Displacement relative to a single reference volume (absolute displacement) and relative to the precedent volume (relative displacement) were calculated for every subject. In our sample, no significant differences were found between the three conditions (i.e., C1, C2 and sham), considering both absolute and relative displacement (all p-values > 0.05; for further data, see **Supplementary Table 2**).

Regions of Interest-Based Functional Connectivity Analyses

Functional connectivity analyses were implemented based on a whole-brain atlas that parcels the brain into a set of anatomical regions of interest (ROIs). The selected atlas was the one developed for the CONN toolbox (Whitfield-Gabrieli and Nieto-Castanon, 2012). This atlas includes a rich set of regions to perform comprehensive whole-brain analyses using ROI-based approaches. More specifically, this atlas includes 132 ROIs, combining the FSL Harvard-Oxford cortical (91 ROIs) and subcortical atlases (15 ROIs) and the cerebellar areas from the Anatomical Automatic Labeling (AAL) atlas (26 ROIs). Individualized time-series of the different ROIs were extracted from the preprocessed and regressed images. In order to obtain a resting-state functional connectivity (rs-FC) measure for each ROI-to-ROI connection in each subject, the acquired ROI time-series were correlated with one another to create correlation matrices, using Pearson product-moment correlations.

Electric Current Computations

SimNIBS 3.0.7 was used to individually calculate the electrical current induced by tDCS based on the finite element method (FEM) and individualized head models derived from the structural MRI datasets ([3]Windhoff et al., 2013; Thielscher et al., 2015). First, T1-weighted anatomical images were used to create individualized tetrahedral FE head meshes of each subject, using MATLAB toolboxes (Nielsen et al., 2018), MeshFix (Attene, 2010), and Gmsh (Geuzaine and Remacle, 2009). These head models contain representations of the scalp, skull, cerebrospinal fluid (including the ventricles), eyeballs, gray-matter and white-matter. Second, the electrode positions (i.e., the center coordinates of the modeled electrodes) were placed on each subject head mesh, according to the locations established for each montage (i.e., C1 and C2). Then, electric current simulations were computed for each condition separately. Following the specific characteristics of the MRI Sponstim electrodes from Neuroelectrics, the electrode shape was set as elliptical, and the size was defined as 2.3 cm of diameter and 1 mm of thickness. The electrode's sponge size was defined as 3.2 cm of diameter and 3 mm of thickness. Tissue and electrode conductivity values were set as default in SimNIBS software (Thielscher et al., 2011; Saturnino et al., 2015). Third, individual results were averaged together for each condition, resulting in group averages and *SD*s of the electric current density distribution. Finally, for each montage, data on the peak fields (99.9th percentile) and the electric current magnitude values within the selected ROIs, based on fMRI findings, were obtained (see sections "Statistical analyses" and "Multifocal tDCS effects on rs-fMR" for further information). The magnitude of the current density (normJ) was used in all the subject-based analyses of this investigation (i.e., those computed with SimNIBS). Current density seems to be particularly useful for dosage determination in terms of the regional quantity of current reaching the brain with advancing age (i.e., Indahlastari et al., 2020). Hence, if not otherwise specified (i.e., as in the originally designed models using a template brain), figures and analysis results reflect the electric current density in all cases, and are expressed as amperes per square meter (A/m^2). Due to technical issues during the generation of the head mesh, related to poor quality of the T1 MRI data, a subject was discarded from these analyses. The segmentations quality from all generated brain images was individually examined and deemed appropriate.

Statistical Analyses

Data analyses were performed using IBM SPSS (IBM Corp. Released 2017. IBM SPSS Statistics for Windows, Version 25.0. Armonk, NY: IBM Corp.) and MATLAB (Version R2019a, The MathWorks Inc., Natick, MA, United States).

Functional Connectivity Statistical Analyses

Resting-state functional connectivity (rs-FC) correlation matrices, permutation testing and pixel correction for multiple comparisons were performed using custom made MATLAB scripts. Functional connectivity differences were compared between conditions using non-parametric permutation testing (Nichols and Holmes, 2002). We chose this method because it does not rely on assumptions about the distribution of the data and correction methods for multiple comparisons can be easily implemented (Theiler et al., 1992).

Time-series data for each subject, ROI and condition were concatenated into a 4D array (i.e., subject x time-point x ROI x condition). Then, correlations between all ROIs for each subject and condition were computed, taking time-points as individual observations in each ROI-to-ROI correlation. This resulted in three correlation matrices (i.e., one for each condition;

[3]www.simnibs.org

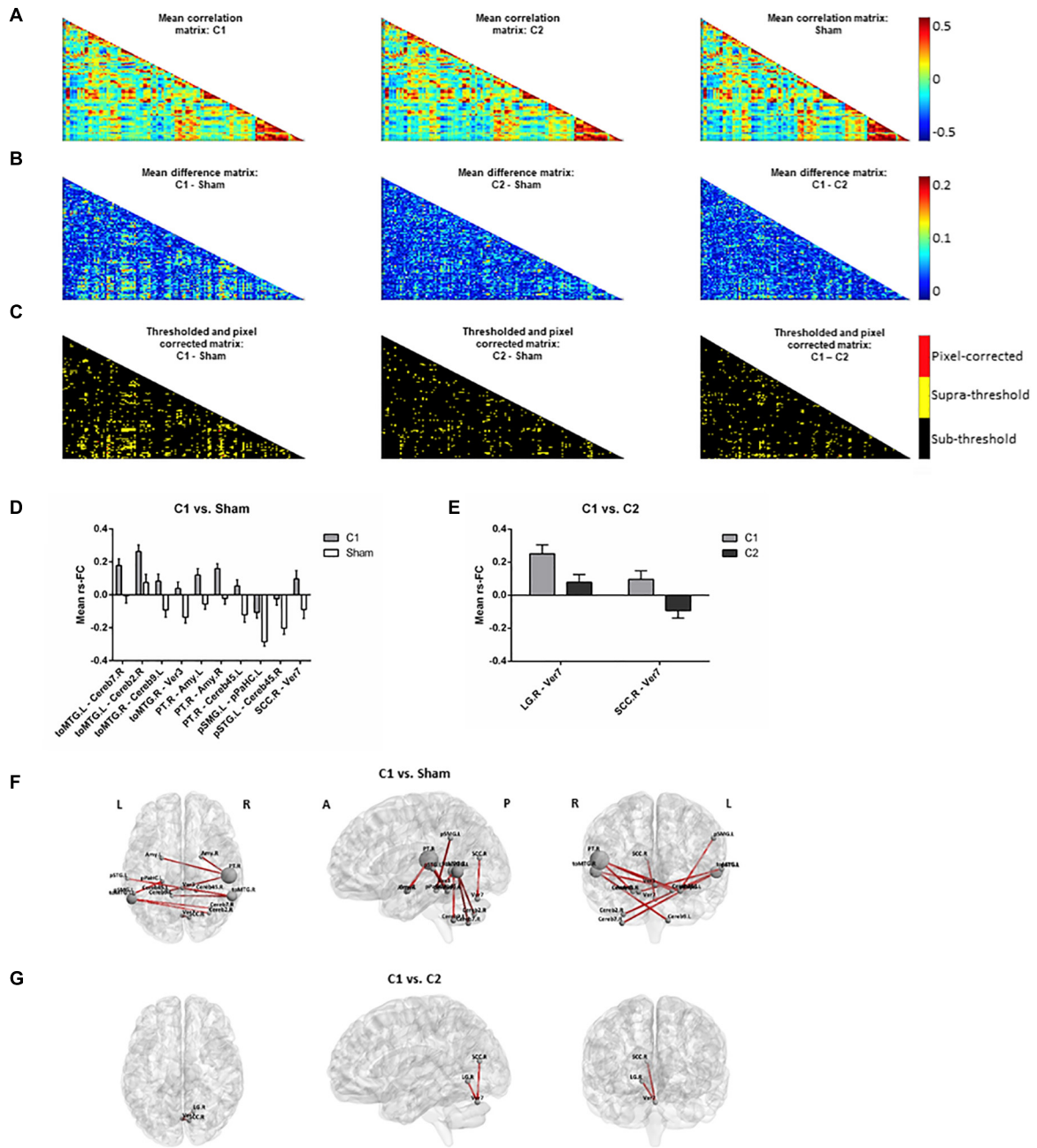

FIGURE 3 | Rs-fMRI analyses. **(A)** Mean correlation matrices for (left to right): C1, C2 and sham. **(B)** Mean difference matrices for (left to right): C1 – Sham, C2 – Sham, C1 – C2. **(C)** Thresholded and pixel-corrected matrices for (left to right): C1 – Sham, C2 – Sham, C1 – C2 (dark: sub-threshold; yellow: supra-threshold; red: pixel-corrected). Bar-plots showing the mean with standard error of the mean (*SEM*) of rs-FC comparing **(D)** C1 vs. Sham and **(E)** C1 vs. C2, computed for visually inspecting the group tendencies in each coupling. Representation of the significant connections for **(F)** C1 vs. Sham and **(G)** C1 vs. C2 on a standard map (left to right: axial, sagittal and coronal view). Note that in Panel **(F)**, selected main hubs (i.e., those ROIs entailing ≥2 significant rs-FC connections when comparing C1 vs. Sham) are displayed with a correspondingly larger size to emphasize them. C1, condition 1; C2, condition 2; toMTG, Middle temporal gyrus, temporo-occipital part; Cereb, Cerebellum; Ver, Vermis; PT, Planum temporale; Amy, Amygdala; pSMG, Supramarginal gyrus, posterior division; pPaHC, Parahippocampal gyrus, posterior division, pSTG, Superior temporal gyrus, posterior division; SCC, Supracalcarine cortex; LG, Lingual gyrus; L, left; R, right; A, anterior; P, posterior.

Figure 3A) with three dimensions each (i.e., ROI x ROI x subject). Then, differences between the means of the correlation matrices, for each pair of conditions and across subjects, were computed for each ROI x ROI correlation matrix point (**Figure 3B**) and compared with the null-hypotheses distribution generated by randomly shuffling the condition labels over subjects and repeating this procedure for 1000 iterations (**Figure 3C**, $\alpha = 0.05$, supra-threshold: in yellow). The resulting comparison matrices

were corrected for multiple comparisons using pixel correction (Cohen, 2014; **Figure 3C**, pixel-corrected: in red). This procedure consists in picking the largest and smallest test statistic values of each permutation -which results in two distributions of extreme values- and then setting the thresholds for statistical significance to be the values corresponding to the 97.5 percentile of the largest value and the 2.5 percentile of the smallest value. Pixel correction was preferred as compared to the more common cluster-based methods because the nature of our data (i.e., correlation matrices) does not require that significant differences are spatially clustered.

Electric Current and Further Statistical Examinations

Furthermore, differences regarding the magnitude of the peak fields (99.9th percentile) between C1 and C2 were compared using a paired sample *t*-test. Additional paired sample *t*-tests were used to test for electric current magnitude differences between experimental conditions for each of the main ROIs selected based on rs-fMRI analyses. ROIs were selected and considered as main hubs when they involved ≥ 2 significant rs-FC couplings that survived multiple comparisons using pixel correction. Moreover, Pearson product-moment correlation was used to explore the association between tDCS-induced rs-fMRI effects and the magnitude of calculated current density estimates in the selected ROIs. More specifically, tDCS-induced functional changes in each particular coupling that survived pixel correction were linked to the selected ROIs' electric current magnitude values when this fell within the rs-FC connection. Finally, to compare head movement and tDCS-related adverse events differences between the experimental groups, a one-way repeated measures ANOVA was used. In these analyses, data distribution was tested for normality with the Shapiro-Wilk test ($p > 0.05$; Shapiro and Wilk, 1965; Razali and Wah, 2011). Non-parametric tests were used in cases where parametric tests were not appropriate. These non-parametric tests are explicitly stated when necessary. No adjustment for multiple comparisons was applied in these exploratory statistical analyses. All these tests were two-tailed and α was set at 0.05.

RESULTS

Multifocal Transcranial Direct Current Stimulation Effects on Resting-State Functional Magnetic Resonance Imaging

The two tDCS conditions differently influenced rs-fMRI connectivity. When comparing C1 against sham, some specific connections (i.e., a total of 10 resting-state couplings) significantly increased their coactivation (**Figures 3D,F**). Many of the affected connections involved temporal and temporo-occipital areas and distinct cerebellar regions. In particular, three temporal areas emerged as main hubs (i.e., those with ≥ 2 significant rs-FC couplings). These regions were the left and right temporo-occipital middle temporal gyri (toMTG.L and toMTG.R, respectively) and the right planum temporale (PT.R), which fall in the posterior part of the temporal lobe. Remarkably, C1 was also able to modulate structures entailing the limbic system, such as the amygdala and the hippocampal formation. When contrasting C1 against C2, two connections were detected to be significantly different (**Figures 3E,G**). These results represented occipital-cerebellar couplings. Particularly, we observed significant modification of the connections between the right lingual gyrus (LG.R) and the right supracalcarine cortex (SCC.R) and the seventh lobule of the vermis (Ver7). No differences were observed between C2 and sham.

Electric Current Simulations

The means and *SDs* of electric current density distributions induced by C1 and C2 are displayed in **Figure 4A** (for C1) and **Figure 4B** (for C2). Individually modeled electric current density distributions are displayed in **Supplementary Figure 1** (for C1) and **Supplementary Figure 2** (for C2). The electric current density distribution induced by C1 predominantly included the inferior parietal lobule as well as temporal and occipital regions. In contrast, the electric current density induced by C2 showed a more anteriorly centered distribution principally encompassing the precentral, superior and, in a lesser extent, the middle frontal gyri. Moreover, as expected for the C2, the electric current magnitude within the posteromedial and occipital areas was very low. As can be further observed, the originally designed patterns created with the Colin27 template and the average simulated configurations obtained with our aged individuals were entirely anatomically consistent (see **Figures 2E,F**, **4A,B**).

Furthermore, C1 reached statistically significant higher peak fields (99.9th percentile) as compared to C2 ($t = 10.716$; $p < 0.001$; **Figure 4C**). Additionally, the electric current magnitude values extracted from the three main ROIs identified on the rs-fMRI analyses (i.e., toMTG.L, toMTG.R and PT.R), were, as expected, significantly higher in C1 when compared to C2 (toMTG.L: $t = 19.986$, $p < 0.001$; toMTG.R: $t = 18.473$, $p < 0.001$; PT.R: Wilcoxon signed-rank test, $Z = 4.000$; $p < 0.001$; **Figure 4D**).

Associations Between Resting-State Functional Magnetic Resonance Imaging Modulation and Induced Electric Current

Lastly, correlation analyses between tDCS-induced rs-fMRI changes and the magnitude of the calculated current density values were performed. We observed that those subjects who showed increased coactivation in C1 compared to sham in the toMTG.R – Ver3 coupling also presented lower induced electric current magnitude estimates in C1 ($r = -0.401$, $p = 0.028$; **Figure 4E**). In addition, those subjects who showed higher coactivation at C1 compared to sham in the toMTG.R – Cereb9.L also presented a negative association with the induced electric current magnitude values in C1, however, this association was not statistically significant ($r = -0.358$, $p = 0.052$; **Figure 4F**). Thus, it was observed that, although in the majority of cases (67.7% for the toMTG.R – Ver3 coupling; 64.5% for toMTG.R – Cereb9.L coupling) an increase in coactivation happened with certain levels of induced current, in those subjects with higher current density estimates, a functional coactivation reduction most likely occurred (see **Figures 4E,F**). Of note, since no significant differences were observed between C2 and sham, we focused these analyses to C1, which was significantly different from sham.

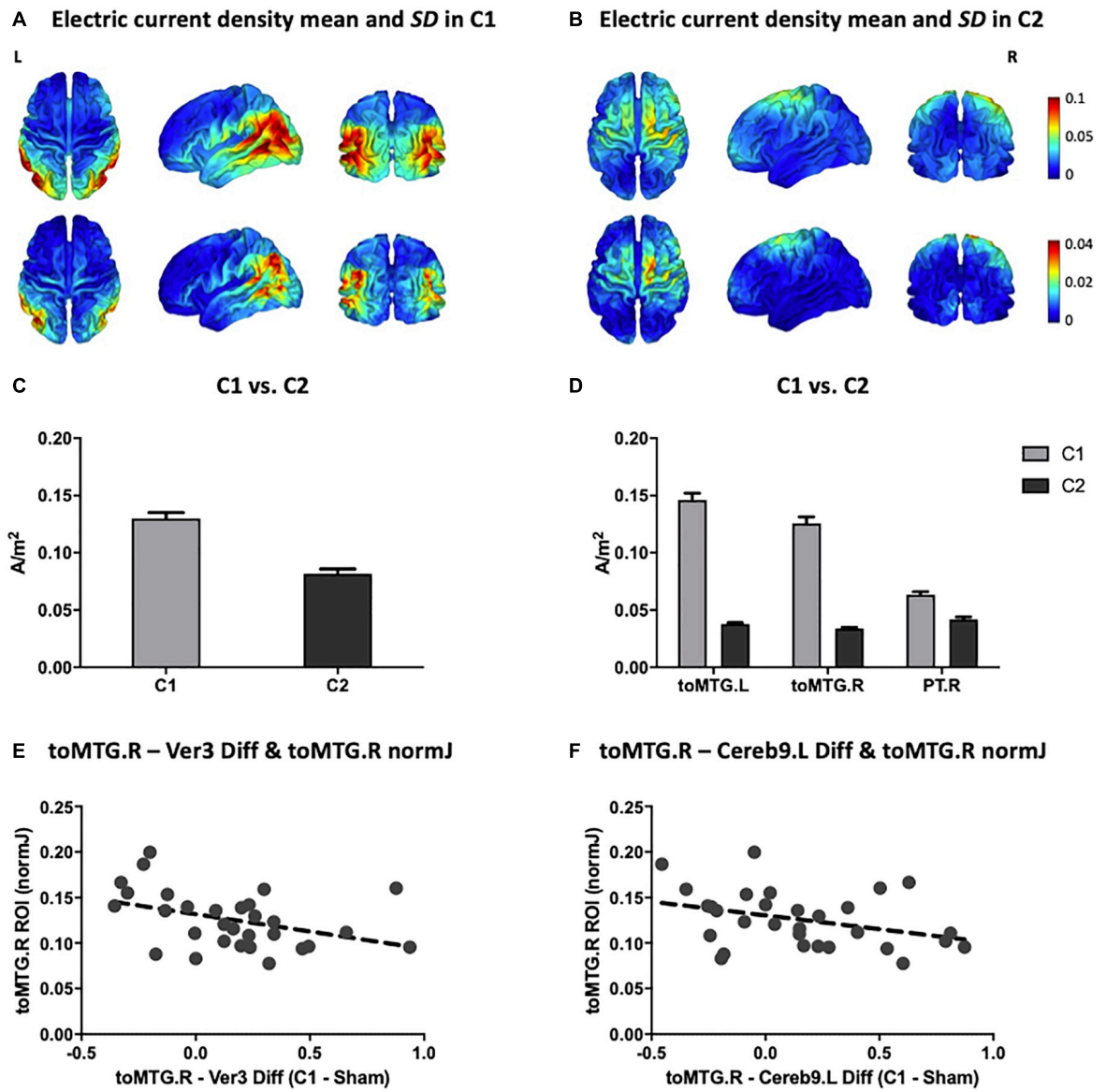

FIGURE 4 | Multifocal tDCS simulated electric current distributions. Anatomical pattern of the electric current density mean (top) and *SD* (bottom) for all subjects in **(A)** C1 and **(B)** C2 (in A/m^2 units). **(C)** Comparison between C1 and C2 of the mean magnitude of the peak fields (99.9th percentile; in A/m^2 units). **(D)** Comparison between C1 and C2 of the electric current magnitude extracted from the three main hubs detected on the rs-fMRI analyses (i.e., toMTG.L, toMTG.R and PT.R; in A/m^2 units). **(E,F)** Scatter plots showing the associations between multifocal tDCS-induced changes in rs-fMRI connectivity estimates and electric current magnitude values (in A/m^2 units). Data in **(C,D)** are presented with mean with *SEM*. C1, condition 1; C2, condition 2; toMTG, Middle temporal gyrus, temporo-occipital part; PT, Planum temporale; Ver, Vermis; Cereb, Cerebellum; L, left; R, right; Diff, difference.

DISCUSSION

This represents, to the best of our knowledge, the first study investigating the impact of two distinct multifocal tDCS montages on rs-fMRI in healthy aging. Our results showed that: (I) multifocal tDCS modulates rs-FC in a montage-dependent manner in older adults. (II) Moreover, the functional impact is consistent with the spatial distribution of the induced electric current on the brain. (III) Finally, specific individual tDCS-induced rs-fMRI responses are related with the magnitude of the calculated electric current estimates, which might be in line with the stochastic resonance hypothesis (see below).

In this investigation, we observed that multifocal tDCS can modulate brain dynamics as measured through rs-fMRI connectivity amongst older adults. Furthermore, network-based tDCS appears to anatomically modulate functional connectivity in a manner dependent with the simulated electric current distribution. In this vein, the impact of transcranial stimulation was particularly evident when comparing C1 to sham. Three temporal regions emerged as the principal modulated regions: the

left and right toMTG and the right PT. A relevant modulatory effect between these cortical nodes and the cerebellum was detected, though the modulation of cerebellar areas was less specific. Moreover, in other cortical temporo-parietal areas, such as the posterior divisions of the superior temporal and the supramarginal gyri, rs-FC was also modulated. In addition, the connectivity of subcortical regions, such as the amygdala and the hippocampal formation, which are core areas of the limbic system, was also modified. Of note, this system has been associated with emotion, motivation, and memory (Morgane et al., 2005), which are processes of particular significance in advancing age (i.e., Liu et al., 2020). In the present investigation, the main rs-fMRI results when contrasting C1 against sham (i.e., considering the main hubs; **Figure 3F**) topographically correspond with the estimated electric current distribution on the brain, as the largest electric current values in C1 were observed also in the inferior parietal and particular temporo-occipital brain regions (see **Figure 4A**). Furthermore, these results were consistent with the position of the electrodes that delivered the highest stimulation intensities in C1 (see **Figure 2G** and **Table 1**), namely P3 and P4 (with positive polarity), as well as P7 and P8 (with negative polarity). Interestingly, P3 and P4 electrode positions in the international 10-10 system are anatomically located above the inferior parietal lobule and principally encompass the Brodmann's area 39 (BA39; Koessler et al., 2009). Moreover, the P7 and P8 electrodes are situated above the middle occipital and inferior temporal gyri and mainly include Brodmann's areas 37 and 19, respectively (BA37 and BA19; Koessler et al., 2009). Hence, the highest intensity electrodes (regardless of the polarity) topographically covered the temporo-parieto-occipital junction (i.e., De Benedictis et al., 2014). In consequence, in the C1 montage, we observed, at the group level, a clear topographical association between the electrode's assembly and injected current intensities, the corresponding calculated electric current density distribution in the cortical surface, and the neuroimaging results obtained with rs-fMRI data in our experimental design. Of note, no clear multifocal tDCS effects were observed at the rs-fMRI level in C2, potentially because the delivered stimulation was not sufficient to induce an observable functional connectivity modulation in the studied aging brains (for a visual inspection, compare **Figures 4A,B**, and see **Figures 4C,D** plots).

In previous literature, considerable inter-individual variability in response to distinct NIBS protocols has been observed (i.e., Hamada et al., 2013; López-Alonso et al., 2014; Wiethoff et al., 2014). These reports highlight the importance of identifying the individual predictors of NIBS effects, particularly in older adults, where substantial attempts have been made to modulate and optimize brain function and the associated cognitive performance (i.e., Antonenko et al., 2018; Nilakantan et al., 2019). In the present study we focused on the magnitude of the simulated electric current density as a potential factor contributing to such variability. In this vein, we investigated whether dissimilar individual differences in rs-fMRI modulation were related to the electric current magnitude estimates within the designated main ROIs. We observed that, in specific functional couplings, the higher the magnitude of calculated current values, the lower the coactivation increment. Thus, it is conceivable that aged individuals with dissimilar neuroanatomical characteristics (which relates to distinct simulated current density parameters) may require differential stimulation intensities to result in optimal modulations of functional brain connectivity. The hypothesis of the stochastic resonance might provide a mechanistic explanation of this state-dependency observation. According to Polanía et al. (2018), the stochastic resonance is a phenomenon referring to a situation in which a signal that is too weak to be detected by a sensor might be enhanced by adding an optimal level of noise. This assumption proposes that in a non-linear system, as the brain is, there are optimal noise levels for neural processing, and only intermediate, but not high or low levels of noise, can led to higher discriminability of the signal of interest. In this vein, the presence of neural noise (that can be added by means of NIBS) might confer to neurons more sensitivity to a given range of weak inputs, thereby rendering the signal stronger, or even synchronized (for a review, see Miniussi et al., 2013). This phenomenon has been reported in previous experimental NIBS studies, both using transcranial magnetic stimulation (TMS; Abrahamyan et al., 2011) and conventional tDCS (Peña-Gómez et al., 2011). More precisely, Abrahamyan et al. (2011) demonstrated that visual sensitivity can be improved with the right amounts of noise induced by means of TMS to the visual cortex. Further, in a previous study from our group, it was observed that distinct personality traits (introverts vs. extraverts), which might entail distinct baseline levels of brain activity, responded behaviorally different to the same tDCS protocol. The authors explained these results within the stochastic resonance paradigm, claiming that introverts, with higher levels of intrinsic neural activity, could have reached the threshold more easily than extraverts with a relatively weak electrical stimulation (see Peña-Gómez et al., 2011). Our data, using multifocal tDCS, appear to be consistent with the hypothesis that specific amounts of current density are required to produce an optimal neural effect (i.e., an increase in functional coactivation). On the contrary, both not delivering enough electrical current in the targeted brain structures (i.e., as could have occurred in C2), as well as a supplying supposedly excessive electrical current, could result in suboptimal neural effects (i.e., a functional coactivation reduction). In this vein, our results shows that the induced electric current magnitude estimates, which are contingent to the individual head and brain anatomy (Thielscher et al., 2011; Miranda et al., 2013), might entail a feasible predictive value regarding NIBS effects in aging when considered within this noise generation hypothesis.

Altogether, our data show that multifocal non-invasive stimulation models and protocols are capable to effectively modulate precise fMRI configurations in older adults. These observations may have important future implications for the cognitive neuroscience of aging field, since many of the neural basis regarding cognitive functioning, longitudinal trajectories

and inter-individual differences, including the development of theoretical models, have been mainly based on studies employing this imaging technology (Grady, 2012; Cabeza et al., 2018; Vaqué-Alcázar et al., 2020). Furthermore, fMRI changes can effectively track the positive impact of behavioral interventions aimed to ameliorate cognition in the elderly (Duda and Sweet, 2020), including its combined effects with NIBS (Antonenko et al., 2018). Therefore, and as opposed to the use of conventional tDCS montages, the possibility of *a priori* designing particular NIBS-based interventions of regional-specific fMRI patterns may offer a valuable and refined approach for studies intended to optimize complex brain configurations amongst older individuals, or to investigate the impact of interventions in clinical trials. Moreover, the obtained tDCS results at the individual level are aligned with the notion that an exhaustive neuroanatomical characterization is critical to determine the right amount of stimulation required to produce optimal neurophysiological effects in each subject.

LIMITATIONS

The present study is not without limitations. First, it is worth noting that the present investigation focused on the large-scale brain networks that hypothetically sustain cognitive aging, but not in cognitive performance itself. Hence, forthcoming studies should make an effort to unify the various levels of brain description (i.e., cells, networks, behavior) toward a comprehensive characterization of brain–behavior relationships in advanced age. Furthermore, although the observed results in fMRI data are unlikely to be due to poor control of the experimental conditions, our study could have improved methodologically by several different means, for instance, by using a sham condition for each real stimulation condition. Moreover, it is worth noting that our original modelings designed with Stimweaver were based on the template Colin27. Models based on aged brains or on individual MRIs could have improved the multifocal tDCS montage for both conditions. Furthermore, even though our individually generated models topographically matched the originally designed, future experimental investigations should incorporate both a T1- and a T2-weigthed acquisitions to optimize the electric current simulation procedures. Further in this line, it is pertinent for T1 images to be acquired without the stimulation cap assembled to avoid potential confounders in the segmentation process. Finally, it must be recognized that in all simulation-based electric current planning systems, there is uncertainty about the precise conductivity values that should be used for the different tissues and materials when creating and analyzing a model for a particular montage (see for further detail Miranda et al., 2013; Saturnino et al., 2019). Notwithstanding, notable advances are being achieved in this vein (Huang et al., 2017).

CONCLUSION

Present results highlight that multifocal electrical stimulation protocols are capable of modulating neural dynamics in the elderly. Moreover, this functional modulation is related with the simulated electric current distribution on the brain. Thus, applying network-based procedures might entail a novel feasible approach to accurately target and modulate specific fMRI networks and connections critically involved in the cognitive aging process. Further, we have shown that the estimated magnitude of current density is a relevant factor accounting for the individual variability to NIBS in aged populations. Gathering knowledge about these variables will allow us to ultimately refine the parameters of transcranial stimulation to boost the brain and the potential cognitive benefits derived from NIBS-based interventions in advanced age.

DATA AVAILABILITY STATEMENT

The raw data and data processing code supporting the conclusions of this article will be made available by the authors, without undue reservation.

ETHICS STATEMENT

The studies involving human participants were reviewed and approved by the Ethics Committee of the University of Barcelona (IRB 00003099). The patients/participants provided their written informed consent to participate in this study.

AUTHOR CONTRIBUTIONS

KA-P, LV-A, and DB-F designed and conducted the study and prepared the manuscript draft with important intellectual input from RP-A, CS-P, NB, RS, GR, MN, and AP-L. KA-P and LV-A completed the data collection. KA-P, LV-A, and RP-A performed the data analysis. All authors reviewed the manuscript.

FUNDING

This work was supported by grants from the Spanish Ministry of Economy and Competitiveness (MINECO/FEDER; PSI2015-64227-R) and the Spanish Ministry of Science, Innovation and Universities (MICIU/FEDER; RTI2018-095181-B-C21) to DB-F, which was also supported by an ICREA Academia 2019 grant award. KA-P was supported by a postdoctoral fellowship associated with the MICIU/FEDER; RTI2018-095181-B-C21 grant. LV-A was supported by a postdoctoral fellowship associated with the MINECO/FEDER PSI2015-64227-R grant (reference number, BES-2016-077620). MN was supported by the German Ministry of Education and Research (TRAINSTIM, grant 01GQ1424E). AP-L was supported by the Sidney R. Baer Jr. Foundation, the National Institutes of Health (NIH R01 MH100186, R01 NS073601, R01 HD069776, R21 MH099196, R21 NS082870, R21 NS085491, and R21 HD07616), Harvard Catalyst | The Harvard Clinical and Translational Science Center (NCRR and the NCATS NIH, UL1 RR025758),

DARPA (via HR001117S0030) and the Football Players Health Study at Harvard University. The project that gave rise to these results also received the support of a fellowship from "la Caixa" Foundation (ID 100010434). The fellowship code is LCF/BQ/DI19/11730050. The present study was also partially funded by EU Horizon 2020 project "Healthy minds 0–100 years: Optimizing the use of European brain imaging cohorts ("Lifebrain")," (Grant Agreement Number: 732592. Call: Societal challenges: Health, demographic change and well-being). This research was furthermore supported by the Government of Catalonia (2017SGR748).

ACKNOWLEDGMENTS

We are indebted to the Magnetic Resonance Imaging Core Facility (IDIBAPS) and the SimNIBS developers for the technical help.

SUPPLEMENTARY MATERIAL

The Supplementary Material for this article can be found online at: https://www.frontiersin.org/articles/10.3389/fnagi.2021.725013/full#supplementary-material

REFERENCES

Abellaneda-Pérez, K., Vaqué-Alcázar, L., Perellón-Alfonso, R., Bargalló, N., Kuo, M. F., Pascual-Leone, A., et al. (2020). Differential tDCS and tACS effects on working memory-related neural activity and resting-state connectivity. *Front. Neurosci.* 13:1440. doi: 10.3389/fnins.2019.01440

Abellaneda-Pérez, K., Vaqué-Alcázar, L., Solé-Padullés, C., and Bartrés-Faz, D. (2019a). Combining non-invasive brain stimulation with functional magnetic resonance imaging to investigate the neural substrates of cognitive aging. *J. Neurosci. Res.* doi: 10.1002/jnr.24514 [Epub ahead of print].

Abellaneda-Pérez, K., Vaqué-Alcázar, L., Vidal-Piñeiro, D., Jannati, A., Solana, E., Bargalló, N., et al. (2019b). Age-related differences in default-mode network connectivity in response to intermittent theta-burst stimulation and its relationships with maintained cognition and brain integrity in healthy aging. *Neuroimage* 188, 794–806. doi: 10.1016/j.neuroimage.2018.11.036

Abrahamyan, A., Clifford, C. W., Arabzadeh, E., and Harris, J. A. (2011). Improving visual sensitivity with subthreshold transcranial magnetic stimulation. *J. Neurosci.* 31, 3290–3294. doi: 10.1523/JNEUROSCI.6256-10.2011

Antal, A., Alekseichuk, I., Bikson, M., Brockmöller, J., Brunoni, A. R., Chen, R., et al. (2017). Low intensity transcranial electric stimulation: safety, ethical, legal regulatory and application guidelines. *Clin. Neurophysiol.* 128, 1774–1809. doi: 10.1016/j.clinph.2017.06.001

Antonenko, D., Külzow, N., Sousa, A., Prehn, K., Grittner, U., and Flöel, A. (2018). Neuronal and behavioral effects of multi-day brain stimulation and memory training. *Neurobiol. Aging* 61, 245–254. doi: 10.1016/j.neurobiolaging.2017.09.017

Attene, M. (2010). A lightweight approach to repairing digitized polygon meshes. *Vis. Comput.* 26, 1393–1406. doi: 10.1007/s00371-010-0416-3

Betzel, R. F., Byrge, L., He, Y., Goñi, J., Zuo, X. N., and Sporns, O. (2014). Changes in structural and functional connectivity among resting-state networks across the human lifespan. *Neuroimage* 102 (Pt 2), 345–357. doi: 10.1016/j.neuroimage.2014.07.067

Bressler, S. L., and Menon, V. (2010). Large-scale brain networks in cognition: emerging methods and principles. *Trends Cogn. Sci.* 14, 277–290. doi: 10.1016/j.tics.2010.04.004

Cabeza, R., Albert, M., Belleville, S., Craik, F. I. M., Duarte, A., Grady, C. L., et al. (2018). Maintenance, reserve and compensation: the cognitive neuroscience of healthy ageing [published correction appears in Nat Rev Neurosci. 2018 Dec;19(12):772]. *Nat. Rev. Neurosci.* 19, 701–710. doi: 10.1038/s41583-018-0068-2

Cao, M., Wang, J. H., Dai, Z. J., Cao, X. Y., Jiang, L. L., Fan, F. M., et al. (2014). Topological organization of the human brain functional connectome across the lifespan. *Dev. Cogn. Neurosci.* 7, 76–93. doi: 10.1016/j.dcn.2013.11.004

Chan, M. Y., Park, D. C., Savalia, N. K., Petersen, S. E., and Wig, G. S. (2014). Decreased segregation of brain systems across the healthy adult lifespan. *Proc. Natl. Acad. Sci. U.S.A.* 111, E4997–E5006. doi: 10.1073/pnas.1415122111

Cohen, M. X. (2014). *Analyzing Neural Time Series Data: Theory and Practice*. Cambridge, MA: The MIT Press.

Damoiseaux, J. S., Rombouts, S. A., Barkhof, F., Stam, C. J., Smith, S. M., Beckmann, C. F., et al. (2006). Consistent resting-state networks across healthy subjects. *Proc. Natl. Acad. Sci. U.S.A.* 103, 13848–13853. doi: 10.1073/pnas.0601417103

De Benedictis, A., Duffau, H., Paradiso, B., Grandi, E., Balbi, S., Granieri, E., et al. (2014). Anatomo-functional study of the temporo-parieto-occipital region: dissection, tractographic and brain mapping evidence from a neurosurgical perspective. *J. Anat.* 225, 132–151. doi: 10.1111/joa.12204

Dosenbach, N. U., Nardos, B., Cohen, A. L., Fair, D. A., Power, J. D., Church, J. A., et al. (2010). Prediction of individual brain maturity using fMRI [published correction appears in Science. 2010 Nov 5;330(6005):756]. *Science* 329, 1358–1361. doi: 10.1126/science.1194144

Duda, B. M., and Sweet, L. H. (2020). Functional brain changes associated with cognitive training in healthy older adults: a preliminary ALE meta-analysis. *Brain Imaging Behav.* 14, 1247–1262. doi: 10.1007/s11682-019-00080-0

Fernández-Cabello, S., Valls-Pedret, C., Schurz, M., Vidal-Piñ;eiro, D., Sala-Llonch, R., Bargallo, N., et al. (2016). White matter hyperintensities and cognitive reserve during a working memory task: a functional magnetic resonance imaging study in cognitively normal older adults. *Neurobiol. Aging* 48, 23–33. doi: 10.1016/j.neurobiolaging.2016.08.008

Ferreira, L. K., and Busatto, G. F. (2013). Resting-state functional connectivity in normal brain aging. *Neurosci. Biobehav. Rev.* 37, 384–400. doi: 10.1016/j.neubiorev.2013.01.017

Fischer, D. B., Fried, P. J., Ruffini, G., Ripolles, O., Salvador, R., Banus, J., et al. (2017). Multifocal tDCS targeting the resting state motor network increases cortical excitability beyond traditional tDCS targeting unilateral motor cortex. *Neuroimage* 157, 34–44. doi: 10.1016/j.neuroimage.2017.05.060

Geuzaine, C., and Remacle, J. F. (2009). Gmsh: a 3-D finite element mesh generator with built-in pre- and post-processing facilities. *Int. J. Numer. Methods Eng.* 79, 1309–1331. doi: 10.1002/nme.2579

Grady, C. (2012). The cognitive neuroscience of ageing. *Nat. Rev. Neurosci.* 13, 491–505. doi: 10.1038/nrn3256

Grady, C., Sarraf, S., Saverino, C., and Campbell, K. (2016). Age differences in the functional interactions among the default, frontoparietal control, and dorsal attention networks. *Neurobiol. Aging* 41, 159–172. doi: 10.1016/j.neurobiolaging.2016.02.020

Hamada, M., Murase, N., Hasan, A., Balaratnam, M., and Rothwell, J. C. (2013). The role of interneuron networks in driving human motor cortical plasticity. *Cereb. Cortex* 23, 1593–1605. doi: 10.1093/cercor/bhs147

Holland, R., Leff, A. P., Josephs, O., Galea, J. M., Desikan, M., Price, C. J., et al. (2011). Speech facilitation by left inferior frontal cortex stimulation. *Curr. Biol.* 21, 1403–1407. doi: 10.1016/j.cub.2011.07.021

Huang, Y., Liu, A. A., Lafon, B., Friedman, D., Dayan, M., Wang, X., et al. (2017). Measurements and models of electric fields in the in vivo human brain during transcranial electric stimulation [published correction appears in Elife. 2018 Feb 15;7:]. *Elife* 6:e18834. doi: 10.7554/eLife.18834

Indahlastari, A., Albizu, A., O'Shea, A., Forbes, M. A., Nissim, N. R., Kraft, J. N., et al. (2020). Modeling transcranial electrical stimulation in the aging brain. *Brain Stimul.* 13, 664–674. doi: 10.1016/j.brs.2020.02.007

Koessler, L., Maillard, L., Benhadid, A., Vespignani, H., Braun, M., Felblinger, J., et al. (2009). Automated cortical projection of EEG sensors: anatomical

correlation via the international 10-10 system. *Neuroimage* 46, 64–72. doi: 10.1016/j.neuroimage.2009.02.006

Liu, K. Y., Reeves, S., McAleese, K. E., Attems, J., Francis, P., Thomas, A., et al. (2020). Neuropsychiatric symptoms in limbic-predominant age-related TDP-43 encephalopathy and Alzheimer's disease. *Brain* 143, 3842–3849. doi: 10.1093/brain/awaa315

López-Alonso, V., Cheeran, B., Río-Rodríguez, D., and Fernández-Del-Olmo, M. (2014). Inter-individual variability in response to non-invasive brain stimulation paradigms. *Brain Stimul.* 7, 372–380. doi: 10.1016/j.brs.2014.02.004

Meinzer, M., Lindenberg, R., Antonenko, D., Flaisch, T., and Flöel, A. (2013). Anodal transcranial direct current stimulation temporarily reverses age-associated cognitive decline and functional brain activity changes. *J. Neurosci.* 33, 12470–12478. doi: 10.1523/JNEUROSCI.5743-12.2013

Miniussi, C., Harris, J. A., and Ruzzoli, M. (2013). Modelling non-invasive brain stimulation in cognitive neuroscience. *Neurosci. Biobehav. Rev.* 37, 1702–1712. doi: 10.1016/j.neubiorev.2013.06.014

Miranda, P. C., Mekonnen, A., Salvador, R., and Ruffini, G. (2013). The electric field in the cortex during transcranial current stimulation. *Neuroimage* 70, 48–58. doi: 10.1016/j.neuroimage.2012.12.034

Morgane, P. J., Galler, J. R., and Mokler, D. J. (2005). A review of systems and networks of the limbic forebrain/limbic midbrain. *Prog. Neurobiol.* 75, 143–160. doi: 10.1016/j.pneurobio.2005.01.001

Nashiro, K., Sakaki, M., Braskie, M. N., and Mather, M. (2017). Resting-state networks associated with cognitive processing show more age-related decline than those associated with emotional processing. *Neurobiol. Aging* 54, 152–162. doi: 10.1016/j.neurobiolaging.2017.03.003

Nichols, T. E., and Holmes, A. P. (2002). Nonparametric permutation tests for functional neuroimaging: a primer with examples. *Hum. Brain Mapp.* 15, 1–25. doi: 10.1002/hbm.1058

Nielsen, J. D., Madsen, K. H., Puonti, O., Siebner, H. R., Bauer, C., Madsen, C. G., et al. (2018). Automatic skull segmentation from MR images for realistic volume conductor models of the head: assessment of the state-of-the-art. *Neuroimage* 174, 587–598. doi: 10.1016/j.neuroimage.2018.03.001

Nilakantan, A. S., Mesulam, M. M., Weintraub, S., Karp, E. L., VanHaerents, S., and Voss, J. L. (2019). Network-targeted stimulation engages neurobehavioral hallmarks of age-related memory decline. *Neurology* 92, e2349–e2354. doi: 10.1212/WNL.0000000000007502

Nitsche, M. A., Cohen, L. G., Wassermann, E. M., Priori, A., Lang, N., Antal, A., et al. (2008). Transcranial direct current stimulation: state of the art 2008. *Brain Stimul.* 1, 206–223. doi: 10.1016/j.brs.2008.06.004

Nitsche, M. A., and Paulus, W. (2000). Excitability changes induced in the human motor cortex by weak transcranial direct current stimulation. *J. Physiol.* 527 (Pt 3), 633–639. doi: 10.1111/j.1469-7793.2000.t01-1-00633.x

Park, J., Carp, J., Kennedy, K. M., Rodrigue, K. M., Bischof, G. N., Huang, C. M., et al. (2012). Neural broadening or neural attenuation? Investigating age-related dedifferentiation in the face network in a large lifespan sample. *J. Neurosci.* 32, 2154–2158. doi: 10.1523/JNEUROSCI.4494-11.2012

Peña-Gómez, C., Vidal-Piñeiro, D., Clemente, I. C., Pascual-Leone, Á, and Bartrés-Faz, D. (2011). Down-regulation of negative emotional processing by transcranial direct current stimulation: effects of personality characteristics. *PLoS One* 6:e22812. doi: 10.1371/journal.pone.0022812

Perceval, G., Flöel, A., and Meinzer, M. (2016). Can transcranial direct current stimulation counteract age-associated functional impairment? *Neurosci. Biobehav. Rev.* 65, 157–172. doi: 10.1016/j.neubiorev.2016.03.028

Petersen, R. C., and Morris, J. C. (2005). Mild cognitive impairment as a clinical entity and treatment target. *Arch. Neurol.* 62, 1160–1167. doi: 10.1001/archneur.62.7.1160

Petersen, S. E., and Sporns, O. (2015). Brain networks and cognitive architectures. *Neuron* 88, 207–219. doi: 10.1016/j.neuron.2015.09.027

Polanía, R., Nitsche, M. A., and Ruff, C. C. (2018). Studying and modifying brain function with non-invasive brain stimulation. *Nat. Neurosci.* 21, 174–187. doi: 10.1038/s41593-017-0054-4

Power, J. D., Barnes, K. A., Snyder, A. Z., Schlaggar, B. L., and Petersen, S. E. (2012). Spurious but systematic correlations in functional connectivity MRI networks arise from subject motion [published correction appears in Neuroimage. 2012 Nov 1;63(2):999]. *Neuroimage* 59, 2142–2154. doi: 10.1016/j.neuroimage.2011.10.018

Power, J. D., Schlaggar, B. L., and Petersen, S. E. (2015). Recent progress and outstanding issues in motion correction in resting state fMRI. *Neuroimage* 105, 536–551. doi: 10.1016/j.neuroimage.2014.10.044

Razali, N. M., and Wah, Y. B. (2011). Power comparisons of shapiro-wilk, kolmogorov-smirnov, lilliefors and anderson-darling tests. *J. Stat. Model. Anal.* 2, 21–33.

Rossi, S., Antal, A., Bestmann, S., Bikson, M., Brewer, C., Brockmöller, J., et al. (2021). Safety and recommendations for TMS use in healthy subjects and patient populations, with updates on training, ethical and regulatory issues: expert guidelines. *Clin. Neurophysiol.* 132, 269–306. doi: 10.1016/j.clinph.2020.10.003

Rossi, S., Hallett, M., Rossini, P. M., Pascual-Leone, A., and Safety of Tms Consensus Group (2009). Safety, ethical considerations, and application guidelines for the use of transcranial magnetic stimulation in clinical practice and research. *Clin. Neurophysiol.* 120, 2008–2039. doi: 10.1016/j.clinph.2009.08.016

Ruffini, G., Fox, M. D., Ripolles, O., Miranda, P. C., and Pascual-Leone, A. (2014). Optimization of multifocal transcranial current stimulation for weighted cortical pattern targeting from realistic modeling of electric fields. *Neuroimage* 89, 216–225. doi: 10.1016/j.neuroimage.2013.12.002

Sala-Llonch, R., Bartrés-Faz, D., and Junqué, C. (2015). Reorganization of brain networks in aging: a review of functional connectivity studies. *Front. Psychol.* 6:663. doi: 10.3389/fpsyg.2015.00663

Sala-Llonch, R., Junqué, C., Arenaza-Urquijo, E. M., Vidal-Piñeiro, D., Valls-Pedret, C., Palacios, E. M., et al. (2014). Changes in whole-brain functional networks and memory performance in aging. *Neurobiol. Aging.* 35, 2193–2202. doi: 10.1016/j.neurobiolaging.2014.04.007

Saturnino, G. B., Antunes, A., and Thielscher, A. (2015). On the importance of electrode parameters for shaping electric field patterns generated by tDCS. *Neuroimage* 120, 25–35. doi: 10.1016/j.neuroimage.2015.06.067

Saturnino, G. B., Thielscher, A., Madsen, K. H., Knösche, T. R., and Weise, K. (2019). A principled approach to conductivity uncertainty analysis in electric field calculations. *Neuroimage* 188, 821–834. doi: 10.1016/j.neuroimage.2018.12.053

Shapiro, S. S., and Wilk, M. B. (1965). An Analysis of variance test for normality (complete samples). *Biometrika* 52, 591–611. doi: 10.2307/2333709

Smith, S. M., Fox, P. T., Miller, K. L., Fox, P. M., Mackay, C. E., Filippini, N., et al. (2009). Correspondence of the brain's functional architecture during activation and rest. *Proc. Natl. Acad. Sci. U.S.A.* 106, 13040–13045. doi: 10.1073/pnas.0905267106

Spreng, R. N., Stevens, W. D., Viviano, J. D., and Schacter, D. L. (2016). Attenuated anticorrelation between the default and dorsal attention networks with aging: evidence from task and rest. *Neurobiol. Aging.* 45, 149–160. doi: 10.1016/j.neurobiolaging.2016.05.020

Tatti, E., Rossi, S., Innocenti, I., Rossi, A., and Santarnecchi, E. (2016). Non-invasive brain stimulation of the aging brain: state of the art and future perspectives. *Ageing Res. Rev.* 29, 66–89. doi: 10.1016/j.arr.2016.05.006

Theiler, J., Eubank, S., Longtin, A., Galdrikian, B., and Doyne Farmer, J. (1992). Testing for nonlinearity in time series: the method of surrogate data. *Physica D* 58, 77–94. doi: 10.1016/0167-2789(92)90102-S

Thielscher, A., Antunes, A., and Saturnino, G. B. (2015). Field modeling for transcranial magnetic stimulation: a useful tool to understand the physiological effects of TMS? *Annu. Int. Conf. IEEE Eng. Med. Biol. Soc.* 2015, 222–225. doi: 10.1109/EMBC.2015.7318340

Thielscher, A., Opitz, A., and Windhoff, M. (2011). Impact of the gyral geometry on the electric field induced by transcranial magnetic stimulation. *Neuroimage* 54, 234–243. doi: 10.1016/j.neuroimage.2010.07.061

Tomasi, D., and Volkow, N. D. (2012). Aging and functional brain networks. *Mol. Psychiatry* 17, 471–558. doi: 10.1038/mp.2011.81

van den Heuvel, M. P., and Sporns, O. (2013). An anatomical substrate for integration among functional networks in human cortex. *J. Neurosci.* 33, 14489–14500. doi: 10.1523/JNEUROSCI.2128-13.2013

Van Dijk, K. R., Sabuncu, M. R., and Buckner, R. L. (2012). The influence of head motion on intrinsic functional connectivity MRI. *Neuroimage* 59, 431–438. doi: 10.1016/j.neuroimage.2011.07.044

Vaqué-Alcázar, L., Sala-Llonch, R., Abellaneda-Pérez, K., Coll-Padrós, N., Valls-Pedret, C., Bargalló, N., et al. (2020). Functional and structural correlates

of working memory performance and stability in healthy older adults. *Brain Struct. Funct.* 225, 375–386. doi: 10.1007/s00429-019-02009-1

Vaqué-Alcázar, L., Sala-Llonch, R., Valls-Pedret, C., Vidal-Piñeiro, D., Fernández-Cabello, S., Bargalló, N., et al. (2017). Differential age-related gray and white matter impact mediates educational influence on elders' cognition. *Brain Imaging Behav.* 11, 318–332. doi: 10.1007/s11682-016-9584-8

Vidal-Piñeiro, D., Valls-Pedret, C., Fernández-Cabello, S., Arenaza-Urquijo, E. M., Sala-Llonch, R., Solana, E., et al. (2014). Decreased default mode network connectivity correlates with age-associated structural and cognitive changes. *Front. Aging Neurosci.* 6:256. doi: 10.3389/fnagi.2014.00256

Whitfield-Gabrieli, S., and Nieto-Castanon, A. (2012). Conn: a functional connectivity toolbox for correlated and anticorrelated brain networks. *Brain Connect.* 2, 125–141. doi: 10.1089/brain.2012.0073

Wiethoff, S., Hamada, M., and Rothwell, J. C. (2014). Variability in response to transcranial direct current stimulation of the motor cortex. *Brain Stimul.* 7, 468–475. doi: 10.1016/j.brs.2014.02.003

Windhoff, M., Opitz, A., and Thielscher, A. (2013). Electric field calculations in brain stimulation based on finite elements: an optimized processing pipeline for the generation and usage of accurate individual head models. *Hum. Brain Mapp.* 34, 923–935. doi: 10.1002/hbm.21479

Conflict of Interest: RS and GR works for Neuroelectrics. MN serves on the scientific advisory board for Neuroelectrics and NeuroDevice. AP-L serves on the scientific advisory boards for Starlab Neuroscience, Neuroelectrics, Axilum Robotics, Constant Therapy, NovaVision, Cognito, Magstim, Nexstim and Neosync, and is listed as an inventor on several issued and pending patents on the real-time integration of transcranial magnetic stimulation with electroencephalography and magnetic resonance imaging.

The remaining authors declare that the research was conducted in the absence of any commercial or financial relationships that could be construed as a potential conflict of interest.

Publisher's Note: All claims expressed in this article are solely those of the authors and do not necessarily represent those of their affiliated organizations, or those of the publisher, the editors and the reviewers. Any product that may be evaluated in this article, or claim that may be made by its manufacturer, is not guaranteed or endorsed by the publisher.

frontiers in Aging Neuroscience

STUDY PROTOCOL
published: 02 December 2021
doi: 10.3389/fnagi.2021.758765

Repetitive Transcranial Magnetic Stimulation for Alzheimer's Disease Based on Apolipoprotein E Genotyping: Protocol for a Randomized Controlled Study

Naili Wei and Jian Chen**

Department of Neurosurgery, The First Affiliated Hospital of Shantou University Medical College, Shantou, China

To date, there is a shortage of effective treatment strategies for Alzheimer's disease (AD), and although repetitive transcranial magnetic stimulation (rTMS) can improve AD cognitive function, there are obvious individual differences, which may be related to different apolipoprotein E (APOE) genotypes. As the risk and pathogenesis of AD varies greatly among different genotypes precise treatment strategies should be implemented depending upon genotype, which has not been proved by clinical studies. Apart from that, the published clinical studies are highly heterogeneous, and therefore, systematic and well-developed randomized controlled Trails (RCT) and demonstration of precise administration protocols are required. To verify this hypothesis, this project designed a RCT study, and randomly divided apoE4 carrier AD and non-carrier AD into high-frequency rTMS (HF-rTMS) or low-frequency rTMS (LF-rTMS) treatment groups. Specifically, 80 patients with AD, namely 48 APOE4 carriers and 32 non-APOE4 carriers will be included in the study. After that, based on different stimulation frequencies of rTMS, they will be divided into the HF-rTMS group and the LF-rTMS group, when patients with AD will be randomly assigned to different treatment groups. After AD patients are involved in the study, their memory, cognition, anxiety, depression and activities of daily living will be tested before and during 2 weeks of rTMS. Furthermore, peripheral blood will be collected before and after treatment to detect changes in pathological indexes via MSD platform (Meso Scale Discovery), while 32-channel EEG data will be also collected to detect and analyze changes in gamma oscillation. In addition, these patients will be followed up for 6 months and their neuropsychological scale was also evaluated every month. At present, our study has included 18 AD patients (10 APOE4 carriers; 8 non-carriers). Our study is still in progress. The grouping has not been unblinded. But the preliminary data demonstrated that non-carriers had better MoCA score improvement than APOE4 carriers. The results indicated that the two populations of AD patients should be treated differently. Thus, this project will provide direction for precision rTMS in AD and also promotes a shift in relevant treatment philosophy.

Clinical Trial Registration: [www.ClinicalTrials.gov], identifier [ChiCTR2100041625].

Keywords: repetitive transcranial magnetic stimulation (rTMS), Alzheimer's disease (AD), APOE genotype, APOE4 carriers, randomized controlled Trail (RCT), preresults

OPEN ACCESS

Edited by:
Yi Guo,
Jinan University, China

Reviewed by:
Yang Bai,
Hangzhou Normal University, China
Hyeon Min Ahn,
Brigham and Women's Hospital and Harvard Medical School, United States

****Correspondence:***
Naili Wei
nlwei@stu.edu.cn
Jian Chen
drchen@stu.edu.cn

Received: *15 August 2021*
Accepted: *03 November 2021*
Published: *02 December 2021*

Citation:
Wei N and Chen J (2021) Repetitive Transcranial Magnetic Stimulation for Alzheimer's Disease Based on Apolipoprotein E Genotyping: Protocol for a Randomized Controlled Study. Front. Aging Neurosci. 13:758765. doi: 10.3389/fnagi.2021.758765

INTRODUCTION

Alzheimer's disease (AD) is a neurodegenerative disease characterized by memory loss and cognitive dysfunction, with a very high prevalence in the middle-aged and elderly population. In this context, hundreds of billions of dollars have been invested in related research and development worldwide, but unfortunately, there are still no drugs with proven efficacy. Moreover, patients may wander and lose their ability to live in the late stages, which is a heavy burden for society and families (Zhou et al., 2019). Therefore, investigating new treatments is urgently needed.

Repetitive transcranial magnetic stimulation (rTMS) is a safe, non-invasive, and inexpensive neuromodulation that can affect the synaptic plasticity of neurons and enhance brain function by adjusting parameters such as stimulation frequency and stimulation intensity (Bestmann, 2008). In recent years, some researchers have tried to adopt rTMS to treat Alzheimer's disease and found that it has a better therapeutic effect (Dong et al., 2018; Chou et al., 2020). The current clinical treatment of Alzheimer's disease with medications has unsatisfactory therapeutic effect. Zhang et al. (2020) reported a meta-analysis of pharmacological treatments showing that improvement of Mini-mental State Examination (MMSE) score standard mean difference (SMD) ranges from −0.29 to 0.49; Lu et al. (2020) also reported another analysis of anti- Aβ agents for mild to moderate Alzheimer's disease suggesting no effect of anti- Aβ drugs vs. the placebo group (SMD of MMSE score improvement: −0.29, 95% CI −0.76–0.17; SMD of ADAScog score improvement: MD: 0.20, 95% CI: −0.40–0.81). In contrast, Chu et al. (2021) reported a promising result. The patients who received high-frequency TMS treatment had a significant improvement in MMSE score (1.65, 0.77–2.54) when compared with sham TMS. In addition, Dong et al. (2018) report also supported the viewpoint that high-frequency rTMS led to a significant improvement in cognition as measured by ADAS-cog (MD = −3.65, 95% CI −5.82 to −1.48). Although the results derived from different study samples, their subjects were AD patients. Although there are no studies designed to compare the differences in therapeutic effects between drugs and rTMS, these data point to the possibility that rTMS is superior to drug therapy of AD patients.

Unfortunately, the results of the published clinical studies on transcranial magnetic stimulation greatly differ, with different parameters and stimulation targets being used, and a wide variation in stimulation patterns (Dong et al., 2018; Chou et al., 2020). Specifically, there are obvious individual differences in patient response to transcranial magnetic stimulation (Dong et al., 2018; Chou et al., 2020). Therefore, the precise implementation of transcranial magnetic stimulation therapy is crucial.

How to precisely direct the rTMS strategy is remains unsolved. However, recent studies indicate that APOE gene-typing is a possible candidate. The apolipoprotein gene (APOE) that can be classified into E2, E3, and E4 subtypes based on the differences in the bases encoding the rs429358 and rs7412 loci but falls into six genotypes according to the double allele typing. The different genotypes play different roles in the pathogenesis of Alzheimer's disease. The APOE ε2 allele proven to be the strongest genetic protective factor but the APOE ε4 allele was the strongest genetic risk factor for Alzheimer's disease after multiple large scale genome-wide studies (Serrano-Pozo et al., 2021). Several researchers have called for the study and treatment of carriers and non-carriers as different phenotypic groups (Yamazaki et al., 2019; Serrano-Pozo et al., 2021). In addition, the other researchers found that APOE ε4 allele carriers had a different outcome of physical exercise treatment (Cancela-Carral et al., 2021). Therefore, we speculate that different APOE ε4 allele carriers have different outcomes of rTMS.

Its potential mechanism may be related to impairment of the function of GABAergic interneurons (Knoferle et al., 2014; Lenz et al., 2016; Wang et al., 2018). Many studies have suggested that the APOE4 allele can reduce the number and impair the function of GABA interneurons in the brain and increased cortical excitability (Knoferle et al., 2014; Lenz et al., 2016; Wang et al., 2018). This feature can also be confirmed by EEG results. High-frequency gamma oscillations are generally encoded by GABA interneurons in the brain (Traub et al., 2003; Colgin et al., 2009; Buzsaki and Wang, 2012; Gillespie et al., 2016). Inhibition of this neuronal activity can lead to a reduction in gamma oscillations, and the reduction of gamma oscillations in the brain of APOE4 carriers (Traub et al., 2003; Colgin et al., 2009; Buzsaki and Wang, 2012; Gillespie et al., 2016) is closely related to the symptoms of AD (Zhao et al., 2018; Etter et al., 2019; Najm et al., 2019). Transcranial magnetic stimulation can improve gamma oscillation power and amplitude, and improve cognitive function (Barr et al., 2009). These results suggest that the damage to gamma oscillation activities caused by the APOE4 allele may affect the treatment results. In summary, it is clear that the APOE genotype determines the number and function of GABAergic neurons in AD patients, and therefore may be related to the heterogeneity of transcranial magnetic stimulation effects. Considering this background, transcranial magnetic stimulation treatment protocols being implemented should vary with APOE genotypes.

Previous studies have tested the effect of both high-frequency rTMS (HF-rTMS) and low-frequency rTMS (LF-rTMS). Interestingly, it was found that both HF-rTMS of the left dorsolateral prefrontal cortex (L-DLPFC) and LF-rTMS of right dorsolateral prefrontal cortex (R-DLPFC) exhibited significant therapeutic efficacy (Chou et al., 2020). Additionally, Ahmed et al. (2012) reported that LF-rTMS of L-DLPFC also showed significant therapeutic efficacy for mild to moderate dementia. But there are no uniform guidelines or standards to guide the choice of treatment protocol. In terms of experience, most doctors will choose high frequency as the treatment scheme. The present study will adopt the left dorsolateral prefrontal cortex (L-DLPFC) as the intervention target.

We believe that different APOE4 carriers should be given different treatment schemes than non-APOE4 carriers because of the excitability of their neural networks is different. The APOE4 carriers have increased network excitability due to the impairment of GABAergic interneuron function (Najm et al., 2019). Compared with the APOE ε3 allele, APOE ε4 allele increases Ca^{2+} excitability due to lysosome dysregulation

and impaired modulation of Ca^{2+} responses upon changes in extracellular lipids (Larramona-Arcas et al., 2020). Traditional theory suggests that high-frequency rTMS increases cortical excitability by inducing long-duration enhancement potentials, while low-frequency rTMS decreases cortical excitability by inducing long-duration inhibition potentials (Pell et al., 2011). GABAergic neuronal receptor activity is mainly associated with chloride channel opening (Traub et al., 2003), and high-frequency stimulation is more likely to induce long-term potentiation (LTP) (Pell et al., 2011). Hence, high-frequency treatment contributes to more gamma oscillatory activity and better therapeutic effects. However, for APOE4 carriers with more significant loss of GABAergic neurons (Knoferle et al., 2014; Najm et al., 2019), HF treatment may be less effective. In this case, low-frequency therapy may be more suitable for that kind of patients. Therefore, in this study, it is believed that different transcranial magnetic stimulation regimens should be selected for AD patients based on APOE genotypes, so as to obtain precise treatment strategies.

In summary, this paper aims to study the difference in the efficacy of different rTMS strategies in AD patients with different APOE genotypes, and analyze the changes of gamma oscillations.

OBJECTIVES

The primary objective of the study is to analyze the different efficacies of rTMS in AD patients with different APOE genotypes, so as to provide the basis for the precise treatment of AD.

The secondary objective is to analyze the changes in gamma oscillations and pathological indicators in different APOE genotypes, thus being conducive to the precise treatment of AD.

METHODS

The Recruitment and Inclusion of Alzheimer's Disease Patients

The patients are recruited in two main ways: (1) Online recruitment: our recruitment program was announced on our hospital's official website in February this year[1]. Then, all eligible Alzheimer's disease patients could apply for rTMS treatment by filling in the online form.

(2) Hospital system: The hospital information retrieval system are also adopted to obtain information about patients with cognitive impairment and call to ask if they would like to participate in the recruitment program. Then, those who are interested in the program will enter into our patient recruitment diagnostic process.

These candidates applying for rTMS treatment will undergo neuropsychological assessments in the outpatient clinic of our hospital. Then, those with cognitive impairment are recommended for MRI scanning so as to assess the extent of hippocampal atrophy, while those with an MTA score ≥ 2 are the potential AD patients, which are diagnosed by the neuroimaging specialist (**Figure 1**). In addition to that, the data of these patients will be further evaluated by two neurologists. Furthermore, the eligible applicants for a clinical diagnosis of Alzheimer's disease should meet our inclusion criteria and exclusion criteria. Beyond that, they should sign a subject informed consent form with our research team. Here, it should be mentioned that before rTMS treatment, patient blood samples were collected for APOE genotyping (**Table 1**).

The inclusion and exclusion criteria are as follows:

Inclusion criteria

(1) The age ranges from 50 to 85 years old.
(2) Subjective perception of memory loss more than 1 year; MMSE $\leq$ 26 (level of education more than 7 years: MMSE $\leq$ 26; level of education 1–7years: MMSE $\leq$ 24; level of education less than 1 year: MMSE $\leq$ 19).
(3) MRI exhibits medial temporal atrophy (hippocampus, entorhinal cortex, amygdala); MTA visual evaluation scale $\geq$ 2.

Exclusion criteria

(1) There was a history of severe brain lesions or brain surgery, such as brain tumor, hydrocephalus and intracranial hematoma.
(2) The patients have received TMS treatment, transcortical electrical stimulation, deep brain electrical stimulation, or vagus nerve electrical stimulation prior to application.
(3) There are serious complications, such as frequent seizures, brain tumor surgery, intracranial infection, serious heart disease, lung disease, mania, and severe mental disorders.
(4) The patient had an implanted pacemaker, defibrillator, cochlear implant, other nerve stimulator, or steel plate, and could not accept TMS therapy or MRI scanning.
(5) The patient suffers frontotemporal dementia, vascular dementia, Lewy body dementia, or other diseases.
(6) White matter lesions with a Fazekas score $>$ 3 and cerebral infarction in medial temporal lobes were excluded.
(7) Others referred to the NINCDS-ADRDA exclusion criteria (revised—2007) (Dubois et al., 2007).

Exit criteria

(1) Subjects voluntarily withdraw from the study for personal reasons.
(2) Subjects are unable to continue to participate in the study due to a serious medical condition, such as a cardiovascular accident, or those that would have a significant impact on the study results.
(3) Subjects developed serious treatment-related complications, are unable to tolerate the treatment dose or could not complete the associated assay.

Apolipoprotein E Genotyping

DNA was extracted from the patients' peripheral blood. Then, genotyping was performed by snapshot SNP typing. In addition, APOE alleles and genotypes were determined by sequencing rs429358 and rs7412 at exon 4 of the APOE gene. Furthermore,

[1]http://www.stuh.com.cn/index.php/home/view?id=6175

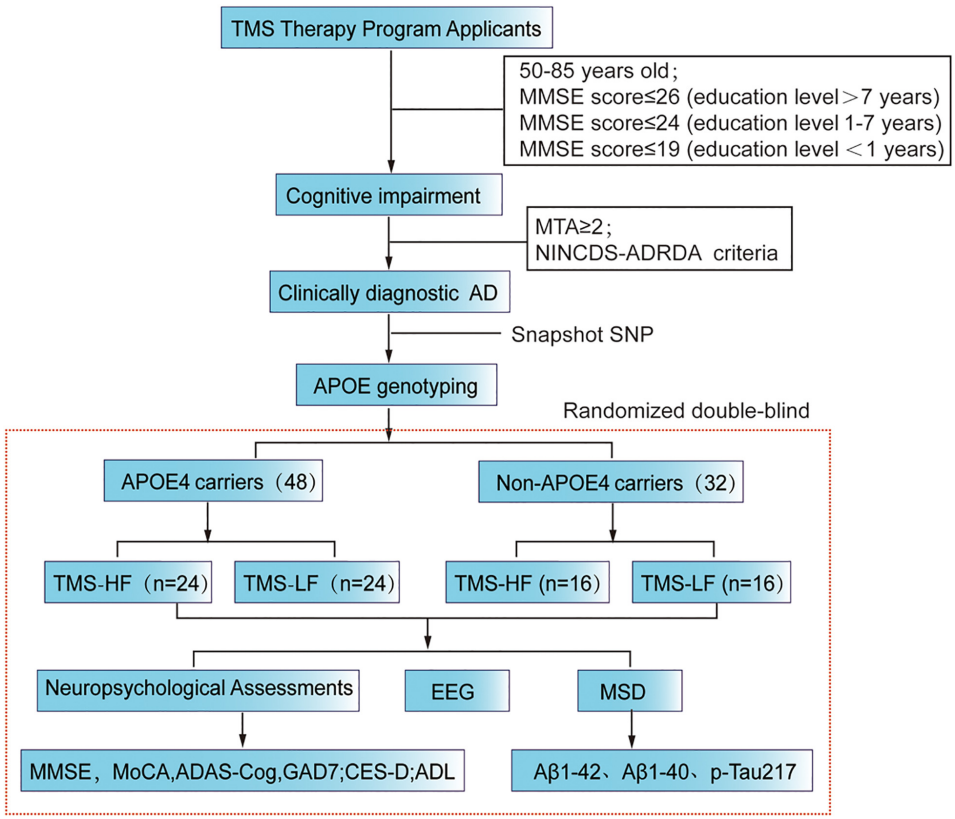

FIGURE 1 | Flow chart of the present RCT study. MMSE, Mini Mental State Examination; rTMS, repetitive transcranial magnetic stimulation; MoCA, Montreal Cognitive Assessment Scale; ADAScog, Assessment Scale-cognitive subscale; Center for Epidemiologic Studies Depression Scale (CES-D); Activity of Daily Living (ADL); MSD, Meso Scale Discovery.

TABLE 1 | APOE genotyping is determined by promoter polymorphisms of two single nucleotides (rs429358 and rs rs7412).

APOE genotypes	S1:rs429358	S2:rs7412
E2/E2	T/T	T/T
E3/E3	T/T	C/C
E4/E4	C/C	C/C
E2/E3	T/T	T/C
E2/E4	T/C	T/C
E3/E4	T/C	C/C

T or C represents the first DNA base of the nucleotides.

APOE status was defined by the possessing one or more copies of E2, E3 and E4, whereas APOE ε4 positive status was confirmed as the ε4/ε4; ε3/ε4 or ε2/ε4 (Risacher et al., 2015). In the experimental steps, 2 ml anticoagulant peripheral venous blood was taken to extract leukocytes, genomic DNA was extracted from blood samples by silicon matrix adsorption column method for PCR amplification of target genes, and then the PCR products were purified. After snapshot extension reaction, sequencing and analysis were carried out. The primer sequences used for genotyping were:rs429358-F: AATC GGAACTGGAGGAACAAC; rs429358-R: GATGGCGCTGAG GCCGCGCTC; rs7412-F: AATCGGAACTGGAGGAACAAC; rs7412-R: GATGGCGCTGAGGCCGCGCTC.

Randomization and Allocation

Stratified Randomized Groups

In this study, 48 APOE4 carrier AD patients (APOE4-AD) and 32 non-APOE4 carrier AD patients (Non-APOE4-AD) will be recruited. Then, they will be assigned to the HF-rTMS group and the LF-rTMS group based on the stratified randomization method: 40 for the HF-rTMS group and 40 for the LF-rTMS group, while in subgroups, 24 patients will be assigned to in the APOE4-HF group, 24 patients will be assigned to the APOE4-LF group, 16 patients will be assigned to non-APOE4-HF group, and 16 will be assigned to the non-APOE4-LF group. The specific process is as follows: Our team members consist of quality control personnel, TMS therapy physicians, neuropsychological assessors and laboratory staff. Specifically, quality control personnel are responsible for quality control of study data and grouping randomization; TMS therapy physicians perform TMS treatment based on information from quality control personnel; neuropsychological assessors conduct neuropsychological assessments before, during and after treatment and follow-up; laboratory staff are in charge of blood sample processing and testing. In addition, the grouping

randomization information will not be released by quality control personnel until the primary endpoint of the study has been met for all program participants at follow-up (**Table 1**).

The postadmission randomization process are performed by the quality control staff. Specifically, the admission sequence of APOE4 carriers and non-carriers was 1–48 and 1–32, respectively, and the admission numbers of carriers and non-carriers were randomized using Excel sheet randomization to assign them within the HF-rTMS and LF-rTMS groups, respectively. When the follow-up of all subjects reached the clinical trial endpoint, the project quality control staff and the project leader verified the grouping information for unblinding and summarized the project data for statistical analysis.

Repetitive Transcranial Magnetic Stimulation Therapy

HF-rTMS group: The rTMS therapy are performed by a transcranial magnetic stimulator (XY-K-JLC-D, Xiangyu Medical, China).

TMS Target: Left Dorsolateral Prefrontal Cortex (L-DLPFC)

The patients accepted 14 consecutive days of TMS therapy (twice a day), with each treatment lasting for 30 min (110% of motor threshold, 20 Hz, 1 s, 29 s interval, 1200 pulses per treatment, 33,600 total sessions).

LF-rTMS group: The rTMS therapy was performed by transcranial magnetic stimulator (XY-K-JLC-D, Xiangyu Medical, China).

TMS Target: Left Dorsolateral Prefrontal Cortex (L-DLPFC)

The patients accepted 14 consecutive days of TMS therapy (twice a day) with each treatment lasting for 30 min (110% of motor threshold, 1 Hz, he stimulation time 40 s, 20 s interval, 1200 pulses per treatment, 33,600 total sessions).

Localization of Transcranial Magnetic Stimulation Target

First, the skull surface position of the left precentral gyrus are located. Specifically, the midpoint of bilateral cerebral hemispheres will be confirmed by that of the patient's bilateral tragus above the skull. Then, the location of the superior sagittal sinus was identified by connecting the nasal root position, the midpoint of bilateral cerebral hemispheres and the external occipital protuberance. It should be mentioned that the midpoint of this line is that of the superior sagittal sinus, which corresponds to the location of the central sulcus. Then, the skull surface position of the hand representation area in the central anterior gyrus was measured by 5 cm left siding from this midpoint in a direction perpendicular to the sagittal line. Furthermore, the left dorsolateral prefrontal region, the target area for rTMS, was located at 20% of the sagittal sinus length from this point in parallel to the sagittal line in a forward translation.

Study Process

After AD patients are included in the study, their neuropsychological scales, including cognition, anxiety, depression, activities of daily living and other scales will be assessed. Then, they will be assigned to HF-rTMS or LF-rTMS group and accept due treatment for 2 weeks. During the treatment, the neuropsychological scales will be assessed every week. In addition, blood test results and 32-channel EEG data will be collected before and after treatment, while a 6-month follow-up will be carried out after treatment (**Figure 1**).

Neuropsychological Assessments

The Mini Mental State Examination (MMSE), Montreal Cognitive Assessment Scale (MoCA) and Alzheimer's Disease Rating Scale cognitive subscales (ADAS-cog) will be used to assess cognitive function, while the Generalized and Center for Epidemiologic Studies Depression Scale (CES-D) will be adopted to assess the mood of all the participants. In addition, daily activity is measured using the Activity of Daily Living (ADL) scale. All scales are tested with common forms and unified guidelines. The evaluators all have received standardized training and they will communicate with the subjects in local language.

EEG Acquisition and Calculation and Analysis of EEG Metrics

EEG data will be collected via a high-density 32-channel EGI system (g.tec) with a sampling rate of 500 Hz and a mastoidea reference. During the recording, patients are instructed to stay awake, relax, and close their eyes for 10 min. Then, a bandpass filter (from 0.5 to 200 Hz) and a notch filter at 50 Hz and 100 Hz were applied. In addition, EEG will be collected under the condition of eyes closed, followed by preprocessing via MATLAB software, such as baseline adjustment, filtering, depression filtering, and referring. Finally, the changes in EEG power and spectra in different frequency bands before and after treatment of different genotypes were analyzed and compared.

EEG metric data will be processed and analyzed by MATLAB 2017. Beyond that, power spectral density (PSD), median spectral frequency (MSF) and spectral entropy measure dynamics of brain signals at a single electrode site are based on spectral frequency content.

For the main analysis, 10 EEG metrics: PSD in delta (1–4 Hz), theta (4–8 Hz), alpha1 (8–10 Hz), alpha2 (10–13 Hz), beta 1(13–20 Hz), beta 1(20–30 Hz), gamma1 (30–48 Hz), and gamma1 (48–100Hz) will be calculated, and then averaged across all epochs (60 s recording).

Outcomes

The primary end point is the quantitative index, namely MMSE, whereas the secondary outcome measures are MoCA, ADAS-cog, GAD-7, CES-D, and ADL.

Sample Size Calculation

The sample size of this project was calculated by Pass software on the basis of previous literature. In this study, the MMSE scores of the HF-rTMS group and the LF-rTMS group were 10.4 ± 1.7

and 10.2 ± 1.8, respectively, before treatment. After 2 weeks of rTMS treatment, their MMSE scores reached 11.2 ± 1.9 and 8.8 ± 2.3, respectively (Ahmed et al., 2012), when the target effect size had 80% power (β = 0.10) and a type I error was 5% (α = 0.05). In addition, the group sample size of 13 and 12 achieved 81% power for detecting a difference of 2.4 between the null hypothesis and that the mean of both groups is 11.2 and the alternative hypothesis that the mean of Group 2 is 8.8 with known group standard deviations of 1.9 and 2.3 and a significance level (alpha) of 0.050 using a two-sided two-sample *t*-test, while the sample size of each subgroup is at least 13. Considering the loss of follow-up, falling off and sample data being eliminated due to data quality, the sample size should be increased by 20%. Thus, the final sample size of each subgroup are at least 16. Furthermore, the ratio of APOE4 carriers to non-APOE4 carriers are set to 3:2 according to the comparison of population samples and our previous study. Other than that, in this study, 80 participants, with 48 APOE4 carriers and 32 non-APOE4 carriers will be recruited.

Quality Control and Quality Assurance

Two neuroscientists, a neuroimaging specialist and an expert in geriatrics, worked together to examine the participants and provide a diagnosis for each participant. In addition, training was provided for all researchers, while all items involved in the test, such as blood samples, EEG data processing and neuropsychological assessments were monitored by the quality control committee who randomly selected data samples to send to a third party for retesting or re-evaluation. Data entry was performed by EpiData Entry software and was also monitored by the quality control committee who further randomly selected the input information and paper information. To control the impacts of clinical treatment, we strictly restricted medication. Oral medication before and during hospitalization as well as during follow-up remained unchanged except for sudden diseases, such as cardiovascular and cerebrovascular accidents and aggravation of primary diseases. If there are errors, the sampling proportion will be expanded, while if the input error proportion is high, a second person needs to check and correct the input data. Moreover, all data were monitored and reviewed by the principal investigator or research coordinators.

Biomarker Test of Blood Samples

Aβ1-42, Aβ1-40, p-tau217 and other indicators of the plasma were detected by liquid phase flow cytometry (using the MSD platform) before and after treatment to evaluate the outcome of pathological indicators. Specifically, blood samples were collected at 7:00 a.m. before and after treatment, and plasma samples were obtained after centrifugation for MSD detection.

Statistical Methods

Statistical Analysis Methods

(1) Descriptive analysis: the counting data was presented as the mean ± standard error; (2) the counting data was compared between groups by performing the continuous correction χ^2-test, when the theoretical frequency of more than 25% cells was less than 5. The Fisher exact probability method was adopted; the independent sample *t*-test was conducted for comparison between groups of normally distributed measures; repeated-measures ANOVA was employed to analyze repeated data between groups in different time. For non-normally distributed measures, the Wilcoxon rank sum (WRS) test was used for comparisons between groups.

Statistical Hypothesis

The primary endpoint of this study was the end of treatment and completion of the 3-month follow-up for all subjects, and its indicator was the MMSE score. Apart from that, the study hypothesis is to demonstrate the superiority of HF-rTMS over LF-rTMS in transcranial magnetic stimulation protocols for patients with Alzheimer's disease. In terms of subgroup analysis, the HF treatment group was preferentially compared with the low-frequency treatment group of non-APOE4 carriers; if the statistical result of *P*-value is less than 0.05, then the comparison between the HF treatment group and the low-frequency treatment group of APOE4 carriers is made in order. If the statistical result of *P*-value is less than 0.0125, then the comparison among the four subgroups is considered significant.

Ethics and Dissemination

This study protocol was been approved by the Clinical Research Ethics Committee of the First Affiliated Hospital of Shantou University Medical College (approval number: 2020-115-XZ2). Apart from that, our team will inform all participants individually of detailed information about our research, while informed consent will be obtained from all participants and/or their legal representatives. In addition, participants will be allowed to withdraw from the study any time, but the reason will be recorded. Furthermore, the results of the study will be reported in peer-reviewed journals and presented at national or international conferences on neuromodulation.

Results in Progress

Our study is still in progress. Our current data are the preliminary data of the RCT study, and the grouping has not been unblinded. We analyzed the demographic informatics of APOE4 carriers and

TABLE 2 | Characteristics of the study cohort.

	APOE4 carriers (*n* = 10)	Non-APOE4 carriers (*n* = 8)	*p*-value
Sex F/M	6/4	5/3	0.914
Age, years	70.3 ± 7.45	73.75 ± 6.27	0.312
Education level, years	7.7 ± 2.98	6.13 ± 5.37	0.44
MMSE score before rTMS	12.6 ± 6.77	15.88 ± 8.54	0.377
MoCA score before rTMS	7.9 ± 4.28	9.25 ± 5.50	0.566
ADAScog score before rTMS	39.13 ± 16.49	34.87 ± 19.03	0.618
MMSE score after rTMS	13.5 ± 6.22	16.63 ± 8.73	0.388
MoCA score after rTMS	8 ± 4.47	11.88 ± 7.72	0.202
ADAScog score after rTMS	37.16 ± 16.39	31.57 ± 21.21	0.536

n, number; F, female; M, male; MMSE, Mini Mental State Examination; rTMS, repetitive transcranial magnetic stimulation; MoCA, Montreal Cognitive Assessment Scale; ADAScog, Assessment Scale-cognitive subscale.

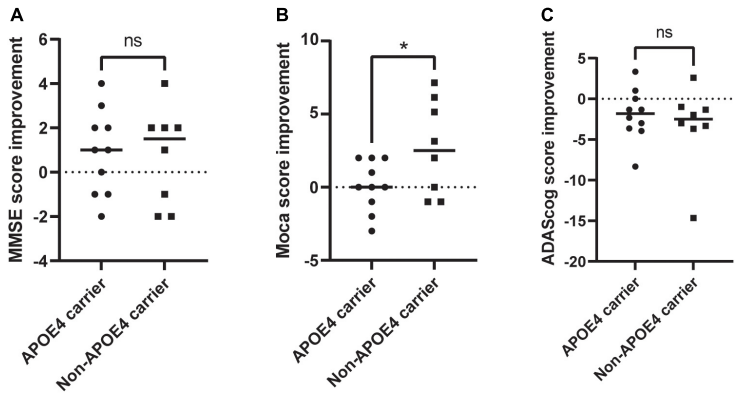

FIGURE 2 | Evaluation of the changes in neuropsychological scale of APOE4 carries and noncarriers pre-rTMS and post-rTMS. **(A)** MMSE improvement; **(B)** MoCA improvement; **(C)** ADAScog improvement. rTMS, repetitive transcranial magnetic stimulation; MoCA, Montreal Cognitive Assessment Scale; ADAScog, Assessment Scale-cognitive subscale. *Indicates of a *P*-value < 0.05.

non-carriers and the changes in cognitive function scores before and after 2 weeks of rTMS treatment. More detailed information was displayed in **Supplementary Table 1**.

To date, 18 patients with clinically diagnosed Alzheimer's disease have been included and have received rTMS treatment for 2 weeks. Among them, ten were APOE4 carriers; eight were non-carriers, and there were no significant differences in age, education or gender (**Table 2**). They were randomly assigned to the high-frequency treatment group or the low-frequency treatment group. Because the study was not blinded, we could not know which subgroup they were assigned to. We could only analyze the overall treatment effect. According to our preliminary results, there was no significant difference in MMSE score, MoCA score except ADAScog (**Supplementary Table 1**) score between the two groups before and after treatment. When comparing the improvement rate of the two groups, there was a significant difference in the improvement of MoCA score between the two groups. For non- carriers, the MoCA score but not the MMSE or ADAScog score improved by 2.65 ± 3.15, while for carriers, it improved by 0.1 ± 1.7 ($t = 2.164$, $p = 0.046$, **Figures 2A–C**).

DISCUSSION

Transcranial magnetic Stimulation (TMS) is a magnetic stimulation technique that uses a transient magnetic field to generate induced currents in the cerebral cortex, thus altering the membrane potential of cortical neurons (Bestmann, 2008). In addition, it is also a painless, non-invasive, safe and reliable tool for non-invasive physiotherapy and research on the central and peripheral nervous systems (Pell et al., 2011). Since the invention of transcranial magnetic stimulation by Anthony Barker from the University of Sheffield in 1985, this technique has been rapidly applied to neuroscience research and clinical practice (Pell et al., 2011). Specifically, in the past 20 years, the number of articles published on TMS has geometrically increased. At present, TMS has been widely used in neuroscience, neurology, psychiatry, rehabilitation medicine, medical psychology and other fields.

At present, there is no effective drug for Alzheimer's disease (Lu et al., 2020; Zhang et al., 2020). Doctors or researchers in many fields are trying variable treatment methods. Transcranial magnetic stimulation is a form of non-invasive nerve regulation, which has very good prospects in the treatment of AD (Dong et al., 2018; Chou et al., 2020; Chu et al., 2021). Several meta-analyses demonstrated the superiority of transcranial magnetic stimulation in the treatment of AD (Dong et al., 2018; Chou et al., 2020; Chu et al., 2021). However, at present, the number of RCTs remain relatively few. Different researchers in previous studies adopted different stimulation targets, intensities, and frequencies, resulting in great differences among these studies. At present, the rTMS protocol continues to rely on empirical selection, and there is no unified understanding of the reference basis. More importantly, according to many published research data, there are great individual differences among different patients in the same research project. This individualized difference also puts forward the demand for accurate rTMS schemes.

Our project hypothesis holds that the treatment scheme can be selected according to the APOE genotyping of Alzheimer's disease. Although our study has not been unblinding, the preliminary results showed the difference in the treatment effect between APOE4 carriers and non-carriers. Thus, it is very necessary to treat APOE4 carriers and non-carriers differently in the treatment scheme. Precise neuromodulation is also the future trend. Furthermore, the current research of our project team is to guide the precise treatment of Alzheimer's disease through different gene phenotypes, thus providing guidance for precise and non-invasive neural regulation of AD, and promoting the transformation of transcranial magnetic stimulation in AD treatment.

ETHICS STATEMENT

The studies involving human participants were reviewed and approved by the Clinical Research Ethics Committee of the First Affiliated Hospital of Shantou University Medical College (approval number: 2020-115-XZ2). The patients/participants

provided their written informed consent to participate in this study. Written informed consent was obtained from the individual(s) for the publication of any potentially identifiable images or data included in this article.

AUTHOR CONTRIBUTIONS

NW: conception, supervision, and design of this article. JC: manuscript editing and research fund. Both authors in the article have approved the submitted version.

FUNDING

This work was supported by grants from the National Natural Science Foundation of China (82001447), the China Postdoctoral Science Foundation (2020M682833), Dengfeng Project for the Construction of High-Level Hospitals in Guangdong Province, the First Affiliated Hospital of Shantou University Medical College Supporting Funding (202003-29), 2020 Li Ka Shing Foundation Cross-Disciplinary Research Grant (2020LKSFG11C), and the Beijing Tsinghua Changgung Hospital Fund (12015C1045).

ACKNOWLEDGMENTS

We thank to the authors who have contributed to the preliminary results of our research. Hui Pan: Grouping and statistical analysis. Xin Zeng: Patient admission treatment plan and supervision. Xinyuan Peng and Yizhi Zeng: rTMS protocol and supervision. Canghao Lu: Patient blood samples and APOE genotyping. Xiaofang Ying, Xinyi Cai, and Kaixun Lin: Neuropsychological Assessments.

SUPPLEMENTARY MATERIAL

The Supplementary Material for this article can be found online at: https://www.frontiersin.org/articles/10.3389/fnagi.2021.758765/full#supplementary-material

REFERENCES

Ahmed, M. A., Darwish, E. S., Khedr, E. M., El Serogy, Y. M., and Ali, A. M. (2012). Effects of low versus high frequencies of repetitive transcranial magnetic stimulation on cognitive function and cortical excitability in Alzheimer's dementia. *J. Neurol.* 259, 83–92. doi: 10.1007/s00415-011-6128-4

Barr, M. S., Farzan, F., Rusjan, P. M., Chen, R., Fitzgerald, P. B., and Daskalakis, Z. J. (2009). Potentiation of gamma oscillatory activity through repetitive transcranial magnetic stimulation of the dorsolateral prefrontal cortex. *Neuropsychopharmacology* 34, 2359–2367. doi: 10.1038/npp.2009.79

Bestmann, S. (2008). The physiological basis of transcranial magnetic stimulation. *Trends Cogn. Sci.* 12, 81–83. doi: 10.1016/j.tics.2007.12.002

Buzsaki, G., and Wang, X. J. (2012). Mechanisms of gamma oscillations. *Annu. Rev. Neurosci.* 35, 203–225. doi: 10.1146/annurev-neuro-062111-150444

Cancela-Carral, J. M., Lopez-Rodriguez, A., and Mollinedo-Cardalda, I. (2021). Effect of physical exercise on cognitive function in older adults' carriers versus noncarriers of apolipoprotein E4: systematic review and meta-analysis. *J. Exerc. Rehabil.* 17, 69–80. doi: 10.12965/jer.2142130.065

Chou, Y. H., Ton That, V., and Sundman, M. (2020). A systematic review and meta-analysis of rTMS effects on cognitive enhancement in mild cognitive impairment and Alzheimer's disease. *Neurobiol. Aging* 86, 1–10.

Chu, C. S., Li, C. T., Brunoni, A. R., Yang, F. C., Tseng, P. T., Tu, Y. K., et al. (2021). Cognitive effects and acceptability of non- invasive brain stimulation on Alzheimer's disease and mild cognitive impairment: a component network meta- analysis. *J. Neurol. Neurosurg. Psychiatry* 92, 195–203. doi: 10.1136/jnnp-2020-323870

Colgin, L. L., Denninger, T., Fyhn, M., Hafting, T., Bonnevie, T., Jensen, O., et al. (2009). Frequency of gamma oscillations routes flow of information in the hippocampus. *Nature* 462, 353–357. doi: 10.1038/nature08573

Dong, X., Yan, L., Huang, L., Guan, X., Dong, C., Tao, H., et al. (2018). Repetitive transcranial magnetic stimulation for the treatment of Alzheimer's disease: a systematic review and meta-analysis of randomized controlled trials. *PLoS One* 13:e0205704. doi: 10.1371/journal.pone.0205704

Dubois, B., Feldman, H. H., Jacova, C., DeKosky, S. T., Barberger-Gateau, P., Cummings, J., et al. (2007). Research criteria for the diagnosis of Alzheimer's disease: revising the NINCDS–ADRDA criteria. *Lancet Neurol.* 6, 734–746. doi: 10.1016/S1474-4422(07)70178-3

Etter, G., van der Veldt, S., Manseau, F., Zarrinkoub, I., Trillaud-Doppia, E., and Williams, S. (2019). Optogenetic gamma stimulation rescues memory impairments in an Alzheimer's disease mouse model. *Nat. Commun.* 10:5322. doi: 10.1038/s41467-019-13260-9

Gillespie, A. K., Jones, E. A., Lin, Y. H., Karlsson, M. P., Kay, K., Yoon, S. Y., et al. (2016). Apolipoprotein E4 causes age-dependent disruption of slow gamma oscillations during hippocampal sharp-wave ripples. *Neuron* 90, 740–751. doi: 10.1016/j.neuron.2016.04.009

Knoferle, J., Yoon, S. Y., Walker, D., Leung, L., Gillespie, A. K., Tong, L. M., et al. (2014). Apolipoprotein E4 produced in GABAergic interneurons causes learning and memory deficits in mice. *J. Neurosci.* 34, 14069–14078. doi: 10.1523/JNEUROSCI.2281-14.2014

Larramona-Arcas, R., Gonzalez-Arias, C., Perea, G., Gutierrez, A., Vitorica, J., Garcia-Barrera, T., et al. (2020). Sex-dependent calcium hyperactivity due to lysosomal-related dysfunction in astrocytes from APOE4 versus APOE3 gene targeted replacement mice. *Mol. Neurodegener.* 15:35. doi: 10.1186/s13024-020-00382-8

Lenz, M., Galanis, C., Müller-Dahlhaus, F., Opitz, A., Wierenga, C. J., Szabó, G., et al. (2016). Repetitive magnetic stimulation induces plasticity of inhibitory synapses. *Nat. Commun.* 7:10020. doi: 10.1038/ncomms10020

Lu, L., Zheng, X., Wang, S., Tang, C., Zhang, Y., Yao, G., et al. (2020). Anti- Aβ agents for mild to moderate Alzheimer's disease: systematic review and meta-analysis. *J. Neurol. Neurosurg. Psychiatry* 91, 1316–1324. doi: 10.1136/jnnp-2020-323497

Najm, R., Jones, E. A., and Huang, Y. (2019). Apolipoprotein E4, inhibitory network dysfunction, and Alzheimer's disease. *Mol. Neurodegener.* 14:24. doi: 10.1186/s13024-019-0324-6

Pell, G. S., Roth, Y., and Zangen, A. (2011). Modulation of cortical excitability induced by repetitive transcranial magnetic stimulation: influence of timing and geometrical parameters and underlying mechanisms. *Prog. Neurobiol.* 93, 59–98. doi: 10.1016/j.pneurobio.2010.10.003

Risacher, S. L., Kim, S., Nho, K., Foroud, T., Shen, L., Petersen, R. C., et al. (2015). APOE effect on Alzheimer's disease biomarkers in older adults with significant memory concern. *Alzheimers Dement.* 11, 1417–1429. doi: 10.1016/j.jalz.2015.03.003

Serrano-Pozo, A., Das, S., and Hyman, B. T. (2021). APOE and Alzheimer's disease: advances in genetics, pathophysiology, and therapeutic approaches. *Lancet Neurol.* 20, 68–80. doi: 10.1016/S1474-4422(20)30412-9

Traub, R. D., Cunningham, M. O., Gloveli, T., LeBeau, F. E., Bibbig, A., Buhl, E. H., et al. (2003). GABA-enhanced collective behavior in neuronal axons underlies persistent gamma-frequency oscillations. *Proc. Natl. Acad. Sci. U.S.A.* 100, 11047–11052. doi: 10.1073/pnas.1934854100

Wang, C., Najm, R., Xu, Q., Jeong, D. E., Walker, D., Balestra, M. E., et al. (2018). Gain of toxic apolipoprotein E4 effects in human iPSC-derived neurons is

ameliorated by a small-molecule structure corrector. *Nat. Med.* 24, 647–657. doi: 10.1038/s41591-018-0004-z

Yamazaki, Y., Zhao, N., Caulfield, T. R., Liu, C. C., and Bu, G. (2019). Apolipoprotein E and Alzheimer disease: pathobiology and targeting strategies. *Nat. Rev. Neurol.* 15, 501–518. doi: 10.1038/s41582-019-0228-7

Zhang, T., Liu, N., Cao, H., Wei, W., Ma, L., and Li, H. (2020). Different doses of pharmacological treatments for mild to moderate alzheimer's disease: a bayesian network meta-analysis. *Front. Pharmacol.* 11:778. doi: 10.3389/fphar.2020.00778

Zhao, N., Liu, C. C., Qiao, W., and Bu, G. (2018). Apolipoprotein E, receptors, and modulation of Alzheimer's disease. *Biol. Psychiatry* 83, 347–357. doi: 10.1016/j.biopsych.2017.03.003

Zhou, M., Wang, H., Zeng, X., Yin, P., Zhu, J., Chen, W., et al. (2019). Mortality, morbidity, and risk factors in China and its provinces, 1990–2017: a systematic analysis for the Global Burden of Disease Study 2017. *Lancet* 394, 1145–1158.

Conflict of Interest: The authors declare that the research was conducted in the absence of any commercial or financial relationships that could be construed as a potential conflict of interest.

Publisher's Note: All claims expressed in this article are solely those of the authors and do not necessarily represent those of their affiliated organizations, or those of the publisher, the editors and the reviewers. Any product that may be evaluated in this article, or claim that may be made by its manufacturer, is not guaranteed or endorsed by the publisher.

frontiers in Aging Neuroscience

ORIGINAL RESEARCH
published: 28 January 2022
doi: 10.3389/fnagi.2021.804362

Prolonged Continuous Theta Burst Stimulation to Demonstrate a Larger Analgesia as Well as Cortical Excitability Changes Dependent on the Context of a Pain Episode

Ying Liu[1], Lina Yu[1], Xianwei Che[2,3] and Min Yan[1]**

[1] Department of Anesthesiology, The Second Affiliated Hospital of Zhejiang University School of Medicine, Hangzhou, China,
[2] Centre for Cognition and Brain Disorders, The Affiliated Hospital of Hangzhou Normal University, Hangzhou, China,
[3] Institute of Psychological Sciences, Hangzhou Normal University, Hangzhou, China

OPEN ACCESS

Edited by:
Yi Guo,
Jinan University, China

Reviewed by:
Zhiguo Zhang,
Shenzhen University, China
Tsung-Hsun Hsieh,
Chang Gung University, Taiwan
Marie-Cécile Niérat,
INSERM U1158 Neurophysiologie Respiratoire Expérimentale et Clinique, France
Alice Witney,
Trinity College Dublin, Ireland

***Correspondence:**
Xianwei Che
xwcheswu@gmail.com;
xianwei.che@hznu.edu.cn
Min Yan
zryanmin@zju.edu.cn

Specialty section:
This article was submitted to Neuroinflammation and Neuropathy, a section of the journal Frontiers in Aging Neuroscience

Received: 29 October 2021
Accepted: 09 December 2021
Published: 28 January 2022

Citation:
Liu Y, Yu L, Che X and Yan M (2022) Prolonged Continuous Theta Burst Stimulation to Demonstrate a Larger Analgesia as Well as Cortical Excitability Changes Dependent on the Context of a Pain Episode. Front. Aging Neurosci. 13:804362. doi: 10.3389/fnagi.2021.804362

A series of neuropathic pain conditions have a prevalence in older adults potentially associated with declined functioning of the peripheral and/or central nervous system. Neuropathic pain conditions demonstrate defective cortical excitability and intermissions, which raises questions of the impact of pain on cortical excitability changes and when to deliver repetitive transcranial magnetic stimulation (rTMS) to maximize the analgesic effects. Using prolonged continuous theta-burst stimulation (pcTBS), a relatively new rTMS protocol to increase excitability, this study was designed to investigate pcTBS analgesia and cortical excitability in the context of pain. With capsaicin application, twenty-nine healthy participants received pcTBS or Sham stimulation either in the phase of pain initialization (capsaicin applied) or pain ascending (20 min after capsaicin application). Pain intensity was measured with a visual-analogic scale (VAS). Cortical excitability was assessed by motor-evoked potential (MEP) and cortical silent period (CSP) which evaluates corticospinal excitability and GABAergic intracortical inhibition, respectively. Our data on pain dynamics demonstrated that pcTBS produced a consistent analgesic effect regardless of the time frame of pcTBS. More importantly, pcTBS delivered at pain initialization induced a larger pain reduction and a higher response rate compared to the stimulation during pain ascending. We further provide novel findings indicating distinct mechanisms of pcTBS analgesia dependent on the context of pain, in which pcTBS delivered at pain initialization was able to reverse depressed MEP, whereby pcTBS during pain ascending was associated with increased CSP. Overall, our data indicate pcTBS to be a potential protocol in pain management that could be delivered before the initialization of a pain episode to improve rTMS analgesia, potentially through inducing early corticospinal excitability changes that would be suppressed by nociceptive transmission.

Keywords: pcTBS, pain, motor-evoked potential, cortical silent period, cortical excitability

INTRODUCTION

Chronic neuropathic pain results from etiologically diverse disorders affecting the peripheral or the central nervous system (Scholz et al., 2019). A series of neuropathic pain conditions (e.g., postherpetic neuralgia and diabetic neuropathy) has a prevalence in older adults (Cunningham et al., 2016; John and Canaday, 2017; Ponirakis et al., 2019). Transcranial magnetic stimulation (TMS) is a safe and noninvasive form of brain stimulation. Repetitive TMS (rTMS) can induce neuroplastic changes, which have been used to manage chronic pain (Mhalla et al., 2010; Klein et al., 2015; Parker et al., 2016) and other neural degenerative conditions (Ahmed et al., 2012; Rabey et al., 2013). Indeed, high-frequency (≥5 Hz) rTMS over the primary motor cortex (M1) is suggested to be able to reduce neuropathic pain in randomized controlled studies (Hosomi et al., 2013, 2020; Attal et al., 2021). Overall, the clinical application of rTMS in chronic pain is still limited by the response rate, whereby it is close to moderate and far from being excellent at its best (Lefaucheur et al., 2014). It is therefore important to optimize the analgesic efficacy of rTMS.

In clinical settings, there is significant variability in pain intensity between rTMS treatment sessions. More specifically, the progress of a pain episode is associated with pain initialization, pain ascending and stabilizing, and pain reduction gradually. This raises questions of the temporal dynamics of pain, its impact on cortical excitability, and when to deliver treatments to maximize the benefits. Meta-analytic evidence has indicated shortened cortical silent period (CSP) in chronic pain populations (Parker et al., 2016), in which the duration of CSP is thought to indicate $GABA_B$-mediated intracortical inhibition (Werhahn et al., 1999). Moreover, motor-evoked potential (MEP) has been repeatedly demonstrated to be suppressed by both provoked (Farina et al., 2001) and chronic pain (Cosentino et al., 2014; Coppola et al., 2019). These studies demonstrate an inhibitory impact of pain on corticospinal excitability and intracortical inhibition. More importantly, the analgesic effects of rTMS could result from the restoration of defective cortical excitability induced by pain (Lefaucheur et al., 2006; Mhalla et al., 2011). It is therefore important to systemically investigate the analgesic influence of rTMS in the context of pain levels and cortical excitability changes.

Neuropathic pain syndromes are clinically characterized by spontaneous pain which has obvious intermissions. Topical application of capsaicin demonstrates temporal dynamics of pain. In general, pain perception tended to reach a significant level after 20 min of capsaicin application, reached the peak amplitude after 40 min and stabilized for at least 20 min, and then started the descending process from 70 to 80 min onward (Farina et al., 2001; Fierro et al., 2010). This pattern of pain dynamics is suggested to be able to mimic the progress of a pain episode (Frias and Merighi, 2016), which provides a unique opportunity to investigate the analgesic impact of rTMS at different pain levels particularly for neuropathic pain conditions.

The investigation of rTMS protocols is also important for improving rTMS analgesia. Theta-burst stimulation (TBS) mimics the bursts of neuronal firing which results in robust long-term potentiation, that is, the combination of the complex-spike pattern (∼100 Hz) with a theta frequency (∼5 Hz) repetition rate (Larson et al., 1986). Continuous TBS (cTBS) is designed to decrease excitability (Huang et al., 2005), whereby prolonged cTBS (pcTBS, i.e., multiple cTBS being delivered continuously) has recently been demonstrated to increase excitability (Klirova et al., 2020; McCalley et al., 2021). Specifically, pcTBS with two times the duration of cTBS converted the conventional inhibitory effect into a facilitatory one by means of increased MEP (Klirova et al., 2020). More importantly, pcTBS was found to have comparable (De Martino et al., 2019) or even better (Moisset et al., 2015) analgesic effects than standard 10 Hz rTMS (but see Klirova et al., 2020). These findings together call for more studies to validate the analgesic efficacy of pcTBS.

Using the fast and patterned pcTBS protocol, the current study was designed to investigate rTMS analgesia in the context of pain levels. With capsaicin application, participants received pcTBS or Sham stimulation either in the phase of pain initialization or pain ascending. These time frames were adopted as TMS tends to take time to act on cortical excitability (Di Lazzaro et al., 2010; Qiu et al., 2020) and therefore it might be late when the pain reaches peak amplitude. MEP and CSP were also evaluated with the purpose of examining cortical excitability dynamics modulated by both pain and pcTBS. It is hypothesized that pcTBS delivered either in the initialization or the ascending phase of pain would be able to reduce pain experience and to increase MEP and CSP compared to the Sham stimulation. We further sought to compare the analgesic efficacy of pcTBS in different pain contexts and to explore the associated cortical excitability changes.

MATERIALS AND METHODS

Participants

An *a priori* sample size calculation ($\alpha = 0.05$, power = 0.8, effect size = 0.3) indicated a minimum of 24 participants for the study to be sufficiently powered. The effect size of 0.3 was estimated based on the literature using the same stimulation protocol (Klirova et al., 2020). A group of 29 healthy, right-handed, TMS eligible (Rossi et al., 2011) adults were recruited to account for potential dropouts. Exclusion criteria included history or current diagnosis of psychiatric disorder, or use of psychoactive medication, as assessed by the Mini International Neuropsychiatric Interview (MINI) (Sheehan et al., 1998). No participant withdrew from this study, data from 29 participants (age range: 18–65 years, mean ± SD: 27.17 ± 12.44, 15 females) were therefore analyzed. All participants provided written informed consent before study commencement. This study was approved by the Ethics Committee in the Centre for Cognition and Brain Disorders of Hangzhou Normal University (20210330) and was conducted in accordance with the Declaration of Helsinki.

Experimental Design and Procedure

This was a single-blind, crossover, Sham-controlled study (**Figure 1**). Participants visited the lab three times (≥72 h

intervals), receiving a single session of pcTBS in the ascending (S20) or initialization (S0) of pain, or Sham stimulation (the same as pcTBS protocol, with the coil being flipped 90° to the scalp) with the sequence being pseudo randomized and counterbalanced. In each session, participants were exposed to pain induced by capsaicin application. Corticospinal excitability was measured with MEP and CSP before and after pcTBS in 90 min at an interval of 10 min.

Resting Motor Threshold and Corticospinal Excitability

Each session started with the assessment of the resting motor threshold (RMT). RMT was defined as the minimum intensity to induce MEPs > 0.05 mV of the first dorsal interosseous (FDI) muscle in 5/10 trials. Single pulses to the hand region of the left M1 (45° to the midline, handle pointing backward) at 5 s ± 10% jitter intervals were sent by a figure-eight coil connected to a Magstim Rapid^2 system (Magstim Company Ltd., United Kingdom). Coil position was measured relative to the nasion and inion to facilitate consistent re-positioning of the coil between sessions (Che et al., 2019).

Corticospinal excitability was measured with MEP and CSP at rest and during a sustained voluntary FDI muscle contraction, respectively (Hupfeld et al., 2020). The maximal voluntary contraction (MVC) was calculated and 20% of MVC was used for tonic contraction in CSP (Fling and Seidler, 2012). A total of 40 single pulses (20 of each) were consecutively delivered to the hand region of the left M1 at 120% RMT (45° to the midline, handle pointing backward). It is worth noting that CSP was evaluated following MEP as the muscle contraction during CSP may have an impact on MEP (Conforto et al., 2004). Corticospinal excitability was measured before and after pain and pcTBS in 90 min at an interval of 10 min, with the purpose to capture the dynamics of corticospinal excitability modulated by pain and pcTBS.

Pain Protocol

Capsaicin application is a widely used tonic pain protocol that has been demonstrated to evoke tonic heat pain lasting up to 90 min (Farina et al., 2001; Fierro et al., 2010). In this study, capsaicin (Dolpyc Teofarma 1%) was applied over the dorsal surface of the right hand in an area of 2 × 2 cm. Pain experience was measured by using a 0–10 point visual-analogic scale (VAS) (0: no pain, 1–3: mild pain, 4–6: moderate pain, and 7–10: severe pain) in 90 min at an interval of 10 min. Pain measurements were collected whereas corticospinal excitability was evaluated for consistency.

Repetitive Transcranial Magnetic Stimulation

Prolonged continuous theta-burst stimulation (pcTBS) was administered to the left M1 at 80% RMT, consisting of a burst of 3 pulses given at 50 Hz repeated every 5 Hz (Moisset et al., 2015; De Martino et al., 2019). A total of 1,200 pulses were delivered with the TMS coil positioned in a posterior-anterior (PA) direction parallel to the midline. In a pain initialization session (S0), pcTBS was delivered immediately after capsaicin application. Meanwhile, a pain ascending session (S20) delivered pcTBS 20 min after capsaicin application. This time point falls in the middle of the pain ascending phase which in general lasts for 40 min (Farina et al., 2001; Brighina et al., 2011; Mavromatis et al., 2016). The Sham stimulation was delivered using the same pcTBS protocol, with the coil being flipped 90° to the scalp so that the magnetic field would be delivered away from the scalp (Pascual-Leone et al., 1999). It is noted that the Sham stimulation was randomized to these two conditions (S0 or S20) at a 50% chance.

The side effect was assessed with painful sensations at the end of each session (Klein et al., 2015), using a numerical rating scale where 0 indicates no pain and 10 most intensive pain.

Data Analysis

Motor-evoked potential (MEP) was calculated from peak to peak. The calculation of CSP duration was based on the mean consecutive difference (MCD) by Garvey et al. (2001), which was highly recommended in a recent review (Hupfeld et al., 2020). This method is briefly described here: (1) all silent period trials were rectified using the absolute value and then were averaged; (2) the MCD of 100 ms of prestimulus EMG was calculated, in which the MCD is the mean successive difference between individual data points; (3) thresholds were set at ±MCD × 2.66 (i.e., 3 SDs), which covers 99.76% of possible prestimulus EMG data points; (4) silent period onset was determined as the time point at which the poststimulus EMG falls below the variation threshold for three consecutive data points, while the silent period offset was defined as the point at which the poststimulus EMG returns above the variation threshold for three consecutive data points.

Statistical Analyses

Statistical analyses were performed with SPSS (version 22; IBM Corporation, Armonk, NY, United States). We initially checked the normality of pain ratings in different combinations of our two factors (i.e., condition and time) with the Shapiro–Wilk test. The normality test was not violated ($P > 0.05$). A repeated measure two-way ANOVA was performed on pain ratings, with condition (S0, S20, and Sham) and time (T0–T10) being specified as within factors. *Post-hoc* pairwise comparisons were conducted to further explore the significant main and interaction effects, with the α-level set to 0.05 and Bonferroni corrected.

As pain ratings demonstrated a clear pattern of baseline (T0), ascending (T10–T30), stabilizing (T40–T60), and descending (T70–T90) phases (please refer to Results), pain ratings were further averaged within each phase for clarity. Pain ratings were then analyzed using a 3 (condition: S0, S20, and Sham) × 4 (time: baseline, ascending, stabilizing, and descending) repeated measures ANOVA and Bonferroni corrected at 0.05.

Motor-evoked potential and CSP data were also analyzed based on this pattern using three conditions: (S0, S20, and Sham) × 4 (time: baseline, ascending, stabilizing, and descending) two-way ANOVAs.

As the S0- and S20-stimulation tended to show a difference in analgesic efficacy (**Figures 2A,B**), we further compared the analgesic efficacy of these two conditions. Pain reduction of S0- and S20-stimulation was derived relative to the Sham stimulation

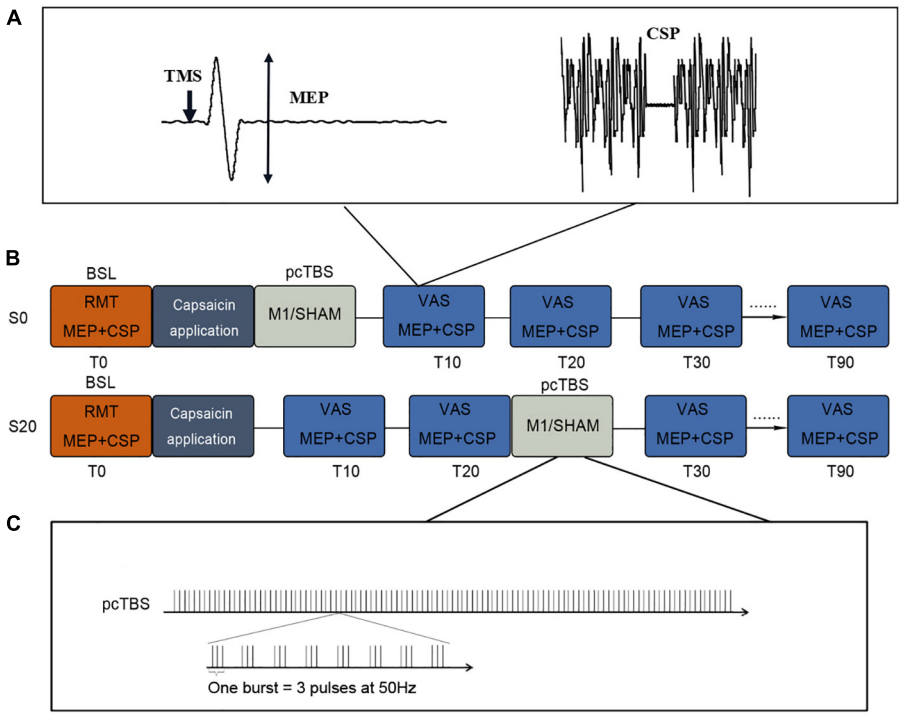

FIGURE 1 | Study design of this study. **(A)** MEP and CSP protocols. **(B)** Study protocol. pcTBS was delivered immediately (S0) or 20 min (S20) after capsaicin application. Sham stimulation was randomized to these two conditions at a 50% chance. Pain intensity (VAS) and cortical excitability (MEP and CSP) were evaluated every 10 min up to 90 min. **(C)** pcTBS protocol. pcTBS consists of a burst of 3 pulses given at 50 Hz repeated every 5 Hz, totaling 1,200 consecutive pulses. RMT, resting motor threshold; MEP, motor-evoked potential; CSP, cortical silent period; VAS, visual analog scale.

[e.g., ($S0_{DESC}$ – $Sham_{DESC}$)/$S0_{DESC}$ × 100%]. We also compared the response rate which was determined by no less than 30% in pain reduction (based on the formula of pain reduction above) in TMS literature (Dworkin et al., 2008). A two-way repeated-measures ANOVA (condition: S0, S20, and Sham; time: stabilizing and descending) and chi-squared (χ^2) statistic were performed on pain reduction and response rate, respectively. It is worth noting that the McNemar test was used for χ^2 statistics which was specifically designed for binary dependent variables in χ^2 statistics (Agresti, 2003). We also performed a series of correlation analyses to establish the relationship between pain reduction and motorcortical excitability changes. As the participants were from differing age groups, we initially examined the relationship between age and pain/MEP/CSP. Changes in pain ratings, MEP, and CSP at each phase were calculated relative to the Sham stimulation. Bivariate or partial (when age had a significant relationship with at least one of the variables) correlations were conducted between changes in pain ratings, MEP, and CSP. We also explored the MEP-to-CSP ratio as it has been used in previous studies (Terada et al., 2016; Latella et al., 2018).

RESULTS

Our data indicated that no participants reported painful sensations by the end of each session.

Effects of Prolonged Continuous Theta-Burst Stimulation on Pain Experience

All of the participants reported no pain at baseline as the capsaicin application took minutes to induce pain. Our data on pain ratings demonstrated a similar pattern of temporal dynamics to the literature. There was a significant time effect on pain ratings ($F_{2.83,79.19}$ = 63.22, $P_{corrected}$ = 0.001, η_p^2 =0.69) (**Figure 2A**). Pairwise comparisons of pain dynamics demonstrated statistically different stages characterized by baseline (T0), ascending (T10–T30, all $P_{corrected} < 0.05$ compared to the predecessor), stabilizing (T40–T60, all $P_{corrected} > 0.05$ compared to the predecessor), and descending (T70–T90, all $P_{corrected} < 0.05$ compared to the peak amplitude T40, and all $P_{corrected} < 0.05$ compared to the predecessor) phases. There was also a significant condition × time interaction effect on pain ratings ($F_{5.89,164.78}$ = 2.38, $P_{corrected}$ = 0.032, η_p^2 =0.08) (**Figure 2A**). Pairwise comparisons indicated that pcTBS at S0 (all $P_{corrected} < 0.05$) and S20 (all $P_{corrected} < 0.05$) decreased pain perception compared to the Sham stimulation from T40 onward to T90, i.e., in the stabilizing and descending phase.

A 3 (condition) × 4 (time) repeated measures ANOVA revealed a significant condition × time interaction effect on pain ($F_{3.89,108.78}$ = 5.19, $P_{corrected}$ = 0.001, η_p^2 =0.16) (**Figure 2B** and **Table 1**). Pairwise comparisons indicated that both the S0- and

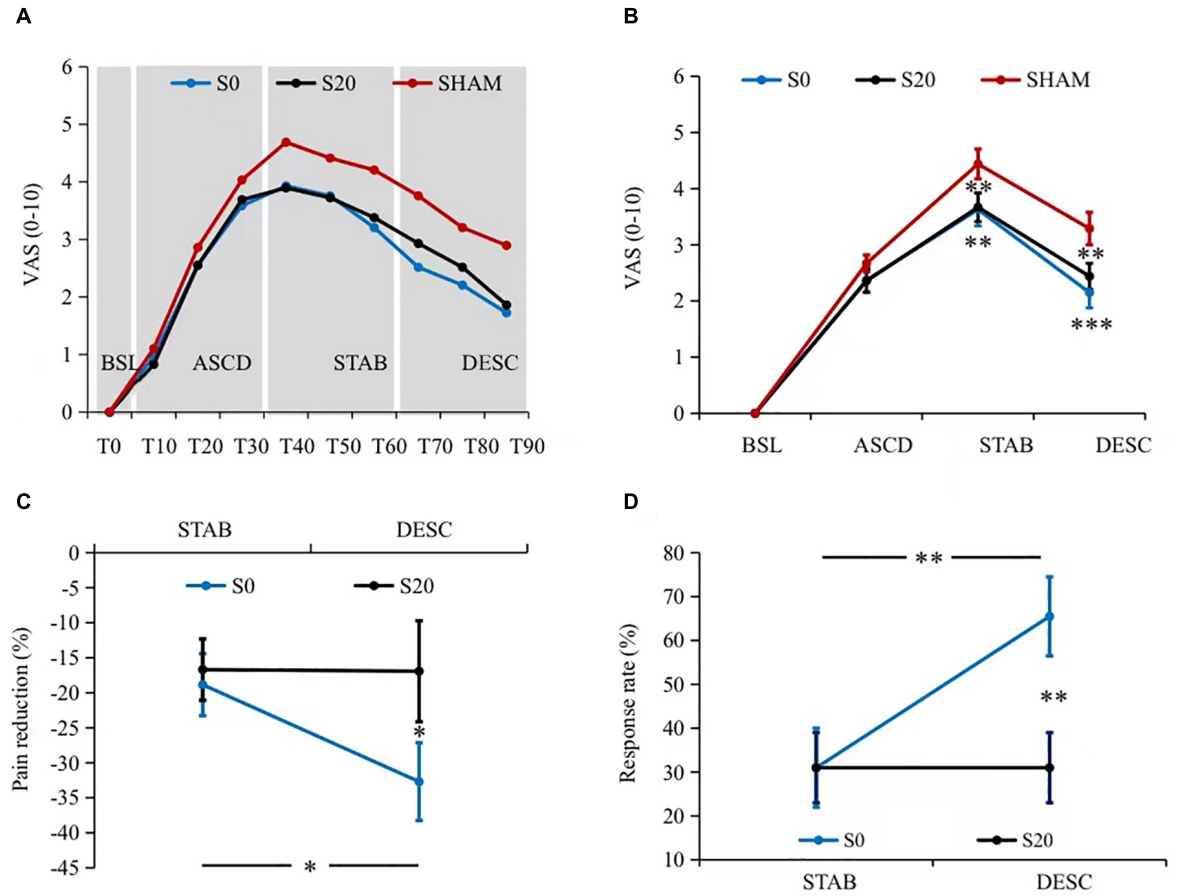

FIGURE 2 | Pain intensity results. **(A)** The dynamics of pain perception. Pain ratings demonstrated a clear pattern of baseline (T0), ascending (T10–T30, all $P_{corrected} < 0.05$ compared to the predecessor), stabilizing (T40–T60, all $P_{corrected} > 0.05$ compared to the predecessor), and descending (T70–T90, all $P_{corrected} < 0.05$ compared to the peak amplitude T40, and all $P_{corrected} < 0.05$ compared to the predecessor) phases. In addition, both the S0- and S20-pcTBS decreased pain from T40 to T90 compared to the Sham stimulation. **(B)** The averaged pain ratings within each phase. Similarly, S0- and S20-pcTBS decreased pain in the stabilizing (all $P_{corrected} < 0.05$) and descending (all $P_{corrected} < 0.05$) stages compared to the Sham stimulation. **(C)** The analgesic efficacy of S0- and S20-pcTBS. S0-pcTBS resulted in a larger pain reduction in the descending phase compared to the S20-pcTBS and that in the stabilizing phase. **(D)** The results of analgesic efficacy in terms of response rate. S0-pcTBS had a higher response rate in the descending phase compared to the S20-pcTBS and that in the stabilizing phase. *, **, and *** denote $P < 0.05$, $P < 0.01$, and $P < 0.001$ compared to the Sham. BSL, baseline; ASCD, ascending; STAB, stabilization; DESC, descending. Please refer to the **Supplementary Material** for figures with all the samples and variances.

S20-pcTBS decreased pain in the stabilizing (S0: $P_{corrected} = 0.003$, S20: $P_{corrected} = 0.001$) and descending (S0: $P_{corrected} = 0.000$, S20: $P_{corrected} = 0.007$) phase compared to the Sham stimulation (S0: $Mean_{STAB} = 3.63$, $Mean_{DESC} = 2.15$; S20: $Mean_{STAB} = 3.67$, $Mean_{DESC} = 2.44$; Sham: $Mean_{STAB} = 4.44$, $Mean_{DESC} = 3.29$).

Our data on the analgesic efficacy indicated a significant condition × time interaction effect on pain ($F_{1,28} = 4.86$, $P_{corrected} = 0.036$, $\eta_p^2 = 0.15$) (**Figure 2C**). Pairwise comparisons indicated that S0-pcTBS ($Mean_{DESC} = -32.69\%$) resulted in a larger pain reduction ($P_{corrected} = 0.048$) in the descending phase compared to the S20 ($Mean_{DESC} = -16.92\%$). Pain reduction in the descending phase ($Mean_{DESC} = -32.69\%$) was also larger ($P_{corrected} = 0.030$) than that in the stabilization stage ($Mean_{STAB} = -18.84\%$) induced by S0-pcTBS. The response rate data indicated a higher response rate ($P_{corrected} = 0.006$) in the S0 ($Mean_{DESC} = 65.5\%$, 19 responders) compared to the S20 condition ($Mean_{DESC} = 31\%$, 9 responders) in the descending phase (**Figure 2D**). The response rate was also higher ($P_{corrected} = 0.006$) in the descending phase ($Mean_{DESC} = 65.5\%$, 19 responders) compared to the stabilization stage ($Mean_{DESC} = 31\%$, 9 responders) in the S0 stimulation.

Effects of Repetitive Transcranial Magnetic Stimulation on Motorcortical Excitability

There was a condition × time interaction effect on MEP ($F_{2.96,82.96} = 2.90$, $P_{corrected} = 0.041$, $\eta_p^2 = 0.09$) (**Figure 3A** and **Table 1**). Pairwise comparisons indicated that capsaicin-induced pain significantly reduced MEP amplitude in all phases (ASCD: $P_{corrected} = 0.023$; STAB: $P_{corrected} = 0.001$; DESC: $P_{corrected} = 0.033$) compared to the baseline in the Sham condition

TABLE 1 | Summaries of ANOVA results.

Source	*df*	Mean square	*F*	*p*	η_p^2
(VAS)					
Condition	2	10.693	18.808	0.000***	0.402
Time	2.222	313.584	109.085	0.000***	0.796
Condition x Time	3.885	3.275	5.189	0.001**	0.156
(MEP)					
Condition	1.435	2.097	4.379	0.030*	0.135
Time	2.302	0.154	1.524	0.223	0.052
Condition x Time	2.963	0.368	2.895	0.041*	0.094
(CSP)					
Condition	1.453	1203.57	3.589	0.050*	0.114
Time	1.795	201.016	2.544	0.094	0.083
Condition x Time	3.624	170.500	2.518	0.050*	0.082

*VAS, visual-analogic scale; MEP, motor evoked potential; CSP, cortical silent period; df, degrees of freedom. *P < 0.05; **P < 0.01; ***P < 0.001.*

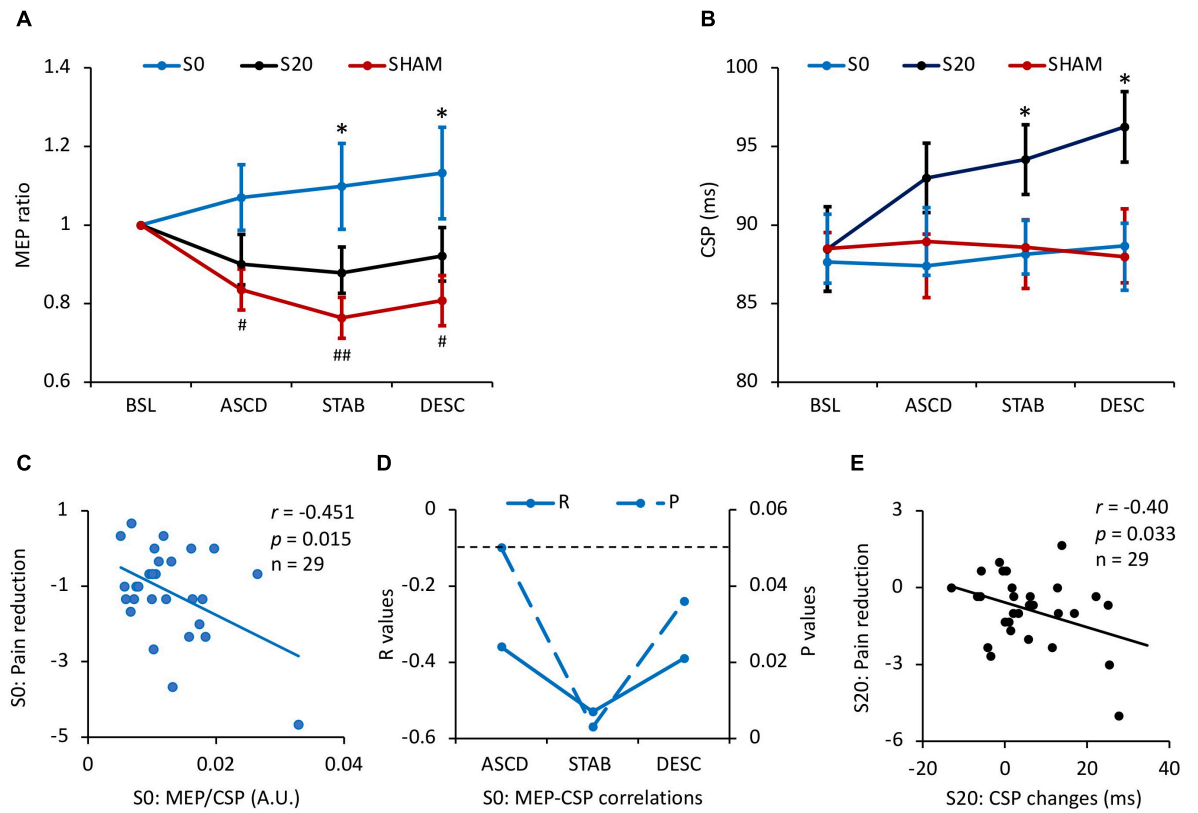

FIGURE 3 | Results of motorcortical excitability and the associations with pain reduction. **(A)** The effects of stimulation on MEP. Pain inhibited MEP in all stages compared to the baseline (all $P_{corrected}$ < 0.05) in the Sham condition, while pcTBS at S0 reversed depressed MEP in the stabilizing ($P_{corrected}$ = 0.022) and descending stages ($P_{corrected}$ = 0.024), and a trend increase in the ascending phase ($P_{corrected}$ = 0.06). **(B)** The effects of pcTBS on CSP. CSP duration was increased by the S20-pcTBS in the stabilizing ($P_{corrected}$ = 0.033) and descending (all $P_{corrected}$ = 0.015) stages compared to the Sham stimulation. **(C)** A significant negative correlation between the early (ascending) MEP/CSP ratio and late (descending) pain reduction in S0-pcTBS. **(D)** The dynamic correlations between MEP and CSP changes in the S0-pcTBS. MEP changes in the early phase (ascending) was negatively associated with CSP changes in the ascending, stabilization, and descending phases. **(E)** A significant negative correlation between the early (stabilization) CSP changes and late (descending) pain reduction in S20-pcTBS. * represents *P* < 0.05 compared to Sham; # and ## represent P < 0.05 and P < 0.01 compared to the baseline. A.U. denotes arbitrary unit. The dash line denotes P < 0.05. Error bars represent mean ± SE; BSL, baseline; ASCD, ascending; STAB, stabilization; DESC, descending. All the correlations are presented with age regressed as a covariate.

($Mean_{ASCD}$ = 0.84, $Mean_{STAB}$ = 0.76, $Mean_{DESC}$ = 0.81). Meanwhile, pcTBS at S0 resulted in larger MEPs in the stabilizing ($P_{corrected}$ = 0.022) and descending stages ($P_{corrected}$ = 0.024), and a trend increase in the ASCD phase ($P_{corrected}$ = 0.06) compared to the Sham stimulation (S0: $Mean_{ASCD}$ = 1.07, $Mean_{STAB}$ = 1.10, $Mean_{DESC}$ = 1.13; Sham: $Mean_{ASCD}$ = 0.84, $Mean_{STAB}$ = 0.76, $Mean_{DESC}$ = 0.81). No significant difference was found between the S0 and S20 conditions ($P_{corrected}$ = 0.38).

In terms of CSP, there was a significant condition × time interaction effect ($F_{3.62,101.47}$ = 2.52, $P_{corrected}$ = 0.050, η_p^2 =0.082) (**Figure 3B** and **Table 1**). Pairwise comparisons indicated that pcTBS at S20 resulted in a larger CSP in the stabilizing ($P_{corrected}$ = 0.022) and descending ($P_{corrected}$ = 0.015) stages compared to the Sham stimulation (S20: $Mean_{STAB}$ = 94.16, $Mean_{DESC}$ = 96.24; Sham: $Mean_{STAB}$ = 88.59, $Mean_{DESC}$ = 87.98). No other significant differences were found between conditions or time (all $P_{corrected} > 0.05$).

Relationship Between Pain Reduction and Cortical Excitability Changes

There was a significant negative correlation between age and baseline CSP across three sessions ($r = -0.42$, $p = 0.02$). We therefore regressed age in the following correlation analyses. We found a significant negative correlation between the early (ascending phase) MEP/CSP ratio and late (descending phase) pain reduction in S0-pcTBS ($r = -0.45$, $p = 0.015$) (**Figure 3C**). Moreover, MEP changes in the early phase (ascending) was negatively associated with CSP changes in the ascending ($r = -0.39$, $p = 0.039$), stabilization ($r = -0.53$, $p = 0.004$), and descending ($r = -0.39$, $p = 0.038$) phases in the S0 stimulation (**Figure 3D**). In terms of S20 stimulation, there was a significant negative correlation ($r = -0.40$, $p = 0.033$) between the early (stabilization) CSP increasement and late (descending) pain reduction (**Figure 3E**).

DISCUSSION

Using the fast and patterned pcTBS protocol, this study was designed to investigate rTMS analgesia in the context of pain. Our data demonstrated a consistent analgesic effect of pcTBS. More importantly, pcTBS delivered at pain initialization induced a larger pain reduction and a higher response rate compared to the stimulation during pain ascending. We also provide novel findings indicating distinct mechanisms of pcTBS analgesia in the context of pain. pcTBS delivered in the phase of pain initialization was able to reverse depressed MEP, whereby pcTBS in the ascending phase of pain was associated with increased CSP.

Our data on pain dynamics demonstrated obvious phases of capsaicin-induced pain, (Farina et al., 2001; Fierro et al., 2010) which provides a unique opportunity to investigate the analgesic impact of rTMS in different phases of a pain episode among chronic pain patients. More importantly, our data demonstrated the consistency of pcTBS analgesia regardless of the time frame to deliver stimulation. Due to the capacity to increase cortical excitability in a short period of time (Klirova et al., 2020; McCalley et al., 2021), studies have begun to evaluate the effect of pcTBS in pain management (Moisset et al., 2015; De Martino et al., 2019; Klirova et al., 2020). Our findings provide direct evidence to support pcTBS analgesia, which is critical for pcTBS to be used in the optimization of rTMS analgesia.

It is important to highlight that pcTBS delivered at pain initialization induced larger analgesia compared to the stimulation during pain ascending, which was characterized by a larger pain reduction and a higher response rate in the descending phase of pain. This is important to many chronic pain conditions as it provides insights on when to deliver treatments to maximize rTMS analgesia. As discussed earlier, neuropathic pain conditions are characterized by clear pain intermissions. Our findings indicate that receiving rTMS before pain initialization or more broadly at the early phase of a pain attack may be able to achieve larger analgesia. However, one needs to be cautious on this conclusion as these two stimulation conditions were close in time and demonstrated similar patterns of analgesia. Nonetheless, we provide evidence to demonstrate dynamic cortical excitability changes associated with the superior analgesic efficacy in the pain initialization condition (see below discussions on excitability mechanisms).

Prolonged continuous theta-burst stimulation (pcTBS) given at different phases of a pain episode may be associated with distinct cortical excitability changes. Our data indicated that pain induction resulted in a significant decrease in MEP amplitude in the absence of pcTBS intervention. This finding is consistent with previous studies in which MEP amplitude was reduced by chronic pain (Lefaucheur et al., 2006; Cosentino et al., 2014; Rittig-Rasmussen et al., 2014; Parker et al., 2016). Reduced motor cortical output is associated with the imbalance of neurotransmission in the central nervous system evoked by the ascending transmission of nociception. Meanwhile, pcTBS delivered during pain initialization increased MEP amplitude from the ascending to the stabilizing and descending stages. Moreover, this pattern of MEP changes aligns nicely with the dynamics of analgesia. In addition, increased "excitation-to-inhibition" ratio (i.e., MEP/CSP) in the early phase of pain was associated with a larger analgesic effect in the late stage of pain induction (**Figure 3C**), providing further evidence to support a mechanism of motorcortical excitability associated with pcTBS analgesia. However, pcTBS delivered in the ascending phase of pain had no impact on MEP amplitude, which indicates the involvement of other mechanisms than motorcortical excitation.

Indeed, pcTBS delivered in the ascending phase of pain enhanced CSP especially in pain stabilizing and descending phases (**Figure 3B**). The cortical silent period is thought to reflect the activity of $GABA_B$-mediated inhibitory circuits acting upon the corticospinal pathway (Siebner et al., 1998; Werhahn et al., 1999). These changes in CSP are in line with significant pain reduction during these two phases which took place from 20 min poststimulation onward. It is worth noting that MEP amplitude was significantly reduced by capsaicin application by this time (see Sham condition). pcTBS may

therefore act on $GABA_B$-mediated intracortical inhibition to reduce pain. Indeed, the balance between cortical excitation and inhibition tends to be disrupted by chronic pain conditions (Barr et al., 2013), and chronic pain is associated with reduced intracortical inhibition (Parker et al., 2016). More importantly, two studies have demonstrated the capacity of rTMS to reverse defective intracortical inhibition in chronic pain patients (Lefaucheur et al., 2006; Mhalla et al., 2011). Our results also indicated that early (i.e., stabilization) CSP increment was associated with a larger pain reduction in the late phase (i.e., descending) (**Figure 3E**). We, therefore, provide the first line of evidence that a single session of pcTBS is sufficient to increase $GABA_B$-mediated intracortical inhibition which is associated with decreased pain.

There were no significant changes in CSP when pcTBS was delivered during the initialization of pain (**Figure 3C**). It is possible that increased motorcortical excitability as indexed by MEP is sufficient to produce pain analgesia. MEP changes in the ascending phase of pain were negatively associated with CSP changes in the ascending, stabilization, and descending phases of pain when pcTBS was delivered during pain initialization. These findings are also consistent with the balance of cortical excitation and inhibition whereby pcTBS during pain initialization may drive early cortical excitation to reduce pain. Overall, we provide interesting findings to indicate superior analgesia when pcTBS is delivered before pain initialization or at the early phase of a pain attack in a broader way. Moreover, this effect is associated with early motorcortical excitability changes which may work against depressed MEP caused by nociceptive transmission. Otherwise, pcTBS may act on the alternative $GABA_B$-mediated intracortical inhibition to modulate the corticospinal pathway when pain stabilized.

There were some limitations in the study. We delivered pcTBS in the initialization and ascending phases of a pain episode without modeling the pain stabilization phase. This was designed as rTMS tends to take time to act, as demonstrated by changes in cortical excitability and pain perception in our data. We averaged data in each phase of pain, especially for the ascending phase whereby pcTBS was delivered right in between, to simplify the profiles of pain dynamic and to highlight the stage effect. Although our data demonstrated the same analgesia between these two methodologies, data presentation of each time point would also be appreciated. The M1 was located using the hotspot methodology. Although the hotspot approach was considered as an effective and efficient method to locate the M1 (Lefaucheur and Nguyen, 2019), a neuronavigation system is able to assist localization and the identification of disease-relevant brain connections and networks mediating positive treatment outcomes (Cash et al., 2020).

Our findings may bear significance for the clinical application of rTMS in pain management. Our data demonstrate a consistent analgesic effect of pcTBS regardless of the context of pain. pcTBS, therefore, represents a potential protocol for pain management that has not been evaluated in chronic pain populations. Moreover, our data demonstrated superior analgesia when pcTBS is delivered at the early compared to the ascending phase of a pain attack. This finding provides direct evidence to optimize rTMS analgesia in terms of when to deliver rTMS treatments. Besides, multiple sessions of pcTBS could be delivered within a single day due to its efficiency and efficacy, with the purpose to accelerate standard rTMS treatment protocols (Blumberger et al., 2018). In addition, our findings indicate distinct mechanisms of pcTBS analgesia when it is delivered at different phases of a pain episode. These findings provide insight for optimizing pcTBS analgesia in which pcTBS protocols can be designed to improve motorcortical excitability or intracortical inhibition dependent on the phases of a pain episode in a treatment session. Findings from this study provide insights on healthy aging and on the management of age-related neurodegenerative conditions. In one way, we demonstrated pcTBS to be able to reduce pain. This is important to healthy aging as a significant portion of old adults suffer from pain conditions (Jones et al., 2016; Sherman et al., 2020) and a range of neuropathic pain conditions (e.g., postherpetic neuralgia and diabetic neuropathy) have a prevalence in older adults (Cunningham et al., 2016; John and Canaday, 2017; Ponirakis et al., 2019). In another way, we provided neuroplastic changes underlying the analgesic effect of pcTBS. These findings add to our understanding of how rTMS can be used to manage age-related neurodegenerative conditions through neuroplastic mechanisms. In addition, our findings on pcTBS analgesia represent an optimizing effort of rTMS efficacy which has clear implications for age-related neurodegenerative conditions such as Alzheimer's disease whereby rTMS has a limited effect (Lefaucheur et al., 2014).

To conclude, this study demonstrated a consistent analgesic effect of pcTBS, which could be delivered before the initialization of a pain episode to improve rTMS analgesia. Moreover, this effect is associated with early motorcortical excitability changes which may work against depressed MEP caused by nociceptive transmission.

DATA AVAILABILITY STATEMENT

All data generated and analyzed during the current study will be available from the first author on reasonable request. Requests to access these datasets should be directed to YL, 350373328@qq.com.

ETHICS STATEMENT

The studies involving human participants were reviewed and approved by the Ethics Committee in the Centre for Cognition and Brain Disorders of Hangzhou Normal University (20210330) and was conducted in accordance with the Declaration of Helsinki. The patients/participants provided their written informed consent to participate in this study.

AUTHOR CONTRIBUTIONS

XC and YL contributed to data acquisition and statistical analysis. YL was a major contributor in writing the

manuscript. XC reviewed and edited the manuscript. All authors contributed to the conception and design of the study, and read as well as approved the final manuscript.

FUNDING

This study was supported by the National Natural Science Foundation of China (4045F41120040), Provincial Advantage Discipline Project (20JYXK034), and Key Medical Disciplines of Hangzhou.

ACKNOWLEDGMENTS

The authors thank all the participants and study sites that took part in this study.

SUPPLEMENTARY MATERIAL

The Supplementary Material for this article can be found online at: https://www.frontiersin.org/articles/10.3389/fnagi.2021.804362/full#supplementary-material

Supplementary Figure 1 | Results of all samples and variances. **(A)** Shows the samples and variances of the averaged pain ratings within each phase. Similarly, S0- and S20-pcTBS decreased pain in the stabilizing (all $P_{corrected} < 0.05$) and descending (all $P_{corrected} < 0.05$) stages compared to the Sham stimulation. **(B)** Indicates the samples and variances of analgesic efficacy of S0- and S20-pcTBS. S0-pcTBS resulted in a larger pain reduction in the descending phase compared to the S20-pcTBS as well as that in the stabilizing phase. **(C)** Shows the samples and variances of MEP. Pain inhibited MEP in all stages compared to the baseline (all $P_{corrected} < 0.05$) in the Sham condition, while pcTBS at S0 reversed depressed MEP in the stabilizing ($P_{corrected} = 0.022$) and descending stages ($P_{corrected} = 0.024$), as well as a trend increase in the ascending phase ($P_{corrected} = 0.06$). **(D)** Shows the samples and variances of pcTBS on CSP. CSP duration was increased by the S20-pcTBS in the stabilizing ($P_{corrected} = 0.033$) and descending (all $P_{corrected} = 0.015$) stages compared to the Sham stimulation.

REFERENCES

Agresti, A. (2003). *Categorical Data Analysis*. Hoboken, NJ: John Wiley & Sons.

Ahmed, M. A., Darwish, E. S., Khedr, E. M., El Serogy, Y. M., and Ali, A. M. (2012). Effects of low versus high frequencies of repetitive transcranial magnetic stimulation on cognitive function and cortical excitability in Alzheimer's dementia. *J. Neurol.* 259, 83–92. doi: 10.1007/s00415-011-6128-4

Attal, N., Poindessous-Jazat, F., de Chauvigny, E., Quesada, C., Mhalla, A., Ayache, S. S., et al. (2021). Repetitive transcranial magnetic stimulation for neuropathic pain: a randomized multicentre sham-controlled trial. *Brain* 144, 3328–3339. doi: 10.1093/brain/awab208

Barr, M. S., Farzan, F., Davis, K. D., Fitzgerald, P. B., and Daskalakis, Z. J. (2013). Measuring GABAergic inhibitory activity with TMS-EEG and its potential clinical application for chronic pain. *J. Neuroimmune Pharmacol.* 8, 535–546. doi: 10.1007/s11481-012-9383-y

Blumberger, D. M., Vila-Rodriguez, F., Thorpe, K. E., Feffer, K., Noda, Y., Giacobbe, P., et al. (2018). Effectiveness of theta burst versus high-frequency repetitive transcranial magnetic stimulation in patients with depression (THREE-D): a randomised non-inferiority trial. *Lancet* 391, 1683–1692. doi: 10.1016/S0140-6736(18)30295-2

Brighina, F., De Tommaso, M., Giglia, F., Scalia, S., Cosentino, G., Puma, A., et al. (2011). Modulation of pain perception by transcranial magnetic stimulation of left prefrontal cortex. *J. Headache Pain* 12, 185–191. doi: 10.1007/s10194-011-0322-8

Cash, R. F. H., Weigand, A., Zalesky, A., Siddiqi, S. H., Downar, J., Fitzgerald, P. B., et al. (2020). Using brain imaging to improve spatial targeting of transcranial magnetic stimulation for depression. *Biol. Psychiatry* 90, 689–700. doi: 10.1016/j.biopsych.2020.05.033

Che, X., Cash, R., Chung, S. W., Bailey, N., Fitzgerald, P. B., and Fitzgibbon, B. M. (2019). The dorsomedial prefrontal cortex as a flexible hub mediating behavioral as well as local and distributed neural effects of social support context on pain: a theta burst stimulation and TMS-EEG study. *Neuroimage* 201:116053. doi: 10.1016/j.neuroimage.2019.116053

Conforto, A. B., Z'Graggen, W. J., Kohl, A. S., Rösler, K. M., and Kaelin-Lang, A. (2004). Impact of coil position and electrophysiological monitoring on determination of motor thresholds to transcranial magnetic stimulation. *Clin. Neurophysiol.* 115, 812–819. doi: 10.1016/j.clinph.2003.11.010

Coppola, G., Di Lorenzo, C., Parisi, V., Lisicki, M., Serrao, M., and Pierelli, F. (2019). Clinical neurophysiology of migraine with aura. *J. Headache Pain* 20:42.

Cosentino, G., Fierro, B., Vigneri, S., Talamanca, S., Paladino, P., Baschi, R., et al. (2014). Cyclical changes of cortical excitability and metaplasticity in migraine: evidence from a repetitive transcranial magnetic stimulation study. *Pain* 155, 1070–1078. doi: 10.1016/j.pain.2014.02.024

Cunningham, A. L., Lal, H., Kovac, M., Chlibek, R., Hwang, S. J., Díez-Domingo, J., et al. (2016). Efficacy of the herpes zoster subunit vaccine in adults 70 years of age or older. *N. Engl. J. Med.* 375, 1019–1032. doi: 10.1056/NEJMoa1603800

De Martino, E., Fernandes, A. M., Galhardoni, R., De Oliveira Souza, C., Ciampi De Andrade, D., and Graven-Nielsen, T. (2019). Sessions of prolonged continuous theta burst stimulation or high-frequency 10 Hz stimulation to left dorsolateral prefrontal cortex for 3 days decreased pain sensitivity by modulation of the efficacy of conditioned pain modulation. *J. Pain* 20, 1459–1469. doi: 10.1016/j.jpain.2019.05.010

Di Lazzaro, V., Profice, P., Pilato, F., Dileone, M., Oliviero, A., and Ziemann, U. (2010). The effects of motor cortex rTMS on corticospinal descending activity. *Clin. Neurophysiol.* 121, 464–473. doi: 10.1016/j.clinph.2009.11.007

Dworkin, R. H., Turk, D. C., Wyrwich, K. W., Beaton, D., Cleeland, C. S., Farrar, J. T., et al. (2008). Interpreting the clinical importance of treatment outcomes in chronic pain clinical trials: IMMPACT recommendations. *J. Pain* 9, 105–121. doi: 10.1016/j.jpain.2007.09.005

Farina, S., Valeriani, M., Rosso, T., Aglioti, S., Tamburin, S., Fiaschi, A., et al. (2001). Transient inhibition of the human motor cortex by capsaicin-induced pain. A study with transcranial magnetic stimulation. *Neurosci. Lett.* 314, 97–101. doi: 10.1016/s0304-3940(01)02297-2

Fierro, B., De Tommaso, M., Giglia, F., Giglia, G., Palermo, A., and Brighina, F. (2010). Repetitive transcranial magnetic stimulation (rTMS) of the dorsolateral prefrontal cortex (DLPFC) during capsaicin-induced pain: modulatory effects on motor cortex excitability. *Exp. Brain Res.* 203, 31–38. doi: 10.1007/s00221-010-2206-6

Fling, B. W., and Seidler, R. D. (2012). Task-dependent effects of interhemispheric inhibition on motor control. *Behav. Brain Res.* 226, 211–217. doi: 10.1016/j.bbr.2011.09.018

Frias, B., and Merighi, A. (2016). Capsaicin, nociception and pain. *Molecules* 21:797. doi: 10.3390/molecules21060797

Garvey, M. A., Ziemann, U., Becker, D. A., Barker, C. A., and Bartko, J. J. (2001). New graphical method to measure silent periods evoked by transcranial magnetic stimulation. *Clin. Neurophysiol.* 112, 1451–1460. doi: 10.1016/s1388-2457(01)00581-8

Hosomi, K., Shimokawa, T., Ikoma, K., Nakamura, Y., Sugiyama, K., Ugawa, Y., et al. (2013). Daily repetitive transcranial magnetic stimulation of primary motor cortex for neuropathic pain: a randomized, multicenter, double-blind, crossover, sham-controlled trial. *Pain* 154, 1065–1072. doi: 10.1016/j.pain.2013.03.016

Hosomi, K., Sugiyama, K., Nakamura, Y., Shimokawa, T., Oshino, S., Goto, Y., et al. (2020). A randomized controlled trial of 5 daily sessions and continuous trial of 4 weekly sessions of repetitive transcranial magnetic stimulation for neuropathic pain. *Pain* 161, 351–360. doi: 10.1097/j.pain.0000000000001712

Huang, Y. Z., Edwards, M. J., Rounis, E., Bhatia, K. P., and Rothwell, J. C. (2005). Theta burst stimulation of the human motor cortex. *Neuron* 45, 201–206.

Hupfeld, K. E., Swanson, C. W., Fling, B. W., and Seidler, R. D. (2020). TMS-induced silent periods: a review of methods and call for consistency. *J. Neurosci. Methods* 346:108950. doi: 10.1016/j.jneumeth.2020.108950

John, A. R., and Canaday, D. H. (2017). Herpes zoster in the older adult. *Infect. Dis. Clin. North Am.* 31, 811–826. doi: 10.1016/j.idc.2017.07.016

Jones, M. R., Ehrhardt, K. P., Ripoll, J. G., Sharma, B., Padnos, I. W., Kaye, R. J., et al. (2016). Pain in the elderly. *Curr. Pain Headache Rep.* 20:23. doi: 10.1201/b14657-4

Klein, M. M., Treister, R., Raij, T., Pascual-Leone, A., Park, L., Nurmikko, T., et al. (2015). Transcranial magnetic stimulation of the brain: guidelines for pain treatment research. *Pain* 156, 1601–1614. doi: 10.1097/j.pain.0000000000000210

Klirova, M., Hejzlar, M., Kostýlková, L., Mohr, P., Rokyta, R., and Novák, T. (2020). Prolonged continuous theta burst stimulation of the motor cortex modulates cortical excitability but not pain perception. *Front. Syst. Neurosci.* 14:27. doi: 10.3389/fnsys.2020.00027

Larson, J., Wong, D., and Lynch, G. (1986). Patterned stimulation at the theta frequency is optimal for the induction of hippocampal long-term potentiation. *Brain Res.* 368, 347–350. doi: 10.1016/0006-8993(86)90579-2

Latella, C., Hendy, A., Vanderwesthuizen, D., and Teo, W. P. (2018). The modulation of corticospinal excitability and inhibition following acute resistance exercise in males and females. *Eur. J. Sport Sci.* 18, 984–993. doi: 10.1080/17461391.2018.1467489

Lefaucheur, J. P., André-Obadia, N., Antal, A., Ayache, S. S., Baeken, C., Benninger, D. H., et al. (2014). Evidence-based guidelines on the therapeutic use of repetitive transcranial magnetic stimulation (rTMS). *Clin. Neurophysiol.* 125, 2150–2206.

Lefaucheur, J. P., Drouot, X., Ménard-Lefaucheur, I., Keravel, Y., and Nguyen, J. P. (2006). Motor cortex rTMS restores defective intracortical inhibition in chronic neuropathic pain. *Neurology* 67, 1568–1574. doi: 10.1212/01.wnl.0000242731.10074.3c

Lefaucheur, J. P., and Nguyen, J. P. (2019). A practical algorithm for using rTMS to treat patients with chronic pain. *Neurophysiol. Clin.* 49, 301–307. doi: 10.1016/j.neucli.2019.07.014

Mavromatis, N., Gagné, M., Voisin, J. I., Reilly, K. T., and Mercier, C. (2016). Experimental tonic hand pain modulates the corticospinal plasticity induced by a subsequent hand deafferentation. *Neuroscience* 330, 403–409. doi: 10.1016/j.neuroscience.2016.06.008

McCalley, D. M., Lench, D. H., Doolittle, J. D., Imperatore, J. P., Hoffman, M., and Hanlon, C. A. (2021). Determining the optimal pulse number for theta burst induced change in cortical excitability. *Sci. Rep.* 11:8726. doi: 10.1038/s41598-021-87916-2

Mhalla, A., Baudic, S., de Andrade, D. C., Gautron, M., Perrot, S., Teixeira, M. J., et al. (2011). Long-term maintenance of the analgesic effects of transcranial magnetic stimulation in fibromyalgia. *Pain* 152, 1478–1485. doi: 10.1016/j.pain.2011.01.034

Mhalla, A., de Andrade, D. C., Baudic, S., Perrot, S., and Bouhassira, D. (2010). Alteration of cortical excitability in patients with fibromyalgia. *Pain* 149, 495–500. doi: 10.1016/j.pain.2010.03.009

Moisset, X., Goudeau, S., Poindessous-Jazat, F., Baudic, S., Clavelou, P., and Bouhassira, D. (2015). Prolonged continuous theta-burst stimulation is more analgesic than 'classical' high frequency repetitive transcranial magnetic stimulation. *Brain Stimul.* 8, 135–141. doi: 10.1016/j.brs.2014.10.006

Parker, R. S., Lewis, G. N., Rice, D. A., and McNair, P. J. (2016). is motor cortical excitability altered in people with chronic pain? A systematic review and meta-analysis. *Brain Stimul.* 9, 488–500. doi: 10.1016/j.brs.2016.03.020

Pascual-Leone, A., Tarazona, F., Keenan, J., Tormos, J. M., Hamilton, R., and Catala, M. D. (1999). Transcranial magnetic stimulation and neuroplasticity. *Neuropsychologia* 37, 207–217. doi: 10.1016/s0028-3932(98)00095-5

Ponirakis, G., Elhadd, T., Chinnaiyan, S., Dabbous, Z., Siddiqui, M., Al-Muhannadi, H., et al. (2019). Prevalence and risk factors for painful diabetic neuropathy in secondary healthcare in Qatar. *J. Diabetes Investig.* 10, 1558–1564. doi: 10.1111/jdi.13037

Qiu, S., Yi, W., Wang, S., Zhang, C., and He, H. (2020). The lasting effects of low-frequency repetitive transcranial magnetic stimulation on resting state EEG in healthy subjects. *IEEE Trans. Neural Syst. Rehabil. Eng.* 28, 832–841. doi: 10.1109/TNSRE.2020.2977883

Rabey, J. M., Dobronevsky, E., Aichenbaum, S., Gonen, O., Marton, R. G., and Khaigrekht, M. (2013). Repetitive transcranial magnetic stimulation combined with cognitive training is a safe and effective modality for the treatment of Alzheimer's disease: a randomized, double-blind study. *J. Neural Transm. (Vienna)* 120, 813–819. doi: 10.1007/s00702-012-0902-z

Rittig-Rasmussen, B., Kasch, H., Fuglsang-Frederiksen, A., Svensson, P., and Jensen, T. S. (2014). Effect of training on corticomotor excitability in clinical neck pain. *Eur. J. Pain* 18, 1207–1216. doi: 10.1002/j.1532-2149.2014.487.x

Rossi, S., Hallett, M., Rossini, P. M., and Pascual-Leone, A. (2011). Screening questionnaire before TMS: an update. *Clin. Neurophysiol.* 122:1686. doi: 10.1016/j.clinph.2010.12.037

Scholz, J., Finnerup, N. B., Attal, N., Aziz, Q., Baron, R., Bennett, M. I., et al. (2019). The IASP classification of chronic pain for ICD-11: chronic neuropathic pain. *Pain* 160, 53–59. doi: 10.1097/j.pain.0000000000001365

Sheehan, D. V., Lecrubier, Y., Sheehan, K. H., Amorim, P., Janavs, J., Weiller, E., et al. (1998). The mini-international neuropsychiatric interview (M.I.N.I.): the development and validation of a structured diagnostic psychiatric interview for DSM-IV and ICD-10. *J. Clin. Psychiatry* 59(Suppl. 20), 22–33; quiz 34–57.

Sherman, K. J., Wellman, R. D., Hawkes, R. J., Phelan, E. A., Lee, T., and Turner, J. A. (2020). T'ai Chi for chronic low back pain in older adults: a feasibility trial. *J. Altern. Complement. Med.* 26, 176–189. doi: 10.1089/acm.2019.0438

Siebner, H. R., Dressnandt, J., Auer, C., and Conrad, B. (1998). Continuous intrathecal baclofen infusions induced a marked increase of the transcranially evoked silent period in a patient with generalized dystonia. *Muscle Nerve* 21, 1209–1212. doi: 10.1002/(sici)1097-4598(199809)21:9<1209::aid-mus15>3.0.co;2-m

Terada, M., Bowker, S., Thomas, A. C., Pietrosimone, B., Hiller, C. E., and Gribble, P. A. (2016). Corticospinal excitability and inhibition of the soleus in individuals with chronic ankle instability. *PM R* 8, 1090–1096. doi: 10.1016/j.pmrj.2016.04.006

Werhahn, K. J., Kunesch, E., Noachtar, S., Benecke, R., and Classen, J. (1999). Differential effects on motorcortical inhibition induced by blockade of GABA uptake in humans. *J. Physiol.* 517(Pt 2), 591–597. doi: 10.1111/j.1469-7793.1999.0591t.x

Conflict of Interest: The authors declare that the research was conducted in the absence of any commercial or financial relationships that could be construed as a potential conflict of interest.

Publisher's Note: All claims expressed in this article are solely those of the authors and do not necessarily represent those of their affiliated organizations, or those of the publisher, the editors and the reviewers. Any product that may be evaluated in this article, or claim that may be made by its manufacturer, is not guaranteed or endorsed by the publisher.

frontiers in Aging Neuroscience

ORIGINAL RESEARCH
published: 07 February 2022
doi: 10.3389/fnagi.2022.807151

Transcranial Direct Current Stimulation on Different Targets to Modulate Cortical Activity and Dual-Task Walking in Individuals With Parkinson's Disease: A Double Blinded Randomized Controlled Trial

*Pei-Ling Wong[1], Yea-Ru Yang[1], Shih-Fong Huang[2], Jong-Ling Fuh[3], Han-Lin Chiang[3] and Ray-Yau Wang[1]**

[1] Department of Physical Therapy and Assistive Technology, National Yang Ming Chiao Tung University, Taipei, Taiwan, [2] Division of Nerve Repair, Department of Neurosurgery, Taipei Veterans General Hospital, Taipei, Taiwan, [3] Division of General Neurology, Department of Neurology, Neurological Institute, Taipei Veterans General Hospital, Taipei, Taiwan

OPEN ACCESS

Edited by:
Junhong Zhou,
Harvard Medical School,
United States

Reviewed by:
Dongning Su,
Capital Medical University, China
On-Yee Lo,
Hinda and Arthur Marcus Institute for Aging Research and Harvard Medical School, United States

***Correspondence:**
Ray-Yau Wang
rywang@nycu.edu.tw
orcid.org/0000-0002-8738-796X

Specialty section:
This article was submitted to Parkinson's Disease and Aging-related Movement Disorders, a section of the journal Frontiers in Aging Neuroscience

Received: 01 November 2021
Accepted: 10 January 2022
Published: 07 February 2022

Citation:
Wong P-L, Yang Y-R, Huang S-F, Fuh J-L, Chiang H-L and Wang R-Y (2022) Transcranial Direct Current Stimulation on Different Targets to Modulate Cortical Activity and Dual-Task Walking in Individuals With Parkinson's Disease: A Double Blinded Randomized Controlled Trial. Front. Aging Neurosci. 14:807151. doi: 10.3389/fnagi.2022.807151

Background: Transcranial direct current stimulation (tDCS) is a non-invasive brain stimulation to modulate cortical activity for improving motor function. However, the information of tDCS stimulation on different brain regions for dual-task walking and cortical modulation in Parkinson's disease (PD) has not yet been compared.

Objective: The objective of this study was to investigate the effects of different tDCS targets on dual-task gait performance and cortical activity in patients with PD.

Methods: A total of 36 participants were randomly assigned to primary motor cortex (M1) tDCS, dorsal lateral prefrontal cortex (DLPFC) tDCS, cerebellum tDCS, or Sham tDCS group. Each group received 20 min of tDCS stimulation, except for the Sham group. Gait performance was measured by the GAITRite system during dual-task walking and single walking. Corticomotor activity of the tibialis anterior (TA) was measured using transcranial magnetic stimulation (TMS). The functional mobility was assessed using the timed up and go (TUG) test.

Results: All participants showed no significant differences in baseline data. Following the one session of tDCS intervention, M1 ($p = 0.048$), DLPFC ($p < 0.001$), and cerebellum ($p = 0.001$) tDCS groups demonstrated significant improvements in dual-task gait speed compared with a pretest. The time × group interaction [$F(3, 32) = 5.125$, $p = 0.005$] was detected in dual-task walking speed. The *post hoc* Tukey's test showed that the differences in gait speed were between the Sham tDCS group and the DLPFC

tDCS group (p = 0.03). Moreover, DLPFC tDCS also increased the silent period (SP) more than M1 tDCS (p = 0.006) and Sham tDCS (p = 0.002).

Conclusion: The results indicate that DLPFC tDCS exerted the most beneficial effects on dual-task walking and cortical modulation in participants with PD.

Clinical trial registration: [http://www.thaiclinicaltrials.org/show/TCTR20200909005], Thai Clinical Trials Registry [TCTR20200909005].

Keywords: tDCS, different targets, single-session effects, dual-task gait, cortical activity, Parkinson's disease

INTRODUCTION

Parkinson's disease (PD) is a degenerative neurological disease due to the loss of dopaminergic neurons in the substantia nigra pars compacta in basal ganglia (BG) (Lees et al., 2009). With impaired interactions among cortico-BG-cerebellar circuits, the deficits in gait performance are frequently seen in individuals with PD (Hausdorff et al., 1998). In addition to classical motor symptoms, cognitive symptoms are widely accepted as part of the clinical feature in individuals with PD. These motor and cognitive impairments increased their difficulties to perform complex daily activities, such as dual-task walking (i.e., responding to a cognitive demanding task while walking) (Benecke et al., 1986; Raffegeau et al., 2019). According to a meta-analysis, the gait speed and stride length decreased under the condition of dual-task walking as compared with single walking in people with PD (Raffegeau et al., 2019). These significant difficulties in dual-task walking may lead to increased disability, fall risks, and decreased quality of life in people with PD (Kelly et al., 2012). Therefore, how to improve the dual-task walking performance is crucial for people with PD.

In addition to deficits in cortico-BG-cerebellar circuits, 33 studies demonstrated abnormal activity in primary motor cortex (M1), dorsal lateral prefrontal cortex (DLPFC), and cerebellum during dual-task performance in patients with PD (Wu and Hallett, 2005; Nieuwhof et al., 2016; Al-Yahya et al., 2019). It has been suggested that abnormal plasticity within M1 reflects a loss of coordination among the BG, cerebellar, and cortical inputs and eventually causes motor impairments in PD (Gaspar et al., 1991; Kishore et al., 2014). The decreased M1 inhibition during resting was reported in people with PD by transcranial magnetic stimulation (TMS) (Rossini et al., 2015), which may be one of the compensations for the cortico-BG-cerebellar deficit. Furthermore, the pattern of hypo-activation between the cortical area and striatum was associated with gait impairment in PD (Shine et al., 2013). Therefore, modulating brain activities might be a strategy for motor improvement, especially the complex movement, such as dual-task walking in individuals with PD.

The transcranial direct current stimulation (tDCS) is a non-invasive technique to modulate cortical excitability (Sánchez-Kuhn et al., 2017). Anodal tDCS has been considered not only to alter cortical excitability but also to exert subcortical effects (Polanía et al., 2012). Fregni et al. (2006) indicated that a single session of M1 tDCS improved upper extremity performance. Moreover, Ferrucci et al. (2016) demonstrated that 5 sessions of cerebellum tDCS decreased the disease severity as indicated by the Unified Parkinson's Disease Rating Scale (UPDRS). The previous study suggested that the lateral cerebellar region plays an important role in the complex motor task, such as dual-task walking (Ilg and Timmann, 2013). Furthermore, a recent review suggested that cerebellum may be the potential tDCS target area to improve the gait performance in people with PD (Potvin-Desrochers and Paquette, 2021). In contrast, as mentioned earlier, walking in daily activities demands interactions between motor and cognitive control, particularly, executive function (Yuan and Raz, 2014). The DLPFC has been recognized as the key area for executive function, and the relative DLPFC activations during gait can be demonstrated *via* dual-task walking (Collette et al., 2005; Beurskens et al., 2014). Evidence also showed that a single session of DLPFC tDCS improved balance and mobility (Manenti et al., 2014; Lattari et al., 2017). Taking together, the potential use of tDCS has been demonstrated for people with PD in neurorehabilitation. However, it is not known whether different tDCS targets would modulate the brain differently to result in different effects on motor performance. Therefore, this study aimed to compare the different tDCS targets in brain modulation and dual-task walking performance in individuals with PD.

MATERIALS AND METHODS

Subjects

This study protocol was approved by the Institutional Review Board of Taipei Veterans General Hospital and Ministry of Health and Welfare. This trial was registered at https://www.clinicaltrials.in.th/(TCTR20200909005) and conformed to the CONSORT checklist. Participants who were diagnosed with idiopathic PD by neurologists (J-LF and H-LC) were recruited from Taipei Veterans General Hospital. The age, gender, duration since the diagnosis of PD, and medications were obtained from the detailed clinical interviews and medical charts. Inclusion criteria were as follows: (1) stages 1–3 on the Hoehn and Yahr scale, (2) ability to walk independently for at least 10 m without

Abbreviations: BG, basal ganglia; CV, coefficients of variation; DLPFC, dorsal lateral prefrontal cortex; DTC, dual-task cost; EMG, electromyography; M1, primary motor cortex; MEP, motor evoked potential; MMSE, Mini-Mental State Examination; PD, Parkinson's disease; RMT, resting motor threshold; SP, silent period; TA, tibialis anterior; tDCS, transcranial direct current stimulation; TMS, transcranial magnetic stimulation; TUG, timed up and go test; UPDRS, Unified Parkinson's Disease Rating Scale.

the use of walking aids, (3) stable medical condition, and (4) a score of ≥ 24 on the Mini-Mental State Examination (MMSE). Exclusion criteria were as follows: (1) history of diseases or conditions known to interfere with participating in this study (e.g., epilepsy or metal implants in the brain) and (2) history of using central nervous system medications other than for PD, e.g., antiepileptic or antidepressant drugs in recent months. In total, 51 individuals were identified as potential subjects. Of these, 36 participants provided informed consent for participation in this study (**Figure 1**).

Experimental Design

This study was a double-blinded, randomized, controlled trial with pre- and post-measurements. An individual who was not involved in this study selected the sealed envelopes to assign participants to one of the four groups (i.e., M1 tDCS group, DLPFC tDCS group, cerebellum tDCS group, and Sham tDCS group) by the block of 2 randomizations. The cortical activities followed by gait performance were measured before (pretest) the real (or Sham) tDCS by the assessor who was blinded to the group assignment (assessor blinded) (**Figure 1**). Participants were blinded to their group assignment (participants blinded) and received one session of real or Sham tDCS for 20 min according to the group assignment. After 20 min of tDCS, all participants were measured the cortical activities immediately after tDCS and gait performance for 30 min after tDCS. All interventions and assessments were carried out with patients in the "on" status.

Intervention

The stimulation was delivered by a current stimulator (Eldith DC Stimulator, NeuroConn, Germany) through a pair of 35 cm^2 electrodes with a maximal output of 2 mA. The stimulation intensity was set to 2 mA for 20 min.

a. M1 tDCS group: The anode was placed over the M1 of the dominant hemisphere (C3 according to EEG 10/20 system), and the cathode was placed over the contralateral supraorbital ridge (Fregni et al., 2006).
b. DLPFC tDCS group: The anode was placed over the DLPFC of the dominant hemisphere (F3 according to EEG 10/20 system), and the cathode was placed over the contralateral supraorbital ridge (Fregni et al., 2006; Lattari et al., 2017).
c. Cerebellum tDCS group: The anode was placed 1 cm below and 2 cm lateral to the inion over the dominant hemisphere, and the cathode was placed over the contralateral supraorbital ridge (Ferrucci et al., 2015).
d. Sham tDCS group: The electrodes were positioned as described in the M1 tDCS group. However, the current was delivered only for the first 60 s, with a ramp up and ramp down for 30 s.

Outcome Measures

Primary Outcome Measures

The primary outcome of this study was dual-task walking performance measured by a GAITRite system (CIR system, Inc., Havertown, PA, United States) (Yang et al., 2019). The GAITRite system is 4.75 m long and 0.9 m wide, and the pressure-sensitive area of the walkway is 4.30 m long and 0.61 m wide. The dual-task walking was walking while performing serial subtracting by three, starting from a randomized 3-digit number at a comfortable speed. The walking trial was repeated three times with 60 s rest in between. The average of the three trials of each walking condition was used for data analysis. Gait parameters of interest were speed, cadence, stride time, stride length, and coefficients of variation (CV) of stride time and stride length. The formula of CV is standard deviation/mean × 100%. A lower CV value means a more consistent gait pattern (Yang et al., 2013). In addition, the dual-task cost (DTC) was calculated to indicate the dual-task interference. The formula of DTC was DTC = (dual-task walking speed – single-task walking speed)/single-task walking speed × 100% (Yang et al., 2019).

Secondary Outcome Measures

The secondary outcomes included corticomotor activity, single walking performance, and functional mobility.

Corticomotor Activity

The resting motor threshold (RMT), motor evoked potentials (MEPs), and silent period (SP) duration of the tibialis anterior (TA) elicited by TMS (Magstim 200 magnetic stimulator; Magstim Company, Whiteland, Dyfed, United Kingdom) were used to indicate the corticomotor activity. The MEPs of TA were recorded by an electromyographic (EMG) machine in response to TMS delivered through a double-cone coil placed on the M1 with participants lying supine wearing a fitted cap marked with a coordinate system (distance, 1 cm). The optimal scalp location (hot spot) was determined by moving the TMS stimulator over the scalp in 1-cm steps. Once the hot spot was identified, a single-pulse TMS was delivered to the location to determine the RMT, as the lowest stimulus intensity necessary to elicit MEPs greater than 0.05-mV peak-to-peak amplitude in at least 5 of 10 consecutive stimuli (Yang et al., 2013). The RMT was expressed as a percentage of maximum stimulator output, which reflects the excitability of motor cortex (Groppa et al., 2012). The MEPs were measured at an intensity of 120% RMT, and the peak-to-peak amplitudes of the MEPs of 10 trials were collected and averaged. The amplitude of MEPs is thought to represent the corticospinal excitability of the M1 (Groppa et al., 2012). Both RMT and MEP were considered to be mediated by the glutamatergic system indicated by the TMS-pharmacological study (Kapogiannis and Wassermann, 2008; Paulus et al., 2008). The SP duration was determined during isometric voluntary contraction of TA. Ten magnetic stimuli were applied at an intensity of 120% RMT, while the participant performed maximum of 20% voluntary contraction. The intensity used in the post-assessment was the same as that used in the pre-assessment. The SP duration was determined from the MEP onset to the recurrence of at least 50% of EMG background activity (Yang et al., 2013). The neurophysiological phenomenon of SP is thought to be due to inhibition mechanisms of the motor cortex mediated through the GABAergic system (Werhahn et al., 1999).

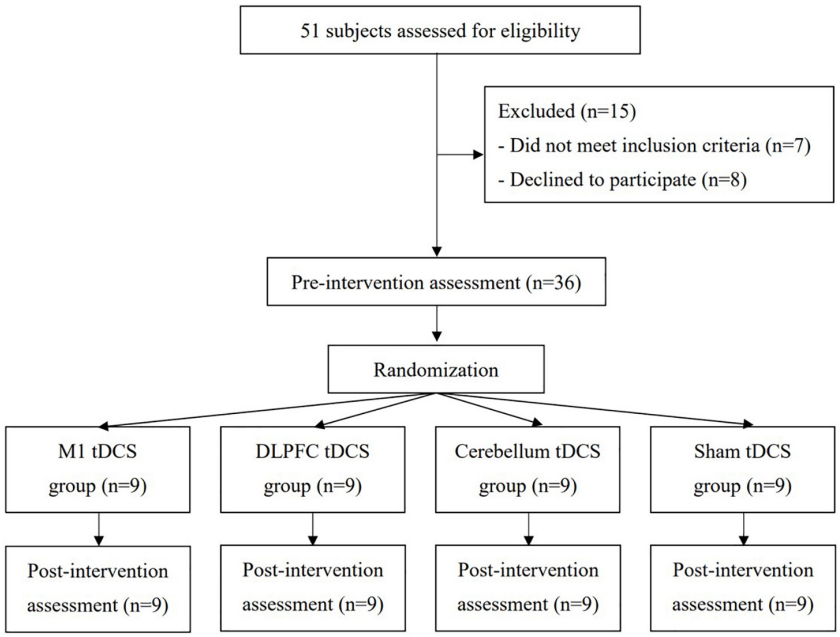

FIGURE 1 | Flowchart of the patient inclusion and study procedures.

Single Walking Performance

The single walking performance was also measured using the GAITRite system. For a single walking performance, the participants walked at their comfortable speed without additional tasking. The average of the three trials was used for data analysis.

Timed Up and Go Test

The timed up and go (TUG) was used to evaluate the functional mobility. The participants were seated in a chair and were instructed to stand up, walk 3 m, turn around, walk back to the chair, and then sit down. We recorded the time needed to complete this task. A high reliability of this test has been documented in individuals with PD (Morris et al., 2001).

Statistical Analysis

All analyses were performed using the SPSS version 24.0. Descriptive statistics [mean ± standard deviation, frequency, or median (interquartile range)] were generated for all variables. The Shapiro–Wilk test was used to assess the normal distributions. The intergroup difference of baseline (pretest) data was analyzed by using the Kruskal–Wallis test and one-way ANOVA for continuous variables or χ^2 test for nominal scales. Accordingly, the two-way repeated measures ANOVA (group × time) was used for intergroup comparisons of dual-task walking, single walking, and TUG performance, followed by the *post hoc* Tukey's test with the Bonferroni correction, which multiplied the uncorrected *p*-values by 6 for multiple comparisons between four groups, if there was group × time effect. The *post hoc* paired *t*-test was used to examine significance between pre- and post-data if there was a significant time effect. The Kruskal–Wallis one-way ANOVA was used for intergroup comparisons of change values in corticomotor activity due to not being normally distributed, followed by the *post hoc* Mann–Whitney *U* tests with the Bonferroni correction. The intragroup difference was thus analyzed by the Wilcoxon signed-rank test. The change values of corticomotor activity were calculated by subtracting the baseline data from the post-intervention data. Statistical significance was set at $p < 0.05$. The sample size was calculated using the G-Power version 3.1.9.7. Although the effect size was 0.85 for tDCS in improving dual-task gait performance in patients with PD (Mishra and Thrasher, 2021), in this study, we chose a relatively smaller effect size of 0.518 according to the study by Kaski et al. (2014). The total sample size was required to be 36 (9 per group) with a power of 0.80 and a two-tailed alpha level of 0.05 to detect a difference in gait performance.

RESULTS

A total of 51 patients were screened for the eligibility of participating in this study. As a result, 36 patients were included in this study and were randomly assigned to the M1 tDCS group (n = 9), DLPFC tDCS group (n = 9), cerebellum tDCS group (n = 9), or Sham tDCS group (n = 9). Participants received 20 min of tDCS according to their group assignment. None of them reported any adverse events or withdrew from this study (**Figure 1**). No significant differences between groups were found in baseline demographic characteristics (**Table 1**) and all outcome measures at the pre-intervention assessment.

Dual-Task Walking Performance

Table 2 shows the dual-task walking performance at pre- and post-intervention for 4 study groups. Regarding the dual-task gait parameters, there was no group effect [$F(3, 32) = 2.237$, $p = 0.103$]

TABLE 1 | Demographic characteristics of included participants with Parkinson's disease.

Group	M1 group (*n* = 9)	DLPFC group (*n* = 9)	Cerebellum group (*n* = 9)	Sham group (*n* = 9)	*P* value
Age (years)	54.20 ± 4.1	50.09 ± 2.4	61.30 ± 7.9	58.30 ± 8.0	0.60
Gender (M/F)	8/1	6/3	2/7	3/6	<0.01
H&Y stage	1.89 ± 0.6	1.67 ± 0.5	2.13 ± 0.6	1.78 ± 0.7	0.75
More affected side (L/R)	2/7	1/8	2/7	1/8	0.85
Duration of diagnosed (months)	93.54 ± 68.2	73.81 ± 39.2	49.11 ± 39.3	100.18 ± 147.0	0.43
UPDRS	33.22 ± 13.1	25.56 ± 17.0	24.22 ± 9.9	23.44 ± 14.7	0.48
MMSE	28.11 ± 1.8	28.89 ± 1.8	27.33 ± 2.2	28.89 ± 2.0	0.29
LEDD (mg)	592.1 ± 208.2	603.89 ± 357.3	468.22 ± 212.1	426.11 ± 243.7	0.41

M, male; F, female; H&Y, Hoehn and Yahr stage; L, left; R, right; MMSE, Mini-Mental State Examination; LEDD: levodopa equivalent daily dosage.

TABLE 2 | Dual task walking performance after different tDCS interventions.

Group	M1 group (*n* = 9)	DLPFC group (*n* = 9)	Cerebellum group (*n* = 9)	Sham group (*n* = 9)	Time	Group	Time × group	*Post-hoc*[a]
					p-value, *F*-value	*p*-value, *F*-value	*p*-value, *F*-value, η^2	
Speed$_{(cm/sec)}$					<0.001, $F(3,32) = 56.616$	0.103, $F(3,32) = 2.237$	0.005, $F(3,32) = 5.125$, 0.325	DLPFC vs. Sham
Pre	97.48 ± 29.2	78.99 ± 26.3	70.74 ± 23.2	90.01 ± 22.4				
Post	107.94 ± 29.6[#]	98.49 ± 24.9[#]	87.54 ± 24.6[#]	92.77 ± 24.4				
Cadence $_{(step/min)}$					<0.001, $F(3,32) = 41.497$	0.182, $F(3,32) = 1.723$	0.005, $F(3,32) = 5.180$, 0.327	–
Pre	108.60 ± 12.9	104.87 ± 20.1	87.24 ± 27.9	108.41 ± 19.2				
Post	113.32 ± 14.2	119.18 ± 16.8[#]	93.33 ± 19.2[#]	111.20 ± 20.5				
ST $_{(sec)}$					0.004, $F(3,32) = 9.628$	0.237, $F(3,32) = 1.487$	0.023, $F(3,32) = 3.649$, 0.255	–
Pre	1.12 ± 0.1	1.19 ± 0.2	1.23 ± 1.0	1.16 ± 0.3				
Post	1.08 ± 0.1	1.02 ± 0.1[#]	1.15 ± 0.3	1.14 ± 0.3				
SL $_{(cm)}$					<0.001, $F(3,32) = 22.069$	0.100, $F(3,32) = 2.267$	0.031, $F(3,32) = 3.340$, 0.238	–
Pre	106.12 ± 22.5	89.02 ± 18.9	84.83 ± 24.6	100.11 ± 18.3				
Post	112.95 ± 22.0[#]	98.32 ± 14.7[#]	92.18 ± 18.8[#]	99.30 ± 18.7				
ST variability $_{(\%)}$					0.047, $F(3,32) = 4.287$	0.832, $F(3,32) = 0.291$	0.239, $F(3,32) = 1.476$, 0.122	–
Pre	5.63 ± 5.5	5.06 ± 4.5	16.23 ± 18.7	4.80 ± 3.1				
Post	3.59 ± 2.5	3.13 ± 1.1	7.34 ± 3.8	4.58 ± 4.1				
SL variability $_{(\%)}$					0.385, $F(3,32) = 0.777$	0.319, $F(3,32) = 1.217$	0.936, $F(3,32) = 0.138$, 0.013	–
Pre	4.64 ± 3.3	5.20 ± 3.0	7.16 ± 4.1	4.38 ± 2.1				
Post	4.11 ± 3.3	4.15 ± 2.0	6.39 ± 3.3	4.46 ± 2.2				
DTC $_{(\%)}$					0.006, $F(3,32) = 8.779$	0.078, $F(3,32) = 2.493$	0.140, $F(3,32) = 1.957$, 0.155	–
Pre	−15.19 ± 17.5	−20.31 ± 25.7	−18.31 ± 22.1	−10.14 ± 11.2				
Post	−12.27 ± 9.0	−13.53 ± 18.4[#]	−13.54 ± 20.0	−8.97 ± 14.0				

Data are presented as the mean ± SD (The Shapiro–Wilk test was used to determine the values are normally distributed). ST, stride time; SL, stride length; DTC, dual task cost. [#]$p < 0.05$ for intragroup comparison (Analyzed using paired t-test). [a]The Tukey's post-hoc test with Bonferroni correction was used to determine the intergroup differences.

but a significant effect of time [$F(3, 32) = 56.616$, $p < 0.001$] and time × group interaction [$F(3, 32) = 5.125$, $p = 0.005$]. The *post hoc* Tukey's test with the Bonferroni correction showed that the differences in gait speed were between the Sham tDCS group and the DLPFC tDCS group ($p = 0.03$) (**Figure 2**). The cadence showed no group effect [$F(3, 32) = 1.723$, $p = 0.182$) but a significant effect of time [$F(3, 32) = 41.497$, $p < 0.001$] and time × group interaction [$F(3, 32) = 5.180$, $p = 0.005$]. However, the *post hoc* Tukey's test with the Bonferroni correction did not show any group difference in cadence. The stride time showed

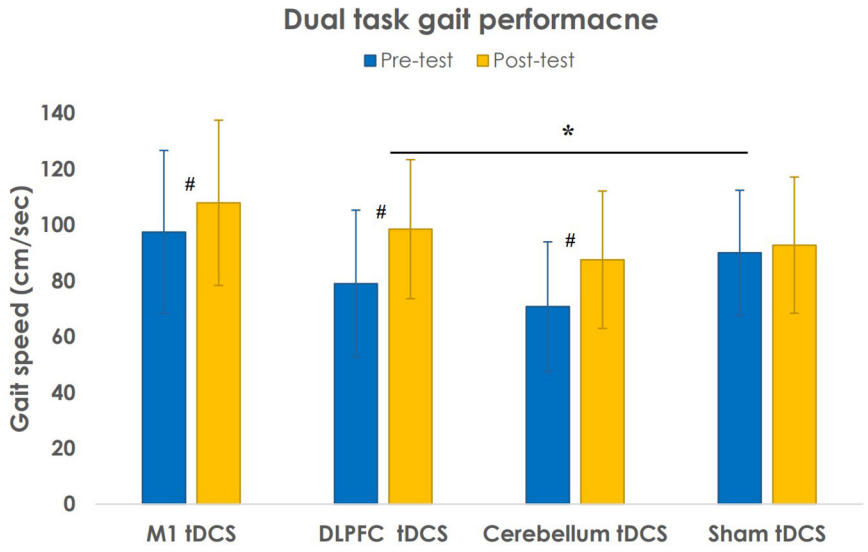

FIGURE 2 | Results of gait speed during dual-task walking performance after different transcranial direct current stimulation (tDCS) stimulations. Data are presented as the mean ± SD. $^{\#}P < 0.05$: intragroup comparison. $^{*}P < 0.05$: intergroup comparison.

no group effect [$F(3, 32) = 1.487$, $p = 0.237$] but a significant effect of time [$F(3, 32) = 9.628$, $p = 0.004$) and time × group interaction [$F(3, 32) = 3.649$, $p = 0.023$]. However, the *post hoc* Tukey's test with the Bonferroni correction did not show any group difference in stride time. The stride length showed no group effect [$F(3, 32) = 2.267$, $p = 0.100$] but a significant effect of time [$F(3, 32) = 22.069$, $p < 0.001$] and time × group interaction [$F(3, 32) = 3.340$, $p = 0.031$]. However, the *post hoc* Tukey's test with the Bonferroni correction did not show any group difference in stride length.

Furthermore, two-way repeated ANOVA indicated several significant time effects. The *post hoc* paired *t*-test showed a significant increase in gait speed [$t(8) = -6.963$, $p < 0.001$], cadence [$t(8) = -6.659$, $p < 0.001$], and stride length [$t(8) = -3.761$, $p = 0.006$] and a decrease in stride time [$t(8) = 4.600$, $p = 0.002$] after DLPFC tDCS intervention. In addition, the *post hoc* paired *t*-tests indicated that patients in cerebellum tDCS group significantly increased in gait speed [$t(8) = -5.231$, $p = 0.001$], cadence [$t(8) = -3.499$, $p = 0.008$], and stride length [$t(8) = -2.610$, $p = 0.031$] and patients in M1 tDCS group significantly increased in gait speed [$t(8) = -2.338$, $p = 0.048$] and stride length [$t(8) = -2.492$, $p = 0.037$] after tDCS intervention.

Corticomotor Activity

Table 3 shows the cortical activity of M1 measured by the TMS before and after tDCS interventions. After the DLPFC tDCS stimulation, the SP of stimulating hemisphere increased significantly more than M1 tDCS ($p = 0.038$) and Sham tDCS ($p = 0.001$) (**Figure 3**). However, there was no significant difference in other groups. In contrast, the corticomotor activity of non-stimulating hemisphere did not change in this study.

Single Walking Performance

Table 4 shows the single walking performance after different tDCS interventions. We found no significant time and group interaction for all gait parameters of single walking but a significant time effect. The *post hoc* paired *t*-test showed that a significant increase in gait speed [$t(8) = -2.528$, $p = 0.035$] and cadence [$t(8) = -3.291$, $p = 0.011$] after DLPFC tDCS intervention. In M1 tDCS group, the *post hoc* paired *t*-test showed a significant increase in stride length [$t(8) = -3.315$, $p = 0.011$] after tDCS intervention.

Timed Up and Go Performance

The results of TUG after different tDCS are shown in **Table 4**. We found no significant group effect [$F(3, 32) = 0.289$, $p = 0.832$], time effect [$F(3, 32) = 0.006$, $p = 0.939$], and group × time interactions [$F(3, 32) = 1.174$, $p = 0.335$]. In addition, there was no significant difference in intragroup comparisons.

DISCUSSION

This randomized, double-blinded, controlled trial was the first study to compare the immediate neuromodulation effects of different tDCS targets on dual-task walking performance in individuals with PD. In this study, we found that only the tDCS on DLPFC increased cortical inhibition and exerted the most beneficial effects to improve dual-task walking in people with PD as compared with tDCS on M1 or Sham tDCS.

In this study, the improvements in dual-task walking coupled with increased SP duration were demonstrated after DLPFC tDCS. The change in dual-task gait speed was highly correlated with change in SP (Spearman's correlation $\rho = 0.733$, $p = 0.025$). Wu et al. (2007) noted that shorter SP duration was associated with worse PD symptoms. We previously found the

TABLE 3 | Corticospinal activity after different tDCS interventions.

Group	M1 group ($n = 9$)		DLPFC group ($n = 9$)		Cerebellum group ($n = 9$)		Sham group ($n = 9$)		p
	Pre	Post	Pre	Post	Pre	Post	Pre	Post	
RMT_{IH} (%)	51.00	55.00	58.00	58.00	65.00	65.00	61.80	62.00	
	(46.00, 58.00)	(50.00, 62.00)	(47.00, 67.00)	(47.00, 70.00)	(60.00, 69.00)	(59.00, 69.00)	(53.50, 73.50)	(53.00, 74.00)	
Change values	2.00 (0.00, 2.00)		0.00 (−1.00, 1.00)		0.00 (−1.00, 0.00)		0.00 (−1.00, 0.00)		0.063
RMT_{CH} (%)	53.00	55.00	56.00	58.00	59.00	60.00	52.00	52.00	
	(49.00, 57.00)	(48.00, 61.0 0)	(49.50, 75.00)	(50.00, 72.00)	(48.00, 63.00)	(53.00, 62.00)	(45.00, 62.00)	(45.00, 62.00)	
Change values	2.00 (−1.00, 3.00)		0.00 (−2.50, 1.50)		2.00 (−1.00, 5.00)				0.312
MEP_{IH} (uV)	418.66	341.38	416.77	315.18	630.78	763.50	329.06	292.61	
	(289.89, 593.17)	(204.45, 773.70)	(276.68, 610.96)	(395.45, 208.47)	(547.20, 858.11)	(361.21, 1068.26)	(159.31, 483.07)	(138.75, 387.26)	
Change values	30.79 (−164.05, 367.42)		−71.10 (−285.29, −41.78)		69.07 (−76.46, 248.79)		−3.01 (−69.25, 8.40)		0.240
MEP_{CH} (uV)	533.55	696.96	408.38	491.19	589.37	516.62	415.82	431.05	
	(315.18, 939.84)	(289.53, 967.77)	(252.60, 580.35)	(333.53, 773.04)	(494.40, 778.99)	(296.92, 750.30)	(247.63, 601.53)	(220.53, 556.67)	
Change values	47.14 (−344.16, 348.62)		67.87 (−59.22, 224.94)		−103.92 (−367.59, 177.84)		−20.77 (−43.49, 8.17)		0.678
SP_{IH} (ms)	144.59	140.02	138.21	139.33	142.29	145.58	141.98	137.44	
	(113.82, 165.44)	(105.91, 163.32)	(118.58, 159.36)	(126.41, 169.31)$^{\#}$	(117.51, 165.21)	(127.09, 157.54)	(118.17, 215.04)	(106.77, 211.84)	
Change values	−5.11 (−13.52, 5.19)		8.50 (3.13, 14.79)^{a,s}		2.48 (−3.36, 9.72)		−5.25 (−8.67, −1.50)		0.007
SP_{CH} (ms)	134.68	132.57	135.59	135.18	136.99	142.94	127.95	135.55	
	(124.78, 151.61)	(118.94, 160.67)	(116.16, 151.57)	(117.18, 148.02)	(123.75, 257.60)	(126.98, 155.93)	(118.98, 141.38)	(121.44, 145.47)	
Change values	2.25 (−14.66, 9.06)		−0.41 (−2.84, 1.85)		0.83 (−3.69, 6.39)		1.84 (−6.51, 13.81)		0.822

Data are presented as the median (Interquartile range) (The Shapiro–Wilk test was used to determine the values are not normally distributed). IH, ipsilateral hemisphere relatively to the stimulating side; CH, contralateral hemisphere relatively to the stimulating side. Change values were calculated by subtracting the baseline data from the post-test data. $^{a}p < 0.05$ *as compared with M1 group;* $^{s}p < 0.05$ *as compared with Sham group.*

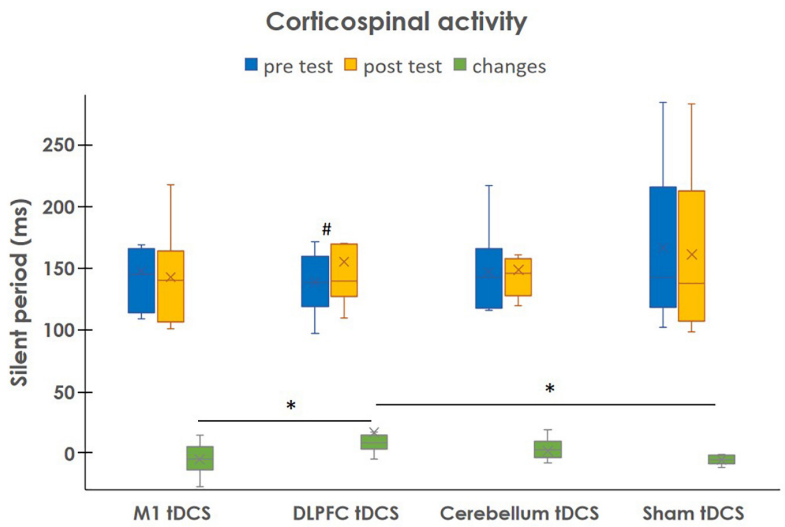

FIGURE 3 | Changes in silent period of ipsilateral hemisphere relatively to the stimulating side after different tDCS stimulations. Data are presented as the median (interquartile range). $^{\#}P < 0.05$: intragroup comparison. $^{*}P < 0.05$: intergroup comparison.

lengthening in SP duration and improvement of single walking performance after the combination of high-frequency repetitive transcranial magnetic stimulation (rTMS) and treadmill training in patients with PD (Yang et al., 2013). Fisher et al. (2008) demonstrated the SP lengthening associated with walking improvements after treadmill training and thus speculated SP lengthening could restore the normal motor processing in people with PD. Recent studies have provided the evidence for the potential of one session of DLPFC tDCS to enhance dopamine release in the striatum (Fonteneau et al., 2018; Fukai et al., 2019). A previous study also reported that dopaminergic treatment could prolong SP duration in patients with PD and suggested that SP may be modulated by the dopamine system (Nakashima et al., 1995). Furthermore, the recent study showed tDCS-induced dopamine release and GABA changes, which contributes to the phenomenon of SP (Bunai et al., 2021). Taking

TABLE 4 | Single walking and timed up and go performance after different tDCS interventions.

Group	M1 group (n = 9)	DLPFC group (n = 9)	Cerebellum group (n = 9)	Sham group (n = 9)	Time	Group	Time × group
					p-value, F-value	p-value, F-value	p-value, F-value, η^2
Single walking							
Speed (cm/sec)					<0.001, $F(3,32) = 15.272$	0.056, $F(3,32) = 2.800$	0.197, $F(3,32) = 1.653$, 0.134
Pre	113.94 ± 22.1	101.14 ± 21.4	87.19 ± 21.8	101.17 ± 18.9			
Post	121.59 ± 26.6	114.30 ± 19.3#	92.18 ± 22.7	103.50 ± 19.4			
Cadence (step/min)					0.012, $F(3,32) = 7.176$	0.117, $F(3,32) = 2.119$	0.058, $F(3,32) = 2.764$, 0.206
Pre	120.09 ± 8.4	116.86 ± 12.0	107.78 ± 11.9	120.26 ± 8.4			
Post	121.41 ± 12.0	124.44 ± 12.5#	112.16 ± 13.3	119.93 ± 10.0			
ST (sec)					0.792, $F(3,32) = 0.070$	0.102, $F(3,32) = 2.250$	0.052, $F(3,32) = 2.858$, 0.211
Pre	1.01 ± 0.1	1.04 ± 0.1	1.12 ± 0.1	0.88 ± 0.3			
Post	1.01 ± 0.1	0.97 ± 0.1	1.09 ± 0.2	1.01 ± 0.1			
SL (cm)					<0.001, $F(3,32) = 16.406$	0.067, $F(3,32) = 2.623$	0.130, $F(3,32) = 2.023$, 0.159
Pre	113.55 ± 18.8	103.31 ± 14.9	96.41 ± 16.4	100.68 ± 14.6			
Post	120.33 ± 19.7#	110.27 ± 11.0	97.59 ± 17.7	102.92 ± 14.0			
ST variability (%)					0.049, $F(3,32) = 4.190$	0.298, $F(3,32) = 1.278$	0.589, $F(3,32) = 0.650$, 0.057
Pre	3.07 ± 1.4	3.08 ± 1.6	6.06 ± 5.5	6.07 ± 9.2			
Post	1.89 ± 0.9	2.90 ± 0.8	3.38 ± 1.2	2.58 ± 1.7			
SL variability (%)					0.134, $F(3,32) = 2.369$	0.743, $F(3,32) = 0.415$	0.496, $F(3,32) = 0.813$, 0.071
Pre	4.10 ± 2.9	3.86 ± 3.1	4.86 ± 3.2	3.68 ± 1.8			
Post	3.56 ± 2.8	4.25 ± 2.9	6.25 ± 3.4	2.53 ± 1.0			
Timed up and go (sec)					0.939, $F(3,32) = 0.006$	0.832, $F(3,32) = 0.289$	0.335, $F(3,32) = 1.174$, 0.099
Pre	9.59 ± 1.9	10.92 ± 2.1	13.56 ± 2.9	11.83 ± 4.0			
Post	9.92 ± 1.9	10.58 ± 1.4	13.26 ± 2.2	12.18 ± 3.3			

Data are presented as the mean ± SD (the Shapiro–Wilk test was used to determine the values are normally distributed).
ST, stride time; SL, stride length.
#P < 0.05 for intragroup comparison (analyzed using paired t-test).

together, the beneficial motor effects of DLPFC tDCS may be related to dopamine release, therefore modulating the cortical inhibition in individuals with PD.

In contrast, dual tasking exacerbates the gait impairments in people with PD, suggesting the overloaded recruitment of prefrontal cortex (cognitive overloaded) under dual-task walking (Strouwen et al., 2015). DLPFC has been recognized as the key area for executive function which involves in many daily activities, especially dual-task walking (Lu et al., 2015). Therefore, we speculated that the improvements in dual-task walking after DLPFC tDCS may also be resulted from direct modulation of DLPFC. In this study, the participants walked faster by 24% under cognitive dual tasking after one session of DLPFC tDCS intervention. Mishra and Thrasher (2021) also reported that the increase of dual-task gait speed after a single session of DLPFC tDCS was more than Sham tDCS in patients with PD. Similarly, tDCS targeting the DLPFC has been reported to improve dual-task gait performance in older adults and people with stroke (Zhou et al., 2021). In contrast, we previously noted that the dual-task gait training for 12 sessions resulted in a 20% improvement of cognitive dual-task walking speed in people with PD (Yang et al., 2019). Therefore, DLPFC tDCS is an effective intervention to immediately improve dual-task walking ability for individuals with PD.

However, it should be mentioned that the DLPFC tDCS group did not improve significantly more in single walking and TUG performance as compared with other groups, although the DLPFC tDCS group showed a pre-post significant improvement in single walking. This may indicate that the dual-task walking performance is more sensitive to reflect the response to intervention, and single walking and TUG performance may need cumulative tDCS interventions for a significant improvement. In addition, it is interesting to note that the RMT and MEP did not change significantly after DLPFC tDCS. Studies have reported that RMT is normal and MEP is variable in people with PD (Lefaucheur, 2005; Rossini et al., 2015). However, decreased SP has been reported consistently in patients with PD (Wu et al., 2007). Therefore, measurement of SP may be a

better indicator to reflect cortical activity changes during disease progression and in response to treatment than RMT and MEP in individuals with PD.

Regarding the cerebellum tDCS, Workman et al. (2020) did not observe a significant single-session effect in single walking performance in people with PD. However, Jayaram et al. (2012) found that one session of anodal cerebellum tDCS resulted in better adaptation on a split-belt treadmill than Sham tDCS in healthy subjects. This study noted that the cerebellum tDCS exerted a significant within-group improvement in dual-task walking but not in single walking and TUG performance. However, such within-group improvement did not couple with significant changes in SP duration. This result lent us to speculate the vestibulocerebellum pathways, which are majorly involved in posture and balance control (Purves et al., 2001), may be modulated by cerebellum tDCS, but this warrants further exploration.

It also drew our attention that one session of anodal tDCS over M1 did not improve the walking performance, and such results were consistent with the results reported by Verheyden et al. (2013). Although Fregni et al. (2006) demonstrated that M1 tDCS improves UPDRS motor scores, limited improvement in the UPDRS gait-related items was noted. Moreover, Schabrun et al. (2016) demonstrated that M1 tDCS did not enhance the effect of dual-task gait training and suggested that M1 tDCS may not be an effective application to improve dual-task walking in individuals with PD. Considering the results of previous studies and this study, it still needs more investigations to establish the beneficial effects of tDCS over M1 on walking performance in people with PD.

Some limitations should be mentioned regarding this study. First, the relatively small number of participants in each group may lead to type II error. The limited sample size and heterogeneity of patients with PD must be considered when generalizing the study results. Second, the included participants were with mild to moderate disease severity (Hoehn and Yahr stages I–III), and the outcomes were measured only at "on" status. Therefore, our findings may only be applicable to individuals with mild to moderate PD at "on" status. Third, we only investigated the post-intervention effects of single-session tDCS, but the maintenance effects or accumulative effects of tDCS are not known. Fourth, we applied 2 mA for all targets because the current with 2 mA was most commonly used in the previous studies, especially in the studies focusing on walking ability (Ferrucci et al., 2015; Liu et al., 2021). However, the best parameter for tDCS in different targets may be different. Therefore, the results may not represent the best effect of tDCS in these targets. Further studies may need to establish the best stimulating intensity of tDCS in various targets. Finally, it has been noted that a single session of DLPFC tDCS could improve cognitive function according to the results of a meta-analysis (Dedoncker et al., 2016). However, we did not measure cognitive performances in this study. Therefore, the cognitive improvement cannot be excluded from the beneficial effects of DLPFC tDCS.

CONCLUSION

The results suggest that one session of DLPFC tDCS can be recommended to improve dual-task walking. Further research is needed to explore the effects of multisessions of DLPFC tDCS.

DATA AVAILABILITY STATEMENT

The raw data supporting the conclusions of this article will be made available by the authors, without undue reservation.

ETHICS STATEMENT

The studies involving human participants were reviewed and approved by Institutional Review Board of Taipei Veterans General Hospital. The patients/participants provided their written informed consent to participate in this study.

AUTHOR CONTRIBUTIONS

P-LW and R-YW conceived and designed the experiments. P-LW performed the experiments. P-LW and Y-RY analyzed the data. J-LF and H-LC confirmed the medical diagnosis of subjects and recruited subjects. P-LW, Y-RY, and S-FH interpreted the data and prepared the manuscript. All authors approved the final manuscript for submission.

FUNDING

This work was supported by grants from the Ministry of Science and Technology, Taiwan (MOST-106-2314-B-010-037-MY3), and the National Health Research Institutes, Taiwan (NHRI-EX110-10913PI).

ACKNOWLEDGMENTS

We would like to thank the study participants.

REFERENCES

Al-Yahya, E., Mahmoud, W., Meester, D., Esser, P., and Dawes, H. (2019). Neural substrates of cognitive motor interference during walking; Peripheral and Central Mechanisms. *Front. Hum. Neurosci.* 12:536. doi: 10.3389/fnhum.2018.00536

Benecke, R., Rothwell, J. C., Dick, J. P., Day, B. L., and Marsden, C. D. (1986). Performance of simultaneous movements in patients with Parkinson's disease. *Brain* 109, 739–757. doi: 10.1093/brain/109.4.739

Beurskens, R., Helmich, I., Rein, R., and Bock, O. (2014). Age-related changes in prefrontal activity during walking in dual-task situations: a fNIRS study. *Int. J. Psychophysiol.* 92, 122–128. doi: 10.1016/j.ijpsycho.2014.03.005

Bunai, T., Hirosawa, T., Kikuchi, M., Fukai, M., Yokokura, M., Ito, S., et al. (2021). tDCS-induced modulation of GABA concentration and dopamine release in the human brain: a combination study of magnetic resonance spectroscopy and positron emission tomography. *Brain Stimul.* 14, 154–160. doi: 10.1016/j.brs.2020.12.010

Collette, F., Olivier, L., Van der Linden, M., Laureys, S., Delfiore, G., Luxen, A., et al. (2005). Involvement of both prefrontal and inferior parietal cortex in dual-task performance. *Brain Res Cogn Brain Res.* 24, 237–51. doi: 10.1016/j.cogbrainres.2005.01.023

Dedoncker, J., Brunoni, A. R., Baeken, C., and Vanderhasselt, M. A. (2016). A Systematic Review and Meta-Analysis of the Effects of Transcranial Direct Current Stimulation (tDCS) Over the Dorsolateral Prefrontal Cortex in Healthy and Neuropsychiatric Samples: influence of Stimulation Parameters. *Brain Stimul.* 9, 501–517. doi: 10.1016/j.brs.2016.04.006

Ferrucci, R., Cortese, F., Bianchi, M., Pittera, D., Turrone, R., Bocci, T., et al. (2016). Cerebellar and motor cortical transcranial stimulation decrease levodopa-induced dyskinesias in Parkinson's disease. *Cerebellum* 15, 43–47. doi: 10.1007/s12311-015-0737-x

Ferrucci, R., Cortese, F., and Priori, A. (2015). Cerebellar tDCS: how to do it. *Cerebellum* 14, 27–30. doi: 10.1007/s12311-014-0599-7

Fisher, B. E., Wu, A. D., Salem, G. J., Song, J., Lin, C. H., Yip, J., et al. (2008). The effect of exercise training in improving motor performance and corticomotor excitability in people with early Parkinson's disease. *Arch. Phys. Med. Rehabil.* 89, 1221–1229. doi: 10.1016/j.apmr.2008.01.013

Fonteneau, C., Redoute, J., Haesebaert, F., Le Bars, D., Costes, N., Suaud-Chagny, M. F., et al. (2018). Frontal transcranial direct current stimulation induces dopamine release in the ventral striatum in human. *Cereb. Cortex.* 28, 2636–2646. doi: 10.1093/cercor/bhy093

Fregni, F., Boggio, P. S., Santos, M. C., Lima, M., Vieira, A. L., Rigonatti, S. P., et al. (2006). Noninvasive cortical stimulation with transcranial direct current stimulation in Parkinson's disease. *Mov. Disord.* 21, 1693–1702. doi: 10.1002/mds.21012

Fukai, M., Bunai, T., Hirosawa, T., Kikuchi, M., Ito, S., Minabe, Y., et al. (2019). Endogenous dopamine release under transcranial direct-current stimulation governs enhanced attention: a study with positron emission tomography. *Transl Psychiatry.* 9:115. doi: 10.1038/s41398-019-0443-4

Gaspar, P., Duyckaerts, C., Alvarez, C., Javoy-Agid, F., and Berger, B. (1991). Alterations of dopaminergic and noradrenergic innervations in motor cortex in Parkinson's disease. *Ann. Neurol.* 30, 365–374. doi: 10.1002/ana.410300308

Groppa, S., Oliviero, A., Eisen, A., Quartarone, A., Cohen, L. G., Mall, V., et al. (2012). A practical guide to diagnostic transcranial magnetic stimulation: report of an IFCN committee. *Clin. Neurophysiol.* 123, 858–882. doi: 10.1016/j.clinph.2012.01.010

Hausdorff, J. M., Cudkowicz, M. E., Firtion, R., Wei, J. Y., and Goldberger, A. L. (1998). Gait variability and basal ganglia disorders: stride-to-stride variations of gait cycle timing in Parkinson's disease and Huntington's disease. *Mov. Disord.* 13, 428–437. doi: 10.1002/mds.870130310

Ilg, W., and Timmann, D. (2013). Gait ataxia–specific cerebellar influences and their rehabilitation. *Mov. Disord.* 15, 1566–1575. doi: 10.1002/mds.25558

Jayaram, G., Tang, B., Pallegadda, R., Vasudevan, E. V., Celnik, P., and Bastian, A. (2012). Modulating locomotor adaptation with cerebellar stimulation. *J. Neurophysiol.* 107, 2950–2957. doi: 10.1152/jn.00645.2011

Kapogiannis, D., and Wassermann, E. M. (2008). Transcranial magnetic stimulation in Clinical Pharmacology. *Cent. Nerv. Syst. Agents Med. Chem.* 8, 234–240. doi: 10.2174/187152408786848076

Kaski, D., Dominguez, R. O., Allum, J. H., Islam, A. F., and Bronstein, A. M. (2014). Combining physical training with transcranial direct current stimulation to improve gait in Parkinson's disease: a pilot randomized controlled study. *Clin. Rehabil.* 28, 1115–1124. doi: 10.1177/0269215514534277

Kelly, V. E., Eusterbrock, A. J., and Shumway-Cook, A. (2012). A review of dual-task walking deficits in people with Parkinson's disease: motor and cognitive contributions, mechanisms, and clinical implications. *Parkinsons Dis.* 2012:918719. doi: 10.1155/2012/918719

Kishore, A., Meunier, S., and Popa, T. (2014). Cerebellar influence on motor cortex plasticity: behavioral implications for Parkinson's disease. *Front. Neurol.* 5:68. doi: 10.3389/fneur.2014.00068

Lattari, E., Costa, S. S., Campos, C., de Oliveira, A. J., Machado, S., and Maranhao Neto, G. A. (2017). Can transcranial direct current stimulation on the dorsolateral prefrontal cortex improves balance and functional mobility in Parkinson's disease? *Neurosci Lett.* 636, 165–169. doi: 10.1016/j.neulet.2016.11.019

Lees, A. J., Hardy, J., and Revesz, T. (2009). Parkinson's disease. *Lancet* 373, 2055–2066. doi: 10.1016/S0140-6736(09)60492-X

Lefaucheur, J. P. (2005). Motor cortex dysfunction revealed by cortical excitability studies in Parkinson's disease: influence of antiparkinsonian treatment and cortical stimulation. *Clin. Neurophysiol.* 116, 244–253. doi: 10.1016/j.clinph.2004.11.017

Liu, X., Liu, H., Liu, Z., Rao, J., Wang, J., Wang, P., et al. (2021). Transcranial Direct Current Stimulation for Parkinson's Disease: a Systematic Review and Meta-Analysis. *Front. Aging Neurosci.* 28:746797. doi: 10.3389/fnagi.2021.746797

Lu, C. F., Liu, Y. C., Yang, Y. R., Wu, Y. T., and Wang, R. Y. (2015). Maintaining Gait Performance by Cortical Activation during Dual-Task Interference: a Functional Near-Infrared Spectroscopy Study. *PLoS One* 10:e0129390. doi: 10.1371/journal.pone.0129390

Manenti, R., Brambilla, M., Rosini, S., Orizio, I., Ferrari, C., Borroni, B., et al. (2014). Time up and go task performance improves after transcranial direct current stimulation in patient affected by Parkinson's disease. *Neurosci Lett.* 580, 74–77. doi: 10.1016/j.neulet.2014.07.052

Mishra, R. K., and Thrasher, A. T. (2021). Transcranial direct current stimulation of dorsolateral prefrontal cortex improves dual-task gait performance in patients with Parkinson's disease: a double blind, sham-controlled study. *Gait Posture* 84, 11–16. doi: 10.1016/j.gaitpost.2020.11.012

Morris, S., Morris, M. E., and Iansek, R. (2001). Reliability of measurements obtained with the Timed "Up & Go" test in people with Parkinson disease. *Phys. Ther.* 81, 810–818. doi: 10.1093/ptj/81.2.810

Nakashima, K., Wang, Y., Shimoda, M., Sakuma, K., and Takahashi, K. (1995). Shortened silent period produced by magnetic cortical stimulation in patients with Parkinson's disease. *J. Neurol. Sci.* 130, 209–214. doi: 10.1016/0022-510x(95)00029-2

Nieuwhof, F., Reelick, M. F., Maidan, I., Mirelman, A., Hausdorff, J. M., Olde Rikkert, M. G., et al. (2016). Measuring prefrontal cortical activity during dual task walking in patients with Parkinson's disease: feasibility of using a new portable fNIRS device. *Pilot Feasibility Stud.* 2:59. doi: 10.1186/s40814-016-0099-2

Paulus, W., Classen, J., Cohen, L. G., Large, C. H., Di Lazzaro, V., Nitsche, M., et al. (2008). State of the art: pharmacologic effects on cortical excitability measures tested by transcranial magnetic stimulation. *Brain Stimul.* 1, 151–163. doi: 10.1016/j.brs.2008.06.002

Polanía, R., Paulus, W., and Nitsche, M. A. (2012). Modulating cortico-striatal and thalamo-cortical functional connectivity with transcranial direct current stimulation. *Hum. Brain Mapp.* 33, 2499–2508. doi: 10.1002/hbm.21380

Potvin-Desrochers, A., and Paquette, C. (2021). Potential Non-invasive Brain Stimulation Targets to Alleviate Freezing of Gait in Parkinson's Disease. *Neuroscience* 468, 366–376. doi: 10.1016/j.neuroscience.2021.05.037

Purves, D., Augustine, G. J., Fitzpatrick, D., Hall, W. C., LaMantia, A. S., McNamara, J. O., et al. (2001). *Neuroscience. second ed.* United States: Sinauer Associates.

Raffegeau, T. E., Krehbiel, L. M., Kang, N., Thijs, F. J., Altmann, L. J. P., Cauraugh, J. H., et al. (2019). A meta-analysis: Parkinson's disease and dual-task walking. *Parkinson. Relat. Disord.* 62, 28–35. doi: 10.1016/j.parkreldis.2018.12.012

Rossini, P. M., Burke, D., Chen, R., Cohen, L. G., Daskalakis, Z., Di Iorio, R., et al. (2015). Non-invasive electrical and magnetic stimulation of the brain, spinal cord, roots and peripheral nerves: basic principles and procedures for routine clinical and research application. An updated report from an I.F.C.N. Committee. *Clin. Neurophysiol.* 126, 1071–1107. doi: 10.1016/j.clinph.2015.02.001

Sánchez-Kuhn, A., Pérez-Fernández, C., Cánovas, R., Flores, P., and Sánchez-Santed, F. (2017). Transcranial direct current stimulation as a motor neurorehabilitation tool: an empirical review. *Biomed. Eng. Online* 16:76. doi: 10.1186/s12938-017-0361-8

Schabrun, S. M., Lamont, R. M., and Brauer, S. G. (2016). Transcranial direct current stimulation to enhance dual-task gait training in Parkinson's disease: a pilot RCT. *PLoS One* 11:e0158497. doi: 10.1371/journal.pone.0158497

Shine, J. M., Matar, E., Ward, P. B., Frank, M. J., Moustafa, A. A., Pearson, M., et al. (2013). Freezing of gait in Parkinson's disease is associated with functional

decoupling between the cognitive control network and the basal ganglia. *Brain* 136, 3671–3681. doi: 10.1093/brain/awt272

Strouwen, C., Molenaar, E. A., Münks, L., Keus, S. H., Bloem, B. R., Rochester, L., et al. (2015). Dual tasking in Parkinson's disease: should we train hazardous behavior? *Expert Rev. Neurother.* 15, 1031–1039. doi: 10.1586/14737175.2015.1077116

Verheyden, G., Purdey, J., Burnett, M., Cole, J., and Ashburn, A. (2013). Immediate effect of transcranial direct current stimulation on postural stability and functional mobility in Parkinson's disease. *Mov. Disord.* 28, 2040–2041. doi: 10.1002/mds.25640

Werhahn, K. J., Kunesch, E., Noachtar, S., Benecke, R., and Classen, J. (1999). Differential effects on motorcortical inhibition induced by blockade of GABA uptake in humans. *J. Physiol.* 517, 591–597. doi: 10.1111/j.1469-7793.1999.0591t.x

Workman, C. D., Fietsam, A. C., Uc, E. Y., and Rudroff, T. (2020). Cerebellar transcranial direct current stimulation in people with Parkinson's disease: a pilot study. *Brain Sci.* 10, 96. doi: 10.3390/brainsci10020096

Wu, A. D., Petzinger, G. M., Lin, C. H., Kung, M., and Fisher, B. (2007). Asymmetric corticomotor excitability correlations in early Parkinson's disease. *Mov Disord.* 22, 1587–1593. doi: 10.1002/mds.21565

Wu, T., and Hallett, M. (2005). A functional MRI study of automatic movements in patients with Parkinson's disease. *Brain* 128, 2250–2259. doi: 10.1093/brain/awh569

Yang, Y. R., Cheng, S. J., Lee, Y. J., Liu, Y. C., and Wang, R. Y. (2019). Cognitive and motor dual task gait training exerted specific training effects on dual task gait performance in individuals with Parkinson's disease: a randomized controlled pilot study. *PLoS One* 14:e0218180. doi: 10.1371/journal.pone.0218180

Yang, Y. R., Tseng, C. Y., Chiou, S. Y., Liao, K. K., Cheng, S. J., Lai, K. L., et al. (2013). Combination of rTMS and treadmill training modulates corticomotor inhibition and improves walking in Parkinson disease: a randomized trial. *Neurorehabil. Neural. Repair.* 27, 79–86.

Yuan, P., and Raz, N. (2014). Prefrontal cortex and executive functions in healthy adults: a meta-analysis of structural neuroimaging studies. *Neurosci. Biobehav. Rev.* 42, 180–192. doi: 10.1016/j.neubiorev.2014.02.005

Zhou, J., Manor, B., Yu, W., Lo, O. Y., Gouskova, N., Salvador, R., et al. (2021). Targeted tDCS Mitigates Dual-Task Costs to Gait and Balance in Older Adults. *Ann. Neurol.* 90, 428–439. doi: 10.1002/ana.26156

Conflict of Interest: The authors declare that the research was conducted in the absence of any commercial or financial relationships that could be construed as a potential conflict of interest.

Publisher's Note: All claims expressed in this article are solely those of the authors and do not necessarily represent those of their affiliated organizations, or those of the publisher, the editors and the reviewers. Any product that may be evaluated in this article, or claim that may be made by its manufacturer, is not guaranteed or endorsed by the publisher.

frontiers in Aging Neuroscience

ORIGINAL RESEARCH
published: 07 February 2022
doi: 10.3389/fnagi.2022.818340

Intermittent Theta Burst Stimulation Increases Natural Oscillatory Frequency in Ipsilesional Motor Cortex Post-Stroke: A Transcranial Magnetic Stimulation and Electroencephalography Study

Qian Ding[1], Songbin Chen[1], Jixiang Chen[1], Shunxi Zhang[1], Yuan Peng[1], Yujie Chen[1], Junhui Chen[1], Xiaotong Li[1], Kang Chen[1], Guiyuan Cai[1], Guangqing Xu[2] and Yue Lan[1]**

[1] Department of Rehabilitation Medicine, Guangzhou First People's Hospital, South China University of Technology, Guangzhou, China, [2] Department of Rehabilitation Medicine, Guangdong Provincial People's Hospital, Guangdong Academy of Medical Sciences, Guangzhou, China

Objective: Intermittent theta burst stimulation (iTBS) has been widely used as a neural modulation approach in stroke rehabilitation. Concurrent use of transcranial magnetic stimulation and electroencephalography (TMS-EEG) offers a chance to directly measure cortical reactivity and oscillatory dynamics and allows for investigating neural effects induced by iTBS in all stroke survivors including individuals without recordable MEPs. Here, we used TMS-EEG to investigate aftereffects of iTBS following stroke.

Methods: We studied 22 stroke survivors (age: 65.2 ± 11.4 years; chronicity: 4.1 ± 3.5 months) with upper limb motor deficits. Upper-extremity component of Fugl-Meyer motor function assessment and action research arm test were used to measure motor function of stroke survivors. Stroke survivors were randomly divided into two groups receiving either Active or Sham iTBS applied over the ipsilesional primary motor cortex. TMS-EEG recordings were performed at baseline and immediately after Active or Sham iTBS. Time and time-frequency domain analyses were performed for quantifying TMS-evoked EEG responses.

Results: At baseline, natural frequency was slower in the ipsilesional compared with the contralesional hemisphere ($P = 0.006$). Baseline natural frequency in the ipsilesional hemisphere was positively correlated with upper limb motor function following stroke ($P = 0.007$). After iTBS, natural frequency in the ipsilesional hemisphere was significantly increased ($P < 0.001$).

Conclusions: This is the first study to investigate the acute neural adaptations after iTBS in stroke survivors using TMS-EEG. Our results revealed that natural frequency is

OPEN ACCESS

Edited by:
Yi Guo,
Jinan University, China

Reviewed by:
Nivethida Thirugnanasambandam, National Brain Research Centre (NBRC), India
Jack Jiaqi Zhang, Hong Kong Polytechnic University, Hong Kong SAR, China
Yuka Okazaki, National Institute for Physiological Sciences (NIPS), Japan

***Correspondence:**
Guangqing Xu
guangchingx@163.com
Yue Lan
bluemooning@163.com

Specialty section:
This article was submitted to Neuroinflammation and Neuropathy, a section of the journal Frontiers in Aging Neuroscience

Received: *19 November 2021*
Accepted: *05 January 2022*
Published: *07 February 2022*

Citation:
Ding Q, Chen S, Chen J, Zhang S, Peng Y, Chen Y, Chen J, Li X, Chen K, Cai G, Xu G and Lan Y (2022) Intermittent Theta Burst Stimulation Increases Natural Oscillatory Frequency in Ipsilesional Motor Cortex Post-Stroke: A Transcranial Magnetic Stimulation and Electroencephalography Study. Front. Aging Neurosci. 14:818340. doi: 10.3389/fnagi.2022.818340

altered following stroke which is related to motor impairments. iTBS increases natural frequency in the ipsilesional motor cortex in stroke survivors. Our findings implicate that iTBS holds the potential to normalize natural frequency in stroke survivors, which can be utilized in stroke rehabilitation.

Keywords: intermittent theta burst stimulation, TMS-EEG, natural frequency, stroke rehabilitation, evoked oscillatory response

INTRODUCTION

Stroke is a debilitating acquired neurological injury and the leading cause of adult disability over the world (Lloyd-Jones et al., 2010). Upper limb motor deficits frequently occur following stroke, which negatively impact quality of life in stroke survivors (Tedesco Triccas et al., 2019). Motor impairment following stroke has been suggested to arise from disruptions of structural and functional integrity at both local and global scales (Bonkhoff et al., 2020). Intermittent theta burst stimulation (iTBS) is a specific form of repetitive transcranial magnetic stimulation (rTMS) that can effectively enhance cortical excitability and modulate oscillatory dynamics in both stimulated area and remote brain regions (Suppa et al., 2016; Ding et al., 2021c). iTBS has been considered as a promising approach for stroke rehabilitation (Corti et al., 2012; Suppa et al., 2016).

Neural effects of iTBS are typically investigated by motor evoked potentials (MEP), which are muscular responses elicited by single-pulse TMS (Talelli et al., 2007; Di Lazzaro et al., 2008; Ding et al., 2021b). However, this approach is not applicable to stroke survivors in whom MEPs are not elicitable. Furthermore, MEPs reflect cortical excitability in only motor cortex but not non-motor brain regions. Concurrent use of TMS and electroencephalography (EEG) (i.e., TMS-EEG) would overcome the drawbacks of MEP measurements, which offers a chance to simultaneously monitor cortical activity in both stimulated area and the interconnected cortical networks (Casula et al., 2021). Importantly, as TMS-EEG can directly measure cortical reactivity and oscillatory dynamics regardless of the integrity of corticospinal tracts (Borich et al., 2016), it allows for investigating neural effects induced by iTBS in stroke survivors without recordable MEPs (Pellicciari et al., 2018).

TMS-EEG signals can be analyzed in both time and time-frequency domains. TMS-evoked potential (TEP) is a complex waveform time-locked to the TMS pulse. TEPs reflect the direct activation of the cortical neurons at the stimulated brain regions (Pellicciari et al., 2018; Tremblay et al., 2019). In the time domain, TEPs can be quantified either by the amplitude and latency of peaks, or by the area under the curve of the rectified signals over the electrodes of interest [i.e., local mean field power (LMFP)] or over the entire surface of the head [i.e., global mean field power (GMFP)] (Tremblay et al., 2019). It has been suggested that LMFP and GMFP take both the width and the amplitude of TEPs into account and do not require an obvious main peak to present (Tremblay et al., 2019). As TEP main peaks are not always present in stroke survivors, LMFP and GMFP have the advantage of quantifying TEPs in stroke studies (Tscherpel et al., 2020). The acute adaptations in LMFP and GMFP after iTBS have been investigated in healthy adults, but results remain inconsistent in current literature (Gedankien et al., 2017; Bai et al., 2021; Ozdemir et al., 2021). Some studies reported no change in LMFP or GMFP after iTBS (Gedankien et al., 2017; Ozdemir et al., 2021), while one study reported reduced GMFP after iTBS (Bai et al., 2021). The adaptations in LMFP and GMFP after iTBS have not been investigated in stroke survivors.

Time-frequency domain analysis offers possibility to study the functional specificity of cortical oscillations in each frequency band [i.e., evoked oscillatory response (EOR)] (Thut and Miniussi, 2009). The adaptations in EOR after iTBS have been investigated in healthy adults, but results were inconsistent (Casula et al., 2016; Chung et al., 2017; Bai et al., 2021). One study reported a reduction in alpha band EOR after iTBS (Bai et al., 2021), while some studies reported an increase in theta (Chung et al., 2017) or beta (Casula et al., 2016) band EOR after iTBS. Besides EOR, time-frequency domain analysis also allows for the study of natural frequency (i.e., the frequency with the maximal power in a specific brain region) (Tremblay et al., 2019). Each brain area preserves its natural frequency of oscillations when stimulated with TMS (Casula et al., 2016). Natural frequency reflects the intrinsic dynamics of the corresponding thalamocortical circuits as well as the intrinsic GABA transmissions and provides important insights in the aftereffects of plasticity-inducing protocols on cortical activities (Rosanova et al., 2009; Tremblay et al., 2019; Ferrarelli and Phillips, 2021). It has been suggested that iTBS elevates the amount of ongoing activity in the connections between the stimulation site and its interconnected brain regions, including the thalamocortical pathway (Bestmann et al., 2004; Suppa et al., 2008). As thalamus is the structure that generates high-frequency oscillations, strengthened thalamocortical connections after iTBS could increase natural frequency in the stimulated brain region (Ferrarelli et al., 2012; Casula et al., 2016). To our knowledge, no study has investigated the adaptations of natural frequency after iTBS in either healthy adults or stroke survivors.

Following stroke, disruption of the intra- and inter-hemispheric network architecture may result in cortical deafferentation from subcortical structures, especially thalamus (Tscherpel et al., 2020). As thalamocortical neurons have been

Abbreviations: iTBS, intermittent theta burst stimulation; rTMS, repetitive transcranial magnetic stimulation; MEP, motor evoked potential; EEG, electroencephalography; TEP, TMS-evoked potential; LMFP, local mean field power; GMFP, global mean field power; EOR, evoked oscillatory response; IH, ipsilesional hemisphere; CH, contralesional hemisphere; FMA, Fugl-Meyer assessment; ARAT, action research arm test; RMT, resting motor threshold; FDI, first dorsal interosseus; M1, primary motor cortex; MSO, maximum stimulator output; ICA, independent component analysis; ERSP, event-related spectral perturbation; LME, linear mixed effects.

implicated in generating fast oscillations (Ferrarelli et al., 2012), impaired thalamocortical connections following stroke may contribute to a slowing of natural frequency in the ipsilesional hemisphere (IH) (Tscherpel et al., 2020). The alterations of natural frequency following stroke has been reported in a recent study (Tscherpel et al., 2020). Tscherpel et al. (2020) observed slowing of IH natural frequency following stroke as well as a positive correlation between natural frequency and motor function in stroke survivors. Based on limited number of studies, it remains unclear whether natural frequency could be used as a biomarker indicating stroke recovery.

In present study, we used concurrent TMS and EEG to investigate the aftereffects of iTBS in stroke survivors. We hypothesized that (1) natural frequency is slower in the ipsilesional compared with the contralesional hemisphere (CH); (2) there is a positive correlation between IH natural frequency and motor function; (3) IH natural frequency is increased after the application of iTBS. These results would have potential implications for understanding the influences of iTBS on cortical oscillatory dynamics in stroke survivors.

MATERIALS AND METHODS

Subjects

Twenty-two stroke survivors were recruited into this study. Each subject provided written, informed consent prior to enrollment and participation. Approval for the experimental procedures was attained from Guangzhou First People's Hospital Human Research Ethics Committee (reference number: K-2021-130-01). The study was carried out in conformity with standards set by the Declaration of Helsinki. Stroke survivors were included if they had a single stroke less than 18 months prior to enrollment. All participants were screened for eligibility to receive TMS and excluded if they were pregnant; using medications that reduce seizure threshold; or any metal or implanted devices that might be affected by TMS (Rossi et al., 2009). As substances like alcohol and caffeine can influence the aftereffects of iTBS, participants were asked not to consume alcohol or caffeine prior to the experiment (Chung et al., 2017). Stroke survivors were excluded from this study if they had cognitive impairment (i.e., the score of Montreal Cognitive Assessment was below 22/30) (Nasreddine et al., 2005) and cannot comprehend or follow three step commands (Ding et al., 2018). Nineteen out of twenty-two stroke survivors were free from lesions in the primary motor cortex (M1). Demographic characteristics are described in **Tables 1**, **2**.

Experimental Procedure

This was a single-session, sham-controlled, randomized single-blinded study. Participants were randomly assigned to the experimental (Active iTBS) and control (Sham iTBS) groups, with eleven participants in each group. Participants were blinded with the group they were assigned to. Upper-extremity component of Fugl-Meyer motor function assessment (FMA) and action research arm test (ARAT) were used to assess motor impairment and upper limb motor function of stroke survivors, respectively. TMS-EEG recordings were performed at baseline and immediately after the completion of iTBS.

Intermittent Theta Burst Stimulation

A NS5000 Magnetic Stimulator (YIRUIDE Medical Co., Wuhan, China) equipped with a 70 mm figure-of-eight coil was used for TMS delivery (biphasic pulses, pulse width = 350 ms). TBS involves the application of a burst of three pulses at 50 Hz repeated at 5 Hz. iTBS involves the application of a 2 s train of TBS repeated every 10 s for a total of 192 s (Huang et al., 2005).

Prior to the application of iTBS, resting motor threshold (RMT) determination was performed in both hands in a random order. Surface electromyography was recorded from the first dorsal interosseus (FDI). Participants were seated comfortably in a chair and were asked to keep their eyes open throughout the experiment (Chung et al., 2017; Ding et al., 2018). During TMS, the coil was positioned tangentially 45 degrees to the midline. Participants were instructed to keep their arms relaxed while determining the optimal scalp position for eliciting maximal responses in the FDI (Ding et al., 2018). RMT was determined as the minimum intensity required to evoke 5 out of 10 MEPs greater than 50 μV at rest (Chen et al., 1998). A neuronavigation system (Visor2, ANT Neuro, Hengelo, Netherlands) was used to ensure consistent coil positioning over the optimal scalp position (i.e., motor hotspot) throughout the experiment (Ding et al., 2021a,c). For the individuals in whom MEPs in the IH cannot be elicited even with 100% MSO (n = 6 in the Active iTBS group and n = 5 in the Sham iTBS group), RMT in the IH was considered as 100% maximum stimulator output (MSO).

iTBS was applied over the motor hotspot in the ipsilesional M1. The iTBS stimulation intensity was set at 70% RMT in the IH (Volz et al., 2016; Ding et al., 2021c). During the application of iTBS, participants were instructed to remain static. As 40% MSO is the upper limit for iTBS with the NS5000 Magnetic Stimulator, iTBS stimulation intensity was set at 40% MSO if the calculated stimulation intensity was greater than 40% MSO (Ding et al., 2021c). For sham stimulation, the same stimulation intensity was used as for iTBS. The TMS coil was held perpendicular to the skull, touching the skull with the rim opposite the handle during sham stimulation (Nettekoven et al., 2014).

Transcranial Magnetic Stimulation-Electroencephalography Recordings

During TMS-EEG recording, participants were seated comfortably in a sound-shielded, dimly lit room. TMS was performed using a NS5000 Magnetic Stimulator (YIRUIDE Medical Co., Wuhan, China) (biphasic pulses, pulse width = 350 ms). A neuronavigation system (Visor2, ANT Neuro, Hengelo, Netherlands) was used during the application of TMS (Ding et al., 2021a).

TMS-evoked EEG responses were recorded using a TMS-compatible EEG cap (ANT Neuro, Enschede, Netherlands) with 64 Ag/AgCl electrodes in a layout based on the extended

TABLE 1 | Patients' demographic and clinical characteristics.

	Age, years	Sex	Paretic side	Type of stroke	Months after stroke onset	UE FMA (0–66)	ARAT (0–57)
	Mean ± SD (range)	Male/ Female	Right /Left	Ischemic/ Hemorrhagic	Mean ± SD (range)	Mean ± SD (range)	Mean ± SD (range)
Active iTBS group (*n* = 11)	62.4 ± 14.0 (35–77)	9/2	5/6	9/2	6.0 ± 4.8 (1–18)	29.1 ± 18.0 (4–58)	28.7 ± 18.2 (0–54)
Sham iTBS group (*n* = 11)	64.4 ± 12.2 (42–79)	9/2	5/6	9/2	4.5 ± 4.1 (1–15)	34.9 ± 21.3 (4–66)	29 ± 22.9 (0–57)

UE FMA refers to upper-extremity component of the Fugl-Meyer Motor Function Assessment, indicating motor impairments in stroke survivors (Fugl-Meyer et al., 1975).
ARAT refers to Action Research Arm Test, indicating upper extremity performance (i.e., coordination and dexterity) in neurological populations (Lang et al., 2006).
SD refers to standard deviation.
No significant difference in chronicity, UE FMA, or ARAT was revealed between subjects in Active and Sham iTBS groups.

international 10–20 system for electrodes placement (Jurcak et al., 2007; Tamburro et al., 2020). All channels were referenced online to CPz and amplified with an eego amplifier (ANT Neuro, Enschede, Netherlands). Data were sampled at 8,000 Hz with impedances kept below 5 kΩ for all channels throughout data collection. To prevent EEG auditory evoked potentials and eye muscle reactions induced by the TMS click, participants wore inserted earplugs during TMS-EEG recordings (Ter Braack et al., 2015; Tscherpel et al., 2020). To minimize bone conduction produced by TMS, we placed a thin layer of plastic film between the TMS coil and the EEG cap during testing (Massimini et al., 2007; Tscherpel et al., 2020).

TMS-EEG testing was performed in both hemispheres in a random order. During TMS-EEG recordings, 50 TMS pulses were applied on M1 (i.e., motor hotspot) in each hemisphere with a 5–8 s interval between two adjacent stimuli. Stimulation intensity was set at 80% RMT. On one hand, this intensity is suggested to be above the threshold of a significant EEG response (Tremblay et al., 2019; Tscherpel et al., 2020). On the other hand, as this intensity is below RMT, muscular responses are unlikely to be induced, which limits reafferent somatosensory feedback that is known to influence on the EEG responses (Tremblay et al., 2019). Of note, for the individuals in whom MEPs in the IH were not elicitable, we used RMT in the CH as a reference for setting stimulation intensities in the IH and defined ipsilesional motor hotspot based on anatomical landmarks (i.e., the hand knob) (Tscherpel et al., 2020).

Data Analysis

Transcranial Magnetic Stimulation-Electroencephalography Analysis

Acquired EEG signals were analyzed off-line using MATLAB2019b (Mathworks, Inc., Natick, MA, United States) with customized scripts. EEGLAB toolbox (version 14.1.2b) (Delorme and Makeig, 2004) and TMSEEG toolbox (Atluri et al., 2016) were used for data preprocessing. Continuous EEG data were epoched around the test TMS pulse (−1,000 to + 1,000 ms). Each data trial was baseline corrected with the mean of the pre-stimulus period from −700 to −200 ms (Atluri et al., 2016; Sun et al., 2018). Data from −5 to 20 ms was discarded to eliminate the large TMS artifact. Trials and channels that were outliers with high-frequency power were labeled and removed by guided visual inspection (Sun et al., 2018) (number of artifact-free trials: Active iTBS group: 44.3 ± 4.5, Sham iTBS group: 44.1 ± 2.2). TMS decay artifacts were cleaned by removing characteristic noise components extracted with independent component analysis (ICA) (number of ICA components removed: Active iTBS group: 4.9 ± 1.1, Sham iTBS group: 4.8 ± 0.8). The signals were then band-pass filtered to 1–45 Hz with a notch filter (50 Hz). After the signals were filtered, a second round of ICA was performed to eliminate other noise components (e.g., ocular, cardiac or muscular artifacts, etc.) (Delorme et al., 2007) (number of ICA components removed: Active iTBS group: 2.5 ± 1.4, Sham iTBS group: 2.7 ± 0.8). Any missing channels were linearly interpolated (number of interpolated channels: Active iTBS group: 5.2 ± 1.3, Sham iTBS group: 5.2 ± 1.6). All channels were then referenced to the average across all electrodes and sampled down to 1,000 Hz.

After preprocessing, EEG data trials were averaged for each recording condition to obtain TEPs. When visualizing the TEPs, we found that electrodes near the stimulating coil suffered from residual artifacts for up to + 30 ms, which cannot be completely cleaned by ICA (Komssi et al., 2004; Rogasch and Fitzgerald, 2013). To be consistent with previous studies (Rogasch and Fitzgerald, 2013; Gordon et al., 2018), data analysis in current study focused on TEPs after + 30 ms from the TMS onset. LMFP was computed as the square root of squared TEPs averaged across the five channels surrounding the stimulated motor cortex (Left motor cortex: C1, C3, FC1, FC3, Cz; Right motor cortex: C2, C4, FC2, FC4, Cz) (Tscherpel et al., 2020). To minimize the effect of possible artifacts occurring at the time of stimulation, LMFP was calculated over a 30–200 ms time window with using the following formula:

$$LMFP(t) = \sqrt{\frac{\left[\sum_i^k \left(V_i\left(t\right) - V_{mean}(t)\right)^2\right]}{K}} \quad (1)$$

where t is time, K is the number of channels, V_i is the voltage in channel i averaged across subjects, and V_{mean} is the averaged voltage in the channels of interest (Casula et al., 2016).

GMFP was computed as the square root of squared TEPs averaged across all active channels on the entire surface of the

TABLE 2 | Stroke characteristics.

Subject number	Sex	Age (years)	Paretic hand	Chronicity (months)	Type of stroke	Lesion location	UE FMA	RMT (MSO%)	iTBS stimulation intensity (MSO%)	iTBS stimulation intensity (RMT%)
S01	M	62	R	4	Ischemic	Basal ganglia	9	100	40	40
S02	M	72	L	2	Ischemic	Basal ganglia, periventricular white matter	43	80	40	50
S03	F	64	R	2	Ischemic	Frontal/temporal/ parietal lobe	4	100	40	40
S04	M	70	L	8	Ischemic	Pons	37	70	40	57
S05	M	57	R	8	Hemorrhagic	Frontal/parietal lobe	47	55	39	71
S06	M	77	L	1	Ischemic	Centrum semiovale, corona radiata, basal ganglia	58	70	40	57
S07	F	35	L	5	Ischemic	Frontal/parietal lobe	49	100	40	40
S08	M	69	R	11	Ischemic	Corona radiata	18	100	40	40
S09	M	70	R	3	Ischemic	Basal ganglia	26	75	40	53
S10	M	75	L	4	Ischemic	Pons	5	100	40	40
S11	M	35	L	18	Hemorrhagic	Basal ganglia	24	100	40	40
C01	M	78	L	3	Ischemic	Corona radiata, basal ganglia	60	70	40	57
C02	M	70	R	2	Ischemic	Basal ganglia	26	75	40	53
C03	M	42	L	6	Hemorrhagic	Pons	21	100	40	40
C04	F	79	R	2	Ischemic	Thalamus/ occipital lobe	36	40	28	70
C05	M	60	R	9	Ischemic	Frontal/parietal/ temporal lobe	4	100	40	40
C06	M	43	L	1	Ischemic	Frontal/parietal lobe, basal ganglia, corona radiata	64	20	14	70
C07	M	75	L	15	Ischemic	Parietal/temporal lobe	9	100	40	40
C08	F	58	R	1	Ischemic	Internal capsule	42	100	40	40
C09	M	68	L	3	Ischemic	Frontal/parietal/ temporal lobe, basil ganglia	66	30	21	70
C10	M	72	R	1	Hemorrhagic	Parietal/temporal lobe	44	40	28	70
C11	M	63	L	6	Ischemic	Basal ganglia, corona radiata, centrum semiovale, frontal lobe	12	100	40	40

UE FMA refers to upper-extremity component of the Fugl-Meyer Motor Function Assessment.
M refers to male, and F refers to female.
L refers to left, and R refers to right.
S01–11 indicate stroke survivors in the Active iTBS group.
C01–11 indicate stroke survivors in the Sham iTBS group.
Stroke lesions of all subjects except S03, S07 and C05 were free from the primary motor cortex.

head. GMFP was calculated over a 30–200 ms time window with using the following formula:

$$GMFP(t) = \sqrt{\frac{\left[\sum_i^k (V_i(t) - V_{mean}(t))^2\right]}{K}} \quad (2)$$

where t is time, K is the number of channels, V_i is the voltage in channel i averaged across subjects, and V_{mean} is the averaged voltages in all active channels (Lehmann and Skrandies, 1980; Pellicciari et al., 2018).

Spectral features in the time-frequency domain were evaluated by computing the event-related spectral perturbation (ERSP) based on Morlet wavelet transform as follows:

$$ERSP(f, t) = \frac{1}{n}\sum_{k=1}^{n} \left|F_k(f,\ t)\right|^2 \quad (3)$$

where for n trials, the spectral estimate F was computed at trial k, at frequency f and time t (Casula et al., 2018; Koch et al., 2020).

EOR was computed by averaging the oscillatory activity of channels surrounding the stimulated motor cortex (Left motor cortex: C1, C3, FC1, FC3, Cz; Right motor cortex: C2, C4, FC2, FC4, Cz). To minimize the effect of TMS artifacts, the frequency values were calculated by averaging the EOR values over a 30–200 ms time window. Subsequently, the spectral power in the frequency ranges between 2–4 Hz (delta), 4–8 Hz (theta), 8–13 Hz (alpha), and 13–30 Hz (beta) was extracted from the wavelet dataset (Pellicciari et al., 2018). Natural frequency was then calculated as the frequency with the largest cumulated ERSP upon stimulated motor cortex between 5–50 Hz (Tremblay et al., 2019; Tscherpel et al., 2020).

Statistical Analysis

Statistical analyses were performed in JMP Pro Version 13.2 (SAS Institute Inc., Cary, NC, United States) and FieldTrip toolbox (Oostenveld et al., 2011) in MATLAB2019b. Non-parametric cluster-based permutation tests by means of the Monte Carlo method were conducted to assess differential changes in LMFP and GMFP after iTBS between groups in each hemisphere. Comparisons were first made across time points for each iTBS condition (within-comparison). Between-group comparisons were performed using change-from-baseline score (i.e., after iTBS–before iTBS) (Chung et al., 2019). Monte Carlo P-values were calculated on 3,000 random permutations, and t-values within every cluster were summed up for cluster-level statistics in each permutation. The proportion of random permutations with larger test statistics than the observed one was the significance probability. Time points were considered significant when > 10 successive t-tests reached the significance threshold ($P < 0.025$) (Casula et al., 2016).

Linear mixed effects (LME) modeling was performed to test differential changes in EOR and natural frequency after iTBS between groups in each hemisphere. Group, Timepoint, and Group × Timepoint interaction were included as fixed effects, and subject was included as a random effect. Timepoint was set as repeated covariance structure. Normality of the residuals was visually assessed for each model with conditional residual quantile-quantile plots, and all were found to reasonably conform to the assumption of normality. *Post hoc* tests were performed when F-tests were significant. Multiple comparisons between Timepoints or Groups were performed with Tukey–Kramer adjustment.

The normality of data was tested using the Kolmogorov-Smirnov test before conducting correlation analyses. For the data that met the normality assumption, Pearson correlations were performed to investigate the relationship between baseline and changes in neurophysiological measures (e.g., LMFP, GMFP, EOR and natural frequency) and subject characteristics (e.g., age, chronicity, FMA, and ARAT). For the data that violated the normality assumption, Spearman correlations were performed instead. For all analyses, statistical significance was established at $P < 0.05$. *Post hoc* power analyses were performed using G*power (Version 3.1) (Faul et al., 2007) and JMP pro (Version 13.2) to determine whether current study had enough power to detect the differences between conditions, which calculated the power (1–β) as a function of α (0.05), the sample size, and the population effect size (Cohen, 1988; Chung et al., 2019).

RESULTS

All participants tolerated iTBS well and no adverse events were reported. TEPs in a representative patient are presented in **Figure 1**.

Local Mean Field Power and Global Mean Field Power

The cluster-based permutation test did not reveal any significant change after Active or Sham iTBS in either hemisphere (P's > 0.05) (**Figure 2**).

Transcranial Magnetic Stimulation-Evoked Oscillatory Response

The LME modeling did not reveal any significant main effect or interaction in any frequency band in either hemisphere (P's > 0.05) (**Figure 3**).

Natural Frequency

At baseline, natural frequency in the IH was significantly slower compared with the CH ($P = 0.006$, power = 0.67) (**Figure 4**).

In the IH, the LME modeling revealed significant main effect of Timepoint and Timepoint × Group interaction [$F_{(1,20)} = 6.00$, $P = 0.024$, power = 0.58; $F_{(1,20)} = 10.73$, $P = 0.004$, power = 0.81, respectively] in natural frequency. *Post hoc* revealed that in the Active iTBS group, natural frequency was significantly increased after iTBS ($P < 0.001$), while in the Sham iTBS group, natural frequency was not significantly changed after iTBS ($P > 0.05$) (**Figure 5**).

In the CH, the LME modeling did not reveal any significant main effect or interaction in natural frequency (P's > 0.05).

Correlation Analysis

Significant positive correlations were observed between baseline IH natural frequency and motor function (including ARAT and FMA) (r's = 0.56 and 0.54, P's = 0.007 and 0.009, power's = 0.81 and 0.77, respectively) (**Figure 6**). No significant correlation was observed between other neurophysiological measures (i.e., LMFP, GMFP and EOR) and subject characteristics (i.e., age, chronicity and motor function) (P's > 0.05).

DISCUSSION

In this study, we conducted concurrent TMS and EEG measurements at baseline and immediately after iTBS in stroke survivors. To our knowledge, this is the first study that used TMS-EEG to investigate the aftereffects of iTBS following stroke. At baseline, natural frequency was slower in the IH compared with CH, and IH natural frequency was positively correlated with

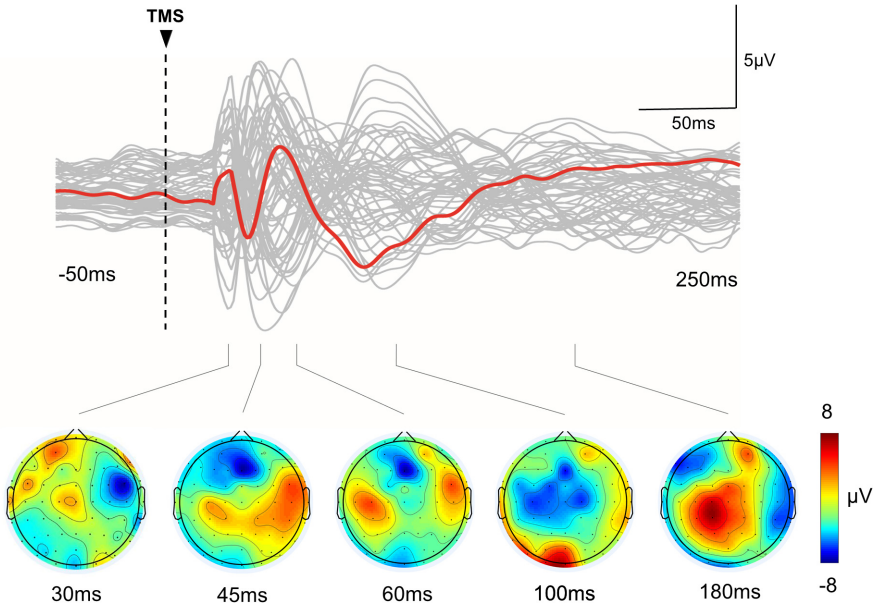

FIGURE 1 | TMS-evoked EEG potentials in a representative subject. Top row: The gray curves represent TEP in each channel, and the red bold curves represent the averaged TEP in the channels surrounding the stimulated motor cortex (C4). Bottom row: Topographic plots of the TMS-evoked responses at 30, 45, 60, 100, and 180 ms post-TMS.

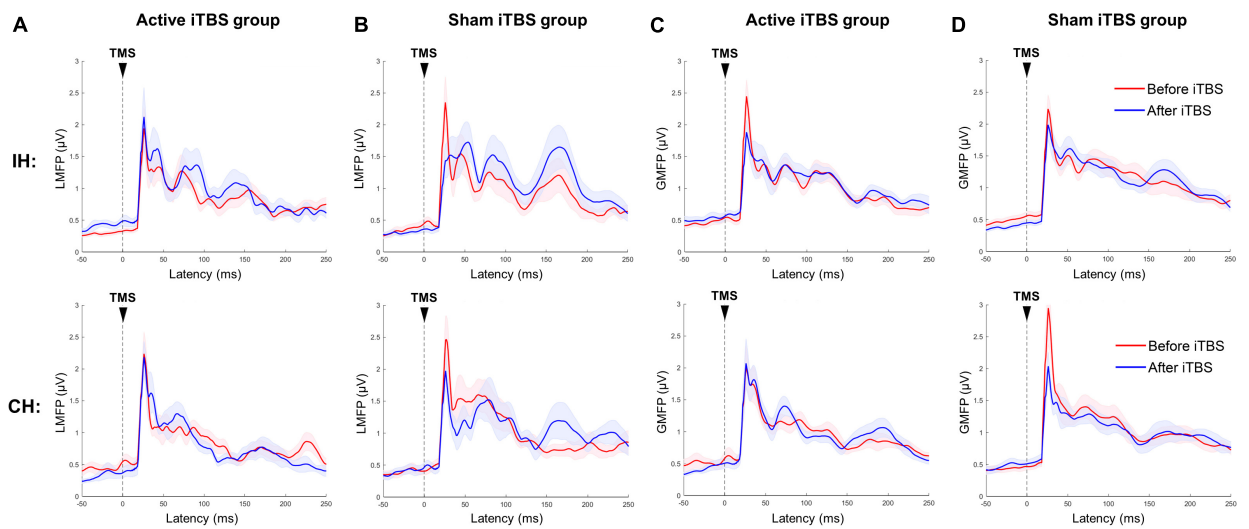

FIGURE 2 | Local and global mean field power changes after iTBS. Data presented are group mean ± standard error. The top panel presents the data in the IH, and the bottom panel presents the data in the CH. **(A,B)** LMFP in the Active and Sham TBS group, respectively. **(C,D)** GMFP in the Active and Sham TBS group, respectively. The red curves represent LMFP or GMFP before iTBS, and the blue curves represent LMFP or GMFP after iTBS. There was no significant change in LMFP or GMFP after iTBS in either group.

upper limb motor function in stroke survivors. We also observed a significant increase in IH natural frequency after iTBS.

Alterations in Natural Frequency Following Stroke

At baseline, natural frequency was significantly slower in the IH compare with CH in stroke survivors. The difference in natural frequency between hemispheres has not been previously investigated following stroke. This is the first study to report an imbalance in natural frequency between hemispheres post-stroke. Similar results have been reported in a recent study (Tscherpel et al., 2020), in which natural frequency was slower in the IH of stroke survivors compared with healthy adults. Natural frequency in the motor cortex has been widely investigated in healthy adults (Rosanova et al., 2009; Ferrarelli et al., 2012;

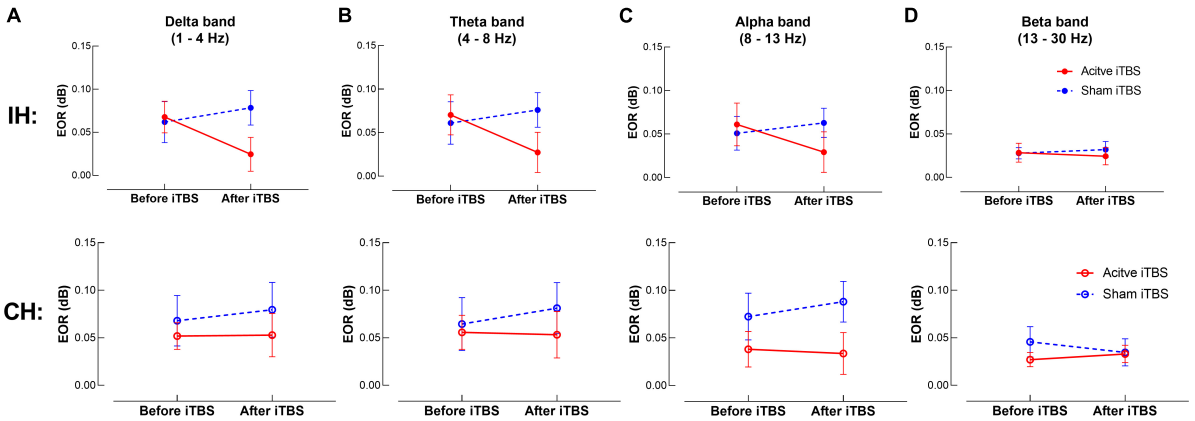

FIGURE 3 | TMS-evoked oscillatory response (EOR) changes after iTBS. Data presented are group mean ± standard error. The top panel presents the data in the IH, and the bottom panel presents the data in the CH. **(A–D)** presents EOR before and after iTBS in the delta, theta, alpha and beta bands, respectively. The red circles represent the Active iTBS group, and the blue circles represent the Sham iTBS group. There was no significant change in EOR after iTBS in any frequency band in either group.

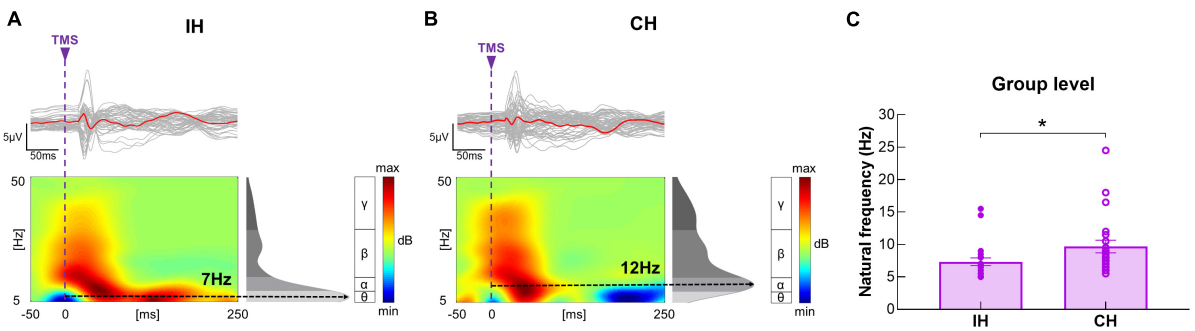

FIGURE 4 | Differences in baseline natural frequency between hemispheres. **(A,B)** Illustration of TEP, ERSP and natural frequency in the IH and CH in a representative subject. The gray curves represent TEP in each channel, and the red bold curves represent the averaged TEP in the channels surrounding the stimulated motor cortex. The ERSP plots show the TMS-evoked oscillatory responses in amplitude and duration, with black dotted lines highlighting the frequency with the highest power (i.e., natural frequency). **(C)** Data presented are group mean ± standard error. Baseline natural frequency was significantly slower in the IH compared with CH in the entire sample. The solid circles represent the IH, and the empty circles represent the CH.

Casula et al., 2016; Tscherpel et al., 2020). In most studies with healthy adults, motor cortex natural frequency falls in the beta band (i.e., 13–30 Hz) (Rosanova et al., 2009; Ferrarelli et al., 2012; Casula et al., 2016; Tscherpel et al., 2020), which appears to be faster than those observed in stroke survivors in current study (7 Hz and 10 Hz in the IH and CH, respectively). As there was no healthy control group at baseline comparison in current study, our results suggest that natural frequency tends to be slower in the IH relative to CH following stroke, but whether natural frequency in both hemispheres (especially CH) is slower in stroke survivors compared with healthy adults needs to be tested in future studies.

We observed a positive correlation between IH natural frequency and paretic hand motor function, that is, the more severely impaired stroke survivors tend to have slower natural frequency in the IH. The same correlation was also reported by Tscherpel et al. (2020). Apart from this cross-sectional correlation, Tscherpel et al. (2020) also reported positive correlations between improvements in the paretic arm motor function and changes in natural frequency during the course of stroke recovery, suggesting that motor recovery following stroke is accompanied by an increase in IH natural frequency. Together, natural frequency provides valuable insights in investigating neural mechanisms underlying motor deficits following stroke and has the potential to be used as a biomarker indicating stroke recovery.

The mechanisms underlying the alterations in natural frequency following stroke remains unclear. One possible mechanism is associated with stroke-related disruption of thalamocortical connections (Tscherpel et al., 2020). Functional magnetic resonance imaging studies have reported substantial disturbance of the intra- and inter- hemispheric network architecture following stroke (Grefkes et al., 2008; Carter et al., 2010), and these alterations have been suggested to be related to motor deficits in stroke survivors (Grefkes et al., 2008; Carter et al., 2010). Lesion-induced cortical deafferentation was observed from subcortical structures, especially thalamus

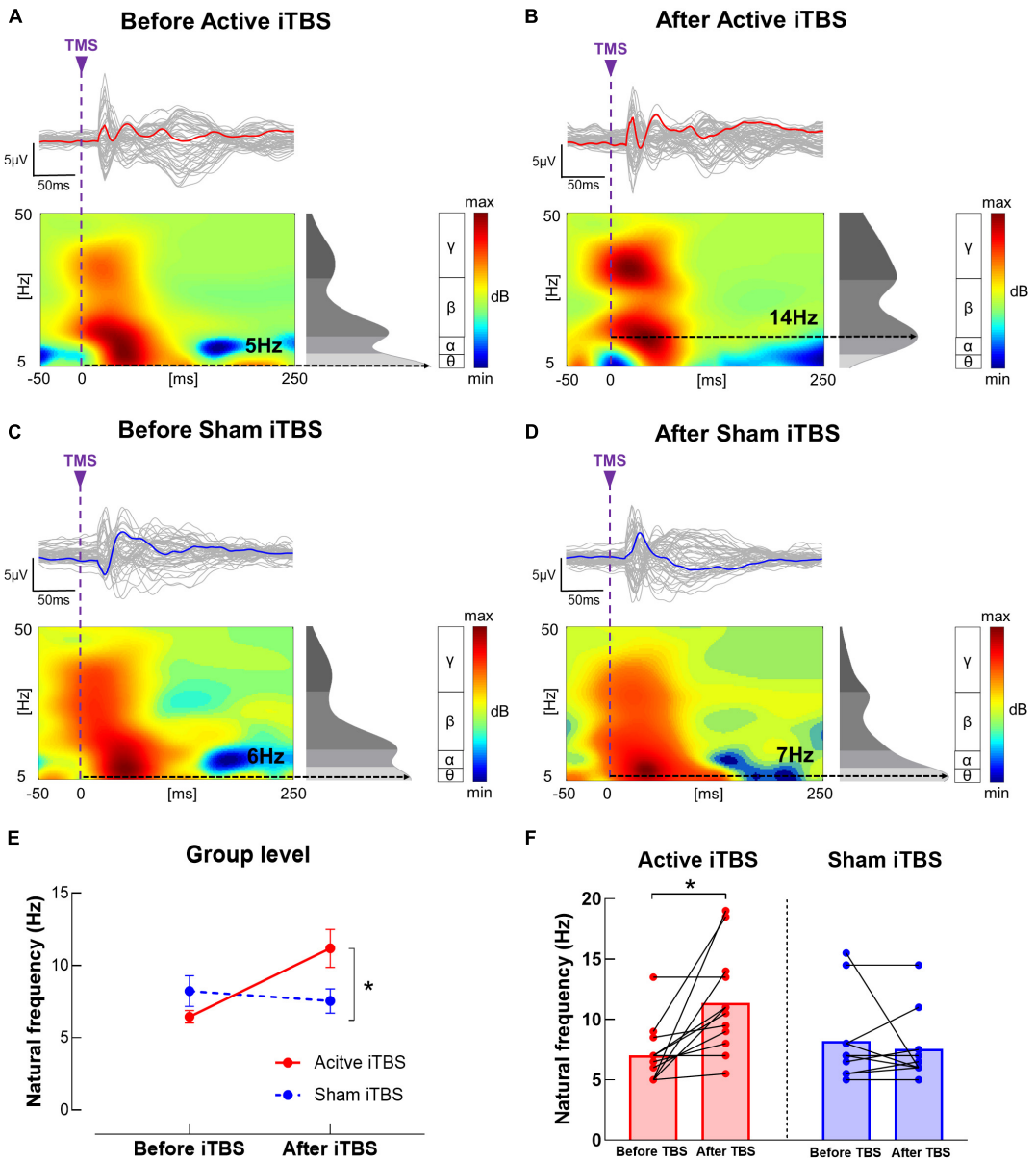

FIGURE 5 | Natural frequency changes after iTBS. **(A–D)** Illustration of TEP, ERSP and natural frequency in the IH before and after iTBS in representative subjects in the Active **(A,B)** and Sham **(C,D)** iTBS groups. The gray curves represent TEP in each channel, and the bold curves represent the averaged TEP in the channels surrounding the stimulated motor cortex. The ERSP plots show the TMS-evoked oscillatory responses in amplitude and duration, with black dotted lines highlighting the frequency with the highest power (i.e., natural frequency). **(E)** Data presented are group mean ± standard error. In the Active iTBS group, IH natural frequency was significantly increased after iTBS; while in the Sham iTBS group, there was no significant change in natural frequency after iTBS. **(F)** Illustration of individual changes in IH natural frequency after iTBS in both groups. The red circles represent the Active iTBS group, and the blue circles represent the Sham iTBS group.

(Tscherpel et al., 2020). As thalamocortical neurons have been implicated in generating fast oscillations (Ferrarelli et al., 2012), disconnection of thalamocortical pathway following stroke may result in reduced IH natural frequency.

Apart from structural disconnections, intrinsic deficits of cortical neurons following stroke could be another mechanism. GABAergic interneurons have been suggested to produce and sustain complex large-scale network oscillations in fast frequency bands (Benes and Berretta, 2001), which are important for integration and synchronous communication between brain regions and are implicated in many brain functions, including fine motor control (Varela et al., 2001; Sohn and Hallett, 2004; Canali et al., 2017). GABA-mediated intracortical inhibition has been reported to be reduced in the IH following stroke (Liepert et al., 2000; Swayne et al., 2008; Ding et al., 2018). Although reduction in GABA-mediated intracortical inhibition may elevate neural plasticity and promote motor recovery in the early stage post-stroke (Clarkson et al., 2010; Huynh et al., 2013), prolonged

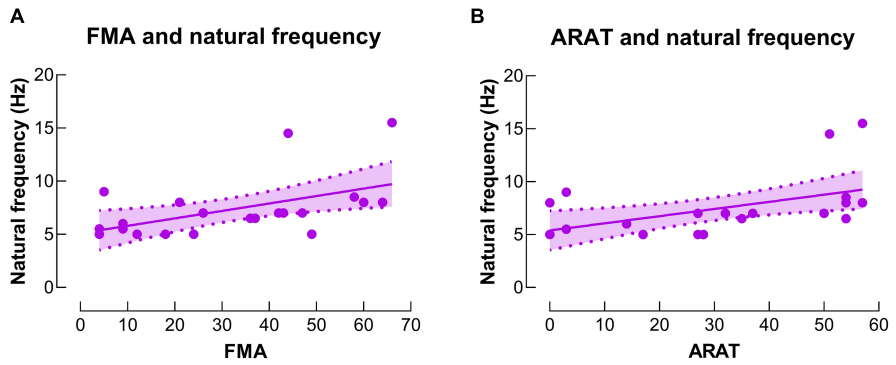

FIGURE 6 | Correlations between natural frequency and motor function. **(A)** There was a significant positive correlation between natural frequency in the IH and upper extremity Fugl-Meyer assessment (FMA) score. **(B)** There was a significant positive correlation between natural frequency in the IH and action research arm test (ARAT) score.

deficiency in GABAergic activity may hamper stroke recovery over a wider time span (Liepert, 2006; Marconi et al., 2011; Ding et al., 2018). As natural frequency has been suggested to reflect intrinsic GABA transmissions (Ferrarelli et al., 2012; Tremblay et al., 2019; Ferrarelli and Phillips, 2021), deficient GABA-mediated inhibitory processes could be associated with slowing of natural frequency following stroke, especially in the individuals with severe motor impairments.

Effects of iTBS on Transcranial Magnetic Stimulation-Evoked Electroencephalography Responses

Transcranial magnetic stimulation-evoked EEG responses were quantified in the time and time-frequency domain in this study. In the time domain, we did not observe any significant change in LMFP or GMFP after iTBS. Several studies have investigated acute adaptations in LMFP and GMFP after iTBS applied on M1 in healthy adults, but the results lack a common thread (Gedankien et al., 2017; Bai et al., 2021; Ozdemir et al., 2021). No significant change in LMFP or GMFP after iTBS was observed in some studies (Gedankien et al., 2017; Ozdemir et al., 2021), but a reduction in GMFP after iTBS was reported in a recent study (Bai et al., 2021). Ozdemir et al. (2021) reported low reproducibility of iTBS-induced modulation of cortical responses (i.e., LMFP and GMFP) across two visits. The authors suggested that iTBS-induced neuromodulation may not be accurately reflected by TMS-EEG time domain parameters, possibly contributing to the inconsistent results in current literature (Ozdemir et al., 2021). Further studies are still needed to investigate whether TMS-EEG time domain parameters are good indicators for iTBS-induced neuromodulation.

In the time-frequency domain, we observed an increase in IH natural frequency after iTBS in stroke survivors. To our knowledge, the adaptation in natural frequency following TBS or rTMS has not been previously investigated in either healthy adults or stroke survivors, although natural frequency has been suggested to provide important insights in the aftereffects of plasticity-inducing protocols on cortical activities (Rosanova et al., 2009; Tremblay et al., 2019; Ferrarelli and Phillips, 2021). The mechanisms underlying the increase in natural frequency after iTBS are still unclear. As neural oscillations in cortical networks originated from interactions between cortical regions and the thalamus, natural frequency in a specific cortical region is thought to reflect the intrinsic dynamic of the corresponding thalamocortical circuits (Casula et al., 2016). It has been suggested that iTBS increases the amount of ongoing activity in the connections between the stimulation site and its interconnected brain regions, including the thalamocortical pathway (Bestmann et al., 2004; Suppa et al., 2008). As thalamus is the structure that generates high-frequency oscillations, strengthened thalamocortical connections after iTBS could increase natural frequency in the stimulated motor cortex (Ferrarelli et al., 2012; Casula et al., 2016).

We did not observe a significant change in EOR after iTBS in any frequency band. To our knowledge, adaptations in EOR after iTBS have only been investigated in healthy adults (Casula et al., 2016; Chung et al., 2017; Bai et al., 2021), but not in stroke survivors. Bai et al. (2021) applied iTBS on M1 and reported a reduction in alpha band EOR after iTBS. Chung et al. (Chung et al., 2017) and Casula et al. (2016) applied iTBS on non-motor areas (i.e., prefrontal cortex, cerebellum) and reported an increase in EOR in theta or beta band, respectively. Different stimulation sites of iTBS may account for inconsistent results among studies, as different brain regions preserve distinct oscillation properties (Rosanova et al., 2009; Tremblay et al., 2019). Different study populations [i.e., stroke survivors in current study *vs.* healthy adults (Bai et al., 2021)] and different methodological details (i.e., stimulation intensity of 80% RMT in current study *vs.* 110% RMT (Bai et al., 2021) for TMS-EEG recordings) may account for the inconsistent results between ours and Bai et al.'s (Bai et al., 2021) study. Based on the limited number of studies that investigated the adaptations in EOR after iTBS, further studies are needed to investigate how EOR is modulated after iTBS.

Clinical Implications

This is the first study that used concurrent TMS-EEG to investigate the aftereffects of iTBS following stroke. Aftereffects

of iTBS are typically investigated by muscle responses induced by single-pulse TMS, which is not applicable to stroke survivors without a measurable MEP (Byblow et al., 2015; Pellicciari et al., 2018). At this regard, TMS-EEG does not rely on the integrity of the corticospinal tract or other efferent and afferent pathways; instead, it directly assesses cortical reactivity and oscillatory dynamics (Borich et al., 2016; Tscherpel et al., 2020). Therefore, TMS-EEG allows for a standardized assessment post-stroke and holds the potential to provide novel biomarkers indicating neuroplastic changes in response to intervention.

As to quantifying TMS-evoked EEG responses, we included natural frequency, a novel TMS-EEG parameter that reflects the intrinsic dynamics of the corresponding thalamocortical circuits as well as the intrinsic GABA transmissions. In line with a recent study (Tscherpel et al., 2020), we observed slowing of natural frequency in the IH as well as a positive correlation between IH natural frequency and motor function in stroke survivors, suggesting that alterations in natural frequency might be associated with motor deficits post-stroke, and natural frequency could be used as a biomarker indicating stroke recovery. Furthermore, IH natural frequency was increased after iTBS, indicating that natural frequency can be normalized by iTBS in stroke survivors and iTBS has the potential to promote motor recovery following stroke.

Limitations

We acknowledge limitations of present study. As a pilot study, the sample size of this study is small (N = 22). The chronicity of stroke survivors who participated in this study were within 18 months, so our findings may not be generalized to more chronic stroke survivors. Furthermore, most subjects in our sample (16 out of 22) were in the subacute phase of stroke (i.e., 1–6 months from stroke onset), which did not allow us to perform subgroup analysis for chronicity in current study. In future work, our results need to be tested in stroke survivors with a wider range of chronicity with larger sample sizes and to perform subgroup analysis for individuals in acute, subacute and chronic phases of stroke.

Auditory and somatosensory potentials arising from the TMS pulses would contaminate the direct cortical response to TMS and confound its interpretation, so strategies are needed to minimize those unwanted stimulation. In current study, we used ear plugs and plastic film under the coil to dampen the auditory and somatosensory stimulation (Massimini et al., 2007; Ter Braack et al., 2015; Tscherpel et al., 2020), but some recent studies suggested that auditory noise masking and foam padding could be more effective in attenuating auditory and somatosensory potentials (Conde et al., 2019; Rocchi et al., 2021). We acknowledge that the lack of using noise masking and foam padding is a limitation of current study. Further TMS-EEG studies are needed to apply noise masking and foam padding to minimize the auditory and somatosensory potentials caused by TMS pulses.

For sham iTBS condition, we used regular TMS coil that is tilted with an edge touching the head. This sham TBS approach produces a clicking sound that is very similar to an active TMS pulse, which has been widely adopted in previous TMS studies (Koch et al., 2009, 2020; Li et al., 2014; Nettekoven et al., 2014; Casula et al., 2016). However, the somatosensory perception produced by this sham TMS approach may not be as strong as active TMS, which possibly affects the arousal level of subjects in the two groups differently. Further studies are needed to use sham TMS coil with better mimic of somatosensory perception produced by active TMS.

Current study delivered only 50 pulses in each hemisphere when testing TMS-EEG (∼44 artifact-free trials), which is a small number of trials compared with many previous studies (Rosanova et al., 2009; Pellicciari et al., 2018; Tscherpel et al., 2020). As TMS-EEG testing was repeated four times in a single session for each subject (i.e., IH and CH, before and after iTBS), it was difficult for many stroke survivors to maintain static for such a long time. Therefore, we did not deliver more TMS pulses for TMS-EEG testing. As suggested in previous studies, adequate number of trials are critical for generating reliable TEPs (Rogasch and Fitzgerald, 2013; Tremblay et al., 2019). We acknowledge that the small number of trials is a limitation in current study which may negatively affect the reliability of current study. Cautions are needed when interpreting our results, and further studies with larger number of trials are needed to be conducted.

Present study took TMS-EEG measurements only at baseline and immediately after iTBS without a follow-up. We acknowledge that it would be more meaningful to take TMS-EEG measurements at multiple time points after iTBS, but it has already been a long experiment for stroke survivors, and many subjects could not tolerate for a longer time of data collection. Further studies are needed to measure TMS-EEG at multiple time points after iTBS.

Conclusion

This is the first study to use concurrent TMS and EEG to investigate the aftereffects of iTBS in following stroke. We observed alterations in natural frequency following stroke which is related to motor impairments. Our results also provide evidence that iTBS increases natural frequency in stroke survivors. Our findings implicate that iTBS has the potential to normalize natural frequency in stroke survivors, which can be utilized in stroke rehabilitation.

DATA AVAILABILITY STATEMENT

The raw data supporting the conclusions of this article will be made available by the authors, without undue reservation.

ETHICS STATEMENT

The studies involving human participants were reviewed and approved by Guangzhou First People's Hospital Human Research Ethics Committee. The patients/participants provided their written informed consent to participate in this study. Written informed consent was obtained from the individual(s) for the publication of any potentially identifiable images or data included in this article.

AUTHOR CONTRIBUTIONS

YL, GX, and QD designed the experiments and wrote the manuscript. JiC and YP recruited the participants. QD, SC, JiC, SZ, XL, JuC, YC, and KC conducted the experiments. QD, SC, GC, and JiC reduced and analyzed the data. QD and YL interpreted the data. All authors contributed to the article and approved the submitted version.

FUNDING

This work was supported by the National Key R&D Program of China [Grant Number 2017YFB1303200 (YL)]; National Science Foundation of China [Grant Numbers 81772438 (YL), 81974357 (YL), 82072548 (GX) and 82102678 (QD)]; the Guangzhou Municipal Science and Technology Program [Grant Number 201803010083 (YL)]; Guangdong Basic and Applied Basic Research Foundation [Grant Number 2020A1515110761 (QD)]; and Guangzhou Postdoctoral Science Foundation (QD).

ACKNOWLEDGMENTS

We would like to thank all our participants for their interest and time investment.

REFERENCES

Atluri, S., Frehlich, M., Mei, Y., Garcia Dominguez, L., Rogasch, N. C., Wong, W., et al. (2016). TMSEEG: A MATLAB-based graphical user interface for processing electrophysiological signals during transcranial magnetic stimulation. *Front. Neural. Circ.* 10:78. doi: 10.3389/fncir.2016.00078

Bai, Z., Zhang, J., and Fong, K. N. K. (2021). Intermittent theta burst stimulation to the primary motor cortex reduces cortical inhibition: a tms-eeg study. *Brain Sci.* 11:1114. doi: 10.3390/brainsci11091114

Benes, F. M., and Berretta, S. (2001). GABAergic interneurons: implications for understanding schizophrenia and bipolar disorder. *Neuropsychopharmacology* 25, 1–27. doi: 10.1016/S0893-133X(01)00225-1

Bestmann, S., Baudewig, J., Siebner, H. R., Rothwell, J. C., and Frahm, J. (2004). Functional MRI of the immediate impact of transcranial magnetic stimulation on cortical and subcortical motor circuits. *Eur. J. Neurosci.* 19, 1950–1962. doi: 10.1111/j.1460-9568.2004.03277.x

Bonkhoff, A. K., Espinoza, F. A., Gazula, H., Vergara, V. M., Hensel, L., Michely, J., et al. (2020). Acute ischaemic stroke alters the brain's preference for distinct dynamic connectivity states. *Brain* 143, 1525–1540. doi: 10.1093/brain/awaa101

Borich, M. R., Wheaton, L. A., Brodie, S. M., Lakhani, B., and Boyd, L. A. (2016). Evaluating interhemispheric cortical responses to transcranial magnetic stimulation in chronic stroke: A TMS-EEG investigation. *Neurosci. Lett.* 618, 25–30. doi: 10.1016/j.neulet.2016.02.047

Byblow, W. D., Stinear, C. M., Barber, P. A., Petoe, M. A., and Ackerley, S. J. (2015). Proportional recovery after stroke depends on corticomotor integrity. *Ann. Neurol.* 78, 848–859. doi: 10.1002/ana.24472

Canali, P., Casarotto, S., Rosanova, M., Sferrazza-Papa, G., Casali, A. G., Gosseries, O., et al. (2017). Abnormal brain oscillations persist after recovery from bipolar depression. *Eur. Psychiatry* 41, 10–15. doi: 10.1016/j.eurpsy.2016.10.005

Carter, A. R., Astafiev, S. V., Lang, C. E., Connor, L. T., Rengachary, J., Strube, M. J., et al. (2010). Resting interhemispheric functional magnetic resonance imaging connectivity predicts performance after stroke. *Ann. Neurol.* 67, 365–375. doi: 10.1002/ana.21905

Casula, E. P., Mayer, I. M. S., Desikan, M., Tabrizi, S. J., Rothwell, J. C., and Orth, M. (2018). Motor cortex synchronization influences the rhythm of motor performance in premanifest huntington's disease. *Mov. Disord.* 33, 440–448. doi: 10.1002/mds.27285

Casula, E. P., Pellicciari, M. C., Bonni, S., Spano, B., Ponzo, V., Salsano, I., et al. (2021). Evidence for interhemispheric imbalance in stroke patients as revealed by combining transcranial magnetic stimulation and electroencephalography. *Hum. Brain Mapp.* 42, 1343–1358. doi: 10.1002/hbm.25297

Casula, E. P., Pellicciari, M. C., Ponzo, V., Stampanoni Bassi, M., Veniero, D., Caltagirone, C., et al. (2016). Cerebellar theta burst stimulation modulates the neural activity of interconnected parietal and motor areas. *Sci. Rep.* 6:36191. doi: 10.1038/srep36191

Chen, R., Tam, A., Butefisch, C., Corwell, B., Ziemann, U., Rothwell, J. C., et al. (1998). Intracortical inhibition and facilitation in different representations of the human motor cortex. *J. Neurophysiol.* 80, 2870–2881. doi: 10.1152/jn.1998.80.6.2870

Chung, S. W., Lewis, B. P., Rogasch, N. C., Saeki, T., Thomson, R. H., Hoy, K. E., et al. (2017). Demonstration of short-term plasticity in the dorsolateral prefrontal cortex with theta burst stimulation: A TMS-EEG study. *Clin. Neurophysiol.* 128, 1117–1126. doi: 10.1016/j.clinph.2017.04.005

Chung, S. W., Sullivan, C. M., Rogasch, N. C., Hoy, K. E., Bailey, N. W., Cash, R. F. H., et al. (2019). The effects of individualised intermittent theta burst stimulation in the prefrontal cortex: A TMS-EEG study. *Hum. Brain Mapp.* 40, 608–627. doi: 10.1002/hbm.24398

Clarkson, A. N., Huang, B. S., Macisaac, S. E., Mody, I., and Carmichael, S. T. (2010). Reducing excessive GABA-mediated tonic inhibition promotes functional recovery after stroke. *Nature* 468, 305–309. doi: 10.1038/nature09511

Cohen, J. (1988). *Statistical power analysis for the behavioral sciences (2nd ed.)*. Hillsdale, NJ: L. Erlbaum Associates.

Conde, V., Tomasevic, L., Akopian, I., Stanek, K., Saturnino, G. B., Thielscher, A., et al. (2019). The non-transcranial TMS-evoked potential is an inherent source of ambiguity in TMS-EEG studies. *Neuroimage* 185, 300–312. doi: 10.1016/j.neuroimage.2018.10.052

Corti, M., Patten, C., and Triggs, W. (2012). Repetitive transcranial magnetic stimulation of motor cortex after stroke: a focused review. *Am. J. Phys. Med. Rehabil.* 91, 254–270. doi: 10.1097/PHM.0b013e318228bf0c

Delorme, A., and Makeig, S. (2004). EEGLAB: an open source toolbox for analysis of single-trial EEG dynamics including independent component analysis. *J. Neurosci. Methods* 134, 9–21. doi: 10.1016/j.jneumeth.2003.10.009

Delorme, A., Sejnowski, T., and Makeig, S. (2007). Enhanced detection of artifacts in EEG data using higher-order statistics and independent component analysis. *Neuroimage* 34, 1443–1449. doi: 10.1016/j.neuroimage.2006.11.004

Di Lazzaro, V., Pilato, F., Dileone, M., Profice, P., Oliviero, A., Mazzone, P., et al. (2008). The physiological basis of the effects of intermittent theta burst stimulation of the human motor cortex. *J. Physiol.* 586, 3871–3879. doi: 10.1113/jphysiol.2008.152736

Ding, Q., Cai, H., Wu, M., Cai, G., Chen, H., Li, W., et al. (2021a). Short intracortical facilitation associates with motor-inhibitory control. *Behav. Brain Res.* 407:113266. doi: 10.1016/j.bbr.2021.113266

Ding, Q., Lin, T., Wu, M., Yang, W., Li, W., Jing, Y., et al. (2021b). Influence of iTBS on the Acute Neuroplastic Change After BCI Training. *Front. Cell. Neurosci.* 15:653487. doi: 10.3389/fncel.2021.653487

Ding, Q., Triggs, W. J., Kamath, S. M., and Patten, C. (2018). Short intracortical inhibition during voluntary movement reveals persistent impairment post-stroke. *Front. Neurol.* 9:1105. doi: 10.3389/fneur.2018.01105

Ding, Q., Zhang, S., Chen, S., Chen, J., Li, X., Chen, J., et al. (2021c). The effects of intermittent theta burst stimulation on functional brain network following stroke: an electroencephalography study. *Front. Neurosci.* 15:755709. doi: 10.3389/fnins.2021.755709

Faul, F., Erdfelder, E., Lang, A. G., and Buchner, A. (2007). G*Power 3: a flexible statistical power analysis program for the social, behavioral, and biomedical sciences. *Behav. Res. Methods* 39, 175–191. doi: 10.3758/bf03193146

Ferrarelli, F., and Phillips, M. L. (2021). Examining and modulating neural circuits in psychiatric disorders with transcranial magnetic stimulation and

electroencephalography: present practices and future developments. *Am. J. Psychiatry* 178, 400–413. doi: 10.1176/appi.ajp.2020.20071050

Ferrarelli, F., Sarasso, S., Guller, Y., Riedner, B. A., Peterson, M. J., Bellesi, M., et al. (2012). Reduced natural oscillatory frequency of frontal thalamocortical circuits in schizophrenia. *Arch. Gen. Psychiatry* 69, 766–774. doi: 10.1001/archgenpsychiatry.2012.147

Fugl-Meyer, A. R., Jaasko, L., Leyman, I., Olsson, S., and Steglind, S. (1975). The post-stroke hemiplegic patient. 1. a method for evaluation of physical performance. *Scand. J. Rehabil. Med.* 7, 13–31.

Gedankien, T., Fried, P. J., Pascual-Leone, A., and Shafi, M. M. (2017). Intermittent theta-burst stimulation induces correlated changes in cortical and corticospinal excitability in healthy older subjects. *Clin. Neurophysiol.* 128, 2419–2427. doi: 10.1016/j.clinph.2017.08.034

Gordon, P. C., Desideri, D., Belardinelli, P., Zrenner, C., and Ziemann, U. (2018). Comparison of cortical EEG responses to realistic sham versus real TMS of human motor cortex. *Brain Stimul.* 11, 1322–1330. doi: 10.1016/j.brs.2018.08.003

Grefkes, C., Eickhoff, S. B., Nowak, D. A., Dafotakis, M., and Fink, G. R. (2008). Dynamic intra- and interhemispheric interactions during unilateral and bilateral hand movements assessed with fMRI and DCM. *Neuroimage* 41, 1382–1394. doi: 10.1016/j.neuroimage.2008.03.048

Huang, Y. Z., Edwards, M. J., Rounis, E., Bhatia, K. P., and Rothwell, J. C. (2005). Theta burst stimulation of the human motor cortex. *Neuron* 45, 201–206.

Huynh, W., Vucic, S., Krishnan, A. V., Lin, C. S., Hornberger, M., and Kiernan, M. C. (2013). Longitudinal plasticity across the neural axis in acute stroke. *Neurorehabil. Neural. Repair* 27, 219–229. doi: 10.1177/1545968312462071

Jurcak, V., Tsuzuki, D., and Dan, I. (2007). 10/20, 10/10, and 10/5 systems revisited: their validity as relative head-surface-based positioning systems. *Neuroimage* 34, 1600–1611. doi: 10.1016/j.neuroimage.2006.09.024

Koch, G., Brusa, L., Carrillo, F., Lo Gerfo, E., Torriero, S., Oliveri, M., et al. (2009). Cerebellar magnetic stimulation decreases levodopa-induced dyskinesias in Parkinson disease. *Neurology* 73, 113–119. doi: 10.1212/WNL.0b013e3181ad5387

Koch, G., Esposito, R., Motta, C., Casula, E. P., DiLorenzo, F., Bonni, S., et al. (2020). Improving visuo-motor learning with cerebellar theta burst stimulation: Behavioral and neurophysiological evidence. *Neuroimage* 208:116424. doi: 10.1016/j.neuroimage.2019.116424

Komssi, S., Kahkonen, S., and Ilmoniemi, R. J. (2004). The effect of stimulus intensity on brain responses evoked by transcranial magnetic stimulation. *Hum. Brain Mapp.* 21, 154–164. doi: 10.1002/hbm.10159

Lang, C. E., Wagner, J. M., Dromerick, A. W., and Edwards, D. F. (2006). Measurement of upper-extremity function early after stroke: properties of the action research arm test. *Arch. Phys. Med. Rehabil.* 87, 1605–1610. doi: 10.1016/j.apmr.2006.09.003

Lehmann, D., and Skrandies, W. (1980). Reference-free identification of components of checkerboard-evoked multichannel potential fields. *Electroencephalogr. Clin. Neurophysiol.* 48, 609–621. doi: 10.1016/0013-4694(80)90419-8

Li, C. T., Chen, M. H., Juan, C. H., Huang, H. H., Chen, L. F., Hsieh, J. C., et al. (2014). Efficacy of prefrontal theta-burst stimulation in refractory depression: a randomized sham-controlled study. *Brain* 137, 2088–2098. doi: 10.1093/brain/awu109

Liepert, J. (2006). Motor cortex excitability in stroke before and after constraint-induced movement therapy. *Cogn. Behav. Neurol.* 19, 41–47. doi: 10.1097/00146965-200603000-00005

Liepert, J., Hamzei, F., and Weiller, C. (2000). Motor cortex disinhibition of the unaffected hemisphere after acute stroke. *Muscle Nerve.* 23, 1761–1763. doi: 10.1002/1097-4598(200011)23

Lloyd-Jones, D., Adams, R. J., Brown, T. M., Carnethon, M., Dai, S., De Simone, G., et al. (2010). Executive summary: heart disease and stroke statistics–2010 update: a report from the American Heart Association. *Circulation* 121, 948–954. doi: 10.1161/CIRCULATIONAHA.109.192666

Marconi, B., Filippi, G. M., Koch, G., Giacobbe, V., Pecchioli, C., Versace, V., et al. (2011). Long-term effects on cortical excitability and motor recovery induced by repeated muscle vibration in chronic stroke patients. *Neurorehabil. Neural. Repair* 25, 48–60. doi: 10.1177/1545968310376757

Massimini, M., Ferrarelli, F., Esser, S. K., Riedner, B. A., Huber, R., Murphy, M., et al. (2007). Triggering sleep slow waves by transcranial magnetic stimulation. *Proc. Natl. Acad. Sci. USA* 104, 8496–8501. doi: 10.1073/pnas.0702495104

Nasreddine, Z. S., Phillips, N. A., Bedirian, V., Charbonneau, S., Whitehead, V., Collin, I., et al. (2005). The montreal cognitive assessment, MoCA: a brief screening tool for mild cognitive impairment. *J. Am. Geriatr. Soc.* 53, 695–699. doi: 10.1111/j.1532-5415.2005.53221.x

Nettekoven, C., Volz, L. J., Kutscha, M., Pool, E. M., Rehme, A. K., Eickhoff, S. B., et al. (2014). Dose-dependent effects of theta burst rTMS on cortical excitability and resting-state connectivity of the human motor system. *J. Neurosci.* 34, 6849–6859. doi: 10.1523/JNEUROSCI.4993-13.2014

Oostenveld, R., Fries, P., Maris, E., and Schoffelen, J. M. (2011). FieldTrip: Open source software for advanced analysis of MEG, EEG, and invasive electrophysiological data. *Comput. Intell. Neurosci.* 2011:156869. doi: 10.1155/2011/156869

Ozdemir, R. A., Boucher, P., Fried, P. J., Momi, D., Jannati, A., Pascual-Leone, A., et al. (2021). Reproducibility of cortical response modulation induced by intermittent and continuous theta-burst stimulation of the human motor cortex. *Brain Stimul.* 14, 949–964. doi: 10.1016/j.brs.2021.05.013

Pellicciari, M. C., Bonni, S., Ponzo, V., Cinnera, A. M., Mancini, M., Casula, E. P., et al. (2018). Dynamic reorganization of TMS-evoked activity in subcortical stroke patients. *Neuroimage* 175, 365–378. doi: 10.1016/j.neuroimage.2018.04.011

Rocchi, L., Di Santo, A., Brown, K., Ibanez, J., Casula, E., Rawji, V., et al. (2021). Disentangling EEG responses to TMS due to cortical and peripheral activations. *Brain Stimul.* 14, 4–18. doi: 10.1016/j.brs.2020.10.011

Rogasch, N. C., and Fitzgerald, P. B. (2013). Assessing cortical network properties using TMS-EEG. *Hum. Brain Mapp.* 34, 1652–1669. doi: 10.1002/hbm.22016

Rosanova, M., Casali, A., Bellina, V., Resta, F., Mariotti, M., and Massimini, M. (2009). Natural frequencies of human corticothalamic circuits. *J. Neurosci.* 29, 7679–7685. doi: 10.1523/JNEUROSCI.0445-09.2009

Rossi, S., Hallett, M., Rossini, P. M., Pascual-Leone, A., and Safety, T. M. S. C. G. (2009). Safety, ethical considerations, and application guidelines for the use of transcranial magnetic stimulation in clinical practice and research. *Clin. Neurophysiol.* 120, 2008–2039. doi: 10.1016/j.clinph.2009.08.016

Sohn, Y. H., and Hallett, M. (2004). Surround inhibition in human motor system. *Exp. Brain Res.* 158, 397–404.

Sun, Y., Blumberger, D. M., Mulsant, B. H., Rajji, T. K., Fitzgerald, P. B., Barr, M. S., et al. (2018). Magnetic seizure therapy reduces suicidal ideation and produces neuroplasticity in treatment-resistant depression. *Transl. Psychiatry* 8:253. doi: 10.1038/s41398-018-0302-8

Suppa, A., Huang, Y. Z., Funke, K., Ridding, M. C., Cheeran, B., Di Lazzaro, V., et al. (2016). Ten years of theta burst stimulation in humans: established knowledge, unknowns and prospects. *Brain Stimul.* 9, 323–335. doi: 10.1016/j.brs.2016.01.006

Suppa, A., Ortu, E., Zafar, N., Deriu, F., Paulus, W., Berardelli, A., et al. (2008). Theta burst stimulation induces after-effects on contralateral primary motor cortex excitability in humans. *J. Physiol.* 586, 4489–4500. doi: 10.1113/jphysiol.2008.156596

Swayne, O. B., Rothwell, J. C., Ward, N. S., and Greenwood, R. J. (2008). Stages of motor output reorganization after hemispheric stroke suggested by longitudinal studies of cortical physiology. *Cereb. Cortex.* 18, 1909–1922. doi: 10.1093/cercor/bhm218

Talelli, P., Greenwood, R. J., and Rothwell, J. C. (2007). Exploring Theta Burst Stimulation as an intervention to improve motor recovery in chronic stroke. *Clin. Neurophysiol.* 118, 333–342. doi: 10.1016/j.clinph.2006.10.014

Tamburro, G., Di Fronso, S., Robazza, C., Bertollo, M., and Comani, S. (2020). Modulation of brain functional connectivity and efficiency during an endurance cycling task: a source-level eeg and graph theory approach. *Front. Hum. Neurosci.* 14:243. doi: 10.3389/fnhum.2020.00243

Tedesco Triccas, L., Meyer, S., Mantini, D., Camilleri, K., Falzon, O., Camilleri, T., et al. (2019). A systematic review investigating the relationship of electroencephalography and magnetoencephalography measurements with sensorimotor upper limb impairments after stroke. *J. Neurosci. Methods* 311, 318–330. doi: 10.1016/j.jneumeth.2018.08.009

Ter Braack, E. M., De Vos, C. C., and Van Putten, M. J. (2015). Masking the auditory evoked potential in TMS-EEG: a comparison of various methods. *Brain Topogr.* 28, 520–528. doi: 10.1007/s10548-013-0312-z

Thut, G., and Miniussi, C. (2009). New insights into rhythmic brain activity from TMS-EEG studies. *Trends Cogn. Sci.* 13, 182–189. doi: 10.1016/j.tics.2009.01.004

Tremblay, S., Rogasch, N. C., Premoli, I., Blumberger, D. M., Casarotto, S., Chen, R., et al. (2019). Clinical utility and prospective of TMS-EEG. *Clin. Neurophysiol.* 130, 802–844. doi: 10.1016/j.clinph.2019.01.001

Tscherpel, C., Dern, S., Hensel, L., Ziemann, U., Fink, G. R., and Grefkes, C. (2020). Brain responsivity provides an individual readout for motor recovery after stroke. *Brain* 143, 1873–1888.

Varela, F., Lachaux, J. P., Rodriguez, E., and Martinerie, J. (2001). The brainweb: phase synchronization and large-scale integration. *Nat. Rev. Neurosci.* 2, 229–239. doi: 10.1038/35067550

Volz, L. J., Rehme, A. K., Michely, J., Nettekoven, C., Eickhoff, S. B., Fink, G. R., et al. (2016). Shaping Early Reorganization of Neural Networks Promotes Motor Function after Stroke. *Cereb. Cortex* 26, 2882–2894. doi: 10.1093/cercor/bhw034

Conflict of Interest: The authors declare that the research was conducted in the absence of any commercial or financial relationships that could be construed as a potential conflict of interest.

frontiers in Aging Neuroscience

ORIGINAL RESEARCH
published: 16 February 2022
doi: 10.3389/fnagi.2022.848380

Long-Term Motor Cortical Electrical Stimulation Ameliorates 6-Hydroxydopamine-Induced Motor Dysfunctions and Exerts Neuroprotective Effects in a Rat Model of Parkinson's Disease

*Chi-Wei Kuo[1,2†], Ming-Yuan Chang[3,4,5†], Ming-Yi Chou[2], Chien-Yuan Pan[2], Chih-Wei Peng[6], Hui-Chiun Tseng[2], Tsu-Yi Jen[7], Xiao-Kuo He[8], Hui-Hua Liu[9], Thi Xuan Dieu Nguyen[1], Pi-Kai Chang[1] and Tsung-Hsun Hsieh[1,10,11]**

[1] School of Physical Therapy and Graduate Institute of Rehabilitation Science, Chang Gung University, Taoyuan City, Taiwan, [2] Department of Life Science, National Taiwan University, Taipei City, Taiwan, [3] Division of Neurosurgery, Department of Surgery, Min-Sheng General Hospital, Taoyuan City, Taiwan, [4] Department of Early Childhood and Family Educare, Chung Chou University of Science and Technology, Yuanlin City, Taiwan, [5] Graduate Institute of Neural Regenerative Medicine, College of Medical Science and Technology, Taipei Medical University, Taipei City, Taiwan, [6] School of Biomedical Engineering, College of Biomedical Engineering, Taipei Medical University, Taipei City, Taiwan, [7] Department of Psychology, National Taiwan University, Taipei City, Taiwan, [8] Department of Rehabilitation Medicine, The Fifth Hospital of Xiamen, Xiamen, China, [9] Department of Rehabilitation Medicine, Sun Yat-sen Memorial Hospital, Sun Yat-sen University, Guangzhou, China, [10] Neuroscience Research Center, Chang Gung Memorial Hospital, Taoyuan City, Taiwan, [11] Healthy Aging Research Center, Chang Gung University, Taoyuan City, Taiwan

OPEN ACCESS

Edited by:
Yi Guo,
Jinan University, China

Reviewed by:
Hamadjida Adjia,
Université de Montréal, Canada
Pratibha Mehta Luthra,
University of Delhi, India

***Correspondence:**
Tsung-Hsun Hsieh
hsieht h@mail.cgu.edu.tw

† These authors have contributed equally to this work

Specialty section:
This article was submitted to Parkinson's Disease and Aging-related Movement Disorders, a section of the journal Frontiers in Aging Neuroscience

Received: *04 January 2022*
Accepted: *26 January 2022*
Published: *16 February 2022*

Citation:
Kuo C-W, Chang M-Y, Chou M-Y, Pan C-Y, Peng C-W, Tseng H-C, Jen T-Y, He X-K, Liu H-H, Nguyen TXD, Chang P-K and Hsieh T-H (2022) Long-Term Motor Cortical Electrical Stimulation Ameliorates 6-Hydroxydopamine-Induced Motor Dysfunctions and Exerts Neuroprotective Effects in a Rat Model of Parkinson's Disease. Front. Aging Neurosci. 14:848380. doi: 10.3389/fnagi.2022.848380

Objective: Cortical electrical stimulation (CES) can modulate cortical excitability through a plasticity-like mechanism and is considered to have therapeutic potentials in Parkinson's disease (PD). However, the precise therapeutic value of such approach for PD remains unclear. Accordingly, we adopted a PD rat model to determine the therapeutic effects of CES. The current study was thus designed to identify the therapeutic potential of CES in PD rats.

Methods: A hemiparkinsonian rat model, in which lesions were induced using unilateral injection of 6-hydroxydopamine (6-OHDA) into the medial forebrain bundle, was applied to identify the therapeutic effects of long-term (4-week) CES with intermittent theta-burst stimulation (iTBS) protocol (starting 24 h after PD lesion observation, 1 session/day, 5 days/week) on motor function and neuroprotection. After the CES intervention, detailed functional behavioral tests including gait analysis, akinesia, open-field locomotor activity, apomorphine-induced rotation as well as degeneration level of dopaminergic neurons were performed weekly up to postlesion week 4.

Results: After the CES treatment, we found that the 4-week CES intervention ameliorated the motor deficits in gait pattern, akinesia, locomotor activity, and apomorphine-induced rotation. Immunohistochemistry and tyrosine hydroxylase staining analysis demonstrated that the number of dopamine neurons was significantly greater in the CES intervention group than in the sham treatment group.

Conclusion: This study suggests that early and long-term CES intervention could reduce the aggravation of motor dysfunction and exert neuroprotective effects in a rat model of PD. Further, this preclinical model of CES may increase the scope for the potential use of CES and serve as a link between animal and PD human studies to further identify the therapeutic mechanism of CES for PD or other neurological disorders.

Keywords: cortical electrical stimulation, Parkinson's disease, gait, locomotor function, neuroprotection, 6-OHDA, rats

INTRODUCTION

Parkinson's disease (PD) is the second-most-frequently diagnosed neurodegenerative disease after Alzheimer's disease and has become a major medical concern that affects 7–10 million individuals, close to 1% of the global population aged over 60 years (Nussbaum and Ellis, 2003; De Lau and Breteler, 2006; Wood-Kaczmar et al., 2006; Gilman, 2007; Kauffman et al., 2007; Reeve et al., 2014). The pathologic hallmark of the disease originates from degeneration of the dopaminergic neurons in the substantia nigra pars compacta (SNpc), which leads to several motor disturbances such as tremor, slowness, stiffness, balance problems, bradykinesia, akinesia, and gait disturbance (Rogers, 1996; Kalia and Lang, 2015; Moller et al., 2016; Sveinbjornsdottir, 2016). Mainstream modern PD treatment involves pharmacological approaches of dopamine supplementation (e.g., levodopa and l-3,4-dihydroxyphenylalanine) or dopamine agonist administration. Although dopaminergic drugs are effective treatments for controlling these symptoms in the initial stage of PD, associated complications such as levodopa-induced dyskinesia, freezing of gait, postural instability, depression, and motor fluctuations are common side effects after 5–10 years of levodopa administration, with the percentage of affected patients increasing over time (Obeso et al., 2000; Connolly and Lang, 2014; Bastide et al., 2015; Espay et al., 2018). Thus, it is still a high unmet need for developing the alternative and non-pharmacological therapeutic approach that can overcome the limitations of current treatment for PD.

Numerous alternative non-pharmacological and neuromodulatory approaches, such as repetitive transcranial magnetic stimulation (rTMS), transcranial direct current stimulation (tDCS), and cortical electrical stimulation (CES), are regarded as promising new therapeutic strategies for inducing the changes in neural activity and plasticity and considered as the new therapeutic strategies for PD (Pascual-Leone et al., 1994; Lefaucheur et al., 2004; Fasano et al., 2008; Elahi and Chen, 2009; Gutierrez et al., 2009; Degardin et al., 2012; De Rose et al., 2012). Among these techniques, compared with rTMS or tDCS, CES is a focused cortical stimulation technique that can provide higher focalization, spatial resolution and accuracy for stimulating a specific area of the motor cortex (Hsieh et al., 2015a). In clinical, CES has been used in neuropathic pain management (Son et al., 2006; Fagundes-Pereyra et al., 2010; Alm and Dreimanis, 2013). In addition, similar to the rTMS and tDCS, a recent animal study suggested that, CES can modulate motor cortical excitability through plasticity-like mechanisms (Hsieh et al., 2015a). Other preclinical studies have also demonstrated that CES can improve functional outcomes in ischemic stroke rats (Adkins-Muir and Jones, 2003; Adkins et al., 2006; Adkins et al., 2008). In human studies, it has been reported that CES of the motor cortex is not only effective in pain relief but also improves cognitive and motor functions in patients with advanced PD (Fasano et al., 2008; Gutierrez et al., 2009; De Rose et al., 2012). Although the CES approach has been reported in several human studies, studies that have applied CES as a long-term treatment in PD animals are few. In addition, several questions, such as what the optimal stimulation protocols and the underlying mechanisms of CES treatment for PD are, remain unclear (Cioni, 2007; Lefaucheur, 2009). Further experimental studies are required to determine the therapeutic value and the indications of CES in the treatment of PD.

For translational purposes, a diseased animal model could be the optimal means of studying the pathogenesis of PD. Such a model may provide a more stable condition, standardized stimulation protocol and controlled method of assessment to eliminate the discrepancies and clarify the treatment outcomes. To date, the detailed long-term effects of CES on PD-related symptoms as well as CES-induced neuroprotective effects have not been studied in PD animal models. Therefore, the current study was designed to identify the therapeutic potentials of CES in a neurotoxin-induced PD rat model. The therapeutic effects of CES were measured using behavioral assessments, including detailed time-course analysis of motor symptoms such as gait pattern, open-field locomotor activity, akinesia, drug-induced rotation and dopamine depletion levels. It was hypothesized that long-term CES intervention would reduce the aggravation of motor dysfunctions and have a neuroprotective effect on dopaminergic neurons in PD rat model. The knowledge obtained in the current study may have translational relevance for developing new therapeutic applications of CES in PD or other neurological disorders.

MATERIALS AND METHODS

Animals

To avoid the hormonal influences on PD lesions (Gillies et al., 2014), experiments were conducted on 16 male Sprague Dawley rats (9 weeks old; body weight, 300–350 g) obtained from the BioLASCO Taiwan Co., Ltd., Taipei City, Taiwan. All rats were housed in a temperature-controlled animal care facility to a 12 h photoperiod (0700–1,900 h light) and temperature of 25°C

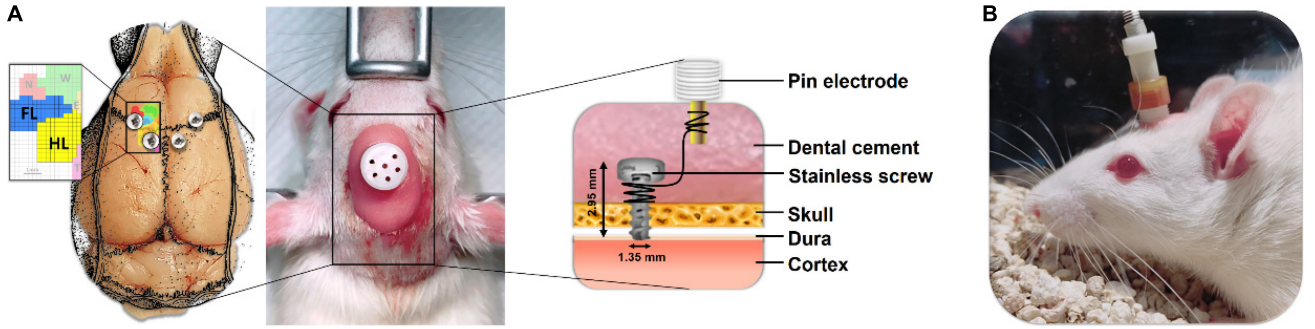

FIGURE 1 | Placement and assembly details of the cortical electrical stimulation (CES) electrodes for the long-term treatment of CES. **(A)** The CES electrodes were positioned at the motor cortex of the forelimb and hindlimb and connected to the six-channel pedestal with wires and fixed with dental cement. **(B)** During the CES treatment, the head electrode pedestal served as the plugin site of the electrode pin to conduct electrical current.

with freely available food and water. All animal procedures were approved by the Institutional Animal Care and Use Committee at Chang Gung University. All efforts were made to minimize the number of rats required for the current study.

Parkinson's Disease Rat Model

In the current study, the classical model of intracerebral injection of neurotoxin 6-hydroxydopamine (6-OHDA) in rats was applied. The animal preparations and procedures for the induction of the PD rat model were in accordance with previous studies (Hsieh et al., 2011; Lee et al., 2012; Hsieh et al., 2015b; Feng et al., 2020). Briefly, rats were anesthetized using intraperitoneal injection of Zoletil 50 (50 mg/kg, i.p. Zoletil, Vibac, Carros, France) with xylazine (10 mg/kg, Rompun, Bayer, Barmen, Germany) and then mounted on a stereotactic apparatus (Model 940, David Kopf Instruments, Tujunga, CA, United States). A 2-cm midline incision was made along the scalp, and the implantation area was carefully cleared with H_2O_2 to expose the bregma line. A 6-hydroxydopamine solution (6-OHDA; 8 μg dissolved in 4 μl 0.02% ascorbic saline, Sigma-Aldrich, Burlington, MA, United States) was injected intracranially into the left medial forebrain bundle at a rate of 0.5 μL/min (AP: –4.3 mm; ML: + 1.6 mm; DV: –8.2 mm) by using a 10-μL microsyringe (84877, Hamilton, OH, United States) in accordance with the stereotaxic brain atlas of Paxinos and Watson (2005). The needle was maintained in the brain for 5 min before being slowly withdrawn to avoid backfilling along the injection tract. After inducing the PD lesion, we verified the effectiveness of PD lesion at 4 weeks post-surgery by using an apomorphine-induced rotational test. The rats that did not exhibit apomorphine-induced contralateral rotation behaviors were excluded for further analysis.

Cortical Electrical Stimulation Electrode Implantation

After 6-OHDA injection, the CES electrode was then implanted on the rat's skull under the same anesthesia. Stainless steel epidural screw electrodes (1.6-mm-diameter pole, 0–80 × 1/16, PlasticsOne Inc., Roanoke, VA, United States) were implanted into the four burr holes. Cortical electrodes were placed epidurally into the primary motor cortex of the forelimb (AP: −1.5 mm from the bregma; ML: ± 4.0 mm from the midline) and hind limb (AP: 1.0 mm from the bregma; ML: ± 1.25 mm from the midline) in accordance with functional rat brain mapping (**Figure 1A**; Fonoff et al., 2009). Four electrodes were inserted into a six-channel pedestal (MS363, Plastics One, Inc., Roanoke, VA, United States) by using wires. The screw electrodes and pedestal were secured to the skull surface with dental acrylic (Lang Dental Mfg., Wheeling, IL, United States). To focally stimulate the motor cortex of the rats, CES was applied from outside through an implantable plastic socket (E363/0 and MS363, Plastics One, Roanoke, VA, United States) (**Figure 1B**).

Cortical Electrical Stimulation Treatment and Experimental Design

To verify the therapeutic effects of CES, the 6-OHDA-induced PD rats were randomly assigned to one of two groups, a sham CES treatment group (n = 8) or a CES treatment group (n = 8; **Figure 2**). In the CES treatment group, awake PD rats were treated with CES and an intermittent theta-burst stimulation (iTBS) protocol (triplets of pulses at 50 Hz, repeated every 200 ms with a 2-s sequence of TBS repeated every 10 s for 20 repetitions to a total of 600 pulses per session) (Huang et al., 2005). Based on our earlier study, the severity of dopamine depletion could be critically involved for the expression of motor plasticity. It might further interfere the improvement of motor performance (Hsieh et al., 2015b). Accordingly, for elucidating the possible therapeutic effects, we therefore conducted to have the early intervention of CES before the onset of symptoms. One day after a PD lesion, the PD animals in the CES treatment group received the CES protocol (1 session/day, 28 consecutive sessions over 4 weeks) (**Figure 2**). The intensity of electrical pulses was set at 80% resting motor threshold, which was defined as the minimal intensity of magnetic stimulation required to elicit minimal forelimb muscle twitches. In the sham CES treatment group, the PD rats also underwent the same CES protocol, but no electrical stimulation was applied at the same time points. All behavioral examinations were performed before and after treatment by a well-trained examiner who was blinded to treatment types. The timetable of behavioral and biochemistry

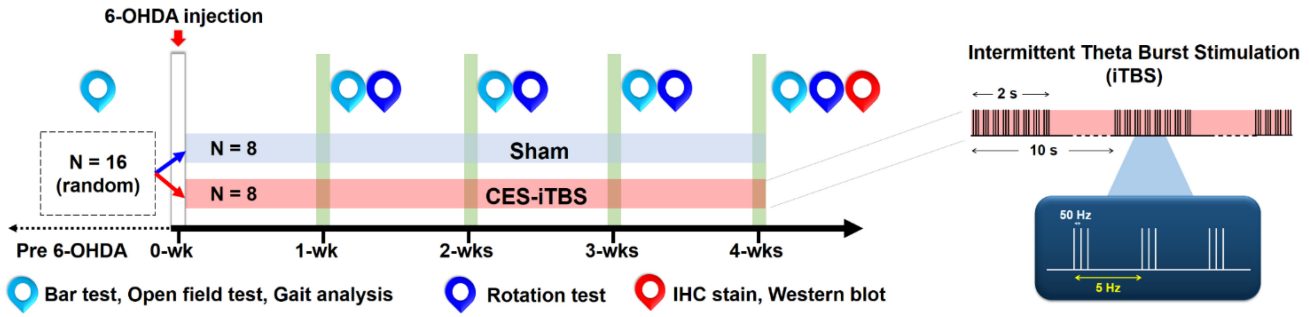

FIGURE 2 | Experimental design for the long-term CES treatment. CES treatment was performed 7 days a week for 4 successive weeks. Behavioral tests, including bar test, open-field test, gait analysis, and apomorphine-induced rotation behavior, were performed weekly to investigate the treatment effects over time. Immunohistochemistry (IHC) and western blot analyses were applied on the week-4 post PD lesion to identify the neuroprotective effects of dopaminergic neurons and fibers following 4 weeks of CES treatment.

analyses is summarized in **Table 1**. Behavioral tests, including the bar test for akinesia, open-field locomotor activity and gait analysis were conducted before as well as every week after the 6-OHDA lesions. Apomorphine-induced rotation was performed every week after PD lesion. Three motor behavior tests (bar test, open field test, gait analysis) were performed in same sequence on same day. The rotational test was conducted on alternate day after motor behavior tests. For each test, there were at least 3 h of resting time between each behavioral test. To identify the neuroprotective effect of CES treatment on dopaminergic neurons and fibers, immunohistochemistry and western blot analysis were conducted at week 4 after PD lesion.

Behavioral Test

The behavioral tests were measured at baseline and weekly for 4 weeks. The tests included bar test for akinesia, open-field locomotor activity, gait pattern, and apomorphine-induced rotation in the 6-OHDA lesioned rats with and without CES treatment.

Akinesia

Akinesia is a cardinal motor symptom of PD. In previous studies, the bar test has been performed to observe the akinesia phenomenon in rat models of PD (Mabrouk et al., 2009; Hsieh et al., 2011). At the outset of the bar test, each rat was placed gently on a platform. Both forelimbs were placed at the same time on a horizontal acrylic bar (0.7 cm diameter), which was held 9 cm above the table surface. The total duration (in seconds) spent from placing of each forepaw on the bar to the first complete removal from the support bar was recorded (Hsieh et al., 2011; Feng et al., 2020; Hsieh et al., 2021). All PD rats were measured over five subsequent trials and the durations of these trials were averaged.

Apomorphine-Induced Rotation Test

To verify the dopamine depletion levels after unilateral 6-OHDA infusion in PD rats, the conventional and reliable apomorphine-induced contralateral rotation test was performed (Creese et al., 1977; Iancu et al., 2005; Metz et al., 2005; Yoon et al., 2007; Hsieh et al., 2011). In brief, the rats were injected with apomorphine (0.5 mg/kg, dissolved in 0.02% ascorbic saline, Sigma-Aldrich, Burlington, MA, United States) and placed in a round bowl with a diameter of 40 cm. The number of rotations in a clockwise (contralateral) direction over 60 min was recorded on video and then manually counted using the trained examiner. Generally, a rotational response of over 300 rotations/h may suggest a maximum of 90% dopaminergic neuronal loss in the substantia nigra (Blandini et al., 2007; Hsieh et al., 2011). The rotation test was used to confirm the effectiveness of 6-OHDA infusion at 4 weeks post PD lesion. The rats that exhibited no contralateral rotation behavior induced by apomorphine were excluded from further analysis.

Open-Field Locomotor Activity

The open-field test was commonly applied to measure general locomotor activity in 6-OHDA induced PD rat model (Silva et al., 2016; Su et al., 2018; Feng et al., 2020). In the open field test, each rat was monitored on video camera in an open-field black plexiglass arena (60 cm × 60 cm × 100 cm in dimension), as previously described (Yang et al., 2016; Feng et al., 2020). The total distance traveled and the movement time of each animal during a 10-min testing period was recorded on a digital camera (C930e, Logitech, Newark, CA, United States) and analyzed using a video-tracking system (Smart v3.0, Panlab SL, Barcelona, Spain). The testing arena was completely cleansed with 75% ethanol in the periods between each rat's test session.

Gait Analysis

To understand the motor behavioral changes in the PD rats before and after CES treatment, a detailed gait analysis was performed to assess gait disturbances in the PD rats. The procedure for measuring gait pattern was as described in previous works (Hsieh et al., 2011; Lee et al., 2012; Hsieh et al., 2021). In brief, the walking track equipment consisted of an enclosed walkway made of transparent plexiglass (80 cm × 6 cm × 12 cm length, width, and height, respectively) with a mirror (tilting at 45°) positioned underneath the walkway. A high-speed and high-resolution camera (PX-100, JVC, Yokohama, Japan) was

TABLE 1 | Timetable of behavioral and biochemical examinations on Parkinson's disease (PD) rat model.

Assay	Weeks after 6-OHDA lesion					
	Pre 6-OHDA	0-wk	1-wk	2-wks	3-wks	4-wks
Bar test	+	−	+	+	+	+
Open field test	+	−	+	+	+	+
Gait analysis	+	−	+	+	+	+
Rotation test	−	−	+	+	+	+
IHC stain	−	−	−	−	−	+
Western blot	-	−	−	−	−	+

positioned in the front of the walkway to capture a sagittal view and a downward view reflected by the mirror. After recording, we captured the image data from each trial and processed them semi-automatically by using the Matrix Laboratory software (MathWorks, version 9.6., R2019a) to identify the sequential footprints. Four spatial parameters (i.e., step length, stride length, base of support, and foot angle) and three temporal gait parameters (i.e., walking speed, stance/swing phase time, and stance/swing ratio) were determined (Hsieh et al., 2011; Lee et al., 2012; Liang et al., 2014).

Histology Investigation

To assess the dopaminergic loss in the nigrostriatal neurons and fibers in PD rats, tyrosine-hydroxylase (TH) staining was performed (Hsieh et al., 2011; Li et al., 2015; Feng et al., 2020). The 6-OHDA-lesioned rats from both groups were sacrificed after behavioral tests at postlesion week 4. The procedure for the TH staining was as described previously (Truong et al., 2006; Hsieh et al., 2011; Hsieh et al., 2015b; Feng et al., 2020). In brief, the rat brains were carefully removed, postfixed with 4% paraformaldehyde fixative solution (PFA), and then placed under 48-h cryoprotection at 4°C with 30% sucrose solution until the brain sank. The cerebral tissues were sectioned into 30-μm-thick coronal blocks by using a cryostat (Leica CM3050 S Cryostat, Miami, FL, United States). The substantia nigra pars compacta (SNpc) and striatum areas were selected. The free-floating sections were quenched for 10 min with 0.3% H_2O_2–phosphate-buffered-saline (PBS) and blocked non-specific antibodies for 1 h with 10% milk. The sections were then incubated with anti-TH rabbit primary antibody (1:1,000, AB152, Millipore, Burlington, MA, United States) at room temperature for 1 h. Thereafter, the sections were washed three times with PBS, incubated with antirabbit secondary antibody (1:200, MP-7401, Vector Labs, Burlingame, CA, United States) at room temperature for 1 h, and placed in 3,3-diaminobenzidine (DAB, SK-4105, Vector Labs, Burlingame, CA, United States) solution for 3–5 min. Finally, the sections were mounted on slides and treated with graded alcohols to dehydrate them. To remove excess dyes and make the samples clear for microscopic observation, the brain tissue sections were cleaned using xylol (Sinopharm, Beijing, China) before being coverslipped in dibutyl phthalate polystyrene xylene. Three brain slices were collected and used for further analysis in each rat. The sections were digitally scanned by using a digital pathology slide scanner (Aperio CS2, Leica Biosystems Inc., Buffalo Grove, IL, United States). The obtained digital images were then converted into binary (8-bit black-and-white) images. In each slide, two fields, including SNpc and striatum in the non-lesioned and lesioned areas were chosen for further analysis. The numbers of TH-positive cells in the SNpc were counted by means of particle analysis using Image-Pro Plus 6.0 software (Media Cybernetics, Bethesda, MD, United States) and these values were then manually validated by two investigators to ensure the correct identification of TH-positive pattern (Hsieh et al., 2021). The percentage of TH-positive cells was calculated in the ipsilateral hemisphere and normalized with respect to the contralateral side (Feng et al., 2020; Hsieh et al., 2021). With regard to the striatal TH-positive fibers, the same image analysis software (Image-Pro Plus 6.0, Media Cybernetics, Bethesda, MD, United States) was used to correct the non-specific background density measured at the corpus callosum, and the optical density of the TH-positive fibers in the striatum of each hemisphere was analyzed separately (Hsieh et al., 2011; Feng et al., 2020; Hsieh et al., 2021). The percentage of TH-positive fibers on the ipsilateral side was normalized and presented with respect to the contralateral side.

Western Blot

Approximately 4 μg of tissue-lysate proteins was fractionated and separated using 12% sodium dodecyl sulfate-polyacrylamide gel and then blotted onto a polyvinylidene difluoride membrane (Millipore, Burlington, MA, United States). To prevent antibodies from binding to the membrane non-specifically, the membrane was blocked with 5% skim milk diluted in Tris-buffered saline with Tween 20 buffer. Dopaminergic neuron levels were calculated using a blotting membrane with indicated primary antibodies, including anti-TH (1:100, Merck, Darmstadt, Germany) and mouse anti-β-actin (1:100, Santa Cruz Biotechnology, Santa Cruz, CA, United States). After incubation with anti-mouse IgG antibodies (enzyme horseradish peroxidase [HRP]; 1:5,000, GeneTex, Irvine, CA, United States) for 1 h at room temperature, the protein intensity was determined using a chemiluminescent HRP substrate (Millipore, Burlington, MA, United States). The bands were digitally scanned, and the intensities were quantified using Image J software (National Institutes of Health, Bethesda, MD, United States).

Data Analysis

Statistical analysis was performed using the SPSS 25.0 package (IBMCorp., Armonk, NY, United States). The significance level was set at $p < 0.05$. The effect of CES treatment for all data measures was assessed using two-way repeated-measures analysis of variance (ANOVA) with protocol (sham vs. CES treatment) used as the between-subjects factor and time (pre-assessment vs. post-assessment) as the within-subject factor. Unpaired *t* tests were performed to compare groups at each time point when the main effect of the group was significant. Furthermore, separate one-way ANOVAs, followed by *post-hoc* Bonferroni tests, were used to compare behavioral, immunohistochemistry and Western blot data at distinct time points as necessary.

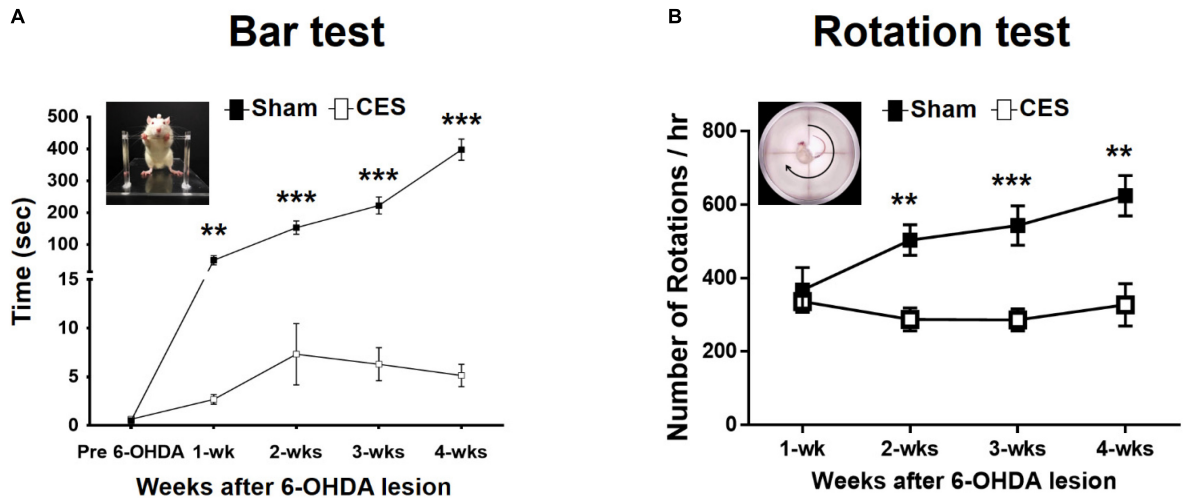

FIGURE 3 | Time-course analysis of bar test **(A)** and apomorphine-induced rotational behavior **(B)** in the sham-CES-treated and CES-treated groups after the 6-hydroxydopamine (6-OHDA) lesions. Values are shown as means ± SEMs. $^{*}p < 0.05$, $^{**}p < 0.01$, and $^{***}p < 0.001$; each indicates significant difference between the two groups.

RESULTS

Effects of Cortical Electrical Stimulation Treatment on Akinesia After 6-Hydroxydopamine Lesion

All behavioral tests were completed in eight PD-lesioned rats that underwent 4 weeks of sham treatment and in another eight such rats that underwent 4 weeks of CES treatment. The akinesia phenomenon was observed using the prelesion and post-6-OHDA-lesion week 1–4 using bar test. Repeated-measures ANOVA revealed significant differences main effects of time ($F_{(4,56)} = 62.483$, $p < 0.001$), group ($F_{(1,14)} = 148.764$, $p < 0.001$), and time × group interaction ($F_{(4,56)} = 59.823$, $p < 0.001$). Moreover, the subsequent *post-hoc t*-tests revealed that the duration in the bar test reached significant differences between the two groups at 1 week ($t = 3.406$; $p = 0.004$), 2 weeks ($t = 6.875$; $p < 0.001$), 3 weeks ($t = 8.084$; $p < 0.001$), and 4 weeks ($t = 11.866$; $p < 0.001$) after the 6-OHDA lesions were observed (**Figure 3A**).

Effects of Cortical Electrical Stimulation Treatment on Apomorphine-Induced Rotation

In this study, we observed the contralateral rotations by using apomorphine-induced rotation tests from postlesion weeks 1–4 to characterize the extent of motor impairment behavior of PD rats with the disease progression. All animals exhibited the apomorphine-induced contralateral rotation behavior at 4 weeks post PD lesion. Therefore, all 16 rats (8 rats for sham CES treatment group and 8 rats for CES treatment group) were included for data analysis. Repeated-measures ANOVA revealed significant differences main effects of time ($F_{(3,42)} = 5.162$, $p = 0.004$), group ($F_{(1,14)} = 14.757$, $p = 0.002$), and time × group interaction ($F_{(3,42)} = 6.678$, $p = 0.001$). Moreover, according to the results of the *post-hoc t*-tests at each time point, the differences were mainly influenced by CES treatment effects, which was chiefly observed in the number of rotations per hour at 2 weeks ($t = 4.146$; $p = 0.001$), 3 weeks ($t = 4.194$; $p = 0.001$), and 4 weeks ($t = 3.735$; $p = 0.002$) after 6-OHDA lesion (**Figure 3B**).

Effects of Cortical Electrical Stimulation Treatment on Open-Field Test Locomotor Activity Levels

The open-field test is a common behavioral test used to evaluate the locomotor activity. The measured outcomes, including walking distance, immobile time and mobile time, were used to investigate the differences in general locomotor activity between the sham and CES treatment groups from the prelesion stage and throughout postlesion weeks 1–4. In the open field test, the overall traveled walking distance between the CES-treated rats and sham-CES treated rats following 6-OHDA PD lesion was calculated (**Figure 4A**). A repeated-measures ANOVA revealed significant differences main effects of time ($F_{(4,56)} = 15.872$, $p < 0.001$), group ($F_{(1,14)} = 29.822$, $p < 0.001$), and time × group interaction ($F_{(4,56)} = 4.325$, $p = 0.004$). Moreover, according to the *post-hoc t*-test results, the differences were mainly influenced by CES treatment effects across every time point, primarily for walking distance at postlesion weeks 1 ($t = -3.415$; $p = 0.004$), 2 ($t = -5.831$; $p < 0.001$), 3 ($t = -4.575$; $p < 0.001$), and 4 ($t = -5.751$; $p < 0.001$; **Figure 4B**). With regard to the immobile time, repeated-measures ANOVA revealed significant differences main effects of time ($F_{(4,56)} = 9.608$, $p < 0.001$), group ($F_{(1,14)} = 14.338$, $p = 0.002$), and time × group interaction ($F_{(4,56)} = 5.851$, $p = 0.001$). Moreover, according to the *post-hoc t*-test results, the differences were mainly driven by CES treatment effects across every time point, primarily for immobile time at postlesion weeks 1 ($t = -2.610$; $p = 0.021$), 2 ($t =$

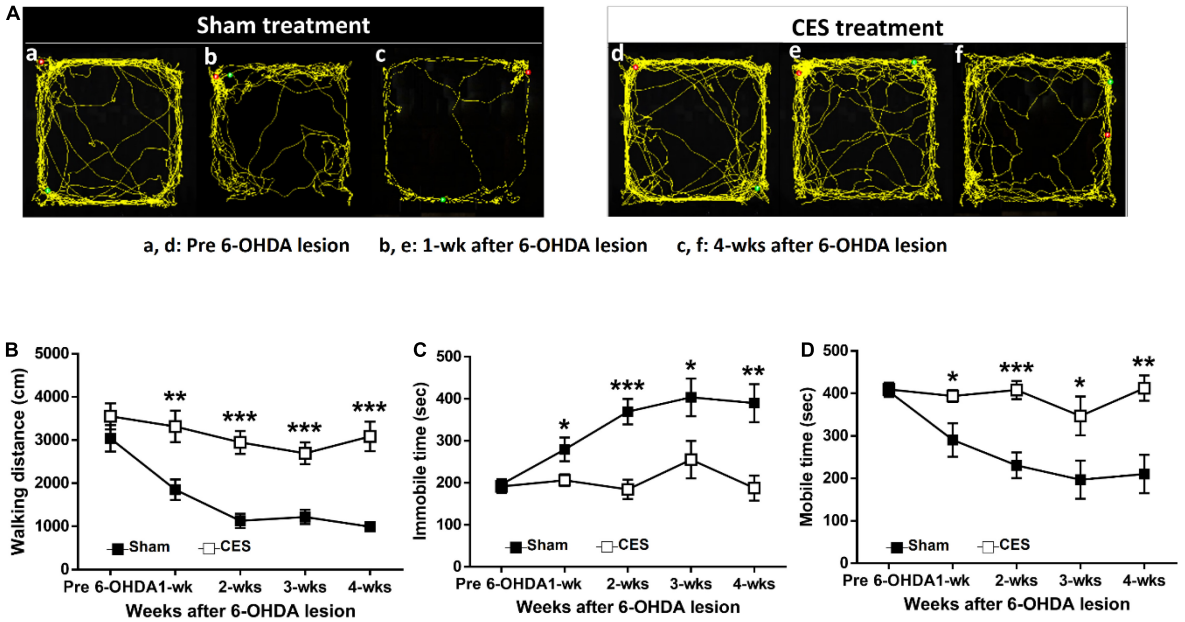

FIGURE 4 | Time-course analysis of locomotor activity assessed by open-field test at before and after 6-OHDA lesions. **(A)** Representative traces of rat movement patterns during the open-field test in the sham- and CES-treaded rats before PD lesions and at postlesion weeks 1 and 4. **(B)** Significant differences were observed between the sham and CES treatment groups in walking distance, **(C)** immobile time, and **(D)** mobile time after PD lesions. Values are expressed as the means ± SEMs. *$p < 0.05$, **$p < 0.01$, and ***$p < 0.001$; each indicates a significant difference between the two groups.

−4.857; $p < 0.001$), 3 ($t = -2.321$; $p = 0.036$), and 4 ($t = -3.727$; $p = 0.002$; **Figure 4C**). With regard to the mobile time, repeated-measures ANOVA revealed significant differences main effects of time ($F_{(4,56)} = 9.539$, $p < 0.001$), group ($F_{(1,14)} = 14.386$, $p = 0.002$), and time × group interaction ($F_{(4,56)} = 5.835$, $p = 0.001$). Furthermore, according to *post-hoc t*-test results, the differences were mainly influenced by CES treatment effects across every time point, primarily in mobile time at postlesion weeks 1 ($t = 2.609$; $p = 0.021$), 2 ($t = 4.858$; $p < 0.001$), 3 ($t = 2.327$; $p = 0.036$), and 4 ($t = 3.727$; $p = 0.002$; **Figure 4D**).

Effects of Cortical Electrical Stimulation Treatment on Gait Pattern

In this study, a quantitative analysis of gait pattern in PD rats with and without CES treatment was performed. **Figure 5A** presents typical footprint images captured from the PD rats that underwent sham and CES treatments before PD lesion and at postlesion week 4. Repeated-measures ANOVA on gait parameters revealed significant time × group interaction in walking speed ($F_{(4,56)} = 15.80$, $p < 0.001$), step length ($F_{(4,56)} = 4.51$, $p = 0.003$), stride length ($F_{(4,56)} = 6.04$, $p < 0.001$), double support time ($F_{(4,56)} = 4.756$, $p = 0.002$), stance phase time ($F_{(4,56)} = 10.488$, $p < 0.001$), suggesting less impairment of gait pattern in the CES treatment group than in the sham CES treated group (**Figures 5B–D,F,G**). No significant group × time interaction was found in base of support ($F_{(4,56)} = 0.65$, $p = 0.632$) and swing phase time ($F_{(4,56)} = 0.901$, $p = 0.47$) (**Figures 5E,H**). *Post-hoc t*-tests between the two groups showed that walking speed, step length, stride length, base of support, double support time and stance phase time reached a significant difference at 2, 3 and 4 weeks after PD lesion (**Figures 5B–G**).

Figure 6A shows footprint images captured from PD rats with sham and CES treatment at week 4 following PD lesion. Repeated measures ANOVA on foot parameters during locomotion revealed significant main effect of group in print length ($F_{(1,14)} = 17.02$, $p = 0.001$), toe spread ($F_{(1,14)} = 6.426$, $p = 0.024$) but not in foot angle ($F_{(1,14)} = 1.254$, $p = 0.282$). The differences were mainly driven by CES treatment according to the results of *post-hoc t*-test at each time point, which chiefly observed in print length and toe spread stride at the 4th week of 6-OHDA lesion (unpaired *t*-tests, $p < 0.05$) (**Figures 6B–D**).

Quantification of Dopaminergic Neuronal Degeneration Levels

To observe the effects of 4-week CES treatment on dopaminergic neurons and fibers in the nigrostriatal pathway, we measured TH-positive cells in the substantia nigra and TH-positive fibers in the striatum by using immunohistochemistry staining. The results of the TH immunohistochemistry in the substantia nigra and striatum in PD rats that received and did not receive CES treatment for the 4 weeks are illustrated in **Figure 7A**. The quantification of TH-positive fiber loss in the striatum and TH-positive cell loss in the substantia nigra at 4 weeks post PD lesion are presented in **Figure 7B**. PD rats that received CES treatment exhibited a greater preservation of TH-positive fibers in the striatum ($t = 26.879$, $p < 0.001$) and TH-positive cells in the substantia nigra ($t = 7.055$, $p = 0.002$) compared with sham treatment group.

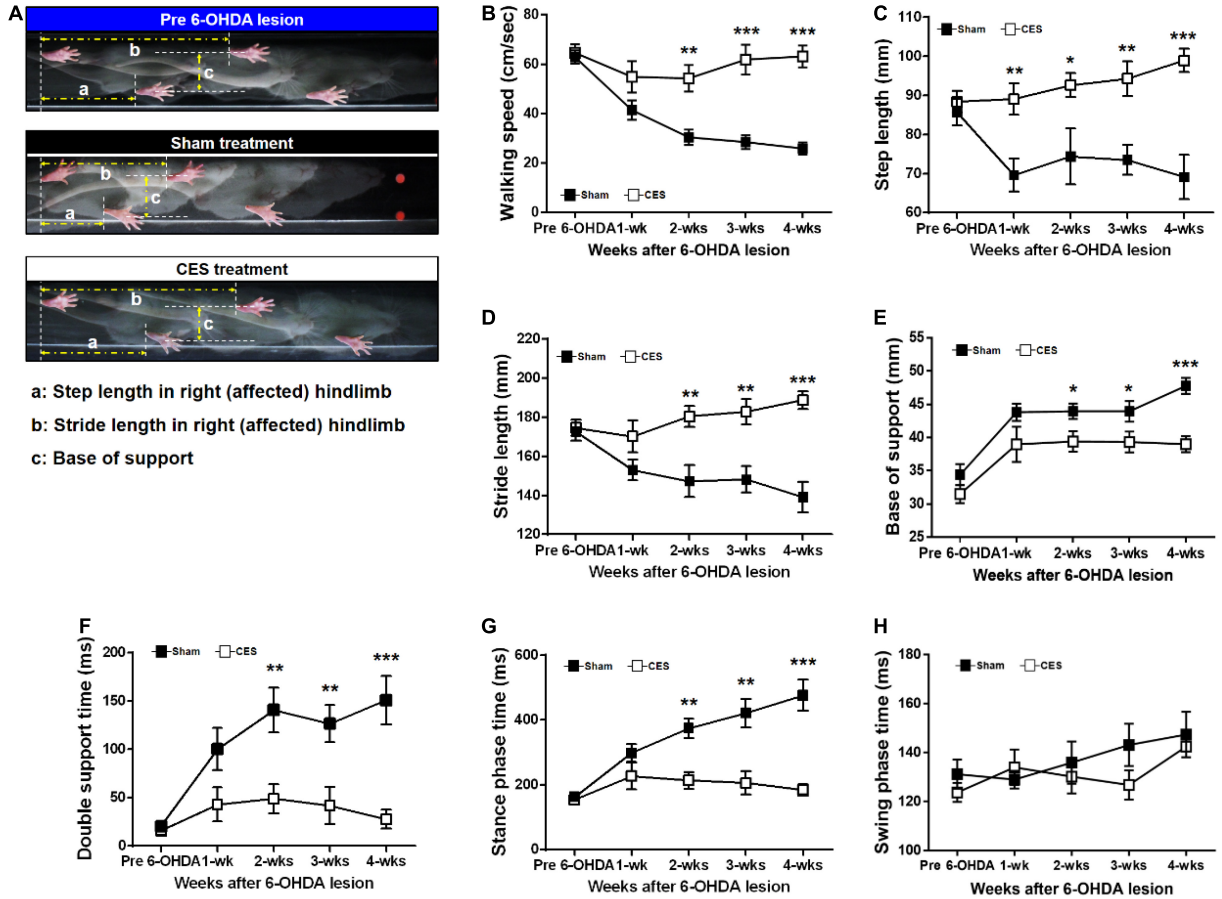

FIGURE 5 | (A) Characteristics of stepping of rat (as indicated by footprints) during walkway locomotion prior to PD lesion and postlesion week 4 for a sham treatment group rat and a CES-treated rat. Time-course changes in walking speed **(B)**, step length **(C)**, stride length **(D)**, base of support **(E)**, double support time **(F)**, stance phase time **(G)**, and swing phase time **(H)** in the sham-treated and CES-treated PD rats over the 4 weeks of observation. Notably, the walking speed, step, and stride lengths decreased significantly in the sham CES treatment group but were less affected in the CES treatment group. Gradual increases in the base of support were found in both groups, but the CES treatment group exhibited a lower increase than the sham treatment group. $^{*}p < 0.05$, $^{**}p < 0.01$, and $^{***}p < 0.001$, each of which indicated significant differences between two groups at each time point (unpaired *t*-tests).

Furthermore, we examined the expression levels of TH protein of the lesioned striatum in the sham or CES treatment group through western blotting. The TH levels in the striatum are illustrated in **Figure 7C**. Compared with the CES treatment group, the sham treatment group exhibited lower TH levels in the striatum. *Post-hoc* test in TH levels showed significant difference between the sham-treated and CES-treated PD rats ($t = 8.576$; $p < 0.01$; **Figure 7D**).

DISCUSSION

In the current study, we evaluated the effects of CES treatment in a 6-OHDA induced PD rat model. We performed several comprehensive quantitative assessments under various aspects of motor function (all of which are commonly affected in PD patients) to identify the therapeutic effects over the 4 weeks of CES treatment. We found that such a long-term CES treatment with iTBS protocol could mitigate 6-OHDA-induced motor dysfunction and potentially exert a neuroprotective effect on dopaminergic neurons and fibers. After 4 weeks of CES intervention, several types of motor behavioral impairment were reduced. In addition, the histological results revealed greater preservation of dopaminergic neurons and striatal fibers in the CES treated group than in the sham-treated group, a finding that was verified through western blotting, further indicating the neuroprotective effect of CES. To the best of our knowledge, this is the first study to comprehensively investigate the therapeutic effects of CES on several aspects of motor function in a PD rat model. These data could enhance the growing body of basic and clinical research on the efficacy of CES in PD treatment.

In this study, CES with iTBS protocol was applied to induce changes in long-term potentiation and plasticity in disease progression. The pattern of neurodegeneration in PD involves abnormal neuronal activities in the basal ganglia–thalamo–cortical circuits. For example, the usual effect of the facilitation of thalamic projections to the motor cortex

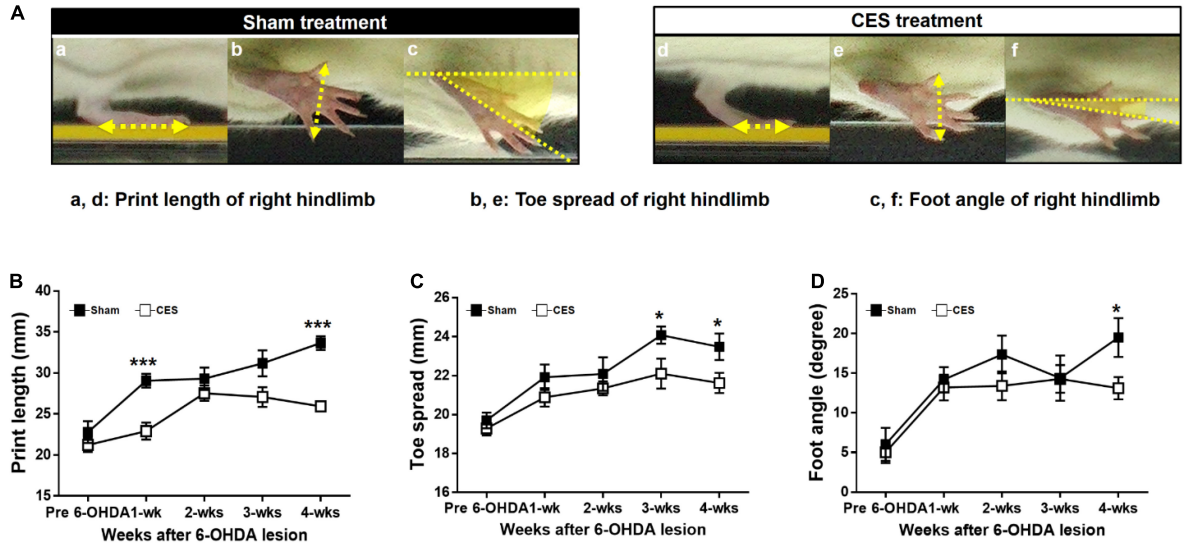

FIGURE 6 | Characteristics of footprint during walkway locomotion in PD rats with sham-treatment or CES treatment after 4 weeks PD lesion **(A)**. Time-course changes in print length **(B)**, toe spread **(C)**, and foot angle **(D)** in the sham- and CES-treated PD rats over 4 weeks of observation. Note that the print length, toe spread, and foot angle increased in the sham CES treatment group but less affected in the CES treatment group. $^{*}p < 0.05$, $^{**}p < 0.01$, and $^{***}p < 0.001$, significant differences between two groups at each time point (unpaired *t*-tests).

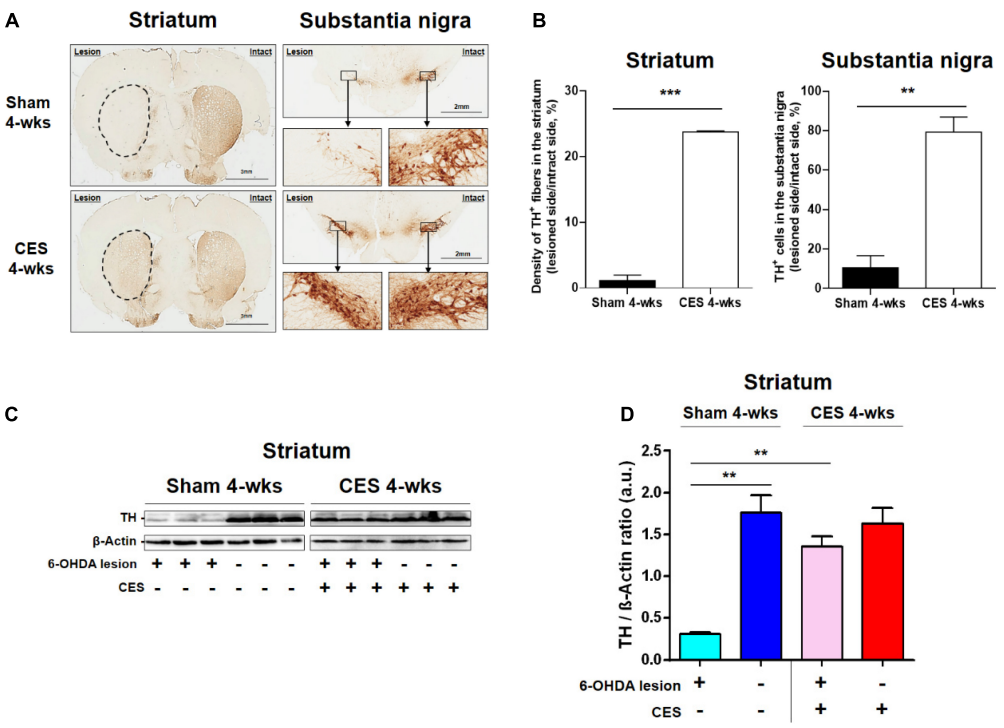

FIGURE 7 | (A) Representative TH-positive fibers in the striatum and TH-positive neurons in the substantia nigra pars compacta from the sham-treated and CES-treated rats at 4 weeks after PD lesion. **(B)** Comparison of the average TH-positive fibers and neurons between sham and CES treatment groups. **(C)** Expression of TH in the striatum represented through a western blot for PD rats that received sham ($n = 3$) and CES ($n = 3$) treatments at 4 weeks after PD lesion. **(D)** Quantitative analysis of relative protein levels of TH in the striatum in the sham and CES treatment groups. $^{**}p < 0.01$, $^{***}p < 0.001$, each of which indicates a significant difference between the two groups.

is reduced in PD, resulting in deactivation or hypoactivation of cortical motor areas, and thus, reduced motor output during movement (Wichmann and Delong, 1996; Lefaucheur, 2005; Pasquereau et al., 2015). Functional neuroimaging studies have also indicated that the motor cortex is impaired in both the early and late stages of PD. For example, hypoactivation in the primary motor cortex seems to be observed preferentially by functional magnetic resonance imaging (fMRI) in early, untreated patients (Ellaway et al., 1995; Buhmann et al., 2003). By contrast, hyperactivity of the motor cortex has more often been found in patients with more advanced PD (Sabatini et al., 2000; Haslinger et al., 2001). It indicates that the motor cortex may be attributed to a compensatory cortical reorganization due to the disease progression (Rascol et al., 1998). The available anatomical, physiological, and imaging-based studies suggest that PD results from dopamine loss in the basal ganglia, which induces neuronal discharge abnormalities within the entire motor circuit (Delong and Wichmann, 2007). In addition to the basal ganglia pathway, at the cortical level, this manifests in the form of abnormalities in cortical activation patterns during movement tasks (Delong and Wichmann, 2007). Thus, in addition to the basal ganglia circuit, targeting the motor circuitry in neuromodulation approaches can be also be considered as a therapeutic strategy for PD. Previous research has demonstrated that both long-term potentiation and depression-like plasticity of the motor cortex are impaired in individuals with PD (Kishore et al., 2011; Suppa et al., 2011). On the basis of histological and behavioral investigations, our earlier study suggested that such impaired motor plasticity is strongly associated with the loss of dopaminergic nigral cells and striatal fibers (Hsieh et al., 2015b). Thus, in the present study, the early intervention of brain stimulation was designed to induce superior neuroprotective effects and CES-induced motor functional changes in the PD rats.

Until now, the therapeutic effects and potential mechanisms of CES in the treatment of PD have remained unclear. The animal models may help provide greater insight into these mechanisms. In the histological results of IHC staining in the two groups, CES treatment could effectively reduce the degeneration level of TH-positive fibers and TH-positive cells. We also found that 6-OHDA-lesioned rats treated with CES for 4 weeks registered reductions in akinesia and gait disturbances. These results are consistent with the findings of a human study that demonstrated the effectiveness of CES in improving cognitive and motor function in patients with advanced PD (Fasano et al., 2008; Gutierrez et al., 2009; De Rose et al., 2012). Although the optimal stimulation parameters of CES remain unclear, a suitable animal model of the disease could help identify an effective stimulation protocol, including adjustment and optimization of frequency, polarity, and current level, allowing rapid screening and neurophysiological analysis in PD animal studies. Future research is still required to clarify the mechanisms underlying the effects of CES and explore and optimize CES protocols in PD.

Moreover, the western blot results verified the TH protein levels, indicating that long-term CES intervention might not only ameliorate the deterioration of motor behavior caused by 6-OHDA lesions but also promote the retention of more dopaminergic neurons under the threat of neurotoxin. Most motor functions were significantly well preserved after 3–4 weeks of CES treatment. Based our previous study, after 24 h of the 6-OHDA injection, the degeneration of dopaminergic neurons and striatum terminal was observed (Hsieh et al., 2011). Hence, combined with the histological and behavioral results, this study suggests that early (starting from directly after the appearance of PD lesions) and long-term (4-week) CES intervention may help mitigate the threat of neurodegeneration, maintain motor functions and reduce dopaminergic neuron death. Similar to our findings, earlier studies reported that rTMS could induce neuroprotective effects in stroke and brain injury animal models (Ljubisavljevic et al., 2015; Sasso et al., 2016). The neuroprotective effects on dopaminergic cells or fibers could be related to anti-inflammatory effects (e.g., tumor necrosis factor-alpha, TNF-α or cyclooxygenase-2, COX-2), upregulation of neurotrophic factor (e.g., brain-derived neurotrophic factor, BDNF; glial cell line-derived neurotrophic factor, GDNF) or reduction of astrogliosis and microglial activation (glial fibrillary acidic protein, GFAP; ionized calcium binding adaptor molecule 1, Iba-1) induced by long-term CES intervention (Yang et al., 2010; Lee et al., 2013; Sasso et al., 2016; Cacace et al., 2017). Because the exact mechanism underlying these effects remains unclear, further investigation is required to clarify these potential mechanisms underlying the neuroprotective effects of CES in PD.

CONCLUSION

This study provided a clearer picture of the progressive changes in PD-related symptoms with or without CES treatment and documented the efficacy of CES in ameliorating motor dysfunctions and inducing the neuroprotective effect of the dopaminergic system in a 6-OHDA-induced PD rat model. The long-term CES treatment model used in this study may help bridge the gap between animal and human studies of PD. Future research is still required to further clarify the underlying mechanisms, allowing improved CES protocols and more effective therapies in PD and other neurological diseases to be developed for humans.

DATA AVAILABILITY STATEMENT

The raw data supporting the conclusions of this article will be made available by the authors, without undue reservation.

ETHICS STATEMENT

The animal study was reviewed and approved by the Institutional Animal Care and Use Committee, Chang Gung University IACUC Approval No: CGU15-151, Period of Protocol: valid from August 01, 2016 to July 30, 2019.

AUTHOR CONTRIBUTIONS

C-WK, C-WP, and T-HH conceived and designed the experiments. C-WK, H-CT, P-KC, T-YJ, and T-HH performed the experiments. T-HH, M-YuC, C-YP, and C-WP provided the equipment. C-YP, C-WP, X-KH, H-HL, and T-HH developed the methodology. C-WK, H-HL, X-KH, H-CT, and T-HH analyzed the data. C-WK, M-YuC, M-YiC, X-KH, H-HL, TN, and T-HH contributed to the writing and editing the manuscript. All authors contributed to the article and approved the submitted version.

FUNDING

This study was supported by grants from the Ministry of Science and Technology, Taiwan (MOST 108-2314-B-182-015-MY3, 109-2314-B-182-029-MY3 to T-HH, and MOST 109-2221-E-038-005-MY3 to C-WP), Chang Gung Medical Foundation, Taiwan (CMRPD1H0463 and CMRPD1K0671 to T-HH), Industry-Academy Cooperation Project of Chang Gung University (QCRPD657, SCRPD1H0061, SCRPD1K0351, and SCRPD1K0611 to T-HH), and Min-Sheng General Hospital (Grant Nos. 1090003 and 2020003 to M-YuC).

REFERENCES

Adkins, D. L., Campos, P., Quach, D., Borromeo, M., Schallert, K., and Jones, T. A. (2006). Epidural cortical stimulation enhances motor function after sensorimotor cortical infarcts in rats. *Exp. Neurol.* 200, 356–370. doi: 10.1016/j.expneurol.2006.02.131

Adkins, D. L., Hsu, J. E., and Jones, T. A. (2008). Motor cortical stimulation promotes synaptic plasticity and behavioral improvements following sensorimotor cortex lesions. *Exp Neurol* 212, 14–28. doi: 10.1016/j.expneurol.2008.01.031

Adkins-Muir, D. L., and Jones, T. A. (2003). Cortical electrical stimulation combined with rehabilitative training: enhanced functional recovery and dendritic plasticity following focal cortical ischemia in rats. *Neurol Res* 25, 780–788. doi: 10.1179/016164103771953853

Alm, P. A., and Dreimanis, K. (2013). Neuropathic pain: transcranial electric motor cortex stimulation using high frequency random noise. Case report of a novel treatment. *J Pain Res* 6, 479–486. doi: 10.2147/JPR.S44648

Bastide, M. F., Meissner, W. G., Picconi, B., Fasano, S., Fernagut, P. O., Feyder, M., et al. (2015). Pathophysiology of L-dopa-induced motor and non-motor complications in Parkinson's disease. *Prog. Neurobiol.* 132, 96–168.

Blandini, F., Levandis, G., Bazzini, E., Nappi, G., and Armentero, M. T. (2007). Time-course of nigrostriatal damage, basal ganglia metabolic changes and behavioural alterations following intrastriatal injection of 6-hydroxydopamine in the rat: new clues from an old model. *Eur. J. Neurosci.* 25, 397–405. doi: 10.1111/j.1460-9568.2006.05285.x

Buhmann, C., Glauche, V., Sturenburg, H. J., Oechsner, M., Weiller, C., and Buchel, C. (2003). Pharmacologically modulated fMRI–cortical responsiveness to levodopa in drug-naive hemiparkinsonian patients. *Brain* 126, 451–461. doi: 10.1093/brain/awg033

Cacace, F., Mineo, D., Viscomi, M. T., Latagliata, E. C., Mancini, M., Sasso, V., et al. (2017). Intermittent theta-burst stimulation rescues dopamine-dependent corticostriatal synaptic plasticity and motor behavior in experimental parkinsonism: Possible role of glial activity. *Mov. Disord.* 32, 1035–1046. doi: 10.1002/mds.26982

Cioni, B. (2007). Motor cortex stimulation for Parkinson's disease. *Acta Neurochir. Suppl.* 97, 233–238. doi: 10.1007/978-3-211-33081-4_26

Connolly, B. S., and Lang, A. E. (2014). Pharmacological treatment of Parkinson disease: a review. *JAMA* 311, 1670–1683. doi: 10.1001/jama.2014.3654

Creese, I., Burt, D. R., and Snyder, S. H. (1977). Dopamine receptor binding enhancement accompanies lesion-induced behavioral supersensitivity. *Science* 197, 596–598. doi: 10.1126/science.877576

De Lau, L. M., and Breteler, M. M. (2006). Epidemiology of Parkinson's disease. *Lancet Neurol.* 5, 525–535.

De Rose, M., Guzzi, G., Bosco, D., Romano, M., Lavano, S. M., Plastino, M., et al. (2012). Motor cortex stimulation in Parkinson's disease. *Neurol. Res. Int.* 2012:502096.

Degardin, A., Devos, D., Defebvre, L., Destee, A., Plomhause, L., Derambure, P., et al. (2012). Effect of intermittent theta-burst stimulation on akinesia and sensorimotor integration in patients with Parkinson's disease. *Eur. J. Neurosci.* 36, 2669–2678. doi: 10.1111/j.1460-9568.2012.08158.x

Delong, M. R., and Wichmann, T. (2007). Circuits and circuit disorders of the basal ganglia. *Arch. Neurol.* 64, 20–24. doi: 10.1001/archneur.64.1.20

Elahi, B., and Chen, R. (2009). Effect of transcranial magnetic stimulation on Parkinson motor function–systematic review of controlled clinical trials. *Mov. Disord.* 24, 357–363. doi: 10.1002/mds.22364

Ellaway, P. H., Davey, N. J., Maskill, D. W., and Dick, J. P. (1995). The relation between bradykinesia and excitability of the motor cortex assessed using transcranial magnetic stimulation in normal and parkinsonian subjects. *Electroencephalogr. Clin. Neurophysiol.* 97, 169–178. doi: 10.1016/0924-980x(94)00336-6

Espay, A. J., Morgante, F., Merola, A., Fasano, A., Marsili, L., Fox, S. H., et al. (2018). Levodopa-induced dyskinesia in Parkinson disease: Current and evolving concepts. *Ann. Neurol.* 84, 797–811. doi: 10.1002/ana.25364

Fagundes-Pereyra, W. J., Teixeira, M. J., Reyns, N., Touzet, G., Dantas, S., Laureau, E., et al. (2010). Motor cortex electric stimulation for the treatment of neuropathic pain. *Arq. Neuropsiquiatr.* 68, 923–929.

Fasano, A., Piano, C., De Simone, C., Cioni, B., Di Giuda, D., Zinno, M., et al. (2008). High frequency extradural motor cortex stimulation transiently improves axial symptoms in a patient with Parkinson's disease. *Mov. Disord.* 23, 1916–1919. doi: 10.1002/mds.21977

Feng, X. J., Huang, Y. T., Huang, Y. Z., Kuo, C. W., Peng, C. W., Rotenberg, A., et al. (2020). Early transcranial direct current stimulation treatment exerts neuroprotective effects on 6-OHDA-induced Parkinsonism in rats. *Brain Stimul.* 13, 655–663. doi: 10.1016/j.brs.2020.02.002

Fonoff, E. T., Pereira, J. F. Jr., Camargo, L. V., Dale, C. S., Pagano, R. L., Ballester, G., et al. (2009). Functional mapping of the motor cortex of the rat using transdural electrical stimulation. *Behav Brain Res* 202, 138–141. doi: 10.1016/j.bbr.2009.03.018

Gillies, G. E., Pienaar, I. S., Vohra, S., and Qamhawi, Z. (2014). Sex differences in Parkinson's disease. *Front. Neuroendocrinol.* 35:370–384. doi: 10.1016/j.yfrne.2014.02.002

Gilman, S. (2007). *Neurobiology of Disease*. Burlington, Mass: Elsevier Academic Press.

Gutierrez, J. C., Seijo, F. J., Alvarez Vega, M. A., Fernandez Gonzalez, F., Lozano Aragoneses, B., and Blazquez, M. (2009). Therapeutic extradural cortical stimulation for Parkinson's Disease: report of six cases and review of the literature. *Clin. Neurol. Neurosurg.* 111, 703–707. doi: 10.1016/j.clineuro.2009.06.006

Haslinger, B., Erhard, P., Kampfe, N., Boecker, H., Rummeny, E., Schwaiger, M., et al. (2001). Event-related functional magnetic resonance imaging in Parkinson's disease before and after levodopa. *Brain* 124, 558–570. doi: 10.1093/brain/124.3.558

Hsieh, T. H., Chen, J. J., Chen, L. H., Chiang, P. T., and Lee, H. Y. (2011). Time-course gait analysis of hemiparkinsonian rats following 6-hydroxydopamine lesion. *Behav. Brain. Res.* 222, 1–9. doi: 10.1016/j.bbr.2011.03.031

Hsieh, T. H., He, X. K., Liu, H. H., Chen, J. J., Peng, C. W., Liu, H. L., et al. (2021). Early Repetitive Transcranial Magnetic Stimulation Exerts Neuroprotective Effects and Improves Motor Functions in Hemiparkinsonian Rats. *Neural Plast.* 2021:1763533. doi: 10.1155/2021/1763533

Hsieh, T. H., Huang, Y. Z., Chen, J. J. J., Rotenberg, A., Chiang, Y. H., Chien, W. S. C., et al. (2015a). Novel Use of Theta Burst Cortical Electrical Stimulation for Modulating Motor Plasticity in Rats. *J. Med. Biol. Eng.* 35, 62–68. doi: 10.3389/fncir.2021.693073

Hsieh, T. H., Huang, Y. Z., Rotenberg, A., Pascual-Leone, A., Chiang, Y. H., Wang, J. Y., et al. (2015b). Functional Dopaminergic Neurons in Substantia Nigra

are Required for Transcranial Magnetic Stimulation-Induced Motor Plasticity. *Cereb. Cortex.* 25, 1806–1814. doi: 10.1093/cercor/bht421

Huang, Y. Z., Edwards, M. J., Rounis, E., Bhatia, K. P., and Rothwell, J. C. (2005). Theta burst stimulation of the human motor cortex. *Neuron* 45, 201–206.

Iancu, R., Mohapel, P., Brundin, P., and Paul, G. (2005). Behavioral characterization of a unilateral 6-OHDA-lesion model of Parkinson's disease in mice. *Behav. Brain Res.* 162, 1–10. doi: 10.1016/j.bbr.2005.02.023

Kalia, L. V., and Lang, A. E. (2015). Parkinson's disease. *Lancet* 386, 896–912.

Kauffman, T. L., Barr, J. O., and Moran, M. L. (2007). *Geriatric Rehabilitation Manual*. Edinburgh; N Y: Churchill Livingstone Elsevier.

Kishore, A., Joseph, T., Velayudhan, B., Popa, T., and Meunier, S. (2011). Early, severe and bilateral loss of LTP and LTD-like plasticity in motor cortex (M1) in de novo Parkinson's disease. *Clin. Neurophysiol.* 123, 822–828. doi: 10.1016/j.clinph.2011.06.034

Lee, H. Y., Hsieh, T. H., Liang, J. I., Yeh, M. L., and Chen, J. J. (2012). Quantitative video-based gait pattern analysis for hemiparkinsonian rats. *Med. Biol. Eng. Comput.* 50, 937–946. doi: 10.1007/s11517-012-0933-5

Lee, J. Y., Kim, S. H., Ko, A. R., Lee, J. S., Yu, J. H., Seo, J. H., et al. (2013). Therapeutic effects of repetitive transcranial magnetic stimulation in an animal model of Parkinson's disease. *Brain Res.* 1537, 290–302. doi: 10.1016/j.brainres.2013.08.051

Lefaucheur, J. P. (2005). Motor cortex dysfunction revealed by cortical excitability studies in Parkinson's disease: influence of antiparkinsonian treatment and cortical stimulation. *Clin. Neurophysiol.* 116, 244–253. doi: 10.1016/j.clinph.2004.11.017

Lefaucheur, J. P. (2009). Treatment of Parkinson's disease by cortical stimulation. *Expert Rev. Neurother.* 9, 1755–1771.

Lefaucheur, J. P., Drouot, X., Von Raison, F., Menard-Lefaucheur, I., Cesaro, P., and Nguyen, J. P. (2004). Improvement of motor performance and modulation of cortical excitability by repetitive transcranial magnetic stimulation of the motor cortex in Parkinson's disease. *Clin. Neurophysiol.* 115, 2530–2541. doi: 10.1016/j.clinph.2004.05.025

Li, H., Lei, X., Yan, T., Li, H., Huang, B., Li, L., et al. (2015). The temporary and accumulated effects of transcranial direct current stimulation for the treatment of advanced Parkinson's disease monkeys. *Sci. Rep.* 5:12178. doi: 10.1038/srep12178

Liang, J. I., Lin, P. C., Chen, M. Y., Hsieh, T. H., Chen, J. J., and Yeh, M. L. (2014). The effect of tenocyte/hyaluronic acid therapy on the early recovery of healing Achilles tendon in rats. *J. Mater. Sci. Mater. Med.* 25, 217–227. doi: 10.1007/s10856-013-5036-9

Ljubisavljevic, M. R., Javid, A., Oommen, J., Parekh, K., Nagelkerke, N., Shehab, S., et al. (2015). The Effects of Different Repetitive Transcranial Magnetic Stimulation (rTMS) Protocols on Cortical Gene Expression in a Rat Model of Cerebral Ischemic-Reperfusion Injury. *PLoS One* 10:e0139892. doi: 10.1371/journal.pone.0139892

Mabrouk, O. S., Marti, M., Salvadori, S., and Morari, M. (2009). The novel delta opioid receptor agonist UFP-512 dually modulates motor activity in hemiparkinsonian rats via control of the nigro-thalamic pathway. *Neuroscience* 164, 360–369. doi: 10.1016/j.neuroscience.2009.08.058

Metz, G. A., Tse, A., Ballermann, M., Smith, L. K., and Fouad, K. (2005). The unilateral 6-OHDA rat model of Parkinson's disease revisited: an electromyographic and behavioural analysis. *Eur. J. Neurosci.* 22, 735–744. doi: 10.1111/j.1460-9568.2005.04238.x

Moller, J. C., Menig, A., and Oechsner, M. (2016). [Neurorehabilitation in Parkinson's disease]. *Praxis (Bern 1994)* 105, 377–382.

Nussbaum, R. L., and Ellis, C. E. (2003). Alzheimer's disease and Parkinson's disease. *N. Engl. J. Med.* 348, 1356–1364.

Obeso, J. A., Rodriguez-Oroz, M. C., Chana, P., Lera, G., Rodriguez, M., and Olanow, C. W. (2000). The evolution and origin of motor complications in Parkinson's disease. *Neurology* 55, S13–S20.

Pascual-Leone, A., Valls-Sole, J., Wassermann, E. M., and Hallett, M. (1994). Responses to rapid-rate transcranial magnetic stimulation of the human motor cortex. *Brain* 117(Pt 4), 847–858. doi: 10.1093/brain/117.4.847

Pasquereau, B., Delong, M. R., and Turner, R. S. (2015). Primary motor cortex of the parkinsonian monkey: altered encoding of active movement. *Brain* 39, 127–143. doi: 10.1093/brain/awv312

Paxinos, G., and Watson, C. (2005). *The Rat Brain in Stereotaxic Coordinates*. Amsterdam: Elsevier Academic Press.

Rascol, O., Sabatini, U., Brefel, C., Fabre, N., Rai, S., Senard, J. M., et al. (1998). Cortical motor overactivation in parkinsonian patients with L-dopa-induced peak-dose dyskinesia. *Brain* 121(Pt 3), 527–533. doi: 10.1093/brain/121.3.527

Reeve, A., Simcox, E., and Turnbull, D. (2014). Ageing and Parkinson's disease: why is advancing age the biggest risk factor? *Ageing Res. Rev.* 14, 19–30. doi: 10.1016/j.arr.2014.01.004

Rogers, M. W. (1996). Disorders of posture, balance, and gait in Parkinson's disease. *Clin. Geriatr. Med.* 12, 825–845.

Sabatini, U., Boulanouar, K., Fabre, N., Martin, F., Carel, C., Colonnese, C., et al. (2000). Cortical motor reorganization in akinetic patients with Parkinson's disease: a functional MRI study. *Brain* 123(Pt 2), 394–403.

Sasso, V., Bisicchia, E., Latini, L., Ghiglieri, V., Cacace, F., Carola, V., et al. (2016). Repetitive transcranial magnetic stimulation reduces remote apoptotic cell death and inflammation after focal brain injury. *J. Neuroinflammation* 13:150. doi: 10.1186/s12974-016-0616-5

Silva, T. P., Poli, A., Hara, D. B., and Takahashi, R. N. (2016). Time course study of microglial and behavioral alterations induced by 6-hydroxydopamine in rats. *Neurosci. Lett.* 622, 83–87. doi: 10.1016/j.neulet.2016.04.049

Son, B. C., Lee, S. W., Choi, E. S., Sung, J. H., and Hong, J. T. (2006). Motor cortex stimulation for central pain following a traumatic brain injury. *Pain* 123, 210–216. doi: 10.1016/j.pain.2006.02.028

Su, R. J., Zhen, J. L., Wang, W., Zhang, J. L., Zheng, Y., and Wang, X. M. (2018). Time-course behavioral features are correlated with Parkinson's diseaseassociated pathology in a 6-hydroxydopamine hemiparkinsonian rat model. *Mol. Med. Rep.* 17, 3356–3363. doi: 10.3892/mmr.2017.8277

Suppa, A., Marsili, L., Belvisi, D., Conte, A., Iezzi, E., Modugno, N., et al. (2011). Lack of LTP-like plasticity in primary motor cortex in Parkinson's disease. *Exp. Neurol.* 227, 296–301. doi: 10.1016/j.expneurol.2010.11.020

Sveinbjornsdottir, S. (2016). The clinical symptoms of Parkinson's disease. *J. Neurochem.* 139(Suppl. 1), 318–324.

Truong, L., Allbutt, H., Kassiou, M., and Henderson, J. M. (2006). Developing a preclinical model of Parkinson's disease: a study of behaviour in rats with graded 6-OHDA lesions. *Behav. Brain Res.* 169, 1–9. doi: 10.1016/j.bbr.2005.11.026

Wichmann, T., and Delong, M. R. (1996). Functional and pathophysiological models of the basal ganglia. *Curr. Opin. Neurobiol.* 6, 751–758. doi: 10.1016/s0959-4388(96)80024-9

Wood-Kaczmar, A., Gandhi, S., and Wood, N. W. (2006). Understanding the molecular causes of Parkinson's disease. *Trends Mol. Med.* 12, 521–528. doi: 10.1016/j.molmed.2006.09.007

Yang, L. Y., Greig, N. H., Huang, Y. N., Hsieh, T. H., Tweedie, D., Yu, Q. S., et al. (2016). Post-traumatic administration of the p53 inactivator pifithrin-alpha oxygen analogue reduces hippocampal neuronal loss and improves cognitive deficits after experimental traumatic brain injury. *Neurobiol. Dis.* 96, 216–226. doi: 10.1016/j.nbd.2016.08.012

Yang, X., Song, L., and Liu, Z. (2010). The effect of repetitive transcranial magnetic stimulation on a model rat of Parkinson's disease. *Neuroreport* 21, 268–272. doi: 10.1097/WNR.0b013e328335b411

Yoon, M. C., Shin, M. S., Kim, T. S., Kim, B. K., Ko, I. G., Sung, Y. H., et al. (2007). Treadmill exercise suppresses nigrostriatal dopaminergic neuronal loss in 6-hydroxydopamine-induced Parkinson's rats. *Neurosci. Lett.* 423, 12–17. doi: 10.1016/j.neulet.2007.06.031

Conflict of Interest: The authors declare that the research was conducted in the absence of any commercial or financial relationships that could be construed as a potential conflict of interest.

Publisher's Note: All claims expressed in this article are solely those of the authors and do not necessarily represent those of their affiliated organizations, or those of the publisher, the editors and the reviewers. Any product that may be evaluated in this article, or claim that may be made by its manufacturer, is not guaranteed or endorsed by the publisher.

frontiers in Aging Neuroscience

ORIGINAL RESEARCH
published: 21 February 2022
doi: 10.3389/fnagi.2022.814560

Low-Intensity Focused Ultrasound Stimulation Ameliorates Working Memory Dysfunctions in Vascular Dementia Rats *via* Improving Neuronal Environment

Faqi Wang[1†], Qian Wang[1†], Ling Wang[2,3], Jing Ren[1], Xizi Song[1,3], Yutao Tian[1,3], Chenguang Zheng[2,3], Jiajia Yang[1,2,3] and Dong Ming[1,2,3*]*

[1] Academy of Medical Engineering and Translational Medicine, Tianjin University, Tianjin, China, [2] College of Precision Instruments and Optoelectronics Engineering, Tianjin University, Tianjin, China, [3] Tianjin Key Laboratory of Brain Science and Neuroengineering, Tianjin, China

OPEN ACCESS

Edited by:
Yi Guo,
Jinan University, China

Reviewed by:
Muhammad Ikram,
Gyeongsang National University, South Korea
Jianbo Tang,
Southern University of Science and Technology, China

***Correspondence:**
Jiajia Yang
jiajia.yang@tju.edu.cn
Dong Ming
richardming@tju.edu.cn

[†]*These authors share first authorship*

Specialty section:
This article was submitted to Alzheimer's Disease and Related Dementias, a section of the journal Frontiers in Aging Neuroscience

Received: *13 November 2021*
Accepted: *24 January 2022*
Published: *21 February 2022*

Citation:
Wang F, Wang Q, Wang L, Ren J, Song X, Tian Y, Zheng C, Yang J and Ming D (2022) Low-Intensity Focused Ultrasound Stimulation Ameliorates Working Memory Dysfunctions in Vascular Dementia Rats via Improving Neuronal Environment. Front. Aging Neurosci. 14:814560. doi: 10.3389/fnagi.2022.814560

Working memory impairment is one of the remarkable cognitive dysfunctions induced by vascular dementia (VD), and it is necessary to explore an effective treatment. Recently, low-intensity focused ultrasound stimulation (LIFUS) has been found notable neuroprotective effects on some neurological diseases, including VD. However, whether it could ameliorate VD-induced working memory impairment was still not been clarified. The purpose of this study was to address this issue and the underlying mechanism. We established VD rat model using the bilateral common carotid artery occlusion (BCCAO) and applied the LIFUS (center frequency = 0.5 MHz; I_{spta} = 500 mW/cm^2, 10 mins/day) to bilateral medial prefrontal cortex (mPFC) for 2 weeks since 2 weeks after the surgery. The main results showed that the LIFUS could significantly improve the performance of VD rats in the specific working memory tasks (delayed nonmatch-to-sample task and step-down task), which might be associated with the improved synaptic function. We also found the improvement in the cerebral blood flow (CBF) and reduced neuroinflammation in mPFC after LIFUS treatment indicated by the inhibition of Toll-like receptor (TLR4)/nuclear factor kappa B (NF-κB) pathway and the decrease of proinflammatory cytokines. The amelioration of CBF and neuroinflammation may promote the living environment of the neurons in VD which then contribute to the survival of neurons and the improvement in synaptic function. Taken together, our findings indicate that LIFUS targeted mPFC can effectively ameliorate reward-based spatial working memory and fear working memory dysfunctions induced by VD *via* restoring the living environment, survivability, and synaptic functions of the neurons in mPFC of VD rats. This study adds to the evidence that LIFUS could become a promising and non-invasive treatment strategy for the clinical treatment of central nervous system diseases related to cognitive impairments in the future.

Keywords: low intensity focused ultrasound, vascular dementia, working memory, cerebral blood flow, synaptic function, neuroinflammation

INTRODUCTION

Dementia is a common public health problem in the world with alarming increases in the prevalence. Additionally, the vascular dementia (VD) is a very frequent form of dementia only after Alzheimer's disease (AD). The prevalence rises with age, with a risk of VD roughly doubling every 5.3 years (O'Brien and Thomas, 2015). However, unlike AD, no curative treatment is yet available for VD in clinic at present (O'Brien and Thomas, 2015; Eguchi et al., 2018). VD is a progressive disease caused by long-term chronic cerebral hypoperfusion (CCH). Cerebral ischemia is a critical cause of neuronal loss and synaptic disintegration. Recent evidence suggests that CCH is associated with systemic inflammation before neurological symptoms develop in VD (Poh et al., 2020). Neuroinflammation caused by cerebral ischemia could aggravate the damage of neurons (Wang et al., 2020). Both in clinical and in basic research, it has been found that VD affects many cognitive abilities including working memory (Venkat et al., 2015). Working memory is a crucial component of memory processes, and it is necessary for higher cognitive and executive functions, which include comprehension, language, learning, reasoning, and thinking (Baddeley, 2010; Riley and Constantinidis, 2015). Although it has been shown that working memory impairment is one of the remarkable symptoms after VD (Blom et al., 2019), there is still a lack of effective treatment methods for working memory impairment caused by VD. Therefore, there is an urgent need for novel and effective treatment strategies.

The prefrontal cortex (PFC) plays a critical role for resilient information maintenance during whole performing working memory tasks (Eriksson et al., 2015). In addition, the medial prefrontal cortex (mPFC), a subregion of PFC, is essential for cognitive process including working memory (Euston et al., 2012; Xu et al., 2019). Prior studies have found that the mPFC plays an important role in a variety of working memory processes, which include spatial working memory (Toepper et al., 2014; Hallock et al., 2016; Tamura et al., 2017), emotional working memory (Smith et al., 2018; Manelis et al., 2020), olfactory working memory (Liu et al., 2014; Nguyen et al., 2020), and tactile working memory (Esmaeili and Diamond, 2019). Therefore, mPFC may become a promising target for improving the working memory impairments caused by VD.

Non-invasive brain stimulation technologies have gradually played an important role in the researches of neuroscience and neurological diseases in recent decades. Low-intensity focused ultrasound stimulation (LIFUS), as an emerging non-invasive neuromodulation, has been rapidly developed with the advantage of excellent targeting, penetration depth, and spatial resolution (Yuan et al., 2021). Among previous animal reports, LIFUS has been proved to be useful in treating various neurological and psychiatric diseases such as ischemic brain injury (Guo et al., 2015; Li et al., 2017), depression (Zhang et al., 2019, 2021), and dementia (Huang et al., 2017; Eguchi et al., 2018; Bobola et al., 2020). Although low-intensity ultrasound therapy has been used to modulate cognitive impairments induced by VD, whether LIFUS targeting the mPFC could ameliorate the working memory impairment and the underlying mechanisms are still unknown. A series of previous studies have found that LIFUS could promote cerebral angiogenesis in rodents (Huang et al., 2017; Li et al., 2017; Eguchi et al., 2018). Meanwhile, chronic cerebral ischemia is one of the main pathogenic factors of VD. Therefore, promoting cerebral angiogenesis may be one of the mechanisms for LIFUS treating VD. Among several studies on therapeutic applications of LIFUS, it has been found that ultrasound stimulation can suppress the neuroinflammation induced by lipopolysaccharide (LPS) both *in vivo* and *in vitro* by modulation of Toll-like receptor (TLR4)/nuclear factor kappa B (NF-κB) pathway (Liu et al., 2017; Chen et al., 2019; Chang et al., 2020). Therefore, we hypothesized that the antiinflammatory effect of LIFUS may be one of the potential mechanisms for ameliorating the cognitive impairments induced by VD.

Thus, this study aims to explore the effects of LIFUS on working memory impairments induced by VD and the underlying mechanisms. Here, we first showed that LIFUS targeted mPFC could restore specific working memory dysfunctions induced by VD. Additionally, it could improve Nissl bodies expression and synaptic functions in mPFC of VD rats. Furthermore, the underlying mechanism may be that LIFUS could increase the CBF and inhibit the TLR4/NF-κB pathway. Overall, our findings reveal that the LIFUS targeted mPFC may be a potential therapeutic method in central nervous system diseases related to cognitive impairments.

MATERIALS AND METHODS

Animals

Twenty-five adult male Wistar rats (170–210 g) were purchased from Beijing Vital River Laboratory Animal Technology Co. Before the experiment, animals were housed five per cage and allowed to acclimate for 1 week. The house environment was controlled at 23°C ± 2°C and 5060% humidity with a 12-h light–dark cycle (with lights on and off at 20:00 and 8:00, respectively). Unless otherwise specified, rats could receive food and water *ad libitum*. All experiments' procedures were carried out following the Animal Management Rules of the Ministry of Health of the People's Republic of China and approved by the Animal Research Ethics Committee of Tianjin Hospital.

Vascular Dementia Model

The VD model was established by typical bilateral common carotid artery occlusion (BCCAO). Rats were fasted but free to water, 6 h before the surgery. Following that, rats were anesthetized using 10% chloral hydrate (350 mg/kg, i.p., Beijing Dingguo Changsheng Biotechnology Co., Ltd., Beijing, China). After anesthesia, atropine (0.09 ml/kg, i.p., Shanghai full woo Biotechnology (Zhumadian)Co., Ltd., Shanghai, China) was used to inhibit salivary secretion. Then, the VD rats underwent the BCCAO surgery as previously published (Yang et al., 2017). First, a ventral midline incision was made in the neck and the muscle retracted on either side of the trachea to expose both the right and left common carotid arteries, around which

loose threads were placed. Second, the vessel was fully ligated, and the wound was sutured. During the surgery, the rats were maintained normal respiratory tract and body temperature with a homeothermic monitoring system (RWD, Shenzhen, China). After the surgery, rats were injected flurbiprofen axetil (0.45 ml/kg, i.p., Beijing Tide Pharmaceutical Co., Ltd., Beijing, China) for postoperative analgesia. After coming to their senses, all rats were reared in the animal house and given free access to food and water.

Low-Intensity Focused Ultrasound Stimulation Procedure

The LIFUS system consists of (1) two function generators (DG4162 and DG822, RIGOL, Beijing, China), (2) a custom-designed radio frequency amplifier (SWA400A, North Star, Shijia zhuang, China), (3) a 0.5MHz single element immersion transducer (V318, Olympus, Tokyo, Japan), and (4) a custom-designed acoustic collimator (Zhang et al., 2019). The schematic diagram of LIFUS system is shown in **Figure 1A**. The LIFUS parameters used in this study were as follows (shown in **Figure 1B**): center frequency = 0.5 MHz; pulse repetition frequency (PRF) = 2.0 kHz; the number of cycles = 150 (0.3 ms tone burst duration, TBD); the sonication duration (SD) = 0.5 s; the interstimulus interval (ISI) = 2 s, and the spatial peak temporal average intensity (I_{spta}) = 500 mW/cm^2. The targets of LIFUS are the bilateral mPFC. In addition, the LIFUS treatment was performed daily for 10 min on each side. During the LIFUS, all rats were mounted on the stereotaxic apparatus (RWD, Shenzhen, China) and anesthetized with 1% isoflurane (RWD, Shenzhen, China). Before applying the LIFUS, the hair on the bilateral mPFC was shaved. The other rats in either CON or VD groups underwent the same procedures including anesthesia but without LIFUS.

Experimental Procedure

First, twenty-five rats were randomly divided into control group (CON, n = 8) and VD model group (n = 17). The rats in VD model group received the BCCAO surgery and recovered for 2 weeks. Due to the survival rate of surgery being about 70%, twelve rats of the VD model group survived. Then, the survival rats were randomly divided into two subgroups, VD group (VD model rats without LIFUS, n = 6) and VD + LIFUS group (VD model rats with LIFUS treatment, n = 6). VD + LIFUS group was treated by LIFUS daily for 14 days starting after 2 weeks' recovery whereas CON and VD groups with sham LIFUS. At the end of the LIFUS, the behavioral tests were performed to evaluate the effects of LIFUS on working memory. After all behavioral tests, the cerebral blood flow (CBF) was measured to examine the change of ischemia. In addition, the histological and western blotting analyses were performed to explore the underlying mechanisms. The experimental schedule is shown in **Figure 1C**.

Behavioral Tests

All behavioral tests were carried out in a dimly lit and quiet room and during the dark phase of the light–dark cycle. In every behavioral test, the equipment and the objects used were cleaned with 75% ethanol solution and water in order between each trial to eliminate odor cues.

Elevated-Plus Maze Task

A standard elevated-plus maze was used to assess the anxiety-associated behavior. When starting the test, rats were placed into the center square facing a same open arm and allowed to explore freely for 5 min. The activity track of each rat was recorded by Smart video tracking software (Panlab, Holliston, United States). The evaluation indexes were the number of entries into open arms and the percentage of residence time in the open arms.

Delayed Nonmatch-to-Sample Task

This test was performed to evaluate spatial working memory based on a reward using a standard Y maze equipment. The delayed nonmatch-to-sample task includes three periods: (1) adaptation period, (2) training period, and (3) testing period. In the 4 days' adaptation period, all groups were restricted drinking water and could drink water for 2 h daily to maintain their water desire. Before the training period, rats underwent 3 days of habituation in the Y maze that they could visit three arms (all with 150 μl water) freely for 10 min. In the 2-day training period, only two arms (baited arms) were placed 150 μl water. The rats were forced to explore each baited arm in turn 30 min daily for reward. During the 4-day testing period, each rat underwent 10 trials per day. Each trial contained three stages. First, the rat was placed into the starting arm and forced into one of the baited arms randomly obtaining a 150 μl water reward (sample stage). Next, the rat returned the starting arm for a thirty-s delay stage. Then, both baited arms were accessible for the rat during the choice stage. But the rat could get a 150 μl water reward only when it chose the baited arm which was different from that during the sample stage and this trial was recorded as "correct." The rat was immediately guided back to the starting arm waiting for next trial whether this trial was correct or not. The interval between the two trials was 60 s. The evaluation indexes were the correct rate and reaction time. The reaction time was defined as the time spent from start to choice point (30 cm away from the end of baited arms).

Novel Object Recognition Test

This test was performed to evaluate working memory of objects based on natural proclivity for exploring novelty. The task contained three periods: (1) habituation period, (2) familiarization period, and (3) testing period. During the habituation periods, the rats were allowed to explore the empty experimental box (60 cm × 60 cm) freely for habituation for 8 min. After 24 h, the rats were allowed to freely explore the box for 5 min with two identical objects placed in opposite corners during the familiarization period. One h later, the rats were placed in the same box again for the test period. During the test period, the rats were also allowed to freely explore the box for 5 min but one of the two familiar objects in the familiarization period was replaced with a novel object.

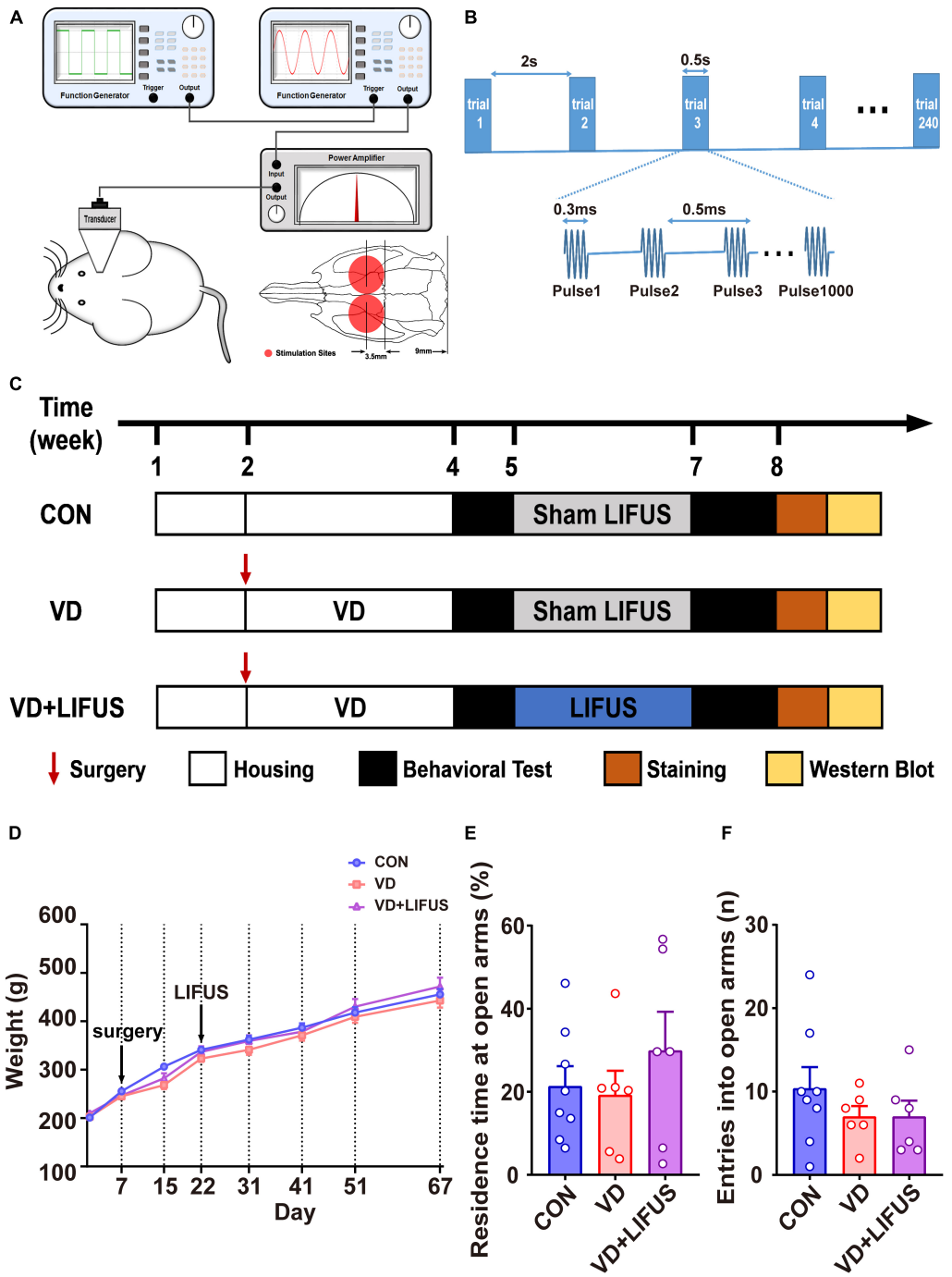

FIGURE 1 | (A) Illustration of LIFUS system. **(B)** Illustration of LIFUS parameters. **(C)** The timeline of the whole experiment. **(D)** Changes in body weight during the experiment (CON, *n* = 8; VD, *n* = 6; VD + LIFUS, *n* = 6). **(E,F)** The residence time at open arms **(E)** and entries into open arms in the OPT (CON, *n* = 8; VD, *n* = 6; VD + LIFUS, *n* = 6).

Define exploration as touching or sniffing the object with the forepaws and/or nose. The exploration time of the familiar object (TF) and the novel object (TN) during the testing period was recorded. The discrimination ratio was calculated as TN/(TN + TF).

Step-Down Task

This test was performed to evaluate fear working memory based on the fear environment using a step-down reaction box. The bottom of the step-down reaction box is made of parallel stainless-steel bars that can apply electrical stimulation

to create a fearful environment for rats. In addition, an insulated platform is placed at the corner of the box. The task also includes three periods: (1) adaptation period, (2) training period, and (3) testing period. In the adaptation period, the rats were allowed to explore the step-down reaction box freely for 5 min without electrical stimulation. The training period was performed after 24 h. During the training period, the rats were placed on the platform in the reaction box. When the rats jumped off the platform, a 0.4 mA electrical stimulation would be applied continuously at an interval of 2 s until the rat jumps on the platform. If one rat could not jump on the platform within 90 s, this rat would be regarded as failed. After 90 min, the rats were placed on the platform again without electrical stimulation. The duration time of test period was 3 min, and the latency of rats jumping off the platform was recorded. Define jumping off the platform as all four claws leaving the platform. The evaluation indexes were the latency to step-down, time on the platform, and the number of down the platform.

Laser Speckle Contrast Imaging

At the end of all behavioral tests, the laser speckle contrast imaging (LSCI) was carried out to measure CBF by a commercial laser speckle blood flow imager (RFLSI Pro, RWD, Shenzhen, China). To measure the CBF, the rats were mounted on the stereotaxic apparatus (RWD, Shenzhen, China) under anesthesia with 1% isoflurane. The scalp was cut along the midline to expose the skull after shaving the hair. The tissues on the surface of skull were cleaned carefully (Li et al., 2017). Then, using a skull drill (RWD, Shenzhen, China) slowly thinned a 6 mm × 10 mm rectangular cranial window (centered at 1 mm posterior to the bregma). The skull was thinned until the cortical blood vessels were clearly visible. During the whole process, the normal saline was used to cool the skull avoiding brain tissue damaged by excessive temperature. Then, the position of the skull window was placed under the laser speckle imager for laser speckle imaging. The evaluation indexes were the number of vascular branches and the blood flow of the main vein.

Histological Analysis

In the histological analysis, hematoxylin–eosin staining (HE) was used to detect the morphological changes of neurons in PFC of rats (each group, n = 2). The Nissl staining was used to detect the density of Nissl body in rats PFC (each group, n = 2). The changes of morphology and density of dendritic spines were measured by the Golgi-cox staining (CON, n = 6; VD, n = 4; VD + LIFUS, n = 4). After the LSCI, all the rats were sacrificed with urethane and perfused with 0.1 M phosphate buffer saline (PBS, pH = 7.4) immediately. For Golgi-cox staining, the brains of rats were removed into the Golgi-cox solution right now. After 12 days, the PFC was sectioned into 150-μm thick slices in coronal plane with an oscillating microtome (Leica VT1200S, Germany). In addition, spine counting was carried out in a single dendrite in each neuron. The dendritic spines were classified into four different types: thin, mushroom, stubby, and branched. The total density of dendritic spines was expressed as the mean of dendritic spines in per unit length. On the other hand, the quantification of dendritic spines according to shape was expressed as a ratio in relation to total dendritic spines (i.e., number of spines of a given shape/total number of spines in each dendrite) (Risher et al., 2014; Bello-Medina et al., 2016). In addition, the rats for HE and Nissl staining were perfused with freshly prepared 4% paraformaldehyde in PBS immediately after PBS perfusion. Then, the brains were embedded in OCT compound (Tissue-Tek, Miles) at −20°C. Later, the PFC was sectioned into 15-μm thick slices in coronal plane with by Cryostat Microtome (Leica CM1860UV, Germany).

Western Blotting Analysis

After the above test, the other rats were also sacrificed and perfused with PBS, and their mPFC was removed at 0°C and stored at −80°C. The procedure of western blotting analysis was described as previously published (Wang et al., 2018). The primary antibodies used in this study included the following: (1) inflammatory protein: anti-TLR4 (1:1000, Wanleibio, WL00196), anti-JNK (1:1000, Wanleibio, WL01295), anti-p-JNK (1:1000, CST, 4668), anti-NF-κB (1:1000, Abcam, ab16502), anti-IL-6 (1:1000, Wanleibio, WL02841); (2) synaptic functional protein: anti-SYP (1:2000, Abcam, ab32594), anti-NR2B (1:1000, Abcam, ab65783) and PSD95 (1:2000, GeneTex, GTX133091), anti-CaMKII (1:1000, Abcam, ab134041); (3) anti-GAPDH (1:1000, GeneTex, GTX627408). The secondary antibodies used in this study included (1) rabbit IgG antibody (HRP) (1:5000, GeneTex, GTX213110-01); (2) mouse IgG antibody (HRP) (1:5000, GeneTex, GTX213111-01).

Statistical Analysis

All data were analyzed by IBM SPSS Statistics 20 software. The results of rats' weight and delayed nonmatch-to-sample task were analyzed using repeated measures ANOVA. The other results were all analyzed by one-way ANOVA. LSD multiple-comparison test was performed for comparisons between groups. Data are expressed as the average ± standard error of the mean (SEM). The value of $p < 0.05$ is considered to be significant.

RESULTS

Low-Intensity Focused Ultrasound Stimulation Ameliorates Working Memory Dysfunctions Induced by Vascular Dementia

To verify whether LIFUS could cause adverse reactions in rats, we tested the weight changes in the rats during the experiment and detected the anxiety-like behavior of rats through the elevated-plus maze task. The result of weight changes showed that during the whole experiment, the weight of the three groups showed a similar increasing trend, and there was no statistical difference among the three groups (**Figure 1D**). At the same time, the results of elevated-plus maze task showed no significant difference among the three groups, which indicates that VD modeling and LIFUS process did not induce anxiety

behavior in rats (**Figures 1E,F**). In addition, we tested the performance of rats in different working memory tasks to verify the effect of LIFUS on working memory impairments in VD rats. The results of different working memory tasks showed that LIFUS significantly improved the performance of working memory tasks in VD rats, which includes the delayed nonmatch-to-sample task and step-down task (**Figure 2**). In the delayed nonmatch-to-sample task, the response time gradually decreased with the increase of training times, and there was significant difference among the three groups (repeated measures ANOVA, $F(2, 16) = 5.196$, $p = 0.018$). Compared with CON group, the response time of VD group was significantly longer ($p = 0.005$) (**Figure 2A**). On the 2nd day, the response time of VD group was longer than that in the other groups (one-way ANOVA, $F(2,16) = 4.908$, $p = 0.022$; CON vs. VD: $p < 0.01$; VD vs. VD + LIFUS: $p < 0.05$) (**Figure 2C**). On the 4th day, the response time of both VD and VD + LIFUS group was longer than that in the CON group ($p < 0.05$) (**Figure 2D**). Moreover, the increasing trend of correct rate with the increase of training times was similar among the three groups, and no significant difference was found (**Figure 2B**). However, on the 4th day, the VD group had a significantly poor performance on making the right choice than other groups (one-way ANOVA, $F(2,16) = 6.063$, $p = 0.011$; CON vs. VD: $p < 0.01$; VD vs. VD + LIFUS: $p < 0.05$) (**Figure 2E**). The results of step-down task also showed the LIFUS improved the working memory impairment induced by VD. The VD group had a poor performance in step-down task that the latency of VD group was significantly shorter than CON group, whereas performance of VD + LIFUS group was reversed (one-way ANOVA,$F(2,16) = 4.672$,$p = 0.025$; CON vs. VD: $p < 0.05$; VD vs. VD + LIFUS: $p < 0.05$) (**Figure 2F**). There were no significant differences in other indicators of step-down task (**Figures 2G,H**), nor in the novel object recognition test (**Figure 2I**). Taken together, these results of behavioral tests suggest that LIFUS can significantly ameliorate working memory dysfunctions induced by VD without inducing adverse reactions such as weight loss and anxiety-like behavior.

Low-Intensity Focused Ultrasound Stimulation Increases Cerebral Blood Flow in the Vascular Dementia Rats

The CBF was measured to test the effect of LIFUS on global cerebral ischemia in VD rats. The results are shown in the **Figure 3**. **Figure 3A** shows the typical CBF imaging of three groups. There were abundant vascular branches in CON and VD + LIFUS group, not VD group. The statistical results of the blood flow of the main vein and number of vascular branches are shown in the **Figures 3B,C**, respectively. Although there was difference in blood flow of the main vein among three groups, they were not significant (**Figure 3B**). Compared with

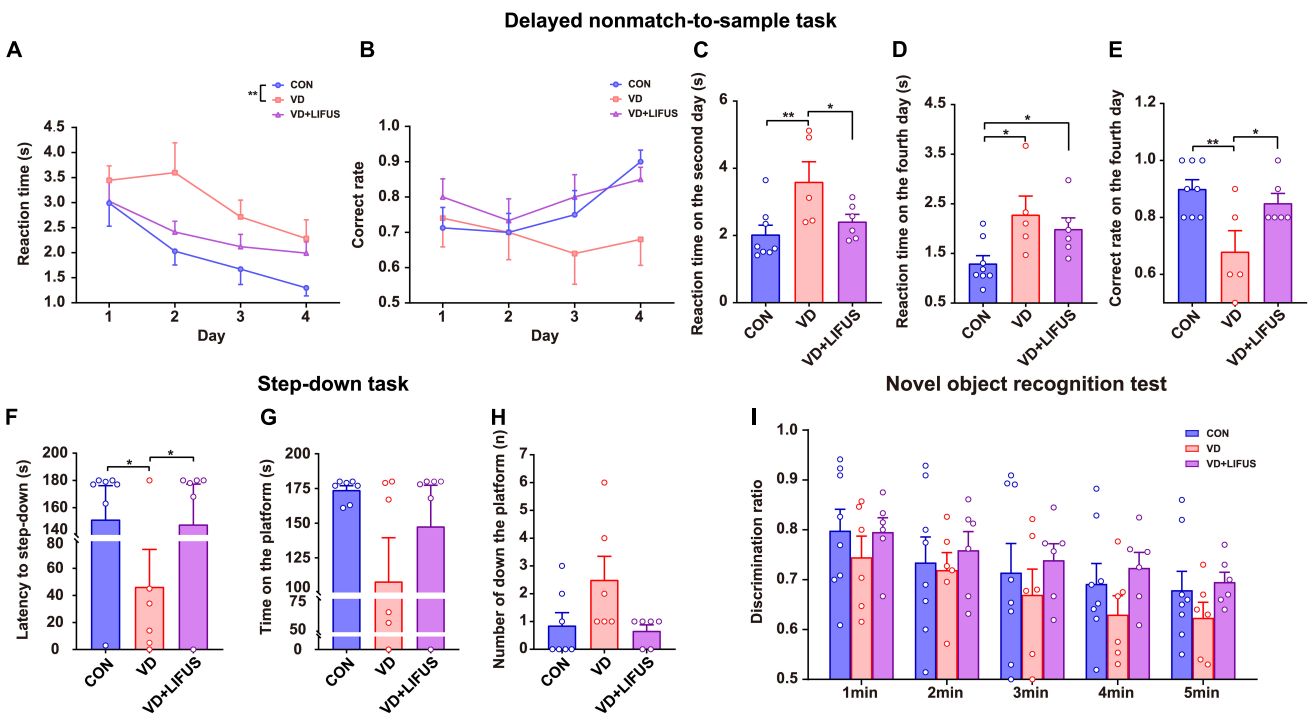

FIGURE 2 | Effect of LIFUS on working memory dysfunctions in the VD rats. **(A–E)** The average response time of 4-day task **(A)**, average accuracy of 4-day task **(B)**, average reaction time on day 2 **(C)**, average reaction time on day 4 **(D)**, and average correct rate on day 4 **(E)** in the delayed nonmatch-to-sample task (CON, $n = 8$; VD, $n = 5$; VD + LIFUS, $n = 6$). **(F–H)** The latency of the step-down **(F)**, time on the platform **(G)**, and number of down the platform **(H)** in the step-down task (CON, $n = 8$; VD, $n = 5$; VD + LIFUS, $n = 6$). **(I)** The discrimination ratio for new objects during the test period 1–5 min in the novel object recognition test. Data are expressed as mean ± SEM. $^*p < 0.05$, $^{**}p < 0.01$ (CON, $n = 8$; VD, $n = 6$; VD + LIFUS, $n = 6$).

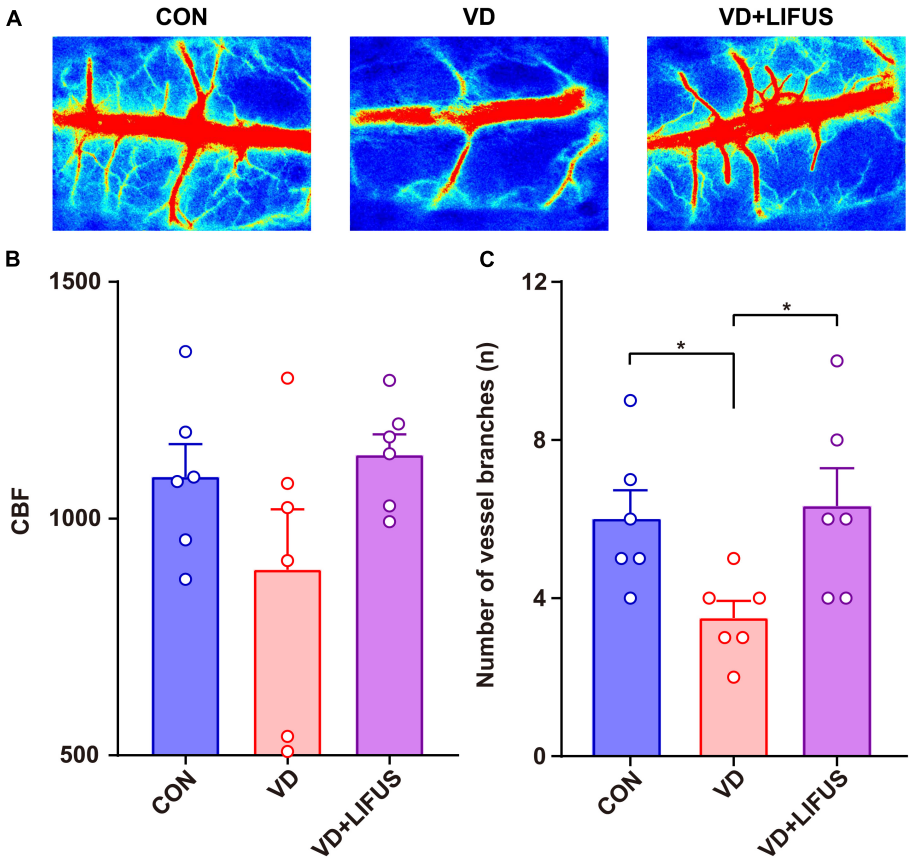

FIGURE 3 | Effect of LIFUS on blood flow in VD rats. **(A)** Typical diagrams of brain flow in the region of interest in three groups. **(B)** The average blood flow of main vein. **(C)** The number of vascular branches. Data are expressed as mean ± SEM. *$p < 0.05$ (CON, VD, VD + LIFUS, $n = 6$).

CON and VD + LIFUS group, the number of vascular branches in VD groups decreased significantly (one-way ANOVA, F (2, 15) = 4.420, $p = 0.031$; CON vs. VD: $p < 0.05$; VD vs. VD + LIFUS: $p < 0.05$) (**Figure 3C**). These results indicate that LIFUS targeting the mPFC can increase global CBF in VD rats and suggest that the improvements of working memory in VD rats by the LIFUS may be associated with increased vascular branches and blood flow.

Low-Intensity Focused Ultrasound Stimulation Improves the Survivability of the Neurons and Ability of Protein Synthesis in the Vascular Dementia Rats

The HE was performed to test the effect of LIFUS on the morphological changes of neurons in the rats. The number of nucleus in the PFC of VD group significantly reduced, and the arrangement of neurons was loosen and pyknosis appeared compared with CON group, whereas these were all reversed after LIFUS (**Figure 4A**). In addition, to evaluate the effects on protein synthesis of neurons in the PFC after ultrasound treatment, we observed the Nissl body expression in different groups. The **Figure 4B** shows the typical expression of Nissl bodies in PFC of the three groups. We can observe that compared with the other groups, the distribution of Nissl bodies in VD group was looser. Additionally statistically, the number of Nissl bodies in VD group was significantly decreased (one-way ANOVA, $F(2,45) = 9.318$, $p < 0.001$; CON vs. VD: $p < 0.001$; VD vs. VD + LIFUS, $p = 0.002$) (**Figure 4C**). The above results show that the LIFUS can enhance the survival ability and protein synthesis ability of neurons in PFC of VD rats.

Low-Intensity Focused Ultrasound Stimulation Enhances the Density of Dendritic Spines and Expression of Synaptic Proteins in the Vascular Dementia Rats

Next, we examined the effects of LIFUS on synaptic structure and expression of synaptic proteins. The typical examples of expression of dendritic spines in the PFC of the three groups showed that the density of dendritic spines in VD group was less than that in CON and VD + LIFUS group (**Figure 5A**). This point was further proved by the statistical results (one-way ANOVA, $F(2,102) = 20.311$, $p < 0.001$; CON vs. VD, $p < 0.001$; VD vs. VD + LIFUS, $p < 0.001$) (**Figure 5B**). By analyzing the proportion of various subtypes of dendritic spines, we found

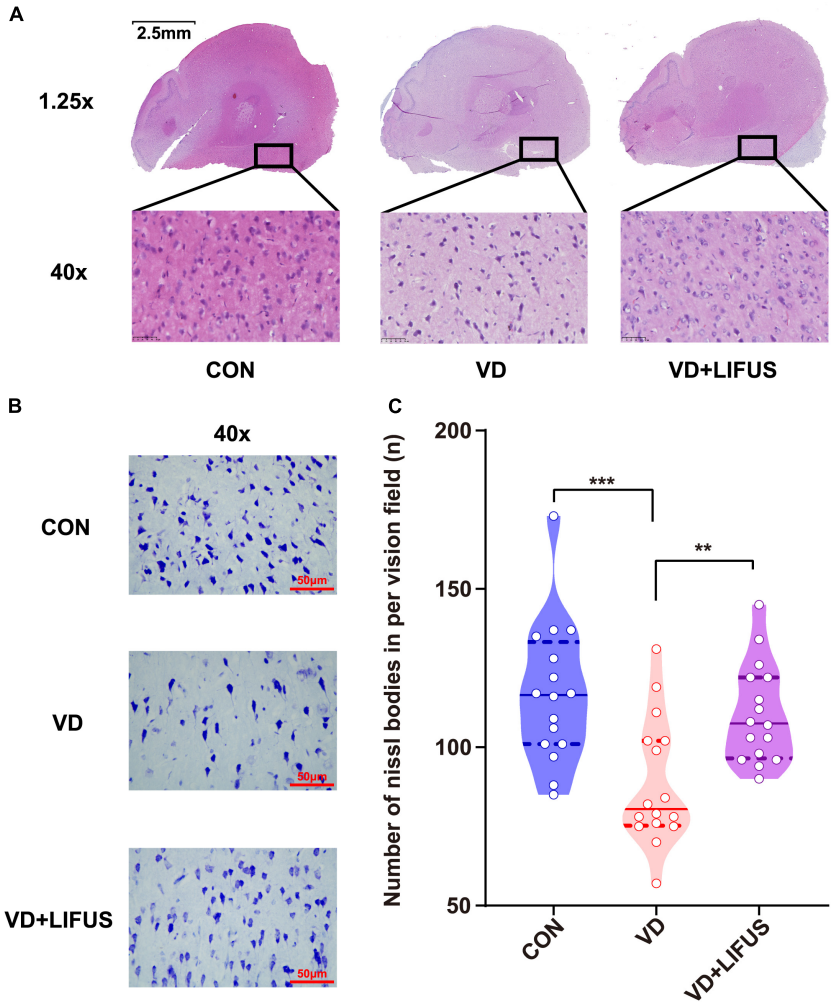

FIGURE 4 | Effect of LIFUS on the morphological changes of the neurons and ability of protein synthesis in the VD rats. **(A)** Typical diagrams of HE in three groups. **(B)** Typical diagrams of Nissl staining in three groups. **(C)** The statistical results of the number of Nissl bodies. Data are expressed as mean ± SEM. $^{**}p < 0.01$, $^{***}p < 0.001$ (CON, VD, VD + LIFUS, $n = 2$).

that the proportion of mushroom type, not other subtypes, in VD group was significantly lower than other two groups (one-way ANOVA, $F(2,102) = 3.907$, $p = 0.023$; CON vs. VD, $p = 0.022$; VD vs. VD + LIFUS, $p = 0.015$) (**Figures 5C–F**). The **Figures 6A–D** show the statistical results of synaptic protein expression levels. Compared with CON group, the expression of NR2B, PSD-95, and CaMKII decreased in VD group without statistical difference. Moreover, the expression of NR2B, PSD-95, CaMKII, and SYP was increased in VD + LIFUS group, and there was significant difference between NR2B and SYP (NR2B: $F(2,101) = 7.521$, $p = 0.001$, CON vs. VD + LIFUS, $p < 0.05$; SYP: $F(2,101) = 7.194$, $p = 0.001$, CON vs. VD + LIFUS, $p < 0.001$). In addition, the expression of NR2B, CaMKII, and SYP in VD + LIFUS group was increased significantly than those in VD group (NR2B: $F(2,101) = 7.521$, $p = 0.001$, VD vs. VD + LIFUS, $p < 0.001$; CaMKII: $F(2,101) = 3.738$, $p = 0.031$, VD vs. VD + LIFUS, $p < 0.05$; SYP: $F(2,101) = 7.194$, $p = 0.001$, VD vs. VD + LIFUS, $p = 0.007$). The above results show that the LIFUS can increase the density of dendritic spines and the proportion of mushroom shaped dendritic spines and improve the expression of synaptic proteins in the mPFC of VD rats.

Low-Intensity Focused Ultrasound Stimulation Inhibits the TLR4/NF-κB Pathway and Decreases Proinflammatory Cytokines in the Vascular Dementia Rats

After that, we detected whether the TLR4/NF-κB pathway and proinflammatory cytokines were involved the improvements of working memory in VD rats by the LIFUS. As shown in **Figures 7A–F**, the protein expression levels of TLR4, JNK, NF-κB, and the proinflammatory IL-6 in mPFC of VD group were significantly increased compared with these in CON group (TLR4: $F(2,151) = 10.404$, $p < 0.001$, CON vs. VD, $p < 0.001$;

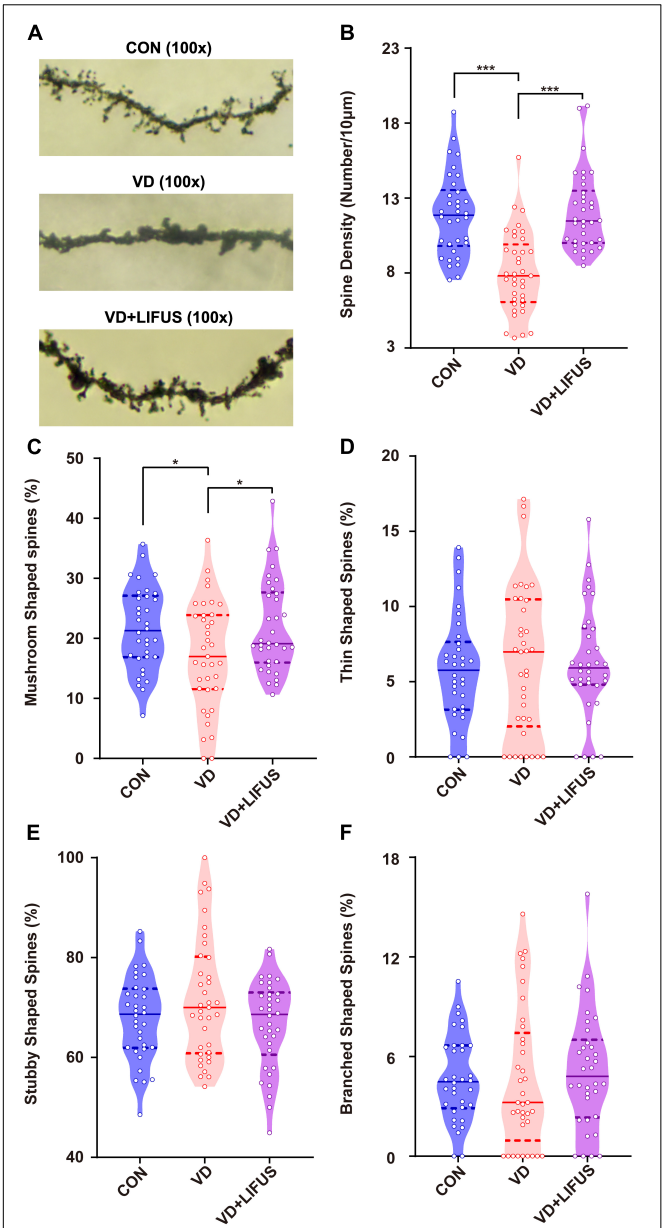

FIGURE 5 | Effect of LIFUS on the density of dendritic spines. **(A)** Typical diagrams of Golgi-cox staining in three groups. **(B)** The spine density in three groups. **(C–F)** The percentage of the mushroom shaped spines, thin shaped spines, stubby shaped spines, and branched shaped spines. Data are expressed as mean ± SEM. *$p < 0.05$, *** $p < 0.001$ (CON, $n = 6$; VD, $n = 4$; VD + LIFUS, $n = 4$).

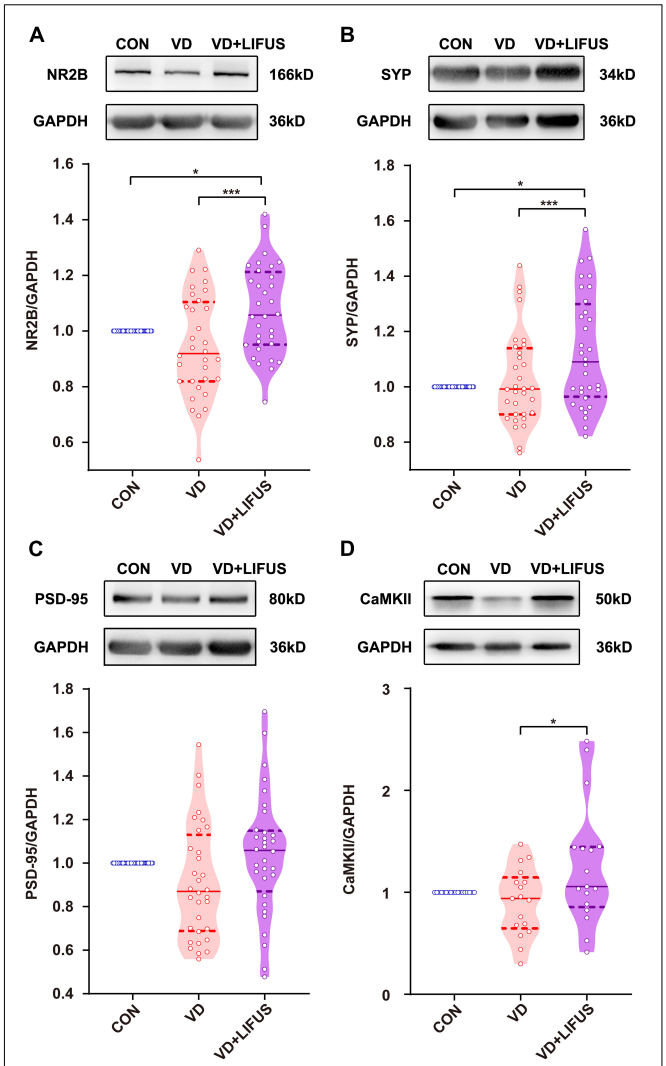

FIGURE 6 | Effect of LIFUS on the expression of synaptic proteins. **(A–D)** The expression of NR2B, SYP, PSD-95, and CaMKII. Data are expressed as mean ± SEM. *$p < 0.05$, *** $p < 0.001$ (CON, $n = 6$; VD, $n = 4$; VD + LIFUS, $n = 4$).

JNK: $F(2,136) = 19.521$, $p < 0.001$, CON vs. VD, $p < 0.001$; NF-κB: $F(2,178) = 10.167$, $p < 0.001$, CON vs. VD, $p < 0.001$; IL-6: $F(2,169) = 9.130$, $p < 0.001$, CON vs. VD, $p < 0.05$). Meanwhile, the LIFUS significantly inhibited the expression of these proteins in mPFC (TLR4: VD vs. VD + LIFUS, $p < 0.001$; JNK: VD vs. VD + LIFUS, $p < 0.001$; NF-κB: VD vs. VD + LIFUS, $p < 0.001$; IL-6: VD vs. VD + LIFUS, $p < 0.001$). However, the p-JNK and ratio of p-JNK/JNK in VD + LIFUS group were significantly higher than the other group (p-JNK: $F(2,117) = 10.404$, $p < 0.001$, CON vs. VD + LIFUS, $p < 0.001$, VD vs. VD + LIFUS, $p < 0.05$; p-JNK/JNK: $F(2,117) = 19.521$, $p < 0.001$, CON vs. VD + LIFUS, $p < 0.001$, VD vs. VD + LIFUS, $p < 0.001$) (**Figures 7A–F**). The above results show that the LIFUS can decrease proinflammatory cytokines, such as IL-6, by inhibiting the TLR4/NF-κB pathway in the VD rats.

DISCUSSION

In this study, we first provides the experimental evidence that LIFUS, targeting the mPFC, markedly improves specific working memory impairments in VD rats. Furthermore, our results support the hypotheses that promoting CBF

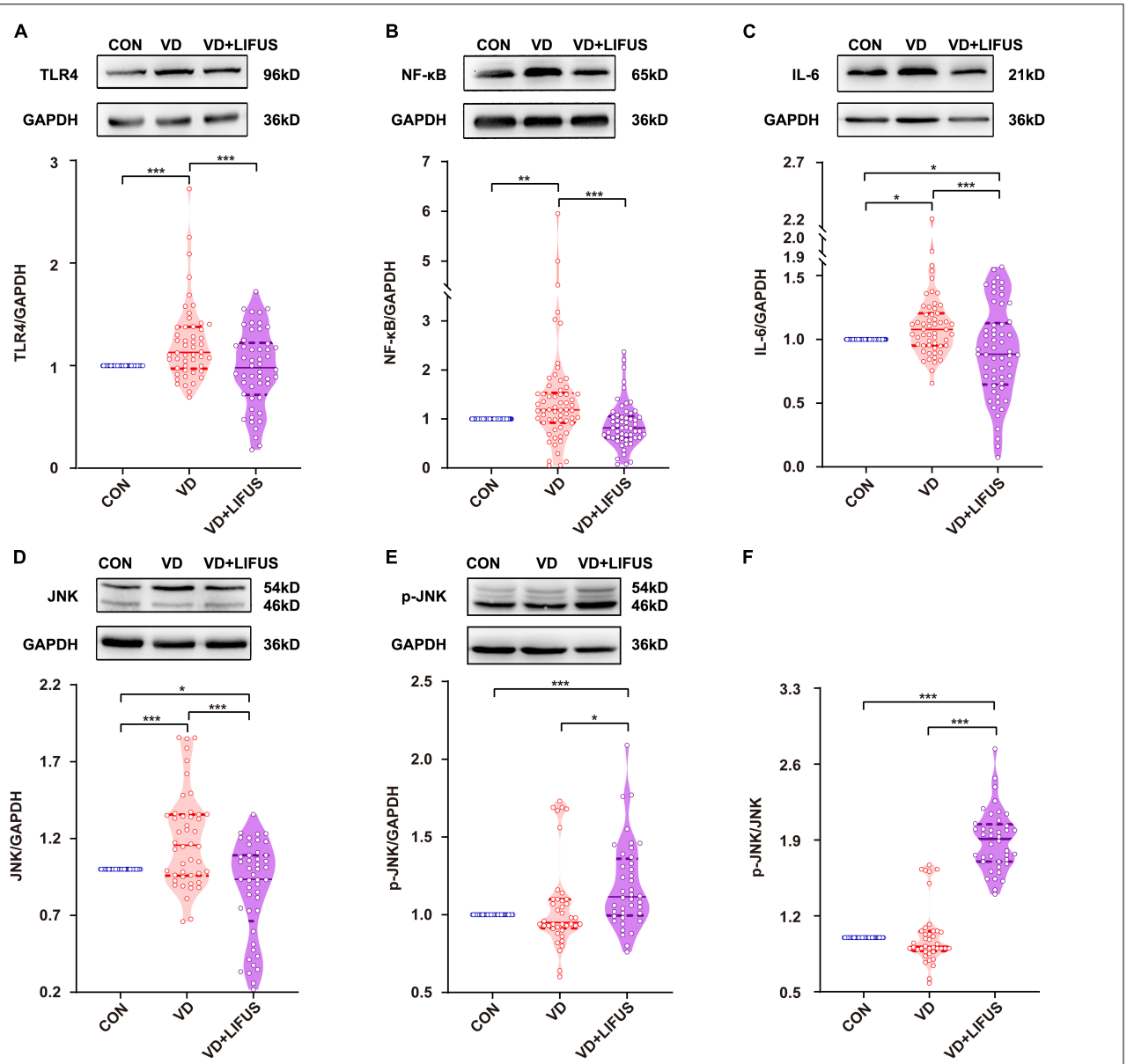

FIGURE 7 | Effect of LIFUS on the expression of neuroinflammatory related proteins. **(A–F)** The expression of TLR4, NF-κB, IL-6, JNK, p-JNK, and ratio of p-JNK/JNK. Data are expressed as mean ± SEM. $^{*}p < 0.05$, $^{**}p < 0.01$, $^{***}p < 0.001$ (CON, $n = 6$; VD, $n = 4$; VD + LIFUS, $n = 4$).

and antiinflammatory may be the potential mechanisms for ameliorating the cognitive impairments induced by VD.

There is extensive research on ultrasound stimulation treating the cognitive impairments in different animal models (Huang et al., 2017; Eguchi et al., 2018; Chen et al., 2019). These researches suggested that LIFUS could affect the different cognitive functions while stimulating different brain regions involved in different cognitive processes. Therefore, the targeted brain region is one of the key factors that affect the efficacy of LIFUS. It has been recognized that mPFC is essential for social, affective functions and cognitive process including working memory (Etkin et al., 2011; Euston et al., 2012; Hiser and Koenigs, 2018; Xu et al., 2019). Meanwhile, excitation of the PFC using brain stimulation technology, such as transcranial current stimulation, optogenetic and chemogenetic neuromodulation, can regulate the working memory *via* modulating the neural activities and neural oscillations in the PFC (Alekseichuk et al., 2016; Abbas et al., 2018; Nagai et al., 2020; Upright and Baxter, 2020). Thus, mPFC might be an effective targeted brain region, which we focused in this study to investigate the neural modulation function of LIFUS. However, it was still not clear the specific action of LIFUS under our experimental condition. Therefore, three kinds of behavioral tasks were carried out to evaluate the different types working memory. Interestingly,

we found that LIFUS could affect the reward-based spatial working memory and fear working memory task but not object recognition memory. We speculated that it might be associated with the decision-making on risk and reward function of mPFC (Der-Avakian and Markou, 2012; Euston et al., 2012; Pitts et al., 2016; Hiser and Koenigs, 2018; Murray and Rudebeck, 2018) and negative emotion including fear as well (Etkin et al., 2011; Euston et al., 2012; Giustino and Maren, 2015; Hiser and Koenigs, 2018). These functions of mPFC are believed to rely on the neural activities and neural oscillations during distinct task processes (Der-Avakian and Markou, 2012; Eriksson et al., 2015; Giustino and Maren, 2015; Riley and Constantinidis, 2015; Murray and Rudebeck, 2018). Additionally, a series of studies found that ultrasound stimulation, including focused ultrasound and transcranial pulsed ultrasound stimulation, could stimulate intact brain circuits and modulate the neuronal oscillations (Tufail et al., 2010; Yuan et al., 2016a,b). So, we believe that the improvements in specific working memory impairments may be due to the regulation of neural oscillations in mPFC by LIFUS, although this needs to be verified in the subsequent experiments.

As discussed above, changes in neural activities and neural oscillations could affect working memory. The origin of them thus become important as well which depend on synaptic function. So, we evaluated the changes of synaptic function by analyzing the synaptic structure and synaptic protein (Wang et al., 2013). In previous study, it has been reported that the LIFUS could modulate structural and functional synaptic plasticity in rat hippocampus by increasing the density of dendritic spines and the expression level of GluN2A (Huang et al., 2019). Consistent with previous results, we found that the LIFUS not only improved the density of dendritic spines and the expression of synaptic proteins, including the NR2B, PSD-95, CaMKII, and SYP, but also improved the ability of protein synthesis in the mPFC of VD rats. Hence, we believed that the improvements in synaptic structure and synaptic protein contributed to facilitate neural activity in mPFC, thereby improving cognitive behavior.

Then, how LIFUS could improve synaptic function? Previous studies have demonstrated that angiogenesis and antiinflammation may be the two neuroprotection effects activated by the ultrasound stimulation (Kim et al., 2017; Li et al., 2017; Liu et al., 2017; Eguchi et al., 2018; Chen et al., 2019; Chang et al., 2020). Several experiments suggested that LIFUS could lead to angiogenesis in VD and cerebral ischemia rodents, thereby promoting the survival of neurons (Li et al., 2017; Eguchi et al., 2018). On the other hand, a serious of studies found that ultrasound stimulation suppresses LPS-induced proinflammatory responses by regulating TLR4/NF-κB pathway and release of proinflammatory cytokines *in vivo* and *in vitro* (Liu et al., 2017; Chen et al., 2019; Chang et al., 2020). Therefore, we explored the underlying mechanism from CBF and neuroinflammation, respectively. Our results about CBF and neuroinflammation were in agreement with those of previous studies. On the one hand, we found that LIFUS increased vascular branches and blood flow in mPFC, which is consistent with previous results. Hence, the alleviated hemodynamic compromise and the improved CBF observed in this study should be one mechanism of LIFUS treating the VD. On the other hand, the past findings are consistent with our results that the expressions of TLR4, NF-κB, and IL-6 decreased significantly after LIFUS treatment. Hence, antiinflammation may be another neuroprotection mechanism of LIFUS treating the VD. However, there is a difference that p-JNK expression was significantly

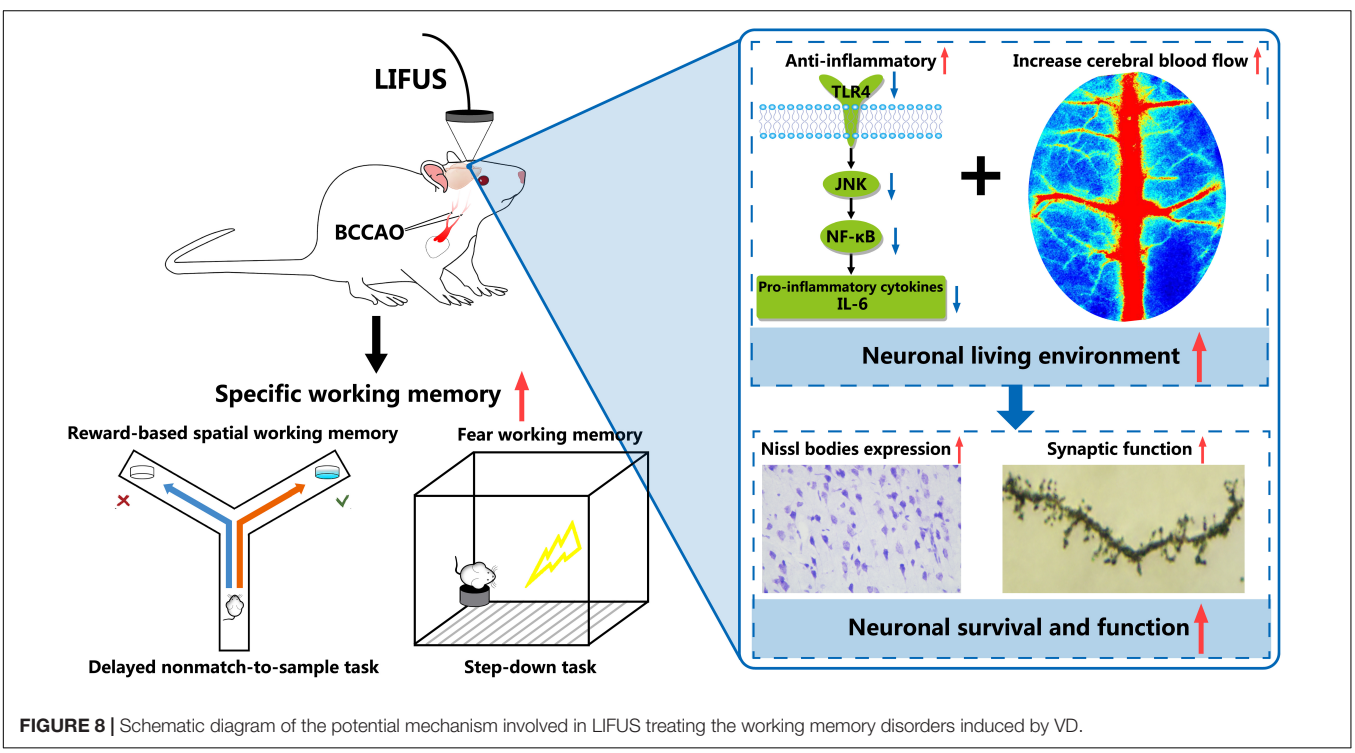

FIGURE 8 | Schematic diagram of the potential mechanism involved in LIFUS treating the working memory disorders induced by VD.

increased after LIFUS treatment. This disparity may be due to the reason that JNK, the activities of which are stimulated by many physiological, pathological, and environmental cues, are involved in diverse and sometimes even opposing cell functions (Xia and Karin, 2004). The previous studies have found that the significant upregulation of p-JNK2 could enhance the proliferation and neuronal differentiation of rat embryonic neural stem cells (Jiao et al., 2017). Additionally, the ischemia –hypoxia could activate JNK signaling and results in proliferation of neural stem cells (Chen et al., 2010; Cai et al., 2014). Meanwhile, ultrasound stimulation has been found to promote the proliferation of HaCaT keratinocytes, osteoblasts, and human chondrocyte cell by activating JNK (Choi et al., 2007; Chiu et al., 2008; Leng et al., 2018). LIFUS used in this study may be induced the proliferation of neural cells *via* activating JNK, although the exact mechanisms and pathways remain to be investigated.

Overall, as shown in **Figure 8**, we demonstrated that LIFUS treatment significantly ameliorated the reward and fear-based working memory dysfunctions, the survivability of the neurons, and synaptic functions in VD rats. These beneficial effects of LIFUS might be due to the increase in the CBF and inhibit the TLR4/NF-κB pathway. Our findings indicated that LIFUS could be a novel therapeutic technique for the treatment of central nervous system diseases related to cognitive impairments.

DATA AVAILABILITY STATEMENT

The original contributions presented in the study are included in the article/**Supplementary Material**, further inquiries can be directed to the corresponding authors.

ETHICS STATEMENT

The animal study was reviewed and approved by Animal Research Ethics Committee of Tianjin Hospital.

AUTHOR CONTRIBUTIONS

FW performed the surgery, behavioral test, LIFUS procedure, and wrote the manuscript. QW performed the all experiments and analyzed the data. LW and JR contributed to behavioral test and the western blotting experiment. XS contributed to the LIFUS procedure. YT and CZ contributed to design the study and revised the manuscript. CZ, YT, and JY obtained the funding. JY and DM designed the study, revised the manuscript, and gave final approval of the manuscript. All authors contributed to the article and approved the submitted version.

FUNDING

This research was supported by grants from the National Natural Science Foundation of China (81871517) awarded to JY, from the National Natural Science Foundation of China (32071103) awarded to YT, and from the National Natural Science Foundation of China (81870847) awarded to CZ.

SUPPLEMENTARY MATERIAL

The Supplementary Material for this article can be found online at: https://www.frontiersin.org/articles/10.3389/fnagi.2022.814560/full#supplementary-material

REFERENCES

Abbas, A. I., Sundiang, M. J. M., Henoch, B., Morton, M. P., Bolkan, S. S., Park, A. J., et al. (2018). Somatostatin Interneurons Facilitate Hippocampal-Prefrontal Synchrony and Prefrontal Spatial Encoding. *Neuron* 100, 926–939.e3. doi: 10.1016/j.neuron.2018.09.029

Alekseichuk, I., Turi, Z., Amador de Lara, G., Antal, A., and Paulus, W. (2016). Spatial Working Memory in Humans Depends on Theta and High Gamma Synchronization in the Prefrontal Cortex. *Curr. Biol.* 26, 1513–1521. doi: 10.1016/j.cub.2016.04.035

Baddeley, A. (2010). Working memory. *Curr. Biol.* 20, R136–R140. doi: 10.1016/j.cub.2009.12.014

Bello-Medina, P. C., Flores, G., Quirarte, G. L., McGaugh, J. L., and Prado Alcala, R. A. (2016). Mushroom spine dynamics in medium spiny neurons of dorsal striatum associated with memory of moderate and intense training. *Proc. Natl. Acad. Sci. U.S.A.* 113, E6516–E6525. doi: 10.1073/pnas.1613680113

Blom, K., Koek, H. L., Zwartbol, M. H. T., van der Graaf, Y., Kesseler, L., Biessels, G. J., et al. (2019). Subjective cognitive decline, brain imaging biomarkers, and cognitive functioning in patients with a history of vascular disease: the SMART-Medea study. *Neurobiol. Aging* 84, 33–40. doi: 10.1016/j.neurobiolaging.2019.07.011

Bobola, M. S., Chen, L., Ezeokeke, C. K., Olmstead, T. A., Nguyen, C., Sahota, A., et al. (2020). Transcranial focused ultrasound, pulsed at 40 Hz, activates microglia acutely and reduces Abeta load chronically, as demonstrated in vivo. *Brain Stimul.* 13, 1014–1023. doi: 10.1016/j.brs.2020.03.016

Cai, M., Zhou, Y., Zhou, B., and Lou, S. (2014). Hypoxic conditioned medium from rat cerebral cortical cells enhances the proliferation and differentiation of neural stem cells mainly through PI3-K/Akt pathways. *PLoS One* 9:e111938. doi: 10.1371/journal.pone.0111938

Chang, J. W., Wu, M. T., Song, W. S., and Yang, F. Y. (2020). Ultrasound Stimulation Suppresses LPS-Induced Proinflammatory Responses by Regulating NF-kappaB and CREB Activation in Microglial Cells. *Cereb. Cortex* 30, 4597–4606. doi: 10.1093/cercor/bhaa062

Chen, T. T., Lan, T. H., and Yang, F. Y. (2019). Low-Intensity Pulsed Ultrasound Attenuates LPS-Induced Neuroinflammation and Memory Impairment by Modulation of TLR4/NF-kappaB Signaling and CREB/BDNF Expression. *Cereb. Cortex* 29, 1430–1438. doi: 10.1093/cercor/bhy039

Chen, X., Tian, Y., Yao, L., Zhang, J., and Liu, Y. (2010). Hypoxia stimulates proliferation of rat neural stem cells with influence on the expression of cyclin D1 and c-Jun N-terminal protein kinase signaling pathway in vitro. *Neuroscience* 165, 705–714. doi: 10.1016/j.neuroscience.2009.11.007

Chiu, Y. C., Huang, T. H., Fu, W. M., Yang, R. S., and Tang, C. H. (2008). Ultrasound stimulates MMP-13 expression through p38 and JNK pathway in osteoblasts. *J. Cell Physiol.* 215, 356–365. doi: 10.1002/jcp.21322

Choi, B. H., Choi, M. H., Kwak, M. G., Min, B. H., Woo, Z. H., and Park, S. R. (2007). Mechanotransduction pathways of low-intensity ultrasound in C-28/I2 human chondrocyte cell line. *Proc. Inst. Mech. Eng. H.* 221, 527–535. doi: 10.1243/09544119JEIM201

Der-Avakian, A., and Markou, A. (2012). The neurobiology of anhedonia and other reward-related deficits. *Trends Neurosci.* 35, 68–77. doi: 10.1016/j.tins.2011.11.005

Eguchi, K., Shindo, T., Ito, K., Ogata, T., Kurosawa, R., Kagaya, Y., et al. (2018). Whole-brain low-intensity pulsed ultrasound therapy markedly improves cognitive dysfunctions in mouse models of dementia - Crucial roles of

endothelial nitric oxide synthase. *Brain Stimul.* 11, 959–973. doi: 10.1016/j.brs.2018.05.012

Eriksson, J., Vogel, E. K., Lansner, A., Bergstrom, F., and Nyberg, L. (2015). Neurocognitive Architecture of Working Memory. *Neuron* 88, 33–46. doi: 10.1016/j.neuron.2015.09.020

Esmaeili, V., and Diamond, M. E. (2019). Neuronal Correlates of Tactile Working Memory in Prefrontal and Vibrissal Somatosensory Cortex. *Cell Rep.* 27, 3167–3181.e3. doi: 10.1016/j.celrep.2019.05.034

Etkin, A., Egner, T., and Kalisch, R. (2011). Emotional processing in anterior cingulate and medial prefrontal cortex. *Trends Cogn. Sci.* 15, 85–93. doi: 10.1016/j.tics.2010.11.004

Euston, D. R., Gruber, A. J., and McNaughton, B. L. (2012). The role of medial prefrontal cortex in memory and decision making. *Neuron* 76, 1057–1070. doi: 10.1016/j.neuron.2012.12.002

Giustino, T. F., and Maren, S. (2015). The Role of the Medial Prefrontal Cortex in the Conditioning and Extinction of Fear. *Front. Behav. Neurosci.* 9:298. doi: 10.3389/fnbeh.2015.00298

Guo, T. F., Li, H. D., Lv, Y. F., Lu, H. Y., Niu, J. H., Sun, J. F., et al. (2015). Pulsed Transcranial Ultrasound Stimulation Immediately After The Ischemic Brain Injury is Neuroprotective. *IEEE Trans. Biomed. Eng.* 62, 2352–2357. doi: 10.1109/Tbme.2015.2427339

Hallock, H. L., Wang, A., and Griffin, A. L. (2016). Ventral Midline Thalamus Is Critical for Hippocampal-Prefrontal Synchrony and Spatial Working Memory. *J. Neurosci.* 36, 8372–8389. doi: 10.1523/JNEUROSCI.0991-16.2016

Hiser, J., and Koenigs, M. (2018). The Multifaceted Role of the Ventromedial Prefrontal Cortex in Emotion, Decision Making, Social Cognition, and Psychopathology. *Biol. Psychiatry* 83, 638–647. doi: 10.1016/j.biopsych.2017.10.030

Huang, S. L., Chang, C. W., Lee, Y. H., and Yang, F. Y. (2017). Protective Effect of Low-Intensity Pulsed Ultrasound on Memory Impairment and Brain Damage in a Rat Model of Vascular Dementia. *Radiology* 282, 113–122. doi: 10.1148/radiol.2016160095

Huang, X., Lin, Z., Wang, K., Liu, X., Zhou, W., Meng, L., et al. (2019). Transcranial Low-Intensity Pulsed Ultrasound Modulates Structural and Functional Synaptic Plasticity in Rat Hippocampus. *IEEE Trans. Ultrason. Ferroelectr. Freq. Control* 66, 930–938. doi: 10.1109/TUFFC.2019.2903896

Jiao, Q., Li, X., An, J., Zhang, Z., Chen, X., Tan, J., et al. (2017). Cell-Cell Connection Enhances Proliferation and Neuronal Differentiation of Rat Embryonic Neural Stem/Progenitor Cells. *Front. Cell Neurosci.* 11:200. doi: 10.3389/fncel.2017.00200

Kim, E., Anguluan, E., and Kim, J. G. (2017). Monitoring cerebral hemodynamic change during transcranial ultrasound stimulation using optical intrinsic signal imaging. *Sci. Rep.* 7:13148. doi: 10.1038/s41598-017-13572-0

Leng, X., Shang, J., Gao, D., and Wu, J. (2018). Low-intensity pulsed ultrasound promotes proliferation and migration of HaCaT keratinocytes through the PI3K/AKT and JNK pathways. *Braz. J. Med. Biol. Res.* 51:e7862. doi: 10.1590/1414-431X20187862

Li, H., Sun, J., Zhang, D., Omire-Mayor, D., Lewin, P. A., and Tong, S. (2017). Low-intensity (400 mW/cm(2), 500 kHz) pulsed transcranial ultrasound preconditioning may mitigate focal cerebral ischemia in rats. *Brain Stimul.* 10, 695–702. doi: 10.1016/j.brs.2017.02.008

Liu, D., Gu, X., Zhu, J., Zhang, X., Han, Z., Yan, W., et al. (2014). Medial prefrontal activity during delay period contributes to learning of a working memory task. *Science* 346, 458–463. doi: 10.1126/science.1256573

Liu, S. H., Lai, Y. L., Chen, B. L., and Yang, F. Y. (2017). Ultrasound Enhances the Expression of Brain-Derived Neurotrophic Factor in Astrocyte Through Activation of TrkB-Akt and Calcium-CaMK Signaling Pathways. *Cereb. Cortex* 27, 3152–3160. doi: 10.1093/cercor/bhw169

Manelis, A., Iyengar, S., Swartz, H. A., and Phillips, M. L. (2020). Prefrontal cortical activation during working memory task anticipation contributes to discrimination between bipolar and unipolar depression. *Neuropsychopharmacology* 45, 956–963. doi: 10.1038/s41386-020-0638-7

Murray, E. A., and Rudebeck, P. H. (2018). Specializations for reward-guided decision-making in the primate ventral prefrontal cortex. *Nat. Rev. Neurosci.* 19, 404–417. doi: 10.1038/s41583-018-0013-4

Nagai, Y., Miyakawa, N., Takuwa, H., Hori, Y., Oyama, K., Ji, B., et al. (2020). Deschloroclozapine, a potent and selective chemogenetic actuator enables rapid neuronal and behavioral modulations in mice and monkeys. *Nat. Neurosci.* 23, 1157–1167. doi: 10.1038/s41593-020-0661-3

Nguyen, R., Venkatesan, S., Binko, M., Bang, J. Y., Cajanding, J. D., Briggs, C., et al. (2020). Cholecystokinin-Expressing Interneurons of the Medial Prefrontal Cortex Mediate Working Memory Retrieval. *J. Neurosci.* 40, 2314–2331. doi: 10.1523/JNEUROSCI.1919-19.2020

O'Brien, J. T., and Thomas, A. (2015). Vascular dementia. *Lancet* 386, 1698–1706. doi: 10.1016/s0140-6736(15)00463-8

Pitts, E. G., Taylor, J. R., and Gourley, S. L. (2016). Prefrontal cortical BDNF: a regulatory key in cocaine- and food-reinforced behaviors. *Neurobiol. Dis.* 91, 326–335. doi: 10.1016/j.nbd.2016.02.021

Poh, L., Fann, D. Y., Wong, P., Lim, H. M., Foo, S. L., Kang, S.-W., et al. (2020). AIM2 inflammasome mediates hallmark neuropathological alterations and cognitive impairment in a mouse model of vascular dementia. *Mol. Psychiatry* 26, 4544-4560. doi: 10.1038/s41380-020-00971-5

Riley, M. R., and Constantinidis, C. (2015). Role of Prefrontal Persistent Activity in Working Memory. *Front. Syst. Neurosci.* 9:181. doi: 10.3389/fnsys.2015.00181

Risher, W. C., Ustunkaya, T., Singh Alvarado, J., and Eroglu, C. (2014). Rapid Golgi analysis method for efficient and unbiased classification of dendritic spines. *PLoS One* 9:e107591. doi: 10.1371/journal.pone.0107591

Smith, R., Lane, R. D., Alkozei, A., Bao, J., Smith, C., Sanova, A., et al. (2018). The role of medial prefrontal cortex in the working memory maintenance of one's own emotional responses. *Sci. Rep.* 8:3460. doi: 10.1038/s41598-018-21896-8

Tamura, M., Spellman, T. J., Rosen, A. M., Gogos, J. A., and Gordon, J. A. (2017). Hippocampal-prefrontal theta-gamma coupling during performance of a spatial working memory task. *Nat. Commun.* 8:2182. doi: 10.1038/s41467-017-02108-9

Toepper, M., Markowitsch, H. J., Gebhardt, H., Beblo, T., Bauer, E., Woermann, F. G., et al. (2014). The impact of age on prefrontal cortex integrity during spatial working memory retrieval. *Neuropsychologia* 59, 157–168. doi: 10.1016/j.neuropsychologia.2014.04.020

Tufail, Y., Matyushov, A., Baldwin, N., Tauchmann, M. L., Georges, J., Yoshihiro, A., et al. (2010). Transcranial pulsed ultrasound stimulates intact brain circuits. *Neuron* 66, 681–694. doi: 10.1016/j.neuron.2010.05.008

Upright, N. A., and Baxter, M. G. (2020). Effect of chemogenetic actuator drugs on prefrontal cortex-dependent working memory in nonhuman primates. *Neuropsychopharmacology* 45, 1793–1798. doi: 10.1038/s41386-020-0660-9

Venkat, P., Chopp, M., and Chen, J. (2015). Models and mechanisms of vascular dementia. *Exp. Neurol.* 272, 97–108. doi: 10.1016/j.expneurol.2015.05.006

Wang, L., Wang, F., Liu, S., Yang, X., Yang, J., and Ming, D. (2018). VEGF attenuates 2-VO induced cognitive impairment and neuronal injury associated with the activation of PI3K/Akt and Notch1 pathway. *Exp. Gerontol.* 102, 93–100. doi: 10.1016/j.exger.2017.12.010

Wang, M., Yang, Y., Wang, C. J., Gamo, N. J., Jin, L. E., Mazer, J. A., et al. (2013). NMDA receptors subserve persistent neuronal firing during working memory in dorsolateral prefrontal cortex. *Neuron* 77, 736–749. doi: 10.1016/j.neuron.2012.12.032

Wang, X. X., Zhang, B., Xia, R., and Jia, Q. Y. (2020). Inflammation, apoptosis and autophagy as critical players in vascular dementia. *Eur. Rev. Med. Pharmacol. Sci.* 24, 9601–9614. doi: 10.26355/eurrev_202009_23048

Xia, Y., and Karin, M. (2004). The control of cell motility and epithelial morphogenesis by Jun kinases. *Trends Cell Biol.* 14, 94–101. doi: 10.1016/j.tcb.2003.12.005

Xu, P., Chen, A., Li, Y., Xing, X., and Lu, H. (2019). Medial prefrontal cortex in neurological diseases. *Physiol. Genom.* 51, 432–442. doi: 10.1152/physiolgenomics.00006.2019

Yang, J., Yao, Y., Wang, L., Yang, C., Wang, F., Guo, J., et al. (2017). Gastrin-releasing peptide facilitates glutamatergic transmission in the hippocampus and effectively prevents vascular dementia induced cognitive and synaptic plasticity deficits. *Exp. Neurol.* 287(Pt 1), 75–83. doi: 10.1016/j.expneurol.2016.08.008

Yuan, Y., Yan, J., Ma, Z., and Li, X. (2016a). Effect of noninvasive focused ultrasound stimulation on gamma oscillations in rat hippocampus. *Neuroreport* 27, 508–515. doi: 10.1097/WNR.0000000000000572

Yuan, Y., Yan, J., Ma, Z., and Li, X. (2016b). Noninvasive Focused Ultrasound Stimulation Can Modulate Phase-Amplitude Coupling between Neuronal Oscillations in the Rat Hippocampus. *Front. Neurosci.* 10:348. doi: 10.3389/fnins.2016.00348

Yuan, Y., Zhang, K., Zhang, Y., Yan, J., Wang, Z., Wang, X., et al. (2021). The Effect of Low-Intensity Transcranial Ultrasound Stimulation on Neural Oscillation and Hemodynamics in the Mouse Visual Cortex Depends on Anesthesia Level and Ultrasound Intensity. *IEEE Trans. Biomed. Eng.* 68, 1619–1626. doi: 10.1109/TBME.2021.3050797

Zhang, D., Li, H., Sun, J., Hu, W., Jin, W., Li, S., et al. (2019). Antidepressant-Like Effect of Low-Intensity Transcranial Ultrasound Stimulation. *IEEE Trans. Biomed. Eng.* 66, 411–420. doi: 10.1109/TBME.2018.2845689

Zhang, J., Zhou, H., Yang, J., Jia, J., Niu, L., Sun, Z., et al. (2021). Low-intensity pulsed ultrasound ameliorates depression-like behaviors in a rat model of chronic unpredictable stress. *CNS Neurosci. Ther.* 27, 233–243. doi: 10.1111/cns.13463

Conflict of Interest: The authors declare that the research was conducted in the absence of any commercial or financial relationships that could be construed as a potential conflict of interest.

Publisher's Note: All claims expressed in this article are solely those of the authors and do not necessarily represent those of their affiliated organizations, or those of the publisher, the editors and the reviewers. Any product that may be evaluated in this article, or claim that may be made by its manufacturer, is not guaranteed or endorsed by the publisher.

frontiers in Aging Neuroscience

ORIGINAL RESEARCH
published: 10 March 2022
doi: 10.3389/fnagi.2022.828377

The Effects of Electroencephalogram Feature-Based Transcranial Alternating Current Stimulation on Working Memory and Electrophysiology

Lanting Zeng[1†], Mingrou Guo[1†], Ruoling Wu[1,2], Yu Luo[3] and Pengfei Wei[1,4]*

[1] Shenzhen Key Laboratory of Neuropsychiatric Modulation and Collaborative Innovation Center for Brain Science, Guangdong Provincial Key Laboratory of Brain Connectome and Behavior, CAS Center for Excellence in Brain Science and Intelligence Technology, Brain Cognition and Brain Disease Institute, Shenzhen Institute of Advanced Technology, Chinese Academy of Sciences, Shenzhen-Hong Kong Institute of Brain Science, Shenzhen Fundamental Research Institutions, Shenzhen, China, [2] Department of Bioengineering, Imperial College London, London, United Kingdom, [3] Shenzhen Zhongke Huayi Technology Co., Ltd., Shenzhen, China, [4] University of Chinese Academy of Sciences, Beijing, China

OPEN ACCESS

Edited by:
Yi Guo,
Jinan University, China

Reviewed by:
Philip Tseng,
Taipei Medical University, Taiwan
Kristin Sellers,
University of California, San Francisco, United States

****Correspondence:***
Pengfei Wei
pf.wei@siat.ac.cn

[†] These authors have contributed equally to this work and share first authorship

Specialty section:
This article was submitted to Neurocognitive Aging and Behavior, a section of the journal Frontiers in Aging Neuroscience

Received: *03 December 2021*
Accepted: *07 February 2022*
Published: *10 March 2022*

Citation:
Zeng L, Guo M, Wu R, Luo Y and Wei P (2022) The Effects of Electroencephalogram Feature-Based Transcranial Alternating Current Stimulation on Working Memory and Electrophysiology. Front. Aging Neurosci. 14:828377. doi: 10.3389/fnagi.2022.828377

Transcranial alternating current stimulation (tACS) can influence cognitive functions by modulating brain oscillations. However, results regarding the effectiveness of tACS in regulating cognitive performance have been inconsistent. In the present study, we aimed to find electroencephalogram (EEG) characteristics associated with the improvements in working memory performance, to select tACS stimulus targets and frequency based on this feature, and to explore effects of selected stimulus on verbal working memory. To achieve this goal, we first investigated the EEG characteristics associated with improvements in working memory performance with the aid of EEG analyses and machine learning techniques. These analyses suggested that 8 Hz activity in the prefrontal region was related to accuracy in the verbal working memory task. The tACS stimulus target and pattern were then selected based on the EEG feature. Finally, the selected tACS frequency (8 Hz tACS in the prefrontal region) was applied to modulate working memory. Such modulation resulted significantly greater improvements, compared with 40 Hz and sham modulations (especially for participants with weak verbal working memory). In conclusion, using EEG features related to positive behavioral changes to select brain regions and stimulation patterns for tACS is an effective intervention for improving working memory. Our results contribute to the groundwork for future tACS closed-loop interventions for cognitive deterioration.

Keywords: electroencephalogram, transcranial alternating current stimulation, working memory, filter bank common spatial pattern, theta oscillations

INTRODUCTION

Over the past few decades, the development of non-invasive brain stimulation (NIBS) techniques has provided a new and effective approach to modulate memory for both researchers and clinicians (Rombouts et al., 2005; Reinhart and Nguyen, 2019; Misselhorn et al., 2020; Benussi et al., 2021; Grover et al., 2021). Among NIBS techniques, transcranial alternating current stimulation (tACS)

can alter specific frequencies of brain oscillations in predefined brain regions and further modulate human cognition (Zaehle et al., 2010; Vosskuhl et al., 2015; Riddle et al., 2021). Working memory deterioration is a key feature of cognitive decline in old age (Li et al., 2001). Although some researchers have proposed that NIBS can help to regulate memory and attenuate age-related cognitive decline (Reinhart and Nguyen, 2019; Klink et al., 2020; Krebs et al., 2021), results regarding the effectiveness of tACS in regulating working memory performance have been inconsistent. Given that verbal and visual working memory involve different cognitive structures, these inconsistencies may have been due to improper selection of stimulation targets and parameters. Therefore, in the current study, we want to select tACS stimulus targets and frequency based on the electroencephalogram (EEG) characteristics associated with improvements in verbal working memory, and to explore the effect of selected stimulus on verbal working memory.

Several studies have indicated that theta and gamma tACS can improve verbal working memory. Based on the positive association between gamma band activity and task performance reported in previous studies, Hoy et al. (2015) applied 40 Hz tACS to the F3-contralateral supraorbital area in 18 healthy participants. Participants underwent 20 min of tES (40 Hz or sham) while completing a verbal two-back task, as well as two-back and three-back tasks before and after tACS. Compared with sham-tACS and transcranial direct current stimulation (tDCS), 40 Hz tACS resulted in increased performance in terms of d prime (an accuracy discriminability index). Biel et al. (2021) also recently reported that frontoparietal in-phase and in-phase focal theta tACS substantially improved verbal three-back task performance when compared with placebo stimulation.

However, some studies have reported that tACS was not effective or was only effective in a limited number of people for verbal working memory. For example, Pahor and Jaušovec (2018) applied tACS over many regions (F3-F4, F3-P3, F4-P4, and P3-P4) in healthy adults to investigate working memory using two-back and three-back tasks. The rationale of the electrode montage and frequency band was based on previous correlational research, which showed that frontotemporal theta and gamma frequency bands are involved in working memory. Nevertheless, only theta-tACS improved performance on the three-back task in the F4-P4 region. In an earlier study, Vosskuhl et al. (2015) applied individual theta frequency stimulation at Pz-FPz. When compared with sham stimulation, tACS was associated with improved short-term memory performance. However, there was no significant difference in improvements on the verbal three-back task between tACS and sham stimulation. Abellaneda-Pérez et al. (2020) further compared the effects of tDCS and 6-Hz tACS applied at F3-FP2 in healthy participants, reporting no significant difference in verbal n-back task performance among the experimental groups (sham, tDCS, and tACS), but they observed that tDCS and tACS exert different modulatory effects on fMRI-derived network dynamics.

In the abovementioned studies, stimulation targeted the prefrontal, frontal, and parietal lobes using theta and gamma frequencies. In NIBS studies, specific targets and parameters for stimulation are usually selected in the following two ways: (a) frequency bands and regions are determined based on previously reported findings regarding their association with verbal working memory or (b) the parameters are simply selected based on those used in previous studies. While these methods have been somewhat successful, there is no guarantee that each combination of parameters will regulate working memory.

We hypothesized that after identifying the brain regions and frequency bands associated with working memory, further exploration of changes in EEG activity that correspond to positive behavioral changes can help to improve the effectiveness of tACS by enabling researchers to set stimulation targets and parameters based on such EEG activity. Repeated assessments of verbal working memory and EEG activity may therefore help to elucidate the electrophysiological features that vary with improvements in behavioral performance. To test this hypothesis, we conducted two experiments that mainly focused on working memory. Experiment 1 was an EEG study, wherein participants completed three n-back tasks, and the electrophysiological features related to improvements in working memory were extracted. In Experiment 2, the participants were divided into three groups and received different frequencies of online tACS: the frequency in group 1 was the evident band in Experiment 1, the frequency in group 2 was the non-evident band in Experiment 1, and group 3 was the sham group. The results of the comparison between group 1 and the other groups can answer the research question.

EXPERIMENT 1: ELECTROENCEPHALOGRAM FEATURES RELATED TO PERFORMANCE

Materials and Methods

Participants

A total of 35 healthy adults aged 22–26 years of age participated in Experiment 1. All participants had normal or corrected-to-normal vision and were right-handed.

In Experiment 1, ten participants were excluded because they did not complete the experiment and 25 participants (five females; mean age 23.76 $\pm$ 1.14 years) were included in the analyses.

When analyzing the results of Experiment 1, we considered that some volunteers would exhibit naturally high performance on the verbal working memory task, leading to a ceiling effect over multiple measurements that may impede identification of the EEG characteristics associated with improvements in performance. We also considered that individuals with high and low levels of verbal working memory ability may exhibit differences in EEG activity and that the same tES parameter may exert different modulatory effects in each group (Daffner et al., 2011; Tseng et al., 2012). For the behavioral analyses, participants were divided into two groups based on their performance in block 1. The grouping method was selected in reference to previous studies (Daffner et al., 2011; Tseng et al., 2012). The scores of the three-back and four-back tasks were summed. The participants who scored lower than the median scores were

assigned to the low-performance (LP) group, while those who scored higher than the median scores were assigned to the high-performance (HP) group. Following grouping, four participants were excluded due to extreme values [target accuracy (target-ACC) or reaction time (RT) exceeding two standard deviations from the mean]. The final LP and HP groups included nine and 12 participants, respectively.

For the EEG analyses, two participants were excluded because they had not sufficient number of good quality EEG trials after artifact removal (LP group: $n = 8$; HP group: $n = 11$).

This study was approved by the Ethics Committee of the Shenzhen Institute of Advanced Technology. The experimental procedures conformed to the principles of the Declaration of Helsinki regarding human experimentation. All participants provided oral consent, signed informed consent documents, and received 270RMB for their participation.

Experimental Design and Schedule

In Experiment 1, all subjects received the same treatment. Participants were required to visit the laboratory twice to complete three n-back tasks (blocks 1, 2, and 3). On day 1, participants performed the block 1 n-back task. After 1 week, the subjects returned to the laboratory and completed blocks 2 and 3. There was a 10 min break between blocks 2 and 3. In each task, task-state EEG data were recorded.

N-Back Task

Kirchner (1958) first proposed the n-back task. Subsequently, the n-back task has been widely employed to investigate and measure working memory. In Experiment 1, we employed the two-back task as an exercise, and the three-back and four-back tasks to measure the working memory performance of volunteers. As illustrated in **Figure 1**, in n-back task (e.g., two-back task), each trial started with a stimulus consisting of an uppercase letter presented for 2 s, followed by a fixation "+" for 0.5 s. After the n-th trial (e.g., second in the two-back task), participants were required to determine whether the current letter was the same as the previous n-th letter (e.g., second in the two-back task). If they were the same, the participants were required to press the "match" button, and the current trial was defined as a target trial. Otherwise, the participants pressed the "non-match" button, and the current trial was defined as a non-target trial. The accuracy of the target trials is defined as "target-ACC." For each trial, participants had 2.5 s to respond and were instructed to press the button as quickly as possible. The instructions were similar in the three-back and four-back tasks.

Each load condition (three-back and four-back) had one sequence of 60 + n trials. Each sequence consisted of 20 trials for targets and 40 trials for non-targets. To help participants understand the n-back task requirements, practice trials were provided for each task. Each n-back task took 10–15 min to complete. The paradigms were programmed in MATLAB using PsychToolbox (Brainard, 1997; Pelli, 1997).

Electrophysiological Recordings

The EEG was recorded during each n-back task with an online reference against the CPz electrode using a 64-channel wireless EEG amplifier with a sampling rate of 1,000 Hz (NeuSen. W64, Neuracle, Changzhou, China). The ground electrode was located on the forehead (between the FPz and Fz electrodes). Electrode impedances were maintained at <5 kΩ.

Initial Electroencephalogram Analysis

Initial EEG analysis includes two steps: (a) EEG signal preprocessing to remove artifacts and to improve the reliability of data and; (b) preliminary exploration of brain regions and frequency bands with the activity corresponding to improvements in performance.

For EEG signal preprocessing, all data were analyzed using EEGLAB version 13.0.0b running in MATLAB (The MathWorks, Untied States). Only correctly responded trials were used in the analysis. Preprocessing steps included filtering (1–48 Hz), epoching (1,000 ms before and 1,500 ms after stimulus onset), baseline correction (500 ms before stimulus onset), and large artifact removal. Ocular artifacts were removed from the independent component analysis (ICA) results. The EEG data were then average-referenced. Finally, epochs that contained signals >100 μV from baseline were rejected.

In the second step, we used the function *pop_newtimef* (Arnaud Delorme, CNL/Salk Institute; Delorme and Makeig, 2004) in EEGLAB for time-frequency analysis to compare the changes of EEG activity between block 1 and block 3. The number of cycles in each [3 0.5] (It means that the wavelet used to measure the amount and phase of the data in each successive, overlapping time window will begin with a 3-cycle wavelet (with a Hanning-tapered window applied). The '0.5' here means that the number of cycles in the wavelets used for higher frequencies will continue to expand slowly, reaching 50% (1 minus 0.5) of the number of cycles in the equivalent FFT window at its highest frequency. This controls the shapes of the individual time/frequency windows measured by the function and their shapes in the resulting time/frequency panes.), analysis wavelet was (3 0.5), the padratio was 2, and the window length was 350 ms. Meanwhile, the filter bank common spatial pattern (FBCSP) was used to explore spatio-frequency modes corresponding to improvements in performance.

Filter bank common spatial pattern is a machine learning approach used to extract the optimal spatial features from different frequency bands (Ang et al., 2008). The original FBCSP algorithm consists of four steps: (1) band filtering, (2) spatial filtering, (3) mutual information (MI)-based feature selection, and (4) classification. MI is a useful statistical measure that can be used to quantify the relationship between variables (Timme and Lapish, 2018). Here, we dropped the classification step. Instead, we focused on the spatio-frequency modes (i.e., the brain regions and frequency bands) of the selected features. **Figure 2** illustrates the workflow. To begin this process, FIR band-pass filters were employed to filter the EEG signals into three frequency bands: theta (4–8 Hz), alpha (8–13 Hz), and beta (13–30 Hz). $E_{i,q} \in \mathbb{R}^{C \times T}$ denotes the i-th trial of the q-th frequency band EEG. In the spatial filtering step, we first calculated a spatial filter $W_{i,q}$ for each frequency band using the CSP algorithm (Pfurtscheller and Neuper, 2001; Blankertz et al., 2007). Notably, ${W_{i,q}}^{-1}$ is the spatial distribution pattern of

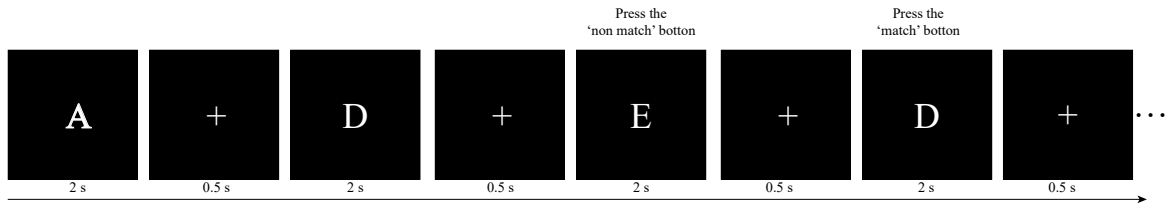

FIGURE 1 | Illustration of the two-back task paradigm in this study. For the first two letters, participants were not required to press buttons, but keep the letters in their mind instead. Subsequently, for each letter, participants were required to determine whether the current letter was the same as the previous second letter. In this case, the third letter should be compared with the first ("E" vs. "A": non-match) and the fourth should be compared with the second one ("D" vs. "D": match).

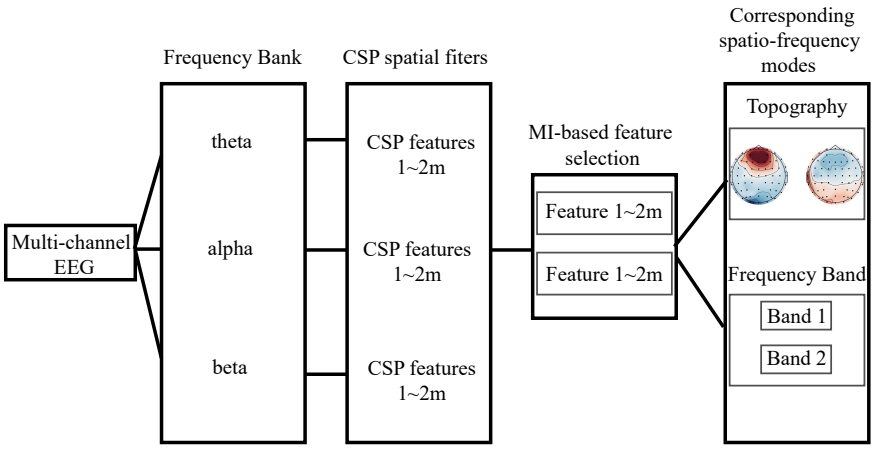

FIGURE 2 | The workflow of filter bank common spatial pattern-based spatio-frequency mode selection. We first filtered the raw electroencephalogram into three frequency bands and then performed spatial filtering to obtain the common spatial pattern (CSP) features. Based on the mutual information, we selected the two most discriminate features and determined their associated spatio-frequency modes.

EEG signals. The spatial filter $W_{i,q}$ was then applied to the EEG matrix $E_{i,q}$,

$$Z_{i,q} = W_q E_{i,q} \quad (1)$$

where the projected EEG matrix is $Z_{i,q} \in \mathbb{R}^{C \times T}$. We selected the m first and rows of $Z_{i,q}$ to maximize the variation for one class while minimizing the variance for the other class. The normalized feature vector $X_{i,q}^p$ was then computed as follows:

$$X_{i,q}^p = \log\left[\frac{var\left(Z_{i,q}^p\right)}{\sum_{i=1}^{2m} var(Z_{i,q}^p)}\right], p \in \{1, 2, ..., 2m\} \quad (2)$$

In the third step, the MI-based feature selection method was adopted to find the spatio-frequency modes containing the most discriminating features (Battiti, 1994). We defined the binary labels set as $l \in L = \{0, 1\}$, where label 0 is for the lower-capacity subjects and label 1 is for the higher-capacity subjects. The MI $I(X_{i,q}^p; L)$ (MI-value) was defined as (Cover, 1999):

$$I\left(X_{i,q}^p; l\right) = H\left(X_{i,q}^p\right) - H\left(X_{i,q}^p \,\middle|\, L\right) \quad (3)$$

where the entropy for the T-dimensional feature vector $X_{i,q}^p$ is

$$H\left(X_{i,q}^p\right) = -\sum_{i=1}^{T} p\left(X_{i,q}^p\right) \log_2 p\left(X_{i,q}^p\right) \quad (4)$$

and the conditional entropy for the random variable $X_{i,q}^p$ and L is

$$H\left(X_{i,q}^p \,\middle|\, L\right) = -\sum_{l \in L} p\left(l \,\middle|\, X_{i,q}^p\right) \log_2 p\left(l \,\middle|\, X_{i,q}^p\right) \quad (5)$$

We selected the top two largest MI values for each n-back test. The corresponding brain regions and frequency bands were considered the most important spatio-frequency modes for n-back performance discrimination.

Graph Convolutional Neural Network

We adapted the original Graph Convolutional Neural Network (GCNN) by adding an attention layer to capture brain network dynamics and identify the channel providing the greatest contribution to the n-back tasks. The GCNN is a generalized version of the convolutional neural network (CNN) (Defferrard et al., 2016). By employing spectral graph theory (Chung and Graham, 1997), GCNN can reveal the underlying topological information of high-dimensional data. In the second step, we investigated the intrinsic spatial patterns of multichannel EEG data using a GCNN model, in which each vertex represents an EEG channel and each edge represents the connection between two electrodes. Although the GCNN approach is effective for elucidating the spatial patterns of multichannel EEG, one limitation is the requirement for a fixed graph representation. In other words, the adjacent matrix must be predetermined

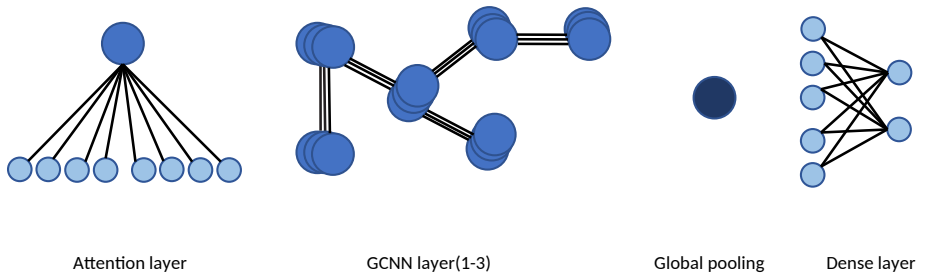

FIGURE 3 | The architecture of the attention based GCNN. The network consists of an attention layer, three GCNN layers, a global pooling layer, and a dense layer. The graph attention mechanism in the first layer learns the dynamic adjacent matrix and the graph features.

before applying the GCNN to the data. However, the brain states of participants can exhibit time variance during long recording periods. Consequently, inspired by graph attention network (GAT) methods (Veličković et al., 2017), we adapted the original GCNN by adding an attention layer to capture brain network dynamics and identify the channel providing the greatest contribution in the n-back tasks (see **Figure 3**).

By definition, a graph can be represented as $G = \{V, E, A\}$, in which V is the set of vertices with the number of N $|V|$. A represents the adjacent matrix, in which each entry denotes the connection relationship (i.e., the edge) between two vertices. The set of input features can be denoted as $h = \{\overrightarrow{h}_1, \overrightarrow{h}_2, \overrightarrow{h}_3, \cdots, \overrightarrow{h}_4\}$, where each feature vector corresponds to a vertex. We first initialized the adjacent matrix randomly. The initial adjacent matrix can be updated by the graph attention layer (Veličković et al., 2017) during the training process. The updating rule is presented as follows:

First, the graph attention layer computes the attention coefficient matrix $\alpha \in \mathbb{R}^{F' \times F'}$,where F' is the size of the output feature set. The coefficients can be computed as

$$\alpha_{i,j} = \frac{\exp\left(LeakyReLU\left(\overrightarrow{w}^T\left[A\overrightarrow{h}_i \parallel A\overrightarrow{h}_j\right]\right)\right)}{\sum_{k\in N_i}\exp\left(LeakyReLU\left(\overrightarrow{w}^T\left[A\overrightarrow{h}_i \parallel A\overrightarrow{h}_k\right]\right)\right)} \quad (6)$$

where N_i is the set of adjacent vertices of the vertex i, $\overrightarrow{w} \in \mathbb{R}^{2F'}$ is the parameter vector of the graph attention layer, and $\parallel$ is the concatenation operation.

The adjacent matrix A can be updated by multiplying the coefficient matrix and the original adjacent matrix, as follows:

$$A' = \alpha A \quad (7)$$

Meanwhile, the graph attention layer also updates the feature set according to the following:

$$\overrightarrow{h}'_i = \sigma\left(\sum_{j\in N_i}\alpha_{i,j}A\overrightarrow{h}_i\right) \quad (8)$$

Then, two GCNN layers are used to classify the performance of the participants. L denotes the Laplacian matrix, which can be written as

$$\mathrm{L} = \mathrm{D}-\mathrm{W} \in \mathbb{R}^{N\ N} \quad (9)$$

where D represents the degree matrix. L can then be decomposed as follows:

$$\mathrm{L} = \mathrm{U}\Lambda\mathrm{U}^{\mathrm{T}} \quad (10)$$

The convolution in the non-Euclidean domains can be computed as

$$\mathrm{y} = \mathrm{g}_\theta(\mathrm{L})\,\mathrm{x} = \mathrm{g}_\theta\left(\mathrm{U}\Lambda\mathrm{U}^{\mathrm{T}}\right)\mathrm{x} = \mathrm{U}\mathrm{g}_\theta(\Lambda)\,\mathrm{U}^{\mathrm{T}}\mathrm{x} \quad (11)$$

where g_θ is the non-parametric filter with learnable parameters. A fully connected layer is then adopted to predict behavioral performance.

Further Electroencephalogram Analysis

Further EEG analysis is based on the results of initial EEG analysis and GCNN to explore the frequency (4, 5, 6, 7, and 8 Hz) that most covariate with improvements in performance. To obtain the EEG activity patterns that most closely corresponded to the integer frequency values of 4, 5, 6, 7, and 8 Hz, we changed the padratio to 8 in further EEG analysis, and compared the changes of each integer frequency (4, 5, 6, 7, and 8 Hz) activity between block 1 and block 3. We measured the MI between power features (4, 5, 6, 7, and 8 Hz) and n-back performance to investigate which frequency was more sensitive to changes in behavior. Specifically, the frequency with the largest MI magnitude is chosen as the stimulation frequency and was applied to modulate working memory.

Results

Behavioral Analyses

The target-ACC of the n-back task was analyzed using a mixed-design analysis of variance (ANOVA) employing one between-subject factor of group (HP or LP) and two within-subject factors of back (three-back or four-back) and block (block 1, 2, or 3). As shown in **Figure 4**, the main effect of block was significant ($F_{2,38} = 23.015$, $p < 0.001$, MSE = 3,266.76, $\eta^2 = 0.55$), suggesting that target-ACC increased as the participants practiced more (target-$ACC_{block\ 3}$ > target-$ACC_{block\ 2}$ > target-$ACC_{block\ 1}$, $ps < 0.05$). The main effect of back was also significant ($F_{1,19} = 25.778$, $p < 0.001$, MSE = 5,831.80, $\eta^2 = 0.58$), suggesting that target-ACC was significantly better on the four-back than the three-back task ($ps < 0.05$). The main effect of group was significant ($F_{1,19} = 15.003$, $p = 0.001$, MSE = 5,630.21,

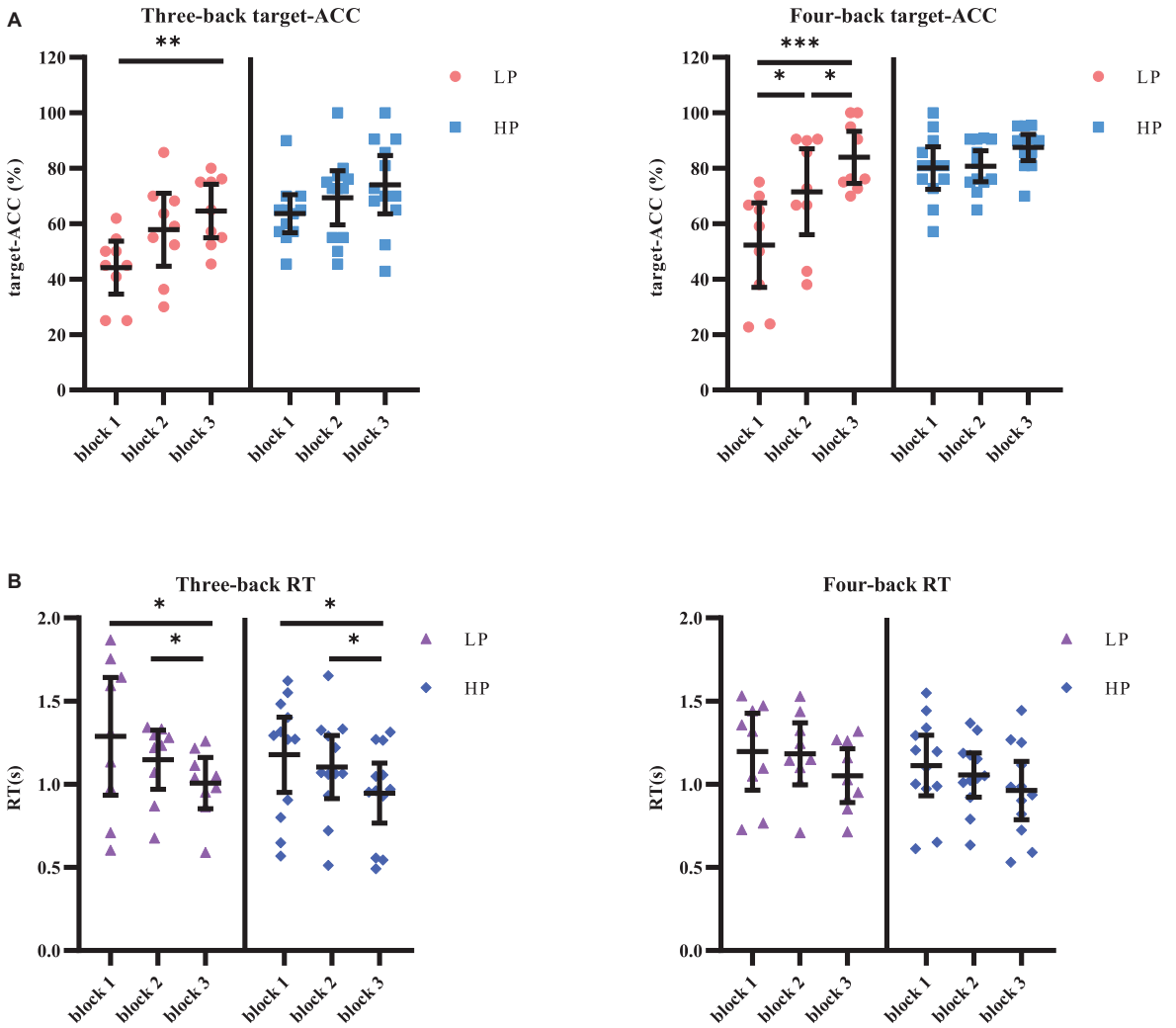

FIGURE 4 | Target-ACC and RT of each group for each back and each block in Experiment 1. **(A)** Scatterplots with individual data points of target-ACC in three-back and four-back tasks. **(B)** Scatterplots with individual data points of RT in three-back and four-back tasks. Error bars are 95%-confidence intervals around the estimates. "*" $p < 0.05$, "**" $p < 0.01$, and "***" $p < 0.001$.

$\eta^2 = 0.44$), suggesting that target-ACC was significantly better among the HP group than among the LP group ($ps < 0.05$). We also observed a significant interaction effect between block and group ($F_{2,38} = 6.02$, $p = 0.005$, MSE = 828.77, $\eta^2 = 0.24$), suggesting that target-ACC increased with practice in the LP group (target-$ACC_{block\ 3}$ > target-$ACC_{block\ 1}$, target-$ACC_{block\ 3}$ > target-$ACC_{block\ 1}$, $ps < 0.05$). In the HP group, only block 3 target-ACC was significantly greater than that in block 1. Further comparisons indicated that target-ACC significantly improved as the number of practice trials increased in the LP group (three-back: target-$ACC_{block\ 3}$ > target-$ACC_{block\ 1}$, $ps < 0.05$; four-back: target-$ACC_{block\ 3}$ > target-$ACC_{block\ 2}$ > target-$ACCb_{lock\ 1}$, $ps < 0.05$). However, this effect was not observed in the HP group.

The same mixed-design ANOVA was conducted for the RT of the correct target trials. Only the main effect of block was significant ($F_{1.49,28.22} = 13.26$, $p < 0.001$, MSE = 0.43, $\eta^2 = 0.41$, with Greenhouse–Geisser correction), suggesting that the RT decreased as the participants practiced more ($RT_{block\ 1}$ > $RT_{block\ 3}$, $RT_{block\ 2}$ > $RT_{block\ 3}$, $ps < 0.05$). Further comparisons indicated that RT significantly decreased as the number of practice trials increased in the relatively simple three-back task (for three-back, $RT_{block\ 1}$ > $RT_{block\ 3}$, $RT_{block\ 2}$ > $RT_{block\ 3}$, $ps < 0.05$, in both the HP and LP groups), but not in the relatively difficult four-back task.

In block 3, the target-ACC was significantly higher than block 1 within the LP group rather than the HP group, which indicates that the division of the two group is appropriate. RT was affected by the difficulty of the task, and the practice effect was only observed in the simpler three-back task.

Initial Electroencephalogram Analyses

After EEG signal preprocessing, we conducted an initial analysis to explore the brain regions and frequency bands exhibiting

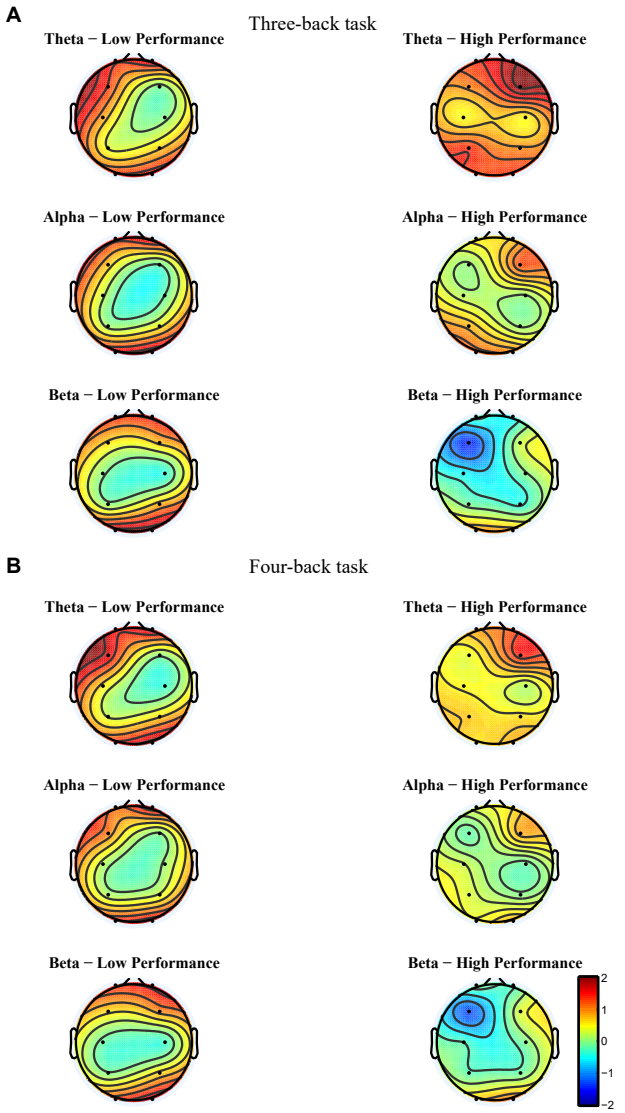

FIGURE 5 | Event-related synchronization from block 1 to block 3 of each group for each band and each back in Experiment 1. **(A)** The power change from block 1 to block 3 in three-back task. **(B)** The power change from block 1 to block 3 in four-back task. The more tend to red, the more positive changes. The more tend to blue, the more negative changes. The color of the central region for each group and each frequency band tends to be green, suggesting that the power of central region tend to remain unchanged among practices.

changes that corresponded to increases in target-ACC in the LP group. For each frequency band (i.e., theta, alpha, and beta) and each block (i.e., block 1 and block 3), the average power between 100 and 700 ms was computed and was further averaged among the two n-back tasks. **Figure 5** shows the event-related synchronization distribution from block 1 to block 3 ($Power_{\text{block 3}} - Power_{\text{block 1}}$). According to this figure, the power seemed relatively stable in the central and parietal regions, regardless of the group or frequency band. Compared with those in block 1, theta and alpha activity was significantly enhanced in the prefrontal, frontal, and occipital lobes in block 3. Considering that the occipital lobe is more involved in visual processing, while the prefrontal and frontal lobes are more closely related to working memory processing, we conducted further analyses on theta and alpha activity in the prefrontal and frontal lobes. After preliminary identification of brain regions and frequencies, the theta and alpha power in Fp1, Fp2, F3, and F4 of the n-back task was analyzed using a mixed-design ANOVA employing one between-subject factor of group (HP or LP) and two within-subject factors of back (three-back or four-back) and block (block 1, 2, or 3). For theta activity, the main effect of block was significant ($F_{2,34} = 5.18$, $p = 0.011$, MSE = 22.99, $\eta^2 = 0.23$) in Fp1, $\text{power}_{\text{block 3}}$ was significantly greater than $\text{power}_{\text{block 1}}$, and $\text{power}_{\text{block 2}}$ was significantly greater than $\text{power}_{\text{block 1}}$. For theta activity, the main effect of block was significant ($F_{2,34} = 6.39$, $p = 0.004$, MSE = 26.12, $\eta^2 = 0.27$) in Fp2, $\text{power}_{\text{block 3}}$ was significantly greater than $\text{power}_{\text{block 1}}$, and $\text{power}_{\text{block 2}}$ was significantly greater than $\text{power}_{\text{block 1}}$. For theta activity, the main effect of block was significant ($F_{2,34} = 7.30$, $p = 0.002$, MSE = 16.79, $\eta^2 = 0.30$) in F3, and $\text{power}_{\text{block 2}}$ was significantly greater than $\text{power}_{\text{block 1}}$. For alpha activity, the main effect of block was significant ($F_{2,34} = 3.86$, $p = 0.031$, MSE = 16.06, $\eta^2 = 0.19$) in Fp2, and $\text{power}_{\text{block 3}}$ was significantly greater than $\text{power}_{\text{block 1}}$. No other main effects were significant (see **Table 1**). These findings suggested that, when compared with other combinations (i.e., theta in frontal region, alpha in frontal region, and alpha in prefrontal region), theta activity in the prefrontal region exhibited trends similar to those observed for changes in behavior [i.e., compared with block 1, the behavioral performance (target-ACC and RT) and theta activity in block 3 were changed significantly].

Meanwhile, to determine the most discriminative spatio-frequency, we performed quantitative analysis on the 2m (m = 2) selected spatial features by measuring MI. We selected the top two largest MI values for each test (see **Table 2**) and visualized the corresponding EEG topographies (see **Figure 6**). **Table 2** and **Figure 6** show that all selected MI values were obtained from the lower band (theta and alpha) activities in frontal and prefrontal region, indicating that lower band activities in frontal and prefrontal region can provide more information for predicting performance on the n-back test (i.e., more sensitive to n-back performance differences). In particular, among the three tests, the features extracted from the theta band had larger MI values than those extracted from the alpha band, aside from those in the three-back test. Thus, we believe that theta band activity in frontal and prefrontal region may be a better indicator of changes in working memory performance.

Graph Convolutional Neural Network

We use an adapted graph attention mechanism to capture brain network dynamics and find the channel contributing most to performance in the n-back tasks. The proposed model achieved a classification accuracy of 80.4%. We selected the top 15 largest weights from the output optimal adjacent matrix and normalized the chosen weights. The edge between Fp1 and Fp2 had the largest

TABLE 1 | The analysis results of theta and alpha in prefrontal and frontal regions.

Frequency	Channel	Main effect	Pairwise comparisons
Theta (4–8 Hz)	Fp1	Block (block 2 > block 1, block 3 > block 1, $p < 0.05$)	/
	Fp2	Block (block 2 > block 1, block 3 > block 1, $p < 0.05$)	For four-back, block 3 > block 1 ($p < 0.05$) in the LP group
	F3	Block (block 2 > block 1, block 3 > block 1, $p < 0.05$)	For three-back, block 3 > block 1 ($p < 0.05$) in the LP group
	F4	/	/
Alpha (9–12 Hz)	Fp1	/	/
	Fp2	Block (block 3 > block 1, $p < 0.05$)	For three-back, block 3 > block 1 ($p < 0.05$) in the LP group
	F3	/	/
	F4	/	/

TABLE 2 | The largest MI values in each frequency bands and the corresponding components.

Test	Component (CSP)	Frequency band	MI
Three-back	CSP3	θ	0.2677
	CSP1	**α**	**0.3264**
	CSP0	β	0.1241
	CSP0	γ	0.1436
Four-back	**CSP2**	**θ**	**0.2808**
	CSP3	α	0.2636
	CSP0	β	0.1395
	CSP0	γ	0.1921

CSP, common spatial pattern; MI, mutual information. The bold text indicates the spatio-frequency modes with the largest MI values.

weight at 0.78, suggesting that the functional connection between Fp1 and Fp2 was most important for n-back task performance.

The result of GCNN was similar to the initial EEG analysis, indicating that the brain activity in prefrontal region was associated with the changes in working memory performance.

Further Electroencephalogram Analysis

In further EEG analysis, we investigated which frequency activity change (4, 5, 6,7, and 8 Hz) is most closely related to the improvements in behavior. The same mixed-design ANOVA was conducted for EEG powers of 4, 5, 6, 7, and 8 Hz in Fp1 and Fp2. **Table 3** lists the significant results. We observed that 8 Hz activity in the prefrontal region (especially Fp2) was most closely related to target-ACC. Specifically, for both three- and four-back tasks, 8 Hz activity and target-ACC were significantly greater in block 3 than in block 1 in the LP group, as was the target-ACC. Prefrontal activity at 6 and 7 Hz appeared to be related to both target-ACC and RT.

Meanwhile, we measured the MI between power features (4, 5, 6, 7, and 8 Hz) of the two selected regions (Fp1 and Fp2) and n-back performance (see **Table 4**). We observed that the 8 Hz power of both regions had larger MI values than other frequencies. Since the magnitude of MI is an indicator of shared information between variables, we inferred that dependency was greatest between 8 Hz power and n-back task performance when compared with that for the other four frequency–performance pairs.

Considering the specificity of the stimulus, these findings indicated that applying 8-Hz stimulation to the prefrontal lobe may be effective for improving verbal working memory performance.

Summary

Electroencephalogram analysis indicated that 8 Hz activity in the prefrontal lobe was associated with the correct response rate in the verbal working memory task, while 6 and 7 Hz activity appeared to be associated with both the correct response rate and response time. Dependency was greatest between 8 Hz power in the prefrontal cortex and n-back task performance when compared with that for the other four frequency–performance pairs. In addition, machine learning results suggested that the functional connection between Fp1 and Fp2 was most important for performance in the n-back tasks. These EEG and machine learning results were used to design Experiment 2, in which the prefrontal lobe was selected as the target for stimulation at a frequency of 8 Hz. In Experiment 2, we compared the modulatory effects of 8 Hz (selected stimulation), 40 Hz (control) and sham stimulation on verbal working memory.

EXPERIMENT 2

Materials and Methods

Participants

In Experiment 2, we recruited 67 young healthy volunteers, but only 48 were included in the behavioral data analysis (20–30 years old). The exclusion criteria were as follows: (1) participants who did not follow the instructions, (2) participants who had outstanding performance in pre-stimulation (target-ACC of >90% in the pre-stimulation tasks), and (3) extreme values (target-ACC or RT exceeding 2 SD from the mean). Among the 48 included participants, 12 were excluded from the EEG analysis because of poor signal quality, and 36 participants (12 females; mean age 23.67 ± 1.97 years) were included in the analyses.

All participants had normal or corrected-to-normal vision and were right-handed. A preliminary questionnaire screening with each subject ensured that all inclusion criteria for transcranial electric stimulation applications were met [i.e., no history of neuropsychiatric disorders (e.g., epilepsy), no brain injuries, no

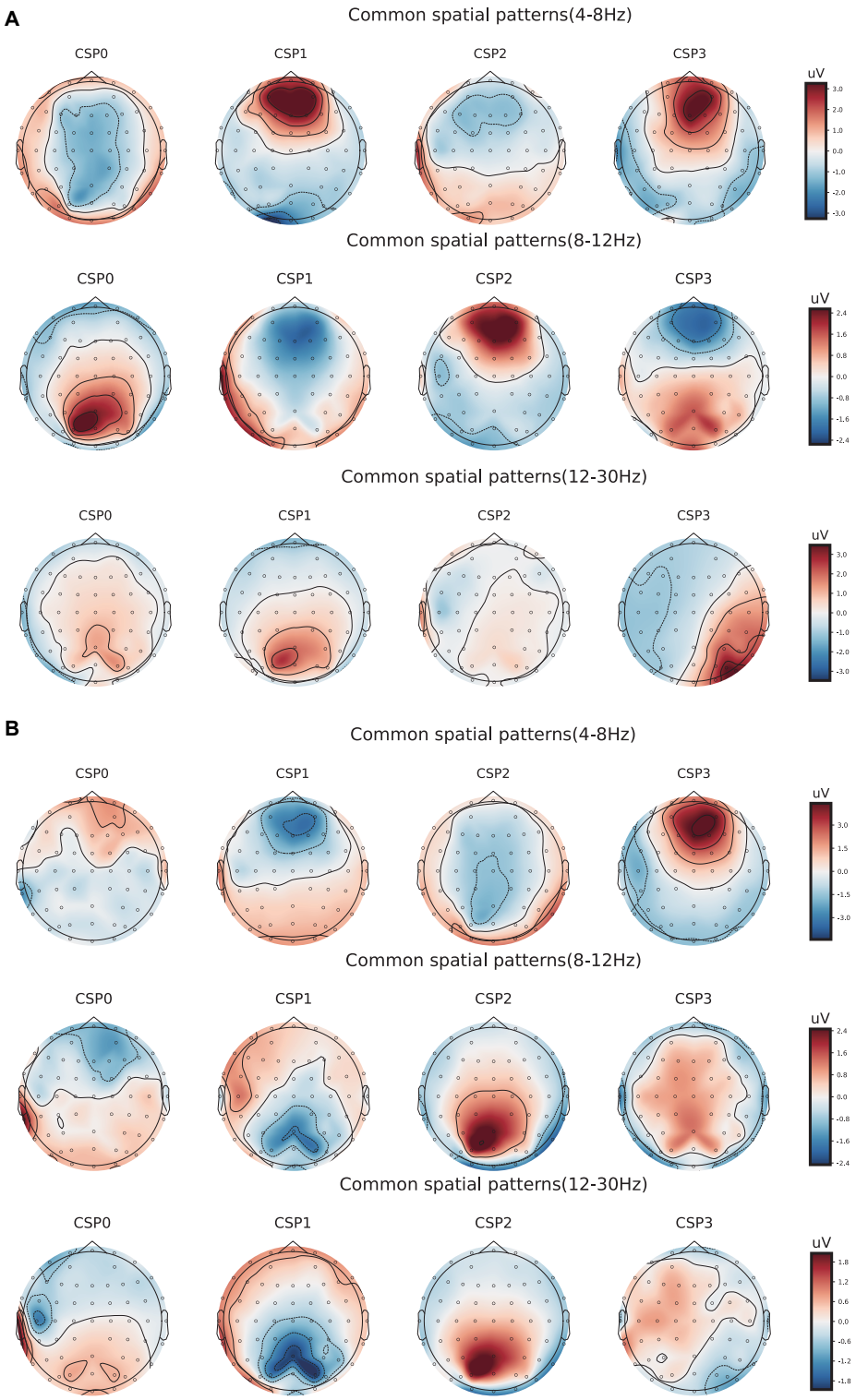

FIGURE 6 | Electroencephalogram topography showing the spatial distribution of the most discriminate features and the associated frequency bands. **(A)** Electroencephalogram topography of three-back task. From top to bottom, each row displays the most important spatio-frequency modes for the theta, alpha, and beta bands, respectively. **(B)** Electroencephalogram topography of four-back task.

TABLE 3 | The analysis results of 4, 5, 6, 7, and 8 Hz in prefrontal.

Channel	Frequency	Main effect	Pairwise comparisons
Fp1	4 Hz	Block (block 2 > block 1, $p < 0.05$)	/
	5 Hz	Block (block 2 > block 1, block 3 > block 1, $p < 0.05$)	/
	6 Hz	Block (block 2 > block 1, block 3 > block 1, $p < 0.05$)	/
	7 Hz	Block (block 2 > block 1, block 3 > block 1, $p < 0.05$)	/
	8 Hz	Block (block 2 > block 1, $p < 0.05$)	/
Fp2	4 Hz	Block (block 3 > block 1, $p < 0.05$)	/
	5 Hz	Block (block 3 > block 1, $p < 0.05$)	/
	6 Hz	Block (block 2 > block 1, block 3 > block 1, $p < 0.05$)	For three-back, block 3 > block 1 ($p < 0.05$) in the HP group. For four-back, block 3 > block 1 ($p < 0.05$) in the LP group.
	7 Hz	Block (block 2 > block 1, block 3 > block 1, $p < 0.05$)	For three-back, block 3 > block 1 ($p < 0.05$) in the HP group. For four-back, block 3 > block 1 ($p < 0.05$) in the LP group
	8 Hz	Block (block 2 > block 1, block 3 > block 1, $p < 0.05$)	For three-back, block 3 > block 1 ($p < 0.05$) in the LP group. For four-back, block 3 > block 1 ($p < 0.05$) in the LP group.

TABLE 4 | The mutual information between 4, 5, 6, 7, and 8 Hz power and working memory performance in the two selected regions.

Channel Frequency (Hz)	Fp1	Fp2
4	0	0.002
5	0.006	0
6	0	0.003
7	0.002	0.003
8	0.009	0.012

pregnancy, no intake of neuroleptic or hypnotic medications, and no metallic or electrical implants in the body].

This study was approved by the Ethics Committee of the Shenzhen Institute of Advanced Technology, and all experimental procedures conformed to the principles of the Helsinki Declaration regarding human experimentation. All participants provided oral consent, signed informed consent documents, and received 200RMB for their participation.

Experimental Design and Schedule

Experiment 2 was conducted using a single-blinded sham-controlled design. Participants were randomly divided into a selected group (n = 14), sham group (n = 18), and control group (n = 16). They completed three sessions (pre-stimulation, stimulation, and post-stimulation). Each session included one n-back task (blocks 1, 2, or 3). In the pre-stimulation session, resting-state EEG data were collected for 5 min before the block 1 n-back task. The participants then underwent tACS while performing the block 2 n-back tasks in the stimulation session. The post-stimulation session was the same as that in the pre-stimulation session. Task-state EEG data were recorded for block 1 (the pre-stimulation session) and block 3 (the post-stimulation session). Finally, subjects completed an electrical stimulation sensitivity questionnaire to report their experiences regarding phosphenes, dizziness, tingling, and itching.

N-Back Tasks

Compared with the n-back tasks of Experiment 1, those in Experiment 2 included an additional five-back task to further investigate the effect of tACS on performance on a more difficult working memory task. In addition, there are nine sequences in total, and each back included three sequences. Each sequence contained 33 + n trials, including 11 target trials and 22 non-target trials.

Electroencephalogram Recordings and Data Preprocessing

Electroencephalogram data recording, processing, and time-frequency analyses were the same as those in Experiment 1.

Transcranial Alternating Current Stimulation

Transcranial alternating current stimulation was delivered *via* a pair of 4.5 cm × 5.5 cm gel electrodes connected to a battery-driven stimulator. The gel electrode impedances were <500 Ω. One of the electrodes was placed over FP1-AP7 and the other was placed over FP2-AF8. The stimulation intensity was 2.0 mA (peak-to-peak current) and was applied for 20 min during the stimulation session in Experiment 2. The selected group received 8 Hz tACS (8 Hz group) and the control group received 40 Hz tACS (40 Hz group). The sham group was also equipped with tACS electrodes but did not receive stimulation.

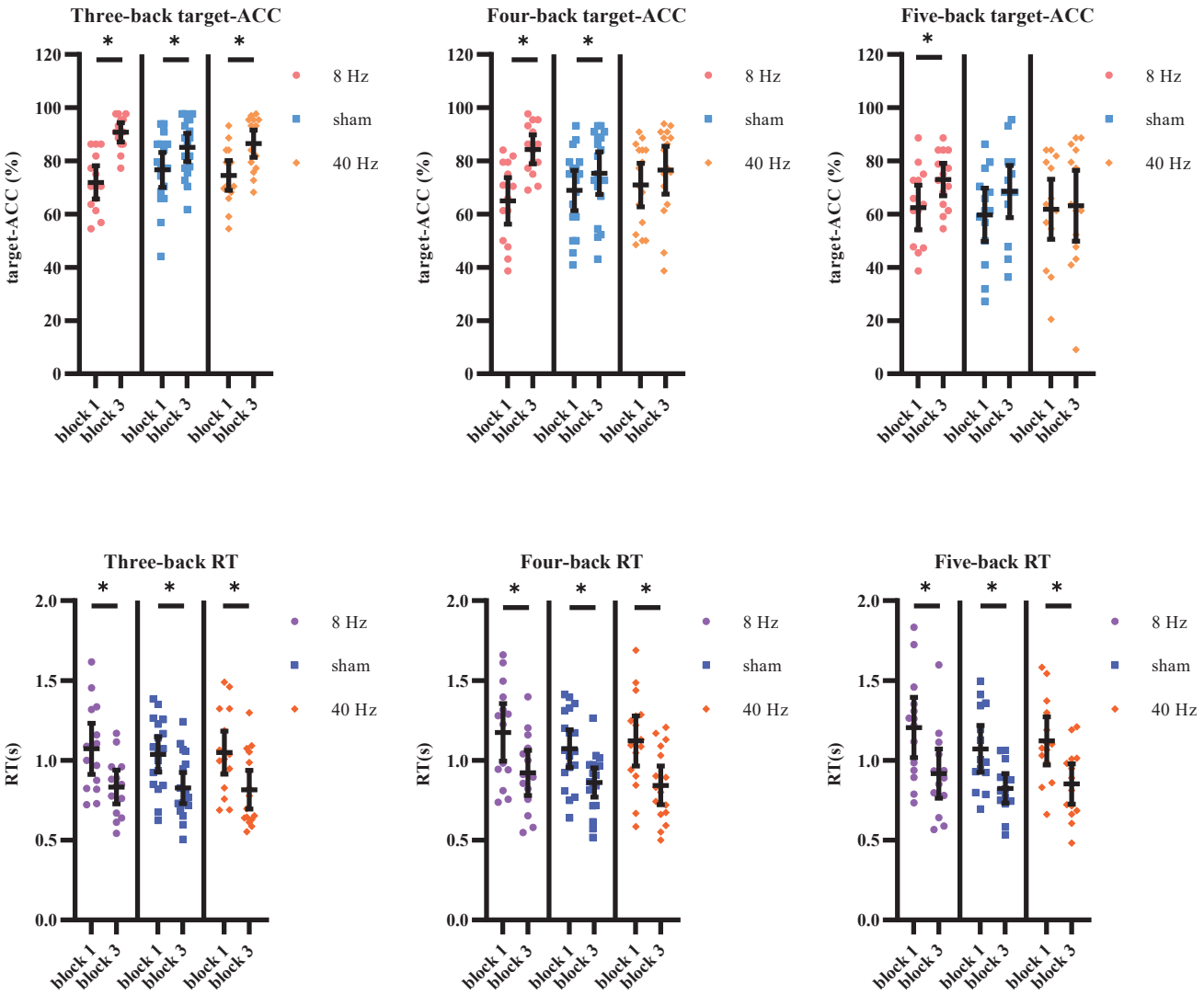

FIGURE 7 | Target-ACC and RT of each group for each back and each block in Experiment 2. **(A)** Scatterplots with individual data points of target-ACC in three-back, four-back, and five-back tasks. **(B)** Scatterplots with individual data points of RT in three-back, four-back, and five-back tasks. Error bars are 95%-confidence intervals around the estimates. "*"$p < 0.05$, "**"$p < 0.01$, and "****"$p < 0.001$.

Results

Behavioral Analyses

The target-ACC of the n-back task was analyzed using a mixed-design ANOVA employing one between-subject factor of group (8 Hz, 40 Hz, or sham) and two within-subject factors of back (three-back, four-back, or five-back) and block (block 1 or 2). As shown in **Figure 7A**, the main effect of block was significant ($F_{1,39} = 62.56$, $p < 0.001$, MSE = 6,059.908, $\eta^2 = 0.62$), suggesting that target-ACC was greater in block 3 than in block 1. The main effect of back was also significant ($F_{1.56,60.87} = 42.90$, $p < 0.001$, MSE = 611.80, $\eta^2 = 0.52$, with Greenhouse–Geisser correction), suggesting that target-ACC decreased significantly as the difficulty of the task increased (target-$ACC_{three-back}$ > target-$ACC_{four-back}$ > target-$ACC_{five-back}$, $ps < 0.001$). We also observed a significant interaction effect between block and group ($F_{2,39} = 7.11$, $p = 0.002$, MSE = 689.06, $\eta^2 = 0.27$), suggesting that target-ACC was significantly greater for block 3 than for block 1 at 8 Hz, 40 Hz, and in the sham condition ($ps < 0.05$). The interaction effect between back and block ($F_{2,78} = 3.38$, $p = 0.039$, MSE = 178.69, $\eta^2 = 0.08$) was also significant, suggesting that target-ACC was significantly greater in block 3 than in block 1 for three-back, four-back, and five-back tasks ($ps < 0.05$). Further comparisons indicated that block 3 target-ACC in the 8 Hz group was significantly higher than that in block 1 for the three-back, four-back, and five-back tasks ($ps < 0.05$). Furthermore, in the sham group, target-ACC was significantly higher in block 3 than in block 1 for the three-back and four-back ($ps < 0.05$). However, in the 40 Hz group, target-ACC was significantly greater in block 3 than in block 1 for the three-back task only.

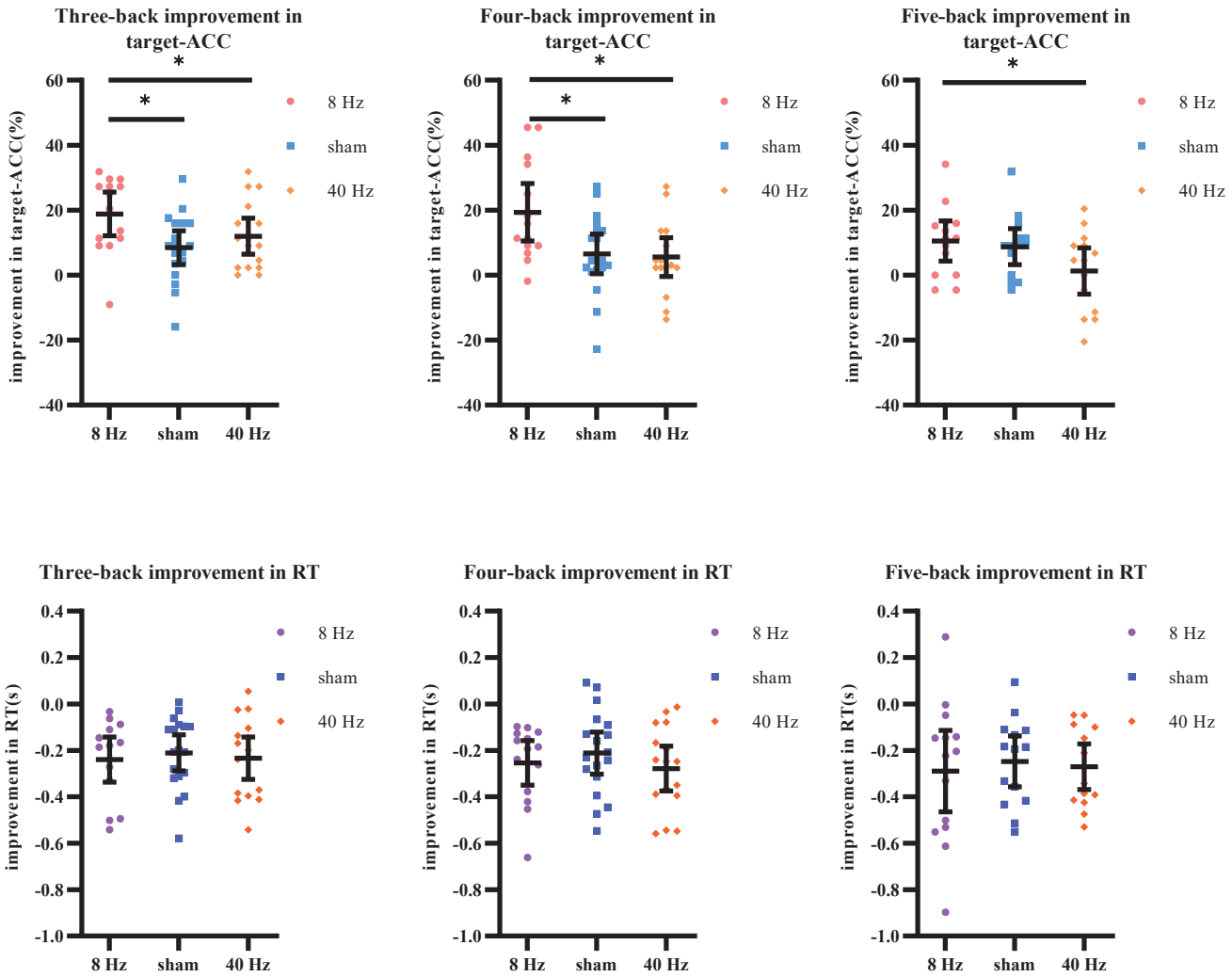

FIGURE 8 | Improvement in target-ACC and RT of each group for each back in Experiment 2. **(A)** Scatterplots with individual data points of improvement in target-ACC for three-back, four-back, and five-back tasks. **(B)** Scatterplots with individual data points of improvement in RT for three-back, four-back, and five-back tasks. Error bars are 95%-confidence intervals around the estimates. "*"$p < 0.05$, "***"$p < 0.01$, and "****"$p < 0.001$.

The same mixed-design ANOVA was conducted to examine RT for correct target trials. As shown in **Figure 7B**, the main effect of block was significant ($F_{1,39} = 87.58$, $p < 0.001$, MSE = 4.18, $\eta^2 = 0.69$), suggesting that block 3 RTs were shorter than those in block 1. The main effect of back was also significant ($F_{1.59,62.18} = 25.12$, $p < 0.001$, MSE = 0.16, $\eta^2 = 0.39$, with Greenhouse–Geisser correction), suggesting that RT increased significantly as the difficulty of the task increased ($RT_{four-back} > RT_{three-back}$, $RT_{five-back} > RT_{three-back}$, $ps < 0.001$). Further comparisons indicated that RT was significantly shorter in block 3 than in block 1 for all three groups (8 Hz, 40 Hz, and sham) and in all three task conditions (three-back, four-back, and five-back) ($ps < 0.05$).

As shown above, the strong practice effect resulted in better performance in block 3 than in block 1. Therefore, we used the improvements in target-ACC (i.e., $target\text{-}ACC_{block\ 3} - target\text{-}ACC_{block\ 1}$) and RT (i.e., $RT_{block\ 3} - RT_{block\ 1}$) as behavioral indices to compare which stimulation setting induced the greatest improvements in verbal working memory. Improvements in target-ACC in each n-back task were analyzed using a mixed-design ANOVA employing one between-subject factor of group (8 Hz, 40 Hz, or sham) and one within-subject factor of back (three-back, four-back, or five-back). As shown in **Figure 8**, the main effect of back was significant ($F_{2,78} = 3.38$, $p = 0.039$, MSE = 357.38, $\eta^2 = 0.08$), indicating a smaller degree of improvement in target-ACC in the five-back task than in the three-back task. The main effect of group was significant ($F_{2,39} = 7.11$, $p = 0.002$, MSE = 1,378.12, $\eta^2 = 0.27$), indicating that the target-ACC improvement was significantly greater in the 8 Hz group than in the 40 Hz and sham groups ($ps < 0.05$). Further comparisons revealed that

the target-ACC improvement of 8 Hz group was significantly greater than that of the 40-Hz group and sham group ($ps < 0.05$) in the three-back and four-back tasks. In the five-back task, the improvement in target-ACC was significantly greater in the 8 Hz group than in the 40 Hz group ($ps < 0.05$). The same analysis was conducted to examine improvements in RT. However, no significant effects were observed in the RT analysis.

We further aimed to explore the effects of the three stimulation conditions on verbal working memory in the HP and LP groups, which were determined based on performance in block 1. Scores for the three-back, four-back, and five-back tasks were summed, and participants who scored lower than the median were assigned to the LP group, while those who scored higher than the median were assigned to the HP group. Eventually, the volunteers were divided into six groups: LP group receiving 8-Hz stimulation (LP-8 Hz) ($n = 6$), HP group receiving 8-Hz stimulation (HP-8 Hz) ($n = 8$), LP group receiving sham stimulation (LP-sham) ($n = 10$), HP group receiving sham stimulation (HP-sham) ($n = 8$), LP group receiving 40-Hz stimulation (LP-40 Hz) ($n = 8$), and HP group receiving 40-Hz stimulation (HP-40 Hz) ($n = 8$). The target-ACC of the n-back task was analyzed using a mixed-design ANOVA employing one between-subject factor of group (LP-8 Hz, HP-8 Hz, LP-sham, HP-sham, LP-40 Hz, and HP-40 Hz) and two within-subject factors of back (three-back, four-back, or five-back) and block (block 1 or 3).

As shown in **Figure 9A**, the main effect of block was significant ($F_{1,36} = 69.90$, $p < 0.001$, MSE = 6,183.12, $\eta^2 = 0.66$), suggesting that target-ACC was significantly greater in block 3 than in block 1. The main effect of back was also significant ($F_{1.49,53.44} = 51.48$, $p < 0.001$, MSE = 6,607.74, $\eta^2 = 0.59$, with Greenhouse–Geisser correction), suggesting that target-ACC decreased significantly as the difficulty of the task increased (target-$ACC_{three-back}$ > target-$ACC_{four-back}$ > target-$ACC_{five-back}$, $ps < 0.001$). The main effect of group was significant ($F_{5,36} = 19.47$, $p < 0.001$, MSE = 4,190.33, $\eta^2 = 0.73$), suggesting a complex difference between groups. We also observed a significant interaction effect between block and group ($F_{5,36} = 4.46$, $p = 0.003$, MSE = 394.32, $\eta^2 = 0.38$), indicating that target-ACC in block 3 was significantly greater than that in block 1 in both the LP-sham and HP-sham groups ($ps < 0.05$). The analysis also indicated that block 3 target-ACC was significantly greater than block 1 target-ACC in the LP-8 Hz and HP-8 Hz groups ($ps < 0.001$). Further comparisons indicated that target-ACC in block 3 was significantly greater than that in block 1 in the three-back, four-back, and five-back tasks within the LP-8 Hz group ($ps < 0.05$). Within the HP-8 Hz group, block 3 target-ACC was greater than block 1 target-ACC for the three- and four-back tasks only ($ps < 0.05$). We also observed improvements in target-ACC between block 1 and 3 of the three-back task in the LP-40 Hz, HP-40 Hz, and HP-sham group ($ps < 0.05$). Target-ACC was significantly greater in block 3 than in block 1 for the five-back task in the LP-sham group ($p < 0.05$).

To weaken the influence of practice effect on the results, the target-ACC improvement in the n-back task was analyzed using a mixed-design ANOVA employing one between-subject factor of group (LP-8 Hz, HP-8 Hz, LP-sham, HP-sham, LP-40 Hz, and HP-40 Hz) and one within-subject factor of back (three-back, four-back, or five-back). As shown in **Figure 9B**, the main effect of group was significant ($F_{5,36} = 4.46$, $p = 0.003$, MSE = 788.64, $\eta^2 = 0.38$), indicating that the target-ACC improvement was significantly greater in the LP-8 Hz group than in the other groups. Further comparisons revealed that the target-ACC improvement was significantly greater in the LP-8 Hz group than in the LP-sham, HP-sham, LP-40 Hz, and HP-40 Hz groups in the three-back and four-back tasks ($ps < 0.05$). In the five-back task, the target-ACC improvement of the LP-8 Hz group was significantly greater than that of the LP-40 Hz and HP-40 Hz groups ($ps < 0.05$). As our previous analysis revealed no differences in the effects of the three stimulation conditions on RT, we did not analyze RT results here.

Electroencephalogram Analyses

The theta power in Fp1 and Fp2 during the n-back task was analyzed using a mixed-design ANOVA employing one between-subject factor of group (8 Hz, 40 Hz, or sham) and two within-subject factors of back (three-back, four-back, or five-back) and block (block 1 or 2). In Fp1, the main effect of block was significant ($F_{1,33} = 4.23$, $p = 0.048$, MSE = 95.32, $\eta^2 = 0.11$), and the theta power was significantly greater in block 3 than in block 1. Further comparisons indicated that theta power during the three-back and four-back tasks was significantly greater in block 3 than in block 1 in the 8 Hz group ($ps < 0.05$), while that during the five-back task was only marginally significantly greater ($ps = 0.056$). No significant effects were observed in the 40 Hz and sham groups. In Fp2, the main effect of block was marginal significant ($ps = 0.056$), and the theta power was greater in block 3 than in block 1. Furthermore, no effect was significant in the theta power analysis for Fp2.

In addition, we explored the effects of the three stimulation conditions on EEG activity associated with verbal working memory in the HP and LP groups. The theta power in Fp1 and Fp2 during the n-back task was analyzed using a mixed-design ANOVA employing one between-subject factor of group (LP-8 Hz, HP-8 Hz, LP-sham, HP-sham, LP-40 Hz, and HP-40 Hz) and two within-subject factors of back (three-back, four-back, or five-back) and block (block 1 or 2). No effect was significant in the theta power analysis for either Fp1 or Fp2.

Adverse Effects Ratings

Participants were required to rate their adverse experiences during and after stimulation. The questionnaire used a four-point Likert scale ranging from 1 (none) to 4 (extreme). Overall, tACS was well-tolerated. For 8-Hz and 40-Hz stimulation, participants reported phosphenes (100%), dizziness (40%), tingling (73.33%), and itching (46.67%) during stimulation. These effects were attenuated after the stimulation, and participants reported phosphenes (3.45%), dizziness (24.14%), tingling (0%), and itching (6.9%). According to the one-way ANOVA, most of the ratings of adverse experiences that occurred during

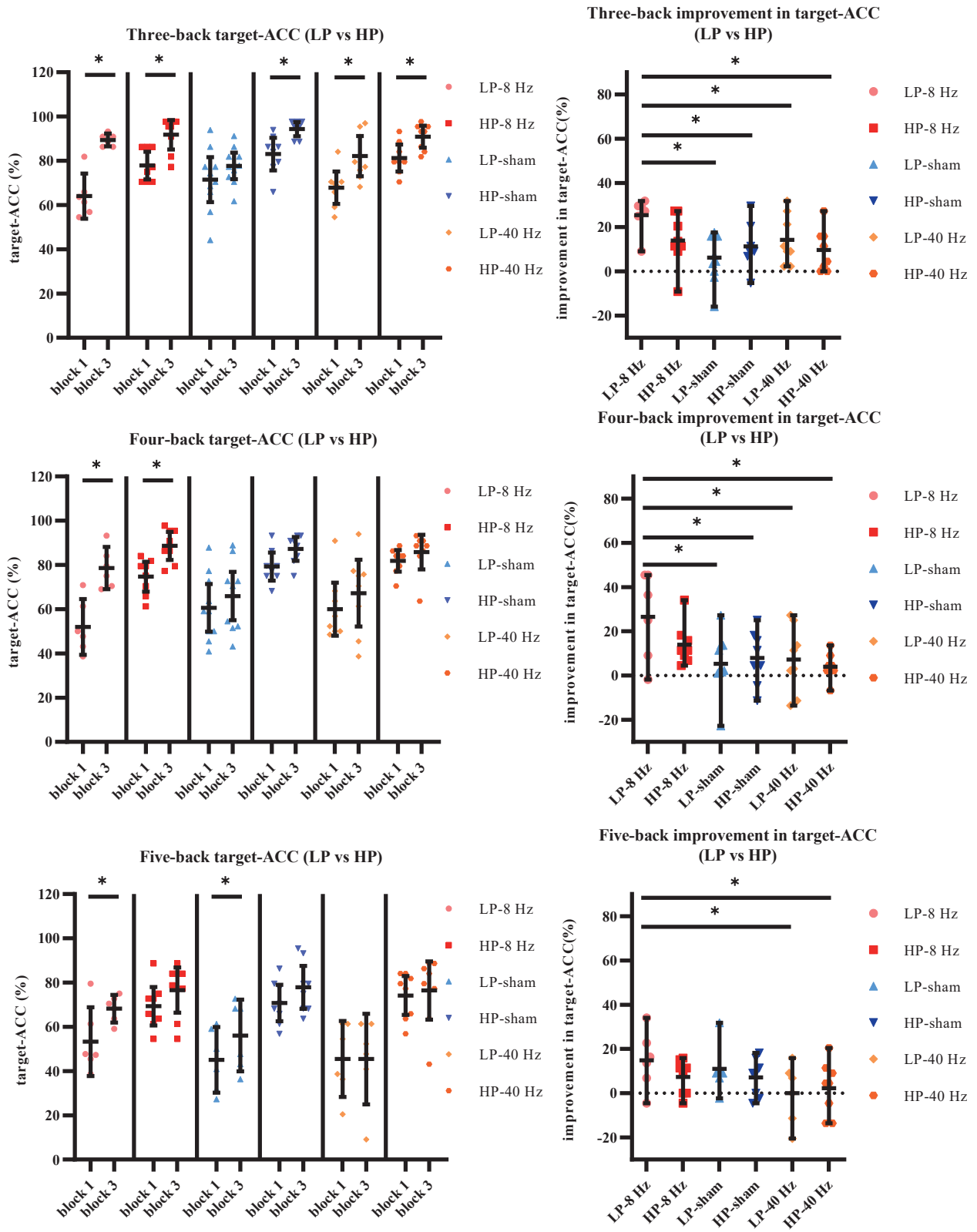

FIGURE 9 | Further analysis result of LP and HP in Experiment 2. **(A)** Scatterplots with individual data points of target-ACC for three-back, four-back, and five-back tasks. **(B)** Scatterplots with individual data points of improvement in target-ACC for three-back, four-back, and five-back tasks. Error bars are 95%-confidence intervals around the estimates. "*"$p < 0.05$, "**"$p < 0.01$, and "****"$p < 0.001$.

stimulation significantly differed between groups, including phosphenes ($F_{2,45}$ = 20.52, $p < 0.001$), tingling ($F_{2,45}$ = 14.15, $p < 0.001$), and itching ($F_{2,45}$ = 3.71, p = 0.032). For phosphenes and tingling, the ratings of the 8 Hz and 40 Hz groups were significantly greater than those of the sham group ($ps < 0.001$). For itching, the rating of the 40 Hz group was significantly greater than that of the sham group (p = 0.034). However, the rating of dizziness that occurred during stimulation did not significantly differ between the groups ($F_{2,45}$ = 1.52, p = 0.230). The ratings of adverse experiences that occurred after stimulation did not significantly differ between groups.

DISCUSSION

Electroencephalogram Activities Related to Positive Behavior Changes

In Experiment 1, participants completed three n-back tasks (blocks 1, 2, and 3). There was an one-week interval between block 1 and block 2 and a ten-minutes break between block 2 and block 3. The result showed that the practice effect was not affected by the interval time. Practice effect of target-ACC was mainly affected by participant's naturally verbal working memory capacity. Low performance subjects showed stronger practice effects than high performance participants. Practice effect of RT was mainly affected by the task difficulty. Subjects showed stronger practice effect in relatively simple three-back task than in relatively difficult four-back task.

In initial EEG analysis, we first targeted the EEG characteristic regions and frequency bands by observing the differences of the topographic maps between block 3 and block 1. We found that theta and alpha activation of block 3 was greater than block 1 in prefrontal and frontal regions. Specifically, theta activity in the prefrontal region exhibited trends similar to those observed for changes in behavior. Meanwhile, the result of FBCSP suggested that theta band activity in frontal and prefrontal regions may be a better indicator of changes in working memory performance. In addition, we used an adapted graph attention mechanism to capture the brain network dynamics and to find the channel contributing most to the performance in n-back tasks. The result was similar to EEG analysis, finding that brain activity in prefrontal region was associated with the changes in working memory performance. Thus, we concluded that theta activity in prefrontal region was associated with improvements in verbal working memory performance.

In further EEG analysis, we investigated the brain oscillations of different frequencies to see which frequency band is most closely associated with improvements in behavioral performance. The result indicated that 8 Hz activity in the prefrontal lobe was associated with the correct response rate in the verbal working memory task, while 6 and 7 Hz activity appeared to be associated with both the correct response rate and response time. Considering the specificity of the stimulus, these findings indicated that applying 8-Hz stimulation to the prefrontal lobe may be effective for improving verbal working memory performance.

The Modulatory Effects of 8 Hz (Selected Stimulation), 40 Hz (Control), and Sham Stimulation on Verbal Working Memory

In Experiment 2, we compared the modulatory effects of 8 Hz (selected stimulation), 40 Hz (control), and sham stimulation on verbal working memory. For the behavioral index of target-ACC, strong practice effects presented in most conditions. Therefore, we used the improvements in target-ACC and RT as behavioral indices to compare which stimulation setting induced the greatest improvements in verbal working memory. The target-ACC improvement of 8 Hz group was significantly greater than that 40 Hz group and sham group in the three-back and four-back tasks. However, no significant effects were observed in RT analysis. These results aligned with the conclusion of Experiment 1 that 8 Hz activity in prefrontal region was associated with the correct response rate in verbal working memory task.

We further explored the effects of three stimulation conditions on verbal working memory in HP and LP groups, which were determined based on performance in block 1. In a relatively simple three-back task, target-ACC of most of subjects became higher in block 3. In relatively difficult four-back and five-back tasks, only LP-8 Hz group maintained a stable and significant improvement in target-ACC. The improvements in target-ACC of LP-8 Hz group was significantly greater than 40 Hz and sham group. The target-ACC of verbal working memory was improved significantly using 8 Hz stimulation than 40 Hz and sham stimulation (especially for participants with low level of verbal working memory).

Overall, accordance to with several previous studies (Vosskuhl et al., 2015; Pahor and Jaušovec, 2018; Abellaneda-Pérez et al., 2020; Biel et al., 2021), our findings indicated that theta band activity was strongly associated with verbal working memory, and that theta tACS improved verbal working memory performance. Moreover, our study extends these findings, as we investigating the EEG characteristics correspond to the improvements in working memory performance in both HP and LP groups. Our analysis revealed that the changes in 8 Hz activity prefrontal region exhibited trends similar to those for the correct response rate in verbal working memory tasks. These results may indicate that 8 Hz activity in prefrontal region supports response accuracy. In Experiment 2, we applied 8 Hz tACS in prefrontal region, representing the biggest difference between the current investigation and previous studies. Although our stimulus targets and frequencies differed from those used in previous research, the performance of verbal working memory was improved significantly by using 8 Hz stimulation than 40 Hz and sham stimulation (especially for participants with low level of verbal working memory). The result suggested that 8 Hz tACS at prefrontal region had an effective intervention on improving verbal working memory.

In EEG analysis, the theta power of prefrontal region during n-back tasks was greater in block 3 than block 1 in 8 Hz group. No significant effects were observed in 40 Hz and sham groups.

The results suggested that after 8 Hz tACS, brain oscillations of the theta frequency band was improved. It is worth considering that the degree of change in EEG is relatively subtle compared to the change in behavior.

Conclusion

The results of Experiment 1 showed that prefrontal lobe theta power was particularly sensitive to the amount of practice. Specifically, 8 Hz activity in the prefrontal region was related to improvements in response accuracy among participants with low verbal working memory ability, while activity at 6 and 7 Hz was related to both response accuracy and RT. Meanwhile, machine learning also indicated that frontal lobe theta power (especially for 8 Hz activity) is sensitive to improvements in performance. In Experiment 2, we utilized a frequency of 8 Hz to target the prefrontal region during tACS. The results of Experiment 2 showed that 8 Hz tACS could effectively improve performance on verbal n-back tasks, and the brain oscillations of the theta frequency band increased after stimulation. In addition, when 8 Hz stimulation was delivered, the target-ACC improvement was significantly higher in the LP group than other participants in sham and 40 Hz groups. These results suggest that applying 8 Hz electrical stimulation to the prefrontal region can effectively improve verbal working memory performance (especially in individuals with low ability), while stimulation at 40 Hz and sham stimulation exert no such effects. In conclusion, using EEG features related to positive behavioral changes to select brain regions and stimulation patterns for tACS is an effective intervention for improving working memory.

Significance

The current study indicated that employing 8 Hz tACS in the prefrontal region can improve performance on n-back tasks that assess working memory. Delivery of tACS at 8 Hz may be especially helpful for improving verbal working memory in participants with generally low initial ability. Moreover, few studies to date have focused on stimulation at Fp1 and Fp2.

More importantly, the current study provides new insight into the selection of appropriate parameters for tACS. Researchers can first investigate the neurophysiological features associated with positive behavioral changes in specific cognitive tasks. Then, selecting tACS targets and parameters based on the feature. This method could be particularly helpful when the source of brain oscillations of specific cognitive functions is not clearly understood. For example, most tACS can influence the superficial regions of brain cortex only (Brunyé, 2018). The spatial resolution of EEG is relatively low. If stimulation of superficial brain regions can causally influence cognitive function, the experiment could indicate that the specific superficial brain region is involved in cognitive function. Using the same logic, different combinations of neurophysiological and stimulation approaches can also be employed to study the mechanisms of cognitive functions and aid the development of interventions for various mental disorders.

Limitations

The current study applied various analyses to determine the EEG features associated with improvements in verbal working memory performance. The results of these analyses were not homogeneous. The final selection of the parameters was a balance between the results of these analyses. Therefore, the selection of the parameters was not stable, meaning that selection may depend on the number and types of analyses used. If more analyses are included, the results may be more inconsistent, which may make selection difficult. However, the number of analyses was not a key feature of the current paradigm. It is important to determine the parameters of tACS by analyzing the electrophysiological online signal, regardless of the number of analyses employed. In addition, the target region for stimulation was very large and may have covered at least four channel sites in the EEG cap. This shortcoming was mainly attributed to the tACS design. The more specific the region, the smaller the electrode, and the more pain the participants would experience. This pain could drastically reduce cognitive function because it constitutes a significant distraction.

Finally, the approach utilized in the current study may be inconvenient because it requires at least two separate experiments. It has been suggested that individualized stimulation may be better. For example, researchers could analyze the neurophysiological data for each participant immediately after the first test of cognitive function and immediately apply the stimulation in the same experiment. In this scenario, the difference between correct and incorrect trials could be revealed by rapid analyses or machine learning methods. However, these issues are much more complicated in practice. For example, correct trials do not fully reflect true judgment; participants may press a button based on guesswork. Although researchers could subtract the false alarm rate from the target-ACC to evaluate function, the number of correct trials wherein participants respond by guessing would be unknown. Including these trials in the analyses will greatly reduce the reliability of the analyses that aim to differentiate correct and incorrect trials because different participants might have different tendencies to guess. In addition, the number of correct and incorrect trials is difficult to control, and they would directly influence the results of the analyses.

Further Study

Further studies could employ the same procedures in a cohort of older adults to investigate whether this method is effective in improving the working memory of the older adults and those with cognitive decline.

In addition, more cognitive tasks that are used to assess working memory could be included in future studies, employing a similar design to Experiments 1 and 2. By doing this, the differences and the common brain activities of working memory among various tasks could be revealed, which may help to explain the inconsistent results of previous studies.

Future studies should employ AI training to improve cognitive function. Although the differentiation between correct and incorrect trials may be difficult, differentiation of HP and LP groups using AI is feasible. The current study already trained AI

to differentiate the two groups. In further studies, this AI could analyze all trials in the first session and classify the case as HP or LP. In the second session, half of the cases in each group would receive the corresponding stimulation. Comparison of the stimulated and non-stimulated cases in the LP group may be more convincing because the two sessions would include the same participants and comparison within a group might make the difference greater.

DATA AVAILABILITY STATEMENT

All datasets generated for this study are included in the article.

ETHICS STATEMENT

The studies involving human participants were reviewed and approved by Ethics Committee of the Shenzhen Institute of Advanced Technology. The patients/participants provided their written informed consent to participate in this study.

AUTHOR CONTRIBUTIONS

PW designed the study. MG and LZ contributed to the literature search, data collection, data analysis, and interpretation of the results. YL provided hardware support for the experiment and participated in data collection. RW was responsible for machine learning data analysis. All authors contributed to the writing of this manuscript.

FUNDING

This work was supported in part by the National Key R&D Program of China (2021ZD0203902 and 2018YFA0701403) and the Youth Innovation Promotion Association of the Chinese Academy of Sciences (2017413).

REFERENCES

Abellaneda-Pérez, K., Vaqué-Alcázar, L., Perellón-Alfonso, R., Bargalló, N., Kuo, M.-F., Pascual-Leone, A., et al. (2020). Differential tDCS and tACS effects on working memory-related neural activity and resting-state connectivity. *Front. Neurosci.* 13:1440. doi: 10.3389/fnins.2019.01440

Ang, K. K., Chin, Z. Y., Zhang, H., and Guan, C. (2008). "Filter bank common spatial pattern (FBCSP) in brain-computer interface," in *2008 IEEE International Joint Conference on Neural Networks*, (Piscataway: IEEE), 2390–2397.

Battiti, R. (1994). Using mutual information for selecting features in supervised neural net learning. *IEEE Trans. Neural Netw.* 5, 537–550. doi: 10.1109/72.298224

Benussi, A., Cantoni, V., Cotelli, M. S., Cotelli, M., Brattini, C., Datta, A., et al. (2021). Exposure to gamma tACS in Alzheimer's disease: a randomized, double-blind, sham-controlled, crossover, pilot study. *Brain Stimul.* 14, 531–540. doi: 10.1016/j.brs.2021.03.007

Biel, A. L., Sterner, E., Röll, L., and Sauseng, P. (2021). Modulating verbal working memory with fronto-parietal transcranial electric stimulation at theta frequency: does it work? *Eur. J. Neurosci.* 55, 405–425. doi: 10.1111/ejn.15563

Blankertz, B., Dornhege, G., Krauledat, M., Müller, K. R., and Curio, G. (2007). The non-invasive Berlin Brain–Computer Interface: fast acquisition of effective performance in untrained subjects. *Neuroimage* 37, 539–550. doi: 10.1016/j.neuroimage.2007.01.051

Brainard, D. H. (1997). The psychophysics toolbox. *Spat. Vis.* 10, 433–436. doi: 10.1163/156856897x00357

Brunyé, T. T. (2018). Modulating spatial processes and navigation via transcranial electrical stimulation: a mini review. *Front. Hum. Neurosci.* 11:649. doi: 10.3389/fnhum.2017.00649

Chung, F. R. K., and Graham, F. C. (1997). *Spectral Graph Theory*. Providence: American Mathematical Soc.

Cover, T. M. (1999). *Elements of Information Theory*. Hoboken: John Wiley & Sons.

Daffner, K. R., Chong, H., Sun, X., Tarbi, E. C., Riis, J. L., McGinnis, S. M., et al. (2011). Mechanisms underlying age- and performance-related differences in working memory. *J. Cogn. Neurosci.* 23, 1298–1314. doi: 10.1162/jocn.2010.21540

Defferrard, M., Bresson, X., and Vandergheynst, P. (2016). "Convolutional neural networks on graphs with fast localized spectral filtering," in *NIPS'16: Proceedings of the 30th International Conference on Neural Information Processing Systems*, (Barcelona: Neural Information Processing Systems), 3844–3852.

Delorme, A., and Makeig, S. (2004). EEGLAB: an open source toolbox for analysis of single-trial EEG dynamics including independent component analysis. *J. Neurosci. Methods* 134, 9–21. doi: 10.1016/j.jneumeth.2003.10.009

Grover, S., Nguyen, J. A., Viswanathan, V., and Reinhart, R. M. (2021). High-frequency neuromodulation improves obsessive–compulsive behavior. *Nat. Med.* 27, 232–238. doi: 10.1038/s41591-020-01173-w

Hoy, K. E., Bailey, N., Arnold, S., Windsor, K., John, J., Daskalakis, Z. J., et al. (2015). The effect of γ-tACS on working memory performance in healthy controls. *Brain Cogn.* 101, 51–56. doi: 10.1016/j.bandc.2015.11.002

Kirchner, W. K. (1958). Age differences in short-term retention of rapidly changing information. *J. Exp. Psychol.* 55, 352–358. doi: 10.1037/h0043688

Klink, K., Peter, J., Wyss, P., and Klöppel, S. (2020). Transcranial electric current stimulation during associative memory encoding: comparing tACS and tDCS effects in healthy aging. *Front. Aging Neurosci.* 12:66. doi: 10.3389/fnagi.2020.00066

Krebs, C., Peter, J., Wyss, P., Brem, A. K., and Klöppel, S. (2021). Transcranial electrical stimulation improves cognitive training effects in healthy elderly adults with low cognitive performance. *Clin. Neurophysiol.* 132, 1254–1263. doi: 10.1016/j.clinph.2021.01.034

Li, S. C., Lindenberger, U., and Sikström, S. (2001). Aging cognition: from neuromodulation to representation. *Trends Cogn. Sci.* 5, 479–486. doi: 10.1016/s1364-6613(00)01769-1

Misselhorn, J., Göschl, F., Higgen, F. L., Hummel, F. C., Gerloff, C., and Engel, A. K. (2020). Sensory capability and information integration independently explain the cognitive status of healthy older adults. *Sci. Rep.* 10:22437. doi: 10.1038/s41598-020-80069-8

Pahor, A., and Jaušovec, N. (2018). The effects of theta and gamma tACS on working memory and electrophysiology. *Front. Hum. Neurosci.* 11:651. doi: 10.3389/fnhum.2017.00651

Pelli, D. G. (1997). The Video Toolbox software for visual psychophysics: transforming numbers into movies. *Spat. Vis.* 10, 437–442.

Pfurtscheller, G., and Neuper, C. (2001). Motor imagery and direct brain-computer communication. *Proc. IEEE.* 89, 1123–1134. doi: 10.1109/5.939829

Reinhart, R. M. G., and Nguyen, J. A. (2019). Working memory revived in older adults by synchronizing rhythmic brain circuits. *Nat. Neurosci.* 22, 820–827. doi: 10.1038/s41593-019-0371-x

Riddle, J., McFerren, A., and Frohlich, F. (2021). Causal role of cross-frequency coupling in distinct components of cognitive control. *Prog. Neurobiol.* 202:102033. doi: 10.1016/j.pneurobio.2021.102033

Rombouts, S. A., Barkhof, F., Goekoop, R., Stam, C. J., and Scheltens, P. (2005). Altered resting state networks in mild cognitive impairment and mild

Alzheimer's disease: an fMRI study. *Hum. Brain Mapp.* 26, 231–239. doi: 10.1002/hbm.20160

Timme, N. M., and Lapish, C. (2018). A tutorial for information theory in neuroscience. *eNeuro* 5:ENEURO.0052-18.2018. doi: 10.1523/ENEURO.0052-18.2018

Tseng, P., Hsu, T. Y., Chang, C. F., Tzeng, O. J., Hung, D. L., Muggleton, N. G., et al. (2012). Unleashing potential: transcranial direct current stimulation over the right posterior parietal cortex improves change detection in low-performing individuals. *J. Neurosci.* 32, 10554–10561. doi: 10.1523/jneurosci.0362-12.2012

Veličković, P., Cucurull, G., Casanova, A., Romero, A., Liò, P., and Bengio, Y. (2017). Graph attention networks. *arXiv* [preprint]. Available online at: https://arxiv.org/abs/1710.10903v1 (accessed October 30, 2017).

Vosskuhl, J., Huster, R. J., and Herrmann, C. S. (2015). Increase in short-term memory capacity induced by down-regulating individual theta frequency via transcranial alternating current stimulation. *Front. Hum. Neurosci.* 9:257. doi: 10.3389/fnhum.2015.00257

Zaehle, T., Rach, S., and Herrmann, C. S. (2010). Transcranial alternating current stimulation enhances individual alpha activity in human EEG. *PLoS One* 5:e13766. doi: 10.1371/journal.pone.0013766

Conflict of Interest: YL was employed by Shenzhen Zhongke Huayi Technology Co. Ltd.

The remaining authors declare that the research was conducted in the absence of any commercial or financial relationships that could be construed as a potential conflict of interest.

frontiers in Aging Neuroscience

ORIGINAL RESEARCH
published: 15 March 2022
doi: 10.3389/fnagi.2022.847223

Optimized Magnetic Stimulation Induced Hypoconnectivity Within the Executive Control Network Yields Cognition Improvements in Alzheimer's Patients

Guixian Xiao[1,2,3†], Yue Wu[1,2,3†], Yibing Yan[1,2,3†], Liying Gao[1,2,3], Zhi Geng[4,5,6], Bensheng Qiu[7], Shanshan Zhou[1,2,3], Gongjun Ji[1,2,3], Xingqi Wu[1,2,3], Panpan Hu[1,2,3*] and Kai Wang[1,2,3,4,5*]*

[1] Department of Neurology, The First Affiliated Hospital of Anhui Medical University, Hefei, China, [2] The School of Mental Health and Psychological Sciences, Anhui Medical University, Hefei, China, [3] Institute of Artificial Intelligence, Hefei Comprehensive National Science Center, Hefei, China, [4] Anhui Province Key Laboratory of Cognition and Neuropsychiatric Disorders, Hefei, China, [5] Collaborative Innovation Center for Neuropsychiatric Disorders and Mental Health, Hefei, China, [6] Department of Neurology, Second People's Hospital of Hefei City, The Hefei Affiliated Hospital of Anhui Medical University, Hefei, China, [7] Center for Biomedical Imaging, University of Science and Technology of China, Hefei, China

OPEN ACCESS

Edited by:
Yi Guo,
Jinan University, China

Reviewed by:
Liyong Wu,
Capital Medical University, China
Tianzhen Chen,
Shanghai Jiao Tong University, China
Chunming Xie,
Southeast University, China

***Correspondence:**
Xingqi Wu
wuxingqi09@163.com
Panpan Hu
hpppanda9@126.com
Kai Wang
wangkai1964@126.com

[†]These authors share first authorship

Specialty section:
This article was submitted to Alzheimer's Disease and Related Dementias, a section of the journal Frontiers in Aging Neuroscience

Received: 01 January 2022
Accepted: 07 February 2022
Published: 15 March 2022

Citation:
Xiao G, Wu Y, Yan Y, Gao L, Geng Z, Qiu B, Zhou S, Ji G, Wu X, Hu P and Wang K (2022) Optimized Magnetic Stimulation Induced Hypoconnectivity Within the Executive Control Network Yields Cognition Improvements in Alzheimer's Patients. Front. Aging Neurosci. 14:847223. doi: 10.3389/fnagi.2022.847223

Alzheimer's disease (AD) is a severe neurodegenerative disease, which mainly manifests as memory and progressive cognitive impairment. At present, there is no method to prevent the progression of AD or cure it, and effective intervention methods are urgently needed. Network-targeted intermittent theta burst stimulation (iTBS) may be effective in alleviating the cognitive symptoms of patients with mild AD. The abnormal function of the dorsolateral prefrontal cortex (DLPFC) within executive control network (ECN) may be the pathogenesis of AD. Here, we verify the abnormality of the ECN in the native AD data set, and build the relevant brain network. In addition, we also recruited AD patients to verify the clinical effects of DLPFC-targeted intervention, and explor the neuro-mechanism. Sixty clinically diagnosed AD patients and 62 normal controls were recruited to explore the ECN abnormalities. In addition, the researchers recruited 20 AD patients to explore the efficacy of 14-session iTBS treatments for targeted DLPFC interventions. Functional magnetic resonance imaging and neuropsychological assessment of resting state were performed before and after the intervention. Calculate the changes in the functional connectivity of related brain regions in the ECN, as well as the correlation between the baseline functional connectivity and the clinical scoring scale, to clarify the mechanism of the response of iTBS treatment to treatment. Our results showed that compared with normal control samples, the brain function connection between the left DLPFC and the left IPL within the ECN of AD patients was significantly enhanced (t = 2.687, p = 0.008, FDR-corrected p = 0.045). And we found that iTBS stimulation significantly reduced the functional magnetic resonance imaging signal between the left DLPFC and the left IPL in the ECN (t = 4.271, p < 0.001, FDR-corrected p = 0.006),

and it was related to the improvement of the patient's clinical symptoms ($r = -0.470$, $p = 0.042$). This work provides new insights for targeted brain area interventions. By targeted adjusting the functional connection of ECN to improve the clinical symptoms and cognitive function of AD patients.

Keywords: Alzheimer's disease, executive control network, intermittent theta burst stimulation (iTBS), dorsolateral prefrontal cortex, cognitive function

INTRODUCTION

Alzheimer's disease (AD) is a severe neurodegenerative disease that mainly manifests as memory and progressive cognitive impairment (Molteni and Rossetti, 2017). Data from the 2018 Annual Report of the World Alzheimer's Disease (Prince and Matthew, 2018) show that there are approximately 50 million AD patients in the world at present, and the incidence continues to rise. AD has become the seventh cause of death in the world, and it is one of the most important health and social crises of the 21st century (Prince and Matthew, 2018). AD patients are mainly treated with drugs (Blennow et al., 2006), but these drug treatments can only delay the course of the disease to a certain extent, and they cause adverse reactions (Mielke et al., 2012). At present, there is no method to prevent the progression of AD or cure it (Godyn et al., 2016). With the advancement of science and technology, physical therapy methods have gradually been applied to the field of neurodegenerative diseases, such as transcranial magnetic stimulation (TMS) and transcranial electrical stimulation.

The abnormal function of the executive control network (ECN) may be the pathogenesis of AD (Dhanjal and Wise, 2014; Zhao et al., 2018, 2019). Studies have shown that the impaired response of the ECN during verbal memory contributes to the decline in memory performance (Dhanjal and Wise, 2014). Heterogeneity exists in previous studies, which may be related to different ECN construction methods (Shirer et al., 2012; Li et al., 2019). The research on ECN encompasses the dorsolateral prefrontal cortex (DLPFC) related to working memory and attention; the inferior parietal lobule (IPL) related to bottom-up attention and episodic memory; middle frontal gyrus (MFG) related to executive ability; and middle temporal gyrus (MTG) related to language function (Seeley et al., 2007; Vincent et al., 2008; Liu et al., 2021). Previous studies based on *a priori* selection of brain networks have shown that the functional connectivity between specific central executive networks and different areas of the brain is weakened (Dhanjal and Wise, 2014; Joo et al., 2016; Cai et al., 2017), which may explain the impairment and severity of cognitive function in AD patients (Chandra et al., 2019; Jones et al., 2019). Research on the functional connectivity of the resting state MRI of AD shows that DLPFC dysfunction in the early stage of AD manifests as memory impairment, especially the impairment of its executive components (Kaufman et al., 2010; Kumar et al., 2017; Puttaert et al., 2020). As an important node of the ECN (Seeley et al., 2007), understanding the functional mechanisms of the DLPFC and other brain areas of the ECN is important for designing effective interventions for patients with AD. At present, magnetic resonance imaging (TMS) can improve cognition by targeting the network through functional magnetic resonance imaging.

Targeted cortical-hippocampal network TMS stimulation in adults increases the functional connection between the cortex-hippocampal network area, which demonstrates their role in improving the associative memory function (Wang et al., 2014). A study on the effect of high-frequency TMS on network-targeted stimulation showed that it promoted the recall ability of participants to a greater extent (Nilakantan et al., 2019). Repetitive TMS (rTMS) is a non-invasive, green treatment that can stimulate brain nerves through the skull without attenuation. At present, TMS mainly treats diseases by adjusting the balance between excitement and inhibition of the brain in both directions in clinical practice; rTMS can generate excitatory postsynaptic potentials, resulting in abnormal excitement of the nerves in the stimulated part, while low-frequency stimulation is the opposite. TMS is generally considered to mainly affect the cerebral cortex, relying on cognitive circuits in the subcortex and other deep structures, such as the cingulate gyrus and hippocampus. The DLPFC is located in the lateral cerebral cortex, usually close to the stimulation area, which stimulates the cognitive function and clinical symptoms of DLPFC and is expected to benefit from TMS (Miniussi and Rossini, 2011; Brunoni and Vanderhasselt, 2014; Penolazzi et al., 2015; Cappon et al., 2016).

Cognition is a broad concept. Different cognitive functions are maintained by different brain networks and are affected by stimulation techniques to varying degrees. Whether intervention in the DLPFC of AD patients can compensate for the functional connection within the ECN, and the relevance of cognitive function and the ECN is still unclear. In this study, we mainly explored the effect of the iTBS on targeted DLPFC within the ECN in AD patients to determine whether they can improve memory function and clinical symptoms by regulating the activities of the frontal and parietal lobes. We predicted that left-DLPFC-targeted iTBS stimulation improves cognitive function clinical symptoms in AD. The improvement of clinical symptoms was related to the change of functional connections within the ECN.

MATERIALS AND METHODS

Participants

This study mainly recruited AD patients aged 50–85 in the neurology clinic or ward of the First Affiliated Hospital of Anhui Medical University. All AD patients satisfying the diagnostic criteria for probable Alzheimer's disease based on the National Institute of Neurological and Communicative Disorders and

Stroke and the Alzheimer's Disease and Related Disorders Association (NINCDS-ADRDA) criteria (McKhann et al., 1984, 2011). The clinical dementia rating (CDR) was between 0.5 and 2 points. Scored 10–27 on the Mini-Mental State Examination (MMSE). Treatment with donepezil at a steady dose for at least 3 months prior to iTBS until the treatment was completed. The exclusion criteria were as follows: patients with a history of drug abuse, alcoholism, or mental illness; patients with severe heart, lung, liver, and kidney dysfunction; acute and chronic infection; patients with craniocerebral trauma or severe cerebrovascular disease; and allergic constitution. For the normal controls (NCs), we recruited right-handed people who matched the AD group in age and gender. The exclusion criteria were participates without Alzheimer's disease. The rest exclusion criteria for NCs were the same as those for AD patients.

The study was approved by the Anhui Medical University Ethics Committee, and all NCs and patients signed informed consent forms.

Process

A total of 60 patients with AD were recruited during the first phase of the study; 62 age- and gender-matched NCs were also recruited. All participants were given a complete set of cognitive assessment scales by professional clinicians to assess their cognitive abilities and clinical symptoms. The resting state fMRI data were used to analyze the functional relationships between different parts of the ECN. In the second phase of the study we conducted an intervention study. A total of 20 AD patients were included. Each participant needed to be treated once a day for two consecutive weeks. After the first assessment and completion of the MRI scan, the resting motor threshold (RMT) was measured (Schutter and van Honk, 2006). During the completion of treatment, all patients received a stable dose of donepezil. All patients received complete neuropsychological tests and multimodal MRI scans before receiving iTBS treatment and within 24 h after the last stimulation treatment.

Clinical Symptoms and Multi-Domain Cognition Assessments

The neuropsychology of the patients was assessed by a clinical investigator. The following neuropsychological test battery including the CDR, Global Deterioration Scale (GDS), Lawton-Brody Activities of Daily Living (ADL) scale, Montreal Cognitive Assessment (MoCA, Mandarin-version), Mini-mental State Examination (MMSE), AD8 scale and the Neuropsychiatric Inventory (NPI) were administered to evaluate whole cognitive function and clinical symptoms (Lezak et al., 2004). The CDR is a widely used multidimensional assessment of an individual's internal cognitive, behavioral, and functional decline, based on the individual's previously acquired abilities in these areas. The GDS is a set of staging methods developed by Reisberg et al. (1982) to assess the symptoms of AD. There were seven stages ranging from normal (no cognitive decline) to very severe cognitive decline. The scale was scored by interviewing patients and caregivers and was not objective. The higher the score, the more severe the symptoms. The CDR and GDS were used to grade the severity of AD and other dementias, which were widely used multidimensional assessment of an individual's internal cognitive, behavioral, and functional decline, based on the individual's previously acquired abilities in these areas (Reisberg et al., 1982; Morris, 1993). The ADL is mainly used to assess the daily living ability of the subjects. The AD8 is an assessment tool for rapid screening for cognitive abnormalities. The MMSE and MOCA were used to assess participants' overall cognitive function. The NPI scale is used to assess the mental and behavioral symptoms of dementia patients. Based on the caregiver's perception of the patient's behavior and perceived distress. The Hachinski Ischemic Scale (HIS) was mainly used for the differential diagnosis of Alzheimer's disease and vascular dementia. The severity of emotional symptoms in AD patients was evaluated by Hamilton Anxiety Scale and Hamilton Depression Scale. The Chinese version of the Auditory Verbal Learning Test (CAVLT, A/B), Clock-Drawing Test (CDT), Stroop test (Color/Word/Interference), Color Trail Test A/B (CTT A/B), Verbal Fluency Test (VFT) and Digital Span (forward/backward) were used to evaluate multiple cognitive domains. The Boston Naming Test (BNT) was used to investigate the ability of naming. Among them, CAVLT, Digital Span, and MMSE, A/B versions were adopted in the study and randomly used.

Transcranial Magnetic Stimulation Intervention

Personalization and Image Navigation Transcranial Magnetic Stimulation

Individualized and image-navigated TMS uses individual 3D-T1 images to develop individualized targets for the stimulation for each participant. The stimulus target was defined as a sphere of the brain area of interest with a radius of 10 mm centered on the Montreal Neurology Institute (MNI) coordinates (−38, 44, 26) in standard magnetic resonance space (Mir-Moghtadaei et al., 2015; Wang et al., 2020; Wu et al., 2021). SPM[1] were used to standardize and segment individualized magnetic resonance images and the TMS-target (Ji et al., 2017) to convert MNI coordinates to personalized TMS targets. The generated individualized stimulation targets and magnetic resonance images were all imported to the frameless navigation system (Visor 2.0). During stimulation, the same researcher placed the figure-eight MagStim coil under the navigation of Visor 2.0 and the connection point of the coil on the brain area of the stimulation target, which was a tangent to the skull, making the coil handle and the brain midline 45° angle oblique to the rear.

Intermittent θ Explosive Magnetic Stimulation

The parameters of iTBS were as follows: Resting Motor Threshold (RMT, more than 5 out of 10 consecutive stimuli can evoke the minimum motor evoked potential amplitude of the first dorsal extensor pollicis brevis muscle of >50 μV stimulus intensity) with a stimulation intensity of 70% (Schutter and van Honk, 2006). Each iTBS sequence released 600 pulses for a total of three sequences; each had an interval of 15 minutes and there were 1,800 pulse stimulations in total. For every 200 milliseconds,

[1]https://www.fil.ion.ucl.ac.uk/spm/software/spm8/

three pulses were continuously applied at a frequency of 50 Hz; each stimulation lasted for 2 s, with an interval of 8 s for rest, lasting for 192 s (Huang et al., 2005; Wang et al., 2020; Wu et al., 2020). The iTBS treatment was administered using a 70 mm air-cooled figure-of-eight coil and MagStim[2] stimulator. To prevent hearing damage during treatment, the participants wore earplugs, closed their eyes during the process and at rest, and maintained a comfortable sitting posture. Before, during, and after the treatment, additional dialog between the participants and the researcher was avoided; the participants were asked if they had any symptoms of discomfort after the stimulation.

Resting-State Functional Magnetic Resonance

Data Acquisition

The rs-fMRI image acquisition for all participants was mainly carried out at the Imaging Center of the University of Science and Technology of China, Hefei, Anhui Province. During the scan, all participants were asked not to fall asleep, close their eyes, not think about anything special, and keep their bodies still. A 3.0T MRI scanner (Discovery GE750w; GE Healthcare, Buckinghamshire, United Kingdom) composed of 217 echo plane imaging bodies was used for functional imaging. A total of 188 slices of T1-weighted anatomical images were acquired (voxel size = 1 mm × 1 mm × 1 mm; Repetition time = 8.16 ms; Echo time = 3.18 ms; flip angle = 12°; field of view = 256 mm × 256 mm; slice thickness = 1 mm). The parameters for rs-fMRI uses EPI scanning sequence were as follows (a total of 9,982 images were collected): Repetition time = 2,400 ms; slice thickness = 3 mm, Echo time = 30 ms, continuous slices = 46, voxel size = 3 mm × 3 mm × 3 mm), Flip angle = 90°, matrix size = 64 × 64, field of view = 192 mm × 192 mm.

rs-fMRI Preprocessing

We preprocess resting state functional magnetic resonance imaging data mainly using resting state functional magnetic resonance imaging toolkit (DPARSF) and SPM8[2](Chao-Gan and Yu-Feng, 2010). After deleting the first five volumes of data, the data was preprocessed, including slice time correction, head movement correction, spatial normalization, and smoothing. There was no significant difference in head movement between the two groups. And participants with a maximum displacement of 3 mm in any of the x, y, or z directions of head movement during the entire scan were excluded. We resampled the voxel size to 3 mm × 3 mm × 3 mm. Spatial normalization is performed using MNI's standard EPI template. A 4 mm full-width half-maximum Gaussian filter is used for spatial smoothing. The removal of physiological high-frequency noise and low-frequency drift is performed by linear detrending and time bandpass (0.01–0.08 Hz) filtering (Cordes et al., 2001). In order to eliminate the influence of interference covariates, we perform linear regression on head movement parameters, global average signal, brain white matter signal, and cerebrospinal fluid signal (Fox et al., 2009).

[2]www.fil.ion.ucl.ac.uk/spm/software/spm8

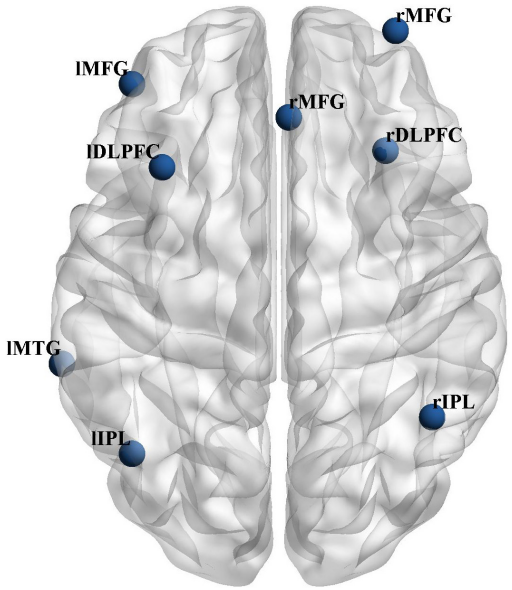

FIGURE 1 | Location of the bilateral ECN seeds.

Resting-State Functional Connection Analysis

The locations of these subdivided seeds are shown in **Figure 1**. To explore the abnormal functional connections and clusters between the ECN structures, five bilateral seed points were selected from the ECN, based on previous studies (Fox et al., 2009) (see **Supplementary Table 1**). Create a spherical seed point with a radius of 3.5-mm around each seed point coordinate (Kennis et al., 2015). The BOLD time series of voxels between the seed regions are averaged to generate the reference time series of the seed region for each seed region.

Statistical Analysis

The analysis was performed using SPSS23 (v 23.0, IBM, Armonk, NY, United States). Cross-sectional neuropsychological assessment data was statistically analyzed using the independent sample *t*-test, and the paired *t*-test was used to assess changes in neuropsychological assessment data before and after treatment. Pearson correlation analysis was used to do correlation analysis. The Fisher z-transform is used to normalize the correlation ROI signals. Individual z-signals was used for analysis. And the obtained test value was corrected using FDR. FDR correction is to correct each *p*-value and convert it to *q*-value. $q = p \times n/rank$, where rank refers to the order in which *p*-values are sorted from the smallest to the largest. The probability value $p < 0.05$ (two-tailed) was considered to be statistically significant.

RESULTS

Demographic and Clinical Information in Baseline

Participant demographic and clinical information are shown in **Table 1**. The average age and education (±standard

deviation) in years were 64.508 (±9.005) for AD/63.984 (±7.623) for NCs and 8.783 (±4.694) for AD/9.540 (±4.099) for NCs, respectively. Their Hakinski Ischemic Scale (HIS) scores were 1.117 ± 0.691; all were less than 4. There were no significant differences in gender, age, and education between the AD and control groups. In the AD group, the MMSE, MoCA, NPI, ADL, CDR, and GDS were worse than those of the same age group. According to the multidimensional cognitive assessment, the AD group performed significantly worse on tests that assessed memory (immediate recall, delayed recall, and recognition), sub-tests that assessed information processing (DS-F/B, Trail Making Test A/B, and Stroop interference Test), and tests that assessed language function (VFT) in **Table 1**.

Group Difference Within Executive Control Network in Baseline

The results of the seed point RSFC within the network between groups show that in the ECN, compared with the NCs, the functional connections in the network between left DLPFC and left IPL (t = 2.687, p = 0.008, FDR-corrected p = 0.045), left MFG and left IPL (t = 2.770, p = 0.007, FDR-corrected p = 0.045), left MFG and right IPL (t = 3.387, p = 0.001, FDR-corrected p = 0.012), left IPL and right IPL (t = 2.871,

TABLE 1 | The demographic and clinical characteristics and neuropsychological test results of the Alzheimer's Patients and normal controls in the cross-sectional study.

Variable	Alzheimer's patients [n = 60, means (SD)]	Healthy controls [textitn = 62, means (SD)]	χ^2/t	p-value
Demographic				
Gender (M/F)	26/34	26/36	0.024	0.876
Age (years)	64.508(9.005)	63.984(7.623)	0.350	0.727
Education (years)	8.783(4.694)	9.540(4.099)	–0.959	0.342
Clinical characteristics				
HIS	1.117(0.691)	0.968(0.567)	1.305	0.194
NPI-frequency * severity	11.086(12.9110)	0.063(0.504)	**6.498**	**<0.0001****
NPI-distress	4.069(5.057)	0.016(0.126)	**6.102**	**<0.0001****
ADL	31.103(11.243)	20.175(0.555)	**7.395**	**<0.0001****
CDR	1.026(0.581)	0.071(0.176)	**12.020**	**<0.0001****
GDS	3.828(0.704)	1.317(0.715)	**19.438**	**<0.0001****
Neuropsychological tests				
AD8	5.071(2.100)	0.952(1.223)	**11.479**	**<0.0001****
MMSE	18.000(6.250)	28.873(1.601)	**13.174**	**<0.0001****
MoCA	11.852(5.822)	25.444(3.605)	**15.572**	**<0.0001****
HAMA	4.733(4.153)	2.937(3.636)	**2.556**	**0.012***
HAMD	3.696(3.421)	2.952(3.381)	1.155	0.250
CDT	1.650(1.219)	3.902(0.436)	**–13.386**	**<0.0001****
Memory				
CAVLT - immediately	2.521(1.644)	8.851(1.775)	**–20.581**	**<0.0001****
CAVLT - delay	0.590(1.203)	9.778(2.661)	**–24.907**	**<0.0001****
CAVLT - recognition	10.295(4.112)	14.317(1.045)	**–7.411**	**<0.0001****
Attention				
digit span test(forward)	5.818(1.634)	6.968(1.576)	**–3.887**	**<0.0002*****
digit span test(backward)	3.127(1.187)	4.333(1.426)	**–5.013**	**<0.0001****
Executive function				
Stroop Color test	42.825(35.050)	21.537(6.402)	**4.197**	**<0.0001****
Stroop Word test	69.120(59.354)	30.304(10.147)	**4.526**	**<0.0001****
Stroop Interference test	99.169(83.708)	20.425(16.741)	**6.483**	**<0.0001****
Trail Making A	199.429(137.609)	70.482(23.389)	**6.008**	**<0.0001****
Trail Making B	372.821(245.119)	128.731(47.240)	**7.266**	**<0.0001****
Linguistic function				
VFT - animal	9.839(3.296)	17.206(3.802)	**–11.226**	**<0.0001****
BNT	16.426(4.817)	26.377(4.499)	**–11.051**	**<0.0001****

M, male; F, female; HIS, Hachinski Ischemic Scale; NPI, Neuropsychiatric Inventory; NA, not applicable; ADL, Lawton-Brody Activities of Daily Living; CDR, Clinical Dementia Rating; GDS, Global Deterioration Scale, MMSE, Mini-mental State Examination; MoCA, Montreal Cognitive Assessment Test; HAMA, Hamilton Anxiety Rating Scale; HAMD, Hamilton Depression Rating Scale; CDT, Clock Drawing Test; CAVLT, Chinese version of the Auditory Verbal Learning Test; VFT, Verbal Fluency Test; BNT, Boston Naming Test; [a]: Chi-squared test; [b]: Mann-Whitney U test; [c]: Independent sample T test.
**p < 0.05; **p < 0.01; ***p < 0.001; ****p < 0.0001.*

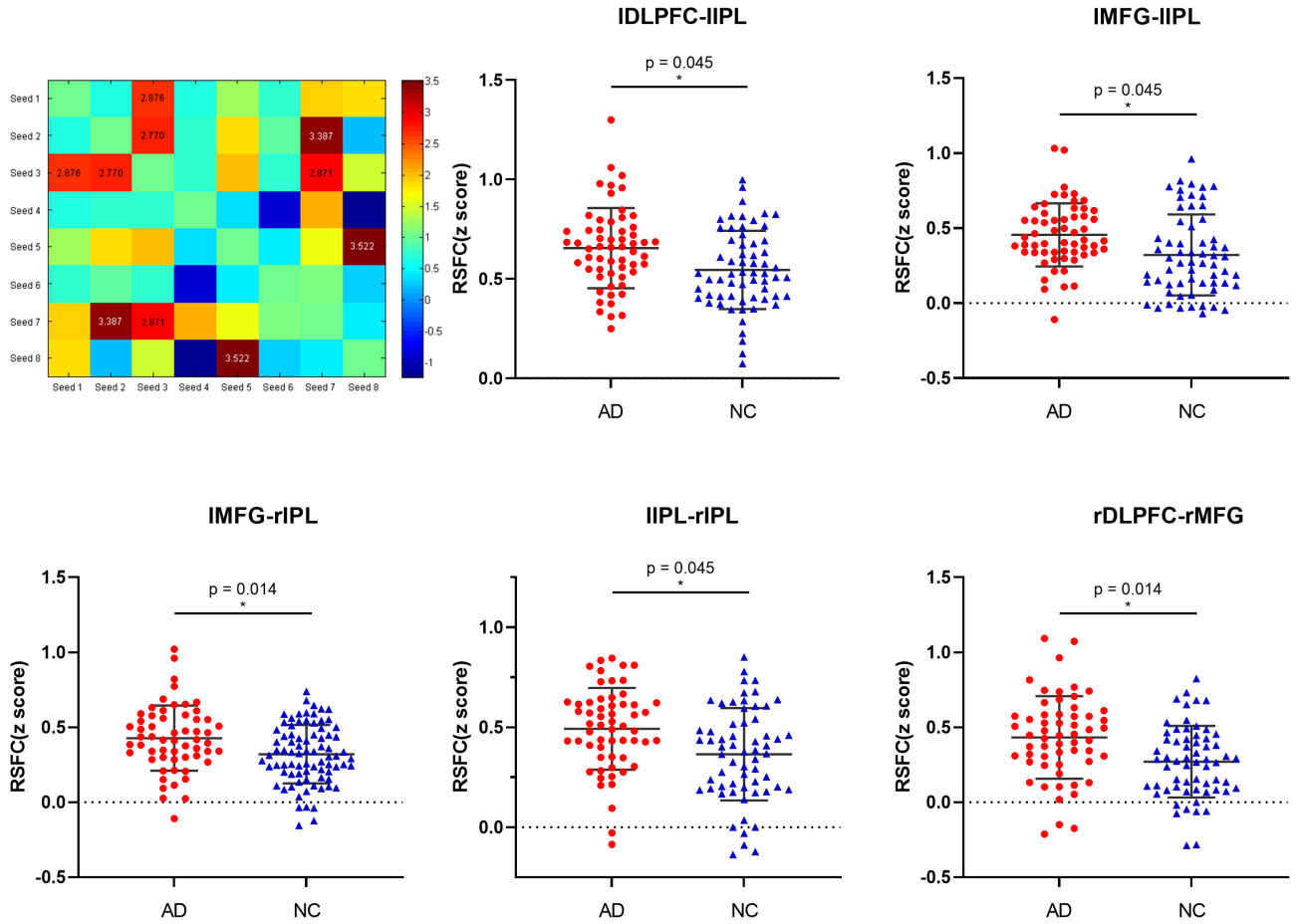

FIGURE 2 | The differences in resting-state functional connectivity (mean *Z*-value) within the bilateral ECN seeds between the AD patients and normal controls.

$p = 0.005$, FDR-corrected $p = 0.045$), right DLPFC and right MFG ($t = 3.522$, $p = 0.001$, FDR-corrected $p = 0.014$) was significantly increased in AD patients (see **Figure 2** and **Supplementary Table 2**). There was no significant difference in the functional connectivity of the resting state within the remaining network in the groups.

Correlation Analysis of Resting-State Functional Connection Within the Executive Control Network in Two Groups

The correlation analysis of RSFC within the bilateral seeds in the ECN showed that the strength of the functional connection in the ECN was significantly correlated with cognition, respectively. In AD group, correlation analysis shows that the functional connection strength between the left DLPFC and the right DLPFC was negatively correlated to VFT ($r = -0.272$, $p = 0.046$), and positively correlated with AD8 ($r = 463$, $p = 0.003$), GDS ($r = 0.323$, $p = 0.015$), and CTT-B ($r = 0.350$, $p = 0.039$). Correlation analysis in NC group shows that the functional connection strength between the left DLPFC and the left IPL is related to CAVLT-immediate ($r = -0.303$, $p = 0.017$), CAVLT-delay ($r = -0.310$, $p = 0.014$) and CTT-B ($r = -0.271$, $p = 0.045$) is negatively correlated. The analysis of the remaining cognition in each group was shown in **Table 2**.

Improvement of Clinical Symptoms Within the Executive Control Network of Alzheimer's Disease Patients After Intermittent Theta Burst Stimulation

It can be found that iTBS can significantly improve the overall cognitive function, daily function, mental behavioral symptoms, and multiple cognitive functions of AD patients ($P < 0.05$). The results show that iTBS can significantly improve the overall cognitive function of AD patients, including MoCA ($t = -5.229$, $p < 0.001$), MMSE ($t = -5.3449$, $p < 0.001$), CAVLT-immediately ($t = -4.129$, $p < 0.001$), CAVLT-delay ($t = -4.129$, $p < 0.001$), CAVLT-recognition ($t = -3.256$, $p = 0.004$) and BNT ($t = -3.685$, $p = 0.002$) significantly improved after stimulation. In addition, both the family members and caregivers of AD patients found a certain degree of improvement after iTBS treatment, which was reflected

in the score of the NPI-frequency × severity (t = 3.427, p = 0.003) and NPI-distress (t = 3.209, p = 0.005), as described in **Table 3**.

The Resting-State Functional Connection Changes Within the Executive Control Network and Correlation Analysis After Intermittent Theta Burst Stimulation

The cognitive function assessment and rs-fMRI imaging studies of a total of 20 patients were included in the study. One patient had a large head movement and was deleted from the analysis. Finally, the data of 19 patients were included in the analysis. The seed point-whole brain RSFC analysis showed that the strength of the functional connection between the left DLPFC and the left IPL (t = 4.271, p < 0.001, FDR-corrected p = 0.006) decreased significantly after treatment (see **Figure 3** and **Supplementary Table 3**). Correlation analysis showed that the improvement of GDS after iTBS stimulation was correlated with the changes in lDLPFC-lIPL strength in the ECN (r = −0.470, p = 0.042).

DISCUSSION

Our study found a significant cognitive decline in AD patients compared with normal controls, and RSFC analysis found enhanced functional connectivity of various seed points within the ECN, which was associated with cognitive function. Longitudinal analysis showed a significant increase in the MMSE, MoCA scores of patients with AD after 2 weeks of treatment. The improvements in the overall clinical neuropsychiatric symptoms, severity, and ability to live daily were observed during the pre-post phase. Cognitive performance across multi-domains improved significantly, especially on tests related to memory (CAVLT, MoCA, and VFT) and attention. In addition, this study revealed the underlying neural mechanism for iTBS related to improvement in the clinical symptoms of AD. This improvement was achieved by changing the functional connection between

TABLE 2 | Pearson correlation analysis of RSFC within the ECN after iTBS stimulation in AD patients and normal controls.

Alzheimer's patients (n = 60)				Normal controls (n = 62)			
Seed	**Neuropsycholo-gical test**	***R***	***p*-value**	**Seed**	**Neuropsycholo-gical test**	***R***	***p*-value**
Seed1-Seed5	AD8	0.463	0.003**	Seed1-Seed3	CAVLT- immediately	−0.303	0.017*
	GDS	0.323	0.015*		CAVLT-delay	−0.310	0.014*
	VFT	−0.272	0.046*		CTT-B	−0.271	0.045*
	CTT-B	0.350	0.039*	Seed1-Seed5	Stroop Color test	0.307	0.016*
Seed1-Seed6	HAMD	0.296	0.030*	Seed1-Seed6	CDT	−0.281	0.030*
Seed1-Seed8	CTT-B	0.524	0.001**	Seed1-Seed7	GDS	0.280	0.028*
Seed2-Seed6	CDT	−0.360	0.006**		CTT-B	0.294	0.029*
	HAMA	0.296	0.024*	Seed1-Seed8	CDT	−0.274	0.034*
	HAMD	0.389	0.004**	Seed2-Seed3	CTT-B	−0.280	0.038*
	NPI-frequency*severity	0.336	0.012*	Seed2-Seed5	VFT	0.258	0.199*
	VFT	−0.411	0.003**	Seed2-Seed6	NPI-frequency*severity	−0.315	0.013*
Seed3-Seed4	HAMA	0.294	0.025*		NPI-distress	−0.315	0.013*
	HAMD	0.301	0.027*	Seed3-Seed4	Stroop Word test	0.312	0.014*
	ADL	0.272	0.045*	Seed3-Seed5	Stroop Color test	0.256	0.047*
	DS(backward)	−0.274	0.047*	Seed3-Seed7	MMSE	0.300	0.018*
	BNT	−0.460	0.001**	Seed4-Seed7	AD8	0.279	0.028*
Seed3-Seed6	HAMA	0.276	0.036*		Stroop Word test	0.282	0.028*
	HAMD	0.378	0.005**	Seed4-Seed8	Stroop Word test	0.253	0.049*
Seed4-Seed5	DS(backward)	−0.292	0.034*	Seed6-Seed7	NPI-frequency*severity	−0.325	0.01*
Seed4-Seed6	HAMD	0.326	0.016*		NPI-distress	−0.325	0.01*
	NPI-frequency*severity	0.278	0.040*		Stroop Color test	0.307	0.016*
Seed5-Seed8	AD8	0.367	0.020*		Stroop Word test	0.344	0.007**
	VFT	−0.303	0.026*	Seed6-Seed8	Stroop Color test	0.298	0.02*
Seed7-Seed8	MMSE	0.336	0.010**		Stroop Word test	0.270	0.035*
	MoCA	0.270	0.040*	Seed7-Seed8	HAMD	−0.263	0.039*
	CAVLT-delay	0.285	0.030*				

NPI, Neuropsychiatric Inventory; NA, not applicable; ADL, Lawton-Brody Activities of Daily Living; GDS, Global Deterioration Scale, MMSE, Mini-mental State Examination; MoCA, Montreal Cognitive Assessment Test; HAMA, Hamilton Anxiety Rating Scale; HAMD, Hamilton Depression Rating Scale; CDT, Clock Drawing Test; CAVLT, Chinese version of the Auditory Verbal Learning Test; CTT, Color Trail Test; VFT, Verbal Fluency Test; DS, Digit Span test; BNT, Boston Naming Test.
**p < 0.05; **p < 0.01.*

the dorsolateral prefrontal lobe and the subparietal lobules in the executive control network. However, this study had no significant effect on CDR and GDS grading, the executive function (including Stroop Interference test and Trail Making A/B) and verbal fluent test.

The overall cognitive function of AD patients, including memory function, attention, executive function and language function, orientation function, computing function, and visual-spatial function, was impaired, which was consistent with the reports of previous studies (Binetti et al., 1996; Baudic et al., 2006; Hodges, 2006; Kirova et al., 2015). RSFC analysis showed that the functional connectivity of each network node in the ECN was abnormal. Compared with normal controls, the functional connectivities of the left DLPFC and left IPL; left IPL and left MFG; left IPL and right IPL; left IPL and right IPL; and right DLPFC and right MFG were enhanced in AD patients. This abnormal pattern of enhanced functional connectivity may be caused by compensatory functional effects in the brain of AD patients (Crosson et al., 2013). Compared with healthy controls, AD patients had impairments of memory, attention, and executive function, and the abnormality of functional connectivity was related to some cognitive subdomains, which may be related to the adjustment of the working memory, attention, thinking, logical reasoning, and other advanced cognitive functions (Zhao et al., 2005; Lantrip et al., 2017). Previous studies also found that the cross-network functional connection of the triple network model (ECN, default mode network, salience network) of AD patients was significantly impaired, and the interaction of the triple-network model was impaired, which may have led to the decline of cognitive function (Li et al., 2019).

The iTBS can significantly improve the overall cognitive function, the ability of daily living, and mental behavior symptoms of AD patients. This result is consistent with the reports of previous studies (Ahmed et al., 2012; Balconi and Ferrari, 2012; Chou et al., 2020). This may be because targeted left-DLPFC iTBS stimulation may have increased the excitability and function. The abnormality of the ECN of AD patients may

TABLE 3 | Improvement clinical characteristics and cognitive function after iTBS treatment in AD patients.

Variable	pre [*n* = 19, means (SD)]	post [*n* = 19, means (SD)]	*t*	*p*-value
Clinical characteristics				
NPI-frequency*severity	8.05(10.54)	3.16(5.81)	3.427	0.003**
NPI-distress	2.47(2.91)	1.31(1.91)	3.209	0.005**
ADL	29.10(8.59)	27.47(8.20)	3.759	0.001**
CDR	0.87(0.46)	0.81(0.48)	1.455	0.163
GDS	3.89(0.74)	3.63(0.76)	2.041	0.056
Neuropsychological tests				
MMSE	19.26(4.73)	21.58(5.75)	−5.349	< 0.0001****
MoCA	12.94(5.53)	15.68(6.53)	−5.229	< 0.0001****
HAMA	4.53(3.18)	2.84(2.31)	2.191	0.042*
HAMD	3.89(3.62)	1.53(2.17)	3.316	0.004**
CDT-4	1.42(0.84)	2.37(1.06)	−4.869	< 0.0001***
Memory				
CAVLT-immediately	2.69(2.18)	4.13(2.65)	−4.129	0.001**
CAVLT-delay	1.79(2.80)	3.53(3.93)	−3.124	0.006**
CAVLT-recognition	11.68(2.43)	13.05(2.15)	−3.256	0.004**
Attention				
digit span test(forward)	5.58(1.89)	6.21(1.68)	−2.721	0.014*
digit span test(backward)	3.26(1.59)	3.79(1.31)	−3.293	0.004**
Executive function				
Stroop Color test	44.38(28.51)	37.42(23.94)	2.304	0.034*
Stroop Word test	63.30(36.46)	54.57(31.32)	2.947	0.009**
Stroop Interference test	91.27(53.58)	81.28(50.48)	1.442	0.168
Trail Making A	245.95(180.38)	229.89(152.80)	1.430	0.170
Trail Making B	414.49(279.86)	399.52(268.05)	1.121	0.279
Linguistic function				
VFT-animal	9.47(4.13)	10.79(4.53)	−1.492	0.153
BNT	16.95(6.25)	19.58(5.98)	−3.685	0.002**

M, male; F, female; HIS, Hachinski Ischemic Scale; NPI, Neuropsychiatric Inventory; NA, not applicable; ADL, Lawton-Brody Activities of Daily Living; CDR, Clinical Dementia Rating; GDS, Global Deterioration Scale, MMSE, Mini-mental State Examination; MoCA, Montreal Cognitive Assessment Test; HAMA, Hamilton Anxiety Rating Scale; HAMD, Hamilton Depression Rating Scale; CDT, Clock Drawing Test; CAVLT, Chinese version of the Auditory Verbal Learning Test; VFT, Verbal Fluency Test; BNT, Boston Naming Test.

*$p < 0.05$; **$p < 0.01$; ***$p < 0.001$; ****$p < 0.0001$.

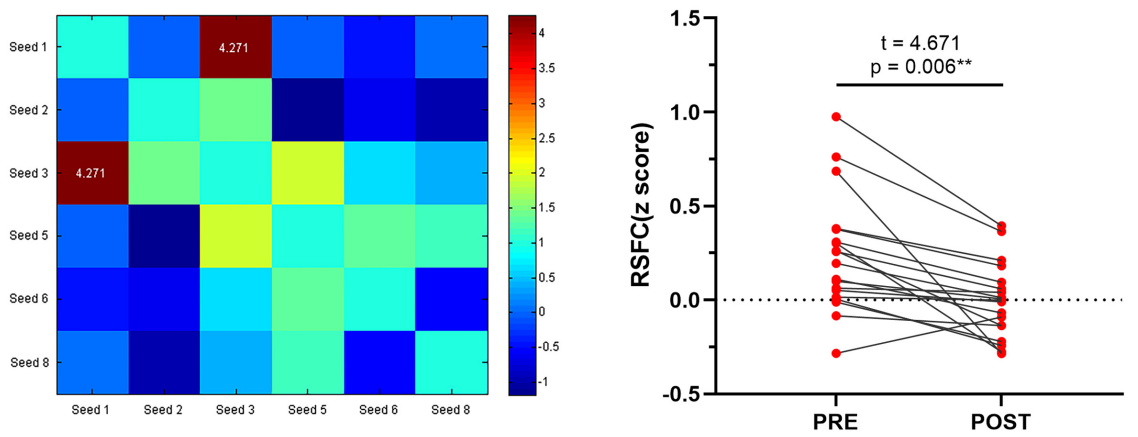

FIGURE 3 | Differences before and after iTBS treatment in the Alzheimer's Patients in the ECN.

be related to its function (Li et al., 2019). TMS is usually used to understand the function of a single brain area, but this ignores the fact that TMS may affect the network through network nodes (Cameron et al., 2020). Studies have found that TMS targeting of the left DLPFC can improve memories of young people and patients with healthy aging and affect network functions (Vidal-Pineiro et al., 2014; Wang et al., 2014; Nilakantan et al., 2017; Kim et al., 2018). As the core node of the executive control network (Seeley et al., 2007), our study showed that targeted stimulation of the left DLPFC may further affect the excitability of the ECN. The change of functional connectivity between the left DLPFC and left IPL within the ECN after stimulation was correlated with the improvement of GDS, which indicated that correcting the abnormalities in the executive control network may be related to the improvement of cognitive function (Dhanjal and Wise, 2014). A possible neurological explanation for the improvement of clinical symptoms in AD patients is that iTBS is designed to counteract maladaptive neuroplasticity and promote adaptive changes. Decreased activity in these areas may be due to iTBS-induced neural stimulants that show more efficient or less laborious processing at different levels (Koechlin and Summerfield, 2007). This hypothesis is consistent with the neural efficiency hypothesis, which holds that individuals with improved cognitive ability have lower cortical metabolic rates (Kar and Wright, 2014). This is supported by previous literature, which has shown that high-frequency iTBS of the left DLPFC may be a useful supplement for the treatment of AD.

There are still several deficiencies in this study. First, the sample size was small. Second, this study was carried out only based on the effectiveness results of previous studies without setting up a control group, which may be mixed with the practice effect. Therefore, future studies with a larger sample size and longer intervention duration and placebo control group are needed to further verify the conclusion of this study. The stimulus targets in this study were based on the conventional therapeutic targets used in our laboratory in the past (Wang et al., 2020; Wu et al., 2021). In future treatments, we can use the abnormally linked brain regions of the ECN obtained from the study as stimulus targets. In addition, future studies could use electroencephalogram techniques combined with MRI to further explore the relationship between changes in neural brain networks and behavioral outcomes during TMS, especially the effect of baseline neural activity characteristics on intervention outcomes.

In summary, this study suggests that the improvement of psychobehavioral symptoms and cognitive dysfunction in AD patients may be related to the changes of RSFC in different brain regions of bilateral ECN. Our study provided preliminary findings that pinpoint the effect of iTBS for the left DLPFC on the clinical symptoms and RSFC between the lDLPFC and lIPL of the ECN of AD patients. This discovery will facilitate the development of effective targeted-left DLPFC non-invasive interventions for the cognitive rehabilitation of patients with AD.

DATA AVAILABILITY STATEMENT

The raw data supporting the conclusions of this article will be made available by the authors, without undue reservation.

ETHICS STATEMENT

The studies involving human participants were reviewed and approved by the Anhui Medical University Ethics Committee, and all NCs and patients signed informed consent forms. The patients/participants provided their written informed consent to participate in this study. Written informed consent was obtained from the individual(s) for the publication of any potentially identifiable images or data included in this article.

AUTHOR CONTRIBUTIONS

All authors contributed significantly to, and approved, the content of this manuscript.

FUNDING

This study was supported by the Natural Science Foundation of China (grant numbers 82090034 to KW and 82101498 to XW), the National key Research and Development program of China (grant number 2016YFC1300604 to WL), the 2021 Youth Foundation Training Program of the First Affiliated Hospital of Anhui Medical University (no. 2021kj19).

SUPPLEMENTARY MATERIAL

The Supplementary Material for this article can be found online at: https://www.frontiersin.org/articles/10.3389/fnagi.2022.847223/full#supplementary-material

REFERENCES

Ahmed, M. A., Darwish, E. S., Khedr, E. M., El Serogy, Y. M., and Ali, A. M. (2012). Effects of low versus high frequencies of repetitive transcranial magnetic stimulation on cognitive function and cortical excitability in Alzheimer's dementia. *J. Neurol.* 259, 83–92. doi: 10.1007/s00415-011-6128-4

Balconi, M., and Ferrari, C. (2012). Emotional memory retrieval. rTMS stimulation on left DLPFC increases the positive memories. *Brain Imaging Behav.* 6, 454–461. doi: 10.1007/s11682-012-9163-6

Baudic, S., Barba, G. D., Thibaudet, M. C., Smagghe, A., Remy, P., and Traykov, L. (2006). Executive function deficits in early Alzheimer's disease and their relations with episodic memory. *Arch. Clin. Neuropsychol.* 21, 15–21. doi: 10.1016/j.acn.2005.07.002

Binetti, G., Magni, E., Padovani, A., Cappa, S. F., Bianchetti, A., and Trabucchi, M. (1996). Executive dysfunction in early Alzheimer's disease. *J. Neurol. Neurosurg. Psychiatry* 60, 91–93. doi: 10.1136/jnnp.60.1.91

Blennow, K., de Leon, M. J., and Zetterberg, H. (2006). Alzheimer's disease. *Lancet* 368, 387–403. doi: 10.1016/s0140-6736(06)69113-7

Brunoni, A. R., and Vanderhasselt, M. A. (2014). Working memory improvement with non-invasive brain stimulation of the dorsolateral prefrontal cortex: a systematic review and meta-analysis. *Brain Cogn.* 86, 1–9. doi: 10.1016/j.bandc.2014.01.008

Cai, S., Peng, Y., Chong, T., Zhang, Y., von Deneen, K. M., Huang, L., et al. (2017). Differentiated effective connectivity patterns of the executive control network in progressive MCI: a potential biomarker for predicting AD. *Curr. Alzheimer Res.* 14, 937–950. doi: 10.2174/1567205014666170309120200

Cameron, I. G. M., Cretu, A. L., Struik, F., and Toni, I. (2020). The Effects of a TMS double perturbation to a cortical network. *eNeuro* 7:ENEURO.0188-19.2019. doi: 10.1523/ENEURO.0188-19.2019

Cappon, D., Jahanshahi, M., and Bisiacchi, P. (2016). Value and efficacy of transcranial direct current stimulation in the cognitive rehabilitation: a critical review since 2000. *Front. Neurosci.* 10:157. doi: 10.3389/fnins.2016.00157

Chandra, A., Dervenoulas, G., Politis, M., and Neuroimaging, I. (2019). Magnetic resonance imaging in Alzheimer's disease and mild cognitive impairment. *J. Neurol.* 266, 1293–1302. doi: 10.1007/s00415-018-9016-3

Chao-Gan, Y., and Yu-Feng, Z. (2010). DPARSF: a MATLAB toolbox for "Pipeline" data analysis of resting-state fMRI. *Front. Syst. Neurosci.* 4:13. doi: 10.3389/fnsys.2010.00013

Chou, Y. H., Ton That, V., and Sundman, M. (2020). A systematic review and meta-analysis of rTMS effects on cognitive enhancement in mild cognitive impairment and Alzheimer's disease. *Neurobiol. Aging* 86, 1–10. doi: 10.1016/j.neurobiolaging.2019.08.020

Cordes, D., Haughton, V. M., Arfanakis, K., Carew, J. D., Turski, P. A., Moritz, C. H., et al. (2001). Frequencies contributing to functional connectivity in the cerebral cortex in "resting-state" data. *AJNR Am. J. Neuroradiol.* 22, 1326–1333.

Crosson, B. G. A., McGregor, K. M., Wierenga, C. E., and Meinzer, M. (2013). "The impact of aging on neural systems for language," in *Neuropsychology: Science and Practice*, eds S. Koffler, J. Morgan, I. S. Baron, and M. F. Greiffenstein (Oxford: Oxford University Press), 149–188.

Dhanjal, N. S., and Wise, R. J. (2014). Frontoparietal cognitive control of verbal memory recall in Alzheimer's disease. *Ann. Neurol.* 76, 241–251. doi: 10.1002/ana.24199

Fox, M. D., Zhang, D., Snyder, A. Z., and Raichle, M. E. (2009). The global signal and observed anticorrelated resting state brain networks. *J. Neurophysiol.* 101, 3270–3283. doi: 10.1152/jn.90777.2008

Godyn, J., Jonczyk, J., Panek, D., and Malawska, B. (2016). Therapeutic strategies for Alzheimer's disease in clinical trials. *Pharmacol. Rep.* 68, 127–138. doi: 10.1016/j.pharep.2015.07.006

Hodges, J. R. (2006). Alzheimer's centennial legacy: origins, landmarks and the current status of knowledge concerning cognitive aspects. *Brain* 129, 2811–2822. doi: 10.1093/brain/awl275

Huang, Y. Z., Edwards, M. J., Rounis, E., Bhatia, K. P., and Rothwell, J. C. (2005). Theta burst stimulation of the human motor cortex. *Neuron* 45, 201–206. doi: 10.1016/j.neuron.2004.12.033

Ji, G. J., Yu, F., Liao, W., and Wang, K. (2017). Dynamic aftereffects in supplementary motor network following inhibitory transcranial magnetic stimulation protocols. *Neuroimage* 149, 285–294. doi: 10.1016/j.neuroimage.2017.01.035

Jones, S. A., De Marco, M., Manca, R., Bell, S. M., Blackburn, D. J., Wilkinson, I. D., et al. (2019). Altered frontal and insular functional connectivity as pivotal mechanisms for apathy in Alzheimer's disease. *Cortex* 119, 100–110. doi: 10.1016/j.cortex.2019.04.008

Joo, S. H., Lim, H. K., and Lee, C. U. (2016). Three large-scale functional brain networks from resting-state functional MRI in subjects with different levels of cognitive impairment. *Psychiatry Investig.* 13, 1–7. doi: 10.4306/pi.2016.13.1.1

Kar, K., and Wright, J. (2014). Probing the mechanisms underlying the mitigation of cognitive aging with anodal transcranial direct current stimulation. *J. Neurophysiol.* 111, 1397–1399. doi: 10.1152/jn.00736.2013

Kaufman, L. D., Pratt, J., Levine, B., and Black, S. E. (2010). Antisaccades: a probe into the dorsolateral prefrontal cortex in Alzheimer's disease. a critical review. *J. Alzheimers Dis.* 19, 781–793. doi: 10.3233/JAD-2010-1275

Kennis, M., Rademaker, A. R., van Rooij, S. J., Kahn, R. S., and Geuze, E. (2015). Resting state functional connectivity of the anterior cingulate cortex in veterans with and without post-traumatic stress disorder. *Hum. Brain Mapp.* 36, 99–109. doi: 10.1002/hbm.22615

Kim, S., Nilakantan, A. S., Hermiller, M. S., Palumbo, R. T., VanHaerents, S., and Voss, J. L. (2018). Selective and coherent activity increases due to stimulation indicate functional distinctions between episodic memory networks. *Sci. Adv.* 4:eaar2768. doi: 10.1126/sciadv.aar2768

Kirova, A. M., Bays, R. B., and Lagalwar, S. (2015). Working memory and executive function decline across normal aging, mild cognitive impairment, and Alzheimer's disease. *Biomed Res. Int.* 2015:748212. doi: 10.1155/2015/748212

Koechlin, E., and Summerfield, C. (2007). An information theoretical approach to prefrontal executive function. *Trends Cogn. Sci.* 11, 229–235. doi: 10.1016/j.tics.2007.04.005

Kumar, S., Zomorrodi, R., Ghazala, Z., Goodman, M. S., Blumberger, D. M., Cheam, A., et al. (2017). Extent of dorsolateral prefrontal cortex plasticity and its association with working memory in patients with Alzheimer disease. *JAMA Psychiatry* 74, 1266–1274. doi: 10.1001/jamapsychiatry.2017.3292

Lantrip, C., Gunning, F. M., Flashman, L., Roth, R. M., and Holtzheimer, P. E. (2017). Effects of transcranial magnetic stimulation on the cognitive control of emotion: potential antidepressant mechanisms. *J. ECT* 33, 73–80. doi: 10.1097/YCT.0000000000000386

Lezak, M. D., Howieson, D. B., Loring, D. W., and Fischer, J. S. (2004). *Neuropsychological Assessment*, 4th Edn. Oxford: Oxford University Press.

Li, C., Li, Y., Zheng, L., Zhu, X., Shao, B., Fan, G., et al. (2019). Abnormal brain network connectivity in a triple-network model of Alzheimer's disease. *J. Alzheimers Dis.* 69, 237–252. doi: 10.3233/JAD-181097

Liu, G., Jiao, K., Zhong, Y., Hao, Z., Wang, C., Xu, H., et al. (2021). The alteration of cognitive function networks in remitted patients with major depressive disorder: an independent component analysis. *Behav. Brain Res.* 400:113018. doi: 10.1016/j.bbr.2020.113018

McKhann, G., Drachman, D., Folstein, M., Katzman, R., Price, D., and Stadlan, E. M. (1984). Clinical-diagnosis of Alzheimers disease report of the NINCADS-ADRDA work group under the auspices of department of health and human services task foecr on Alzheimers disease. *Neurology* 34, 939–944. doi: 10.1212/wnl.34.7.939

McKhann, G. M., Knopman, D. S., Chertkow, H., Hyman, B. T., Jack, C. R., Kawas, C. H., et al. (2011). The diagnosis of dementia due to Alzheimer's disease: recommendations from the national institute on Aging-Alzheimer's Association workgroups on diagnostic guidelines for Alzheimer's disease. *Alzheimers Dement.* 7, 263–269. doi: 10.1016/j.jalz.2011.03.005

Mielke, M. M., Leoutsakos, J. M., Corcoran, C. D., Green, R. C., Norton, M. C., Welsh-Bohmer, K. A., et al. (2012). Effects of food and drug administration-approved medications for Alzheimer's disease on clinical progression. *Alzheimers Dement.* 8, 180–187. doi: 10.1016/j.jalz.2011.02.011

Miniussi, C., and Rossini, P. M. (2011). Transcranial magnetic stimulation in cognitive rehabilitation. *Neuropsychol. Rehabil.* 21, 579–601. doi: 10.1080/09602011.2011.562689

Mir-Moghtadaei, A., Caballero, R., Fried, P., Fox, M. D., Lee, K., Giacobbe, P., et al. (2015). Concordance between BeamF3 and MRI-neuronavigated target sites for repetitive transcranial magnetic stimulation of the left dorsolateral prefrontal cortex. *Brain Stimul.* 8, 965–973. doi: 10.1016/j.brs.2015.05.008

Molteni, M., and Rossetti, C. (2017). Neurodegenerative diseases: the immunological perspective. *J. Neuroimmunol.* 313, 109–115. doi: 10.1016/j.jneuroim.2017.11.002

Morris, J. C. (1993). The clinical dementia rating (CDR): current version and scoring rules. *Neurology* 43, 2412–2414. doi: 10.1212/wnl.43.11.2412-a

Nilakantan, A. S., Bridge, D. J., Gagnon, E. P., VanHaerents, S. A., and Voss, J. L. (2017). Stimulation of the posterior cortical-hippocampal network enhances precision of memory recollection. *Curr. Biol.* 27, 465–470. doi: 10.1016/j.cub.2016.12.042

Nilakantan, A. S., Mesulam, M. M., Weintraub, S., Karp, E. L., VanHaerents, S., and Voss, J. L. (2019). Network-targeted stimulation engages neurobehavioral hallmarks of age-related memory decline. *Neurology* 92, e2349–e2354. doi: 10.1212/WNL.0000000000007502

Penolazzi, B., Bergamaschi, S., Pastore, M., Villani, D., Sartori, G., and Mondini, S. (2015). Transcranial direct current stimulation and cognitive training in the rehabilitation of Alzheimer disease: a case study. *Neuropsychol. Rehabil.* 25, 799–817. doi: 10.1080/09602011.2014.977301

Prince, M. G., and Matthew, P. (2018). *World Alzheimer Report*. London: Alzheimer's Disease International.

Puttaert, D., Coquelet, N., Wens, V., Peigneux, P., Fery, P., Rovai, A., et al. (2020). Alterations in resting-state network dynamics along the Alzheimer's disease continuum. *Sci. Rep.* 10:21990. doi: 10.1038/s41598-020-76201-3

Reisberg, B., Ferris, S. H., de Leon, M. J., and Crook, T. (1982). The Global Deterioration scale for assessment of primary degenerative dementia. *Am. J. Psychiatry* 139, 1136–1139. doi: 10.1176/ajp.139.9.1136

Schutter, D. J., and van Honk, J. (2006). A standardized motor threshold estimation procedure for transcranial magnetic stimulation research. *J. ECT* 22, 176–178. doi: 10.1097/01.yct.0000235924.60364.27

Seeley, W. W., Menon, V., Schatzberg, A. F., Keller, J., Glover, G. H., Kenna, H., et al. (2007). Dissociable intrinsic connectivity networks for salience processing and executive control. *J. Neurosci.* 27, 2349–2356. doi: 10.1523/JNEUROSCI.5587-06.2007

Shirer, W. R., Ryali, S., Rykhlevskaia, E., Menon, V., and Greicius, M. D. (2012). Decoding subject-driven cognitive states with whole-brain connectivity patterns. *Cereb. Cortex* 22, 158–165. doi: 10.1093/cercor/bhr099

Vidal-Pineiro, D., Martin-Trias, P., Arenaza-Urquijo, E. M., Sala-Llonch, R., Clemente, I. C., Mena-Sanchez, I., et al. (2014). Task-dependent activity and connectivity predict episodic memory network-based responses to brain stimulation in healthy aging. *Brain Stimul.* 7, 287–296. doi: 10.1016/j.brs.2013.12.016

Vincent, J. L., Kahn, I., Snyder, A. Z., Raichle, M. E., and Buckner, R. L. (2008). Evidence for a frontoparietal control system revealed by intrinsic functional connectivity. *J. Neurophysiol.* 100, 3328–3342. doi: 10.1152/jn.90355.2008

Wang, J. X., Rogers, L. M., Gross, E. Z., Ryals, A. J., Dokucu, M. E., Brandstatt, K. L., et al. (2014). Targeted enhancement of cortical-hippocampal brain networks and associative memory. *Science* 345, 1054–1057. doi: 10.1126/science.1252900

Wang, L., Chen, X., Wu, Y., He, K., Xu, F., Xiao, G., et al. (2020). Intermittent theta burst stimulation (iTBS) adjustment effects of schizophrenia: results from an exploratory outcome of a randomized double-blind controlled study. *Schizophr. Res.* 216, 550–553. doi: 10.1016/j.schres.2019.12.008

Wu, X., Ji, G. J., Geng, Z., Zhou, S., Yan, Y., Wei, L., et al. (2020). Strengthened theta-burst transcranial magnetic stimulation as an adjunctive treatment for Alzheimer's disease: an open-label pilot study. *Brain Stimul.* 13, 484–486. doi: 10.1016/j.brs.2019.12.020

Wu, X., Wang, L., Geng, Z., Wei, L., Yan, Y., Xie, C., et al. (2021). Improved cognitive promotion through accelerated magnetic stimulation. *eNeuro* 8:ENEURO.0392-20.2020. doi: 10.1523/eneuro.0392-20.2020

Zhao, M. G., Toyoda, H., Lee, Y. S., Wu, L. J., Ko, S. W., Zhang, X. H., et al. (2005). Roles of NMDA NR2B subtype receptor in prefrontal long-term potentiation and contextual fear memory. *Neuron* 47, 859–872. doi: 10.1016/j.neuron.2005.08.014

Zhao, Q., Lu, H., Metmer, H., Li, W. X. Y., and Lu, J. (2018). Evaluating functional connectivity of executive control network and frontoparietal network in Alzheimer's disease. *Brain Res.* 1678, 262–272. doi: 10.1016/j.brainres.2017.10.025

Zhao, Q., Sang, X., Metmer, H., Swati, Z., Lu, J., and NeuroImaging, I. (2019). Functional segregation of executive control network and frontoparietal network in Alzheimer's disease. *Cortex* 120, 36–48. doi: 10.1016/j.cortex.2019.04.026

Conflict of Interest: The authors declare that the research was conducted in the absence of any commercial or financial relationships that could be construed as a potential conflict of interest.

Publisher's Note: All claims expressed in this article are solely those of the authors and do not necessarily represent those of their affiliated organizations, or those of the publisher, the editors and the reviewers. Any product that may be evaluated in this article, or claim that may be made by its manufacturer, is not guaranteed or endorsed by the publisher.

frontiers in Aging Neuroscience

ORIGINAL RESEARCH
published: 30 March 2022
doi: 10.3389/fnagi.2022.879006

The Infraslow Frequency Oscillatory Transcranial Direct Current Stimulation Over the Left Dorsolateral Prefrontal Cortex Enhances Sustained Attention

Jingwen Qiao[1], Xinyu Li[2], Youhao Wang[1], Yifeng Wang[3], Gen Li[3], Ping Lu[3] and Shouyan Wang[1,4]**

[1] Academy for Engineering and Technology, Fudan University, Shanghai, China, [2] Department of Electronic Engineering, Fudan University, Shanghai, China, [3] Institute of Brain and Psychological Sciences, Sichuan Normal University, Chengdu, China, [4] Institute of Science and Technology for Brain-Inspired Intelligence, Fudan University, Shanghai, China

Background: The vigilance fluctuation and decrement of sustained attention have large detrimental consequences to most tasks in daily life, especially among the elderly. Non-invasive brain stimulations (e.g., transcranial direct current stimulation, tDCS) have been widely applied to improve sustained attention, however, with mixed results.

Objective: An infraslow frequency oscillatory tDCS approach was designed to improve sustained attention.

Methods: The infraslow frequency oscillatory tDCS (O-tDCS) over the left dorsolateral prefrontal cortex at 0.05 Hz was designed and compared with conventional tDCS (C-tDCS) to test whether this new protocol improves sustained attention more effectively. The sustained attention was evaluated by reaction time and accuracy.

Results: Compared with the C-tDCS and sham, the O-tDCS significantly enhanced sustained attention by increasing response accuracy, reducing response time, and its variability. These effects were predicted by the evoked oscillation of response time at the stimulation frequency.

Conclusion: Similar to previous studies, the modulation effect of C-tDCS on sustained attention is weak and unstable. In contrast, the O-tDCS effectively and systematically enhances sustained attention by optimizing vigilance fluctuation. The modulation effect of O-tDCS is probably driven by neural oscillations at the infraslow frequency range.

Keywords: infraslow frequency oscillatory tDCS, left dorsolateral prefrontal cortex, sustained attention, steady-state brain response, variability

OPEN ACCESS

Edited by:
Junhong Zhou,
Harvard Medical School,
United States

Reviewed by:
Dongning Su,
Capital Medical University, China
Zhu Liu,
Capital Medical University, China

****Correspondence:***
Shouyan Wang
shouyan@fudan.edu.cn
Yifeng Wang
wyf@sicnu.edu.cn

Specialty section:
This article was submitted to Neurocognitive Aging and Behavior, a section of the journal Frontiers in Aging Neuroscience

Received: *18 February 2022*
Accepted: *28 February 2022*
Published: *30 March 2022*

Citation:
Qiao J, Li X, Wang Y, Wang Y, Li G, Lu P and Wang S (2022) The Infraslow Frequency Oscillatory Transcranial Direct Current Stimulation Over the Left Dorsolateral Prefrontal Cortex Enhances Sustained Attention. Front. Aging Neurosci. 14:879006. doi: 10.3389/fnagi.2022.879006

INTRODUCTION

Sustained attention, the ability to maintain a goal-directed behavior for extended periods of time (Schouwenburg et al., 2021), is the key to most activities in daily life, such as driving vehicles, lifeguarding, as well as industrial and air traffic control. This capacity has been linked to the activation in brain cortical networks, especially the prefrontal regions (Brosnan et al., 2018). Aging and age-related disease often diminish the cortical activation, leading to diminished sustained

attention [e.g., the vigilance decrement and fluctuation (Brosnan et al., 2018; Esterman and Rothlein, 2019; Sharma et al., 2019)], altering the functional independence in older adults and those with mild cognitive impairment and Alzheimer's disease.

With the advancement of the neural modulation technique, recent studies have implemented the non-invasive brain stimulation technique, primarily the transcranial direct current stimulation (tDCS), to help restore sustained attention in older adults (Cruz and Fong, 2017; Brosnan et al., 2018; Indahlastari et al., 2021). Studies have shown that the tDCS targeting the dorsolateral prefrontal cortex (DLPFC) can help prevent the vigilance decrement during sustained attention tasks (Mcintire et al., 2014; Nelson et al., 2014). Using anodal stimulation over the right PFC, Brosnan et al. (2018), for example, observed a marginally significant tDCS effect on sustained attention tasks in older adults. However, other studies observed contradictory results. For example, Luna et al. (2020) exerted a high-definition tDCS over the right DLPFC and right posterior parietal cortex (PPC) while subjects doing attention tasks and found the brain stimulation mitigates the executive but not the arousal vigilance decrement. Some recent reviews and meta-analyses suggested that many factors, including but not limited to stimulation parameters, individual differences, learning effect, and task difficulty, are responsible for these inconsistent results (Reteig et al., 2017; Al-Shargie et al., 2019). These variances in the effect of tDCS on sustained attention suggested that more studies are needed to optimize the design of tDCS montage (i.e., current parameter and the stimulation protocols) for sustained attention (Al-Shargie et al., 2019), which may ultimately improve the efficacy of tDCS on sustained attention.

The attention fluctuates in the order of seconds to minutes (Esterman and Rothlein, 2019), which are independent of vigilance decrement (Esterman et al., 2014a). The time scale of attentional fluctuations is mainly situated in the infraslow frequency range (0.01–0.1 Hz) of the fluctuations of neural activity and behavioral performance, indicating the close links among neural, behavioral, and attentional fluctuations (Palva and Palva, 2012; Esterman and Rothlein, 2019). Therefore, using tDCS to modulate this infraslow frequency may hold great promise to enhance sustained attention, which, however, has not been examined.

In this study, we thus aimed to enhance sustained attention by modulating attentional fluctuations with infraslow-frequency-oscillatory tDCS (O-tDCS). We expected the O-tDCS to effectively modulate attentional fluctuations due to three reasons. First, the infraslow neural oscillations have been recorded in the thalamocortical circuit, which is closely associated with infraslow arousal fluctuations *via* neural networks and neurotransmitters (Hughes et al., 2011; Ballinger et al., 2016; Kobayashi et al., 2017). The high consistency of infraslow fluctuations among electrophysiological recordings and psychophysical time series during various kinds of continuous performance tasks (CPTs) was further demonstrated (Helps et al., 2010; Palva and Palva, 2012), suggesting that the infraslow fluctuations of behavioral performance are linked to neural activities. Second, the attention lapses in patients with attention deficit hyperactivity disorder fluctuated within the infraslow frequency range, especially around 0.05 Hz (Yordanova et al., 2011; Karalunas et al., 2013; Adamo et al., 2014), indicating that the infraslow frequency fluctuations are a potential intervention target of sustained attention. Third, the infraslow frequency task stimulations have been demonstrated to evoke strong steady-state brain responses (SSBRs) in cognitive-specific networks (Wang et al., 2016, 2018a, 2019a), implying that non-invasive brain stimulations within the infraslow frequency range could modulate neural fluctuations as well as associated behaviors. The above evidence indicated that the O-tDCS at a particular infraslow frequency (e.g., 0.05 Hz) may effectively enhance sustained attention.

Therefore, in this within-subject pilot study, we applied anodal 0.05 Hz (i.e., the potential target frequency of attention lapses) (Yordanova et al., 2011) O-tDCS over the left DLPFC (i.e., the core brain region pertaining to sustained attention and that has been widely used the target of traditional tDCS for enhancing the sustained attention) when performing the gradual-onset CPT (gradCPT). The gradCPT is a revised CPT with gradual transitions between stimuli, which can evaluate sustained attention processing with high reliability (Esterman et al., 2013). We hypothesized that as compared to controls (i.e., C-tDCS and sham), O-tDCS can significantly improve sustained attention as assessed by the performance of gradCPT, including attention focus and stability, inhibitory control, attention lapses, and infraslow fluctuations of behavioral performance.

MATERIALS AND METHODS

Subjects

A total of 21 healthy graduate students at Fudan University participated in this study (i.e., 11 men and 10 women, age: 26.47 ± 1.91 years). All subjects had no reported history of neurological or psychiatric disorders, had a normal or corrected-to-normal vision, with intact cognitive function as assessed by the total score of mini-mental state examination (MMSE) greater than 27, and were right-handed determined by the Edinburgh Handedness Inventory (Oldfield, 1971). Subjects were asked to avoid any intake of alcohol or caffeine for 24 h prior to testing. Written informed consent form was obtained prior to their participation in the study. The ethical approval of the study was granted by the School of Life Sciences, Fudan University.

Study Protocol

Each subject underwent three study visits consisting of the performance of gradCPTs before, during, and after receiving one session of either O-tDCS, C-tDCS, or sham stimulation. Each test lasted for 8 min and was successively conducted before, during the second half of the 20-min stimulation, and after stimulation. Each session lasted for about 40 min (**Figure 1A**). A questionnaire about tDCS side effects was filled in at the end of each session. Of note, these successive tests might trigger the practice effect or fatigue effect, reducing some experimental effects, e.g., vigilance decrement. Therefore, three stimulation conditions were conducted in a randomized order to balance the possible impact of practice effect or fatigue effect on stimulation conditions. Furthermore, these three visits were separated by at

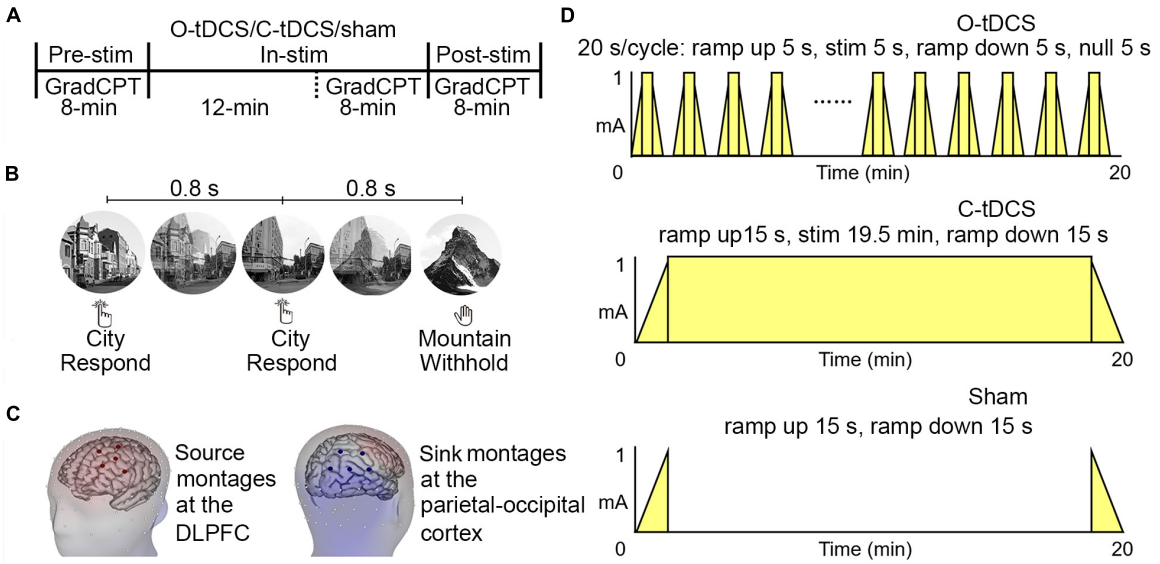

FIGURE 1 | The illustration of experimental procedure. **(A)** Stimulation procedure. Each stimulation condition consists of three phases, namely, pre-stim, in-stim, and post-stim. The gradual-onset continuous performance task (GradCPT) is performed once in each phase. **(B)** GradCPT program. The scenes were randomly presented with 90% city (i.e., the go stimulation) and 10% mountain (i.e., the no-go stimulation). The gradual transition of one image to another used the linear pixel-by-pixel interpolation, where the complete transition occurred over 800 ms. **(C)** Stimulation location. The source montages were placed over the left dorsal lateral prefrontal cortex (corresponding to AF3, F1, F3, F5, and FC3 of the 10–20 EEG system), while the sink montages were placed over the right-back of the head (corresponding to CP4, CP6, P2, P4, and PO4 of the 10–20 EEG system). **(D)** Stimulation protocol. Each stimulation condition lasts for 20 min with different patterns of ramp-up, stimulation, and ramp down.

least 72 h between each to eliminate the potential carryover effect of the prior stimulation. The participants were blinded to the type of tDCS. The C-tDCS and sham served as the active control condition and baseline condition, respectively.

The Gradual-Onset Continuous Performance Task

The gradCPT represents a unique combination of task features, in that, it requires frequent overt responses and removes abrupt stimulus onsets that may exogenously capture attention (Rosenberg et al., 2013). It was selected to measure sustained attention due to its very high reliability for both behavioral and neural measurements compared with other sustained attention tasks (Rosenberg et al., 2016). As shown in **Figure 1B**, stimuli in the gradCPT were round, grayscale photographs containing 10 mountain scenes and 10 city scenes. These scenes were randomly presented with 90% city (i.e., the go stimulation) and 10% mountain (i.e., the no-go stimulation), without allowing the identical scene to repeat on consecutive trials. The gradual transition of one image to another used the linear pixel-by-pixel interpolation, where the complete transition occurred over 800 ms. Participants were asked to press the space bar on the keyboard for each city scene but withhold their responses for mountain scenes. The reaction time (RT) was defined as the delayed time of response relative to the beginning (0%) of each image transition. The response accuracy was emphasized without reference to speed. However, given that the next image would replace the current image in 800 ms, a response deadline was implicit in the task (refer to RT analysis). The MATLAB software (MathWorks) and Psychophysics Toolbox (Brainard, 1997) were used to present stimuli and collect responses.

Transcranial Direct Current Stimulation Protocol

The tDCS was delivered with the 128-channel Geodesic Transcranial Electrical Neuromodulation (GTEN) system (Philips Neuro, Eugene, OR, United States). For the C-tDCS, the 1 mA total constant current was delivered for 20 min through five prefrontal source channels (the maximum current density was focused on the left DLPFC) to five sink channels, located at the parietal-occipital area (**Figure 1C**). Source/sink electrodes were positioned at the same location across three stimulation conditions. The time for ramping up and ramping down was 15 s at the beginning and end of the stimulation, respectively. For the O-tDCS, the stimulation current fluctuated between 0 and 1 mA, with 5 s on/5 s off periods, and rising and falling slopes of 5 s; thus, resulting in a 0.05 Hz oscillating stimulation, totally applied for 20 min. For the sham condition, no constant current was delivered except at the first and last 15 s, respectively (**Figure 1D**). To minimize sensation from the current injection, the Elefix conductive paste for the stimulating electrodes was mixed with a lidocaine solution for both stimulation and sham.

Reaction Time Analysis

The RTs were analyzed following previous studies about gradCPT (Esterman et al., 2013, 2014b). Since the RT was calculated relative to the beginning of each image transition, an RT of 800 ms indicates a button press at the moment an image was 100%

coherent and not mixed with the successive image. An RT shorter than 800 ms indicates that the current image was still in the process of transitioning from the previous, whereas an RT longer than 800 ms indicates that the current image was in the process of transitioning to the subsequent image. On rare trials with highly deviant RTs (before the 70% coherence of image n or after the 40% coherence of image n + 1) or multiple button presses, an iterative algorithm maximized correct responses as follows. First, the algorithm assigned unambiguous correct responses, leaving few ambiguous button presses (<5% of trials). Second, an ambiguous press was assigned to an adjacent trial if one of two successive trials had no response. If two successive trials had no response, the press was assigned to the closest trial, unless one was a no-go target, in which, case subjects were given the benefit of the doubt that they correctly omitted. Third, if there were multiple presses that could be assigned to any one trial, the fastest response was considered a valid response. Finally, if more than two successive trials had no response and some trials cannot be assigned with the proper response, the missing RTs to cities and mountains were filled up with the median of RTs of each type of scene (city or mountain) in each run, respectively. After those processes, the mean and standard deviation (SD) of RTs for each run were calculated. The lower mean and SD of RT represented higher attention focus and attention stability, respectively (Yamashita et al., 2021).

Accuracy Analysis

Trials in which participants responded to mountains were considered commission errors. The failure of response suppression to mountains reflects a lower inhibitory control level. Trials in which participants failed to respond to cities were considered omission errors, which is possibly due to the lack of attention focus or attention lapses (Egeland and Kovalik-Gran, 2010).

Vigilance Decrement

According to previous experience in parameter optimization (Esterman et al., 2013), vigilance decrements were calculated with a 2 min sliding window around performance measures of interest (i.e., commission error, omission error, RT_mean, and RT_SD), where the first window contained 0–2 min and the last contained 6–8 min. The window moved with a step of 1 trial. A linear slope (computed as the rate of change per minute) was then calculated for each run. Vigilance decrements were determined if slopes are larger than zero in one-sample *t*-tests.

Power Analysis

The time series of RTs in each run was transformed to the frequency domain with the fast Fourier transform (FFT) (Wang et al., 2016). The frequency resolution was 0.0021 Hz (sampling rate/sampled data: 1.25 Hz/600). The power spectrum of each run was obtained to test whether the O-tDCS evoked low-frequency behavioral oscillations.

Predictive Analysis

To evaluate whether the enhanced sustained attention was driven by the enhanced power of behavioral oscillations, we used the value of power at 0.05 Hz to predict other indicators of sustained attention. The leave-one-out approach was used to estimate the predicted value of each indicator of each subject. Indicators under the O-tDCS and sham conditions during stimulation were recruited in the linear regression model to construct the relationship between power at 0.05 Hz and the commission error, omission error, RT_mean, and RT_SD. The least-square method was used to determine the predicted values of commission error, omission error, RT_mean, and RT_SD.

Statistical Analysis

The three stimulation types (i.e., O-tDCS, C-tDCS, and sham) by three tests (i.e., pre-stim, in-stim, and post-stim) repeated measures analysis of variance (ANOVA) was performed on the power of each frequency point. The 3×3 ANOVA was also performed on remaining indicators, including the mean and SD of RTs, commission errors, omission errors, and slope. The *post hoc* analysis was conducted with the paired-sample *t*-test if there was a significant interaction between the stimulation type and test. Since predicted values were lower than observed values, Spearman's correlation was performed to test the relationship between observed values and predicted values of the commission error, omission error, RT_mean, and RT_SD (Rosenberg et al., 2016). The Greenhouse-Geisser correction was used if the equal variance was not assumed. Bonferroni's correction ($p < 0.05$) was used if there were multiple comparisons for each indicator.

RESULTS

All the subjects completed the assessments before and after the stimulation. No side effects or adverse events were reported.

The Oscillatory Transcranial Direct Current Stimulation Enhanced Inhibitory Control and Reduced Attention Lapses

As shown in **Figure 2A** and **Table 1**, significant main effects of stimulation and test as well as their interaction for commission errors were observed, suggesting that stimulations enhance inhibitory control. The *post hoc* analysis revealed significantly reduced commission errors by the O-tDCS than the C-tDCS [$t(20) = -2.727$, $p = 0.013$, Cohen's $d = -1.22$ for in-stim, $t(20) = -5.62$, $p < 0.001$, Cohen's $d = -2.513$ for post-stim] and sham [$t(20) = -5.555$, $p < 0.001$, Cohen's $d = -2.484$ for in-stim, $t(20) = -5.274$, $p < 0.001$, Cohen's $d = -2.359$ for post-stim] as well as marginally significant reduction of commission errors by the C-tDCS than sham [$t(20) = -2.159$, $p = 0.043$, Cohen's $d = -0.966$ for in-stim, $t(20) = -2.82$, $p = 0.011$, Cohen's $d = -1.261$ for post-stim]. Compared with pre-stim, the commission errors were reduced only by the O-tDCS under in-stim and post-stim [pre-stim vs. in-stim: $t(20) = 6.173$, $p < 0.001$, Cohen's $d = 2.761$; pre-stim vs. post-stim: $t(20) = 5.724$, $p < 0.001$, Cohen's $d = 2.56$].

Similarly, the main effect of stimulation and the interaction of stimulation by test for omission errors were significant (**Figure 2A** and **Table 1**), indicating that stimulations reduce attention lapses. The omission errors were reduced only by

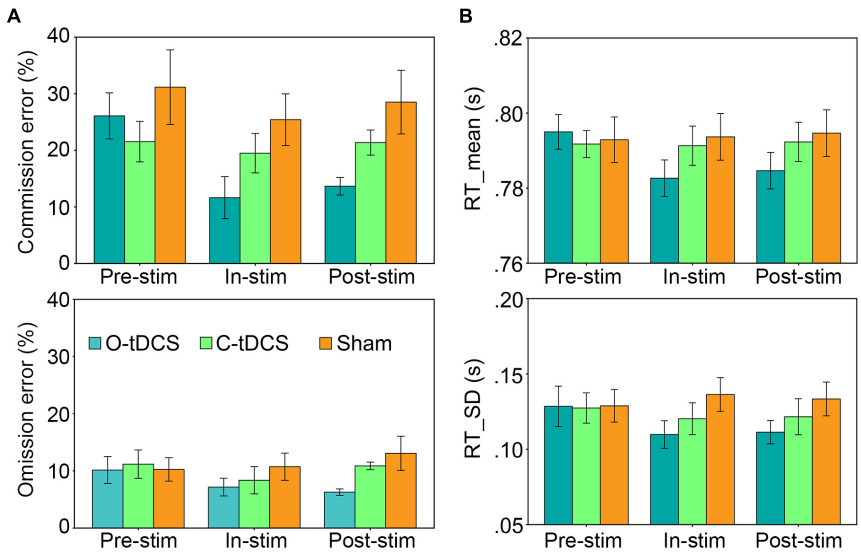

FIGURE 2 | The oscillatory transcranial direct current stimulation (O-tDCS) improved accuracy and reduced the mean and SD of reaction time (RT) under pre-stim, in-stim, and post-stim. **(A)** Accuracy. **(B)** RT. Error bars show the 95% confidence interval.

TABLE 1 | The ANOVA results for all indicators.

		Main effect of stimulation			Main effect of test			Interaction		
		F(2,40)	*P*	η_p^2	*F*(2,40)	*P*	η_p^2	*F*(4,80)	*P*	η_p^2
Commission error		21.318	<0.001	0.516	11.778	**<0.001**	0.371	4.781	**0.002**	0.193
Omission error		14.621	**<0.001**	0.422	2.460	0.098	0.110	3.971	**0.015**	0.166
RT	Mean	2.486	0.096	0.111	2.313	0.112	0.104	5.408	**0.001**	0.213
	SD	5.444	**0.008**	0.214	2.380	0.123	0.106	4.043	**0.005**	0.168
Commission error slope		1.444	0.248	0.067	1.981	0.151	0.090	2.032	0.121	0.092
Omission error slope		0.251	0.779	0.012	2.452	0.099	0.109	2.636	0.062	0.116
RT slope	Mean	0.689	0.508	0.033	4.034	**0.025**	0.168	1.145	0.341	0.054
	SD	0.691	0.507	0.033	1.067	0.353	0.051	0.980	0.423	0.047
Power at 0.05 Hz		4987.964	**<0.001**	0.996	1056.153	**<0.001**	0.981	1161.539	**<0.001**	0.983

The bold values means p < 0.05.

the O-tDCS compared with sham [$t(20) = -2.709$, $p = 0.014$, Cohen's $d = -1.212$ for in-stim, $t(20) = -4.68$, $p < 0.001$, Cohen's $d = -2.093$ for post-stim]. Compared with pre-stim, the omission errors were reduced only by the O-tDCS under in-stim [$t(20) = -2.439$, $p = 0.024$, Cohen's $d = -1.091$] and post-stim [$t(20) = -3.066$, $p = 0.006$, Cohen's $d = -1.371$].

Overall, the O-tDCS reduced both commission errors and omission errors than the C-tDCS and sham. The modulation effect of O-tDCS on commission errors and omission errors was even larger after stimulation than during stimulation. The commission errors and omission errors were lower under C-tDCS than under sham, but no significant difference was achieved.

The Oscillatory Transcranial Direct Current Stimulation Improved Attention Focus and Stability

Although there was only a significant main effect of stimulation for the SD of RT, the interaction of stimulation and test was significant for both mean and SD of RT (**Table 1** and **Figure 2B**), suggesting that stimulations improve attention focus and stability. The *post hoc* analysis showed that only the O-tDCS significantly reduced both the mean [$t(20) = -2.939$, $p = 0.008$, Cohen's $d = -1.314$ for in-stim, $t(20) = -2.672$, $p = 0.015$, Cohen's $d = -1.195$ for post-stim] and SD [$t(20) = -4.552$, $p < 0.001$, Cohen's $d = -2.036$ for in-stim, $t(20) = -3.296$, $p = 0.004$, Cohen's $d = -1.474$ for post-stim] of RT, while the C-tDCS reduced the SD [$t(20) = -2.222$, $p = 0.038$, Cohen's $d = -0.994$ for in-stim] of RT with marginal significance compared with that in sham. In contrast, only the O-tDCS reduced the mean and SD of RT under in-stim [$t(20) = -3.75$, $p = 0.001$, Cohen's $d = -1.677$ for mean, $t(20) = -3.334$, $p = 0.003$, Cohen's $d = -1.491$ for SD] and post-stim [$t(20) = -3.142$, $p = 0.005$, Cohen's $d = -1.405$ for mean, $t(20) = -2.894$, $p = 0.009$, Cohen's $d = -1.294$ for SD] compared with pre-stim.

There Was No Vigilance Decrement

There was no stimulation effect for the slope as all slope values were close to zero (mean = -0.002; ranged from −0.177 to 0.104). In other words, there was no vigilance decrement in this study. However, the sliding window analysis replicated the

aforementioned results about attention lapses, attention focus, attention stability, and inhibitory control that the O-tDCS reduced all accuracy and RT indicators under in-stim and post-stim (**Figure 3**), suggesting that the O-tDCS enhances sustained attention across the time of the whole task.

The Oscillatory Transcranial Direct Current Stimulation Enhanced the Power of Reaction Time Oscillations at the Stimulation Frequency

The O-tDCS evoked remarkable oscillations in the RT around the stimulation frequency. Significant interaction of stimulation and task was observed within 0.031–0.063 Hz, peaking at 0.05 Hz (**Figure 4A**). During stimulation, the power of RT oscillations at the stimulation frequency was tremendously enhanced by the O-tDCS more than 4 times of the C-tDCS [$t(20) = 76.45$, $p < 0.001$, Cohen's $d = 34.189$] and sham [$t(20) = 90.897$, $p < 0.001$, Cohen's $d = 40.65$], which reduced to about 3 times of the C-tDCS [$t(20) = 46.11$, $p < 0.001$, Cohen's $d = 20.621$] and sham [$t(20) = 48.676$, $p < 0.001$, Cohen's $d = 21.769$] after stimulation. Only the O-tDCS enhanced the power of RT oscillations at 0.05 Hz for in-stim [$t(20) = 70.699$, $p < 0.001$, Cohen's $d = 31.618$] and post-stim [$t(20) = 48.393$, $p < 0.001$, Cohen's $d = 21.642$] compared with pre-stim (**Figure 4B**).

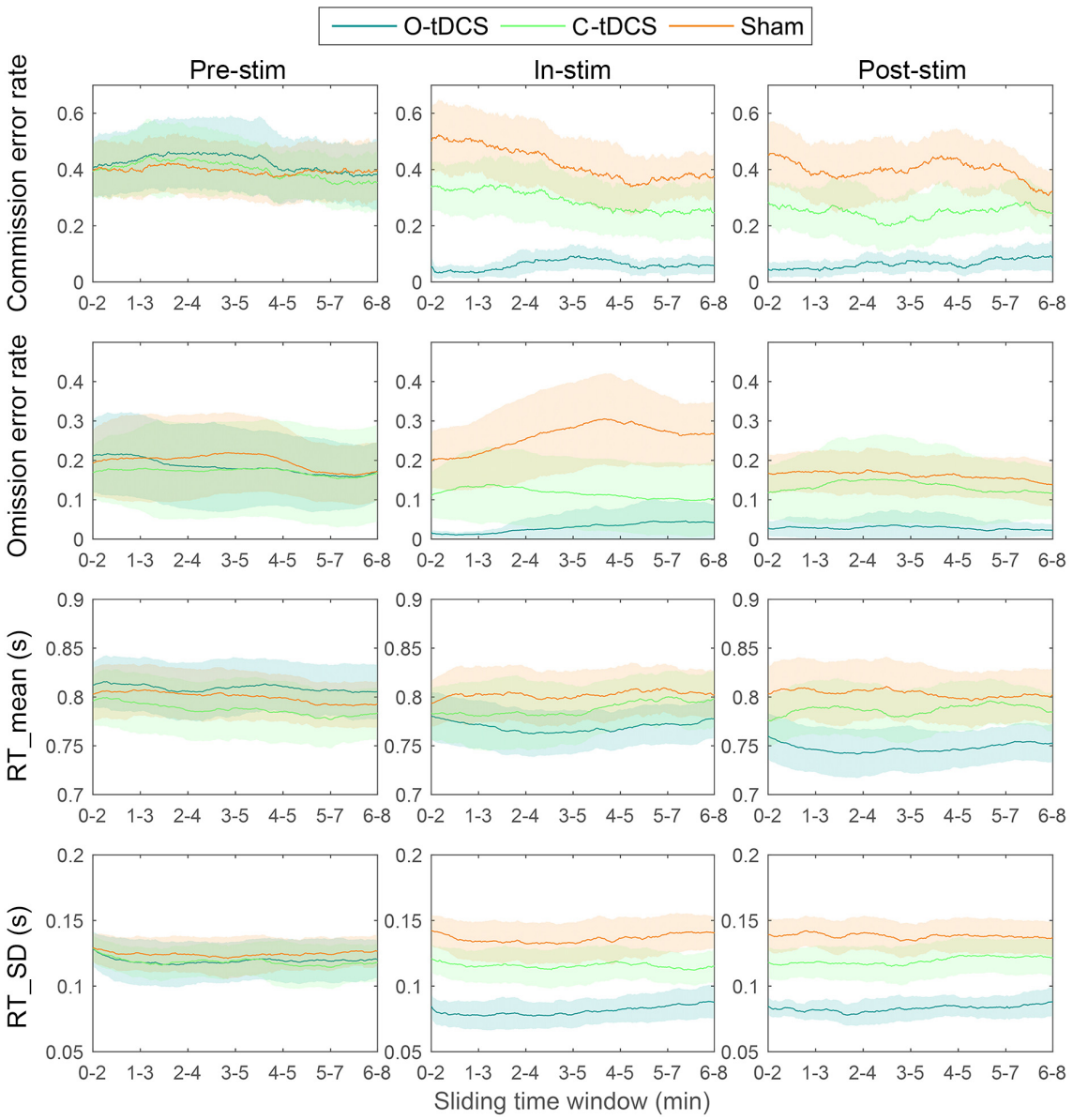

FIGURE 3 | The vigilance decrement effect. There was no vigilance decrement as well as stimulation and test effects indicated by the slope. Lines show the mean values. Shadows show the 95% confidence intervals.

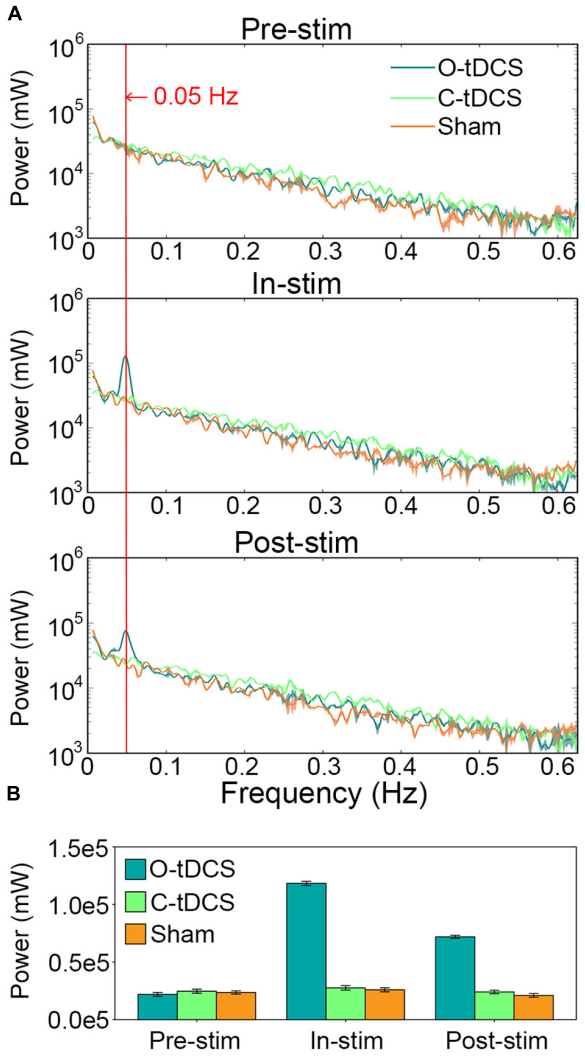

FIGURE 4 | The O-tDCS enhanced the power of RT oscillations at the stimulation frequency. **(A)** The power spectrum of RT fluctuations. **(B)** The power at 0.05 Hz. Lines and charts show the mean value of all subjects. Shadows and error bars show the 95% confidence intervals.

Further analysis revealed that the power at 0.05 Hz effectively predicted commission error, omission error, RT_mean, and RT_SD during stimulation. The correlations between observed values and predicted values were all significant [$r = 0.601$, $p < 0.001$ for commission error; $r = 0.516$, $p < 0.001$ for omission error; $r = 0.37$, $p = 0.016$ for RT_mean, and $r = 0.509$, $p = 0.001$ for RT_SD].

DISCUSSION

Based on the low-frequency SSBR and fluctuations of sustained attention, we designed a low-frequency O-tDCS to modulate sustained attention in normal young adults. The results of this pilot study suggested that compared with C-tDCS and sham, the O-tDCS hold great promise to enhance sustained attention, including inhibitory control, attention lapses, attention focus, and attention stability. The power of RT oscillations at the stimulation frequency (0.05 Hz) could predict these effects, suggesting that the low-frequency fluctuations may modulate the effect of O-tDCS on sustained attention. These observations indicate that the O-tDCS is a promising strategy to improve sustained attention.

Stimulation effects on the performance accuracy and RT supported the overload theory. The underload theory and overload theory are two main psychological theories about the mechanisms of sustained attention (Thomson et al., 2015). Both theories postulate that the total amount of available attentional resources is fixed over time, while resources required by task decrease over time. However, the underload theory proposes that people redirect resources to task-unrelated thoughts as time progresses due to the low requirement of resources of the simple and tedious CPT (Smallwood and Schooler, 2015). In contrast, the overload theory postulates that a large amount of resources is required by the CPT. Resources are drained by the task over time and are increasingly devoted to counter motor impulsivity (Caggiano and Parasuraman, 2004). The tDCS excites cortical activity, thus providing more available resources for completing cognitive tasks and challenging the basic hypothesis of the underload theory and overload theory (Chase et al., 2020). However, available resources are usually more than resources required by the task (Thomson et al., 2015). Those additional resources, therefore, may have minimal impact on the task, leading to no significant modulation effect of the C-tDCS on sustained attention. In contrast, the O-tDCS reduced attention lapses and improved attention focus and attention stability, indicating that it increases resources devoted to the task. Furthermore, the O-tDCS reduced inhibitory control, indicating that it increased resources directed toward motor impulsivity, in line with the overload theory (Thomson et al., 2015). Therefore, the effective modulation of sustained attention requires more resources devoted to specific aspects of the task.

Where are these resources come from? Power analysis revealed dramatically enhanced power of RT oscillations at the stimulation frequency. The enhanced power represents greater variability of psychophysical performance over time (Palva and Palva, 2012). Although the neural correlation was not detected, we assumed that the enhanced power was evoked by periodic oscillations of cortical excitability modulated by the O-tDCS (Chase et al., 2020) due to the consistency of brain activity and behavior performance demonstrated by SSBR studies (Wang et al., 2014, 2015, 2016, 2018a). Greater variability has been suggested to provide greater dynamic range and kinetic energy for the adaptability and efficiency of neural systems, allowing them to achieve a variety of possible states and operate in an optimal probabilistic Bayesian manner (Garrett et al., 2013; Wang et al., 2019b, 2020a). Considering that the O-tDCS operated within the frequency range of the intrinsic fluctuations of sustained attention (Castellanos et al., 2005; Palva and Palva, 2018) and the evoked power of RT oscillations could systematically predict sustained attention performances, it may suggest that the improved attention focus, attention stability,

attention lapses, and inhibitory control are associated with an optimized sustained attention system through the low-frequency resonance of neural excitability.

Although there are many factors that affect the effect of tDCS (Reteig et al., 2017; Al-Shargie et al., 2019), the O-tDCS significantly enhanced sustained attention in multiple aspects for almost all subjects compared with the C-tDCS and sham. These differences cannot be caused by task, subject, and learning factors due to the counterbalanced and perfectly matched design here. Therefore, we suggested that the oscillatory paradigm matters. Specifically, the intrinsic frequency of attentional fluctuations may provide a precise target for non-invasive brain stimulation. Considering that different brain and psychological functions have various frequency characteristics (Palva and Palva, 2018; Wang et al., 2020a), the O-tDCS in this frequency range may evoke the strongest resonance while eliminating noises and distractions at other frequencies (e.g., the modulation effect only appeared around the stimulation frequency). The strong effect and high signal-to-noise ratio may overwhelm a number of factors diminishing the effectiveness of tDCS. Due to a lack of neural recording, this hypothesis warrants further verification.

Some limitations and future directions should be noted. First, there was no modulation effect on vigilance decrements. Although vigilance decrements have been suggested to appear in the gradCPT (Esterman et al., 2013; Rosenberg et al., 2013), they were lack for all indicators and under all conditions in the current study, which may be caused by practice effect or fatigue effect in the within-subject design. In other words, these successive tests may keep subjects' vigilance at a lower level, so that there is no longer a vigilance decrement. Future studies should use the between-subject design to test how the O-tDCS separately influences the vigilance decrement and attention fluctuations. Second, the neural correlation of the modulation effect of O-tDCS on sustained attention has not been detected. Therefore, we cannot determine whether the O-tDCS truly optimizes the sustained attention network or generally optimizes cognitive-related networks because all the intrinsic brain networks operate in this frequency band (Achard et al., 2006; Thompson and Fransson, 2015; Wang et al., 2018b, 2020b). If the latter is true, the O-tDCS would enhance many other cognitions rather than limited in sustained attention. More cognition assessments were needed to test this hypothesis. Third, it was not clear how long this modulation effect lasts. The effect on omission error was even larger after stimulation than during stimulation while that on other indicators was reduced. It seems that the washout period for the O-tDCS effect lasts for at least 8–10 min and possibly longer than one day. However, the exact time of the washout period for the stimulation effect cannot be determined in this study and should be tested in future studies.

CONCLUSION

The O-tDCS effectively and systematically enhances sustained attention by modulating its main subcomponents. The modulation effect of O-tDCS is probably driven by neural oscillations at the infra-slow frequency range.

DATA AVAILABILITY STATEMENT

The raw data supporting the conclusions of this article will be made available by the authors, without undue reservation.

ETHICS STATEMENT

The studies involving human participants were reviewed and approved by Ethics Committee, School of Life Sciences, Fudan University. The patients/participants provided their written informed consent to participate in this study.

AUTHOR CONTRIBUTIONS

SW, YiW, and JQ were responsible for the design of the whole experiments. JQ, XL, YoW, GL, and PL carried out the experiments, data acquisition, and analysis. JQ completed the manuscript writing. All authors contributed to the article and approved the submitted version.

FUNDING

This research was supported by the National Special Program of China (No. 2021ZD0200400), Shanghai Municipal Science and Technology Major Project (No. 2018SHZDZX01), ZJ Lab, and Shanghai Center for Brain Science and Brain Inspired Technology, the National Natural Science Foundation of China (62177035), National Key R&D Program of China (No. 2018YFC1705800), Shanghai Municipal Science and Technology Major Project (No. 2021SHZDZX0103), and the 111 Project (No. B18015).

ACKNOWLEDGMENTS

We acknowledge the assistance of Han Zhang and Zijian Cheng for assistance related to experiments.

REFERENCES

Achard, S., Salvador, R., Whitcher, B., Suckling, J., and Bullmore, E. (2006). A resilient, low-frequency, small-world human brain functional network with highly connected association cortical hubs. *J. Neurosci.* 26, 63–72. doi: 10.1523/JNEUROSCI.3874-05.2006

Adamo, N., Martino, A. D., Esu, L., Petkova, E., Johnson, K., Kelly, S., et al. (2014). Increased response-time variability across different cognitive tasks in children with ADHD. *J. Atten. Disord.* 18, 434–446. doi: 10.1177/1087054712439419

Al-Shargie, F., Tariq, U., Mir, H., Alawar, H., Babiloni, F., and Al-Nashash, H. (2019). Vigilance decrement and enhancement techniques: a review. *Brain Sci.* 9:178. doi: 10.3390/brainsci9080178

Ballinger, E. C., Ananth, M., Talmage, D. A., and Role, L. W. (2016). Basal forebrain cholinergic circuits and signaling in cognition and cognitive decline. *Neuron* 91, 1199–1218. doi: 10.1016/j.neuron.2016.09.006

Brainard, D. H. (1997). The psychophysics toolbox. *Spat. Vis.* 10, 433–436.

Brosnan, M. B., Arvaneh, M., Harty, S., Maguire, T., O'CONNELL, R., Robertson, I. H., et al. (2018). Prefrontal modulation of visual processing and sustained attention in aging, a tDCS-EEG coregistration approach. *J. Cogn. Neurosci.* 30, 1630–1645. doi: 10.1162/jocn_a_01307

Caggiano, D. M., and Parasuraman, R. (2004). The role of memory representation in the vigilance decrement. *Psychon. Bull. Rev.* 11, 932–937. doi: 10.3758/BF03196724

Castellanos, F. X., Sonuga-Barke, E. J., Scheres, A., Di Martino, A., Hyde, C., and Walters, J. R. (2005). Varieties of attention-deficit/hyperactivity disorder-related intra-individual variability. *Biol. Psychiatry* 57, 1416–1423. doi: 10.1016/j.biopsych.2004.12.005

Chase, H. W., Boudewyn, M. A., Carter, C. S., and Phillips, M. L. (2020). Transcranial direct current stimulation: a roadmap for research, from mechanism of action to clinical implementation. *Mol. Psychiatry* 25, 397–407. doi: 10.1038/s41380-019-0499-9

Cruz, P., and Fong, K. (2017). Transcranial direct current stimulation on cognitive functions in older adults with mild cognitive impairment: a pilot study. *Asian J. Gerontol. Geriatr.* 12, 33–34.

Egeland, J., and Kovalik-Gran, I. (2010). Measuring several aspects of attention in one test: The factor structure of Conners's continuous performance test. *J. Atten. Disord.* 13, 339–346. doi: 10.1177/1087054708323019

Esterman, M., Noonan, S. K., Rosenberg, M., and Degutis, J. (2013). In the zone or zoning out? Tracking behavioral and neural fluctuations during sustained attention. *Cereb. Cortex* 23, 2712–2723. doi: 10.1093/cercor/bhs261

Esterman, M., Reagan, A., Liu, G., Turner, C., and Degutis, J. (2014a). Reward reveals dissociable aspects of sustained attention. *J. Exp. Psychol. Gen.* 143, 2287–2295. doi: 10.1037/xge0000019

Esterman, M., Rosenberg, M. D., and Noonan, S. K. (2014b). Intrinsic fluctuations in sustained attention and distractor processing. *J. Neurosci.* 34, 1724–1730. doi: 10.1523/JNEUROSCI.2658-13.2014

Esterman, M., and Rothlein, D. (2019). Models of sustained attention. *Curr. Opin. Psychol.* 29, 174–180. doi: 10.1016/j.copsyc.2019.03.005

Garrett, D. D., Kovacevic, N., Mcintosh, A. R., and Grady, C. L. (2013). The modulation of BOLD variability between cognitive states varies by age and processing speed. *Cereb. Cortex* 23, 684–693. doi: 10.1093/cercor/bhs055

Helps, S. K., Broyd, S. J., James, C. J., Karl, A., Chen, W., and Sonugabarke, E. J. (2010). Altered spontaneous low frequency brain activity in attention deficit/hyperactivity disorder. *Brain Res.* 1322, 134–143. doi: 10.1016/j.brainres.2010.01.057

Hughes, S. W., Lõrincz, M. L., Parri, H. R., and Crunelli, V. (2011). Infra-slow (< 0.1 Hz) oscillations in thalamic relay nuclei: basic mechanisms and significance to health and disease states. *Prog. Brain Res.* 193, 145–162. doi: 10.1016/B978-0-444-53839-0.00010-7

Indahlastari, A., Hardcastle, C., Albizu, A., Alvarez-Alvarado, S., Boutzoukas, E. M., Evangelista, N. D., et al. (2021). A systematic review and meta-analysis of transcranial direct current stimulation to remediate age-related cognitive decline in healthy older adults. *Neuropsychiatr. Dis. Treat.* 17, 971–990. doi: 10.2147/NDT.S259499

Karalunas, S. L., Huangpollock, C. L., and Nigg, J. T. (2013). Is reaction time variability in ADHD mainly at low frequencies? *J. Child Psychol. Psychiatry* 54, 536–544. doi: 10.1111/jcpp.12028

Kobayashi, T., Shimada, Y., Fujiwara, K., and Ikeguchi, T. (2017). Reproducing infra-slow oscillations with dopaminergic modulation. *Sci. Rep.* 7:2411. doi: 10.1038/s41598-017-02366-z

Luna, F. G., ROMáN-Caballero, R., Barttfeld, P., LUPIáñEZ, J., and MARTíN-ARéVALO, E. (2020). A high-definition tDCS and EEG study on attention and vigilance: brain stimulation mitigates the executive but not the arousal vigilance decrement. *Neuropsychologia* 142:107447. doi: 10.1016/j.neuropsychologia.2020.107447

Mcintire, L. K., Mckinley, R. A., Goodyear, C., and Nelson, J. (2014). A comparison of the effects of transcranial direct current stimulation and caffeine on vigilance and cognitive performance during extended wakefulness. *Brain Stimul.* 7, 499–507. doi: 10.1016/j.brs.2014.04.008

Nelson, J. T., Mckinley, R. A., Golob, E. J., Warm, J. S., and Parasuraman, R. (2014). Enhancing vigilance in operators with prefrontal cortex transcranial direct current stimulation (tDCS). *NeuroImage* 85, 909–917. doi: 10.1016/j.neuroimage.2012.11.061

Oldfield, R. C. (1971). The assessment and analysis of handedness: the Edinburgh inventory. *Neuropsychologia* 9, 97–113. doi: 10.1016/0028-3932(71)90067-4

Palva, J. M., and Palva, S. (2012). Infra-slow fluctuations in electrophysiological recordings, blood-oxygenation-level-dependent signals, and psychophysical time series. *NeuroImage* 62, 2201–2211. doi: 10.1016/j.neuroimage.2012.02.060

Palva, S., and Palva, J. M. (2018). Roles of brain criticality and multiscale oscillations in temporal predictions for sensorimotor processing. *Trends Neurosci.* 41, 729–743. doi: 10.1016/j.tins.2018.08.008

Reteig, L. C., Talsma, L. J., Van Schouwenburg, M. R., and Slagter, H. A. (2017). Transcranial electrical stimulation as a tool to enhance attention. *J. Cogn. Enhanc.* 1, 10–25. doi: 10.1007/s41465-017-0010-y

Rosenberg, M., Noonan, S., Degutis, J., and Esterman, M. (2013). Sustaining visual attention in the face of distraction: a novel gradual-onset continuous performance task. *Atten. Percept. Psycho.* 75, 426–435. doi: 10.3758/s13414-012-0413-x

Rosenberg, M. D., Finn, E. S., Scheinost, D., Papademetris, X., Shen, X., Constable, R. T., et al. (2016). A neuromarker of sustained attention from whole-brain functional connectivity. *Nat. Neurosci.* 19, 165–171. doi: 10.1038/nn.4179

Schouwenburg, M. R. V., Sligte, I. G., Giffin, M. R., GüNTHER, F., Koster, D., Spronkers, F. S., et al. (2021). Effects of midfrontal brain stimulation on sustained attention. *J. Cogn. Enhanc.* 5, 62–72. doi: 10.1007/s41465-020-00179-z

Sharma, N., Kolekar, M. H., Jha, K., and Kumar, Y. (2019). EEG and cognitive biomarkers based mild cognitive impairment diagnosis. *IRBM* 40, 113–121. doi: 10.1016/j.irbm.2018.11.007

Smallwood, J., and Schooler, J. W. (2015). The science of mind wandering: empirically navigating the stream of consciousness. *Annu. Rev. Psychol.* 66, 487–518. doi: 10.1146/annurev-psych-010814-015331

Thompson, W. H., and Fransson, P. (2015). The frequency dimension of fMRI dynamic connectivity: network connectivity, functional hubs and integration in the resting brain. *NeuroImage* 121, 227–242. doi: 10.1016/j.neuroimage.2015.07.022

Thomson, D. R., Besner, D., and Smilek, D. (2015). A resource-control account of sustained attention: evidence from mind-wandering and vigilance paradigms. *Perspect. Psychol. Sci.* 10, 82–96. doi: 10.1177/1745691614556681

Wang, Y., Ao, Y., Yang, Q., Liu, Y., Ouyang, Y., Jing, X., et al. (2020a). Spatial variability of low frequency brain signal differentiates brain states. *PLoS One* 15:e0242330. doi: 10.1371/journal.pone.0242330

Wang, Y., Chen, W., Ye, L., Biswal, B. B., Yang, X., Zou, Q., et al. (2018a). Multiscale energy reallocation during low-frequency steady-state brain response. *Human Brain Mapp.* 39, 2121–2132. doi: 10.1002/hbm.23992

Wang, Y., Huang, X., Yang, X., Yang, Q., Wang, X., Northoff, G., et al. (2019a). Low-frequency phase-locking of brain signals contribute to efficient face recognition. *Neuroscience* 422, 172–183. doi: 10.1016/j.neuroscience.2019.10.024

Wang, Y., Liu, F., Long, Z., Duan, X., Cui, Q., Yan, J., et al. (2014). Steady-state BOLD response modulates low frequency neural oscillations. *Sci. Rep.* 4:7376. doi: 10.1038/srep07376

Wang, Y., Wang, X., Ye, L., Yang, Q., Cui, Q., He, Z., et al. (2019b). Spatial complexity of brain signal is altered in patients with generalized anxiety disorder. *J. Affect. Disord.* 246, 387–393. doi: 10.1016/j.jad.2018.12.107

Wang, Y., Zhu, L., Zou, Q., Cui, Q., Liao, W., Duan, X., et al. (2018b). Frequency dependent hub role of the dorsal and ventral right anterior insula. *Neuroimage* 165, 112–117. doi: 10.1016/j.neuroimage.2017.10.004

Wang, Y., Zou, Q., Ao, Y., Liu, Y., Ouyang, Y., Wang, X., et al. (2020b). Frequency-dependent circuits anchored in the dorsal and ventral left anterior insula. *Sci. Rep.* 10:16394. doi: 10.1038/s41598-020-73192-z

Wang, Y.-F., Dai, G.-S., Liu, F., Long, Z.-L., Yan, J. H., and Chen, H.-F. (2015). Steady-state BOLD response to higher-order cognition modulates low frequency neural oscillations. *J. Cogn. Neurosci.* 27, 2406–2415. doi: 10.1162/jocn_a_00864

Wang, Y. F., Long, Z., Cui, Q., Liu, F., Jing, X. J., Chen, H., et al. (2016). Low frequency steady-state brain responses modulate large scale functional networks in a frequency-specific means. *Human Brain Mapp.* 37, 381–394. doi: 10.1002/hbm.23037

Yamashita, A., Rothlein, D., Kucyi, A., Valera, E. M., Germine, L., Wilmer, J., et al. (2021). Variable rather than extreme slow reaction times distinguish brain states during sustained attention. *Sci. Rep.* 11:14883. doi: 10.1038/s41598-021-94161-0

Yordanova, J., Albrecht, B., Uebel, H., Kirov, R., Banaschewski, T., Rothenberger, A., et al. (2011). Independent oscillatory patterns determine performance fluctuations in children with attention deficit/hyperactivity disorder. *Brain* 134, 1740–1750. doi: 10.1093/brain/awr107

Conflict of Interest: The authors declare that the research was conducted in the absence of any commercial or financial relationships that could be construed as a potential conflict of interest.

Publisher's Note: All claims expressed in this article are solely those of the authors and do not necessarily represent those of their affiliated organizations, or those of the publisher, the editors and the reviewers. Any product that may be evaluated in this article, or claim that may be made by its manufacturer, is not guaranteed or endorsed by the publisher.

frontiers | Frontiers in Aging Neuroscience

MINI REVIEW
published: 12 April 2022
doi: 10.3389/fnagi.2022.880897

Novel Non-invasive Transcranial Electrical Stimulation for Parkinson's Disease

*Rui Ni[1,2], Ye Yuan[1], Li Yang[1], Qiujian Meng[1], Ying Zhu[1], Yiya Zhong[2], Zhenqian Cao[1], Shengzhao Zhang[1], Wenjun Yao[3], Daping Lv[4], Xin Chen[4], Xianwen Chen[5] and Junjie Bu[1,6]**

[1] Department of Intelligent Medical Engineering, School of Biomedical Engineering, Anhui Medical University, Hefei, China, [2] Department of Life Sciences, Imperial College London, London, United Kingdom, [3] Department of Radiology, The Second Affiliated Hospital of Anhui Medical University, Hefei, China, [4] Department of Neurology, The Fourth Affiliated Hospital of Anhui Medical University, Hefei, China, [5] Department of Neurology, The First Affiliated Hospital of Anhui Medical University, Hefei, China, [6] Department of Neurosurgery, The Fourth Affiliated Hospital of Anhui Medical University, Hefei, China

OPEN ACCESS

Edited by:
Junhong Zhou,
Harvard Medical School,
United States

Reviewed by:
Shaoqiang Han,
First Affiliated Hospital of Zhengzhou University, China
Zongya Zhao,
Xinxiang Medical University, China

***Correspondence:**
Junjie Bu
bujunjie@ahmu.edu.cn

Specialty section:
This article was submitted to Parkinson's Disease and Aging-related Movement Disorders, a section of the journal Frontiers in Aging Neuroscience

Received: *22 February 2022*
Accepted: *15 March 2022*
Published: *12 April 2022*

Citation:
Ni R, Yuan Y, Yang L, Meng Q, Zhu Y, Zhong Y, Cao Z, Zhang S, Yao W, Lv D, Chen X, Chen X and Bu J (2022) Novel Non-invasive Transcranial Electrical Stimulation for Parkinson's Disease. Front. Aging Neurosci. 14:880897. doi: 10.3389/fnagi.2022.880897

Conventional transcranial electrical stimulation (tES) is a non-invasive method to modulate brain activity and has been extensively used in the treatment of Parkinson's disease (PD). Despite promising prospects, the efficacy of conventional tES in PD treatment is highly variable across different studies. Therefore, many have tried to optimize tES for an improved therapeutic efficacy by developing novel tES intervention strategies. Until now, these novel clinical interventions have not been discussed or reviewed in the context of PD therapy. In this review, we focused on the efficacy of these novel strategies in PD mitigation, classified them into three categories based on their distinct technical approach to circumvent conventional tES problems. The first category has novel stimulation modes to target different modulating mechanisms, expanding the rang of stimulation choices hence enabling the ability to modulate complex brain circuit or functional networks. The second category applies tES as a supplementary intervention for PD hence amplifies neurological or behavioral improvements. Lastly, the closed loop tES stimulation can provide self-adaptive individualized stimulation, which enables a more specialized intervention. In summary, these novel tES have validated potential in both alleviating PD symptoms and improving understanding of the pathophysiological mechanisms of PD. However, to assure wide clinical used of tES therapy for PD patients, further large-scale trials are required.

Keywords: transcranial electrical stimulation (tES), Parkinson's disease, closed loop stimulation, neuromodulation, non-invasive treatment

INTRODUCTION

Parkinson's disease (PD) is the second most common neurodegenerative disorder (Wirdefeldt et al., 2011). The diminishing number of pigmented dopaminergic neurons in the substantia nigra and the presence of Lewy bodies are the hallmarks of PD, resulting in both motor and cognitive impairments. The motor symptoms of PD typically include resting tremor, rigidity, and

stoop posture, while the non-motor symptoms involve defects in patients' memory and emotions, sometimes dementia (Beitz, 2014).

The most recent decades were marked by extensive research efforts in developing novel pharmacological and physical therapies to ameliorate symptoms of PD. Levodopa has been widely used in PD treatment and proved to be extremely effective in alleviating motor symptoms during early disease stages. Nevertheless, levodopa has fell short treating non-motor impairments, which are especially common during the late stages of PD (Fabbri et al., 2017). Furthermore, undesirable side effects and drug resistance accompanied by disease progression hindered levodopa efficacy (Nonnekes et al., 2016). Therefore, a pivotal objective of current tES studies is to develop potential therapeutic interventions to relieve both motor and non-motor symptoms.

Over the past decades various neuromodulation techniques have been trialed, including deep brain stimulation (DBS), transcranial magnetic stimulation (TMS), and transcranial electrical stimulation (tES). DBS has now been clinically tested in late-stage PD. However, DBS surgery involves implantation of electrodes into deep brain regions, with significant safety risk (Morishita et al., 2017). Non-invasive stimulation approaches such as TMS have the risk of activating facial muscles, which leads to unpleasant feelings and forestalls double blind clinical trials (Weber et al., 2014). In addition, TMS is relatively expensive and difficult to perform. In contrast, tES has been considered one of the most compelling PD interventions, not only because of its low cost but also because of its safety and ease of operation. tES is a non-invasive neuromodulation method by which a low-intensity current is applied over the subject's scalp, hence facilitating or inhibiting abnormal neuron activity (Ganguly et al., 2020). tES includes transcranial direct current stimulation (tDCS), transcranial alternating current stimulation (tACS), transcranial pulsed current stimulation (tPCS), and transcranial random noise stimulation (tRNS). Since Conventional tDCS is one of the earliest non-invasive neuromodulation methods clinically tested in PD patients, while other tES methods either lack clinical testing in human PD populations, or may not have been studied in the context of PD, therefore this review classify only tDCS that contains one target electrode (anode/cathode) and a return electrode (Nitsche and Paulus, 2000) as the conventional tES.

Although conventional tDCS has shown some encouraging results in alleviating both motor and non-motor symptoms (Boggio et al., 2006; Bueno et al., 2019), in practice, effects of conventional tES fluctuated across different studies (Doruk et al., 2014; Lau et al., 2019). In addition, tDCS is relatively less effective than other existing interventions for PD, and the improvements on symptoms bring by tDCS are highly dependent on the patients' condition. Therefore, in order achieve a promoted efficacy among large population of PD patients to be fully advantageous over other interventions, further development of tDCS is required. Here we present three possible reasons behind such inconsistent reports, each corresponding to a novel tES approach that tries to overcome this constraint.

Conventional tES might modulate the neuronal pathways that are not the main drivers of disease pathology or specific symptoms. Recently, the view that distinct pathologic pathways might be responsible for different PD symptoms has emerged. For example, PD symptoms can be recognized by impaired functional brain networks, which involve multiple brain regions (Boord et al., 2017). However, conventional tES is not able to adapt these novel pathology hypotheses, since it can only activate or suppress the activity of one specific brain region. Thus, novel tES modes target at different pathological pathways have been developed.

Additionally, improvements in behavior solely resulting from tES are often too subtle for accurate recording (Swank et al., 2016; Lau et al., 2019), therefore, some suggested that the cooperation of tES with other interventions might synergize and amplify the therapeutic effect by simultaneous modulating multiple pathways. It is also tempting to question whether the effects of tES would interact with other stimulations, serving as an accelerator of modulating efficiency.

Besides, tES efficacy highly depends on the subjects' condition and considerable discrepancies have been observed following identical stimulation inter or intra- subject. Therefore, the individualization of tES (e.g., closed-loop and brain-informed tES) is also gaining increasing interests owing to its "specialized to neuron response" characteristic. While conventional tDCS cannot automatically respond to these changes, novel stimulation approaches might give real-time individualized responses.

In this review, novel stimulation patterns are discussed and categorized into three groups: novel stimulation approaches, tES combination therapy with other interventions, and closed-loop stimulation. We will first discuss novel stimulation approaches with different modulation mechanisms toward PD. Then, the integrations of existing stimulation approaches with other types of PD intervention strategies will be introduced, and finally, we will analyze the closed-loop stimulation strategy that aims to achieve individualized self-adaptive parameters of stimulation. A detailed method and results of existing novel tES studies toward PD were summarized in **Table 1**.

NOVEL STIMULATION MODES

Conventional tDCS usually target at one specific brain region, thereby excite or inhibit the activity within that region. The most frequently targeted regions for tES in PD studies are summarized in **Table 2**. However, to enable the ability to modulate altered brain circuit or functional network found in PD patients, the invention of novel stimulation modes is required.

Multielectrode Transcranial Electrical Stimulation

Multielectrode tES is an improved version of tES with shared mechanism but multielectrode montages. Currently, multielectrode tES consists of multitarget tES and high-definition tES (hd-tES). Multitarget can modulate multiple regions of interest (Fischer et al., 2017), while hd-tES aims to achieve higher focality by minimizing the electrodes size and multiplying return electrodes (Datta et al., 2009). These two techniques are usually incorporated as a combination in experiments. In PD studies, up

TABLE 1 | The detailed method and results of existing novel tES studies toward PD.

References	Stimulation method	Subjects (*n*)	Electrode montage	Targeted brain regions	Study design for tES	Results
Novel stimulation modes						
Dagan et al. (2018)	Multitarget, hd tDCS	20 PD with FOG	According to the 10–20 EEG system **anodes:** Cz, F3 **cathodes:** AF4, CP1, FC1, FC5	M1 Left DLPFC	Placebo-controlled, double blind, crossover (M1 tDCS, multitarget tDCS, sham) 20 minutes each session	FOG provoking test score↑ gait speed TUG performance↑ accuracy of Stroop test↑
Manor et al. (2021)	Multitarget, hd tDCS	77 PD with FOG	According to the 10–20 EEG system **anodes:** Cz, F3 **cathodes:** AF4, CP1, FC1, FC5	M1 Left DLPFC	Sham-controlled, double-blinded, randomized, 5 sessions per week, 2 weeks then 1 session per week, 5 weeks. 20 minutes each session	FOG provoking test:no improvements Likert global impression scale↑ daily living step counts↑. Mild to moderate PD patients revealed greater improvement and showed reduction in time completing FOG provoking test.
Shill et al. (2011)	tACS	23 PD	**Stimulation electrode:** frontal **reference electrodes:** bilateral mastoids	PFC	Sham-controlled, double-blinded, randomized, 77.5 Hz, 15 mA, 5 continuous stimulation sessions, 2 days break, followed by another 5-day session. 45 min per day.	Total off-medication UPDRS I-III: no improvements
Guerra et al. (2021)	β tACS and γ tACS	18 PD, 16 healthy subjects	According to the 10–20 EEG system **stimulation electrode:** centered over the First dorsal interosseus hotspot **reference electrode:** Pz	**M1**	Placebo-controlled, double blind, crossover (20 Hz, 70 Hz, sham in a session; 2 sessions on and off medication) 1 mA tACS. Each session = 3 blocks 15 s of task under each stimulation per block+ 4 min each stimulation together with TMS	Patients on medication: movement velocity↓ movement amplitude during β tACS compared to γ tACS. short interval intracortical inhibition (SICI)↓ in patients than HS
Krause et al. (2013)	tACS	10 PD–MCI, 10 healthy subjects	**Stimulation electrode:** above the M1 hot spot **reference electrode:** supraorbital region contralateral to the stimulation electrode.	**M1**	Placebo-controlled, double blind, crossover (10 Hz, 20 Hz, sham) 1 mA, 15 min each session	**20 Hz tACS** : finger tapping amplitude variation↓ CMC amplitude↓
Alon et al. (2012)	tPCS+ treadmill	10 PD with FOG	**Positive electrode:** right M1 **reference electrode:** left supraorbital area.	**M1**	Sham-controlled, double-blinded, monophasic, both pulse duration and interpulse intervals are 33.3 μs. week 1 20 min tPCS, week 2 20 min treadmill walking, third week 20 min tPCS.	**tPCS session:** gait speed and amplitude↑, steps backward↓ **treadmill session:** forward step length↑ **tPCS + treadmill session**: steps forward ↓
Monastero et al. (2020)	tRNS	10 PD-MCI	**Stimulation electrode:** left M1 **reference electrode:** contralateral shoulder.	M1	Placebo-controlled, double blind, randomized, crossover (active tRNS, sham) 1.5 mA randomly oscillating between 100–600 Hz 15 min each session	UPDRS total↑ UPDRS lateralized right and left score↑
Stephani et al. (2011)	tRNS	8 non-tremor-dominant idiopathic PD	**Stimulation electrode:** hot spot representing the largest reproducible MEP-response of the contralateral ADM, **reference electrode**:contralateral supraorbital region	M1	Double blind, ± 600 μA, maximum 640 Hz, 10 min	Cortical excitability↓

(Continued)

TABLE 1 | (Continued)

References	Stimulation method	Subjects (*n*)	Electrode montage	Targeted brain regions	Study design for tES	Results
tES combined with other interventions						
Ferrucci et al. (2016)	hd tDCS with drug	9 PD with LIDs	According to EEG 10/20 system M1 tDCS: **stimulation electrode:** C3 and C4 **return electrode:** right deltoid muscle cerebellar tDCS: **stimulating electrode:** cerebellum **return electrode:** buccinator muscle	M1 cerebellar	Placebo-controlled, double blind, crossover (sham, cerebellar tDCS, M1 tDCS) 2 mA, 1 session per day, 5 continuous days, 20 min each session. Each condition at least 1 month separation.	UPDRS IV score↑
Chang et al. (2017)	tACS+ TMS	32 PD with FOG	According to EEG 10/20 system region for tACS **stimulation electrode:** F3 **reference electrode:** FP2	Left DLPFC	Placebo-controlled, double blind, randomized, 1 mA tACS, 1 session per day, 5 consecutive days, 20 min each session.	Executive function↑ in dual-mode PD subjects group compared to rTMS group
Guerra et al. (2020)	iTBS + tACS	16 PD, 16 healthy control	**Stimulating electrode:** centered over the first dorsal interosseus hotspot **reference electrode** :Pz	M1	Placebo-controlled, double blind, crossover (γtACS70 Hz,βtACS20 Hz, sham), 1 session per condition, approximately 3 mins and 30 s per session	iTBS-induced plasticity ↓in the iTBS-sham tACS session in patients, iTBS-γ tACS↑ abnormal plasticity, no long-lasting changes induced in M1 excitability
Kaski et al. (2014)	tDCS+ physical training	16 PD	**Stimulation electrode:** a region 10%–20% anterior to Cz as measured from the midline of the electrode **reference electrode:** inion	SMA	Sham-controlled, double blind, randomized,2 mA, physical training +tDCS and tDCS group, 15 min each group	tDCS+ physical training: gait speed↑ gait performance↑ TUG completing time↓ 6-minute walk test completing time↓ time needed to regain stability in pull test↓.
Conceição et al. (2021)	tDCS+ aerobic exercise	13 PD (only 7 analyzed)	According EGG 10–20 system **Anode**:F3/F4 (contralateral to most affected body side) **cathode:** FP2 or FP1 (contralateral to anode)	Personalized unilateral DLPFC	Placebo-controlled, double blind, cro20 min for each session,	Aerobic exercise + active-tDCS session: choice reaction time↓ step time variability↓ relative Hemoglobin levels in the stimulated hemisphere↓
Fernandez-Lago et al. (2017)	tDCS+ treadmill walking	18 PD	**Anode:** in the hotspot of the tibialis anterior muscle over motor cortex contralateral to the most affected body side **cathode:** supraorbital region contralateral to anode.	M1	Placebo-controlled, double blind, crossover (treadmill, treadmill+ active tDCS, treadmill+ sham tDCS) 2 mA, 20 min each session	No significant changes were found before and after under the tDCS+ treadmill condition.
Manenti et al. (2016)	tDCS+ physical training	20 PD-MCI	According to EGG 10–20 system **anode:** F3/F4 (contralateral to the most affected body side) **cathode:** FP2/FP1 (contralateral to the anode)	Personalized unilateral DLPFC	Placebo-controlled, double blind, randomized 2 mA tDCS per day 5 days per week 2 weeks	tDCS+ physical therapy: PD-CRS frontal-subcortical scale↑ PD-CRS total scale↑ and verbal fluency↑ PD-CRS frontal-subcortical scale and verbal fluency showed a long lasting effect of tDCS even 3 months after stimulation.
Del Felice et al. (2019)	tACS+ physical training	15 PD and 21 healthy subjects	**Stimulation electrode** : brain region where power spectral difference detected between patient and healthy controls, including FC1,FC5,C3,C4,F3,CP5 and PZ. **reference electrode:** ipsilateral mastoid	Personalized	Placebo-controlled, double blind, randomized, crossover (active tACS, sham) 1 mA minimum and 2 mA maximum in sinusoidal current relative β excess: 4 Hz; relative θ excess: 30 Hz, 30 min per day, 5 days per week, 2 weeks one session, with an 8 weeks separation between sessions.	Theta tACS stimulation showed bradykinesia item score↓ MOCA↑ only theta stimulation at right sensorimotor area and left frontal have additional neurophysiological changes: EEG frequencies↓

(Continued)

TABLE 1 | (Continued)

References	Stimulation method	Subjects (*n*)	Electrode montage	Targeted brain regions	Study design for tES	Results
Biundo et al. (2015)	tDCS+ computer training	24 PD-MCI	**Anode** :individual left DLPFC **cathode**: contralateral supraorbital region.	**Left DLPFC**	Placebo-controlled, double blind, crossover (active tDCS/sham tDCS) 20 min active/sham+10 min CT per day, 4 days per week, 4 weeks	**After 4 weeks of stimulation**: attention ↓ execution functions ↓ **at week 16**: story learning test ↑ immediate memory index↑
Lawrence et al. (2018)	tDCS+ computer training	38 PD-MCI	According to EEG 10/20 system region **anode:** F3 **cathode:** FP2	**Left DLPFC**	Controlled, double blind, randomized 1.5 mA, once a week, 4 weeks, 20 min per session.	**Standard Computer training+ tDCS:** executive function↑ attention/working memory↑ memory↑ language↑ activities of daily living↑ **tailored computer training+ tDCS**: executive function↑ memory↑ language↑ **tDCS:** attention/working memory↑ memory↑
Closed loop tES						
Brittain et al. (2013)	tACS	14 tremor-dominant Parkinson's disease	**Stimulation electrode**: hotspot of contralateral motor region for the most pronounced tremor muscles in the most affected upper limb **reference electrode**: shoulder contralateral to the stimulation electrode	M1	Placebo-controlled, double blind, crossover (tACS with nearest tremor frequency, tACS with double tremor frequency, sham) 10 min, 2 mA	Tremor amplitude depends on the phase alignment between tACS and tremor signals Individualized closed loop tACS: 42% ↓ in rest tremor.

↑, increase; ↓, decrease.
M1: primary motor cortex; DLPFC: dorsal lateral prefrontal cortex; PFC: prefrontal cortex; SMA: supplementary motor area; TUG: Timed Up & Go test; FOG: freezing of gait; PD-CRS: The Parkinson's Disease-Cognitive Rating Scale; HHB: hemoglobin.

TABLE 2 | Frequently targeted brain regions for tES in Parkinson's disease.

Brain cortex	Position in 10–20 EEG system	Reasons for targeting
Primary motor cortex (M1) (Boggio et al., 2006; Fregni et al., 2006; Dagan et al., 2018)	C3(left), C4(right), CZ	Motor: planning and execution of movement, dysfunction of M1 was found in PD (Ridding et al., 1995)
Bilateral dorsal lateral prefrontal cortex (DLPFC) (Pereira et al., 2013)	F4 (right), F3(left)	Cognitive: execution function, impaired function of rDLPFC was found in PD (Li et al., 2016; Cai et al., 2021)
Supplementary motor area (sma) (Costa-Ribeiro et al., 2017; Kami et al., 2018; Sadler et al., 2021)	FCz	Motor: planning and execution of movement, connected to diverse cortical or subcortical brain regions (Liotti et al., 2003; Mure et al., 2012)
Pre supplementary motor are(pre-SMA) (Lohse et al., 2020)	Fz	Cognitive: execution function, connected to diverse cortical and subcortical regions (Gan et al., 2020; Nakamura et al., 2001)
Cerebellum (Workman et al., 2020)	Approximately in O1, O2, Oz	Sensorimotor and cognitive function, abnormal activity in PD (Rascol et al., 1997; Yu et al., 2007)
Sensorimotor are(SM) (Ishikuro et al., 2018; Del Felice et al., 2019)	CZ,T7, C3, P7 and P3 T8, C4, P8 and P4	Both cognitive and motor: integration of sensory and motor, controls movement. Impaired function in PD (Bagnato et al., 2006)

to date, only multitarget tDCS and hd-tDCS have been tested in clinical population.

Freezing of gait (FOG) is a characteristic symptom in PD patients and is usually seen as a target disability in PD tES studies. Stemming from both cognitive (failed at decision making) and motor impairments (failed at action) (Nutt et al., 2011), early FOG tDCS studies either targeted on M1 or left dorsolateral prefrontal cortex (lDLPFC) (Rektorova et al., 2007), with M1 stimulation aiming to alleviate FOG through motor improvements, while lDLPFC stimulation used against cognitive defects. Since both stimulation montages seemingly harvested promising results, Dagan et al. assumed that an optimized tES paradigm for FOG should improve motor and cognition at the same time. Using hd multitarget tDCS, both M1 and lDLPFC were selected. In this double-blind crossover trial, each PD FOG patient had undergone all three conditions: single

target (M1) stimulation, dual-target stimulation, and sham. Subjects received 20 min of stimulation for each session with an average electric field strength of 0.25 V/m in the targeted area(s). hd-tDCS targeted at either the DLPFC or M1 was proven to be non-effective, while multitarget hd-tDCS exhibited a significantly improved gait speed and accuracy of the Stroop test (Dagan et al., 2018).

However, skepticism still exists in the assumption that multitarget tDCS would improve FOG performance, as a subsequent clinical trial with a subject population of 70 PD patients revealed the opposite results. After 2 weeks of intense treatment containing 10 stimulation sessions and 5 weeks of mild treatment with 5 stimulation sessions, despite some secondary performance improvements, no significant differences in FOG provoking test and FOG severity score were found (Manor et al., 2021).

In addition, the abovementioned studies did not assess the changes in functional connectivity. It is now generally accepted that the brain consists of many functionally connected networks. The communications and interplays among brain regions are fundamental for complex behaviors (Van Den Heuvel and Pol, 2010). Multitarget hd-tDCS provide the possibility to modulate brain networks, and has proven to be effective in modulating communications between brain regions (Yaqub et al., 2018). PD patients posed reduced functional connectivity in multiple brain networks, such as the default mode network and sensorimotor network (Ruan et al., 2020), therefore, further exploration and modulation of functional networks using multitarget hd-tDCS prove to be an efficient solution.

Transcranial Alternating Current Stimulation

Transcranial alternating current stimulation provides a sinusoidal external current stimulation that could either synchronize or desynchronize with the internal cortical rhythm (Antal and Paulus, 2013). Dissimilar to tDCS, tACS has more viable parameters, such as amplitude, frequency, and phase. Hence, tACS is capable of specifically correcting natural brain oscillations back to normal.

Parkinson's disease patients suffer from pathological changes in internal brain oscillation frequency ranges. Higher theta (4–8 Hz), delta (less than 4 Hz) activities and lower alpha (8–12 Hz), beta (12–30 Hz) activities in the basal ganglia were detected in PD patients (Soikkeli et al., 1991). Additionally, PD patients also exhibit a reduced power of gamma band (25–140 Hz) oscillation (Crone et al., 1998) as well as deviated task-specific neuronal oscillation activity (Possti et al., 2021).

One of the earliest experiments applying tACS toward PD used 77.5 Hz 15 mA current, with the stimulation electrode placed over the forehead and references at mastoids. The total off-medication Unified Parkinson's Disease motor rating scale (UPDRS) of this experiment exhibited no significant difference in scores between early PD patients and sham patients (Shill et al., 2011). Nevertheless, later tACS PD studies have applied more reasonable parameters and successfully improved subjects' behavior. Del Felice et al. constructed a study that considered the baseline neuron activity that fluctuated in different individuals. By comparing PD patients with healthy controls, PD subjects were divided into two experimental groups. If PD subjects had higher relative power than healthy subjects in the range of fast frequencies (i.e., beta waves), tACS was set at 4 Hz. If they had excessive slow frequencies (i.e., theta wave), the tACS frequency was set in the fast frequency range at 30 Hz. Theta stimulation resulted in bradykinesia item improvement in the UPDRS, and cognitive improvements assessed by the Montreal Cognitive Assessment scale (MOCA). Only theta stimulation on sensorimotor area resulted in both behavior improvements and sustained beta rhythm reduction (Del Felice et al., 2019).

Additionally, tACS can be applied to probe and detect the causal relationship between behavior and neuron activity. In a randomized crossover tACS study, the associations between bradykinesia and abnormally altered beta/gamma oscillations in primary motor cortex (M1) were exposed when 1 mA tACS at 20 Hz or 7 Hz was delivered to patients. The stimulation electrode was centered over the first dorsal interosseous hotspot, while the return electrode was centered over the PZ according to the EEG 10–20 system. As a result, the increased beta power led to aggravated bradykinesia, while gamma synchronization entrained by tACS mitigated these symptoms (Guerra et al., 2021).

To clarify how this aberrantly increased beta power is linked with bradykinesia, Krause et al. hypothesized that an increase in beta power contributed to decreased cortico-muscular coupling (CMC); a critical linkage between neurological activity and motor performance that subsequently leads to bradykinesia and akinesia. Ten PD patients and 10 healthy control subjects were recruited for this study. Each participant received three sessions of 1 mA current stimulation targeted at M1, randomly applying 15 min of 10 Hz tACS, 20 Hz tACS, and sham. To determine the effects of each stimulus, the behavior performance of PD was assessed after each session. Only after 20 Hz stimulation did PD patients reveal a more rigid motor performance and a significant reduction in beta band CMC amplitude, while healthy controls experienced no significant difference in CMC and behavioral performance after either 10 or 20 Hz stimulation (Krause et al., 2013).

Despite these positive results, tACS might induce phosphene, namely, the feeling of flickering lights. Phosphene could affect subjects' performance during tasks and impair the reliability of double-blind studies. Even if the phosphene threshold could be increased to 80 Hz when targeting brain regions far from the retina, it was found that maximum phosphene levels could occur between 14 and 20 Hz under an occiput–vertex electrode montage (Schutter and Hortensius, 2010). Thus, solutions are required for those phosphene inducing montages.

Transcranial Pulsed Current Stimulation

Different from conventional tDCS, tPCS provides discontinuous direct current interrupted by either short or long periodical inter-pulse intervals (Ma et al., 2019), thus adding two additional parameters: inter-pulse intervals and pulse durations. Although phosphene might also be induced by tPCS, the overall tolerability toward tPCS is better than tDCS in healthy subjects, with a

significantly reduced feeling of itching, tingling, and eye flashing (Jaberzadeh et al., 2014).

In a Parkinsonian study, a combined tPCS and treadmill strategy was applied for 10 PD freezing of gait(FOG) patients, with both pulse duration and inter-pulse interval of tPCS being 33.3 μs. The tPCS targeted M1 provided 20 min of stimulation with or without concurrent treadmill training. The gait speed and gait amplitude, however, were found to be improved after a single tPCS session but not in the combined group or treadmill alone group (Alon et al., 2012). However, this study did not include sham tPCS as a placebo control, and the reliability of its results was therefore dented. Further studies should take place to further assess the efficacy of tPCS toward PD.

There was a study toward healthy population implicated that the duration of tPCS was not aligned with the lasting time of aftereffects (Vasquez et al., 2016). Thus, the non-linear effects of tPCS together with its unclear mechanisms complicate the process of selecting proper tPCS parameters. Consequently, few PD studies have focused on tPCS.

Transcranial Random Noise Stimulation

Transcranial random noise stimulation delivers alternating currents of random frequencies and amplitudes within a specific range of the spectrum (Carvalho et al., 2018). tRNS has been used as an active control in several neuromodulation studies; nevertheless, tRNS itself can also serve as a possible therapeutic stimulation method for PD. Like tACS, tRNS can also interfere with internal brain oscillations and neuronal activities. In healthy controls, weak tRNS over M1 increased corticospinal excitability during and after stimulation (Terney et al., 2008). In addition, tRNS exhibits a higher perception threshold (Ambrus et al., 2010) and is more effective activating M1 (Moliadze et al., 2014) than anodal tDCS in healthy controls.

In order to assess the potential of tRNS toward PD, a study has combined tRNS with intermittent theta burst stimulation (iTBS) to detect neuron activity alterations. In this study, PD patients who received a maximum 640 Hz 0.5 mA tRNS over M1 showed an adverse effect on the excitability of M1. In contrast, in healthy controls, M1 cortical excitability was enhanced after stimulation, while PD patients exhibited decreased cortical activity (Stephani et al., 2011). This study revealed a difference in tRNS efficacy among different populations. Thus, further assessment of the efficacy of tRNS as a rehabilitation strategy for PD is needed.

In a double-blind study specific to PD with major cognitive impairment (PD-MCI), Monastero et al. applied 1.5 mA tRNS oscillating randomly between 100 and 600 Hz on M1 to 10 PD-MCI subjects. In this study, 10 patients went through two randomized stimulation sessions, one of them being an active tRNS session and the other being sham. As a result, the total UPDRS score of subjects was significantly increased only after the active tRNS session (Monastero et al., 2020). Again, the validity of this result is doubtful due to the limited subject population and the lack of repetitive sessions.

Outlook for Novel Stimulation Modes

Although promising results were shown by these novel approaches of tES, some studies revealed adverse results. For example, identical multitarget hd-tDCS stimuli resulted in controversial responses in two studies, possibly attributed to the different scales of subjects. In the future, numerous studies with larger sample sizes are needed to prove the prevalence of their efficacy toward PD. In addition, due to the substantial variabilities between populations, even if studies have revealed positive results toward healthy subjects or other homologous disorders, the stimulation parameters should be carefully reconsidered when applied to PD patients.

The investigation of tES mechanisms can not only provide insight into finding optimized tES parameters but also help to explore the neurological process behind specific symptoms. Many studies have employed novel tES to investigate the causal relationship between specific oscillation patterns and behaviors. The understanding of behavior mechanisms can in turn help the design of effective interventions, forming a virtuous circle.

Conventional tDCS separates the whole brain into individual functional regions and neglects the brain's functional networks, while novel modes of tES provide the possibility to modulate the communications between regions. Future studies should focus on stimulating the functional connectivity within brain networks.

Although the mechanisms behind tRNS and tPCS are yet uncertain, future exploration of their mechanisms might be extremely advantageous to optimize parameter settings, that will encourage more tRNS and tPCS studies. Therefore, the adjustment of stimulation would be quite challenging and might lead to contradictory results.

In addition, tPCS and tACS both face phosphene problems. Although there are solutions such as masking flicker stimuli to offset the phosphene (Krause et al., 2013), new methods that eliminate phosphene generation are likely better alternatives.

Recently, the tolerability and feasibility of remotely supervised tDCS (rs-tDCS) has been validated in PD patients, and promising therapeutic improvements were shown by rs-tDCS targeted at the DLPFC paired with cognitive training (Dobbs et al., 2018). This remotely supervised tES provides hints for future studies.

Single session tES usually experienced shorter aftereffects, while repetitive sessions of stimulation would harvest longer aftereffects duration. A single session tDCS or tACS (Neuling et al., 2013; Wach et al., 2013) usually leads to aftereffects that last 30 min or so, independent of the stimulation time. However, a study revealed that repetitive sessions of tDCS with short intervals(several minutes) can harvest up to 24 h of offline effects, while longer intervals(several hours) was found with little or no effects on plasticity (Agboada et al., 2020). Future studies are required to validate whether the short interval repetitive tES would results in sustained and wide-spread aftereffects.

TRANSCRANIAL ELECTRICAL STIMULATION COMBINED WITH OTHER INTERVENTION

In addition to the novel stimulation approaches discussed above, the combination of existing tES with another PD therapy can also be recognized as a novel stimulation method.

Transcranial Electrical Stimulation Combined With Drug

Since one limitation of pharmacologic therapy is side effects, it is intriguing to discuss whether the combination of tES and drugs would optimize improvements and lessen side effects at the same time.

In contrast to tDCS experiments where medication is controlled as baseline, in the study of Ferrucci et al., tDCS was provided as a supplementary intervention of levodopa to eliminate L-dopa-induced cognitive and motor impairments. M1 tDCS, cerebellar tDCS, and sham sessions are randomized for each subject, and each session was at least 1 month separated from another. Anodal tDCS (2 mA) was applied for 20 min in 5 consecutive days in each active stimulation session. Although no other cognitive or motor improvements were observed, both M1 and cerebellar tDCS led to a decrease in levodopa-induced dyskinesias in PD patients (Ferrucci et al., 2016).

Transcranial Electrical Stimulation Combined With Transcranial Magnetic Stimulation

Transcranial electrical stimulation can also be combine with TMS to boost the benefits of intervention. Recently, a dual mode tDCS scheme applied anodal tDCS together with repetitive transcranial magnetic stimulation (rTMS). The stimulation electrode of tDCS was placed over the lDLPFC, while TMS targeted M1. This stimulation scheme demonstrated a significant improvement in the executive functions of PD patients under dual-mode stimulation conditions (Chang et al., 2017).

Similarly, tACS delivered at gamma frequency combined with intermittent theta burst stimulation (iTBS) can also repair the damaged brain activity of PD patients. iTBS is a novel rTMS that provides more tolerable and robust action than conventional rTMS (Sanna et al., 2019). In PD patients, the long-term potentiation (LTP)-like plasticity induced by iTBS is impaired in M1 which subsequently damages PD patients' motor learning ability (Ziemann et al., 2006). Concurrently, PD patients also present decreased gamma oscillatory activity in the basal ganglia-thalamo-cortical network. By applying 70 Hz tACS together with iTBS, iTBS-induced LTP-like plasticity in PD patients can be recovered (Guerra et al., 2020). Consequently, behavior improvements of this repairment could be assessed in future studies.

Transcranial Electrical Stimulation Combined With Physical or Cognitive Training

Motor and cognitive training can effectively ameliorate PD symptoms (Sidaway et al., 2006; Leung et al., 2015). Hence it might be possible to harvest the benefits of training and tES by combining these interventions.

In PD-MCI patients, tDCS combined with physical training showed steady cognitive improvements, but no significant additional effects of tDCS was found (Manenti et al., 2016). In line with this finding, Fernández-Lago et al. found that after a single 20 min session of active tDCS stimulation with treadmill walking training, there was no enhancement of tDCS toward sole treadmill walking training (Fernandez-Lago et al., 2017).

In contrast, in another sham-controlled, double-blind crossover study, Kaski et al. applied tDCS at M1 and the premotor cortex, and together with physical training, PD patients were found to have improved gait and balance performance (Kaski et al., 2014). Another study that combined 30 min of aerobic exercise with anodal tDCS targeted at the prefrontal cortex (PFC) revealed a positive impact of this combination on PFC activity, gait, and cognition (Conceição et al., 2021).

For cognitive training, another study combined computer-based cognitive training (CT) with 2 mA tDCS targeted at the DLPFC. This combined intervention was administered 4 times a week for 4 weeks, and at the week 16 follow-up survey, the impairment in executive skill and attention in PD-MCI patients was ameliorated and the immediate memory skill ability increased (Biundo et al., 2015). A later study divided computer-based CT into standard and tailored CT. Standard CT was more general, while tailored CT was specific to types of impairments, but both CT together with tDCS over the lDLPFC at 2 mA, harvested improvements in PD patients' cognitive behavior, such as attention and working memory (Lawrence et al., 2018).

Outlook for Transcranial Electrical Stimulation Combined With Other Interventions

Since different interventions act through distinct mechanisms to alleviate PD symptoms, combined interventions can modulate multiple pathways with higher efficiency. Future studies might be able to provide individualized combination schemes according to patients' symptoms and pathogenic factors, leading to maximized improvements and minimized side-effects in individuals.

Nevertheless, some limitations in combined interventions need to be considered.

First, TMS itself has already faced the problems of tolerability and unblinding toward patients and adding on TMS might worsen the situation.

In addition, although many have applied combination interventions for PD, few of them include control groups to assess the improvement of dual therapy interventions compared to single intervention. Therefore, in some studies, it is uncertain whether these combinations are better, more studies and a larger number of subjects are required for further validation of their effects.

Moreover, determining the framework of combined intervention is also challenging, since several combined stimulation studies have focused on the yet elusive mechanisms. The combination of interventions might support or interact with each other, forming complex response networks. Therefore, it is difficult to decide the dose and timing of interventions. Should these interventions be given together, or which takes precedence? How can the dose be decided to optimize the efficacy while at the same time not resulting in unpleasant feelings or even

damage? These questions need to be solved for a better understanding toward PD.

CLOSED LOOP TRANSCRANIAL ELECTRICAL STIMULATION

It is generally accepted that discrepancies in effects can emerge between individuals when receiving identical stimulation. Similarly, several studies have witnessed deviations in neuronal feedback between different circumstances undergone by the same subject. To date, most tES research on PD has focused on open-loop schemes, providing constant predefined stimulation during the whole experimental process. However, due to these irremovable inter- and intra-subject variabilities, side effects, and low effect sizes may occur during clinical applications (Iturrate et al., 2018). Therefore, closed loop tES, which is self-adaptive toward changes in brain activity, Therefore, closed loop tES has become a hot topic.

Closed loop tES can provide self-adaptive stimulation according to the feedback of brain activity, forming a feedback-control close loop between input and output signals. To be more specific, when a predefined signal is detected(could be both behavior or brain activity) by the sensor, closed loop system should immediately receive the feedback from the sensor and select the corresponding stimulation parameters, then pass to the stimulator to provide real-time control.

Brittain et al. explored a closed loop tACS strategy toward rest tremor, a dominant motor symptom of PD unresolved by dopaminergic therapy. First, the patient-specific tremor frequencies were recorded, then tACS at tremor frequency was applied to M1 at original or double tremor frequencies. The amplitude of tremor was found to be minimized when the tremor signal and tACS were in phase and when stimulation was set at tremor frequency. Then, subjects were stimulated for 30 s at individual optimal tACS phases with arbitrary input. By alignment of internal and external oscillations, the phase of this pathogenic cortical oscillation would be canceled out, hence inhibiting an average of 42% of resting tremors (Brittain et al., 2013). This closed-loop tremor suppression tACS system might provide a basis for future Parkinsonian studies.

Ideally, optimized closed-loop tES should be able to recognize diverse circumstances and select symptom-specific tES parameters, in which case the specificity of stimulation would be improved, like methodology discussed above against rest tremor.

Additionally, an ideal closed loop tES should also automatically switch on when symptoms evoked and switch off when symptoms disappear, reducing the effect of overtreatment, and the financial cost of stimulation. For instance, A research group have designed a closed-loop EEG-tDCS system. They predefined an EEG threshold for automatic stimulation initiation, which in this study was when subjects were performing Stroop test. After the stimulation session, the sensor would again search for any above-threshold event and prepared to initiate another tDCS session. This closed loop EEG-tDCS system had achieved this system achieved 100% correct activation of tDCS in healthy population (Leite et al., 2017).

A recent DBS study on primates verified improved efficiency of closed-loop methodology. By using an adaptive GPi-DBS scheme that responds to signal changes in M1, the improvements in parkinsonian symptoms were greater than normalized DBS at a lower firing rate of GPi (Rosin et al., 2011). There are now closed-loop DBS that provide in-time stimulation corresponding to neuronal signals, harvesting the same therapeutic effects with less energy consumption (Swann et al., 2018).

Current studies applying closed-loop schemes toward PD are mostly focused on DBS, given the preliminary encouraging results, however, conducting a closed-loop tES scheme seems a very promising field in neuronal modulation of PD. Although few closed-loop tES studies focused on PD treatment, the applicability and efficacy of closed- loop tES has been validated in epilepsy (Berenyi et al., 2012; Kozak and Berenyi, 2017) and sleep (Ketz et al., 2018; Cellini et al., 2019; Hubbard et al., 2021).

There are two possible strategies in conducting closed loop tES studies. First, like DBS, tES might be able to track the internal oscillation of the brain, and if any abnormal oscillations were detected, tES would be activated and initiated the stimulation. On the other hand, closed loop tES can monitor the behavior of subjects and apply stimulation corresponding to subjects' performance. For example, in the above study of resting tremors, the amplitude and frequency of tremors were recorded to deliver specific stimulation. These external behavior data would serve as an indicator for stimulation settings. Recently, a study assessed the capability of a smartwatch to track the time when PD patients suffer severe resting tremor outbreaks. In the future, this kind of device might be adopted in a closed-loop PD intervention study, providing precise behavioral data (Powers et al., 2021).

Although no other tES closed-loop study has focused on PD, researchers are trying to investigate novel tES equipment that can satisfy the demands of closed-loop stimulation. For example, a brain-machine interface system that integrate frequency-domain near infrared spectroscopy (fdNIRS) input and tDCS output was designed to enable the application of closed loop tDCS (Miao and Koomson, 2018). In addition, a recently developed tool box called brain electrophysiological recording and stimulation(BEST), had expanded the range of input recording and output stimulation devices with improved compatibility (Hassan et al., 2022). These systems and algorithms would enable the real-time feedback control of input signals by providing a platform for input and output signal integrating and processing, providing technological pilar for future closed-loop studies.

Outlook for Closed Loop Transcranial Electrical Stimulation

Although closed-loop tES studies toward PD are few, adaptive stimulation schemes have gained vast attention since they can deliver individual- or circumstance-specific modulation. Self-adaptive individualized closed-loop scheme can achieve higher efficacy; and closed-loop tES schemes in the future might also be able to automatically switch on when symptoms occur, like closed-loop DBS.

Another serious technical problem for closed loop tES is the time delay between detection of changes in brain conditions and

the response to stimulus. For symptoms with a short provoking duration, the time delay in response might just miss the period of symptoms and become ineffective. Future studies might employ machine learning to predict the occurrence of symptoms so that more precise stimulation could be provided. In addition, using a brain machine interface (BMI) can provide a quicker stimulation response. For example, in a chronic pain study that used BMI in mice to monitor and stimulate the brain, the time delay between characteristics detected and stimulation response was minimized; thus, the pain could be released even when recognizing acute pain signals (Zhang et al., 2021).

Many studies have proposed numerous novel adaptive tACS and tDCS systems that proved to be safe and tolerable in healthy people (Leite et al., 2017; Guo et al., 2019). Building on these results, investigators could adopt those technologies in future closed loop tES studies in clinical PD populations.

CONCLUSION

Novel tES has proven their potential in preventing both motor and cognitive symptoms in PD and has been clinically translated as a supplementary intervention.

Overall, these novel patterns seek to achieve better performance and safety based on achievements made by conventional tES. These three novel tES methods is complementary with each other in a progressive manner. Novel tES approaches provide the possibility to stimulate the brain as functional networks instead of individual regions and have been proved to be effective in most of the PD studies, enhancing current understanding of PD pathology. The development of novel tES modes expanded the choice for combining tES with other intervention strategies and promote the possibility in obtaining the ideal multi-pathway-targeted combination, achieving a "$1 + 1 > 2$" improvement in efficacy as well as a reduced side-effect. Furthermore, considered as the most promising tES strategy, closed loop tES could take individual differences into consideration and adapt to the patient's response, further optimizing therapeutic specificity. Nevertheless, closed-loop tES requires knowledge of pathological mechanisms and optimized stimulation pattern for each symptom, thus help the recognition of symptom-related activity and matching corresponding stimulation for recognized symptom.

Nevertheless, the results between some of the novel tES studies remain inconsistent, which might be resulted from the small sample size in most of the studies. To put novel tES into clinical use, more clinical trials with larger participant numbers are required. In addition, future studies should recognize the brain as a cohort of many functional networks and utilize tES to modulate functional connectivity between functional regions during PD symptoms. Apart from the study design, there should be more studies that investigate closed loop tES, providing higher specificity of stimulation with the lower consumption of energy. Moreover, efforts should be devoted to the invention of novel tES devices with higher operability that can provide in-home stimulation, making this therapy more convenient and available for patients, for example, rs-tES.

Currently, tES strategies lead to undesirable sensations of stimulation that hinder wider applications. Many tES studies are now focusing on temporal interference stimulation, which seems to be almost imperceptible to healthy subjects (Ma et al., 2021). Future studies might adopt this strategy to avoid unblinding of patients in double-blind studies, providing more pleasant stimulation experience for patients.

In conclusion, novel tES patterns have harvested encouraging improvements in both motor and cognitive symptoms of Parkinson's disease despite flaws.

AUTHOR CONTRIBUTIONS

JB, RN, LY, YZu, YY, and QM designed the study. RN compiled and analyzed the data and wrote the manuscript. JB and RN were closely involved in the definition of the manuscript structure. JB, ZC, and YZo provided critical feedback on all the tables and text. JB, WY, and RN provided support for the methodical work and supervision. All authors read and approved the final manuscript.

FUNDING

This work was supported by the Natural Science Foundation of China (32000750), the Anhui Provincial Natural Science Foundation (2008085QH369), the Basic and Clinical Collaborative Research Improvement Project of Anhui Medical University (2020xkjT020), the School Foundation of Anhui Medical University (2019xkj016), Grants for Scientific Research of BSKY (XJ201907) from Anhui Medical University, Scientific Research Improvement Project of Anhui Medical University (2021xkjT018), Natural Science Foundation of Anhui Province of China (2108085MH303), and Major R&D projects of the Ministry of Science and Technology (2021YFC3300504).

REFERENCES

Agboada, D., Mosayebi-Samani, M., Kuo, M. F., and Nitsche, M. A. (2020). Induction of long-term potentiation-like plasticity in the primary motor cortex with repeated anodal transcranial direct current stimulation - Better effects with intensified protocols? *Brain Stimul.* 13, 987–997. doi: 10.1016/j.brs.2020.04.009

Alon, G., Yungher, D. A., Shulman, L. M., and Rogers, M. W. (2012). Safety and immediate effect of noninvasive transcranial pulsed current stimulation on gait and balance in Parkinson disease. *Neurorehabil. Neural. Repair.* 26, 1089–1095. doi: 10.1177/1545968312448233

Ambrus, G. G., Paulus, W., and Antal, A. (2010). Cutaneous perception thresholds of electrical stimulation methods: comparison of tDCS and tRNS. *Clin. Neurophysiol.* 121, 1908–1914. doi: 10.1016/j.clinph.2010.04.020

Antal, A., and Paulus, W. (2013). Transcranial alternating current stimulation (tACS). *Front. Hum. Neurosci.* 7:317. doi: 10.3389/fnhum.2013.00317

Bagnato, S., Agostino, R., Modugno, N., Quartarone, A., and Berardelli, A. (2006). Plasticity of the motor cortex in Parkinson's disease patients on and off therapy. *Mov. Disord.* 21, 639–645. doi: 10.1002/mds.20778

Beitz, J. M. (2014). Parkinson's disease: a review. *Front. Biosci.* 6, 65–74. doi: 10.2741/s415

Berenyi, A., Belluscio, M., Mao, D., and Buzsaki, G. (2012). Closed-loop control of epilepsy by transcranial electrical stimulation. *Science* 337, 735–737. doi: 10.1126/science.1223154

Biundo, R., Weis, L., Fiorenzato, E., Gentile, G., Giglio, M., Schifano, R., et al. (2015). Double-blind Randomized Trial of tDCS Versus Sham in Parkinson Patients With Mild Cognitive Impairment Receiving Cognitive Training. *Brain Stimul.* 8, 1223–1225.

Boggio, P. S., Ferrucci, R., Rigonatti, S. P., Covre, P., Nitsche, M., Pascual-Leone, A., et al. (2006). Effects of transcranial direct current stimulation on working memory in patients with Parkinson's disease. *J. Neurol. Sci.* 249, 31–38. doi: 10.1016/j.jns.2006.05.062

Boord, P., Madhyastha, T. M., Askren, M. K., and Grabowski, T. J. (2017). Executive attention networks show altered relationship with default mode network in PD. *Neuroimage Clin.* 13, 1–8. doi: 10.1016/j.nicl.2016.11.004

Brittain, J. S., Probert-Smith, P., Aziz, T. Z., and Brown, P. (2013). Tremor suppression by rhythmic transcranial current stimulation. *Curr. Biol.* 23, 436–440. doi: 10.1016/j.cub.2013.01.068

Bueno, M. E. B., do Nascimento Neto, L. I., Terra, M. B., Barboza, N. M., Okano, A. H., and Smaili, S. M. (2019). . Effectiveness of acute transcranial direct current stimulation on non-motor and motor symptoms in Parkinson's disease. *Neurosci. Lett.* 696, 46–51. doi: 10.1016/j.neulet.2018.12.017

Cai, M., Dang, G., Su, X., Zhu, L., Shi, X., Che, S., et al. (2021). Identifying mild cognitive impairment in Parkinson's disease with electroencephalogram functional connectivity. *Front. Aging Neurosci.* 381:701499. doi: 10.3389/fnagi.2021.701499

Carvalho, S., Leite, J., and Fregni, F. (2018). *Transcranial alternating current stimulation and transcranial random noise stimulation. Neuromodulation*. Berlin: Elsevier, 1611–1617.

Cellini, N., Shimizu, R. E., Connolly, P. M., Armstrong, D. M., Hernandez, L. T., Polakiewicz, A. G., et al. (2019). Short Duration Repetitive Transcranial Electrical Stimulation During Sleep Enhances Declarative Memory of Facts. *Front. Hum. Neurosci.* 13:123. doi: 10.3389/fnhum.2019.00123

Chang, W. H., Kim, M. S., Park, E., Cho, J. W., Youn, J., Kim, Y. K., et al. (2017). Effect of Dual-Mode and Dual-Site Noninvasive Brain Stimulation on Freezing of Gait in Patients With Parkinson Disease. *Arch. Phys. Med. Rehabil.* 98, 1283–1290. doi: 10.1016/j.apmr.2017.01.011

Conceição, N. R., Gobbi, L. T. B., Nobrega-Sousa, P., Orcioli-Silva, D., Beretta, V. S., Lirani-Silva, E., et al. (2021). Aerobic Exercise Combined With Transcranial Direct Current Stimulation Over the Prefrontal Cortex in Parkinson Disease: Effects on Cortical Activity. Gait, and Cognition. *Neurorehabil. Neural. Repair.* 35, 717–728. doi: 10.1177/15459683211019344

Costa-Ribeiro, A., Maux, A., Bosford, T., Aoki, Y., Castro, R., Baltar, A., et al. (2017). Transcranial direct current stimulation associated with gait training in Parkinson's disease: a pilot randomized clinical trial. *Dev. Neurorehabil.* 20, 121–128. doi: 10.3109/17518423.2015

Crone, N. E., Miglioretti, D. L., Gordon, B., and Lesser, R. P. (1998). Functional mapping of human sensorimotor cortex with electrocorticographic spectral analysis. II. Event-related synchronization in the gamma band. *Brain* 121, 2301–2315. doi: 10.1093/brain/121.12.2301

Dagan, M., Herman, T., Harrison, R., Zhou, J., Giladi, N., Ruffini, G., et al. (2018). Multitarget transcranial direct current stimulation for freezing of gait in Parkinson's disease. *Mov. Disord.* 33, 642–646. doi: 10.1002/mds.27300

Datta, A., Bansal, V., Diaz, J., Patel, J., Reato, D., and Bikson, M. (2009). Gyri-precise head model of transcranial direct current stimulation: improved spatial focality using a ring electrode versus conventional rectangular pad. *Brain Stimul.* 2, 201–7,7e1. doi: 10.1016/j.brs.2009.03.005

Del Felice, A., Castiglia, L., Formaggio, E., Cattelan, M., Scarpa, B., Manganotti, P., et al. (2019). Personalized transcranial alternating current stimulation (tACS) and physical therapy to treat motor and cognitive symptoms in Parkinson's disease: a randomized cross-over trial. *NeuroImage.* 22:101768. doi: 10.1016/j.nicl.2019.101768

Dobbs, B., Pawlak, N., Biagioni, M., Agarwal, S., Shaw, M., Pilloni, G., et al. (2018). Generalizing remotely supervised transcranial direct current stimulation (tDCS): feasibility and benefit in Parkinson's disease. *J. Neuroeng. Rehabil.* 15:114. doi: 10.1186/s12984-018-0457-9

Doruk, D., Gray, Z., Bravo, G. L., Pascual-Leone, A., and Fregni, F. (2014). Effects of tDCS on executive function in Parkinson's disease. *Neurosci. Lett.* 582, 27–31. doi: 10.1016/j.neulet.2014.08.043

Fabbri, M., Coelho, M., Guedes, L. C., Chendo, I., Sousa, C., Rosa, M. M., et al. (2017). Response of non-motor symptoms to levodopa in late-stage Parkinson's disease: Results of a levodopa challenge test. *Parkinsonism Relat. Dis.* 39, 37–43. doi: 10.1016/j.parkreldis.2017.02.007

Fernandez-Lago, H., Bello, O., Mora-Cerda, F., Montero-Camara, J., and Fernandez-Del-Olmo, M. A. (2017). Treadmill Walking Combined With Anodal Transcranial Direct Current Stimulation in Parkinson Disease: A Pilot Study of Kinematic and Neurophysiological Effects. *Am. J. Phys. Med. Rehabil.* 96, 801–808. doi: 10.1097/PHM.0000000000000751

Ferrucci, R., Cortese, F., Bianchi, M., Pittera, D., Turrone, R., Bocci, T., et al. (2016). Cerebellar and Motor Cortical Transcranial Stimulation Decrease Levodopa-Induced Dyskinesias in Parkinson's Disease. *Cerebellum* 15, 43–47. doi: 10.1007/s12311-015-0737-x

Fischer, D. B., Fried, P. J., Ruffini, G., Ripolles, O., Salvador, R., Banus, J., et al. (2017). Multifocal tDCS targeting the resting state motor network increases cortical excitability beyond traditional tDCS targeting unilateral motor cortex. *Neuroimage* 157, 34–44. doi: 10.1016/j.neuroimage.2017.05.060

Fregni, F., Boggio, P. S., Santos, M. C., Lima, M., Vieira, A. L., Rigonatti, S. P., et al. (2006). Noninvasive cortical stimulation with transcranial direct current stimulation in Parkinson's disease. *Mov. Disord.* 21, 1693–1702. doi: 10.1002/mds.21012

Gan, C., Wang, M., Si, Q., Yuan, Y., Zhi, Y., Wang, L., et al. (2020). Altered interhemispheric synchrony in Parkinson's disease patients with levodopa-induced dyskinesias. *NPJ Parkinsons Dis.* 6, 1–7. doi: 10.1038/s41531-020-0116-2

Ganguly, J., Murgai, A., Sharma, S., Aur, D., and Jog, M. (2020). Non-invasive Transcranial Electrical Stimulation in Movement Disorders. *Front. Neurosci.* 14:522. doi: 10.3389/fnins.2020.00522

Guerra, A., Asci, F., D'Onofrio, V., Sveva, V., Bologna, M., Fabbrini, G., et al. (2020). Enhancing Gamma Oscillations Restores Primary Motor Cortex Plasticity in Parkinson's Disease. *J. Neurosci.* 40, 4788–4796. doi: 10.1523/JNEUROSCI.0357-20.2020

Guerra, A., Colella, D., Giangrosso, M., Cannavacciuolo, A., Paparella, G., Fabbrini, G., et al. (2021). Driving motor cortex oscillations modulates bradykinesia in Parkinson's disease. *Brain* 10:awab257. doi: 10.1093/brain/awab257

Guo, D., yan Li, H., and Sun, M. (eds) (2019). *Adaptive alternating current transcranial electrical stimulation (tACS). 2019 6th International Conference on Systems and Informatics (ICSAI)*. Piscataway: IEEE

Hassan, U., Pillen, S., Zrenner, C., and Bergmann, T. O. (2022). The Brain Electrophysiological recording & STimulation (BEST) toolbox. *Brain Stimul.* 15, 109–115.

Hubbard, R. J., Zadeh, I., Jones, A. P., Robert, B., Bryant, N. B., Clark, V. P., et al. (2021). Brain connectivity alterations during sleep by closed-loop transcranial neurostimulation predict metamemory sensitivity. *Netw. Neurosci.* 5, 734–756. doi: 10.1162/netn_a_00201

Ishikuro, K., Dougu, N., Nukui, T., Yamamoto, M., Nakatsuji, Y., Kuroda, S., et al. (2018). Effects of transcranial direct current stimulation (tDCS) over the frontal polar area on motor and executive functions in Parkinson's disease; a pilot study. *Front. Aging Neurosci.* 10:231. doi: 10.3389/fnagi.2018.00231

Iturrate, I., Pereira, M., and Millán, J. D. R. (2018). Closed-loop electrical neurostimulation: challenges and opportunities. *Curr. Opin. Biomed. Eng.* 8, 28–37. doi: 10.3389/fnins.2019.00936

Jaberzadeh, S., Bastani, A., and Zoghi, M. (2014). Anodal transcranial pulsed current stimulation: A novel technique to enhance corticospinal excitability. *Clin. Neurophysiol.* 125, 344–351. doi: 10.1016/j.clinph.2013.08.025

Kami, A. T., Sadler, C., Nantel, J., and Carlsen, A. N. (2018). Transcranial direct current stimulation (TDCS) over supplementary motor area (SMA) improves upper limb movement in individuals with Parkinson's disease. *J. Exerc. Mov. Sport* 50:36. doi: 10.1016/j.clinph.2021.06.031

Kaski, D., Dominguez, R. O., Allum, J. H., Islam, A. F., and Bronstein, A. M. (2014). Combining physical training with transcranial direct current stimulation to improve gait in Parkinson's disease: a pilot randomized controlled study. *Clin Rehabil.* 28, 1115–1124. doi: 10.1177/0269215514534277

Ketz, N., Jones, A. P., Bryant, N. B., Clark, V. P., and Pilly, P. K. (2018). Closed-Loop Slow-Wave tACS Improves Sleep-Dependent Long-Term Memory

Generalization by Modulating Endogenous Oscillations. *J. Neurosci.* 38, 7314–7326. doi: 10.1523/JNEUROSCI.0273-18.2018

Kozak, G., and Berenyi, A. (2017). Sustained efficacy of closed loop electrical stimulation for long-term treatment of absence epilepsy in rats. *Sci. Rep.* 7:6300. doi: 10.1038/s41598-017-06684-0

Krause, V., Wach, C., Sudmeyer, M., Ferrea, S., Schnitzler, A., and Pollok, B. (2013). Cortico-muscular coupling and motor performance are modulated by 20 Hz transcranial alternating current stimulation (tACS) in Parkinson's disease. *Front. Hum. Neurosci.* 7:928. doi: 10.3389/fnhum.2013.00928

Lau, C. I., Liu, M. N., Chang, K. C., Chang, A., Bai, C. H., Tseng, C. S., et al. (2019). Effect of single-session transcranial direct current stimulation on cognition in Parkinson's disease. *CNS Neurosci. Ther.* 25, 1237–1243. doi: 10.1111/cns.13210

Lawrence, B. J., Gasson, N., Johnson, A. R., Booth, L., and Loftus, A. M. (2018). Cognitive Training and Transcranial Direct Current Stimulation for Mild Cognitive Impairment in Parkinson's Disease: A Randomized Controlled Trial. *Park. Dis.* 2018:4318475. doi: 10.1155/2018/4318475

Leite, J., Morales-Quezada, L., Carvalho, S., Thibaut, A., Doruk, D., Chen, C. F., et al. (2017). Surface EEG-Transcranial Direct Current Stimulation (tDCS) Closed-Loop System. *Int. J. Neural. Syst.* 27:1750026. doi: 10.1142/S0129065717500265

Leung, I. H., Walton, C. C., Hallock, H., Lewis, S. J., Valenzuela, M., and Lampit, A. (2015). Cognitive training in Parkinson disease: A systematic review and meta-analysis. *Neurology.* 85, 1843–1851.

Li, Y., Liang, P., Jia, X., and Li, K. (2016). Abnormal regional homogeneity in Parkinson's disease: a resting state fMRI study. *Clin. Radiol.* 71, e28–e34. doi: 10.1016/j.crad.2015.10.006

Liotti, M., Ramig, L., Vogel, D., New, P., Cook, C., Ingham, R., et al. (2003). Hypophonia in Parkinson's disease: neural correlates of voice treatment revealed by PET. *Neurology* 60, 432–440. doi: 10.1212/wnl.60.3.432

Lohse, A., Meder, D., Nielsen, S., Lund, A. E., Herz, D. M., Løkkegaard, A., et al. (2020). Low-frequency transcranial stimulation of pre-supplementary motor area alleviates levodopa-induced dyskinesia in Parkinson's disease: a randomized cross-over trial. *Brain Commun.* 2:fcaa147. doi: 10.1093/braincomms/fcaa147

Ma, R., Xia, X., Zhang, W., Lu, Z., Wu, Q., Cui, J., et al. (2021). High Gamma and Beta Temporal Interference Stimulation in the Human Motor Cortex Improves Motor Functions. *bioRxiv* [Preprint]. doi: 10.1101/2021.03.26.437107

Ma, Z., Du, X., Wang, F., Ding, R., Li, Y., Liu, A., et al. (2019). Cortical Plasticity Induced by Anodal Transcranial Pulsed Current Stimulation Investigated by Combining Two-Photon Imaging and Electrophysiological Recording. *Front. Cell Neurosci.* 13:400. doi: 10.3389/fncel.2019.00400

Manenti, R., Brambilla, M., Benussi, A., Rosini, S., Cobelli, C., Ferrari, C., et al. (2016). Mild cognitive impairment in Parkinson's disease is improved by transcranial direct current stimulation combined with physical therapy. *Mov. Disord.* 31, 715–724.

Manor, B., Dagan, M., Herman, T., Gouskova, N. A., Vanderhorst, V. G., Giladi, N., et al. (2021). Multitarget Transcranial Electrical Stimulation for Freezing of Gait: A Randomized Controlled Trial. *Mov Disord.* 36, 2693–2698. doi: 10.1002/mds.28759

Miao, Y., and Koomson, V. J. A. C. M. O. S. - (2018). Based Bidirectional Brain Machine Interface System With Integrated fdNIRS and tDCS for Closed-Loop Brain Stimulation. *IEEE Trans. Biomed. Circuits Syst.* 12, 554–563. doi: 10.1109/TBCAS.2018.2798924

Moliadze, V., Fritzsche, G., and Antal, A. (2014). Comparing the efficacy of excitatory transcranial stimulation methods measuring motor evoked potentials. *Neural. Plast.* 2014:837141. doi: 10.1155/2014/837141

Monastero, R., Baschi, R., Nicoletti, A., Pilati, L., Pagano, L., Cicero, C. E., et al. (2020). Transcranial random noise stimulation over the primary motor cortex in PD-MCI patients: a crossover, randomized, sham-controlled study. *J. Neural. Transm.*. 127, 1589–1597. doi: 10.1007/s00702-020-02255-2

Morishita, T., Hilliard, J. D., Okun, M. S., Neal, D., Nestor, K. A., Peace, D., et al. (2017). Postoperative lead migration in deep brain stimulation surgery: Incidence, risk factors, and clinical impact. *PLoS One* 12:e0183711. doi: 10.1371/journal.pone.0183711

Mure, H., Tang, C. C., Argyelan, M., Ghilardi, M.-F., Kaplitt, M. G., Dhawan, V., et al. (2012). Improved sequence learning with subthalamic nucleus deep brain stimulation: evidence for treatment-specific network modulation. *J. Neurosci.* 32, 2804–2813. doi: 10.1523/JNEUROSCI.4331-11.2012.

Nakamura, T., Ghilardi, M., Mentis, M., Dhawan, V., Fukuda, M., Hacking, A., et al. (2001). Functional networks in motor sequence learning: abnormal topographies in Parkinson's disease. *Hum. Brain Mapp.* 12, 42–60. doi: 10.1002/1097-0193(200101)12:1<42::aid-hbm40>3.0.co;2-d

Neuling, T., Rach, S., and Herrmann, C. S. (2013). Orchestrating neuronal networks: sustained after-effects of transcranial alternating current stimulation depend upon brain states. *Front. Hum. Neurosci.* 7:161. doi: 10.3389/fncel.2019.00400

Nitsche, M. A., and Paulus, W. (2000). Excitability changes induced in the human motor cortex by weak transcranial direct current stimulation. *J. Physiol.* 527, 633–639. doi: 10.1111/j.1469-7793.2000.t01-1-00633.x

Nonnekes, J., Timmer, M. H., de Vries, N. M., Rascol, O., Helmich, R. C., and Bloem, B. R. (2016). Unmasking levodopa resistance in Parkinson's disease. *Mov. Disord.* 31, 1602–1609. doi: 10.1002/mds.26712

Nutt, J. G., Bloem, B. R., Giladi, N., Hallett, M., Horak, F. B., and Nieuwboer, A. (2011). Freezing of gait: moving forward on a mysterious clinical phenomenon. *Lancet Neurol.* 10, 734–744. doi: 10.1016/S1474-4422(11)70143-0

Pereira, J. B., Junqué, C., Bartrés-Faz, D., Martí, M. J., Sala-Llonch, R., Compta, Y., et al. (2013). Modulation of verbal fluency networks by transcranial direct current stimulation (tDCS) in Parkinson's disease. *Brain Stimul.* 6, 16–24. doi: 10.1016/j.brs.2012.01.006

Possti, D., Fahoum, F., Sosnik, R., Giladi, N., Hausdorff, J. M., Mirelman, A., et al. (2021). Changes in the EEG spectral power during dual-task walking with aging and Parkinson's disease: initial findings using Event-Related Spectral Perturbation analysis. *J. Neurol.* 268, 161–168. doi: 10.1007/s00415-020-10104-1

Powers, R., Etezadi-Amoli, M., Arnold, E. M., Kianian, S., Mance, I., Gibiansky, M., et al. (2021). Smartwatch inertial sensors continuously monitor real-world motor fluctuations in Parkinson's disease. *Sci. Transl. Med.* 13:eabd7865. doi: 10.1126/scitranslmed.abd7865

Rascol, O., Sabatini, U., Fabre, N., Brefel, C., Loubinoux, I., Celsis, P., et al. (1997). The ipsilateral cerebellar hemisphere is overactive during hand movements in akinetic parkinsonian patients. *Brain* 120, 103–110. doi: 10.1093/brain/120.1.103

Rektorova, I., Sedlackova, S., Telecka, S., Hlubocky, A., and Rektor, I. (2007). Repetitive transcranial stimulation for freezing of gait in Parkinson's disease. *Mov. Disord.* 22, 1518–1519.

Ridding, M. C., Inzelberg, R., and Rothwell, J. C. (1995). Changes in excitability of motor cortical circuitry in patients with Parkinson's disease. *Ann. Neurol.* 37, 181–188. doi: 10.1002/ana.410370208

Rosin, B., Slovik, M., Mitelman, R., Rivlin-Etzion, M., Haber, S. N., Israel, Z., et al. (2011). Closed-loop deep brain stimulation is superior in ameliorating parkinsonism. *Neuron* 72, 370–384. doi: 10.1016/j.neuron.2011.08.023

Ruan, X., Li, Y., Li, E., Xie, F., Zhang, G., Luo, Z., et al. (2020). Impaired Topographical Organization of Functional Brain Networks in Parkinson's Disease Patients With Freezing of Gait. *Front. Aging Neurosci.* 12:580564. doi: 10.3389/fnagi.2020.580564

Sadler, C. M., Kami, A. T., Nantel, J., and Carlsen, A. N. (2021). Transcranial direct current stimulation of supplementary motor area improves upper limb kinematics in Parkinson's disease. *Clin. Neurophysiol.* 132, 2907–2915. doi: 10.1016/j.clinph.2021.06.031

Sanna, A., Fattore, L., Badas, P., Corona, G., Cocco, V., and Diana, M. (2019). Intermittent Theta Burst Stimulation of the Prefrontal Cortex in Cocaine Use Disorder: A Pilot Study. *Front. Neurosci.* 13:765. doi: 0.3389/fnins.2019.00765

Schutter, D. J., and Hortensius, R. (2010). Retinal origin of phosphenes to transcranial alternating current stimulation. *Clin. Neurophysiol.* 121, 1080–1084. doi: 10.1016/j.clinph.2009.10.038

Shill, H. A., Obradov, S., Katsnelson, Y., and Pizinger, R. A. (2011). randomized, double-blind trial of transcranial electrostimulation in early Parkinson's disease. *Mov. Disord.* 26, 1477–1480. doi: 10.1002/mds.23591

Sidaway, B., Anderson, J., Danielson, G., Martin, L., and Smith, G. (2006). Effects of long-term gait training using visual cues in an individual with Parkinson disease. *Phys. Ther.* 86, 186–194.

Soikkeli, R., Partanen, J., Soininen, H., Paakkonen, A., and Riekkinen, P. Sr. (1991). Slowing of EEG in Parkinson's disease. *Electroencephalogr. Clin. Neurophysiol.* 79, 159–165.

Stephani, C., Nitsche, M. A., Sommer, M., and Paulus, W. (2011). Impairment of motor cortex plasticity in Parkinson's disease, as revealed by theta-burst-transcranial magnetic stimulation and transcranial random noise stimulation. *Park. Relat. Dis.* 17, 297–298. doi: 10.1016/j.parkreldis.2011.01.006

Swank, C., Mehta, J., and Criminger, C. (2016). Transcranial direct current stimulation lessens dual task cost in people with Parkinson's disease. *Neurosci. Lett.* 626, 1–5. doi: 10.1016/j.neulet.2016.05.010

Swann, N. C., de Hemptinne, C., Thompson, M. C., Miocinovic, S., Miller, A. M., Gilron, R., et al. (2018). Adaptive deep brain stimulation for Parkinson's disease using motor cortex sensing. *J. Neural. Eng.* 15:046006.

Terney, D., Chaieb, L., Moliadze, V., Antal, A., and Paulus, W. (2008). Increasing human brain excitability by transcranial high-frequency random noise stimulation. *J. Neurosci.* 28, 14147–14155. doi: 10.1523/JNEUROSCI.4248-08.2008

Van Den Heuvel, M. P., and Pol, H. E. H. (2010). Exploring the brain network: a review on resting-state fMRI functional connectivity. *Eur. Neuropsychopharmacol.* 20, 519–534. doi: 10.1016/j.euroneuro.2010.03.008

Vasquez, A., Malavera, A., Doruk, D., Morales-Quezada, L., Carvalho, S., Leite, J., et al. (2016). Duration Dependent Effects of Transcranial Pulsed Current Stimulation (tPCS) Indexed by Electroencephalography. *Neuromodulation* 19, 679–688. doi: 10.1111/ner.12457

Wach, C., Krause, V., Moliadze, V., Paulus, W., Schnitzler, A., and Pollok, B. (2013). The effect of 10 Hz transcranial alternating current stimulation (tACS) on corticomuscular coherence. *Front. Hum. Neurosci.* 7:511. doi: 10.3389/fnhum.2013.00511

Weber, M. J., Messing, S. B., Rao, H., Detre, J. A., and Thompson-Schill, S. L. (2014). Prefrontal transcranial direct current stimulation alters activation and connectivity in cortical and subcortical reward systems: a tDCS-fMRI study. *Hum. Brain Mapp.* 35, 3673–3686. doi: 10.1002/hbm.22429

Wirdefeldt, K., Adami, H. O., Cole, P., Trichopoulos, D., and Mandel, J. (2011). Epidemiology and etiology of Parkinson's disease: a review of the evidence. *Eur. J. Epidemiol.* 26, S1–S58. doi: 10.1007/s10654-011-9581-6

Workman, C. D., Fietsam, A. C., Uc, E. Y., and Rudroff, T. (2020). Cerebellar transcranial direct current stimulation in people with Parkinson's disease: a pilot study. *Brain Sci.* 10:96. doi: 10.3390/brainsci10020096

Yaqub, M. A., Woo, S.-W., and Hong, K.-S. (2018). Effects of HD-tDCS on resting-state functional connectivity in the prefrontal cortex: an fNIRS study. *Complexity* 2018, 1-13

Yu, H., Sternad, D., Corcos, D. M., and Vaillancourt, D. E. (2007). Role of hyperactive cerebellum and motor cortex in Parkinson's disease. *Neuroimage* 35, 222–233. doi: 10.1016/j.neuroimage.2006.11.047

Zhang, Q., Hu, S., Talay, R., Xiao, Z., Rosenberg, D., Liu, Y., et al. (2021). A prototype closed-loop brain-machine interface for the study and treatment of pain. *Nat. Biomed. Eng.* doi: 10.1038/s41551-021-00736-7

Ziemann, U., Ilic, T. V., and Jung, P. (2006). Long-term potentiation (LTP)-like plasticity and learning in human motor cortex–investigations with transcranial magnetic stimulation (TMS). *Suppl. Clin. Neurophysiol.* 59, 19–25. doi: 10.1016/s1567-424x(09)70007-8

Conflict of Interest: The authors declare that the research was conducted in the absence of any commercial or financial relationships that could be construed as a potential conflict of interest.

Publisher's Note: All claims expressed in this article are solely those of the authors and do not necessarily represent those of their affiliated organizations, or those of the publisher, the editors and the reviewers. Any product that may be evaluated in this article, or claim that may be made by its manufacturer, is not guaranteed or endorsed by the publisher.

frontiers | Frontiers in Aging Neuroscience

ORIGINAL RESEARCH
published: 25 April 2022
doi: 10.3389/fnagi.2022.827993

Effects of Repetitive Transcranial Magnetic Stimulation on Cerebellar Metabolism in Patients With Spinocerebellar Ataxia Type 3

Xin-Yuan Chen[1†], Yan-Hua Lian[2†], Xia-Hua Liu[1†], Arif Sikandar[3], Meng-Cheng Li[4], Hao-Ling Xu[5], Jian-Ping Hu[4], Qun-Lin Chen[4] and Shi-Rui Gan[3*]*

[1] Department of Rehabilitation Medicine, The First Affiliated Hospital of Fujian Medical University, Fuzhou, China, [2] The School of Health, Fujian Medical University, Fuzhou, China, [3] Department of Neurology, The First Affiliated Hospital of Fujian Medical University, Fuzhou, China, [4] Department of Radiology, The First Affiliated Hospital of Fujian Medical University, Fuzhou, China, [5] Department of Neurology, The 900th Hospital of Joint Logistics Support Force of PLA, Fuzhou, China

OPEN ACCESS

Edited by:
Wei Wu,
Alto Neuroscience, United States

Reviewed by:
Ullrich Wüllner,
University Hospital Bonn, Germany
Junhong Zhou,
Harvard Medical School, United States

***Correspondence:**
Qun-Lin Chen
fychenqunlin@126.com
Shi-Rui Gan
ganshirui@fjmu.edu.cn

[†] These authors have contributed equally to this work and share first authorship

Specialty section:
This article was submitted to Neuroinflammation and Neuropathy, a section of the journal Frontiers in Aging Neuroscience

Received: *02 December 2021*
Accepted: *14 March 2022*
Published: *25 April 2022*

Citation:
Chen X-Y, Lian Y-H, Liu X-H, Sikandar A, Li M-C, Xu H-L, Hu J-P, Chen Q-L and Gan S-R (2022) Effects of Repetitive Transcranial Magnetic Stimulation on Cerebellar Metabolism in Patients With Spinocerebellar Ataxia Type 3. Front. Aging Neurosci. 14:827993. doi: 10.3389/fnagi.2022.827993

Background: Spinocerebellar ataxia type 3 (SCA3) is the most common autosomal dominant hereditary ataxia, and, thus far, effective treatment remains low. Repetitive transcranial magnetic stimulation (rTMS) can improve the symptoms of spinal cerebellar ataxia, but the mechanism is unclear; in addition, whether any improvement in the symptoms is related to cerebellar metabolism has not yet been investigated. Therefore, the purpose of this study was to investigate the effects of low-frequency rTMS on local cerebellar metabolism in patients with SCA3 and the relationship between the improvement in the symptoms and cerebellar metabolism.

Methods: A double-blind, prospective, randomized, sham-controlled trial was carried out among 18 SCA3 patients. The participants were randomly assigned to the real stimulation group (n = 9) or sham stimulation group (n = 9). Each participant in both the groups underwent 30 min of 1 Hz rTMS stimulation (a total of 900 pulses), differing only in terms of stimulator placement, for 15 consecutive days. To separately compare pre- and post-stimulation data (magnetic resonance spectroscopy (MRS) data and the International Cooperative Ataxia Rating Scale (ICARS) score) in the real and sham groups, paired-sample t-tests and Wilcoxon's signed-rank tests were used in the analyses. The differences in the ICARS and MRS data between the two groups were analyzed with independent t-tests and covariance. To explore the association between the changes in the concentration of cerebellar metabolism and ICARS, we applied Pearson's correlation analysis.

Results: After 15 days of treatment, the ICARS scores significantly decreased in both the groups, while the decrease was more significant in the real stimulation group compared to the sham stimulation group ($p < 0.001$). The analysis of covariance further confirmed that the total ICARS scores decreased more dramatically in the real stimulation group after treatment compared to the sham stimulation group ($F = 31.239$, $p < 0.001$). The values of NAA/Cr and Cho/Cr in the cerebellar vermis, bilateral dentate

nucleus, and bilateral cerebellar hemisphere increased significantly in the real stimulation group ($p < 0.05$), but no significant differences were found in the sham stimulation group ($p > 0.05$). The analysis of covariance also confirmed the greater change in the real stimulation group. This study also demonstrated that there was a negative correlation between NAA/Cr in the right cerebellar hemisphere and ICARS in the real stimulation group ($r = -0.831$, $p = 0.02$).

Conclusion: The treatment with rTMS over the cerebellum was found to induce changes in the cerebellar local metabolism and microenvironment in the SCA3 patients. The alterations may contribute to the improvement of the symptoms of ataxia in SCA3 patients.

Keywords: cerebellar metabolism, magnetic resonance spectroscopy, repetitive transcranial magnetic stimulation, spinocerebellar ataxia type 3, international cooperative ataxia rating scale

INTRODUCTION

Spinocerebellar ataxia type 3 (SCA3), also known as Machado–Joseph disease (MJD), is one of the most common types of autosomal dominant neurodegenerative disorders. The manifestation of SCA3 mainly includes gait ataxia, postural imbalance, dysarthria, dysphagia, diplopia, and peripheral neuropathy. Since the pathogenesis of SCA3 has not been fully illustrated, there has not been an effective treatment for this disease so far (Li et al., 2015; Matos et al., 2019; Costa, 2020). There is a growing number of studies applying repetitive transcranial magnetic stimulation (rTMS) in the treatment of spinocerebellar ataxias (SCAs) that has shown promising results (Farzan et al., 2013; Jhunjhunwala et al., 2013; Dang et al., 2019; Manor et al., 2019; Benussi et al., 2020; França et al., 2020). Researchers have observed a marked improvement in the 10-m walk tests and the number of steps in tandem gait and diplopia, particularly after the rTMS treatment, accompanied by an improvement in limb ataxia, as evaluated using the International Cooperative Ataxia Rating Scale (ICARS) (Benussi et al., 2020). Though rTMS can improve the symptoms of SCAs, the mechanism for the improvement is unclear. The previous studies have shown that the therapeutic effect of rTMS on cerebellar ataxia may be due to either the cerebellar modulation of motor cortex excitability by rTMS involving the cerebellar-thalamus-cortical (CTC) pathway (Sanna et al., 2021) or the reduction of oxidative stress, the increase of cerebellar hemispheric blood flow (Ihara et al., 2005), and the effects on cerebellar-cortical plasticity (Song et al., 2020). The magnetic resonance spectroscopy (MRS) provides a non-ionizing and non-invasive method to measure the alteration of cerebellar metabolism (Hall et al., 2012), which has been widely used in the cross-sectional studies of SCAs and admitted as a reliable means in the assessment of the efficacy of SCAs (Lei et al., 2011; Lirng et al., 2012; Adanyeguh et al., 2015; Krahe et al., 2020). Therefore, applying MRS in the detection of the alteration of cerebellar metabolism before and after the rTMS in the SCA3 patients is suitable.

In view of the foregoing, a prospective, randomized, double-blind, sham-controlled study was conducted to investigate the effects of low-frequency rTMS on local intracerebral metabolism in the patients with SCA3 as well as the possible correlation between the alteration of cerebellar metabolism and the improvement of ataxia.

MATERIALS AND METHODS

Ethical Approval and Patient Recruitment

This study was approved by the ethics committee of the First Affiliated Hospital of Fujian Medical University (MRCTA, ECFAH of [2018]201). The registration was recorded in the Chinese Clinical Trial Registry with a unique identifier: ChiCTR1800020133. All the participants signed the informed consent form and any relevant documents. The recruitment of these participants began in December 2018 and ended in October 2019 at the First Affiliated Hospital of Fujian Medical University. The eligibility criteria for the participants were as follows: (1) patients diagnosed with SCA3 and having detectable clinical manifestations; (2) SCA3 patients aged 20–80 years. The participant exclusion criteria were as follows: (1) diagnosed with concomitant epilepsy and dementia (MMSE < 25) or any unstable medical disorder; (2) undergoing neuroleptics or any other current clinical study; (3) a history of seizure, heat convulsion, head injury, neurosurgical interventions, or any metal in the head (outside the mouth); (4) a history of unstable hypertension; (5) a known history of any metallic particles in the eye, implanted cardiac pacemaker, implanted neurostimulators, surgical clips (above the shoulder line), or medical pumps; (6) a history of frequent or severe headaches; (7) a history of migraine, hearing loss, cochlear implants, drug abuse, or alcoholism; and (8) pregnancy or the possibility of pregnancy. The age of onset was defined as the age at which the symptoms associated with SCA3 were first noted by the patient or a close care provider. The duration of the disease was considered to be the time between the age of onset and the age of initial diagnosis.

Study Design and Treatment Protocol

This study was a double-blind, prospective, randomized, sham-controlled trial. A total of 18 SCA3 patients were randomly

allocated to the real or sham stimulation groups using the random number table method (Lim and In, 2019).

A commercially available stimulator (YIDUIDE CCY-I magnetic field stimulator) was utilized for the stimulation in both groups. This trial was completed by 18 (100%) patients. We allocated nine participants (50%) to the real stimulation group; each participant underwent 30 min of 1 Hz rTMS stimulation (a total of 900 pulses) for 15 consecutive days. A total of 9 participants (50%) were assigned to the sham stimulation group; the parameters in the rTMS prescription were the same as those in the real stimulation group. The stimulation coil was placed tangentially above the scalp and centered on the inion in the real stimulation group or vertically in the sham stimulation group (4 cm to the right of the inion and 4 cm to the left of the inion) (Shiga et al., 2002).

Evaluation

The evaluation was done by the trained study staff, who were blind to both intervention arms. The primary outcome measurement was the score of the ICARS (Trouillas et al., 1997). The ICARS is a 100-point scale including 19 items divided into four subscales: postural and gait (PG), limb kinetic function (KF), speech disorders (DS), and oculomotor disorders (OMS). The higher the score is, the poorer the performance is considered to be. The participants' performance was evaluated using the ICARS both before and after the stimulus was applied. The secondary outcome measure was taken on the local cerebellar metabolites consisting of the value of *N*-acetyl aspartate (NAA)/creatine (Cr), and choline complex (Cho)/Cr, detected by a proton magnetic resonance wave (^{1}H-MRS), using a 3.0-Tesla Siemens Skyra scanner before and after the stimulation. The routine sagittal T1-weighted, coronal T1-weighted, and axial T2-weighted fluid-attenuated inversion recovery (T2-FLAIR) sequences were adopted in the multi-planar anatomical positioning of the voxel of interest (VOI). The multi-voxel ^{1}H-MRS sequence was acquired using the following scan parameters: repetition time (TR) = 1,700 ms, echo time (TE) = 135 ms, bandwidth = 1,200 Hz, voxel size = 6.3 mm × 6.3 mm × 15 mm, and total acquisition time = 6 min 53 s. The VOI for each participant was placed at the largest level of the cerebellum, including the bilateral dentate nucleus, cerebellar hemispheres, and the vermis of the cerebellum. The peak areas for NAA at 2.02 parts per million (ppm), Cho at 3.22 ppm, and Cr at 3.03 ppm were automatically calculated by the post-processing software provided by the machine manufacturer. Then, the metabolite intensity ratios, including NAA/Cr and Cho/Cr, for each voxel were acquired. The selection criteria for the voxels in the VOI were as follows: only the voxel with the largest NAA amplitude and good wave quality was selected for analysis when there were multiple voxels simultaneously excited within the VOI.

Data Processing and Statistical Analyses

The analysis of the primary outcome was based on the intention-to-treat principle. Due to the lack of MRS data, the secondary outcome was based on as-treated analysis (Langezaal et al., 2021). Data normality was determined by the Shapiro–Wilk tests in all the analyses. For comparisons of the baseline data between the two groups, a Fisher's exact test was used to analyze gender distribution. To separately compare the pre- and post-stimulation data (MRS data and ICARS score) in the real and sham groups, paired-sample *t*-tests and Wilcoxon signed-rank tests were used in the analyses of normal and abnormal data, respectively. The consecutive variables were analyzed by independent samples *t*-tests for normal data, and Mann–Whitney U tests were used for assessing abnormal data. To confirm the robustness of the primary findings, we used the analysis of covariance to fit additional models with the mean change in the assessment metrics (ICARS and MRS) after the treatment session as the dependent variable, the treatment group as the independent variable, and the corresponding baseline scores as covariates. Pearson correlation analysis was performed to assess the relationship between the MRS data and ICARS scores. The above statistics were analyzed and processed using SPSS 27.0 (SPSS Inc., Chicago, IL, United States). The level of significance was established as $p < 0.05$.

RESULTS

A total of 18 patients participated in this study; nine were randomly assigned to the real stimulation group and nine to the sham stimulation group. No participant dropped out of the study in the sham stimulation group; two participants in the real stimulation group were not included in the imaging data because they were unable to cooperate with the second MRS examination. The flow chart representing all the participants is presented in **Figure 1**. All the participants tolerated the intervention without significant adverse effects throughout the study. There were no significant differences between the two groups for any of the baseline indicators, including age ($p = 0.37$), gender distribution ($p = 1.00$), age of onset ($p = 0.38$), disease duration ($p = 0.95$), NAA/Cr, Cho/Cr ratios, as well as the ICARS scores (**Tables 1**–**3**).

The ICARS scores significantly decreased after treatment in both the groups, while the decrease was more significant in the real stimulation group compared to the sham stimulation group ($p < 0.001$) (**Figure 2**; the comparison of scores of ICARS and its four subscales' domain before and after stimulation in the real and sham intervention groups are provided in **Table 2**). To confirm the robustness of the primary findings, we used the analysis of covariance. The total ICARS scores decreased more dramatically in the real group after treatment compared to the sham group ($F = 31.239$, $p < 0.001$), and three of the four subscales' domain scores had the same decreased pattern as the total ICARS scores as follows: PG ($F = 13.037$, $p = 0.003$), KF ($F = 22.679$, $p < 0.001$), DS (no statistical analysis was performed because there was no change in the results before and after), OMS ($F = 0.261$, $p = 0.617$).

In the real stimulation group, after 15 consecutive days of low-frequency rTMS treatment, the NAA/Cr values in the cerebellar vermis, left and right lateral in the cerebellar hemispheres, and dentate nuclei were all significantly elevated, compared with those before treatment ($p < 0.05$) (**Table 3** and **Figure 3A**). The Cho/Cr values in the above-mentioned brain regions were also obviously elevated compared to those before treatment ($p < 0.05$)

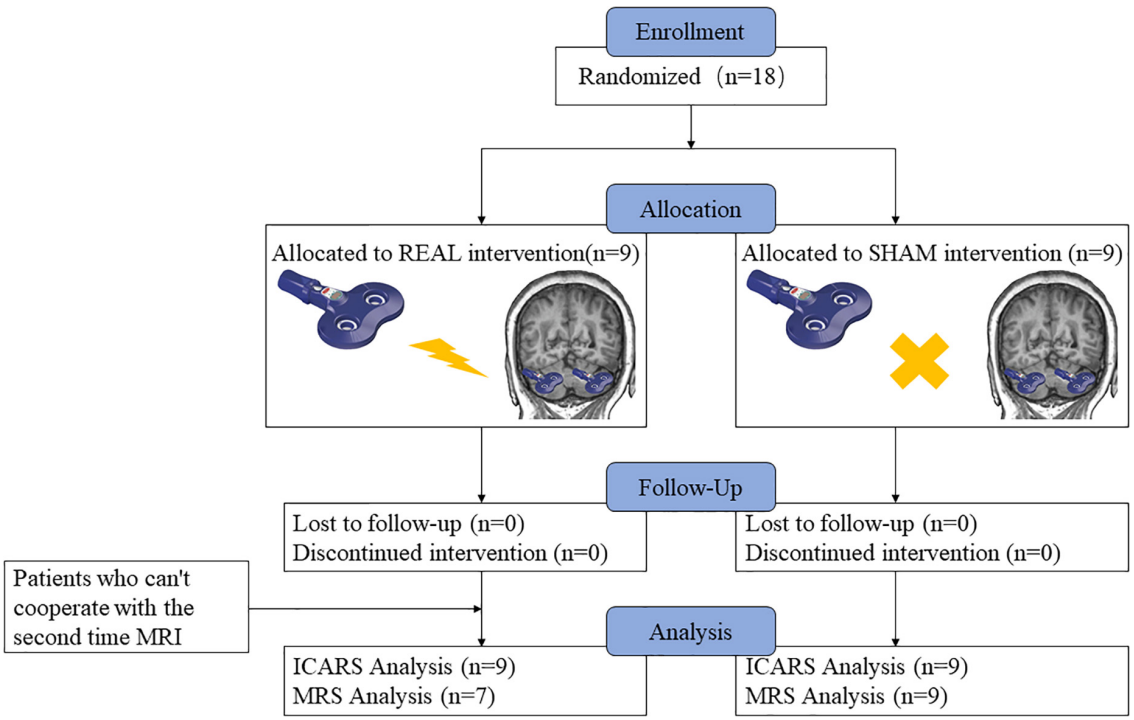

FIGURE 1 | Schematic diagram of the research process. Nine individuals were randomly assigned to the low-frequency rTMS intervention, nine were assigned to the sham intervention, and zero dropped out of the experiment, but two participants in the real stimulation group were not included in the imaging data because they were unable to cooperate with the second MRS examination.

TABLE 1 | The analysis of baseline data from the patients with SCA3.

Characteristic	Real stimulation group	Sham stimulation group	*P* Value
Number	9	9	–
Age, years	37.78 ± 9.28	41.78 ± 9.18	0.37
Gender, M / F	4/5	4/5	1.00
Age at onset (years)	31.44 ± 9.70	35.56 ± 9.51	0.38
Duration of disease (years)	6.33 ± 3.39	6.22 ± 4.15	0.95

TABLE 2 | The comparison of scores of ICARS and its four subscales' domain before and after stimulation in the real and sham intervention groups.

	Real rTMS		Sham rTMS		*P* value[a]	*P* value[b]	*P* value[c]	*P* value[d]
Variables	**Pre-rTMS**	**Post-rTMS**	**Pre-rTMS**	**Post-rTMS**				
ICARS	41.33 ± 15.45	33.56 ± 15.01	29.33 ± 12.04	27.56 ± 12.43	**<0.001[e]**	**0.002[e]**	**0.085[f]**	**<0.001[f]**
PG	17.78 ± 6.40	15.78 ± 6.70	12.33 ± 6.63	11.89 ± 6.70	**0.001[e]**	**0.035[e]**	**0.095[f]**	**0.003[f]**
KF	16.89 ± 7.41	11.22 ± 6.69	12.22 ± 6.04	10.89 ± 6.60	**<0.001[e]**	**0.004[e]**	**0.162[f]**	**<0.001[f]**
DS	3.89 ± 1.62	3.89 ± 1.62	2.33 ± 1.32	2.33 ± 1.32	/*	**0.041[e]**	/*	/*
OMS	2.78 ± 0.97	2.67 ± 0.87	2.67 ± 1.32	2.67 ± 1.12	**0.347[e]**	**1[e]**	**0.842[f]**	**0.588[f]**

*ICARS = the International Cooperative Ataxia Rating Scale; PG = posture and gait; KF = limb kinetic function; DS = speech disorders; OMS = oculomotor disorders. Values are expressed as mean ± standard deviation and median (upper limit, lower limit); the value in bold represents statistical significance. [a]Pre-stimulation vs. post-stimulation in real rTMS. [b]Pre-stimulation vs. post-stimulation in sham rTMS. [c]Comparison between groups (pre-stimulation). [d]Comparison of differences between groups (real vs. sham group). [e]Paired-samples t test. [f]Independent samples t test. *No statistical analysis was performed because there was no change in the results before and after.*

(**Table 3** and **Figure 3B**); on the other hand, in the sham stimulation group, there were no significant differences in either the NAA/Cr and Cho/Cr values in the brain regions noted above both before and after stimulation (**Table 3** and **Figure 4**). The elevations in the NAA/Cr and Cho/Cr values after the stimulation were significantly higher in the real stimulation group than in the

TABLE 3 | The NAA/Cr and Cho/Cr values in the real and sham interventions before and after stimulation.

	Real rTMS		Sham rTMS		*P* value[a]	*P* value[b]	*P* value[c]	*P* value[d]
Variables	**Pre-rTMS**	**Post-rTMS**	**Pre-rTMS**	**Post-rTMS**				
NAA / Cr								
Ce	0.62 ± 0.16	0.96 ± 0.14	0.64 ± 0.11	0.65 ± 0.10	**<0.001[e]**	**0.560[e]**	**0.842[h]**	**<0.001[h]**
L-DN	0.77(0.64,0.80)	1.03(0.99,1.30)	0.82 ± 0.13	0.81 ± 0.15	**0.018[f]**	**0.412[e]**	**0.197[h]**	**0.018[h]**
R-DN	0.70 ± 0.15	1.15 ± 0.17	0.73 ± 0.18	0.77 ± 0.16	**0.007[e]**	**0.172[e]**	**0.726[h]**	**0.009[h]**
L-CH	0.62 ± 0.11	0.95 ± 0.10	0.69 ± 0.08	0.69 ± 0.06	**<0.001[e]**	**0.914[e]**	**0.154[h]**	**<0.001[h]**
R-CH	0.71(0.67,0.78)	1.10(0.97,1.12)	0.83 ± 0.10	0.82 ± 0.07	**0.018[f]**	**0.658[e]**	**0.027[h]**	**<0.001[h]**
Cho / Cr								
Ce	0.81 ± 0.16	1.23 ± 0.17	0.88 ± 0.16	0.84 ± 0.12	**<0.001[e]**	**0.341[e]**	**0.412[h]**	**<0.001[h]**
L-DN	0.92 ± 0.08	1.39 ± 0.39	0.96 ± 0.10	0.97 ± 0.10	**0.021[e]**	**0.899[e]**	**0.325[g]**	**0.021[h]**
R-DN	0.85(0.75,1.00)	1.17(1.11,1.27)	0.89 ± 0.15	0.87 ± 0.13	**0.018[f]**	**0.248[e]**	**0.654[h]**	**0.022[h]**
L-CH	0.86 ± 0.16	1.17 ± 0.08	0.91 ± 0.09	0.89 ± 0.11	**<0.001[e]**	**0.411[e]**	**0.388[h]**	**<0.001[h]**
R-CH	0.88(0.58,0.98)	1.14(1.13,1.23)	0.95 ± 0.12	0.94 ± 0.12	**0.018[f]**	**0.454[e]**	**0.088[h]**	**0.001[h]**

rTMS = repetitive transcranial magnetic stimulation; Ce = cerebellar vermis; L-CH = left cerebellar hemisphere; R-CH = right cerebellar hemisphere; L-DN = left dentate nucleus; R-DN = right dentate nucleus. Values are expressed as mean ± standard deviation and median (upper limit, lower limit); the value in bold represents statistical significance. [a]Pre-stimulation vs. post-stimulation in real rTMS. [b]Pre-stimulation vs. post-stimulation in sham rTMS. [c]Comparison between groups (pre-stimulation). [d]Comparison of differences between groups (real vs. sham group). [e]Paired-samples t test. [f]Wilcoxon signed rank test. [g]Mann-Whitney U test. [h]Independent samples t tests.

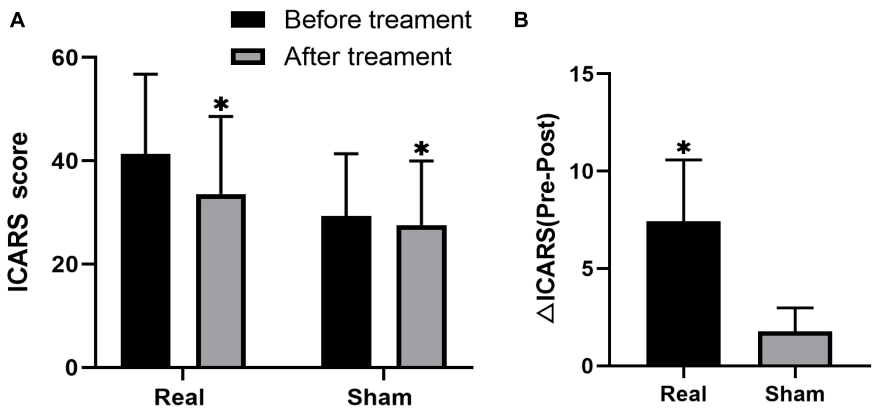

FIGURE 2 | Changes in ICARS score before and after treatment in both groups of real and sham stimulation. The comparison between pre and post stimulation in both groups, respectively **(A)**.The comparison of difference in ICARS (△ICARS) after the stimulation between real and sham stimulation groups **(B)**. *Indicates the significant difference.

sham stimulation group (**Table 3**). The mean change in MRS after treatment using covariance (ANCOVA) showed that the NAA/Cr and Cho/Cr values increased after treatment in the real group compared to the respective scores in the sham group (Ce-NAA / Cr: F = 72.4, $p < 0.001$; Ce-Cho / Cr: F = 73.70, $p < 0.001$; L-CH-NAA / Cr: F = 10.38, $p = 0.007$; L-CH-Cho / Cr: F = 9.41, $p = 0.009$; R-CH-NAA / Cr: F = 22.6, $p < 0.001$; R-CH-Cho / Cr: F = 16.14, $p = 0.001$; L-DN-NAA / Cr: F = 48.24, $p < 0.001$; L-DN-Cho / Cr: F = 61.41, $p < 0.001$; R-DN-NAA / Cr: F = 25.2, $p < 0.001$; R-DN-Cho / Cr: F = 61.15, $p < 0.001$) (Refer to **Table 3** for abbreviations).

In the real stimulation group, the NAA/Cr value changes in the right cerebellar hemisphere were negatively correlated with the changes in the ICARS scores (r = − 0.831, $p = 0.02$), while the changes in the NAA/Cr values in the left cerebellar hemisphere did not correlate with the changes in the ICARS scores (r = − 0.495, $p = 0.259$). No other correlation existed between the remaining indicators.

DISCUSSION

In this study, we conducted a randomized, double-blind, controlled trial among SCA3 patients and found that after the low-frequency rTMS intervention, the NAA/Cr and Cho/Cr values increased and the ataxia symptoms improved. In addition, there was a correlation between the changes in the NAA/Cr values and ICARS scores. Investigating the changes of cerebellar neurochemicals in the SCA3 patients under rTMS intervention is an innovation developed in recent years.

In clinical practice, MRS can non-invasively detect changes in metabolite concentrations in the brain tissue and accurately

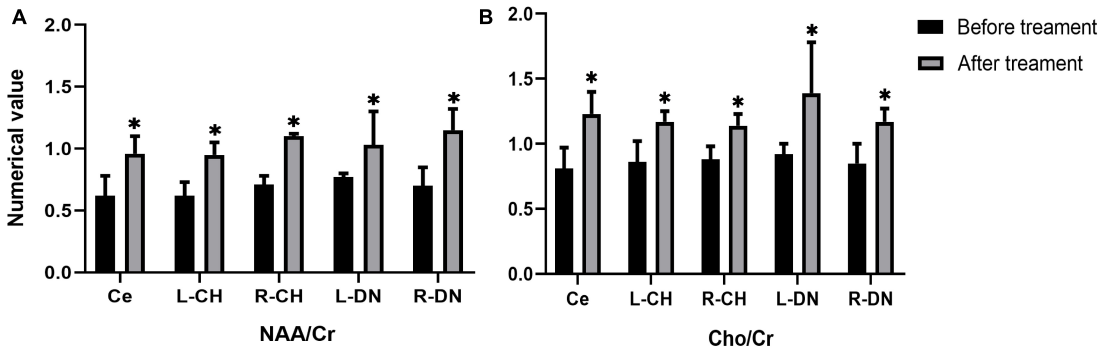

FIGURE 3 | Changes in the values of NAA / Cr **(A)**, and Cho / Cr **(B)** in cerebellar vermis, left and right cerebellar hemisphere, left and right dentate nucleus before and after treatment in the real stimulation group. (Ce representing the cerebellar vermis; L-CH representing the left cerebellar hemisphere; R-CH representing the right cerebellar hemisphere L-DN represents the left dentate nucleus; R-DN represents the right dentate nucleus). *Indicates the significant difference in the comparison between pre and post stimulation.

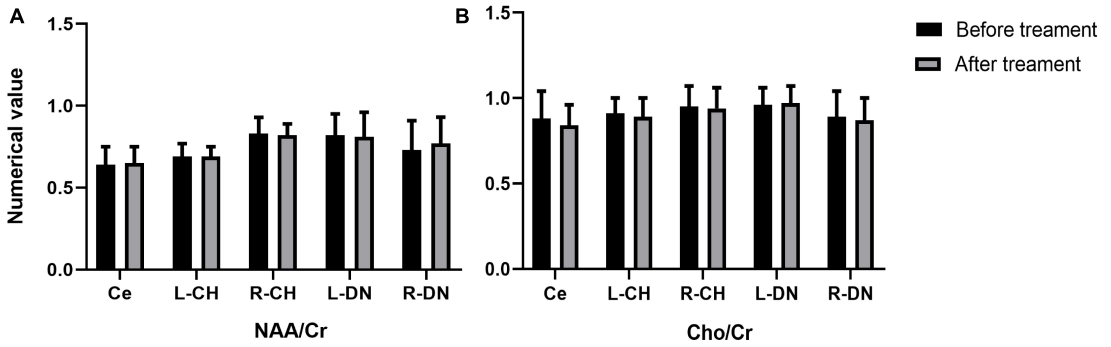

FIGURE 4 | Changes in the values of NAA / Cr **(A)**, and Cho / Cr **(B)** in cerebellar vermis, left and right cerebellar hemisphere, left and right dentate nucleus before and after treatment in the sham stimulation group (Ce representing the cerebellar vermis; L-CH representing the left cerebellar hemisphere; R-CH representing the right cerebellar hemisphere L-DN represents the left dentate nucleus; R-DN represents the right dentate nucleus).

detect NAA, Cho, and Cr in the brain, providing reliable biomarkers for SCA3 (Matos et al., 2019). The NAA represents neuronal viability and integrity (Wang et al., 2012), and creatine (Cr) reflects energy metabolism in the brain (Wang et al., 2012); Cr concentrations in the brain tissue are high and relatively stable. Therefore, NAA and Cr can be used as a reference for comparison between the groups. Choline (Cho) is a marker of cell renewal (Bridges et al., 2018). NAA/Cr indicates neuronal function at the test site, and Cho/Cr reflects glial cell function; therefore, NAA/Cr and Cho/Cr can be used as indicators for neuronal and myelin integrity (Cuypers and Marsman, 2021). Significant pathological damage and atrophy in the patients with SCAs have been shown to result in neuronal loss/dysfunction, and therefore, a decrease in the NAA and Glu (Adanyeguh et al., 2015).

There are studies on the changes in the cerebellar neurometabolites in some diseases under low-frequency rTMS intervention. However, there were no published studies on the changes in the cerebellar neurometabolites in the SCA3 patients with low-frequency rTMS intervention. For the treatment of cognitive function associated with cranial injury, the patient's MRS showed a decrease in both NAA/Cr and Cho/Cr ratios (Zhou et al., 2021). Low-frequency rTMS interfered with *N*-acetyl aspartate (NAAG) synthesis and cell turnover (Bridges et al., 2018) as well as increased NAA levels in the prefrontal and striatal lobes (Hone-Blanchet et al., 2017). Low-frequency rTMS leads to selective changes in the glutamate and gamma-aminobutyric acid concentrations in different brain regions (Yue et al., 2009). It may improve the metabolic activity of NAA and other neuronal cells by stimulating the cortical neurons.

The mechanism by which rTMS affects the neural metabolism in the brain of SCA patients can be explained as follows: low-frequency rTMS inhibits cortical excitability. However, a previous study showed that 1 Hz rTMS led to an increase in the NAA rather than the expected decrease, which may be due to an *in vivo* homeostatic mechanism wherein inhibitory 1 Hz rTMS may paradoxically induce an increase instead of a decrease in the local activity (Fregni et al., 2011). Research has shown that low-frequency rTMS increased brain-derived neurotrophic factor content and nerve growth factor expression, resulting in increased neurometabolic substances (Tan et al., 2013). Among them, the increase in the tCho/tCr ratio may be related to underlying neuroplasticity processes (Flamez et al., 2019). Studies have shown that rTMS can improve motor function in patients,

likely because continuous stimulation with rTMS at the same frequency and intensity can cause uninterrupted excitation or inhibition of neuronal cells, allowing neural networks to reorganize after brain injury, and thus improving clinical symptoms (Zhou et al., 2021). From this, we can speculate that the possible mechanism of low-frequency rTMS in treating SCA3 patients should improve neuronal cell function by modulating the ability of gene expression and regulating the expression of various growth factors.

The Scale for the Assessment and Rating of Ataxia (SARA) is currently the tool of choice to demonstrate the efficacy of the SCA3 disease improvement or symptomatic treatment for ataxia, the most important disease feature, and numerous clinical studies have identified SARA as the preferred method (Saute and Jardim, 2018; Lin et al., 2019; Diallo et al., 2021; Maas et al., 2021). It has also been shown that ICARS and SARA are reliable and valid scales for assessing the severity of ataxia in patients with SCA3/MJD and that the most appropriate scale can be selected according to specific requirements (Zhou et al., 2011). ICARS shows very high inter-rater reliability and is sensitive to a wide range of ataxia symptoms, from very mild to severe (Zhou et al., 2011). There is a correlation between it and the degree of cerebellar lesions (Xing et al., 2017). ICARS outperforms SARA in terms of responsiveness in SCA patients (Perez-Lloret et al., 2021), and many interventional studies have used ICARS alone (Peng et al., 2019; de Oliveira et al., 2021; Leotti et al., 2021), thus, we ultimately chose to use ICARS as the primary clinical outcome parameter.

Both the real and sham groups demonstrated improvement in the ICARS scores. There are many possible reasons behind the improvement in the sham group. First, there may be a placebo effect, which is very common in the intervention studies of cerebellar degeneration (Bier et al., 2003; Zesiewicz et al., 2012); the sham stimulation produced the same noise as the real stimulation and had some scalp perception. Patients were unaware of the difference between the real and sham stimulation because no patient had previously experienced real stimulation. Therefore, patients undergoing sham stimulation did not notice that they were receiving inactive stimulation. Second, all patients were under the supervision of clinical research staff during the study period, which may have been more than their normal care. This may have induced underlying psychological factors in the patients that could have produced a significant treatment effect (Manor et al., 2019). Third, repeated assessment of ICARS over a short time may lead to patient proficiency in the assessment methods, which may then produce improved effects beyond stimulation. We also found an interaction between time and intervention in our results, which suggests a difference in the trend of the outcomes ICARS over time in the two groups. The effect of true stimulation may become more significant as the duration of the intervention increases, but we measured only one time point after treatment, so there may be bias.

Nevertheless, this study has several limitations. First, given that the sample size was small, the evidence collected was limited. Second, since the participants did not receive follow-up care after the study, we were not able to measure the long-term efficacy of low-frequency rTMS on the cerebellar metabolites. Third, although the participants were blind to the assigned treatment, we used a true coil in the sham stimulation group, placed differently than in the real stimulation group, and the patients might have become aware of this difference during the study. This limitation needs to be considered regarding the generalization of the study results. Finally, we conducted a double-blind trial, but the therapist doing the rTMS was not blinded, which may affect the objectivity of the study.

CONCLUSION

Overall, the treatment with rTMS over the cerebellum induced changes in cerebellar local metabolism and microenvironment in SCA3 patients. The alterations may contribute to the improvement of the ataxia symptoms in SCA3 patients.

DATA AVAILABILITY STATEMENT

The raw data supporting the conclusions of this article will be made available by the authors, without undue reservation.

ETHICS STATEMENT

The studies involving human participants were reviewed and approved by the Ethics Committee of First Affiliated Hospital of Fujian Medical University (MRCTA, ECFAH of [2018]201). The patients/participants provided their written informed consent to participate in this study.

AUTHOR CONTRIBUTIONS

X-YC, Y-HL, and X-HL for designed the study, wrote the manuscript, and processed the data. AS and H-LX helped in the transcranial magnetic intervention and patient assessment. J-PH and M-CL contributed to the magnetic resonance scanning and processing. Q-LC and S-RG helped in manuscript preparation and contributed to the supervision of the whole process. All authors reported above for publication was completed and contributed to the article and approved the submitted version.

FUNDING

This work was supported by the National Natural Science Foundation of China (81971082, Beijing; S-RG). This work was also supported by the Fujian Provincial Health Technology Project (2019025, Fujian) and Nursery Fund for Scientific Research of Fujian Medical University (2015MP025, Fujian; X-YC), as well as the Startup Fund for scientific research, Fujian Medical University (2019QH1095, Fujian; X-HL) and the Natural Science Foundation of Fujian Province (2019J01435, Fujian; J-PH).

REFERENCES

Adanyeguh, I. M., Henry, P. G., Nguyen, T. M., Rinaldi, D., Jauffret, C., Valabregue, R., et al. (2015). *In vivo* neurometabolic profiling in patients with spinocerebellar ataxia types 1, 2, 3, and 7. *Mov. Disord. Off. J. Mov. Disord. Soc.* 30, 662–670. doi: 10.1002/mds.26181

Benussi, A., Pascual-Leone, A., and Borroni, B. (2020). Non-invasive cerebellar stimulation in neurodegenerative ataxia: a literature review. *Int. J. Mol. Sci.* 21:1978. doi: 10.3390/ijms21061948

Bier, J. C., Dethy, S., Hildebrand, J., Jacquy, J., Manto, M., Martin, J. J., et al. (2003). Effects of the oral form of ondansetron on cerebellar dysfunction. A multicenter double-blind study. *J. Neurol.* 250, 693–697. doi: 10.1007/s00415-003-1061-9

Bridges, N. R., McKinley, R. A., Boeke, D., Sherwood, M. S., Parker, J. G., McIntire, L. K., et al. (2018). Single session low frequency left dorsolateral prefrontal transcranial magnetic stimulation changes neurometabolite relationships in healthy humans. *Front. Hum. Neurosci.* 12:77. doi: 10.3389/fnhum.2018.00077

Costa, M. (2020). Recent therapeutic prospects for Machado-Joseph disease. *Curr. Opin. Neurol.* 33, 519–526. doi: 10.1097/WCO.0000000000000832

Cuypers, K., and Marsman, A. (2021). Transcranial magnetic stimulation and magnetic resonance spectroscopy: opportunities for a bimodal approach in human neuroscience. *NeuroImage* 224:117394. doi: 10.1016/j.neuroimage.2020.117394

Dang, G., Su, X., Zhou, Z., Che, S., Zeng, S., Chen, S., et al. (2019). Beneficial effects of cerebellar rTMS stimulation on a patient with spinocerebellar ataxia type 6. *Brain Stimul.* 12, 767–769. doi: 10.1016/j.brs.2018.12.225

de Oliveira, C. M., Leotti, V. B., Bolzan, G., Cappelli, A. H., Rocha, A. G., Ecco, G., et al. (2021). Pre-ataxic changes of clinical scales and eye movement in machado-joseph disease: BIGPRO study. *Mov. Disord. Off. J. Mov. Disord. Soc.* 36, 985–994. doi: 10.1002/mds.28466

Diallo, A., Jacobi, H., Tezenas du Montcel, S., and Klockgether, T. (2021). Natural history of most common spinocerebellar ataxia: a systematic review and meta-analysis. *J. Neurol.* 268, 2749–2756. doi: 10.1007/s00415-020-09815-2

Farzan, F., Wu, Y., Manor, B., Anastasio, E. M., Lough, M., Novak, V., et al. (2013). Cerebellar TMS in treatment of a patient with cerebellar ataxia: evidence from clinical, biomechanics and neurophysiological assessments. *Cerebellum (London, England)* 12, 707–712. doi: 10.1007/s12311-013-0485-8

Flamez, A., Wiels, W., Van Schuerbeek, P., De Mey, J., De Keyser, J., and Baeken, C. (2019). The influence of one session of low frequency rTMS on pre-supplementary motor area metabolites in late stage Parkinson's disease. *Clin. Neurophysiol. Off. J. Int. Federat. Clin. Neurophysiol.* 130, 1292–1298. doi: 10.1016/j.clinph.2019.04.720

França, C., de Andrade, D. C., Silva, V., Galhardoni, R., Barbosa, E. R., Teixeira, M. J., et al. (2020). Effects of cerebellar transcranial magnetic stimulation on ataxias: a randomized trial. *Parkinsonism Related Disord.* 80, 1–6. doi: 10.1016/j.parkreldis.2020.09.001

Fregni, F., Potvin, K., Dasilva, D., Wang, X., Lenkinski, R. E., Freedman, S. D., et al. (2011). Clinical effects and brain metabolic correlates in non-invasive cortical neuromodulation for visceral pain. *Eur. J. Pain (London, England)* 15, 53–60. doi: 10.1016/j.ejpain.2010.08.002

Hall, H., Cuellar-Baena, S., Dahlberg, C., In't Zandt, R., Denisov, V., and Kirik, D. (2012). Magnetic resonance spectroscopic methods for the assessment of metabolic functions in the diseased brain. *Curr. Topics Behav. Neurosci.* 11, 169–198. doi: 10.1007/7854_2011_166

Hone-Blanchet, A., Mondino, M., and Fecteau, S. (2017). Repetitive transcranial magnetic stimulation reduces anxiety symptoms, drug cravings, and elevates (1)H-MRS brain metabolites: a case report. *Brain Stimul.* 10, 856–858. doi: 10.1016/j.brs.2017.03.007

Ihara, Y., Takata, H., Tanabe, Y., Nobukuni, K., and Hayabara, T. (2005). Influence of repetitive transcranial magnetic stimulation on disease severity and oxidative stress markers in the cerebrospinal fluid of patients with spinocerebellar degeneration. *Neurol. Res.* 27, 310–313. doi: 10.1179/016164105X39897

Jhunjhunwala, K., Prashanth, D. K., Netravathi, M., Jain, S., Purushottam, M., and Pal, P. K. (2013). Alterations in cortical excitability and central motor conduction time in spinocerebellar ataxias 1, 2 and 3: a comparative study. *Parkinsonism Related Disord.* 19, 306–311. doi: 10.1016/j.parkreldis.2012.11.002

Krahe, J., Binkofski, F., Schulz, J. B., Reetz, K., and Romanzetti, S. (2020). Neurochemical profiles in hereditary ataxias: a meta-analysis of Magnetic Resonance Spectroscopy studies. *Neurosci. Biobehav. Rev.* 108, 854–865. doi: 10.1016/j.neubiorev.2019.12.019

Langezaal, L., van der Hoeven, E., Mont'Alverne, F., de Carvalho, J., Lima, F. O., Dippel, D. W. J., et al. (2021). Endovascular therapy for stroke due to basilar-artery occlusion. *New Engl. J. Med.* 384, 1910–1920. doi: 10.1056/NEJMoa2030297

Lei, L., Liao, Y., Liao, W., Zhou, J., Yuan, Y., Wang, J., et al. (2011). Magnetic resonance spectroscopy of the cerebellum in patients with spinocerebellar ataxia type 3/Machado-Joseph disease. *Zhong Nan Da Xue Xue Bao Yi Xue Ban J. Central South Univ. Med. Sci.* 36, 511–519. doi: 10.3969/j.issn.1672-7347.2011.06.007

Leotti, V. B., de Vries, J. J., Oliveira, C. M., de Mattos, E. P., Te Meerman, G. J., Brunt, E. R., et al. (2021). CAG repeat size influences the progression rate of spinocerebellar ataxia Type 3. *Ann. Neurol.* 89, 66–73. doi: 10.1002/ana.25919

Li, X., Liu, H., Fischhaber, P. L., and Tang, T. S. (2015). Toward therapeutic targets for SCA3: insight into the role of Machado-Joseph disease protein ataxin-3 in misfolded proteins clearance. *Progr. Neurobiol.* 132, 34–58. doi: 10.1016/j.pneurobio.2015.06.004

Lim, C. Y., and In, J. (2019). Randomization in clinical studies. *Korean J. Anesthesiol.* 72, 221–232. doi: 10.4097/kja.19049

Lin, Y. C., Lee, Y. C., Hsu, T. Y., Liao, Y. C., and Soong, B. W. (2019). Comparable progression of spinocerebellar ataxias between Caucasians and Chinese. *Parkinsonism Related Disord.* 62, 156–162. doi: 10.1016/j.parkreldis.2018.12.023

Lirng, J. F., Wang, P. S., Chen, H. C., Soong, B. W., Guo, W. Y., Wu, H. M., et al. (2012). Differences between spinocerebellar ataxias and multiple system atrophy-cerebellar type on proton magnetic resonance spectroscopy. *PLoS One* 7:e47925. doi: 10.1371/journal.pone.0047925

Maas, R., van de Warrenburg, B., and Schutter, D. (2021). Inverse associations between cerebellar inhibition and motor impairment in spinocerebellar ataxia type 3. *Brain Stimul.* 14, 351–357. doi: 10.1016/j.brs.2021.01.020

Manor, B., Greenstein, P. E., Davila-Perez, P., Wakefield, S., Zhou, J., and Pascual-Leone, A. (2019). Repetitive transcranial magnetic stimulation in spinocerebellar ataxia: a pilot randomized controlled trial. *Front. Neurol.* 10:73. doi: 10.3389/fneur.2019.00073

Matos, C. A., de Almeida, L. P., and Nóbrega, C. (2019). Machado-Joseph disease/spinocerebellar ataxia type 3: lessons from disease pathogenesis and clues into therapy. *J. Neurochem.* 148, 8–28. doi: 10.1111/jnc.14541

Peng, H., Liang, X., Long, Z., Chen, Z., Shi, Y., Xia, K., et al. (2019). Gene-Related cerebellar neurodegeneration in SCA3/MJD: a case-controlled imaging-genetic study. *Front. Neurol.* 10:1025. doi: 10.3389/fneur.2019.01025

Perez-Lloret, S., van de Warrenburg, B., Rossi, M., Rodríguez-Blázquez, C., Zesiewicz, T., Saute, J., et al. (2021). Assessment of ataxia rating scales and cerebellar functional tests: critique and recommendations. *Mov. Disord. Off. J. Mov. Disord. Soc.* 36, 283–297. doi: 10.1002/mds.28313

Sanna, A., Follesa, P., Tacconi, P., Serra, M., Pisu, M. G., Cocco, V., et al. (2021). Therapeutic use of cerebellar Intermittent Theta Burst Stimulation (iTBS) in a sardinian family affected by Spinocerebellar Ataxia 38 (SCA 38). *Cerebellum (London, England)*. [Online ahead of print] doi: 10.1007/s12311-021-01313-z

Saute, J., and Jardim, L. B. (2018). Planning future clinical trials for machado-joseph disease. *Adv. Exp. Med. Biol.* 1049, 321–348. doi: 10.1007/978-3-319-71779-1_17

Shiga, Y., Tsuda, T., Itoyama, Y., Shimizu, H., Miyazawa, K. I., Jin, K., et al. (2002). Transcranial magnetic stimulation alleviates truncal ataxia in spinocerebellar degeneration. *J. Neurol. Neurosurg. Psychiatry* 72, 124–126. doi: 10.1136/jnnp.72.1.124

Song, P., Li, S., Wang, S., Wei, H., Lin, H., and Wang, Y. (2020). Repetitive transcranial magnetic stimulation of the cerebellum improves ataxia and cerebello-fronto plasticity in multiple system atrophy: a randomized, double-blind, sham-controlled and TMS-EEG study. *Aging* 12, 20611–20622. doi: 10.18632/aging.103946

Tan, T., Xie, J., Liu, T., Chen, X., Zheng, X., Tong, Z., et al. (2013). Low-frequency (1 Hz) repetitive transcranial magnetic stimulation (rTMS) reverses Aβ (1-42)-mediated memory deficits in rats. *Exp. Gerontol.* 48, 786–794. doi: 10.1016/j.exger.2013.05.001

Trouillas, P., Takayanagi, T., Hallett, M., Currier, R. D., Subramony, S. H., Wessel, K., et al. (1997). International cooperative ataxia rating scale for pharmacological assessment of the cerebellar syndrome. The ataxia

neuropharmacology committee of the world federation of neurology. *J. Neurol. Sci.* 145, 205–211. doi: 10.1016/s0022-510x(96)00231-6

Wang, P. S., Chen, H. C., Wu, H. M., Lirng, J. F., Wu, Y. T., and Soong, B. W. (2012). Association between proton magnetic resonance spectroscopy measurements and CAG repeat number in patients with spinocerebellar ataxias 2, 3, or 6. *PLoS One* 7:e47479. doi: 10.1371/journal.pone.0047479

Xing, W., Liao, X., Guan, T., Xie, F., Shen, L., Liao, W., et al. (2017). [Value of 1H-MRS on SCA3/MJD diagnosis and clinical course]. *Zhong Nan Da Xue Xue Bao Yi Xue Ban J. Central South Univ. Med. Sci.* 42, 291–297. doi: 10.11817/j.issn.1672-7347.2017.03.009

Yue, L., Xiao-lin, H., and Tao, S. (2009). The effects of chronic repetitive transcranial magnetic stimulation on glutamate and gamma-aminobutyric acid in rat brain. *Brain Res.* 1260, 94–99. doi: 10.1016/j.brainres.2009.01.009

Zesiewicz, T. A., Greenstein, P. E., Sullivan, K. L., Wecker, L., Miller, A., Jahan, I., et al. (2012). A randomized trial of varenicline (Chantix) for the treatment of spinocerebellar ataxia type 3. *Neurology* 78, 545–550. doi: 10.1212/WNL.0b013e318247cc7a

Zhou, J., Lei, L., Liao, X., Wang, J., Jiang, H., Tang, B., et al. (2011). Related factors of ICARS and SARA scores on spinocerebellar ataxia type 3/Machado-Joseph disease. *Zhong Nan Da Xue Xue Bao Yi Xue Ban J. Central South Univ. Med. Sci.* 36, 498–503. doi: 10.3969/j.issn.1672-7347.2011.06.005

Zhou, L., Huang, X., Li, H., Guo, R., Wang, J., Zhang, Y., et al. (2021). Rehabilitation effect of rTMS combined with cognitive training on cognitive impairment after traumatic brain injury. *Am. J. Transl. Res.* 13, 11711–11717.

Conflict of Interest: The authors declare that the research was conducted in the absence of any commercial or financial relationships that could be construed as a potential conflict of interest.

Publisher's Note: All claims expressed in this article are solely those of the authors and do not necessarily represent those of their affiliated organizations, or those of the publisher, the editors and the reviewers. Any product that may be evaluated in this article, or claim that may be made by its manufacturer, is not guaranteed or endorsed by the publisher.

Advantages of publishing in Frontiers

OPEN ACCESS
Articles are free to read for greatest visibility and readership

FAST PUBLICATION
Around 90 days from submission to decision

HIGH QUALITY PEER-REVIEW
Rigorous, collaborative, and constructive peer-review

TRANSPARENT PEER-REVIEW
Editors and reviewers acknowledged by name on published articles

Frontiers
Avenue du Tribunal-Fédéral 34
1005 Lausanne | Switzerland

Visit us: www.frontiersin.org
Contact us: frontiersin.org/about/contact

REPRODUCIBILITY OF RESEARCH
Support open data and methods to enhance research reproducibility

DIGITAL PUBLISHING
Articles designed for optimal readership across devices

FOLLOW US
@frontiersin

IMPACT METRICS
Advanced article metrics track visibility across digital media

EXTENSIVE PROMOTION
Marketing and promotion of impactful research

LOOP RESEARCH NETWORK
Our network increases your article's readership